

UNCLASSIFIED

AD 4 1 9 9 9 0

DEFENSE DOCUMENTATION CENTER

FOR

SCIENTIFIC AND TECHNICAL INFORMATION

CAMERON STATION, ALEXANDRIA, VIRGINIA



UNCLASSIFIED

NOTICE: When government or other drawings, specifications or other data are used for any purpose other than in connection with a definitely related government procurement operation, the U. S. Government thereby incurs no responsibility, nor any obligation whatsoever; and the fact that the Government may have formulated, furnished, or in any way supplied the said drawings, specifications, or other data is not to be regarded by implication or otherwise as in any manner licensing the holder or any other person or corporation, or conveying any rights or permission to manufacture, use or sell any patented invention that may in any way be related thereto.

CATALOGED BY ONC

419990

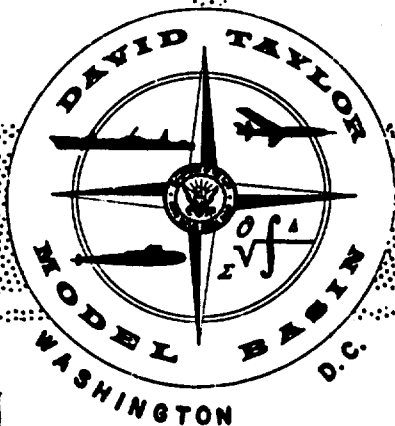
HYDROMECHANICS

AS AD

AERODYNAMICS

STRUCTURAL
MECHANICS

APPLIED
MATHEMATICS



DEPARTMENT OF THE NAVY

SERIES 60

METHODICAL EXPERIMENTS WITH MODELS
OF SINGLE-SCREW MERCHANT SHIPS

by

F. H. Todd, Ph.D

RESEARCH AND DEVELOPMENT REPORT

July 1963

Report 1712

This Document Contains
Missing Page/s That Are
Unavailable In The
Original Document

Best Available Copy

SERIES 60
METHODICAL EXPERIMENTS WITH MODELS
OF SINGLE-SCREW MERCHANT SHIPS

by

F. H. Todd, Ph.D

July 1963

Report 1712

TABLE OF CONTENTS

	Page
CHAPTER I – INTRODUCTION	I-1
CHAPTER II – SELECTION OF THE RANGE OF PROPORTIONS FOR THE SERIES	II-1
CHAPTER III – CHOICE OF HULL FORM FOR THE PARENT MODELS	III-1
CHAPTER IV – CHARACTERISTICS OF SERIES 60 LINES	IV-1
CHAPTER V – RESISTANCE TESTS ON SERIES 60 PARENT MODELS	V-1
CHAPTER VI – EFFECT ON RESISTANCE OF VARIATION IN LCB POSITION	VI-1
CHAPTER VII – EFFECT ON DELIVERED HORSEPOWER (DHP) OF VARIATION IN LCB POSITION	VII-1
CHAPTER VIII – EFFECT ON RESISTANCE AND DHP OF VARIATION IN SHIP PROPORTIONS	VIII-1
CHAPTER IX – DESIGN CHARTS	IX-1
CHAPTER X – EFFECT OF VARIATIONS IN PROPELLER DIAMETER AND SHIP DRAFT AND TRIM	X-1
CHAPTER XI – EFFECT OF VARIATION IN AFTERBODY SHAPE UPON WAKE DISTRIBUTION AND POWER	XI-1
CHAPTER XII – REVIEW OF SERIES 60 PROJECT	XII-1
CHAPTER XIII – POSSIBLE EXTENSION OF SERIES 60 AND FUTURE RESEARCH	XIII-1
APPENDIX A – EFFECTS OF TURBULENCE STIMULATORS	A-1
APPENDIX B – USE OF CONTOURS AND CHARTS	B-1
APPENDIX C – METHODS OF ANALYSIS AND FAIRING OF RESULTS	C-1
APPENDIX D – NUMERICAL EXAMPLE OF USE OF SERIES 60 CHARTS	D-1
APPENDIX E – INTERNATIONAL TOWING TANK CONVERENCE 1957 MODEL-SHIP CORRELATION LINE	E-1
REFERENCES	R-1

FOREWORD

The research on Series 60 was carried out at the David Taylor Model Basin of the United States Navy. The results were published in the first instance in a number of papers before the Society of Naval Architects and Marine Engineers.

From time to time the wish has been expressed that the results of this research should be assembled in a single volume for easy reference and use. The original papers described a great deal of preliminary work carried out before the final Series 60 was adopted, and because they were read at intervals over a period of nearly 10 years, they also contained a certain amount of duplication and connective matter.

The opportunity has therefore been taken to completely rewrite the text, which is new, eliminating the preliminary work and much of the history, and also, it is hoped, most of the errors which are seemingly inevitable in a research of this magnitude.

In presenting the collected results in this new version, the author wishes to express his indebtedness to all the Staff of the Model Basin who have worked on the project since its inception in 1948, particularly those who have been co-authors in the original papers—Capt. F.X. Forest, U.S.N., Mr. J.B. Hadler, Mr. G.R. Stuntz, Dr. P.C. Pien, W.B. Hinterthan, and N.L. Ficken.

Mr. Hadler and Mr. Stuntz have been most helpful in reviewing the present text, although any opinions expressed are those of the author.

The whole project was carried through under the general guidance of a Panel of the Society of Naval Architects and Marine Engineers, the members of which devoted much time and thought to the choice of parameters and the detail design of the Series. The following people served on this Panel from time to time—Professor L.A. Baier, Mr. J.P. Comstock, Mr. H. de Luce, Capt. F.X. Forest, U.S.N., Mr. J.B. Hadler, Admiral C.O. Kell, U.S.N., Professor G.C. Manning, Mr. V.L. Russo and Dr. F.H. Todd—the successive Chairmen being Admiral Kell, Dr. Todd, and Mr. Hadler.

Thanks are especially due to successive Directors of the Model Basin who have throughout supported the research—Admirals C.O. Kell, G.H. Holderness, A.G. Mumma, W.H. Leahy, E.A. Wright, and Captain J.A. Obermeyer—and to the Bureau of Ships which supplied the finance for most of the work under the Fundamental Hydromechanics Research Program, assisted towards the end by the Maritime Administration and the Society of Naval Architects and Marine Engineers.

SYMBOLS

Dimensions

L	Length in general
L_{BP}	Length between perpendiculars (LBP)
L_{WL}	Length on designed waterline
L_S	Length of ship
L_M	Length of model
L_E	Length of entrance
L_X	Length of parallel
L_R	Length of run
B	Beam
H	Draft
Δ	Displacement in tons
∇	Displacement in cubic feet
S	Wetted surface
LCB	Longitudinal centre of buoyancy
$\frac{1}{2} \alpha_E$	Half-angle of entrance on load waterline

Form Coefficients

C_B	Block coefficient
C_X	Midship area coefficient
C_P	Prismatic coefficient
C_{PE}	Prismatic coefficient of entrance
C_{PX}	Prismatic coefficient of parallel body
C_{PR}	Prismatic coefficient of run

\bar{X}_{BP}	Mid-point of LBP
$\frac{x}{L}$	Position of LCB as function of length from forward perpendicular
K_R	Coefficient of bilge radius = $\frac{\text{Bilge radius}}{\sqrt{B \times H}}$
λ	Scale of model to ship

Resistance Coefficients

R	General symbol for resistance
R_F	Frictional resistance
R_R	Residuary resistance
R_T	Total resistance
V	Speed in general
V_S	Speed of ship
V_M	Speed of model
ρ	Mass density of water
g	Acceleration due to gravity
λ	Wave length
$\frac{V}{\sqrt{L}}$	Speed-length ratio
C	Resistance coefficient in general = $\frac{R}{\frac{1}{2}\rho S V^2}$
C_F	Frictional resistance coefficient (ATTC)
C'_F	Frictional resistance coefficient (ITTC)
C_R	Residuary resistance coefficient
C_T	Total resistance coefficient
C_A	Ship correlation allowance coefficient

O_m	Froude resistance coefficient for model
O_s	Froude resistance coefficient for ship
EHI, ehp	Effective or tow rope horsepower = $\frac{RV}{326}$ with R in pounds and V in knots
(K)	Froude speed coefficient = $0.5834 \frac{V}{\Delta^{1/6}}$ with V in knots and Δ in tons
(C)	Froude resistance coefficient = $\frac{EHP}{\Delta^{2/3} V^3} \times 427.1$ with V in knots and Δ in tons.

Propulsion Symbols

D	Diameter of propeller
P	Pitch of propeller
P/D	Pitch ratio
rpm	Revolutions per minute
BAR	Blade area ratio
BTF	Blade thickness fraction
w	Wake fraction (Taylor)
t	Thrust deduction fraction
e_h	Hull efficiency
e_p	Propeller efficiency (open)
e_{rr}	Relative rotative efficiency
DHP, dhp	Delivered horsepower absorbed by propeller
SHP, shp	Shaft horsepower measured in shafting
V_x	Longitudinal velocity of water in wake
V_v	Vertical velocity of water in wake
V_h	Horizontal velocity of water in wake

w_x	Longitudinal wake fraction
w_v	Vertical wake fraction
w_h	Horizontal wake fraction
w_{tr}	Transverse wake fraction compounded of w_v and w_h

CHAPTER I

INTRODUCTION

One of the problems which faces the naval architect at an early stage in the design of any new ship is the determination of the necessary horsepower to fulfill the speed requirements and to assess the effect on this power of making different choices for the size, proportions, and fullness of the ship.

To assist him in this problem, he will have recourse to a number of different sources of data. He will have his own experience to draw upon, covering previous designs and ships built to them, and, possibly, results of model tests carried out in this connection. Then there are available many results of specific model tests published in various technical papers and, in particular, the design data sheets published by the Society of Naval Architects and Marine Engineers (SNAME).¹

Such data, although extremely useful, suffer from the fact that they refer to a large number of models which are unrelated one to the other and in which the variations in design parameters are quite random. Much more valuable are the results of experiments on families of models in which the different design parameters are varied systematically and, so far as is possible in ship design, one at a time. Many such methodical series of model tests have been carried out in the past, perhaps the best known being that due to Admiral D.W. Taylor.² Other such series covering different types of ships have been run by many people,³⁻⁴³ including one by the British Ship Research Association more or less concurrently with the present Series 60 at the David Taylor Model Basin.⁴³

The results of such tests can be expressed in design charts from which the naval architect, by interpolation where necessary, can select a number of forms suitable to a particular problem, determine their relative resistance and propulsive qualities, and so make an informed choice of the best combination of parameters to give minimum power within the other limitations of the design conditions.

Many methodical series of the past are not suitable for modern single-screw merchant ship design for a variety of reasons, and although taken together they cover a large range of values of the usual design parameters, they lack any overall coordinating factor. Also, some doubt exists about the results in a number of the older series because of the absence of any turbulence stimulation on the models.

The need for more systematic information on the design of lines for modern, single-screw ships has been recognized at the Taylor Model Basin for many years. The subject was revived after the war at the meetings of the American Towing Tank Conference (ATTC) and the Hydromechanics Subcommittee of SNAME held in Ann Arbor in 1948. The Society agreed to sponsor the preparation of parent lines suitable for a series of single-screw

¹References are listed on page R-1.

merchant ship forms, and appointed a Panel to select the pattern and range of parameters to be used in the work.* The methods of deriving the parent lines and presenting the data were developed at the Model Basin, and the experiments were carried out there as part of the Bureau of Ships Fundamental Hydromechanics Research Program during the years 1948-1960.

At the time of the inception of this project, there was beginning a great upsurge in the provision of hydromechanic research facilities all over the world, with the certainty that in consequence many programs of research into hull form, in smooth water and in waves, would be initiated. One of the objects of Series 60 was to provide a parent family which, within the type of ship covered, could serve as a starting point for any such work, so that new series might be related one to the other by having a common datum line. Considerable success has been achieved in this way, and parents of the series are being used for research into sea-going qualities of ships, both under ATTC and International Towing Tank Conference (ITTC) sponsorship. Other examples include methodical launching calculations, the effect of bulbous bows on power, the estimation of propeller forces acting on a ship's hull and shafting, and the representation of ships' lines by mathematical methods.

The results of the model experiments have been published before the SNAME from time to time to make them available to the profession as soon as possible; this led inevitably to some duplication and the occurrence of a number of minor errors. In the discussions on these papers, a number of requests have been made that the results be brought together in a single publication. In carrying out this suggestion, much of the preliminary work has been omitted since it did not have any bearing on the ultimate results. Readers who are interested in these historical and development phases of the Series can find a full account in the individual papers. For convenience, these are listed separately on page R-5 immediately following the list of specific references.

* The membership of the Panel is given in the Foreword.

CHAPTER II

SELECTION OF THE RANGE OF PROPORTIONS FOR THE SERIES

At the time of the inception of the program, a survey was made of the current practice in shipbuilding to ensure, as far as possible, that the series would cover the normal range of proportions of modern ships. In the course of this, some 40 individuals and organizations were consulted, and after analyzing these comments, the SNAME Panel agreed upon a series of parent forms and variations which would cover the general field of design for single-screw merchant ships. This was in 1949, and already it is obvious that the Series is no longer adequate for modern single-screw ships, which, on the one hand are being made finer and driven to higher and higher speeds in order to obtain the increased efficiency possible with single-screw as compared with twin-screw propulsion, and on the other hand are being made larger and fuller to achieve the resultant economy in bulk carriers of ore, oil and similar cargoes. At the time of the inception of the program, it appeared that lower and upper limits in block coefficient of 0.60 and 0.80 would be satisfactory, but the intervening years have shown that 0.55 and 0.85 would have been better forecasts. The future extension of the series to such forms would be a very worthwhile project.

The basic parameter chosen for defining the series was block coefficient (C_B). This was used in preference to the prismatic coefficient (C_P) because in the preliminary design stages for merchant ships it is a direct measure of the displacement carried on given dimensions, usually a basic consideration. This approach in no way prevents the use of prismatic coefficient in the subsequent presentation of the results if so desired.

The decision to use C_B in preference to C_P has been a point of comment by numerous contributors to the discussions on the Series 60 papers. In general, the ship designer and operator seem to favor block coefficient. Sir Amos Ayre said that "for the type of ship dealt with, I am pleased to observe that the block coefficient has been chosen as the basic parameter in preference to the prismatic coefficient" (discussion on Reference 44). Mr. Ericson, commenting on the same paper, stated that he "should like . . . to put in a few words which will present the viewpoint of the ship operator himself. First, I should like to endorse the use of the block coefficient as a basic parameter. It is fairly useful in making a study, particularly an economic study, where displacement is considered, which is reflected immediately in the carrying capacity of the vessel."

On the other hand, naval architects and hydrodynamicists have emphasized the merits of the prismatic coefficient as being a more meaningful parameter for interpreting resistance results, although even here some doubts have been expressed by Dr. Weinblum: "Other calculations show the now well-known extreme sensibility of the wave resistance to variations of pure form for a given prismatic coefficient. The wave-resistance values corresponding to two such forms can easily reach a ratio of 3:1, so that sometimes one even is inclined

TABLE 1

Variation of $\frac{L}{B}$, $\frac{B}{H}$, $\frac{\Delta}{\left(\frac{L}{100}\right)^3}$, $\frac{L}{\nabla^{1/3}}$, and LCB Position with C_B for the Parent Models

C_B	0.60	0.65	0.70	0.75	0.80
$\frac{L}{B}$	7.50	7.25	7.00	6.75	6.50
$\frac{B}{H}$	2.50	2.50	2.50	2.50	2.50
$\frac{\Delta}{\left(\frac{L}{100}\right)^3}$	122.0	141.4	163.4	188.2	216.5
$\frac{L}{\nabla^{1/3}}$	6.165	5.869	5.593	5.335	5.092
LCB as percent of L_{BP} from ∇_{BP}	1.5 aft	0.5 aft	0.5 fwd	1.5 fwd	2.5 fwd

to doubt the value of the prismatic coefficient as a standard form parameter" (discussion on Reference 45).

In the present series, the midship area coefficient does not vary very much, and so the resistance qualities can be related either to C_B or C_P without introducing any conflicting situations. Since the results of such a methodical series will essentially be used by the designer, C_B is probably the better choice for presentation of the various curves and contours.

Five block coefficients were chosen, each associated in the first instance with given longitudinal center of buoyancy (LCB) positions, midship area coefficients, length-beam $\left(\frac{L}{B}\right)$ and beam-draft $\left(\frac{B}{H}\right)$ ratios (Table 1 and Figure 1). B and H are the moulded beam and draft in feet, respectively, and L is the length between perpendiculars (L_{BP}) measured from the centerline of the rudder stock to the forward side of stem at the designed load waterline, as adopted by the SNAME in its Model Resistance Data sheets. It corresponds with that used by the classification societies such as the American Bureau of Shipping.

The variation in $\frac{L}{B}$ with C_B was chosen by the panel to take into account the fact that the finer ships were, in general, relatively longer and narrower than the fuller ones.

To cover the general spread of $\frac{L}{B}$, $\frac{B}{H}$, and $\frac{\Delta}{\left(\frac{L}{100}\right)^3}$ for existing designs, and the

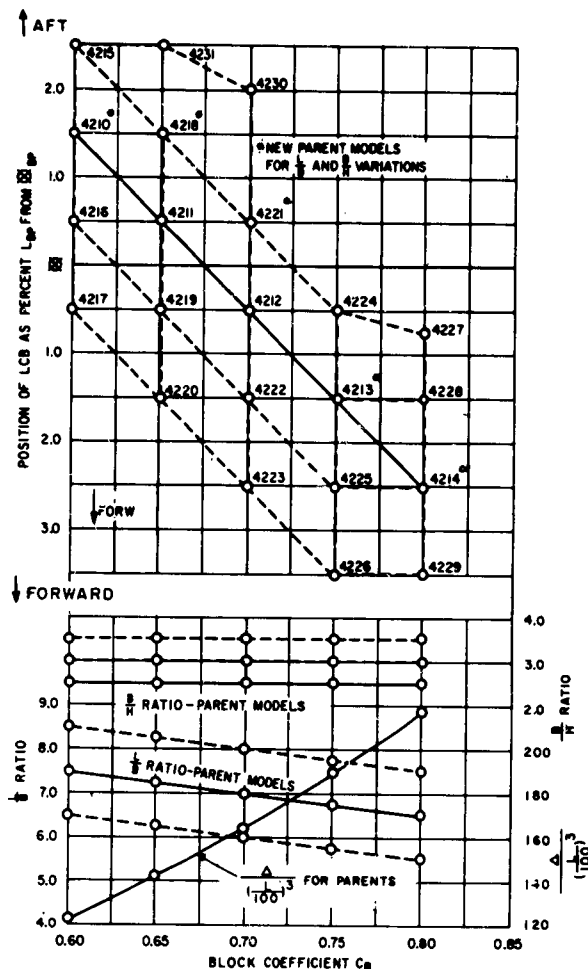


Figure 1 - Variation of Proportions etc.,
with C_B

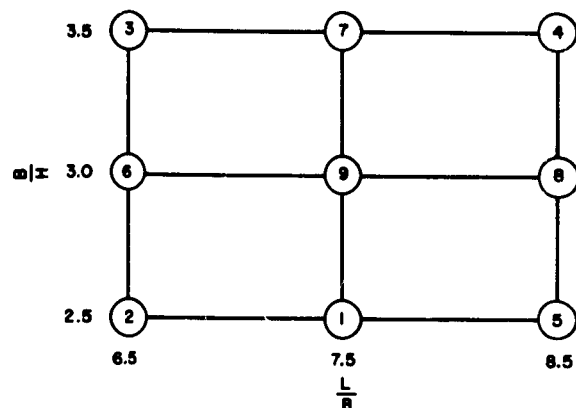


Figure 2 - Typical Variation of $\frac{L}{B}$ and $\frac{B}{H}$
Ratios for a Given Value of C_B

possible variation in LCB position, a grid was adopted as shown by the dotted lines in Figure 1.*

For any one block coefficient and LCB position, a total of nine models was run in which the $\frac{L}{B}$ and $\frac{B}{H}$ ratios were varied. The pattern for a typical case ($C_B = 0.60$) is shown in Figure 2.

*The values of $\frac{L}{B}$, $\frac{B}{H}$, and $\frac{\Delta}{\left(\frac{L}{100}\right)^3}$ are not independent but are related by the expression

$$\frac{\Delta}{\left(\frac{L}{100}\right)^3} = \frac{C_B}{\left(\frac{L}{100}\right)^3 \left(\frac{L}{B}\right)^2 \left(\frac{B}{H}\right)} \times 28570 \text{ with dimensions in feet and displacement in tons, salt water.}$$

CHAPTER III

CHOICE OF HULL FORM FOR THE PARENT MODELS

In the past, the models of most methodical series have been derived from a single parent form by proportioned geometrical changes. When carried to very different proportions and to fullness coefficients suitable to very different values of speed-length ratio $\left(\frac{V}{\sqrt{L}}\right)$, such changes must inevitably lead to unrealistic forms regardless of how good the parent lines might be for the original design conditions. In planning Series 60, therefore, another approach was tried. A review was made of the resistance results of the single-screw merchant ship models available at the Model Basin, and some 20 were selected which appeared to give good performance as judged by a comparison with Taylor's Standard Series. These models covered a range of fullness, and plots were made of sectional area coefficients and waterline half-breadth coefficients to a base of fore- and aft-body prismatic coefficients. Cross curves were then drawn which, while being fair lines, followed the actual points as closely as possible. In this way it was hoped to obtain, by interpolation at the correct values for the parent forms, a series of models which would retain most of the good resistance qualities of the models on which the coefficient curves were based, while also incorporating the changing characteristics necessary to ensure good performance of each model at its appropriate speed-length ratio. At the same time, these parent forms would be related to one another in accordance with a definite graphical pattern. Once the series was complete and the resultant resistance curves available, a form could be quickly obtained by interpolation of the cross curves to fulfill any desired combination of C_B , L , B , H , Δ , and LCB position. Moreover, this design could be immediately associated with a corresponding resistance and effective horsepower.

From these contours, five parent forms were drawn having block coefficients of 0.60, 0.65, 0.70, 0.75 and 0.80, with $\frac{L}{B}$ ratios, $\frac{B}{H}$ ratios, and LCB positions as shown for the parent models in Figure 1. This group of models was designated Series 57 in succession to earlier TMB Series, and the details of their derivation and the results of the model resistance tests were given in a paper before the SNAME in 1951.⁴⁴

The resistance results of Series 57 were compared with those for a number of recent successful modern designs of single-screw ships and found to be disappointing. In view of the apparently good qualities of the models on which the contours were based, this was at first sight surprising. Further investigation suggested that although the departures from the actual design lines made when fairing the contours were small, they may have been critical in certain cases, and also that possibly some of the results of the resistance tests on the chosen models were suffering from the effects of laminar flow. Apparently in ship

models, as in human beings, the selection of good parents does not necessarily lead to better — or even as good — offspring!

Although the original conception of the project was to derive a series of related parent forms which would serve as a point of departure for future model programs, and which therefore should have reasonably good but not necessarily optimum resistance qualities (the quest for which might indeed last forever), it was evident from the very lengthy and valuable discussion on the paper that the members of the profession desired something better in quality than Series 57 as a basis for any such systematic program.

The panel thereupon reviewed the original series and agreed that the real merits of the Series 57 models could best be established by comparison with the performance of actual successful ship designs. In this way, differences in proportions and in *LCB* position could be eliminated and the effects of differences in shape of area curves, waterlines and section shapes evaluated.

Five designs were chosen as being typical of good, modern, single-screw ships, which, of necessity, had to meet many requirements in addition to those of good resistance qualities.

Three of these were Maritime Administration vessels of the MARINER, SCHUYLER OTIS BLAND, and C.2 classes. The other two were Bethlehem Steel Company designs. One was the tanker PENNSYLVANIA. The other did not represent any built ship but was a design for a 0.70 block coefficient ship given by Mr. H. de Luce in his contribution to the discussion on the Series 57 paper.

Models of the first four were available at the Model Basin, and a model of the fifth design was made and tested.

For comparison with each of these, an equivalent Series 57 model was made to lines drawn out from the contours. Each pair of models represented a ship of given length, beam, draft, displacement, and position of *LCB* so that the differences in each case were restricted to the shapes of area, waterline, and section curves.

The results of these model tests are given in full in Reference 45. Briefly, at speeds appropriate to the different fullness coefficients, the Series 57 models were in general somewhat worse than those of the actual ships by amounts up to a maximum of 6 percent.

The area and load waterline (LWL) curves of any pair of these models were not very different in shape or character, and the chief differences lay in the shape of the cross sections. An analysis of the bow and stern lines indicated that the actual ships had, in every case, more U-shaped sections than the Series 57 models, and the Panel decided that new contours should be drawn using the sectional area and waterline curves for these actual designs as guides, thus giving a more U-shaped character to the transverse sections while paying due attention to stability considerations. This change was also expected to lead to improved propulsive efficiencies.

These new contours formed the basis for Series 60.

CHAPTER IV

CHARACTERISTICS OF SERIES 60 LINES

The principal particulars of the Series 60 parent models are set out in Table 2.

Attention must be drawn to a number of details which are important in using the contour charts and resistance results.

a. Midship section area coefficient (C_X)

The midship section has no deadrise, in accordance with current practice, and a linear relation between block coefficient and midship area coefficient was adopted. This relation and the corresponding values of the bilge radius are shown in Figure 3.

b. Position of LCB

Reference to the published data on the selection of a suitable position of the LCB for different fineness coefficients failed to show any unanimity as to the most desirable location,

TABLE 2

Particulars of Parent Forms, Series 60

Model Number.....	4210W	4211W	4212W	4213W	4214W-B4
L_{BP} , ft.....	400.0	400.0	400.0	400.0	400.0
B , ft.....	53.33	55.17	57.14	59.26	61.54
H , ft.....	21.33	22.09	22.86	23.70	24.59
Δ , Tons.....	7,807	9,051	10,456	12,048	13,859
L_B/L_{BP}	0.5	0.472	0.410	0.350	0.290
L_X/L_{BP}	0	0.035	0.119	0.210	0.300
L_K/L_{BP}	0.5	0.493	0.471	0.440	0.410
C_B	0.60	0.650	0.700	0.750	0.800
C_X	0.977	0.982	0.986	0.990	0.994
C_P	0.614	0.661	0.710	0.758	0.805
C_{PF}	0.581	0.651	0.721	0.792	0.861
C_{PA}	0.646	0.672	0.698	0.724	0.750
C_{PB}	0.581	0.630	0.660	0.704	0.761
C_{PR}	0.646	0.667	0.680	0.686	0.695
C_{PV}	0.850	0.871	0.891	0.907	0.920
C_{PVF}	0.910	0.927	0.944	0.961	0.971
C_{PVA}	0.802	0.823	0.842	0.856	0.867
C_W	0.706	0.746	0.785	0.827	0.871
C_{WF}	0.624	0.690	0.753	0.817	0.881
C_{WA}	0.788	0.802	0.818	0.838	0.860
C_{IT}	0.543	0.597	0.653	0.711	0.776
$\frac{1}{2}\alpha_R$, deg.....	7.0	9.1	14.5	22.5	43.0
LWL	406.7	406.7	406.7	406.7	406.7
LCB % LBP from ∇	1.5A	0.5A	0.5F	1.5F	2.5F
L/B	7.50	7.25	7.00	6.75	6.50
B/H	2.50	2.50	2.50	2.50	2.50
$L/\nabla^{1/3}$	6.165	5.869	5.593	5.335	5.092
$S/\nabla^{1/3}$	6.481	6.332	6.200	6.091	6.028
$W.S.$, sq ft.....	27,280	29,410	31,705	34,232	37,200
$K_R = R/\sqrt{BH}$	0.229	0.205	0.181	0.153	0.118

nor did the information for the selected basis models give any clear guidance. All the data showed a progressive movement aft with reducing block or prismatic coefficient, resulting in finer entrances for the models running at the higher speed-length ratios, as one would expect. A linear variation of position of *LCB* with fullness was therefore adopted, as shown in Figure 1. Although arbitrary, this line was in general a mean of the available data. Since the effect of *LCB* position was the next point to be investigated in the program, this line was considered to be an acceptable point of departure.

c. Load waterline half-angle of entrance ($\frac{1}{2} \alpha_E$)

This angle varies from 7.0 to 43 deg, as shown in Table 2 and Figure 4.

d. Sectional area and waterline coefficient contours

The length of parallel body and its fore and aft position for the parent models with the selected position of *LCB* are shown in Figure 4.

The corresponding lengths of entrance and run (L_E and L_R) were determined, each divided into 10 equal intervals, and contours of cross-sectional area coefficients were plotted to a base of prismatic coefficients of entrance and run respectively (C_{PE} and C_{PR}). These contours are shown in Figures 5a and 5b.

The body plans were treated in the same way; contours of waterline half-breadth coefficients to a base of prismatic coefficients of entrance and run are given in Figures 6a to 6p.

The positions of the centroid of volume of the entrance and run are shown in Figures 7 and 8 for different values of the respective prismatic coefficients. (Text continued on page IV-23)

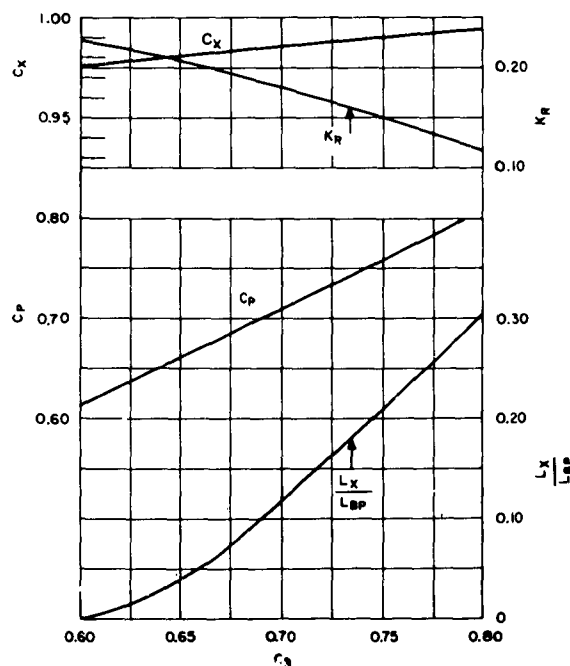


Figure 3 - Variation of C_X , C_P and Bilge Radius with C_B

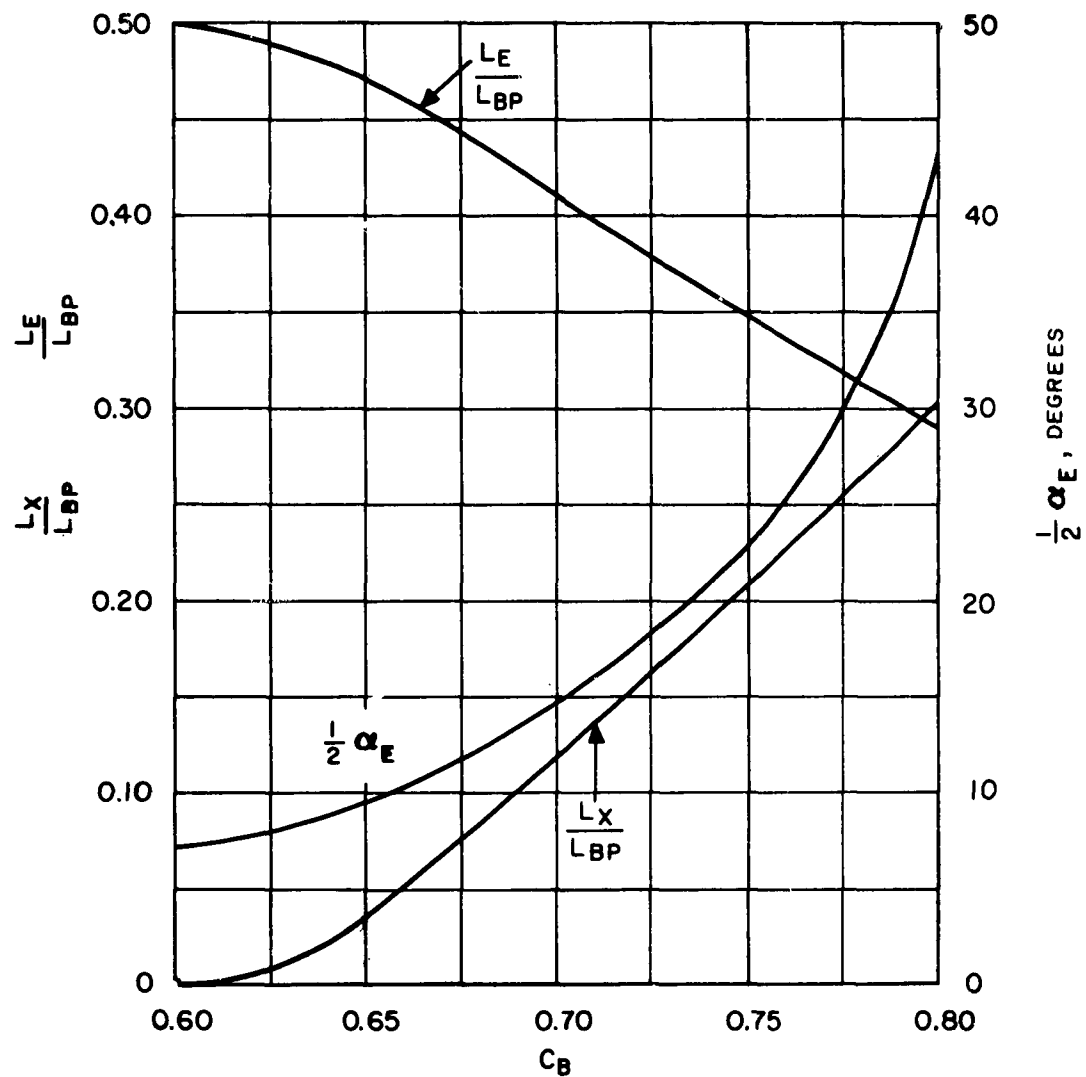
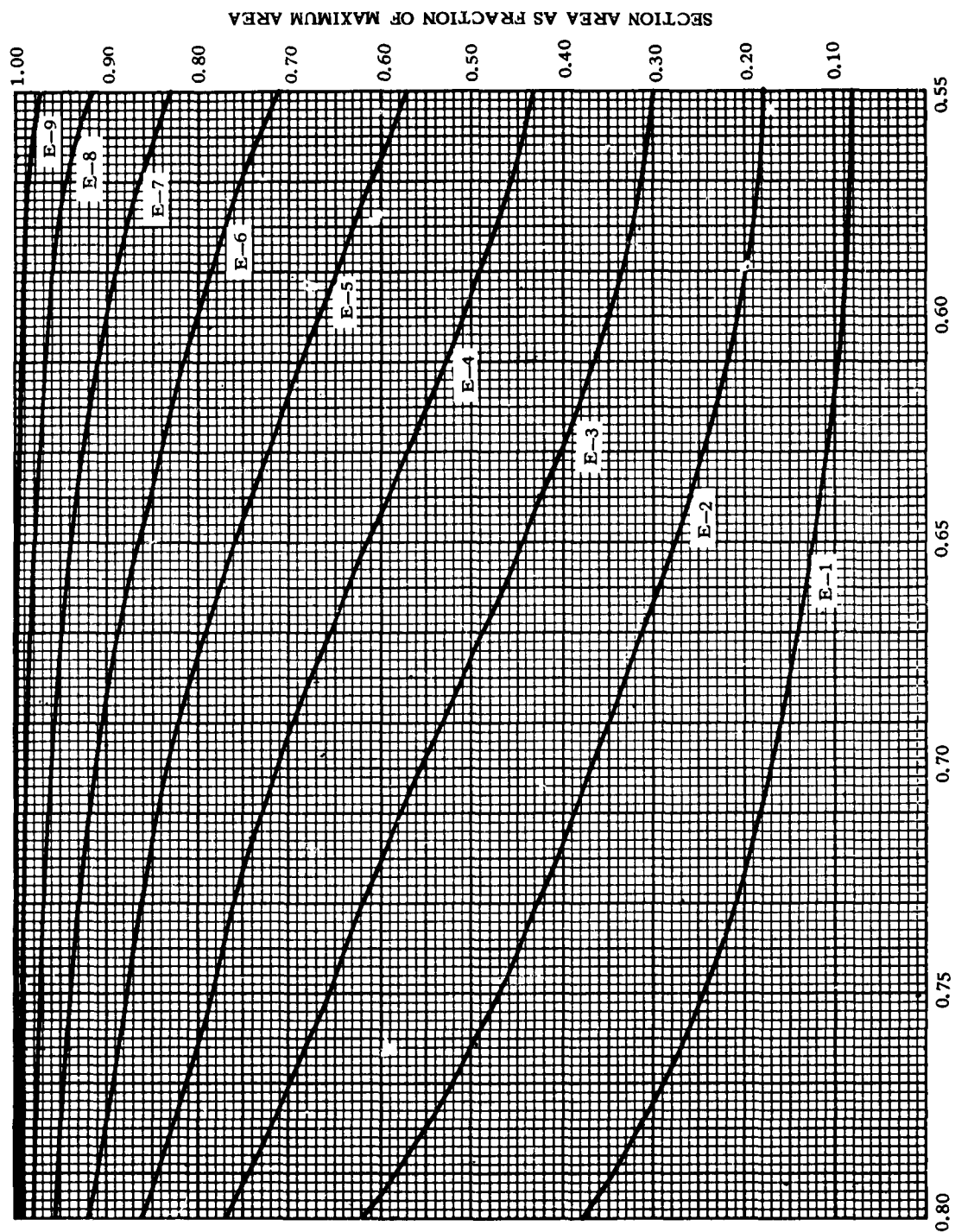


Figure 4 - Variation of Angle of Entrance, Position, and Amount of Parallel Body for Series 60 Parents

Figure 5 - Contours of Cross-Sectional Area Coefficients, Series 60



ENTRANCE PRISMATIC
Figure 5a - Sectional Area Contours, Entrance

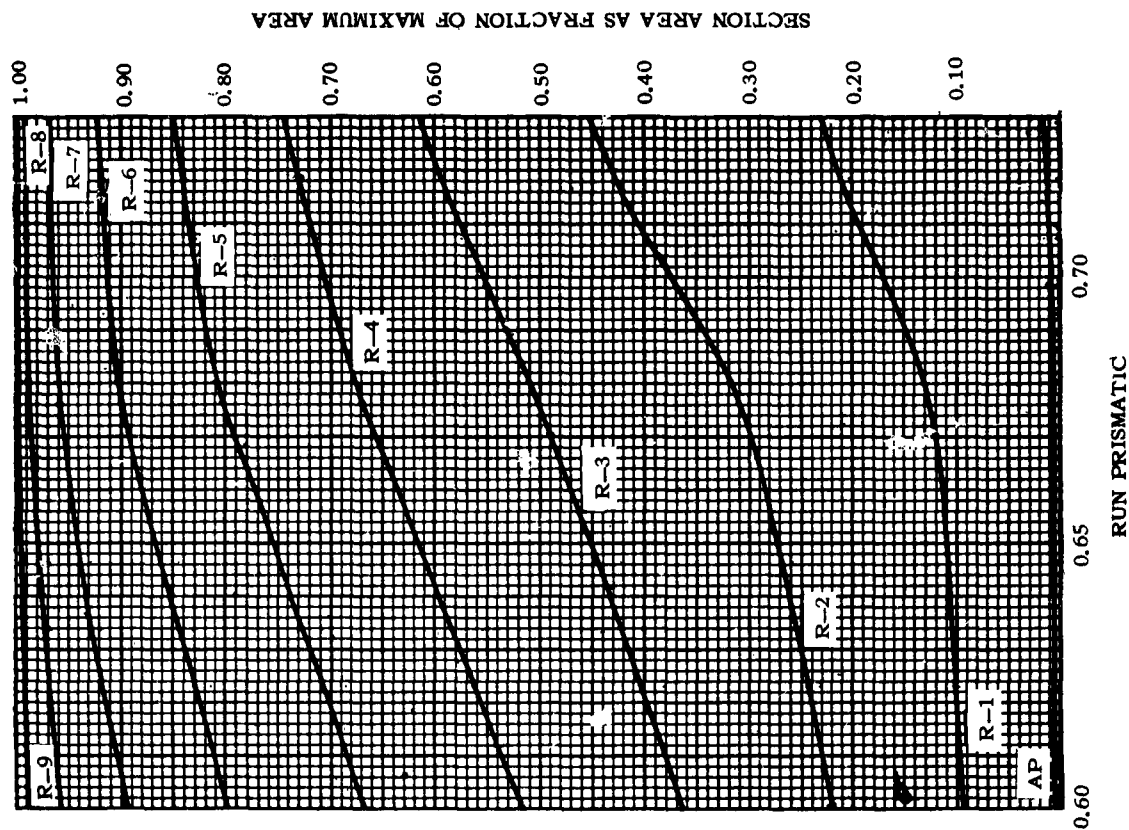


Figure 5b — Sectional Area Contours, Run

Figure 6 — Contours of Waterline Half-Breadth Coefficients, Series 60

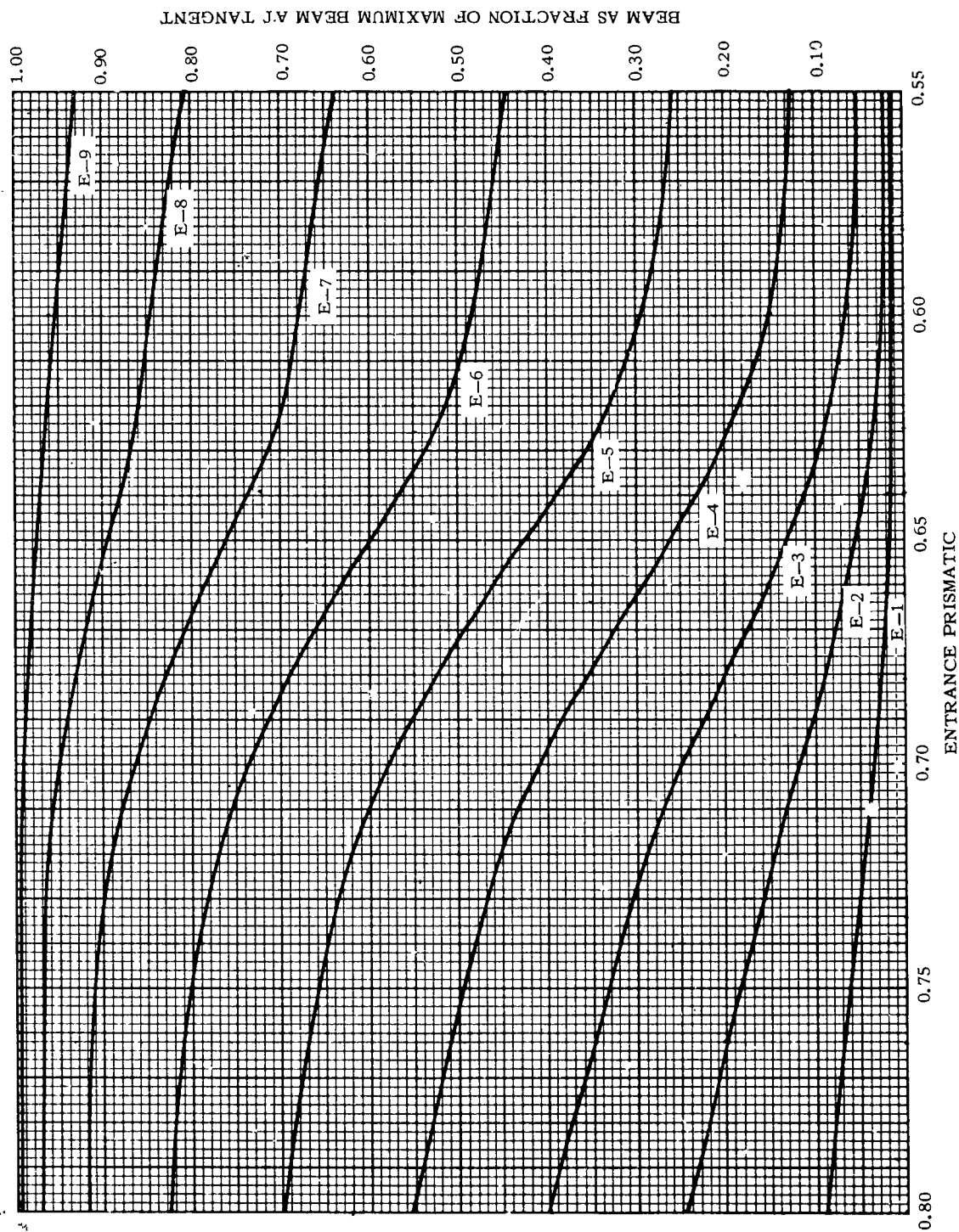


Figure 6a — Tangent Cross Curves, Entrance

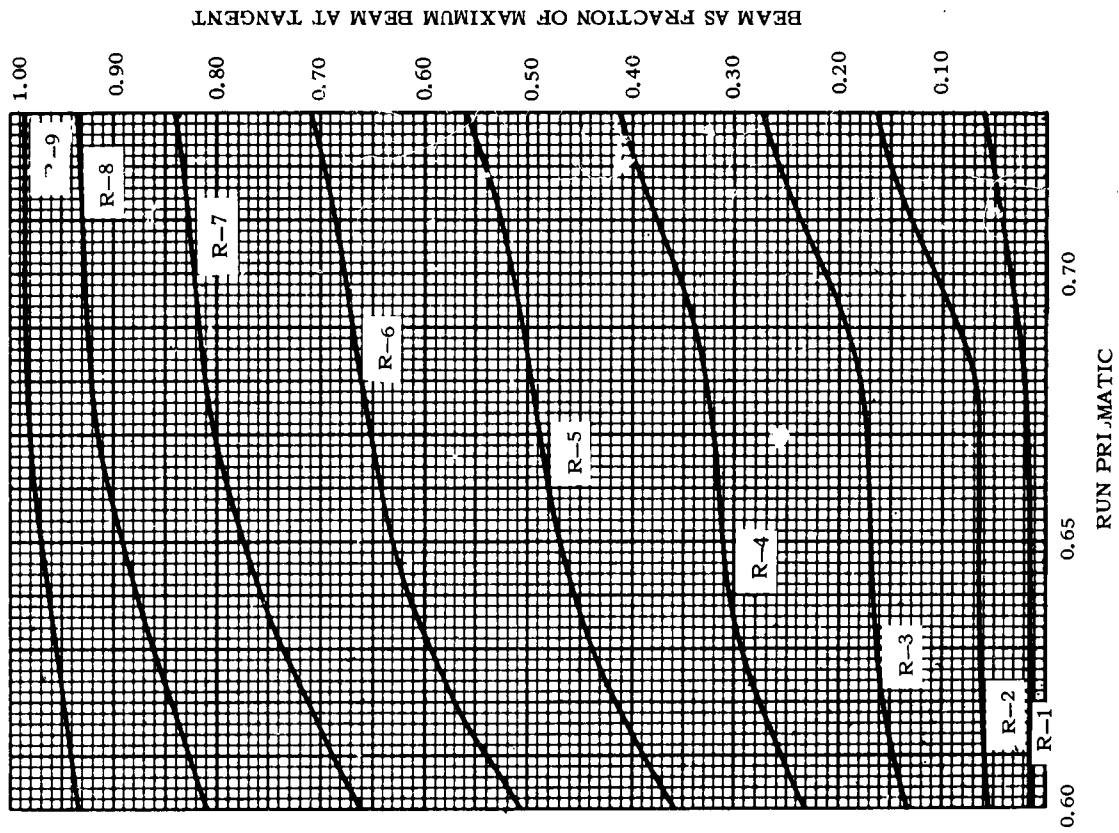


Figure 6b - Tangent Cross Curves Run

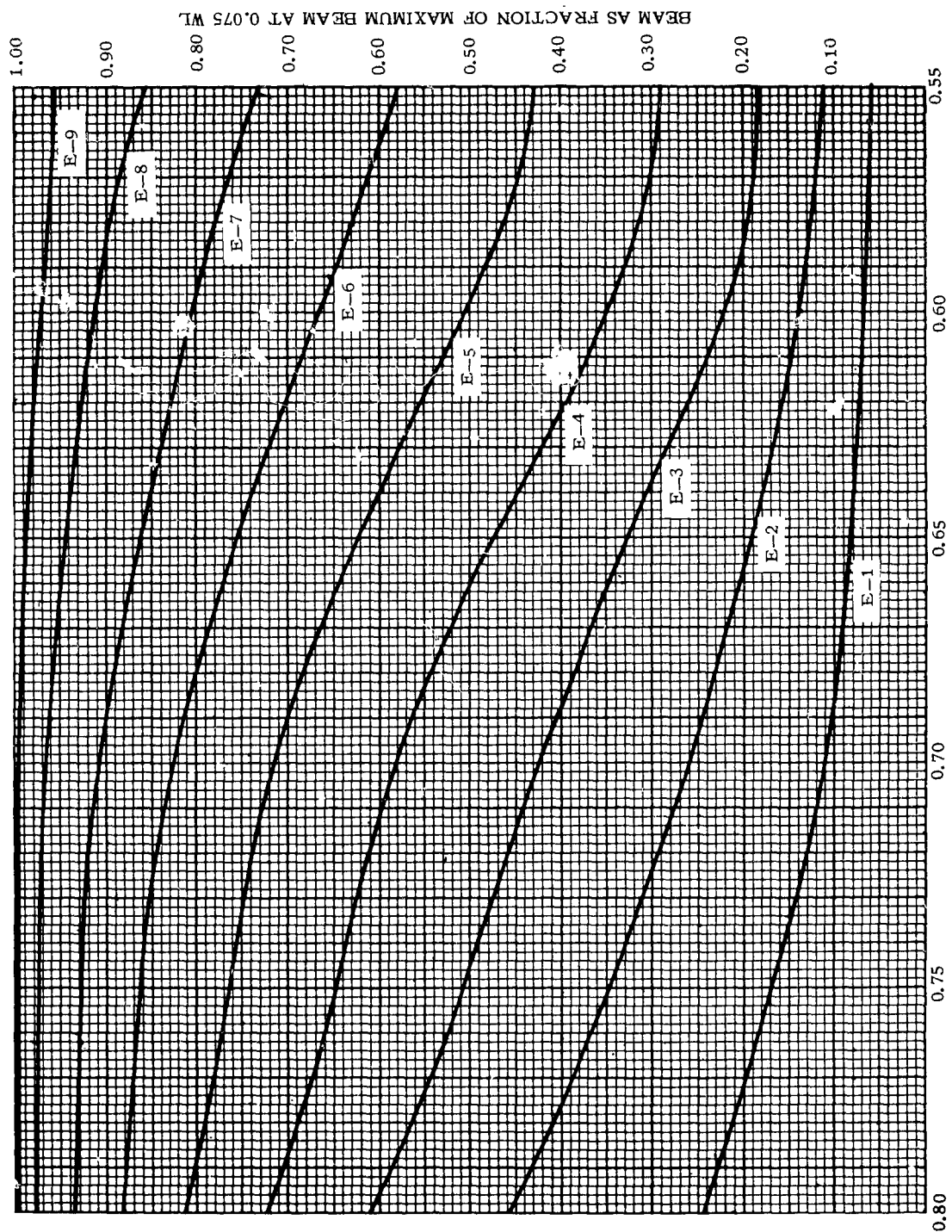


Figure 6c - 0.075 W.L. Cross Curves, Entrance

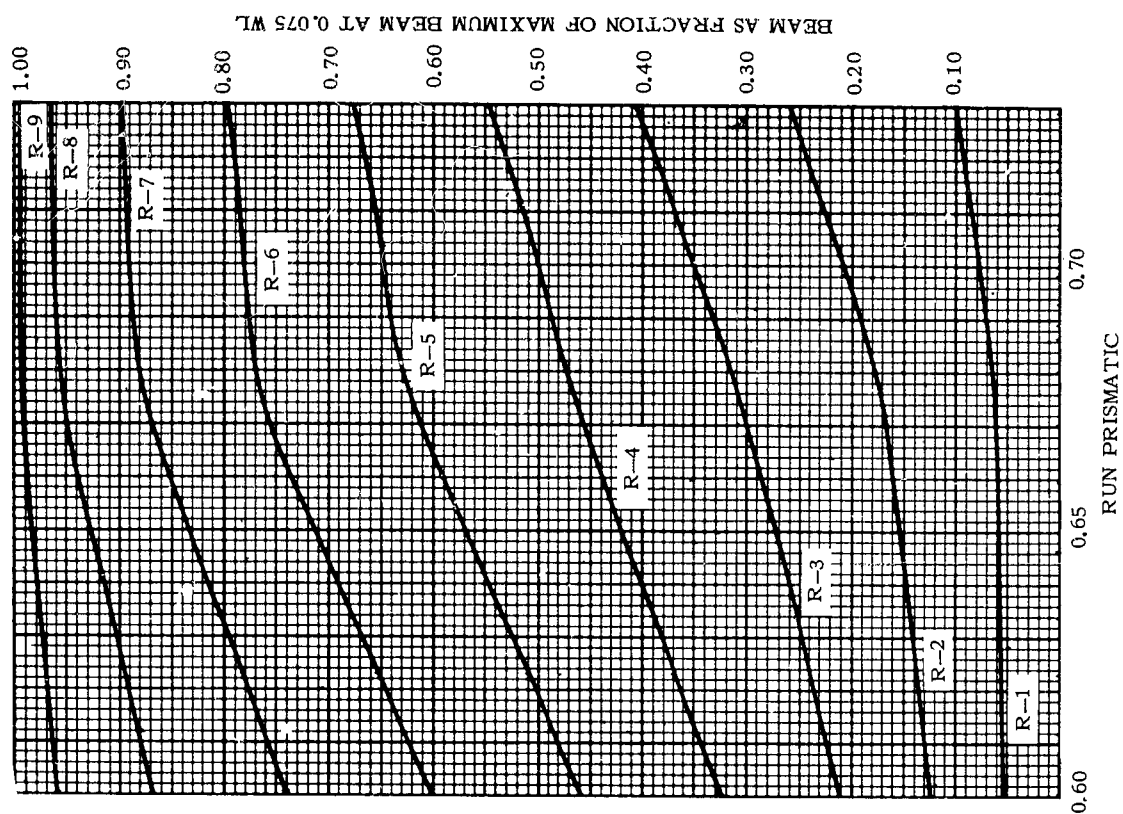


Figure 6d - 0.075 W.L. Cross Curves Run

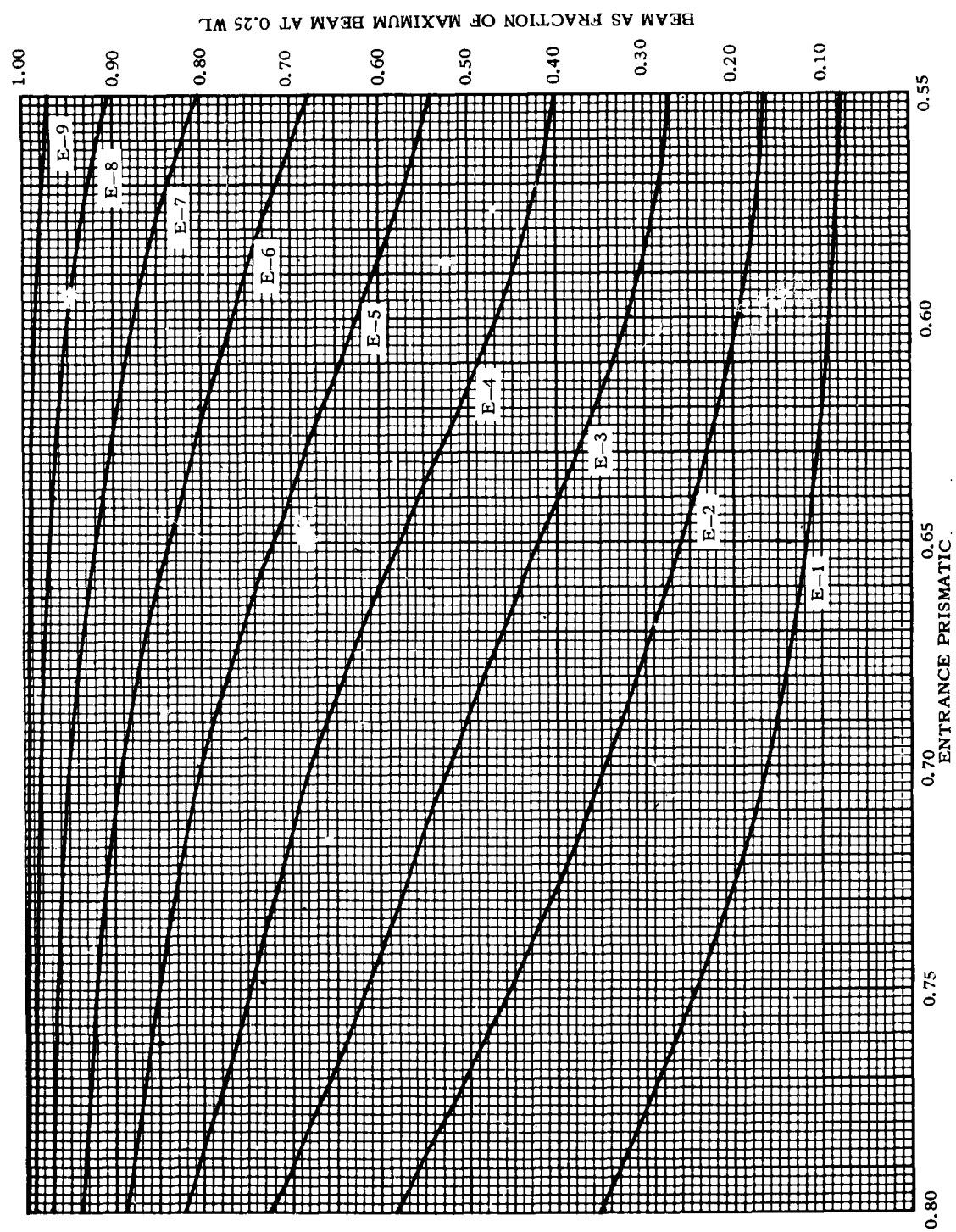


Figure 6e - 0.25 W.L. Cross Curves, Entrance

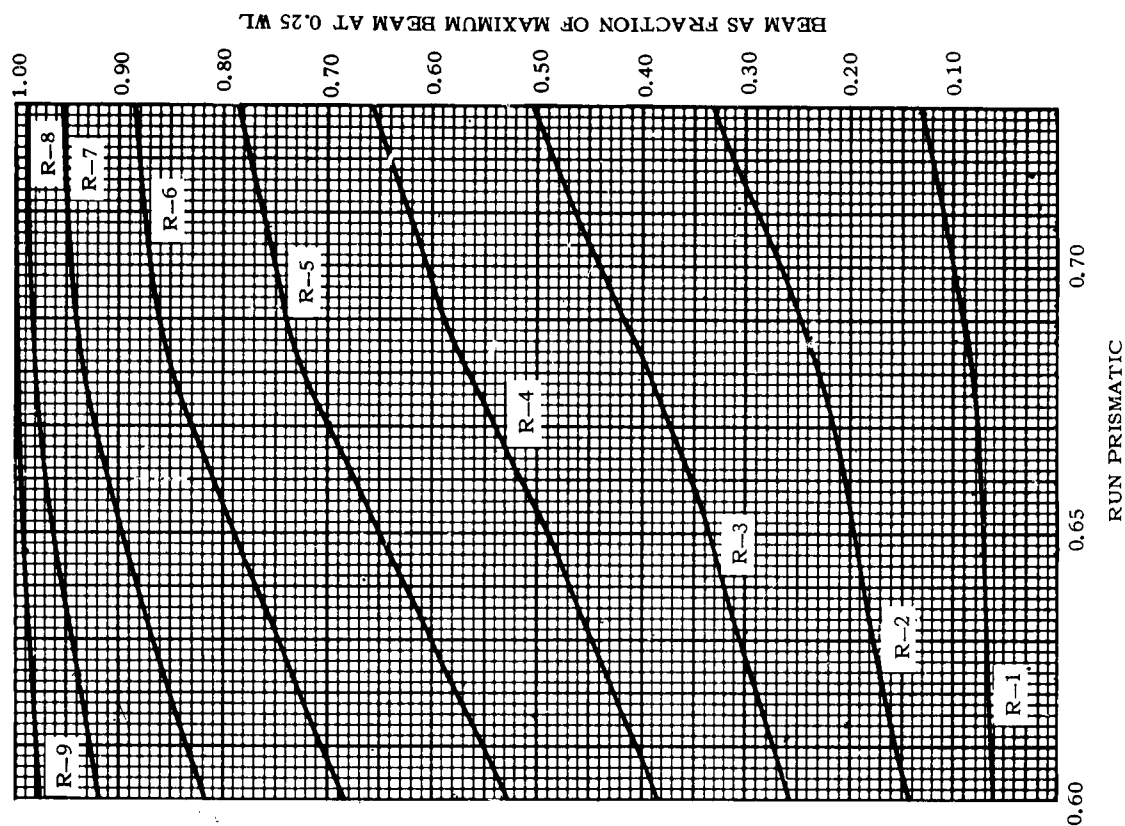


Figure 6f - 0.25 W.L. Cross Curves, Run

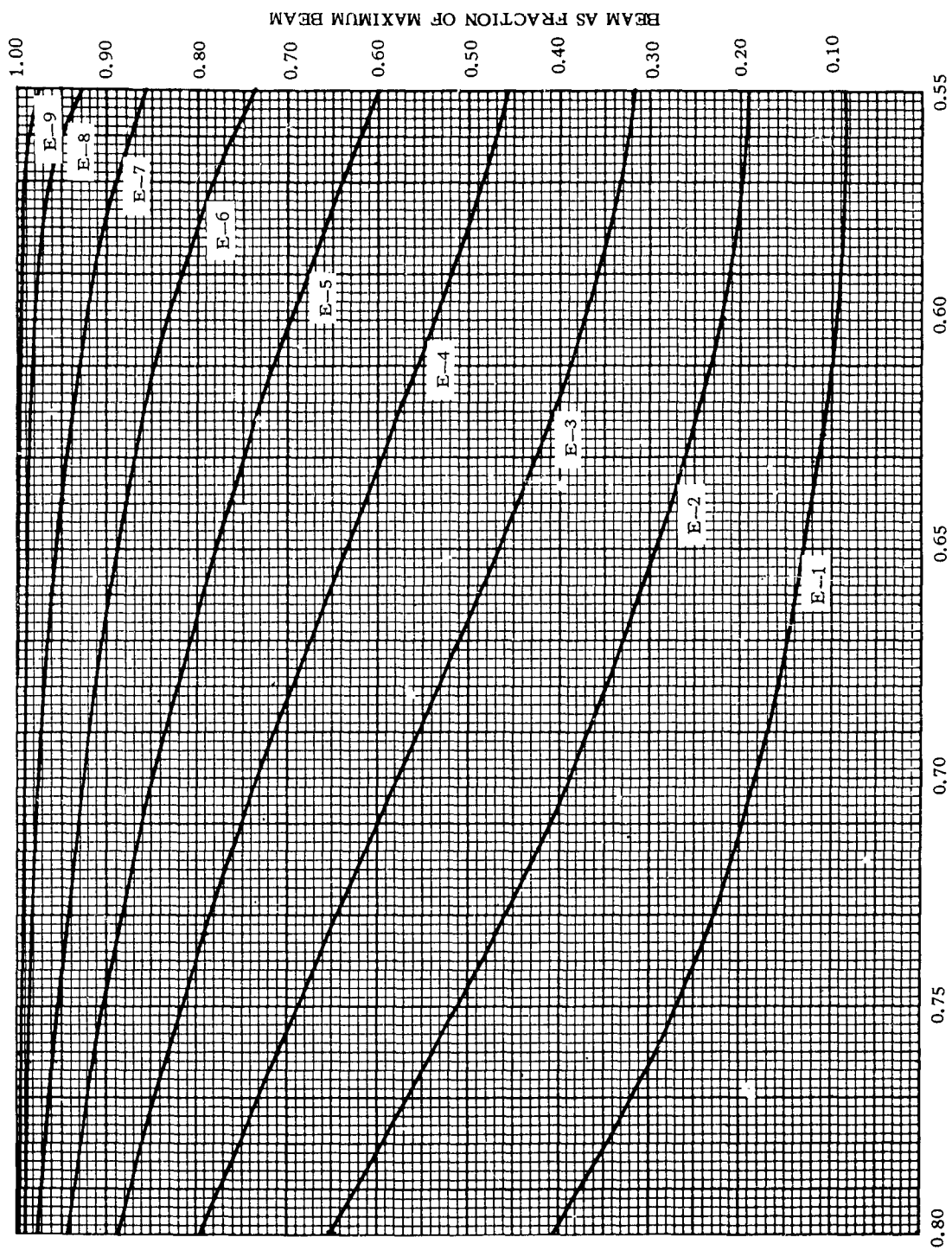


Figure 6g - 0.50 W.L. Cross Curves, Entrance

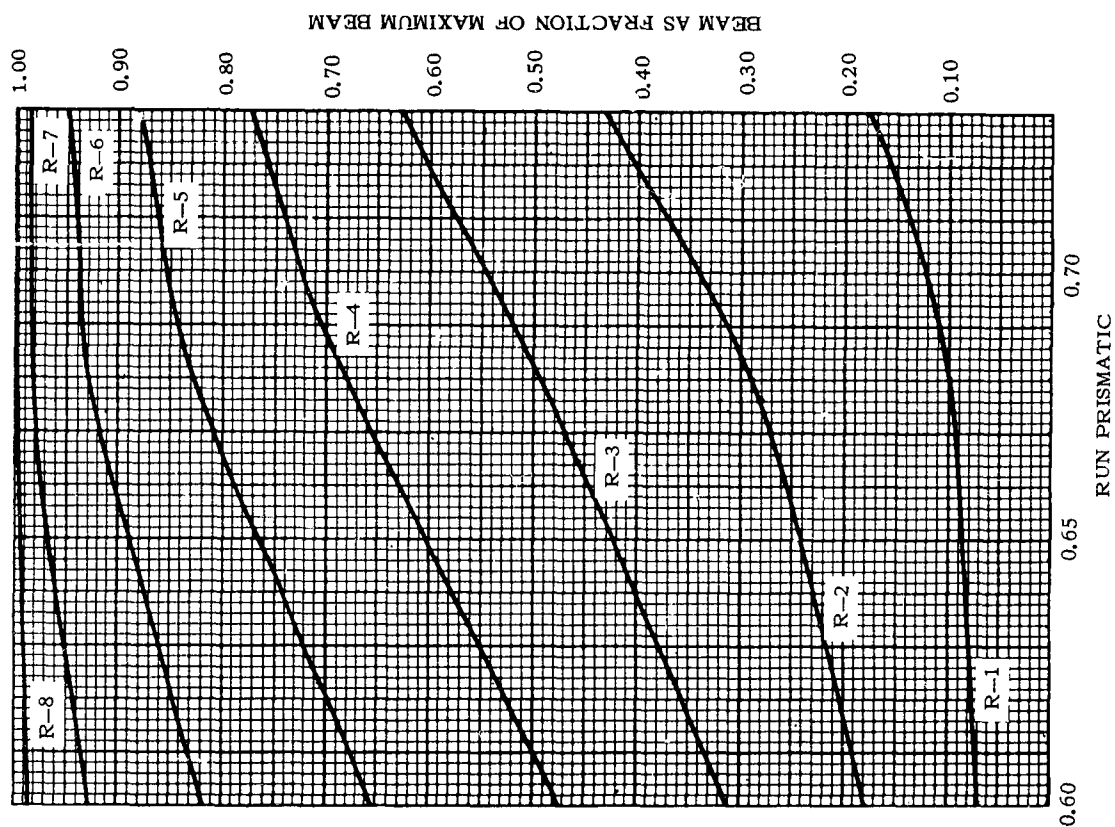


Figure 6h - 0.50 W.L. Cross Curves, Run

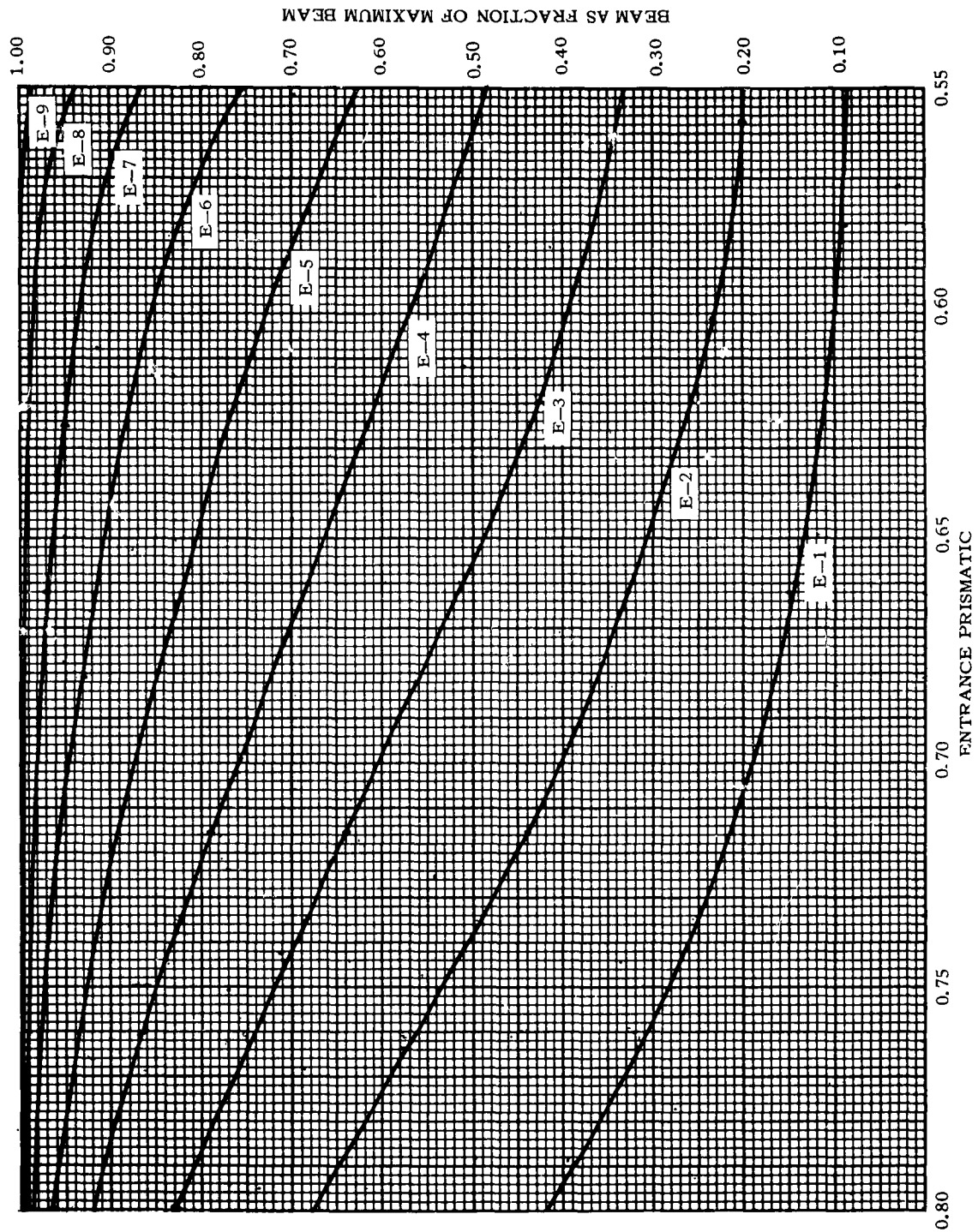


Figure 6i - 0.75 W.L. Cross Curves, Entrance

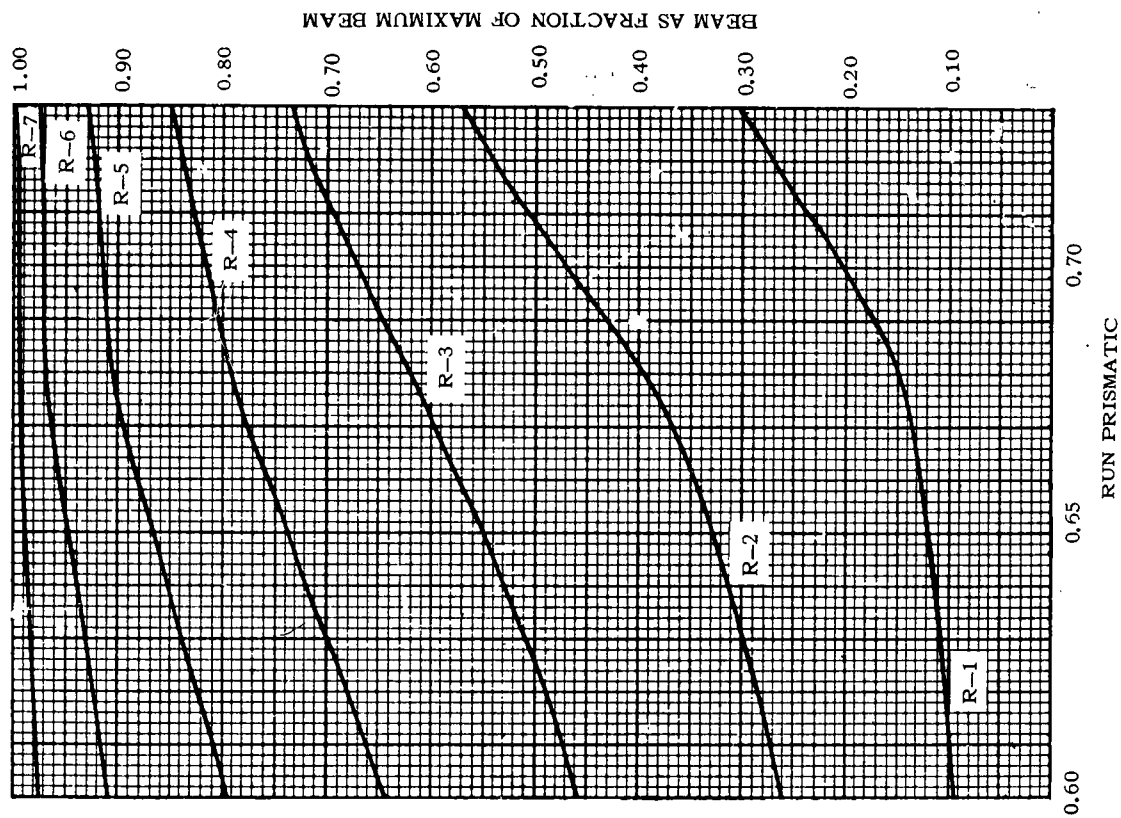


Figure 6j - 0.75 W.L. Cross Curves, Run

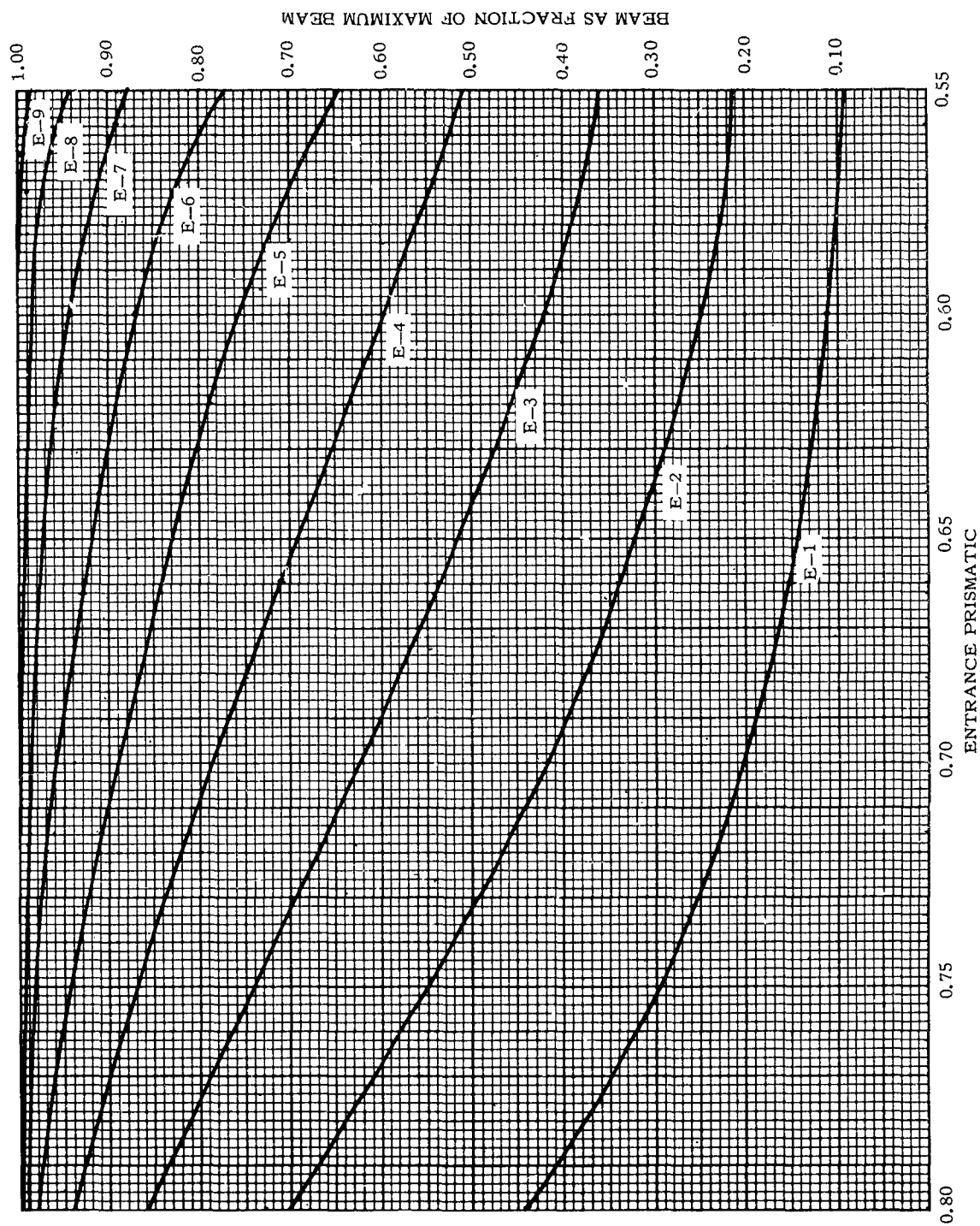


Figure 6k - 1.00 W.L. Cross Curves, Entrance

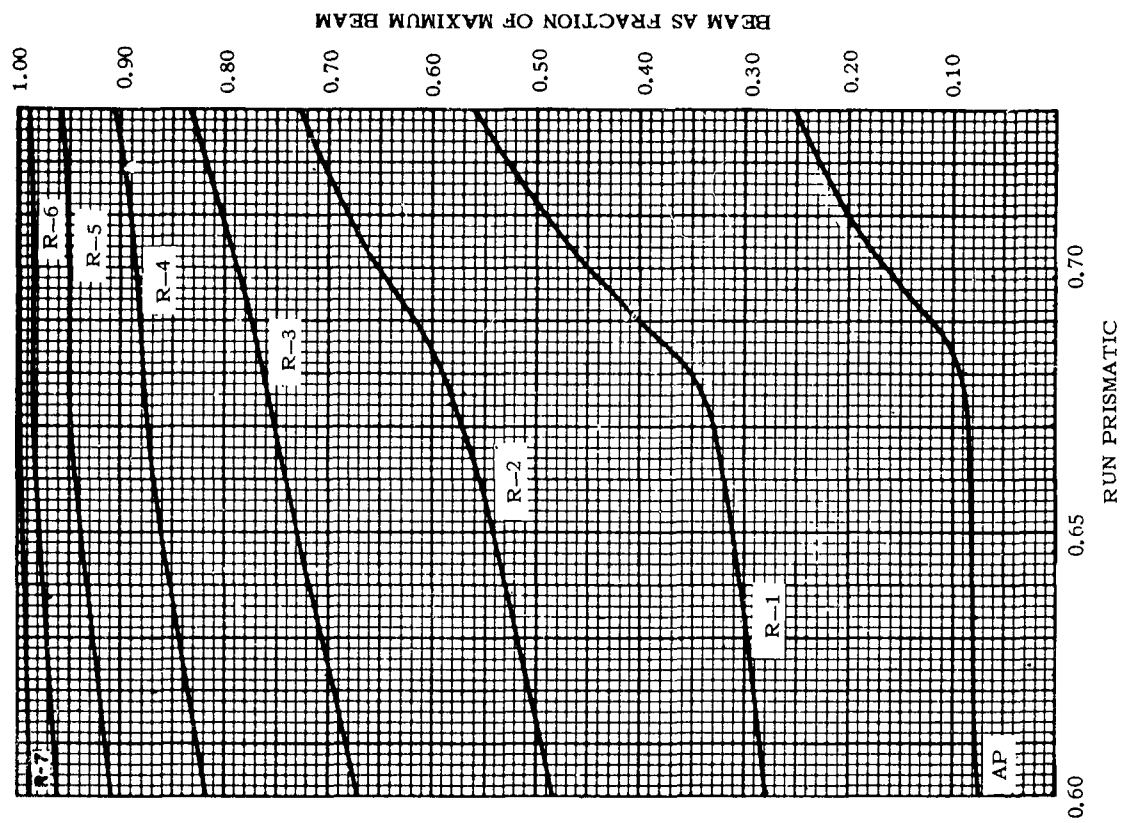
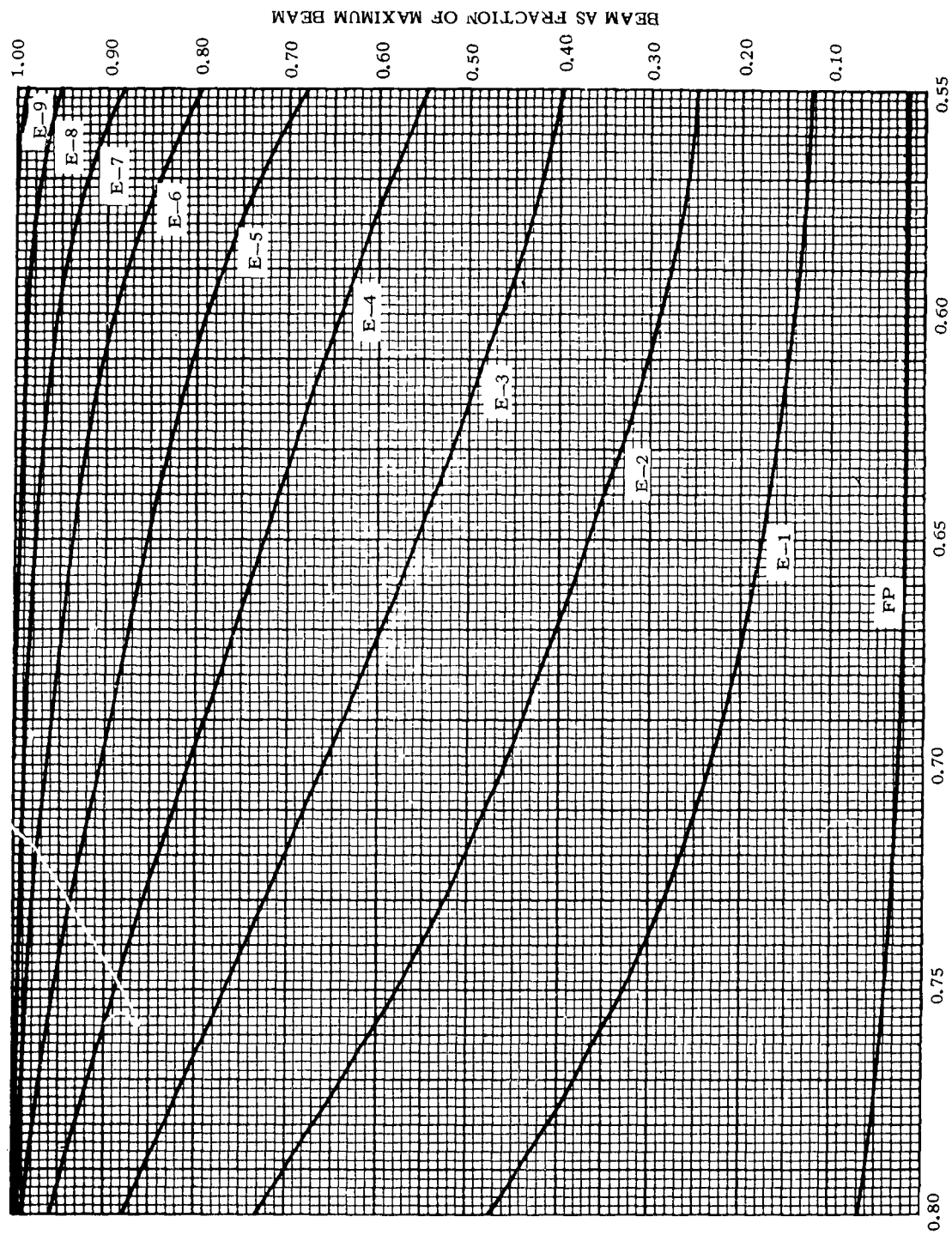


Figure 61 - 1.00 W.L. Cross Curves, Run



ENTRANCE PRISMATIC
Figure 6m - 1.25 W.L. Cross Curves, Entrance

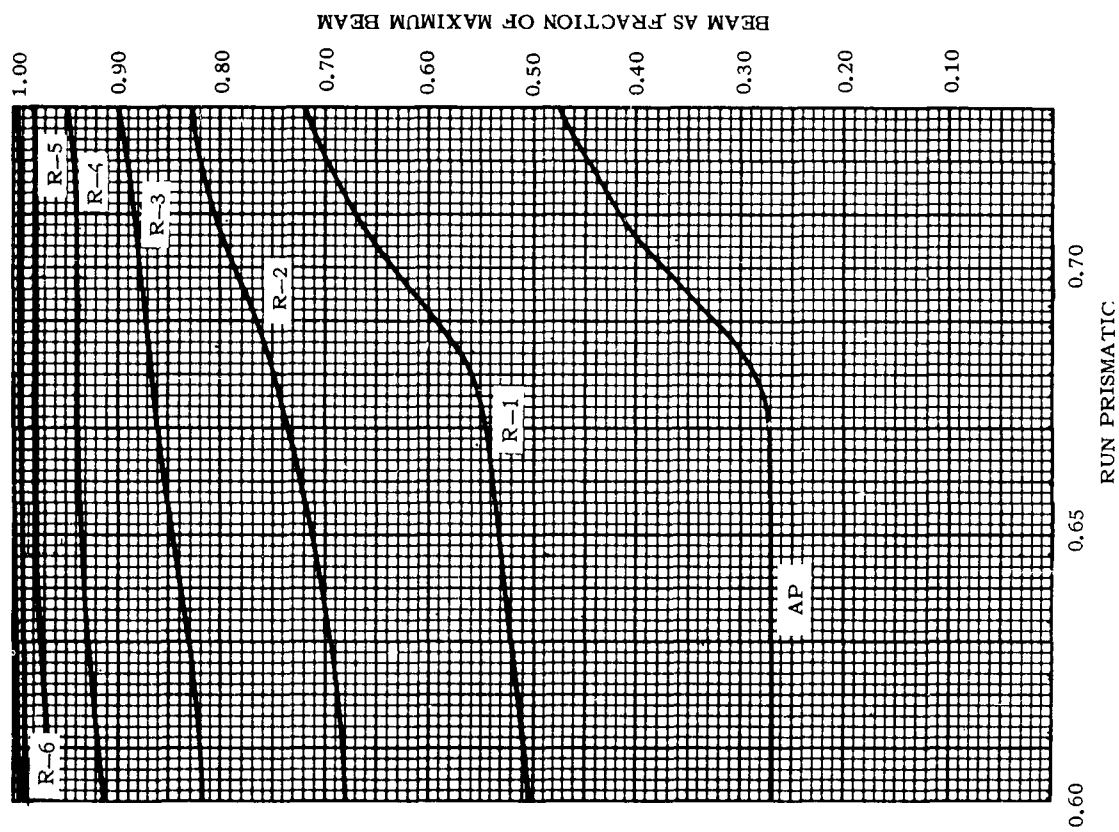


Figure 6n - 1.25 W.L. Cross Curves, Run

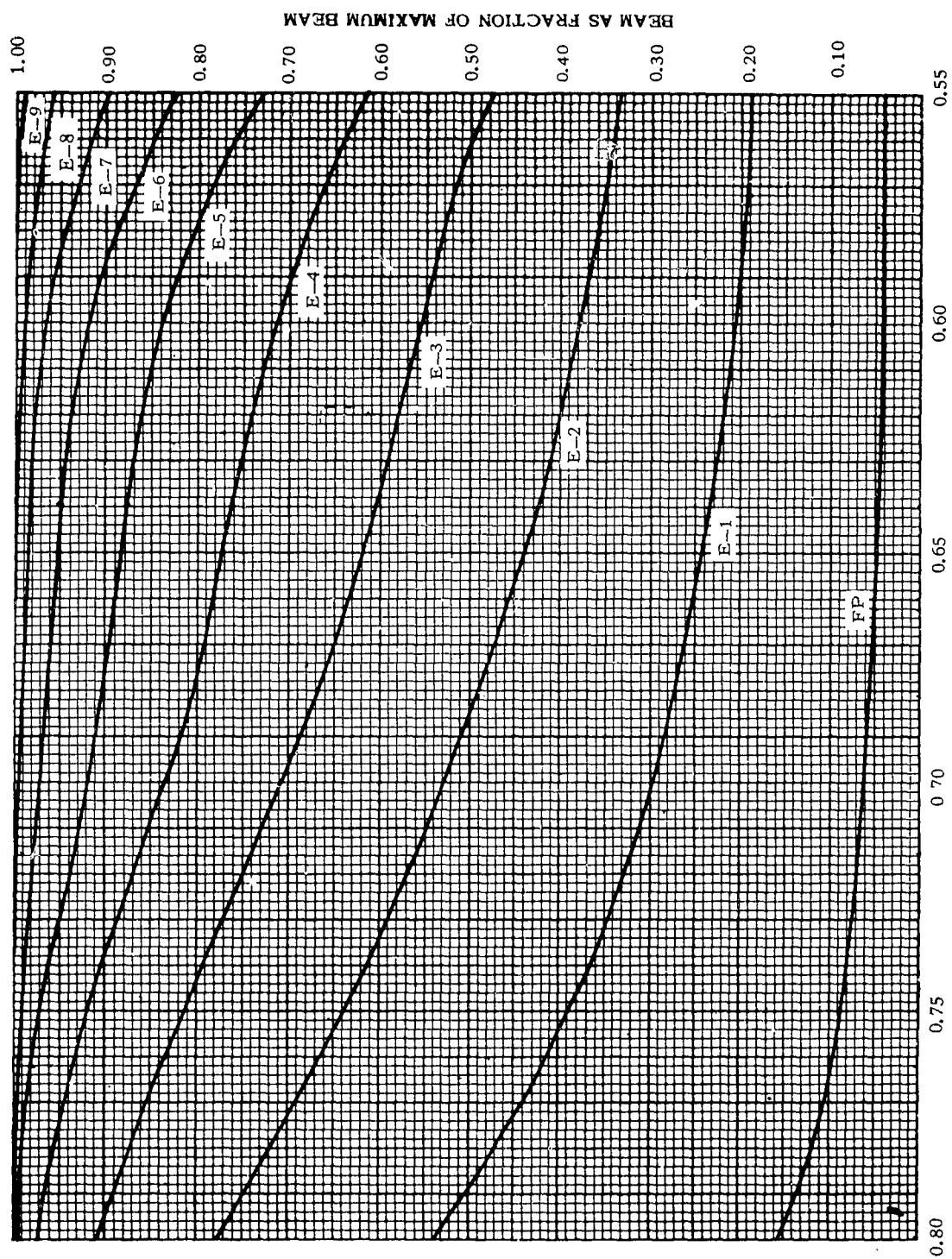


Figure 60 - 1.50 W.L. Cross Curves

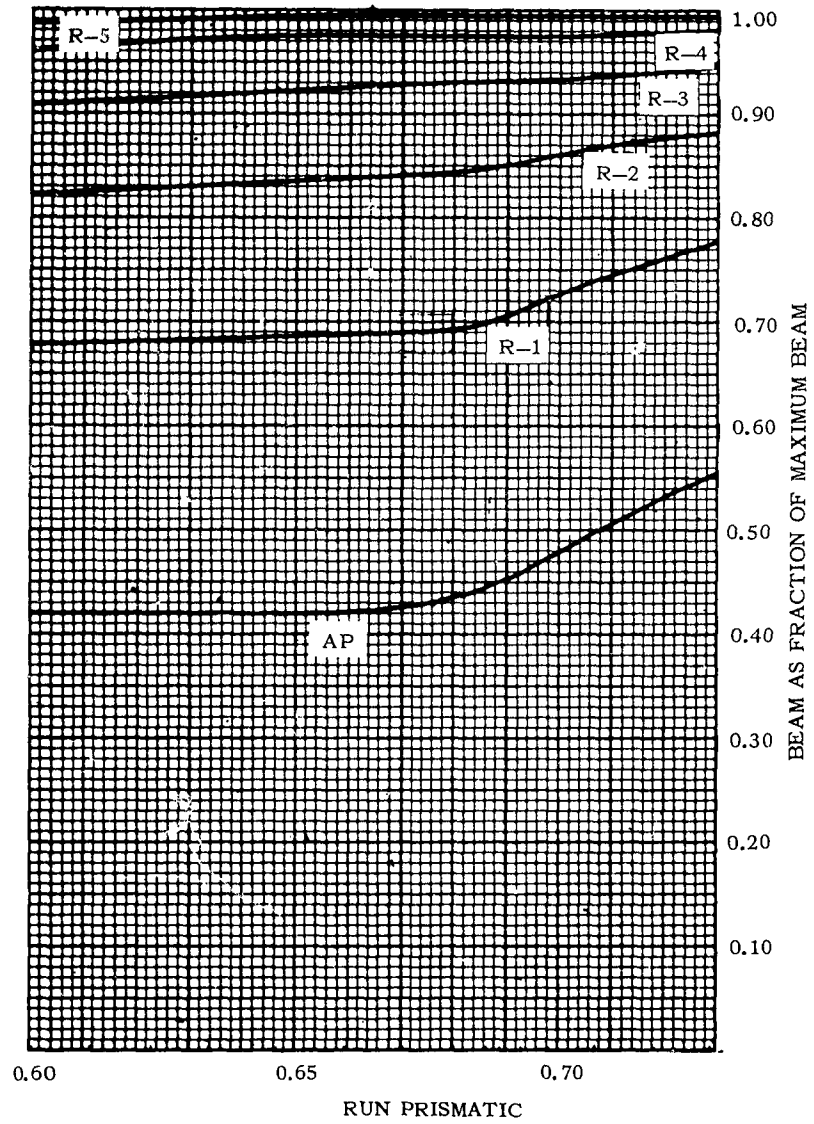


Figure 6p - 1.50 W.L. Cross Curves

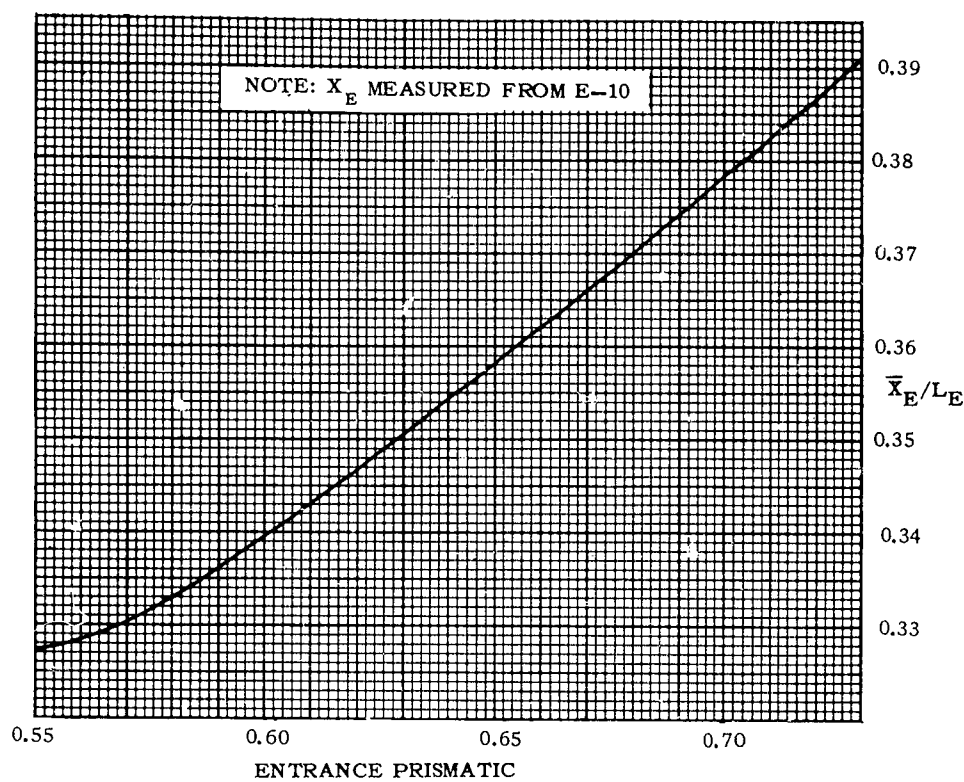


Figure 7 -- Position of Centroid of Volume of Entrance

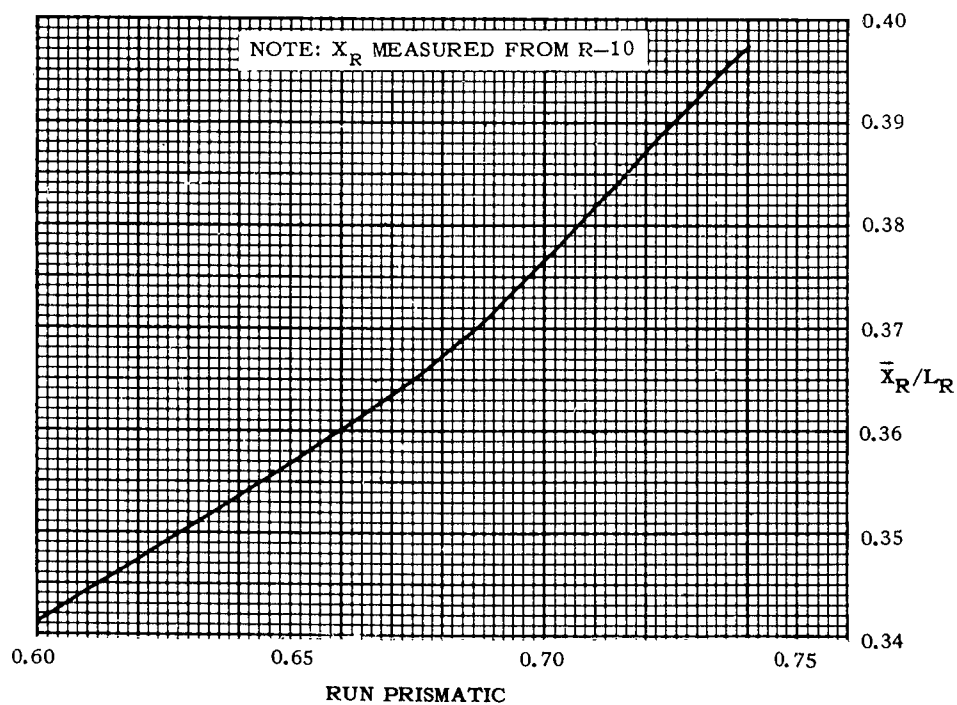


Figure 8 -- Position of Centroid of Volume of Run

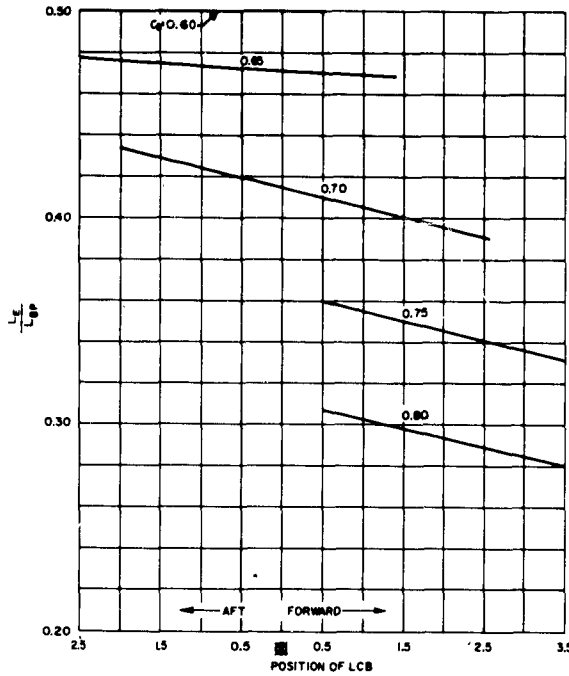


Figure 9 - Ratio of $\frac{L_E}{L_{BP}}$ for Different Values of C_B and Positions of LCB

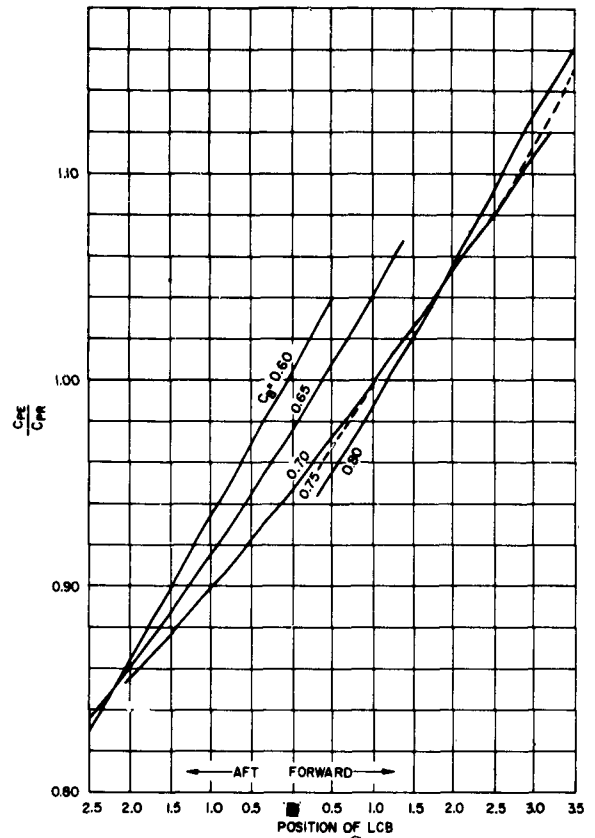


Figure 10 - Ratio of $\frac{C_{PE}}{C_{PR}}$ for Different Values of C_B and Positions of LCB

In order to use the contours to obtain a model having any desired fullness and location of LCB , certain auxiliary curves are necessary. These show:

1. the ratio of length of entrance to total length $\frac{L_E}{L_{BP}}$ (Figure 9) and
2. the ratio of entrance and run prismatic coefficients $\frac{C_{PE}}{C_{PR}}$ for different block

coefficients and positions of LCB (Figure 10).

In a particular case, the dimensions and displacement of the ship and the desired location of the LCB will be determined first from the general design conditions. A number of different solutions may be tried to explore the effects on horsepower, weights, costs, and so on. In any one case, the block, midship area, and prismatic coefficients can be calculated and the length of parallel body (L_X) can be found from Figure 3. Figures 9 and 10 will then give the length of entrance (L_E) and the ratio of prismatic coefficients of entrance and run

$\frac{C_{PE}}{C_{PR}}$. We can then write

$$C_P \times L_{BP} = (C_{PE} \times L_E) + L_X + (C_{PR} \times L_R)$$

from which C_{PE} and C_{PR} can be determined.

These values can be used to enter the area and waterline coefficient contours, and the area curve and lines plan can then be drawn. The stations to which the ordinates refer must be spaced equally along the lengths of entrance and run.

e. Bow and stern contours

These are shown in Figure 11. The stern has an aperture suitable for a single screw with cruiser stern. The bow profile is almost vertical below water, the waterline endings being drawn with a radius. The radius corresponds to 2 in. at 1.1 WL and 24 in. at 1.95 WL for a ship having an *LBP* of 400 ft. (1.00 WL is the designed load waterline.)

f. Although it was realized that the incorporation of a bulb in the bow lines would be of benefit in the finer models of the series, this would have introduced a discontinuity in the graphical representation of the forms. The Panel decided that this was not desirable in a methodical series of this type, and that the effect of bulbs of different shapes and sizes could well be the subject of a future research project of the kind for which Series 60 was designed to be a starting point.

g. Another future research project which might stem from the Series would be concerned with the behavior of such models in waves, and the effect of changes in fullness and proportions upon their motions and speed loss. It was therefore important that the above-water forms should be realistic in terms of sheer and flare, and after consultation with the Maritime Administration, they were drawn out to represent modern average practice.

NOTE: 15 INCH BOW RADIUS AT 1.75 WL
24 INCH BOW RADIUS AT 1.95 WL

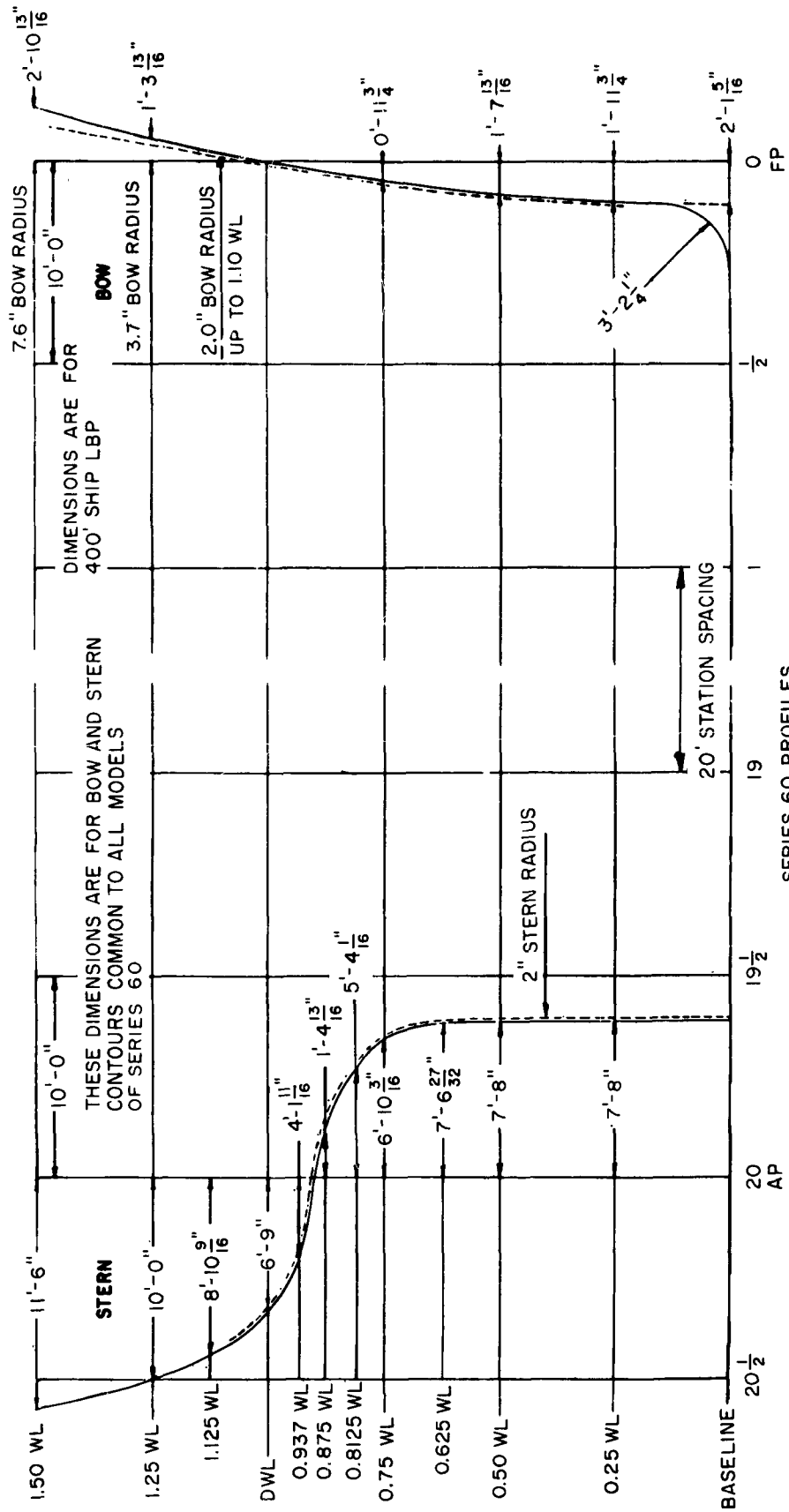


Figure 11 - Bow and Stern Contours

CHAPTER V

RESISTANCE TESTS ON SERIES 60 PARENT MODELS

The five parent models were made to lines drawn out from the new contours and had the numbers and particulars given in Table 2. The lines are shown in Figures 12 through 16; the area curves are given in Figure 17 and the offsets in Tables 3 through 7.

The models were made of wax, 20 ft *LBP*, and towed in the deep-water basin at the Taylor Model Basin, which has a cross section 51 ft wide and 22 ft deep.

Experiments were made with and without turbulence stimulation. The latter was provided by studs, 1/8 in. in diameter, 1/10 in. high, spaced 1 in. apart along a line parallel to the bow contour, the fore and aft position being controlled by the angle of entrance on the LWL as described by Hughes and Allan.⁴⁶

When these series experiments were begun in 1949, the question of turbulence stimulation was under intensive study, and its importance, especially in full models, had only recently been widely appreciated. At that time, there was no agreement as to the best method of stimulating turbulent flow, and indeed the subject is not satisfactorily resolved even today. Several methods were being advocated, the principal ones being sand strips, struts, trip wires and studs. The Series 57 models were run with sand strips, but these were abandoned in favour of studs for the Series 60 parents and *LCB* series. The studs were replaced by trip wires for the final series of variations in $\frac{L}{B}$ and $\frac{B}{H}$ ratios because experience had shown that trip wires gave slightly higher resistances than studs for the full models. Moreover, it was hoped that other experiment tanks would in the future use Series 60 as a point of departure for series work, and most of them used trip wires. In the final presentation based on the $\frac{L}{B}$, $\frac{B}{H}$ Series, the contours all apply to tests made with trip wires. An account of the experiments carried out to evaluate the different types of stimulation is given in Appendix A.

The resistance results from the models have been converted to apply to ships of 400 ft *LBP* and with other dimensions as listed in Table 2. In making this conversion, the ATTC 1947 friction formulation was used together with an addition of +0.0004 for model-ship correlation allowance C_A . The ship values have been expressed as values of C_T and are plotted to a base of $\frac{V}{\sqrt{L_{WL}}}$ in Figure 18.

(Text continued on page V-10)

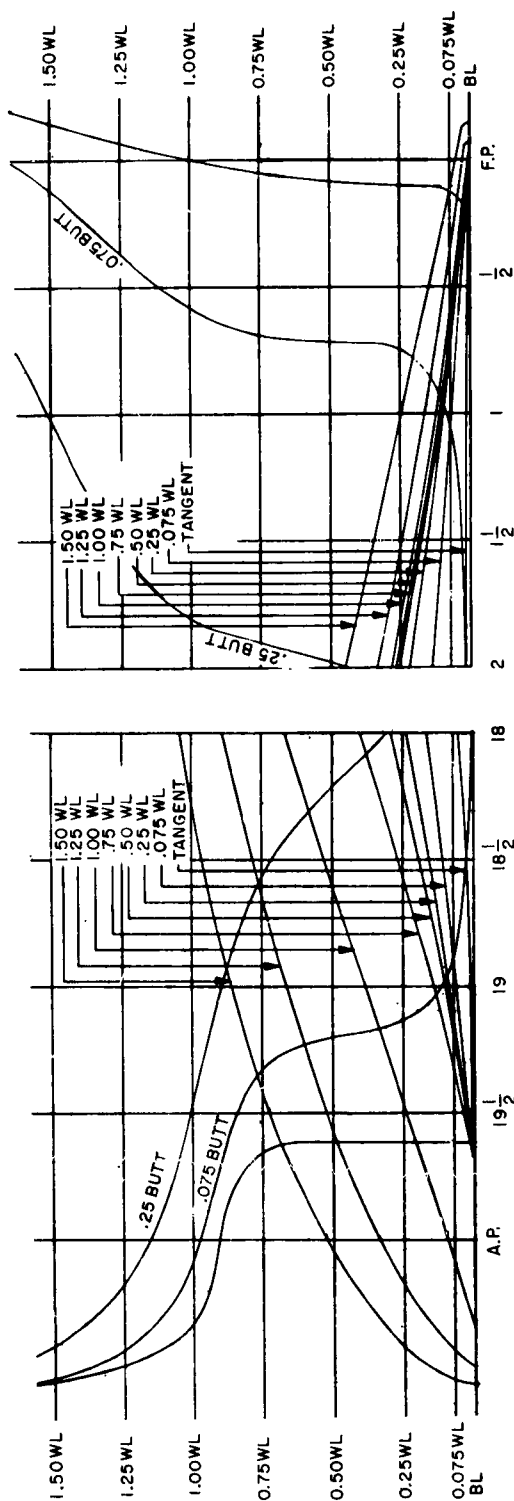


Figure 12a - Stern

Figure 12b - Bow

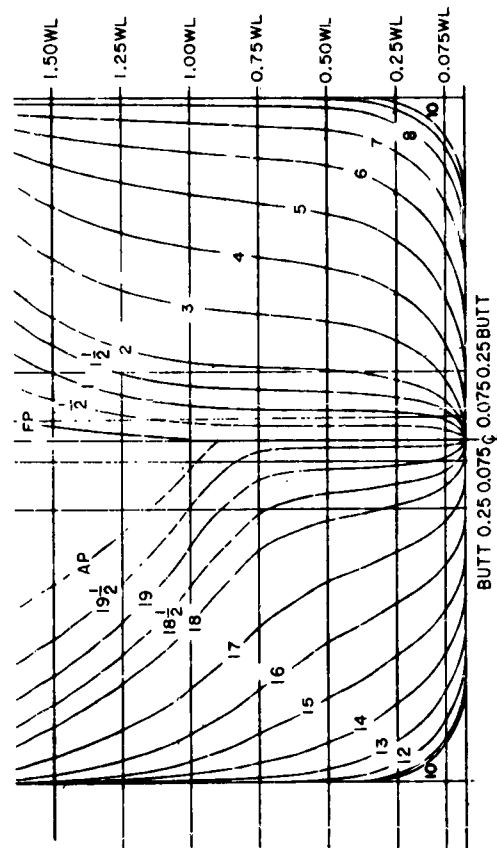


Figure 12c - Body

Figure 12 - Lines of Series 60 Parents. 0.60 C_B (Model 4210W)

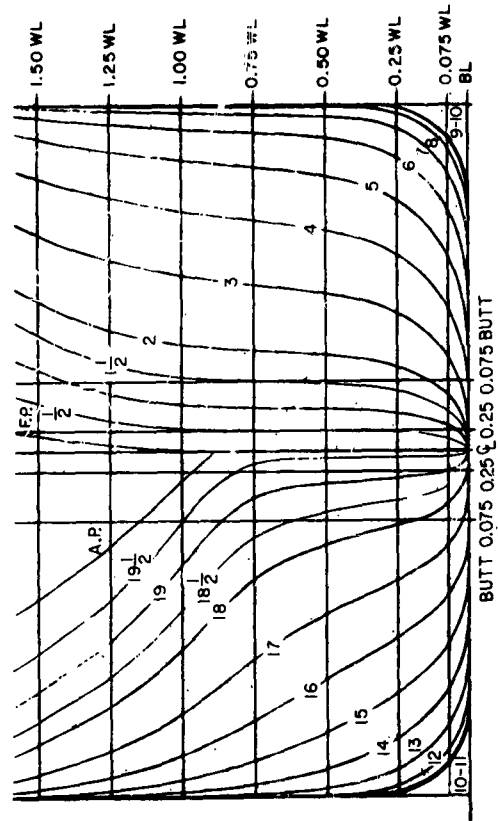
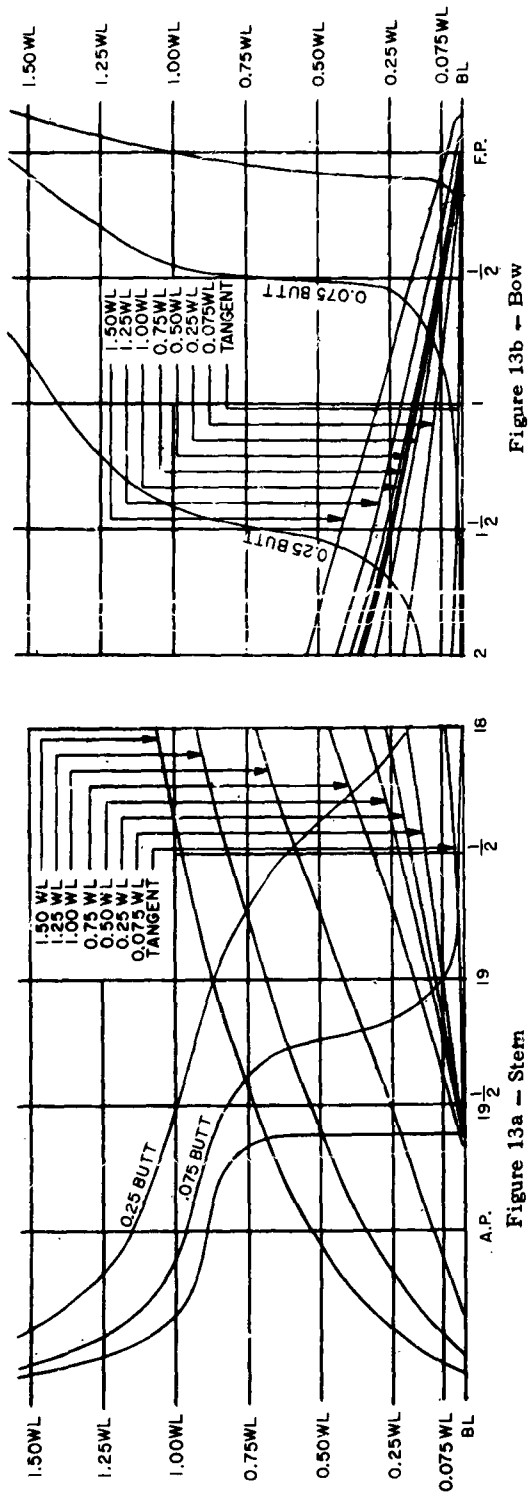


Figure 13 - Lines of Series 60 Parents. 0.65 C_B (Model 4211W)

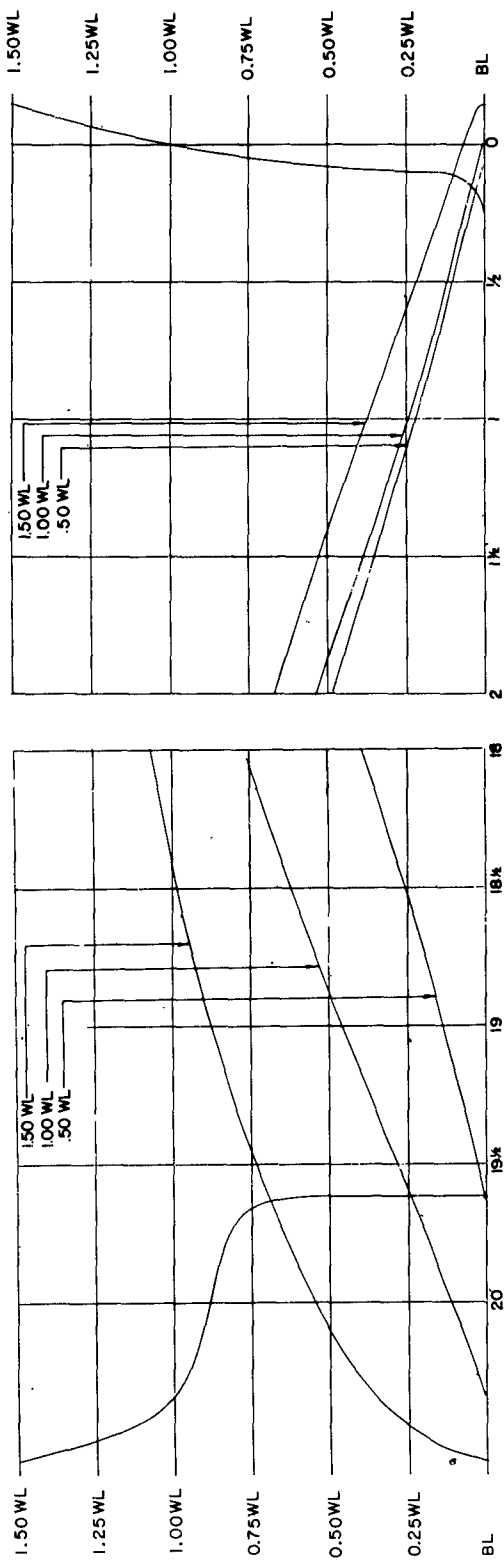


Figure 14a - Stern

Figure 14b - Row

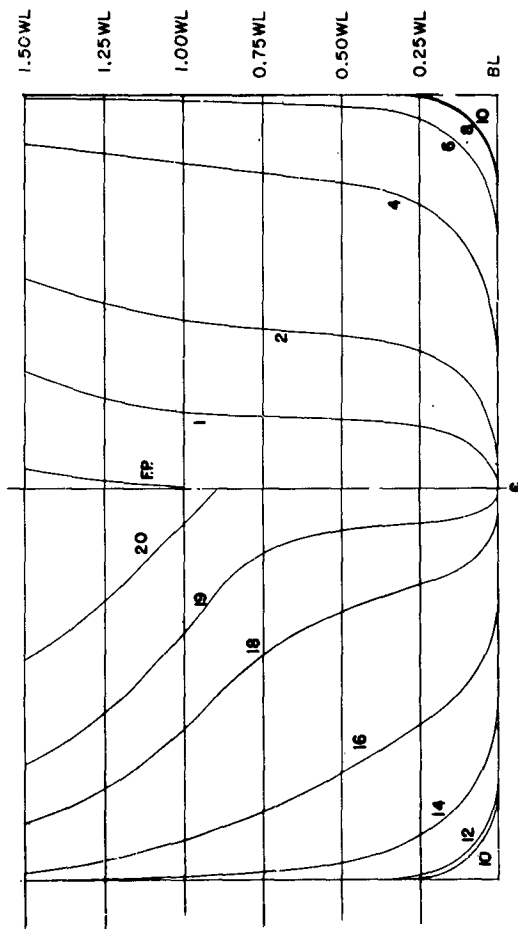


Figure 14c - Body

Figure 14 - Lines of Series 60 Parents. 0.70 C_B (Model 4212V)

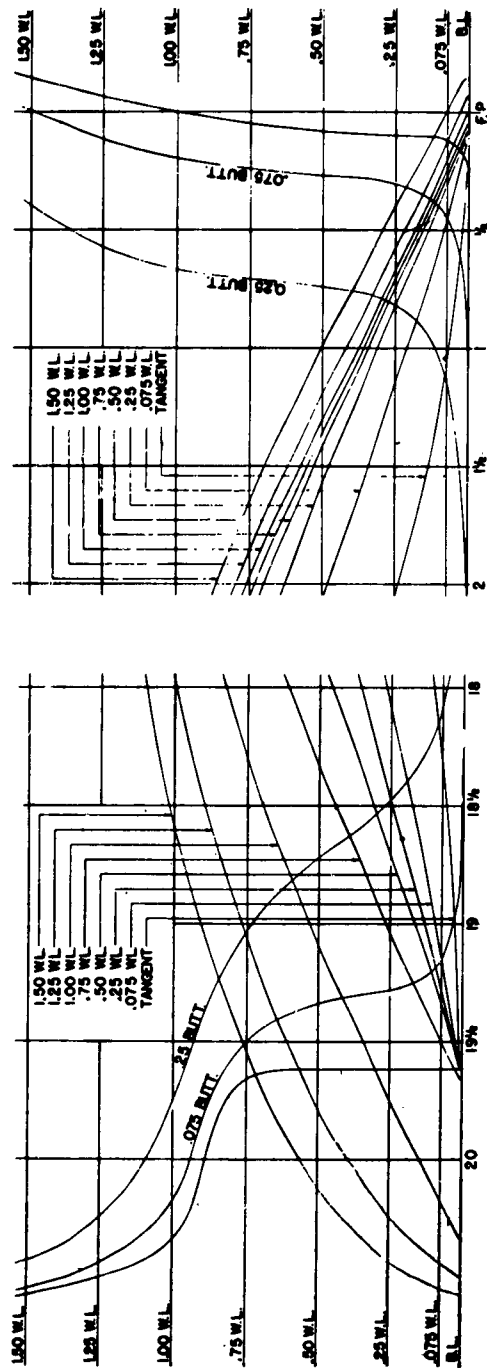


Figure 15b - Bow

Figure 15a - Stern

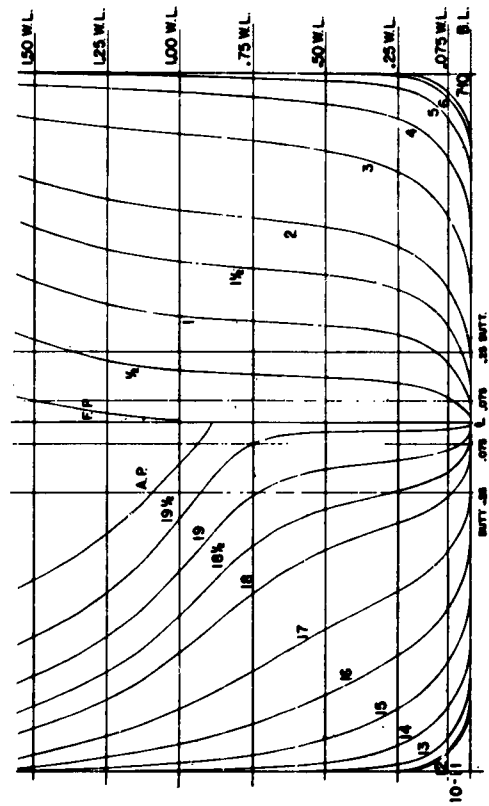


Figure 15c - Body

Figure 15 - Lines of Series 60 Parents: 0.75 C_B (Model 4213W)

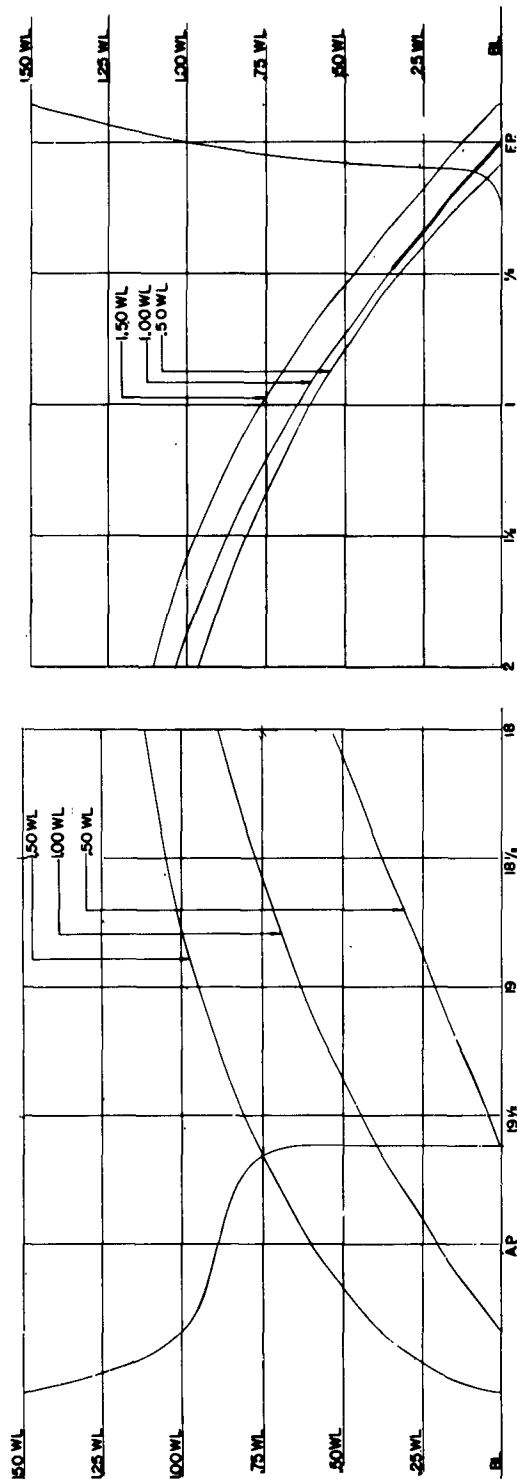


Figure 16a - Stern

Figure 16b - Bow

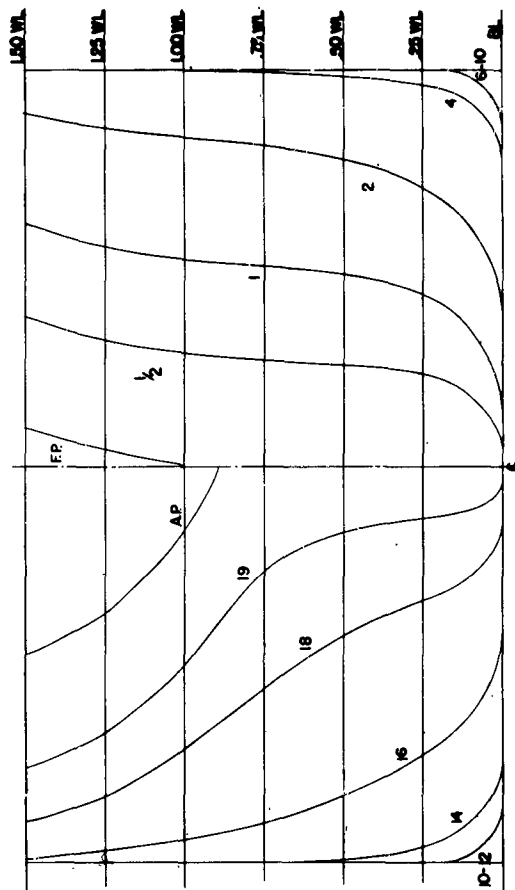


Figure 16c - Body

Figure 16 - Lines of Series 60 Parents. 0.80 C_B (Model 4214WB-4)

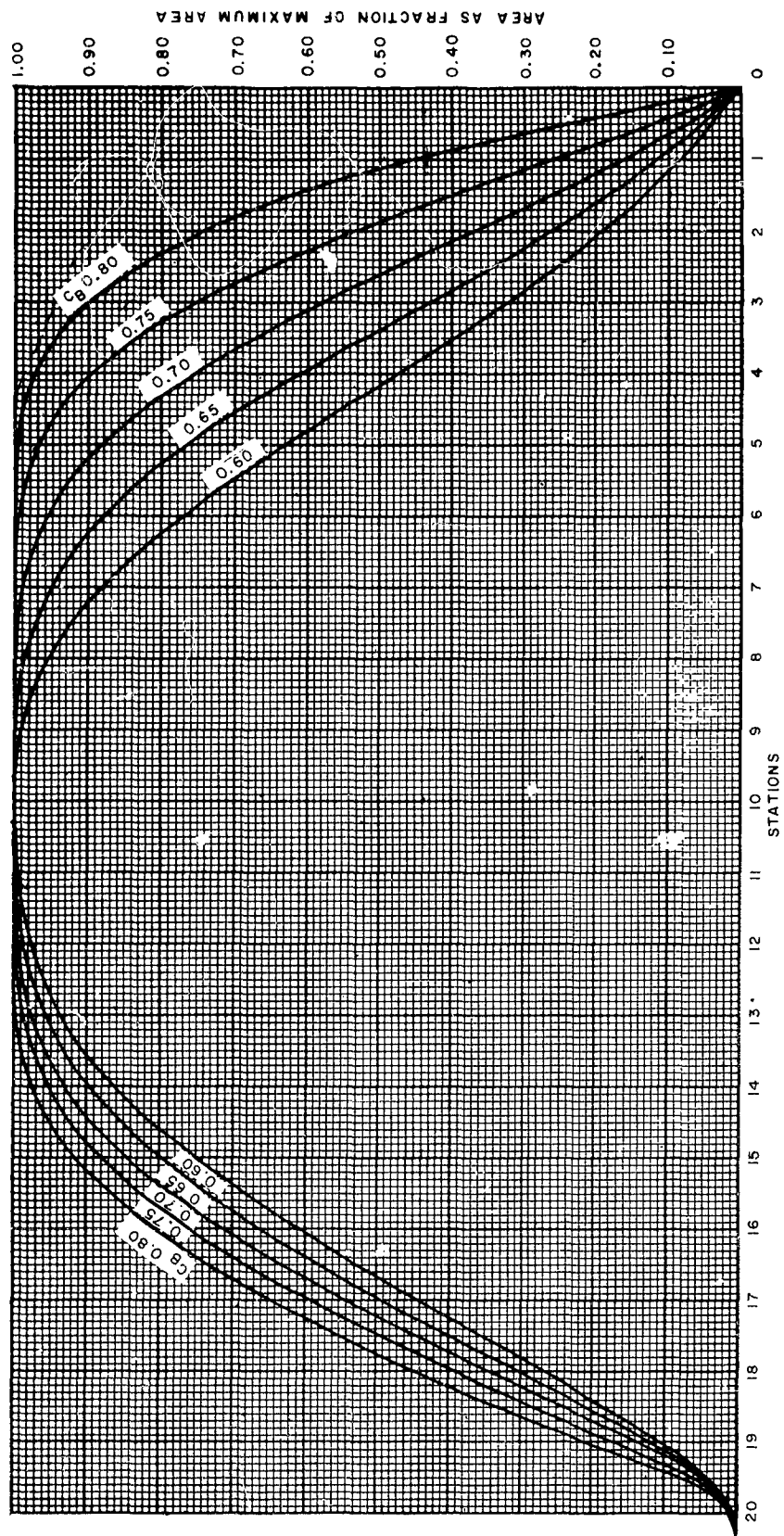


Figure 17 - Area Curves, Series 60 Parents

Table 3 - Table of Offsets-Parent Forms-0.60 Block Coefficient
(Half-breadths of waterline given as fraction of maximum beam on each waterline)

Model = 4210W

W.L. 1.00 is the designed load waterline

Forebody prismatic coefficient = 0.581

Afterbody prismatic coefficient = 0.646

Total prismatic coefficient = 0.614

Sta.	Tan.	Waterlines							Area as fraction of max. area to 1.00 W.L.
		0.075	0.25	0.50	0.75	1.00	1.25	1.50	
FP	0.000	0.000	0.000	0.000	0.000	0.000	0.020	0.042	0.000
1/2	0.009	0.032	0.042	0.041	0.043	0.051	0.076	0.120	0.042
1	0.013	0.064	0.082	0.087	0.090	0.102	0.133	0.198	0.085
1 1/2	0.019	0.095	0.126	0.141	0.148	0.160	0.195	0.278	0.135
2	0.024	0.127	0.178	0.204	0.213	0.228	0.270	0.360	0.192
3	0.055	0.196	0.294	0.346	0.368	0.391	0.440	0.531	0.323
4	0.134	0.314	0.436	0.502	0.535	0.562	0.607	0.683	0.475
5	0.275	0.466	0.589	0.660	0.691	0.718	0.754	0.804	0.630
6	0.469	0.630	0.733	0.802	0.824	0.841	0.862	0.889	0.771
7	0.666	0.779	0.854	0.906	0.917	0.926	0.936	0.946	0.880
8	0.831	0.898	0.935	0.971	0.977	0.979	0.981	0.982	0.955
9	0.945	0.964	0.979	0.996	1.000	1.000	1.000	1.000	0.990
10	1.000	1.000	1.000	1.000	1.000	1.000	1.000	1.000	1.000
11	0.965	0.982	0.990	1.000	1.000	1.000	1.000	1.000	0.996
12	0.882	0.922	0.958	0.994	1.000	1.000	1.000	1.000	0.977
13	0.767	0.826	0.892	0.962	0.987	0.994	0.997	1.000	0.938
14	0.622	0.701	0.781	0.884	0.943	0.975	0.990	0.999	0.863
15	0.463	0.560	0.639	0.754	0.857	0.937	0.977	0.994	0.750
16	0.309	0.413	0.483	0.592	0.728	0.857	0.933	0.975	0.609
17	0.168	0.267	0.330	0.413	0.541	0.725	0.844	0.924	0.445
18	0.065	0.152	0.193	0.236	0.321	0.536	0.709	0.834	0.268
18 1/2	0.032	0.102	0.130	0.156	0.216	0.425	0.626	0.769	0.187
19	0.014	0.058	0.076	0.085	0.116	0.308	0.530	0.686	0.109
19 1/2	0.010	0.020	0.020	0.022	0.033	0.193	0.418	0.579	0.040
AP	0.000	0.000	0.000	0.000	0.000	0.082	0.270	0.420	0.004
Max. half beam	0.710	0.866	0.985	1.000	1.000	1.000	1.000	1.000	

Table 4 - Table of Offsets-Parent Forms-0.65 Block Coefficient
(Half-breadths of waterlines given as fraction of maximum beam on each waterline)

Model = 4211W

W.L. 1.00 is the designed load waterline

Forebody prismatic coefficient = 0.651

Afterbody prismatic coefficient = 0.672

Total prismatic coefficient = 0.661

Sta.	Tan.	Waterlines							Area as fraction of max. area to 1.00 W.L.
		0.075	0.25	0.50	0.75	1.00	1.25	1.50	
FP	0.000	0.000	0.000	0.000	0.000	0.000	0.019	0.045	0.000
1/2	0.008	0.037	0.056	0.058	0.060	0.066	0.090	0.138	0.055
1	0.016	0.081	0.110	0.122	0.126	0.135	0.166	0.236	0.115
1 1/2	0.024	0.125	0.174	0.194	0.204	0.216	0.251	0.336	0.184
2	0.041	0.177	0.244	0.277	0.291	0.308	0.350	0.434	0.261
3	0.109	0.298	0.401	0.455	0.480	0.508	0.552	0.625	0.432
4	0.239	0.452	0.570	0.636	0.667	0.694	0.734	0.788	0.609
5	0.408	0.619	0.729	0.794	0.821	0.842	0.867	0.903	0.765
6	0.604	0.767	0.853	0.905	0.920	0.930	0.946	0.964	0.879
7	0.788	0.886	0.939	0.966	0.972	0.978	0.984	0.991	0.951
8	0.928	0.962	0.982	0.996	0.995	0.997	0.998	1.000	0.987
9	0.999	0.996	0.999	1.000	1.000	1.000	1.000	1.000	0.999
10	1.000	1.000	1.000	1.000	1.000	1.000	1.000	1.000	1.000
11	0.980	0.993	0.996	1.000	1.000	1.000	1.000	1.000	0.998
12	0.922	0.954	0.976	0.997	1.000	1.000	1.000	1.000	0.987
13	0.808	0.873	0.928	0.976	0.992	0.998	1.000	1.000	0.958
14	0.659	0.760	0.837	0.920	0.963	0.984	0.994	1.000	0.898
15	0.492	0.620	0.705	0.813	0.894	0.949	0.980	0.995	0.797
16	0.322	0.460	0.544	0.658	0.778	0.875	0.941	0.976	0.662
17	0.170	0.304	0.377	0.472	0.601	0.755	0.864	0.930	0.492
18	0.066	0.170	0.217	0.270	0.370	0.572	0.736	0.845	0.303
18 1/2	0.034	0.113	0.145	0.178	0.250	0.458	0.651	0.779	0.209
19	0.016	0.063	0.080	0.094	0.135	0.331	0.547	0.693	0.121
19 1/2	0.011	0.020	0.020	0.022	0.037	0.205	0.427	0.581	0.042
AP	0.000	0.000	0.000	0.000	0.000	0.084	0.272	0.426	0.005
Max. half beam*	0.739	0.904	0.992	1.000	1.000	1.000	1.000	1.000	

Table 5 – Table of Offsets—Parent Forms—0.70 Block Coefficient
(Half-breadths of waterlines given as fraction of maximum beam on each waterline)

Model = 4212W
W.L. 1.00 is the designed load waterline

Forebody prismatic coefficient = 0.721
Afterbody prismatic coefficient = 0.698
Total prismatic coefficient = 0.710

Sta.	Tan.	Waterlines							Area as fraction of max. area to 1.00 W.L.
		0.075	0.25	0.50	0.75	1.00	1.25	1.50	
FP	0.000	0.000	0.000	0.000	0.000	0.000	0.020	0.051	0.000
1/2	0.009	0.049	0.072	0.081	0.086	0.094	0.119	0.176	0.076
1	0.026	0.110	0.158	0.177	0.184	0.194	0.229	0.299	0.165
1 1/2	0.054	0.183	0.252	0.281	0.294	0.310	0.350	0.421	0.266
2	0.100	0.266	0.350	0.389	0.407	0.430	0.472	0.536	0.370
3	0.239	0.450	0.550	0.599	0.627	0.655	0.689	0.734	0.579
4	0.437	0.625	0.724	0.778	0.802	0.827	0.851	0.877	0.755
5	0.646	0.783	0.856	0.904	0.920	0.935	0.948	0.961	0.882
6	0.830	0.896	0.942	0.971	0.980	0.985	0.990	0.992	0.958
7	0.939	0.970	0.984	0.994	0.998	1.000	1.000	1.000	0.990
8	0.998	1.000	1.000	1.000	1.000	1.000	1.000	1.000	0.999
9	1.000	1.000	1.000	1.000	1.000	1.000	1.000	1.000	1.000
10	1.000	1.000	1.000	1.000	1.000	1.000	1.000	1.000	1.000
11	1.000	0.997	0.999	1.000	1.000	1.000	1.000	1.000	0.999
12	0.961	0.978	0.989	1.000	1.000	1.000	1.000	1.000	0.994
13	0.855	0.917	0.958	0.993	1.000	1.000	1.000	1.000	0.977
14	0.705	0.815	0.887	0.957	0.980	0.991	0.998	1.000	0.930
15	0.532	0.675	0.768	0.868	0.927	0.961	0.985	0.998	0.844
16	0.344	0.510	0.605	0.726	0.825	0.897	0.950	0.982	0.713
17	0.186	0.338	0.427	0.533	0.658	0.788	0.881	0.939	0.543
18	0.077	0.192	0.245	0.314	0.425	0.614	0.765	0.854	0.343
18 1/2	0.042	0.126	0.165	0.207	0.292	0.499	0.680	0.789	0.239
19	0.023	0.070	0.089	0.107	0.164	0.368	0.572	0.704	0.140
19 1/2	0.014	0.022	0.022	0.024	0.043	0.228	0.444	0.589	0.047
AP	0.000	0.000	0.000	0.000	0.000	0.089	0.286	0.438	0.005
Max. half beam*	0.771	0.926	0.998	1.000	1.000	1.000	1.000	1.000	

Table 6 – Table of Offsets—Parent Forms—0.75 Block Coefficient
(Half-breadths of waterlines given as fraction of maximum beam on each waterline)

Model = 4213W
W.L. 1.00 is the designed load waterline

Forebody prismatic coefficient = 0.792
Afterbody prismatic coefficient = 0.724
Total prismatic coefficient = 0.758

Sta.	Tan.	Waterlines							Area as fraction of max. area to 1.00 W.L.
		0.075	0.25	0.50	0.75	1.00	1.25	1.50	
FP	0.000	0.000	0.000	0.000	0.000	0.000	0.025	0.062	0.000
1/2	0.021	0.075	0.113	0.128	0.138	0.149	0.176	0.235	0.120
1	0.067	0.180	0.251	0.276	0.290	0.304	0.338	0.403	0.261
1 1/2	0.138	0.290	0.380	0.423	0.441	0.460	0.495	0.557	0.401
2	0.235	0.406	0.504	0.560	0.585	0.608	0.639	0.690	0.535
3	0.466	0.625	0.718	0.777	0.806	0.824	0.845	0.867	0.754
4	0.700	0.800	0.870	0.911	0.930	0.943	0.954	0.962	0.845
5	0.883	0.920	0.959	0.978	0.985	0.990	0.994	0.998	0.969
6	0.979	0.983	0.994	0.999	0.999	1.000	1.000	1.000	0.995
7	1.000	1.000	1.000	1.000	1.000	1.000	1.000	1.000	1.000
8	1.000	1.000	1.000	1.000	1.000	1.000	1.000	1.000	1.000
9	1.000	1.000	1.000	1.000	1.000	1.000	1.000	1.000	1.000
10	1.000	1.000	1.000	1.000	1.000	1.000	1.000	1.000	1.000
11	1.000	1.000	1.000	1.000	1.000	1.000	1.000	1.000	1.000
12	0.985	0.992	0.999	1.000	1.000	1.000	1.000	1.000	0.998
13	0.914	0.953	0.979	0.997	1.000	1.000	1.000	1.000	0.987
14	0.784	0.860	0.925	0.976	0.990	0.996	1.000	1.000	0.953
15	0.612	0.728	0.820	0.908	0.953	0.975	0.990	1.000	0.880
16	0.420	0.565	0.667	0.781	0.863	0.921	0.958	0.987	0.760
17	0.242	0.388	0.483	0.592	0.712	0.817	0.899	0.951	0.594
18	0.105	0.225	0.288	0.365	0.488	0.660	0.794	0.875	0.391
18 1/2	0.058	0.151	0.197	0.249	0.354	0.554	0.715	0.812	0.282
19	0.028	0.084	0.109	0.135	0.211	0.427	0.614	0.726	0.172
19 1/2	0.012	0.021	0.025	0.028	0.061	0.278	0.486	0.610	0.060
AP	0.000	0.000	0.000	0.000	0.000	0.115	0.320	0.451	0.006
Max. half beam*	0.807	0.947	1.000	1.000	1.000	1.000	1.000	1.000	

Table 7 - Table of Offsets-Parent Forms-0.80 Block Coefficient
(Half-breadths of waterlines given as fraction of maximum beam on each waterline)

Model = 4214W-B4
W.L. 1.00 is the designed load waterline

Forebody prismatic coefficient = 0.861
Afterbody prismatic coefficient = 0.750
Total prismatic coefficient = 0.805

Sta.	Tan.	Waterlines							Area as fraction of max. area to 1.00 W.L.
		0.075	0.25	0.50	0.75	1.00	1.25	1.50	
FP	0.000	0.000	0.000	0.000	0.000	0.000	0.044	0.098	0.000
1/2	0.053	0.162	0.235	0.258	0.267	0.286	0.318	0.378	0.243
1	0.160	0.324	0.435	0.486	0.505	0.522	0.554	0.613	0.458
1 1/2	0.286	0.467	0.581	0.650	0.681	0.700	0.728	0.779	0.620
2	0.423	0.591	0.702	0.774	0.808	0.830	0.852	0.890	0.746
3	0.696	0.793	0.867	0.921	0.948	0.964	0.975	0.984	0.901
4	0.903	0.929	0.962	0.983	0.994	0.999	1.000	1.000	0.975
5	0.990	0.991	0.995	0.998	1.000	1.000	1.000	1.000	0.997
6	1.000	1.000	1.000	1.000	1.000	1.000	1.000	1.000	1.000
7	1.000	1.000	1.000	1.000	1.000	1.000	1.000	1.000	1.000
8	1.000	1.000	1.000	1.000	1.000	1.000	1.000	1.000	1.000
9	1.000	1.000	1.000	1.000	1.000	1.000	1.000	1.000	1.000
10	1.000	1.000	1.000	1.000	1.000	1.000	1.000	1.000	1.000
11	1.000	1.000	1.000	1.000	1.000	1.000	1.000	1.000	1.000
12	0.996	0.997	1.000	1.000	1.000	1.000	1.000	1.000	0.999
13	0.958	0.976	0.996	1.000	1.000	1.000	1.000	1.000	0.995
14	0.858	0.906	0.958	0.991	1.000	1.000	1.000	1.000	0.974
15	0.686	0.780	0.872	0.941	0.972	0.988	0.996	1.000	0.915
16	0.486	0.625	0.726	0.831	0.900	0.941	0.969	0.991	0.806
17	0.302	0.442	0.542	0.656	0.765	0.851	0.915	0.964	0.649
18	0.146	0.266	0.337	0.427	0.560	0.712	0.832	0.896	0.449
18 1/2	0.092	0.185	0.232	0.298	0.425	0.617	0.764	0.840	0.336
19	0.045	0.105	0.130	0.166	0.263	0.503	0.670	0.760	0.212
19 1/2	0.013	0.026	0.032	0.035	0.071	0.353	0.546	0.644	0.079
AP	0.000	0.000	0.000	0.000	0.000	0.160	0.370	0.476	0.100
Max. half beam	0.850	0.970	1.000	1.000	1.000	1.000	1.000	1.000	

The symbols are defined as follows:
$$C_T = \frac{R}{\frac{1}{2} \cdot \rho \cdot S \cdot v^2}$$

where R is the ship resistance in pounds,

ρ is the mass density of water in $\frac{\text{lb/cu ft}}{g}$,

S is the wetted surface in square feet,

v is the speed of ship in feet per second,

V is the speed of ship in knots, and

L_{WL} is the length of ship on designed load waterline in feet.

The results are also shown in Figure 19 as curves of (C) to a base of (K) . These two "constants," introduced by Froude, are nondimensional, involve only speed and displacement (the two factors which usually control the preliminary design of a merchant ship), and are very useful in comparing forms at this stage. They have been used also in the SNAME Model Resistance Data sheets.

In English units they are defined as

$$(K) = 0.5834 \cdot \frac{V}{\Delta^{1/6}}$$

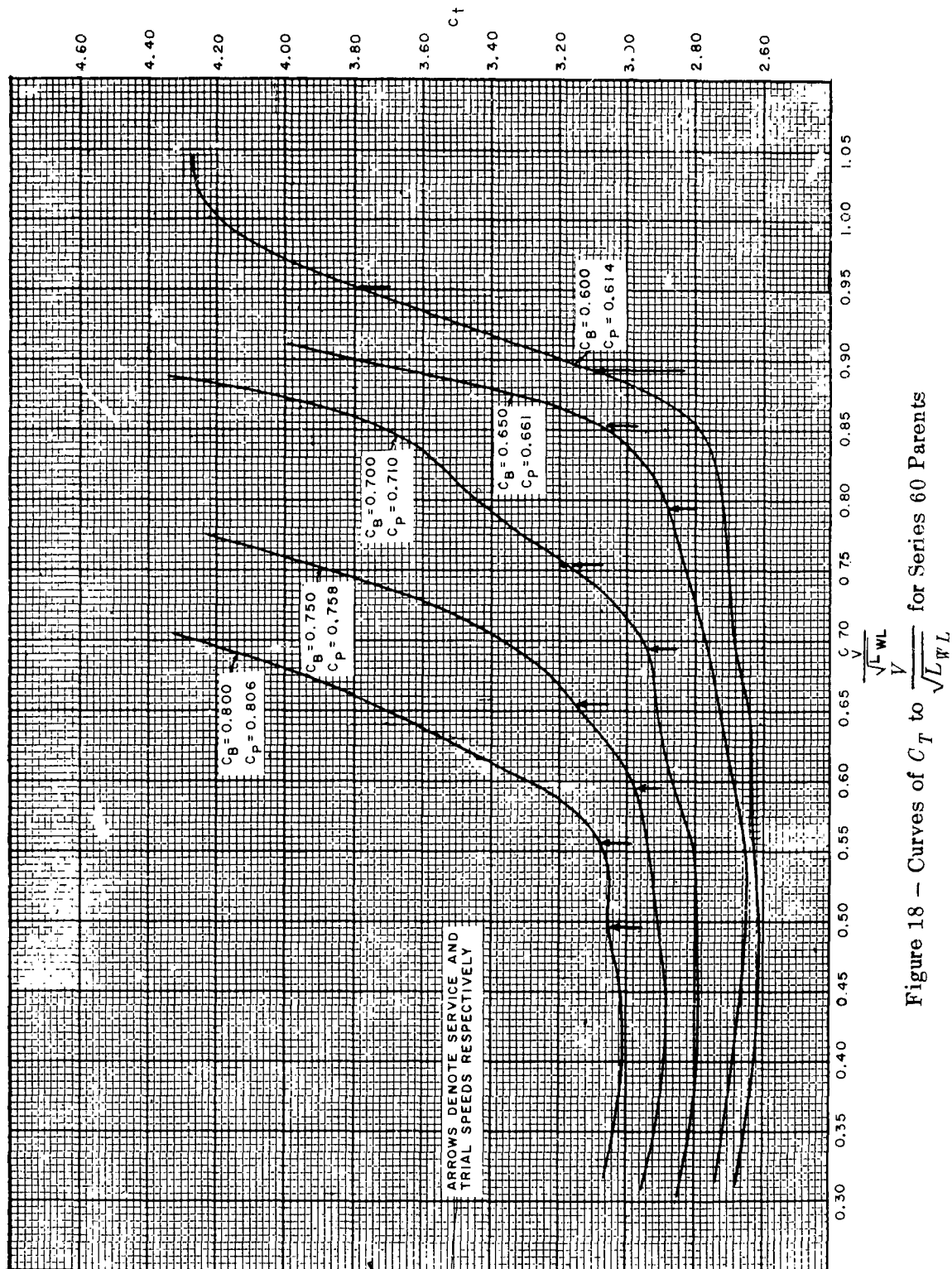


Figure 18 — Curves of C_T to $\frac{\sqrt{L WL}}{V}$ for Series 60 Parents

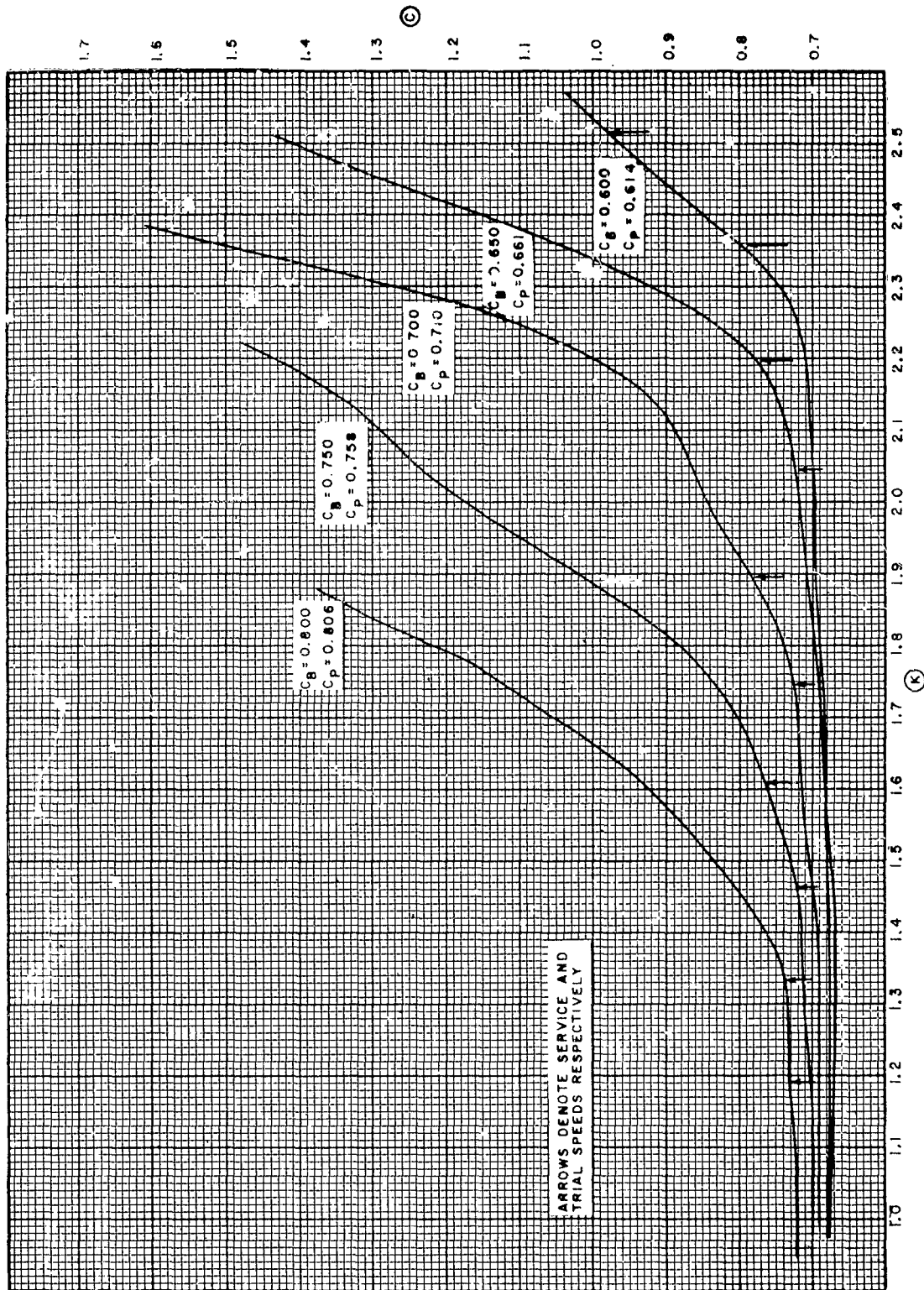


Figure 19 — Curves of C to K for Series 60 Parents

and

$$\textcircled{C} = \frac{\text{ehp} \times 427.1}{\Delta^{2/3} \cdot V^3}$$

where V is the speed of ship in knots

Δ is the displacement of ship in tons salt water, (2240 lb), and

ehp is the towrope horsepower for the ship.

The values of ehp used in calculating \textcircled{C} have been deduced from the model experiments by the use of the ATTC 1947 friction formulation and include the ship correlation allowance of +0.0004. Therefore both the C_T and \textcircled{C} values are based on the same data and are directly comparable in this respect.

$\frac{V}{\sqrt{L_{WL}}}$, $\frac{V}{\sqrt{L_{BP}}}$, and \textcircled{K} are related linearly for any one model. A corresponding set of values is given below, from which any other conversion can be made:

TABLE 8
Relation between C_B , $\frac{V}{\sqrt{L}}$, and \textcircled{K}

Model Number	C_B	$\frac{V}{\sqrt{L_{BP}}}$	$\frac{V}{\sqrt{L_{WL}}}$	\textcircled{K}
4210W	0.60	0.96	0.952	2.515
4211W	0.65	0.86	0.853	2.198
4212W	0.70	0.76	0.754	1.895
4213W	0.75	0.66	0.655	1.609
4214WB-4	0.80	0.56	0.556	1.334

A vast accumulation of model resistance data based on the Froude skin-friction coefficients is available in the transactions of societies and reports of model basins. Since 1948 this method of extrapolation from model to ship and that based on the ATTC 1947 (Schoenherr) line have both been recognized by the ITTC as acceptable for use in all published data. A quick graphical method of mutually converting the \textcircled{C} values based on these two formulations was published by Gertler in 1948.^{47*} The ATTC values used therein include the allowance of +0.0004 for ship correlation allowance, so that the application of this chart to the ATTC \textcircled{C} values given in this present report will yield directly the equivalent \textcircled{C} values based on the Froude coefficients.

*The chart in this report is reproduced as Figure D-4 in Appendix D.

In 1957 at the Madrid Conference, the ITTC agreed upon a new "model-ship correlation line" for use in all published work, which would give ship results differing somewhat from those based either on Froude or the ATTC line. However, pending agreement on the appropriate correlation allowances to use with the new line, it has not come into common usage as yet. When such agreement is reached, a chart similar to that in Reference 47 can easily be constructed.

In comparing a number of closely allied forms, all suitable to fulfill certain design conditions, this $\textcircled{C} - \textcircled{K}$ presentation has the advantage that for a given displacement and speed, \textcircled{K} is the same for all models. An ordinate erected at this value of \textcircled{K} will indicate the relative merits of the forms since \textcircled{C} also involves only the speed and displacement. The other differences in the various hulls can then be considered to determine which features are responsible for the differences in resistance and power.

Before proceeding with the methodical variations in LCB position and hull proportions, the results of the actual ship models and the Series 60 equivalents were compared. For this purpose, the same five designs as before were used as the control models, and equivalent Series 60 models having the same dimensions, displacement, and LCB position were made and tested. The exception was for the MARINER design where the Series 60, 0.60 C_B parent was used in the comparison.

Such comparisons must be made at speeds appropriate to the individual designs, and for this purpose, service and trial speeds have been chosen based on two suggested relations between fullness and speed-length ratio.

The first of these is an old formula first given by F.H. Alexander, but using coefficients suggested by Sir Amos Ayre as being more appropriate to modern ships:

$$\begin{aligned} \frac{V}{\sqrt{L_{BP}}} &= 2(1.08 - C_B) \text{ for trial speed} \\ \frac{V}{\sqrt{L_{BP}}} &= 2(1.05 - C_B) \text{ for service speed} \end{aligned} \quad [1]$$

These formulae give reasonable speeds for the fuller ships, but for the fine ships, such as that of 0.60 C_B , they give speeds which are too high from the standpoint of economic performance.

In 1955, Troost proposed a new formula to define the "sustained sea speed."⁴⁸ Based on a survey of many single-screw models run in the Netherlands Ship Model Basin (NSMB) over some 20 years, the formula generally gives speeds higher than the Alexander service speed for full ships and lower for fine ships, a result in conformity with modern practice. For all forms, the Troost sea speed lies at that point where the \textcircled{C} curve first begins rising steeply, and for some range above it the resistance is varying approximately as the cube of the speed, or the power is varying as V^4 . Troost therefore assumed a trial speed V_T some 6 percent above the sea speed V_s , so that the power on trial at speed V_T is approximately

25 percent greater than the power on trial at speed V_S . This is in keeping with the general design practice that the *service* speed should be attained under *trial* conditions at 80 percent of the maximum continuous power.

Troost defined the speeds as follows:

$$\frac{V_S}{\sqrt{L_{BP}}} = 1.85 - 1.6 C_P \text{ for sustained sea speed} \quad [2]$$

and

$$V_T = 1.06 V_S \text{ for trial speed.}$$

For the Series 60 models, these two formulae lead to the following speeds for ships 400 ft in length.

TABLE 9
List of Alexander and Troost Speeds

C_B	C_P	ALEXANDER SPEEDS (Equation (1))						TROOST SPEEDS (Equation (2))					
		SERVICE			TRIAL			SEA			TRIAL		
		$\frac{V}{\sqrt{L_{BP}}}$	(K)	V knots	$\frac{V}{\sqrt{L_{BP}}}$	(K)	V knots	$\frac{V}{\sqrt{L_{BP}}}$	(K)	V knots	$\frac{V}{\sqrt{L_{BP}}}$	(K)	V knots
0.60	0.614	0.90	2.358	18.0	0.96	2.515	19.20	0.869	2.274	17.38	0.921	2.410	18.42
0.65	0.661	0.80	2.045	16.0	0.86	2.198	17.20	0.792	2.022	15.84	0.839	2.142	16.78
0.70	0.710	0.70	1.746	14.0	0.76	1.895	15.20	0.714	1.781	14.28	0.757	1.889	15.14
0.75	0.758	0.60	1.462	12.0	0.66	1.609	13.20	0.637	1.552	12.74	0.675	1.645	13.50
0.80	0.805	0.50	1.190	10.0	0.56	1.334	11.20	0.562	1.338	11.24	0.596	1.419	11.92

A comparison of these speeds with modern American practice was made by Mr. H. de Luce in his discussion on the first series paper.⁴⁴ He examined the (C) curves for a number of ships and plotted the value of the speed-length ratio $\frac{V^*}{\sqrt{L}}$ against prismatic coefficient for the point on the (C) curve where there was a sharp "upturn" (Figure 20). He drew a mean curve through these points, designated as the mean "upturn" $\frac{V}{\sqrt{L}}$ on Figure 20. This figure also shows the Alexander and Troost lines, and it is clear that the latter conform much more with the general trend of the points and the de Luce line. An examination of the C_T curves for the Series 60 parent models, as given in Figure 18, shows that the values of $\frac{V}{\sqrt{L}}$ for the "upturn" points for these designs also lie very nearly on the Troost "sustained sea speed" line, and the latter would therefore seem to be a close guide to modern design trends (Figure 20).

*Mr. de Luce used L_{BP} for single-screw ships and L_{WL} for twin-screw ships.

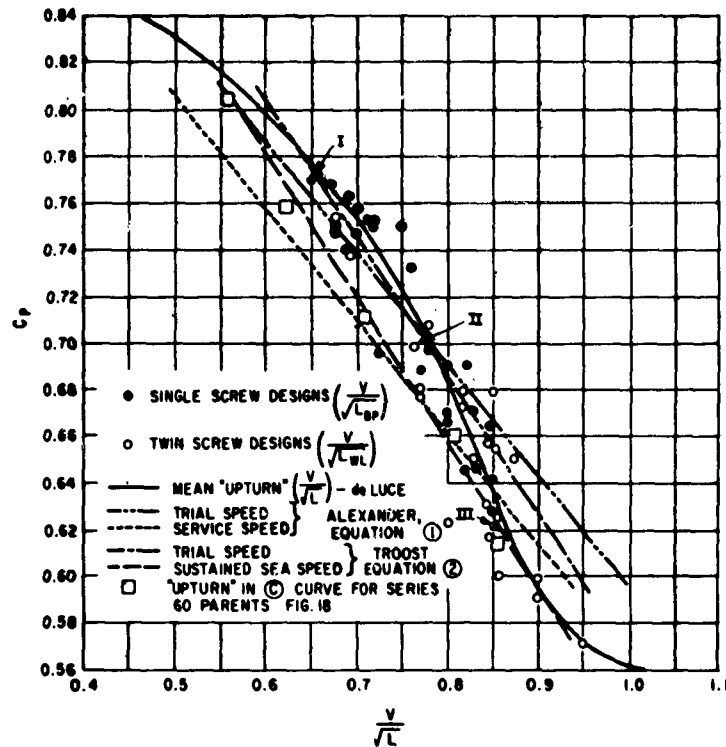


Figure 20 – Comparison of Alexander and Troost Speeds with Modern American Data

Mr. de Luce emphasised the need to relate the “upturn” speed to the speed considered in preparing an actual design. In Figure 21, prismatic coefficients are plotted against the speed-length ratio $\frac{V}{\sqrt{L}}$ corresponding to the speed on trial at designed draft with the machinery developing maximum rated continuous shaft horsepower, mostly taken from actual ship data. The “upturn” curve reproduced from Figure 20 is again a reasonable mean through the trial points, indicating that “many designers over the years have believed it desirable to select dimensions and proportions leading to a flat (C) curve up to the point corresponding to trial speed” (de Luce, discussion on Reference 44).

Designs I, II, and III in Figure 21 represented three modern (1951) designs of good performance. The “upturn” speeds for these three ships are close to the mean line in Figure 20, but the design speeds are higher than the average line in Figure 21 by about 0.05 in terms of $\frac{V}{\sqrt{L}}$. Mr. de Luce stated that all three designs were being “pushed,” I because of the economics of transporting petroleum, and II and III for military considerations; he concluded that for the purpose of evaluating hull form parameters and performance, the “upturn” speed was satisfactory and independent of economic and other considerations. Since 1951, when these comparisons were made, high speed has become more and more a

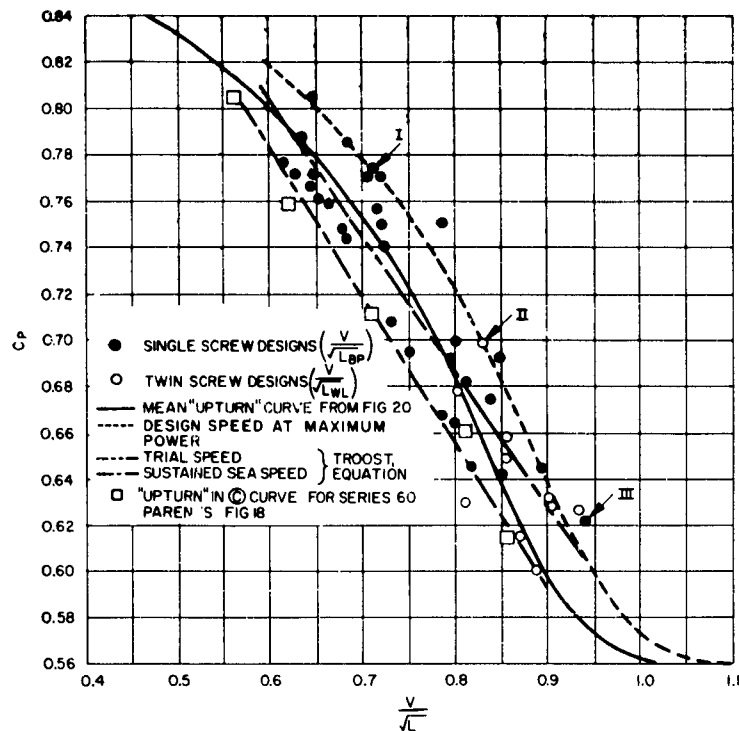


Figure 21 — Relation between Design Speed and Upturn Speed

characteristic of the modern dry-cargo ship, and this has led to the use of block coefficients lower than the range covered by Series 60. Before leaving the discussion of these data for modern American ships, as given by Mr. de Luce, it is interesting to compare the coverage of Series 60 with actual ship proportions. This has been done in Figures 22, 23, and 24 which show the same points as given by de Luce with the addition of the corresponding ones for the Series 60 parents and the limits covered by the whole series.

In general, the coverage for single-screw ships appears to be adequate, with the exception that some models having a $\frac{B}{H}$ value of 2.0 would have been a valuable addition to the program. In regard to the LCB variation, the "upturn" speeds for Series 60 occur in general with the LCB somewhat further aft than in the case of the actual designs, but the latter are covered by the limiting models.

Comparisons between the \textcircled{C} values for the actual ship models and Series 60 equivalents are shown in Figures 25a through 25e.

The MARINER-Class ships (Figure 25a) differed somewhat in coefficients and proportions from the Series 60 parent of 0.60 block coefficient; also, the latter had no bulb at the forefoot. However, the differences were not considered sufficient to justify making an entirely new Series 60 equivalent model.

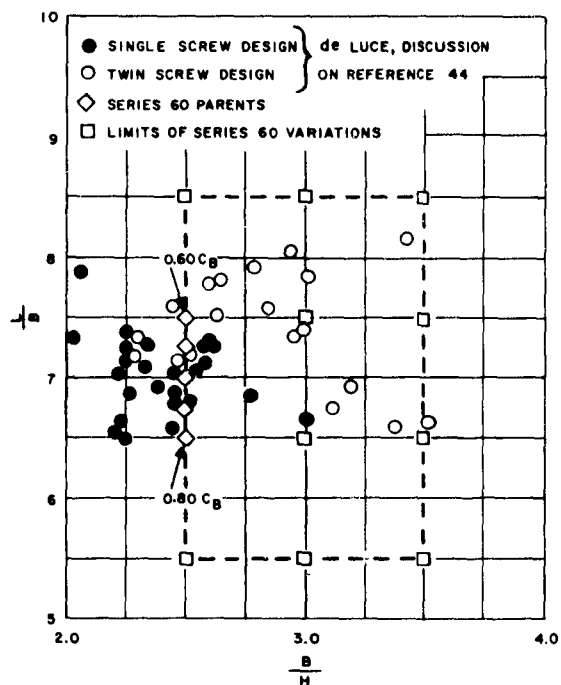


Figure 22 - Comparison of Series 60 with
U. S. Data, $\frac{L}{B}$ and $\frac{B}{H}$

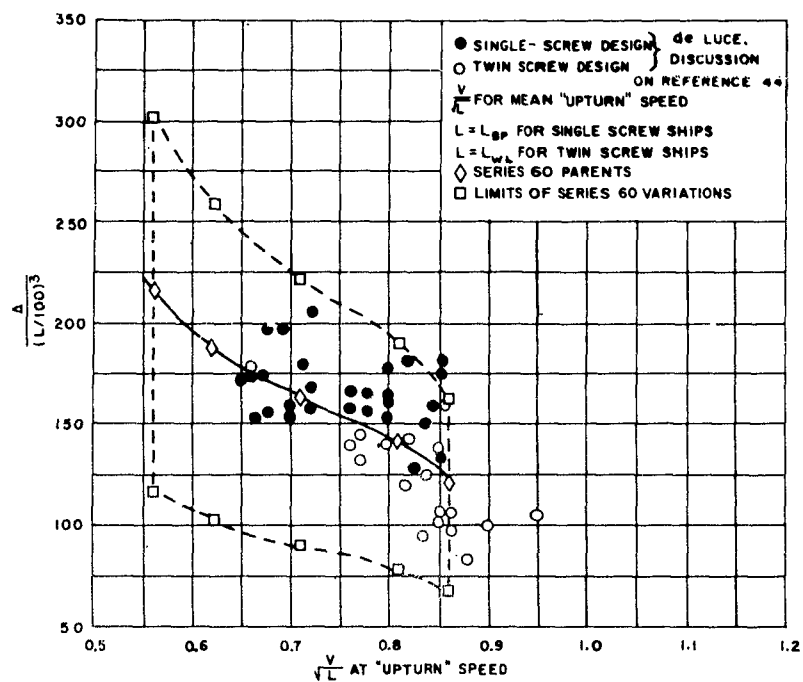


Figure 23 - Comparison of Series 60 with U. S. Data,
 $\frac{V}{\sqrt{L}}$ and $\frac{\Delta}{(L/100)^3}$

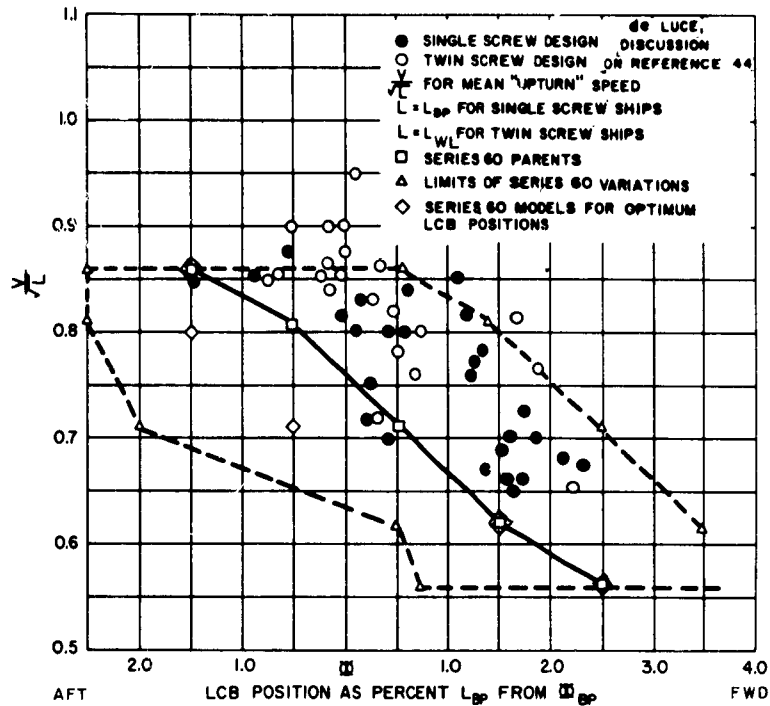


Figure 24 – Comparison of Series 60 with U. S. Data,

$$\frac{V}{\sqrt{L}} \text{ and } LCB$$

Figure 25 – Comparison between the ζ Values for Models of Actual Ships and Series 60 Equivalents

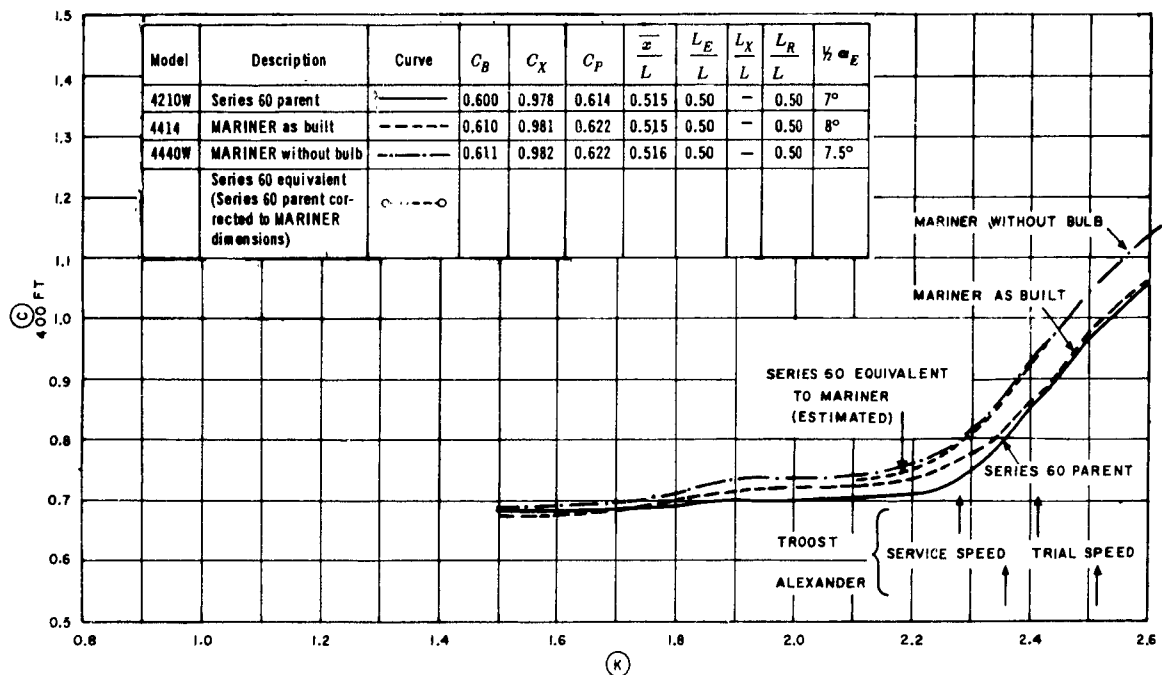


Figure 25a – Comparison, Series 60 and MARINER Class

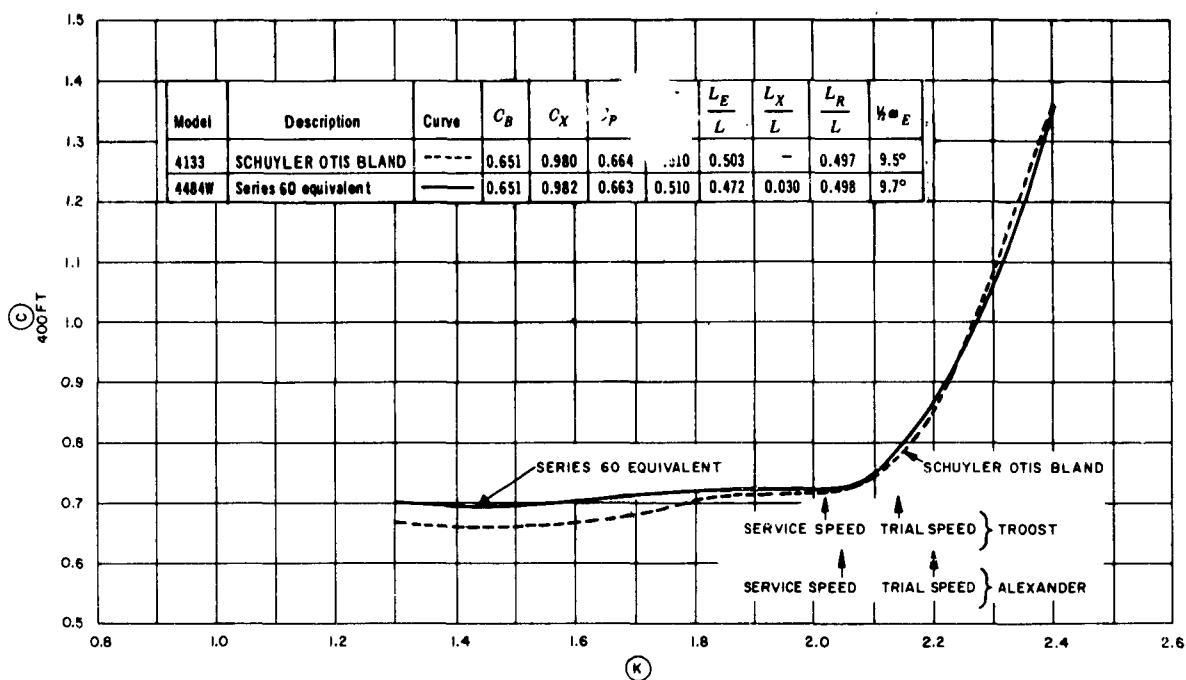


Figure 25b — Comparison, Series 60 and SCHUYLER OTIS BLAND

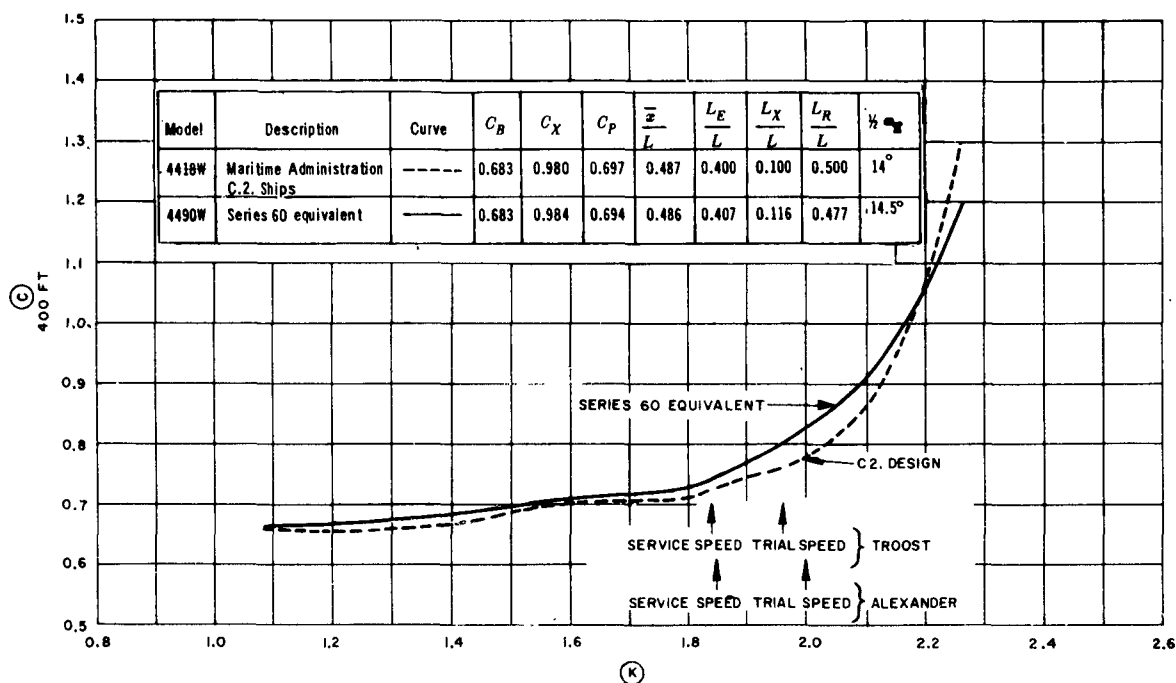


Figure 25c — Comparison, Series 60 and C.2

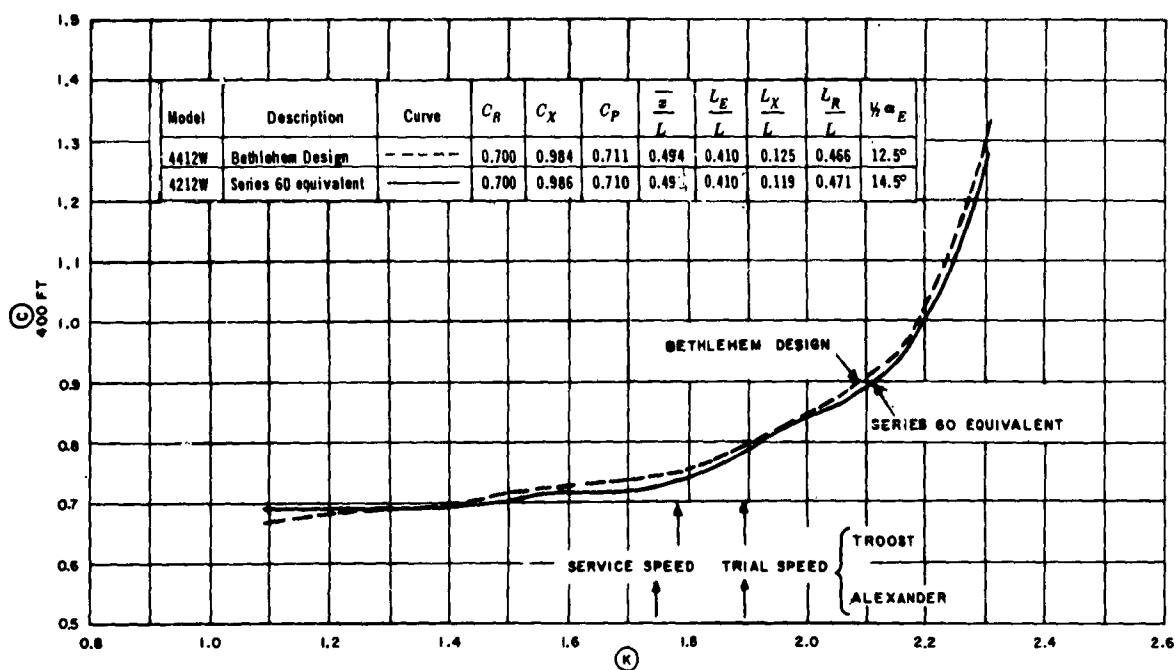


Figure 25d — Comparison, Series 60 and Bethlehem. 0.70 Design

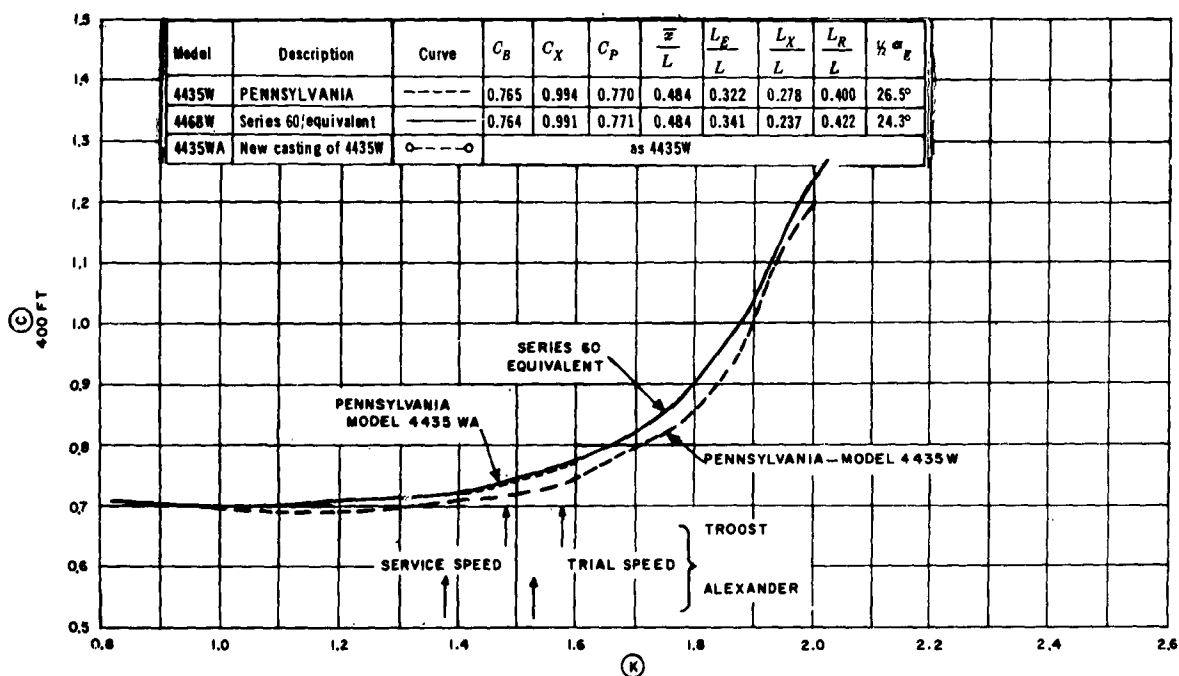


Figure 25e — Comparison, Series 60 and PENNSYLVANIA

The Series 60 parent gave a lower resistance than the MARINER model over the useful speed range, but above this the \textcircled{C} curve turned up more rapidly, at least partly because of the absence of the bulb. However, the Series 60 model was finer than the MARINER (C_B being 0.60 instead of 0.61), and to obtain a better comparison the MARINER model was changed by removing the bulb, and the Series 60 parent resistance was corrected for the difference in fullness and proportions by using Taylor Standard Series data. There was then no appreciable difference in performance over the service and designed speed range.

There was no essential difference in results in the case of SCHUYLER OTIS BLAND, (Figure 25b), the slightly better \textcircled{C} value of the SCHUYLER OTIS BLAND at the trial speeds probably being due to the 2 percent bulb.

The C.2 ship model (Figure 25c) was somewhat better than the equivalent Series 60 model by some 1 percent and 4.5 percent at the service and trial speeds respectively, probably again partly due to a small bulb on the C.2.

The Series 60 equivalent was some 1 to 2 percent better than the 0.70 C_B design, (Figure 25d) in the neighborhood of the service and trial speeds.

Several models of the PENNSYLVANIA (Figure 25e) were made at different times, some in wax and some in wood. There was a certain amount of scatter in the results, influenced to some extent by questions of turbulence stimulation. Over the useful speed range, this difference amounted to some 2 to 4 percent, and the highest results for the PENNSYLVANIA model were the same as those for the equivalent Series 60 model.

No modern cargo vessel design of about 0.80 block coefficient and of approved merit was available for comparison with Series 60. A number of models with a variety of bow and stern shapes were therefore made and run. The sterns were usually U-type, similar to those of Series 60, and the bows ranged from U- to V-forms. In general, the models with the V-shaped bows showed to some advantage, but they did not fit well into the cross-sectional area and waterline contours since the other model lines were predominantly of U-type. The Panel was of the opinion that seagoing merchant ships were unlikely to be built with such fullness coefficients. The somewhat fuller lake steamers would have much greater $\frac{L}{B}$ ratios than those covered by the present series, and in fact were considered to be another problem. The 0.80 C_B model of the series could therefore be considered as really only an end point to which the contours could be anchored. However, subsequent evidence suggests that the form as finally adopted had some intrinsic merits of its own as well as being an "end point" to the series. In the discussion on one Series 60 paper (Reference 45), Professor Baier said that since block coefficients of 0.80 to 0.87 were of particular interest to the Great Lakes region, he had carried out a series of tests with models in this range in the tank at the University of Michigan. He reported that "seven models were designed with rather extreme variations in sections at blocks of 0.857 and 0.872. At each of these block coefficients one form was derived from the contours of Series 60, with some adjustments in the forebody for lake-traffic requirements. It is gratifying to report that these two models were definitely superior to the

other five designs, both in t.r.h.p.* and propulsive coefficients when self-propelled." In Professor Baier's opinion, "the parent form finally adopted by the panel for the 0.80 block was a suitable and wise decision."

As in the case of the lower limit of the series being taken as 0.60 block coefficient, this idea that the 0.80 block model could be treated as an end point seemed a good one at the time, but events have already overtaken the program in this respect also. Just as single-screw ships are now being built with block coefficients well below 0.60, so in the range of supertankers and bulk carriers, designs in the neighborhood of 0.80 to 0.85 block coefficient have become of great importance. There is therefore a good practical case for extending the series at both ends.

In the light of the above survey, the members of the Panel came to the conclusion that the new contours of Series 60 formed a suitable basis for use in defining parent models for a systematic investigation of resistance and propulsive qualities, and it was then possible to proceed to the next phases.

*t.r.h.p. = towrope horsepower or ehp

CHAPTER VI

EFFECT ON RESISTANCE OF VARIATION IN LCB POSITION

In planning the Series 60 parents, a decision had to be made as to the longitudinal distribution of displacement for each model. This distribution is conveniently described, other things being equal, by the position of the *LCB*.

This is an important parameter in ship design for more than one reason. So far as resistance is concerned, the optimum position of the *LCB* depends very much on the speed-length ratio at which the ship is to run. At high values of $\frac{V}{\sqrt{L}}$, it is essential to keep the bow fine to delay the onset of wavemaking resistance; at the same time, the stern cannot be made too full or eddymaking resistance will increase. The result is a ship of overall low block coefficient with the *LCB* aft of midships. For low $\frac{V}{\sqrt{L}}$ values, the stern must still be kept reasonably fine to avoid excessive resistance, but the bow can be made much fuller, since at such speed-length ratios the wavemaking resistance is only a small percentage of the total. The result is a ship with a fine run and full entrance, with the *LCB* forward of amidships. This trend is well illustrated in the Series 60 parents. The prismatic coefficients of the afterbody range only from 0.646 to 0.750 in going from the 0.60 to the 0.80 block coefficient designs, whereas the forebody prismatics go from 0.581 to 0.861. If the efficiency is measured by the resistance per ton of displacement, the fuller ship is the more efficient at low speed-length ratios, and the advantage passes to finer and finer ships as $\frac{V}{\sqrt{L}}$ is increased.

The position of the *LCB* also affects propulsive efficiency for, in general, as it moves forward for a given overall coefficient, wake and thrust deduction both decrease, but the effect of the former usually predominates. Thus it is not unknown for a forward shift of *LCB* to reduce both resistance and propulsive efficiency in such a way that the final shaft horsepower* is increased. Insofar as hydrodynamic efficiency is concerned, the location of *LCB* therefore rests finally on the delivered horsepower* required and not on the resistance, although the latter is an important component of the former.

There is also another feature in ship performance which depends on the *LCB* position, and that is the behaviour in waves, both as regards ship motions and loss of speed. There is little doubt that in the past ships have been built with too full bows, which may have given excellent smooth-water results but have militated greatly against good seagoing qualities. This question is one which should have an early priority in future methodical series testing.

*Shaft horsepower is the power measured in the shafting, for example by torsionmeter. Delivered horsepower is the power absorbed by the propeller.

In the design of a ship, the *LCB* position is also dependent to some extent on considerations other than low power and good sea behavior. Chief of these is the problem of achieving correct trim under a variety of loading conditions, particularly in tankers and other bulk carriers. The tendency to place machinery aft in dry-cargo ships and passenger ships also gives rise to trim problems and in such cases the size of machinery may restrict the hull shape aft and, by requiring additional volume there, also influence the *LCB* position.

In the discussion on one of the Series 60 papers (Reference 63), Professor Manning set out very clearly the importance of *LCB* position in designing the single-screw merchant ship, and one cannot do better than quote his remarks. "Taylor states very clearly that his use of the prismatic coefficient as a major parameter was based on the fact that it is an excellent measure of the longitudinal distribution of the volume of displacement . . . In the case of the Taylor Standard Series, the prismatic coefficient was sufficient in itself as a measure of the longitudinal distribution of displacement by reason of the process used in determining the offsets of all the models of this family and the fact that none of the models had parallel middle body. Whenever a ship has parallel middle body, a substantial change in the longitudinal distribution of the displacement may be made without any change in the prismatic coefficient. For example, if the lengths of entrance, parallel middle body and run are held constant, and the prismatic coefficient of entrance is given to the run, and that for the run to the entrance, the prismatic coefficient of the entire hull has not been altered, but the longitudinal distribution of the displacement certainly has. The wave-making resistance and viscous form-drag have therefore also been changed in substantial magnitude. The difference between the longitudinal distribution of the displacement of vessels which have the same value of prismatic coefficient may be related to differences in the longitudinal position of the centre of buoyancy. This paper (Reference 63) is essentially a study of the effect of changes in the longitudinal position of the centre of buoyancy on the resistance and power required for parallel middle body ships at speeds which reflect current practice. . . From this paper, the ship designer can not only estimate with good precision the position of the centre of buoyancy which gives the least resistance or shaft horsepower, but how much he must pay in terms of these if other conditions favor a different location for this point. The latter is just as important as the former."

For all the above reasons, it was agreed by the Panel that before proceeding to the last phase of this project—the effect upon resistance and propulsion of variations in $\frac{L}{B}$ and $\frac{B}{H}$ ratios—the effect of change in *LCB* position should be investigated for each of the Series 60 parents in order, if possible, to determine the optimum location.

The positions of the *LCB* chosen for the five parent models are shown in Figure 1, together with the variation in these positions for the other 17 models making up the complete set. The positions of *LCB* are shown in Table 10, and the principal particulars of the models are given in Tables 11 through 15.

Table 10 — Pattern of LCB Series Models

C_B	Model numbers				
	Position of LCB as % LBP from $\overline{O}BP$				
0.60....		4215	4210	4216	4217
		2.48A	1.50A	0.51A	0.52F
0.65....	4231	4218	4211	4219	4220
	2.46A	1.54A	0.50A	0.38F	1.37F
0.70....	4230	4221	4212	4222	4223
	2.05A	0.55A	0.50F	1.54F	2.55F
0.75....		4224	4213	4225	4226
		0.48F	1.50F	2.57F	3.46F
0.80....	4227	4228	4214	4229	
	0.76F	1.45F	2.50F	3.51F	

NOTE: Column 3 of model numbers applies to Series 60 Parents.

The lines for each model were drawn out by using the contours of sectional area and waterline coefficients already described. The models are therefore related to one another by the graphical charts, and for a given set of design conditions a unique hull form is determined.

The models were made and the tests carried out in exactly the same manner as described for the parent models. The model results have been converted to apply to ships with 400-ft LBP by using the ATTC line for the friction extrapolation with an addition of +0.0004 for ship correlation allowance, as before.

The ship figures are given in Tables 16 through 20 as values of C_T to a base of

$\frac{V}{\sqrt{L_{WL}}}$ and in Tables 21 through 25 as values of (C) to a base of (K) , all for a standard temperature of 59°F (15°C).

To obtain a visual picture of the resistance results, the (C) values can be plotted as cross curves to a base of LCB location, using (K) as a parameter. When this is done, it is found that for the speeds within the range of economic performance for these models a locus of LCB position to give minimum resistance is usually well defined. At high speeds, beyond the useful range, the minimum lies in general in a region where the LCB is much further aft than was used in any of these experiments.

As might be expected, there is in general no unique relation between block coefficient and optimum LCB location—it depends on what speed is chosen as the criterion for comparison. Figures 26 through 30 show cross-curves of (C) to a base of LCB position for

Table 11 — Principal Particulars of 0.60 Block Coefficient Forms

Model No.	4215	4210	4216	4217
L_{BP} , ft.	400.0	400.0	400.0	400.0
B , ft.	53.33	53.33	53.33	53.33
H , ft.	21.33	21.33	21.33	21.33
D , tons.	7807	7807	7807	7807
L_E/L_{BP}	0.5	0.5	0.5	0.5
L_X/L_{BP}	0	0	0	0
L_R/L_{BP}	0.5	0.5	0.5	0.5
C_B	0.60	0.60	0.60	0.60
C_X	0.977	0.977	0.977	0.977
C_P	0.614	0.614	0.614	0.614
C_{PF}	0.558	0.581	0.603	0.626
C_{PA}	0.671	0.646	0.624	0.602
C_{PE}	0.558	0.581	0.603	0.626
C_{PR}	0.671	0.646	0.624	0.602
C_{PV}	0.857	0.850	0.843	0.839
C_{PVE}	0.910	0.910	0.912	0.919
C_{PVA}	0.818	0.802	0.785	0.770
C_W	0.700	0.706	0.712	0.715
C_{WF}	0.598	0.624	0.646	0.666
C_{WA}	0.802	0.788	0.777	0.765
C_{IT}	0.533	0.543	0.549	0.553
$\frac{1}{2}\alpha_E$, deg.	6.2	7.0	7.6	8.3
L_{WL} , ft.	406.7	406.7	406.7	406.7
LCB % LBP from \overline{O}	2.48A	1.5A	0.51A	0.52F
L/B	7.50	7.50	7.50	7.50
B/H	2.50	2.50	2.50	2.50
$L/\nabla^{1/3}$	6.165	6.165	6.165	6.165
$\Delta/(L/100)^3$	122.0	122.0	122.0	122.0
$S/\nabla^{1/3}$	6.478	6.481	6.504	6.527
WS, sq ft.	27270	27280	27380	27470
$K_R = R/\sqrt{BH}$	0.229	0.229	0.229	0.229
C_{PE}/C_{PR}	0.831	0.899	0.966	1.040

(Text continued on page VI-13)

Table 12 - Principal Particulars of 0.65 Block Coefficient Forms

Model No.....	4231	4218	4211	4219	4220
L_{BP} , ft.....	400.0	400.0	400.0	400.0	400.0
B , ft.....	55.17	55.17	55.17	55.17	55.17
H , ft.....	22.09	22.09	22.09	22.09	22.09
D , tons.....	9092	9051	9051	9051	9065
L_E/L_{BP}	0.477	0.475	0.472	0.470	0.469
L_X/L_{BP}	0.035	0.035	0.035	0.035	0.035
L_R/L_{BP}	0.488	0.490	0.493	0.495	0.496
C_B	0.652	0.650	0.650	0.650	0.650
C_X	0.982	0.982	0.982	0.982	0.982
C_P	0.664	0.661	0.661	0.661	0.662
C_{PF}	0.612	0.628	0.651	0.670	0.692
C_{PA}	0.715	0.694	0.672	0.652	0.632
C_{PE}	0.594	0.609	0.630	0.649	0.672
C_{PR}	0.709	0.688	0.667	0.648	0.630
C_{PV}	0.871	0.874	0.871	0.865	0.862
C_{PVF}	0.920	0.924	0.927	0.929	0.934
C_{PVA}	0.833	0.832	0.823	0.808	0.794
C_W	0.749	0.744	0.746	0.750	0.754
C_{WF}	0.654	0.668	0.690	0.708	0.728
C_{WA}	0.843	0.819	0.802	0.792	0.781
C_{IT}	0.594	0.593	0.597	0.601	0.619
$\frac{1}{2}\alpha_E$, deg.....	7.7	8.3	9.1	11.2	13.8
L_{WL} , ft.....	406.7	406.7	406.7	406.7	406.7
LCB % L_{BP} from \square	2.464	1.544	0.54	0.38F	1.37F
L/B	7.25	7.25	7.25	7.25	7.25
B/H	2.50	2.50	2.50	2.50	2.50
$L/\nabla^{1/4}$	5.860	5.869	5.869	5.869	5.866
$\Delta/(L/100)^3$	142.0	141.4	141.4	141.4	141.5
$S/\nabla^{3/4}$	6.320	6.326	6.328	6.328	6.347
WS, sq ft.....	29380	29380	29390	29390	29480
$K_R = R/\sqrt{BH}$	0.205	0.205	0.205	0.205	0.205
C_{PE}/C_{PR}	0.838	0.885	0.945	1.001	1.067

Table 13 - Principal Particulars of 0.70 Block Coefficient Forms

Model No.....	4230	4221	4212	4222	4223
L_{BP} , ft.....	400.0	400.0	400.0	400.0	400.0
B , ft.....	57.14	57.14	57.14	57.14	57.14
H , ft.....	22.86	22.86	22.86	22.86	22.86
D , tons.....	10441	10456	10456	10456	10456
L_E/L_{BP}	0.434	0.420	0.410	0.400	0.390
L_X/L_{BP}	0.119	0.119	0.119	0.119	0.119
L_R/L_{BP}	0.447	0.461	0.471	0.481	0.491
C_B	0.699	0.700	0.700	0.700	0.700
C_X	0.986	0.986	0.986	0.986	0.986
C_P	0.709	0.710	0.710	0.710	0.710
C_{PF}	0.667	0.700	0.721	0.744	0.766
C_{PA}	0.752	0.721	0.698	0.675	0.654
C_{PE}	0.616	0.642	0.660	0.680	0.700
C_{PR}	0.722	0.698	0.680	0.662	0.647
C_{PV}	0.887	0.890	0.891	0.886	0.880
C_{PVF}	0.932	0.940	0.944	0.948	0.950
C_{PVA}	0.852	0.846	0.842	0.827	0.811
C_W	0.788	0.787	0.785	0.790	0.795
C_{WF}	0.706	0.734	0.753	0.774	0.795
C_{WA}	0.871	0.841	0.818	0.805	0.795
C_{IT}	0.650	0.651	0.653	0.658	0.663
$\frac{1}{2}\alpha_E$	9.3	11.6	14.5	17.1	20.0
L_{WL}	406.7	406.7	406.7	406.7	406.7
LCB % L_{BP} from \square	2.054	0.554	0.5F	1.54F	2.55F
L/B	7.00	7.00	7.00	7.00	7.00
B/H	2.50	2.50	2.50	2.50	2.50
$L/\nabla^{1/4}$	5.593	5.593	5.593	5.593	5.593
$\Delta/(L/100)^3$	163.4	163.4	163.4	163.4	163.4
$S/\nabla^{3/4}$	6.220	6.230	6.200	6.224	6.224
WS, sq ft.....	31777	31859	31705	31830	31828
$K_R = R/\sqrt{BH}$	0.181	0.181	0.181	0.181	0.181
C_{PE}/C_{PR}	0.853	0.920	0.971	1.027	1.082

Table 14 - Principal Particulars of 0.75 Block Coefficient Forms

Model No.	4224	4213	4225	4226
L_{BP} , ft.	400.0	400.0	400.0	400.0
B , ft.	59.26	59.26	59.26	59.26
H , ft.	23.70	23.70	23.70	23.70
D , tons	12048	12048	12048	12038
L_R/L_{BP}	0.360	0.350	0.340	0.332
L_X/L_{BP}	0.210	0.210	0.210	0.210
L_R/L_{BP}	0.430	0.440	0.450	0.458
C_B	0.750	0.750	0.750	0.749
C_X	0.990	0.990	0.990	0.990
C_P	0.758	0.758	0.758	0.757
C_{PF}	0.770	0.792	0.813	0.833
C_{PA}	0.745	0.724	0.702	0.681
C_{PE}	0.680	0.704	0.725	0.748
C_{PR}	0.704	0.686	0.668	0.652
C_{PV}	0.905	0.907	0.903	0.898
C_{PVF}	0.956	0.961	0.959	0.959
C_{PVA}	0.858	0.856	0.846	0.833
C_W	0.828	0.827	0.830	0.834
C_{WF}	0.797	0.817	0.839	0.860
C_{WA}	0.860	0.838	0.821	0.808
C_{IT}	0.708	0.711	0.717	0.722
$\frac{1}{2}\alpha_E$	18.9°	22.5°	27.4°	33.8°
L_{WL} , ft.	406.7	406.7	406.7	406.7
LCB % L_{BP} from \bar{M}	0.48F	1.5F	2.57F	3.46F
L/B	6.75	6.75	6.75	6.75
B/H	2.50	2.50	2.50	2.50
$L/\nabla^{1/4}$	5.335	5.335	5.335	5.337
$\Delta/(L/100)^3$	188.2	188.2	188.2	188.1
$S/\nabla^{1/4}$	6.104	6.091	6.094	6.098
WS, sq ft.	34308	34232	34252	34281
$K_R = R/\sqrt{BH}$	0.153	0.153	0.153	0.153
C_{PE}/C_{PR}	0.966	1.026	1.0853	1.147

Table 15 - Principal Particulars of 0.80 Block Coefficient Forms

Model No.	4227	4228	4214	4229
L_{BP} , ft.	400.0	400.0	400.0	400.0
B , ft.	61.54	61.54	61.54	61.54
H , ft.	24.59	24.59	24.59	24.59
D , tons	13859	13859	13859	13859
L_R/L_{BP}	0.307	0.299	0.290	0.280
L_X/L_{BP}	0.300	0.300	0.300	0.300
L_R/L_{BP}	0.393	0.401	0.410	0.420
C_B	0.800	0.800	0.800	0.800
C_X	0.994	0.994	0.994	0.994
C_P	0.805	0.805	0.805	0.805
C_{PF}	0.822	0.838	0.861	0.881
C_{PA}	0.787	0.772	0.750	0.729
C_{PE}	0.710	0.728	0.761	0.787
C_{PR}	0.730	0.716	0.695	0.678
C_{PV}	0.921	0.920	0.920	0.922
C_{PVF}	0.966	0.967	0.971	0.976
C_{PVA}	0.878	0.874	0.867	0.865
C_W	0.869	0.870	0.871	0.867
C_{WF}	0.845	0.861	0.881	0.897
C_{WA}	0.892	0.878	0.860	0.838
C_{IT}	0.769	0.767	0.776	0.778
$\frac{1}{2}\alpha_E$	26.6°	32.5°	43.0°	52.0°
L_{WL} , ft.	406.7	406.7	406.7	406.7
LCB % L_{BP} from \bar{M}	0.76F	1.45F	2.5F	3.51F
L/B	6.50	6.50	6.50	6.50
B/H	2.50	2.50	2.50	2.50
$L/\nabla^{1/4}$	5.092	5.092	5.092	5.092
$\Delta/(L/100)^3$	216.5	216.5	216.5	216.5
$S/\nabla^{1/4}$	6.011	6.020	6.028	6.025
WS, sq ft.	37098	37148	37200	37183
$K_R = R/\sqrt{BH}$	0.118	0.118	0.118	0.118
C_{PE}/C_{PR}	0.973	1.017	1.095	1.161

Table 16 - Resistance Data as Values of C_T to a Base of $\frac{V}{\sqrt{L_{WL}}}$,

LCB Series 0.60 Block Coefficient Models

(Ship dimensions—400.0 ft x 53.33 ft x 21.33 ft x 7807 tons. Turbulence stimulated by studs)

Model No. LCB as % L_{BP} from $\overline{\text{X}}$		4215 2.48A	4210 1.50A	4216 0.51A	4217 0.62F
$V/\sqrt{L_{WL}}$	Φ	$C_t \times 10^3$ for 400-ft L_{BP}			
0.35	0.925	2.641	2.654	2.620	2.599
0.40	1.057	2.611	2.624	2.604	2.577
0.45	1.189	2.596	2.618	2.597	2.564
0.50	1.321	2.618	2.618	2.602	2.563
0.55	1.453	2.629	2.628	2.613	2.573
0.60	1.585	2.641	2.639	2.627	2.589
0.625	1.651	2.650	2.640	2.632	2.612
0.65	1.717	2.666	2.648	2.653	2.647
0.675	1.783	2.685	2.671	2.681	2.676
0.70	1.849	2.697	2.689	2.706	2.694
0.725	1.915	2.715	2.701	2.712	2.705
0.75	1.981	2.736	2.699	2.718	2.713
0.775	2.047	2.765	2.713	2.711	2.729
0.80	2.113	2.783	2.727	2.727	2.755
0.825	2.179	2.814	2.744	2.794	2.814
0.85	2.245	2.861	2.792	2.873	2.953
0.875	2.312	3.008	2.933	3.003	3.120
0.90	2.378	3.236	3.197	3.252	3.392
0.925	2.444	3.511	3.497	3.627	3.677
0.95	2.510	3.811	3.787	3.952	3.967
0.975	2.576	4.046	4.037	4.157	4.217
1.00	2.642	4.173	4.197	4.292	4.407
1.025	2.708	4.225	4.265	4.382	4.508
1.05	2.774	4.236	4.272	4.412	4.497
1.075	2.840	4.226	4.258	4.408	4.459
1.10	2.906	4.223	4.273	4.413	4.484
1.15	2.938	4.471	4.534	4.656	4.776
1.20	3.170	5.196	5.223	5.188	5.373

Table 17 - Resistance Data as Values of C_T to a Base of $\frac{V}{\sqrt{L_{WL}}}$

LCB Series 0.65 Block Coefficient Models

(Ship dimensions—400.0 ft x 55.17 ft x 22.09 ft x 9051 tons. Turbulence stimulated by studs)

Model No. LCB as % L_{BP} from \bar{X}		4231 2.46A	4218 1.54A	4211 0.50A	4219 0.38F	4220 1.37F
$V/\sqrt{L_{WL}}$	Φ	$C_t \times 10^3$ for 400-ft L_{BP}				
0.25	0.644	2.883	2.745	2.795	2.680	2.675
0.30	0.773	2.840	2.707	2.752	2.652	2.632
0.35	0.902	2.805	2.677	2.717	2.622	2.602
0.40	1.031	2.777	2.649	2.687	2.607	2.597
0.45	1.160	2.760	2.649	2.661	2.601	2.609
0.50	1.289	2.749	2.661	2.650	2.631	2.639
0.55	1.418	2.746	2.676	2.653	2.668	2.673
0.60	1.546	2.746	2.686	2.689	2.696	2.706
0.65	1.675	2.785	2.743	2.727	2.745	2.767
0.675	1.740	2.837	2.777	2.750	2.787	2.807
0.70	1.804	2.888	2.810	2.770	2.830	2.863
0.725	1.869	2.903	2.825	2.800	2.861	2.923
0.75	1.933	2.906	2.841	2.826	2.886	2.986
0.775	1.997	2.899	2.864	2.855	2.919	3.070
0.80	2.062	2.902	2.883	2.886	2.978	3.173
0.825	2.126	2.928	2.913	2.948	3.063	3.298
0.85	2.191	3.012	3.027	3.060	3.242	3.507
0.875	2.255	3.210	3.287	3.340	3.557	3.797
0.90	2.320	3.596	3.799	3.811	4.000	4.176
0.95	2.448	4.721	4.971	5.066	5.246	5.476
1.00	2.577	5.771	5.941	6.201	6.296	6.501
1.05	2.706	6.163	6.313	6.532	6.573	6.832
1.10	2.835	6.104	6.224	6.443	6.542	6.793
1.15	2.964	6.055	6.161	6.316	6.438	6.696
1.20	3.093			6.628		6.918

Table 18 — Resistance Data as Values of C_T to a Base of $\frac{V}{\sqrt{L_{WL}}}$

LCB Series 0.70 Block Coefficient Models

(Ship dimensions—400.0 ft × 57.14 ft × 22.86 ft × 10456 tons. Turbulence stimulated by studs)

Model No.		4230	4221	4212	4222	4223
LCB as % L_{BP} from Ⓢ		2.05A	0.55A	0.50F	1.54F	2.55F
$V/\sqrt{L_{WL}}$	Ⓢ	$C_t \times 10^3$ for 400-ft L_{BP}				
0.25	0.629	2.960	2.829	2.894	2.824	2.752
0.30	0.755	2.932	2.786	2.851	2.776	2.713
0.35	0.881	2.915	2.750	2.815	2.738	2.688
0.40	1.006	2.903	2.729	2.794	2.716	2.681
0.45	1.132	2.900	2.738	2.793	2.742	2.695
0.50	1.258	2.904	2.762	2.796	2.754	2.719
0.55	1.384	2.937	2.793	2.803	2.758	2.760
0.60	1.510	2.971	2.811	2.866	2.836	2.826
0.65	1.636	3.001	2.867	2.915	2.908	2.945
0.675	1.698	3.033	2.896	2.923	2.943	3.041
0.70	1.761	3.054	2.931	2.956	3.003	3.151
0.725	1.824	3.083	2.976	3.039	3.092	3.274
0.75	1.887	3.117	3.050	3.155	3.238	3.448
0.775	1.950	3.171	3.148	3.311	3.451	3.706
0.80	2.013	3.235	3.255	3.445	3.650	4.005
0.85	2.139	3.436	3.495	3.711	4.023	4.675
0.90	2.264	4.220	4.457	4.652	5.152	5.650
0.95	2.390	5.882	6.172	6.602	6.965	7.502
1.00	2.516	7.647	8.002	8.662	8.887	9.627
1.05	2.642	8.693	9.180	9.918	10.330	11.143
1.10	2.768	8.884	9.312	10.049	10.554	11.409
1.15	2.894	8.516	9.126	9.596	10.151	11.006
1.20	3.019			9.222		

Table 19 — Resistance Data as Values of C_T to a Base of $\frac{V}{\sqrt{L_{WL}}}$

LCB Series 0.75 Block Coefficient Models

(Ship dimensions—400.0 ft × 59.26 ft × 23.70 ft × 12048 tons. Turbulence stimulated by studs)

Model No.		4224	4213	4225	4226
LCB as % L_{BP} from Ⓢ		0.48F	1.50F	2.57F	3.46F
$V/\sqrt{L_{WL}}$	Ⓢ	$C_t \times 10^3$ for 400-ft L_{BP}			
0.35	0.860	2.947	2.917	2.892	2.897
0.40	0.983	2.947	2.887	2.875	2.867
0.45	1.106	2.943	2.882	2.877	2.841
0.50	1.229	2.971	2.907	2.887	2.824
0.55	1.352	3.014	2.939	2.878	2.877
0.60	1.474	3.101	2.982	2.899	2.981
0.65	1.597	3.185	3.140	3.151	3.210
0.675	1.659	3.237	3.227	3.314	3.452
0.70	1.720	3.320	3.362	3.525	3.748
0.725	1.782	3.463	3.568	3.803	4.053
0.75	1.843	3.711	3.876	4.156	4.423
0.775	1.904	4.110	4.235	4.630	4.830
0.80	1.966	4.473	4.628	5.093	5.253
0.825	2.027	4.758	4.988	5.403	5.693
0.85	2.089	4.942	5.277	5.662	6.142
0.875	2.150	5.217	5.567	5.977	6.529
0.90	2.212	5.746	6.026	6.481	6.986

Table 20 — Resistance Data as Values of C_T to a Base of $\frac{V}{\sqrt{L_{WL}}}$

LCB Series 0.80 Block Coefficient Models

(Ship dimensions—400.0 ft × 61.54 ft × 24.59 ft × 13859 tons. Turbulence stimulated by studs)

Model No. LCB as % L_{BP} from Ⓚ		4227 0.76F	4228 1.45F	4214 2.50F	4229 3.51F
$V/\sqrt{L_{WL}}$ Ⓚ		$C_T \times 10^3$ for 400-ft L_{BP}			
0.25	0.600	3.472	3.194	3.075	3.090
0.30	0.720	3.452	3.172	3.040	3.055
0.35	0.840	3.434	3.147	3.012	3.017
0.40	0.960	3.432	3.134	2.997	2.992
0.45	1.080	3.444	3.128	2.998	3.016
0.50	1.200	3.476	3.144	3.014	3.059
0.55	1.320	3.528	3.196	3.061	3.146
0.575	1.380	3.564	3.238	3.121	3.256
0.60	1.440	3.616	3.306	3.241	3.441
0.625	1.500	3.682	3.407	3.392	3.690
0.65	1.561	3.785	3.565	3.590	3.987
0.675	1.621	3.945	3.772	3.862	4.297
0.70	1.681	4.175	4.015	4.215	4.622
0.725	1.741	4.463	4.323	4.583	5.038
0.75	1.801	4.843	4.778	5.008	5.718
0.775	1.861	5.475	5.390	5.660	6.580
0.80	1.921	6.393	6.088	6.543	7.378
0.85	2.041	7.222	7.487	7.732	8.737

Table 21 — Resistance Data as Values of C to a Base of K
LCB Series, 0.60 Block Coefficient Models

(Ship dimensions—400.0 ft × 53.33 ft × 21.33 ft × 7807 tons. Turbulence stimulated by studs)

Model No. LCB as % L_{BP} from Ⓚ		4215 2.48A	4210 1.50A	4216 0.51A	4217 0.52F
$V/\sqrt{L_{WL}}$ Ⓚ		C for 400-ft L_{BP}			
0.35	0.925	0.681	0.685	0.679	0.676
0.40	1.057	0.674	0.677	0.675	0.670
0.45	1.189	0.670	0.676	0.673	0.666
0.50	1.321	0.675	0.676	0.674	0.661
0.55	1.453	0.678	0.678	0.677	0.669
0.60	1.585	0.681	0.681	0.680	0.673
0.625	1.651	0.684	0.681	0.682	0.679
0.65	1.717	0.688	0.684	0.687	0.689
0.675	1.783	0.693	0.689	0.694	0.696
0.70	1.849	0.696	0.694	0.701	0.700
0.725	1.915	0.700	0.697	0.702	0.703
0.75	1.981	0.706	0.697	0.704	0.705
0.775	2.047	0.713	0.700	0.702	0.709
0.80	2.113	0.718	0.704	0.706	0.716
0.825	2.179	0.726	0.708	0.724	0.731
0.85	2.245	0.738	0.721	0.744	0.768
0.875	2.312	0.776	0.757	0.778	0.811
0.90	2.378	0.835	0.825	0.842	0.882
0.925	2.444	0.906	0.904	0.940	0.956
0.95	2.510	0.983	0.978	1.024	1.031
0.975	2.576	1.044	1.042	1.077	1.096
1.00	2.642	1.077	1.083	1.118	1.145
1.025	2.708	1.090	1.102	1.135	1.172
1.05	2.774	1.093	1.103	1.143	1.169
1.075	2.840	1.090	1.099	1.142	1.159
1.10	2.906	1.089	1.103	1.143	1.165
1.15	3.038	1.153	1.170	1.206	1.241
1.20	3.170	1.341	1.348	1.344	1.397

Table 22 - Resistance Data as Values of \textcircled{C} to a Base of \textcircled{K}
LCB Series, 0.65 Block Coefficient Models

(Ship dimensions—400.0 ft × 55.17 ft × 22.09 ft × 9051 tons. Turbulence stimulated by studs)

Model No. LCB as % L_{BP} from \textcircled{K}	4231 2.40A	4218 1.54A	4211 0.50A	4219 0.38F	4220 1.37F
$V/\sqrt{L_{WL}}$	\textcircled{C} for 400-ft L_{BP}				
0.25	0.644	0.726	0.691	0.705	0.676
0.30	0.773	0.715	0.682	0.694	0.665
0.35	0.902	0.706	0.674	0.685	0.658
0.40	1.031	0.699	0.667	0.678	0.656
0.45	1.160	0.695	0.667	0.671	0.659
0.50	1.289	0.692	0.670	0.668	0.667
0.55	1.418	0.692	0.674	0.669	0.676
0.60	1.546	0.692	0.676	0.678	0.684
0.65	1.675	0.701	0.691	0.688	0.699
0.675	1.740	0.714	0.699	0.693	0.709
0.70	1.804	0.727	0.708	0.698	0.724
0.725	1.869	0.731	0.711	0.706	0.739
0.75	1.933	0.732	0.715	0.712	0.755
0.775	1.997	0.730	0.721	0.720	0.776
0.80	2.062	0.731	0.726	0.728	0.802
0.825	2.126	0.737	0.734	0.743	0.834
0.85	2.191	0.759	0.762	0.772	0.886
0.875	2.255	0.808	0.828	0.842	0.960
0.90	2.320	0.906	0.957	0.961	1.055
0.95	2.448	1.189	1.252	1.277	1.384
1.00	2.577	1.453	1.496	1.563	1.643
1.05	2.706	1.552	1.590	1.647	1.727
1.10	2.835	1.537	1.567	1.624	1.717
1.15	2.964	1.525	1.551	1.592	1.692
1.20	3.093			1.671	1.748

Table 23 - Resistance Data as Values of \textcircled{C} to a Base of \textcircled{K}
LCB Series, 0.70 Block Coefficient Models

(Ship dimensions—400.0 ft × 57.14 ft × 22.86 ft × 10456 tons. Turbulence stimulated by studs)

Model No. LCB as % L_{BP} from \textcircled{K}	4230 2.05A	4221 0.55A	4212 0.50F	4222 1.54F	4223 2.55F
$V/\sqrt{L_{WL}}$	\textcircled{C} for 400-ft L_{BP}				
0.25	0.629	0.732	0.702	0.715	0.682
0.30	0.755	0.726	0.691	0.704	0.672
0.35	0.881	0.721	0.682	0.695	0.666
0.40	1.006	0.718	0.677	0.690	0.664
0.45	1.132	0.718	0.679	0.690	0.668
0.50	1.258	0.7185	0.685	0.690	0.674
0.55	1.384	0.727	0.693	0.690	0.684
0.60	1.510	0.735	0.697	0.708	0.700
0.65	1.636	0.742	0.711	0.718	0.730
0.675	1.698	0.750	0.718	0.722	0.754
0.70	1.761	0.756	0.727	0.730	0.781
0.725	1.824	0.763	0.738	0.750	0.811
0.75	1.887	0.771	0.756	0.779	0.854
0.775	1.950	0.785	0.781	0.818	0.918
0.80	2.013	0.800	0.807	0.851	0.993
0.85	2.139	0.850	0.867	0.916	1.159
0.90	2.264	1.044	1.106	1.149	1.400
0.95	2.390	1.455	1.531	1.630	1.859
1.00	2.516	1.892	1.985	2.139	2.386
1.05	2.642	2.151	2.277	2.449	2.762
1.10	2.768	2.198	2.310	2.481	2.828
1.15	2.894	2.107	2.264	2.369	2.728
1.20	3.019			2.302	

Table 24 - Resistance Data as Values of \textcircled{C} to a Base of \textcircled{K}
 LCB Series, 0.75 Block Coefficient Models
 (Ship dimensions—400.0 ft \times 59.26 ft \times 23.70 ft \times 12048 tons. Turbulence stimulated by studs)

Model No. LCB as % L_{BP} from \textcircled{K}		4224 0.48F	4213 1.50F	4225 2.57F	4226 3.46F
$V/\sqrt{L_{WL}}$	\textcircled{C}	\textcircled{C} for 400-ft L_{BP}			
0.35	0.860	0.716	0.707	0.702	0.704
0.40	0.983	0.716	0.700	0.698	0.696
0.45	1.106	0.715	0.699	0.698	0.690
0.50	1.229	0.722	0.705	0.701	0.686
0.55	1.352	0.732	0.713	0.698	0.699
0.60	1.474	0.753	0.723	0.704	0.724
0.65	1.597	0.774	0.761	0.765	0.780
0.675	1.659	0.786	0.782	0.804	0.838
0.70	1.720	0.806	0.815	0.855	0.910
0.725	1.782	0.841	0.865	0.923	0.984
0.75	1.843	0.902	0.940	1.008	1.074
0.775	1.904	0.998	1.027	1.124	1.173
0.80	1.966	1.087	1.122	1.236	1.276
0.825	2.027	1.156	1.210	1.311	1.383
0.85	2.089	1.201	1.279	1.374	1.492
0.875	2.150	1.267	1.350	1.450	1.586
0.90	2.212	1.396	1.461	1.573	1.697

Table 25 - Resistance Data as Values of \textcircled{C} to a Base of \textcircled{K}
 LCB Series, 0.80 Block Coefficient Models
 (Ship dimensions—400.0 ft \times 61.54 ft \times 24.59 ft \times 13859 tons. Turbulence stimulated by studs)

Model No. LCB as % L_{BP} from \textcircled{K}		4227 0.76F	4228 1.45F	4214 2.50F	4229 3.51F
$V/\sqrt{L_{WL}}$	\textcircled{C}	\textcircled{C} for 400-ft L_{BP}			
0.25	0.600	0.831	0.766	0.739	0.743
0.30	0.720	0.826	0.760	0.730	0.734
0.35	0.840	0.822	0.754	0.724	0.725
0.40	0.960	0.822	0.751	0.720	0.719
0.45	1.080	0.824	0.750	0.720	0.725
0.50	1.200	0.832	0.754	0.724	0.735
0.55	1.320	0.845	0.766	0.736	0.756
0.575	1.380	0.853	0.776	0.750	0.783
0.60	1.440	0.866	0.792	0.779	0.827
0.625	1.500	0.881	0.817	0.815	0.887
0.65	1.561	0.906	0.855	0.863	0.958
0.675	1.621	0.944	0.904	0.928	1.033
0.70	1.681	1.000	0.962	1.013	1.111
0.725	1.741	1.068	1.036	1.101	1.211
0.75	1.801	1.156	1.145	1.203	1.374
0.775	1.861	1.311	1.292	1.360	1.582
0.80	1.921	1.530	1.459	1.572	1.774
0.85	2.041	1.729	1.795	1.858	2.100

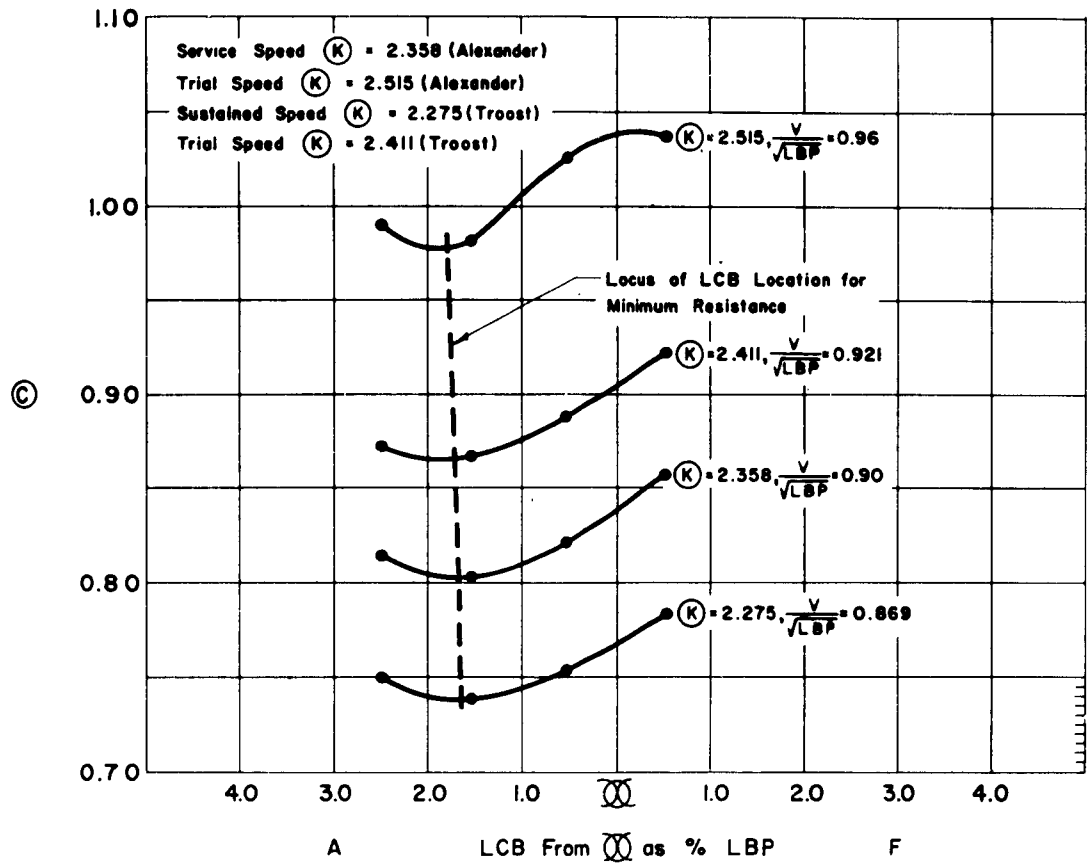


Figure 26 - Cross Curves of ③ on LCB. $C_B = 0.60$

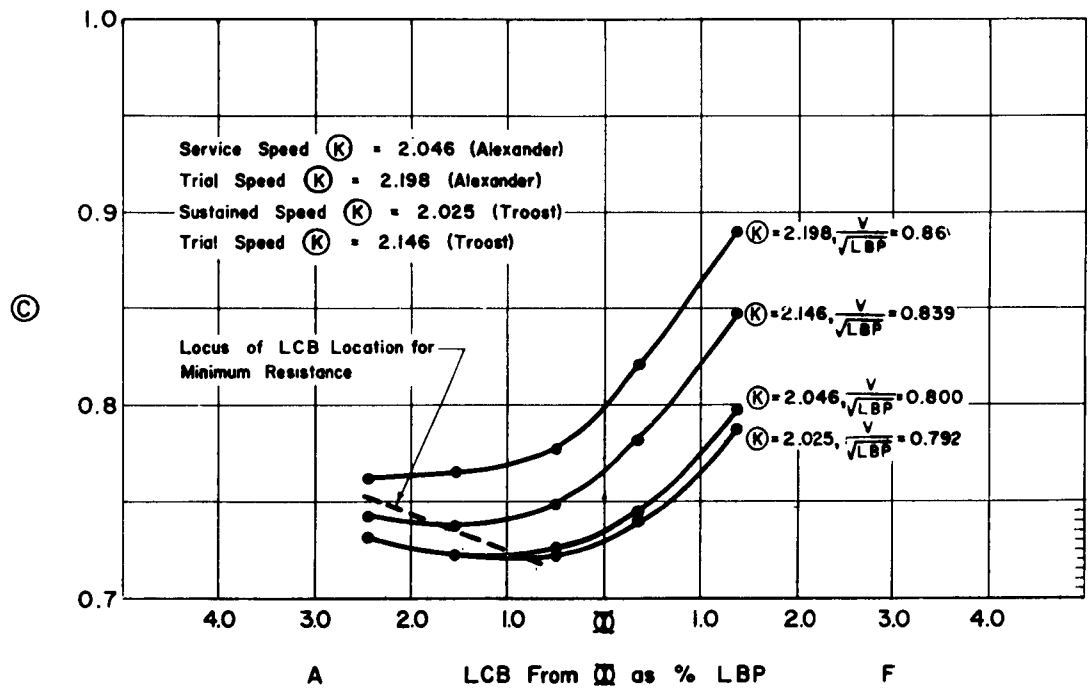


Figure 27 - Cross Curves of ③ on LCB. $C_B = 0.65$

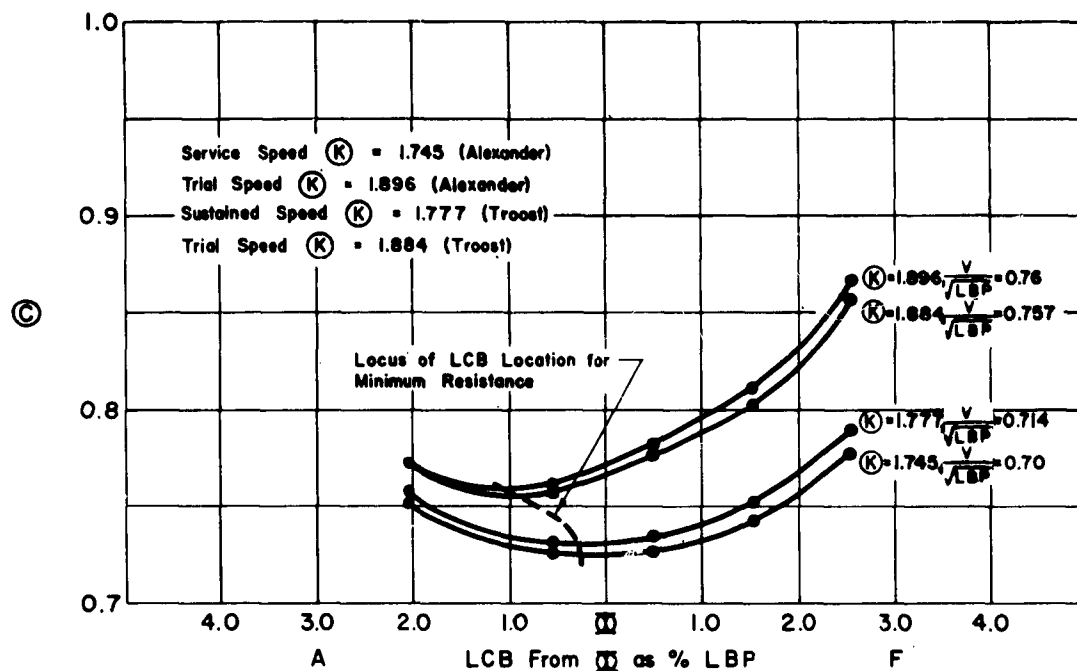


Figure 28 - Cross Curves of (C) on LCB. $C_B = 0.70$

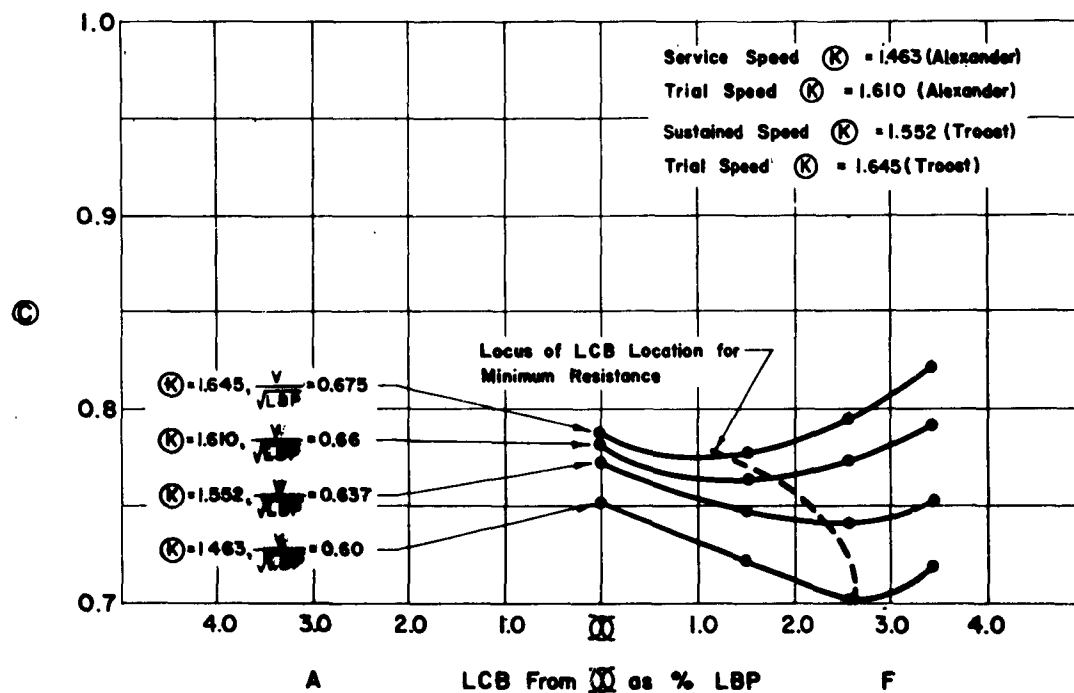


Figure 29 - Cross Curves of (C) on LCB. $C_B = 0.75$

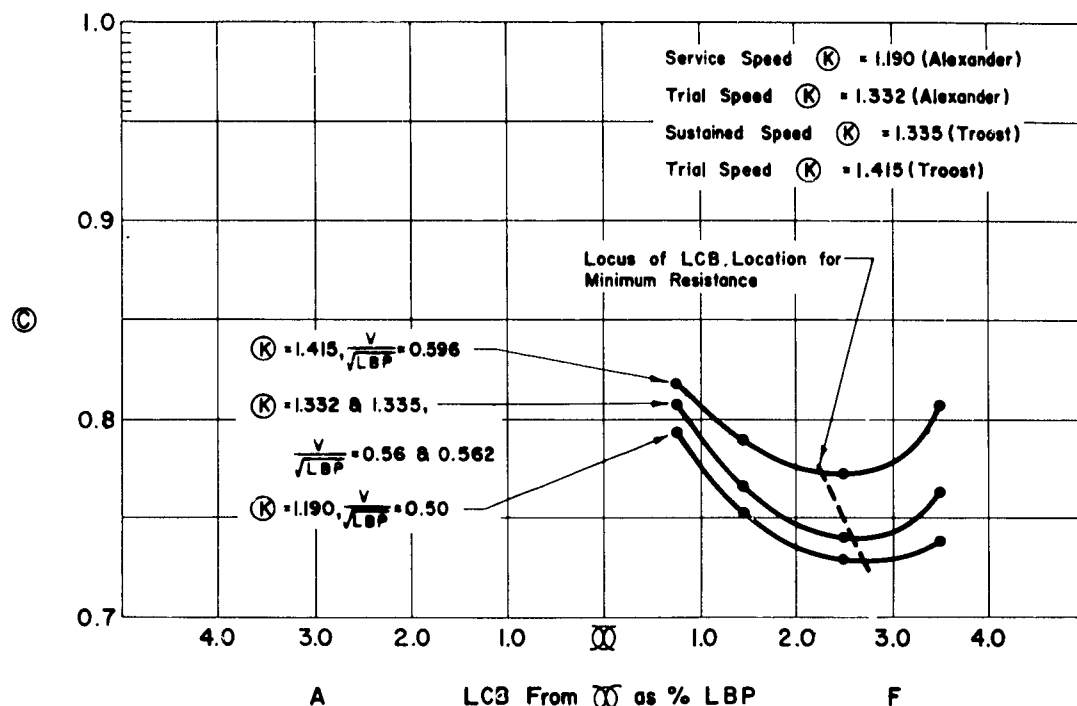


Figure 30 - Cross Curves of (C) on LCB. $C_B = 0.80$

values of (K) corresponding to the Alexander and Troost speeds set out in Table 9. The locus of the LCB position for minimum resistance is indicated on each figure. Table 26 summarizes the data from all five figures.

The optimum LCB locations and the corresponding minimum (C) values are given in Figure 31. This shows how, for a given block coefficient, the optimum LCB location moves aft as the desired speed is increased. When the block coefficient and speed are known, this figure will give the optimum LCB position and the corresponding minimum (C) value which will result if the lines of the ship conform with those of the Series 60 contours. Thus for a block coefficient of 0.65 and a speed corresponding to $(K) = 2.1$, entering Figure 31 on the (K) scale, we find the best position of LCB is 1.45 percent LBP aft of X, the corresponding minimum (C) 400-ft value being 0.73 and $\frac{V}{\sqrt{L_{BP}}} = 0.82$. This chart, in fact, summarizes the conclusions to be drawn from the resistance data and should be of considerable use to designers in all cases where the lines and proportions are not too different from those of the series.

One point of considerable interest which arises from these data is the remarkable constancy of the minimum (C) value at the sustained sea speed as defined by Troost. These speeds are shown in Figure 31; for block coefficients varying from 0.60 to 0.80, the minimum (C) 400-ft values at 0.05 intervals in coefficient are respectively, 0.735, 0.720, 0.730, 0.740, and 0.740.

Table 26 - Comparison of Resistance Results for *LCB* Series

C_B (C_F)	Position of <i>LCB</i> as % <i>LB</i> from \odot	\odot Values for 400-ft Ship							
		Service speed ^a		Trial speed ^a		Sustained speed ^b		Trial speed ^b	
		\odot	\odot	\odot	\odot	\odot	\odot	\odot	\odot
0.60	2.48A	2.358	0.815	2.515	0.990	2.275	0.750	2.411	0.872
(0.614)	1.50A		0.803		0.983		0.736		0.866
	0.51A		0.822		1.027		0.754		0.890
	0.52F		0.858		1.038		0.785		0.922
	Optimum <i>LCB</i> & \odot	1.69A	0.802	1.80A	0.980	1.65A	0.735	1.73A	0.865
0.65	2.46A	2.046	0.731	2.198	0.763	2.025	0.731	2.146	0.741
(0.661)	1.54A		0.723		0.766		0.722		0.739
	0.50A		0.725		0.778		0.722		0.750
	0.38F		0.745		0.822		0.740		0.781
	1.37F		0.797		0.890		0.788		0.849
(0.710)	Optimum <i>LCB</i> & \odot	1.01A	0.722	2.50A	0.763	0.90A	0.720	1.85A	0.740
	2.05A	1.745	0.754	1.896	0.773	1.777	0.759	1.884	0.772
	0.55A		0.726		0.760		0.731		0.757
	0.50F		0.728		0.783		0.735		0.778
(0.758)	1.54F		0.743		0.811		0.752		0.803
	2.55F		0.776		0.866		0.790		0.856
	Optimum <i>LCB</i> & \odot	0.25A	0.725	0.95A	0.757	0.25A	0.730	0.90A	0.754
	0.48F	1.463	0.751	1.610	0.777	1.552	0.768	1.645	0.783
(0.805)	1.50F		0.722		0.765		0.747		0.777
	2.57F		0.702		0.773		0.741		0.795
	3.46F		0.720		0.791		0.752		0.823
	Optimum <i>LCB</i> & \odot	2.60F	0.702	1.70F	0.764	2.30F	0.741	1.20F	0.776
(0.805)	0.76F	1.190	0.792	1.332	0.806	1.335	0.807	1.415	0.819
	1.45F		0.752		0.768		0.769		0.786
	2.50F		0.731		0.739		0.740		0.771
	3.51F		0.736		0.760		0.761		0.807
	Optimum <i>LCB</i> & \odot	2.70F	0.730	2.56F	0.739	2.56F	0.740	2.23F	0.770

^a From Alexander Formula [1] in text.^b From Troost Formula [2] in text.

The optimum locations of *LCB* for Series 60 at the sustained sea speed and trial speed, as defined by Troost, are plotted in Figure 32. If desired, the effect of speed can be brought out by treating it as a parameter for a series of curves such as the two shown. From the cross curves of Figures 26-30, the permissible movement of the *LCB* forward or aft of the optimum position has been determined in order that the minimum \odot value shall not be exceeded by more than 1 percent. The resultant limits are shown as dotted curves in Figure 32 for both sea and trial speeds.

It should be noted that all the Series 60 forms have a vertical stem line but no bulb at the forefoot, and that the recommended *LCB* locations refer to such designs. In the finer forms, it is probable that in many cases a bulb would be fitted which would result in some variation in *LCB* position, depending upon how much the bulb was treated as an addition or how far the extra displacement was used to fine down the load waterline and forebody generally.

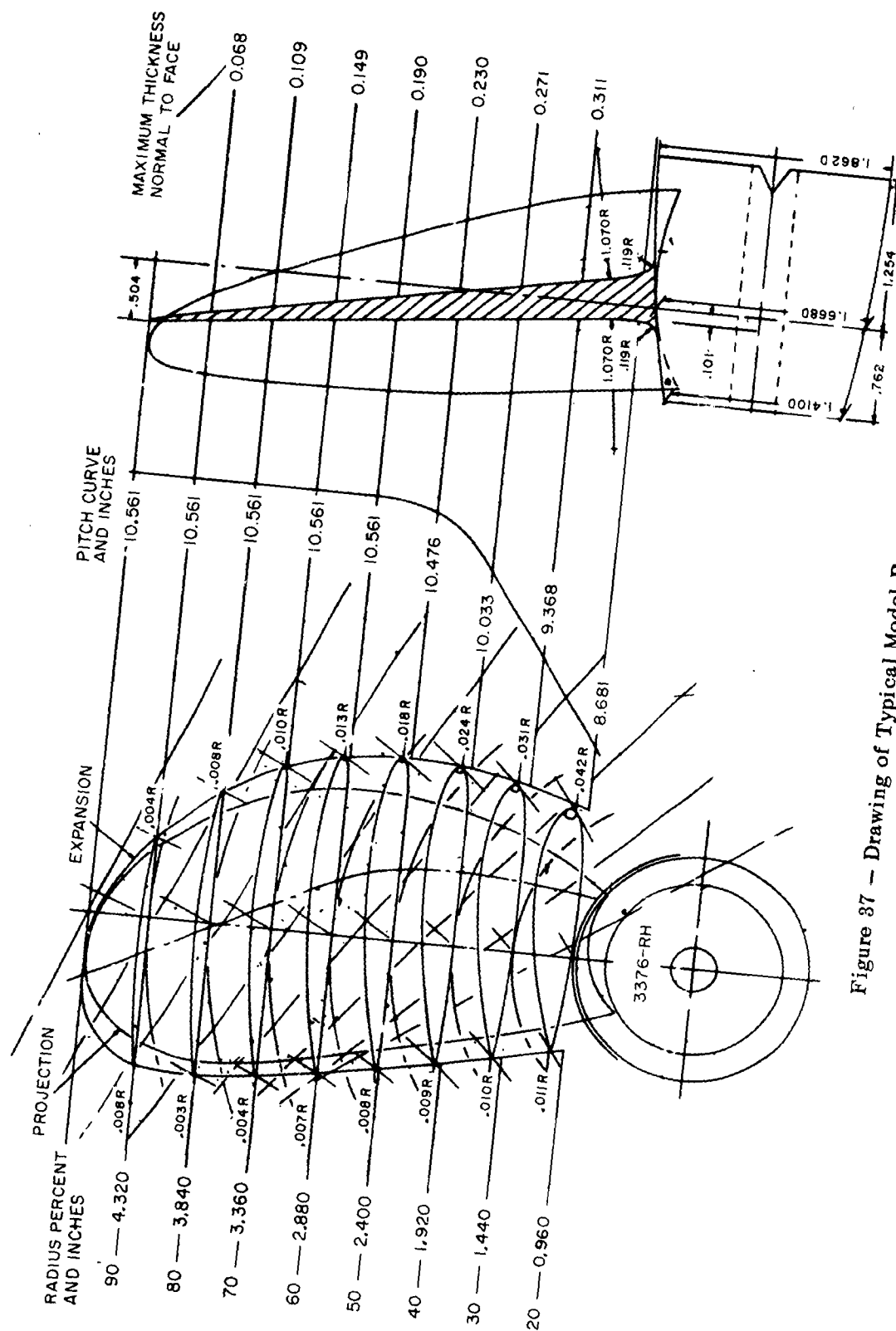


Figure 37 — Drawing of Typical Model Propeller

were calculated using the resistance of the model as measured during the self-propulsion tests, in association with the corresponding values of torque and rpm. This is a correct measure of propulsive efficiency since all the quantities apply to the model in the actual condition of test. However, for a variety of reasons, the actual resistance of the model at that time may not agree exactly with that measured during the original resistance tests, and on which the ehp values are based. The model has a keel piece, rudder, and propeller hub installed, and the surface and shape of the wax model may have changed slightly. The dhp values deduced straight from the torque and rpm will therefore correspond to a different resistance from that used to calculate the ehp values. For this reason, the dhp values have been calculated from the ehp values, using the propulsive efficiencies measured during the propulsion experiments but ignoring the actual torque and rpm values, i.e.,

$$\text{dhp} = \frac{\text{ehp}}{\text{Propulsive efficiency}}$$

In this way there is no inconsistency between the dhp values and the ehp values previously given from the resistance experiments and made when the models were new and in the bare-hull condition with no appendages and a new, clean surface.

The choice of a 600-ft ship to illustrate the propulsion tests was made principally because it was considered more representative of modern ships than the 400 ft chosen for the resistance presentation. This latter is made in coefficient form and may be corrected quite easily to any other desired ship length; most of the resistance data published elsewhere are on the 400-ft basis. The propulsion data, on the other hand, cannot be so corrected, and must be completely recalculated for any other length. Moreover, unless the model has been run at a number of loadings, it is possible to make such correction only for a small change in length.

The results are presented in detail in Tables 27 through 31. The change in wake fraction with movement in *LCB* affects the optimum pitch ratio for the highest propulsive efficiency, but series chart calculations show that this effect does not amount to more than 1 or 2 percent. Cross curves of dhp similar to those of (C) have been drawn for the same four chosen speeds. The data are tabulated in Table 32 and the cross curves are shown in Figure 38. On these have been drawn the loci of optimum *LCB* location to give minimum dhp. Those already derived from the resistance data to give minimum ehp are also shown for purposes of comparison.

In general, the minimum dhp is not so well defined as the minimum ehp, but, within practical limits, the dhp and ehp results agree in defining the same optimum *LCB* loci for each set of models except the fullest — that with $C_B = 0.80$. For this set, the dhp results indicate reducing power the further forward the *LCB*, even beyond the extreme position of 3.51 percent used in the experiments. The ehp results indicate an optimum location at about 2.50 percent of the length forward of midships, and this is a more practical answer — any

Table 27 - Results of Self-Propulsion Experiments, 0.60 Block Coefficient

(All figures are for ship of 600-ft LBP)

Model No. LCB V	4210 1.50 per cent A			4215 2.48 per cent A			4216 0.51 per cent A			4217 0.52 per cent F		
	EHP	N	SHP	EHP	N	SHP	EHP	N	SHP	EHP	N	SHP
12	2304	52.4	2931	2296	51.2	2789	2299	52.0	2796	2273	52.8	2884
13	2940	56.9	3712	2943	55.6	3585	2933	56.7	3608	2896	57.1	3665
14	3685	60.9	4607	3687	60.0	4501	3675	61.3	4560	3631	61.8	4597
15	4549	65.7	5693	4549	64.7	5644	4540	65.9	5689	4499	66.3	5695
16	5545	70.4	7091	5577	69.6	6998	5565	70.7	7053	5575	71.2	7057
17	6730	75.6	8740	6764	74.7	8561	6796	76.1	8713	6796	76.2	8624
18	8063	80.6	10445	8113	79.2	10231	8162	80.9	10518	8145	81.2	10551
19	9531	85.1	12203	9677	83.6	11977	9555	85.9	12360	9635	86.8	12728
20	11219	90.4	14383	11484	88.5	14355	11316	91.1	14696	11445	92.6	15119
20.5	12142	93.0	15667	12454	91.1	15886	12422	93.9	16132	12571	94.6	16606
21	13290	95.5	17292	13631	94.5	17725	13726	96.9	17990	13973	97.7	18458
21.5	14778	98.8	19470	15202	98.1	19976	15253	99.8	20044	15873	101.0	21051
22	16961	102.9	22615	17273	101.6	22727	17297	103.1	22971	18217	104.9	24551
22.5	19533	107.3	26468	19726	105.9	26093	20247	108.3	27324	20887	109.8	28730
23	22469	112.2	30903	22587	110.1	30399	23541	113.6	32248	23818	114.8	33219
23.5	25894	117.4	36165	25772	115.6	35794	26860	119.0	37566	27084	119.7	38146
24	28773	121.9	40755	28864	120.7	41059	29850	123.2	42281	30392	124.6	43170
25	34202	129.8	49354	34363	128.1	49301	35157	130.6	50011	36288	131.9	51839
26	39112	135.5	56196	38795	133.2	55739	40595	137.0	57663	41491	137.6	59443

Table 28 - Results of Self-Propulsion Experiments, 0.65 Block Coefficient

(All figures are for ship of 600-ft LBP)

Model No. LCB V	4211 0.50 per cent A			4218 1.54 per cent A			4219 0.38 per cent F			4220 1.37 per cent F			4231 2.46 per cent A		
	EHP	N	SHP	EHP	N	SHP	EHP	N	SHP	EHP	N	SHP	EHP	N	SHP
10	1475	41.4	1993	1453	41.0	1856	1428	41.8	1833	1427	41.0	1695	1526	41.8	2221
11	1949	45.4	2547	1933	45.3	2453	1898	46.0	2446	1908	45.3	2288	2022	45.8	2905
12	2516	49.6	3238	2526	49.4	3169	2485	50.5	3203	2505	50.0	3051	2613	49.8	3706
13	3200	54.1	4098	3225	53.6	4017	3204	54.9	4134	3226	54.6	3997	3322	53.8	4652
14	4011	58.7	5243	4040	57.9	5031	4046	59.3	5214	4067	59.4	5122	4147	57.9	5728
15	5010	68.1	6472	4992	62.3	6311	5018	63.6	6458	5064	64.4	6501	5116	62.1	6989
16	6172	67.7	7985	6172	67.4	7963	6197	68.3	7965	6267	69.3	8128	6214	66.4	8466
17	7505	72.4	9536	7581	72.5	9858	7627	73.1	9753	7724	74.2	10045	7782	72.3	10763
18	9044	77.0	11594	9113	77.3	11835	9235	78.0	11750	9500	79.2	12337	9369	77.3	12976
19	10818	81.8	13941	10852	82.1	14094	11051	83.3	14371	11641	84.8	15118	11010	81.6	15208
19.5	11789	84.2	15291	11779	82.5	15317	12118	86.1	15903	12910	87.6	16788	11903	83.7	16417
20	12881	87.0	16882	12777	86.8	16681	13319	88.7	17501	14322	90.6	18673	12879	86.0	17788
20.5	14145	90.1	18834	13944	89.2	18347	14800	91.9	19473	16026	94.1	21031	14013	82.5	19436
21	15771	93.8	21458	15565	92.8	20809	16753	95.5	22043	18191	98.0	24062	15469	91.6	21605
21.5	18129	99.0	25534	17803	97.0	24288	19353	99.7	25565	20815	102.4	27865	17477	95.5	24860
22	21555	104.4	31014	21338	102.6	29719	22705	104.4	30559	24031	107.5	32830	20326	100.5	29935
22.5	25864	109.2	37539	25648	108.5	36484	27138	111.0	37797	28204	113.0	39612	24428	106.5	36459
23	31221	115.7	45913	30621	115.0	44703	32600	118.1	46974	33510	119.4	48848	29254	112.4	43991
23.5	37337	121.7	56061	36588	121.9	54527	38626	125.2	57306	40546	127.0	61063	34704	118.9	53064
24	43782	128.8	67048	42542	128.6	65248	44889	132.1	68638	47386	133.7	73353	40734	125.6	64047

Table 29 - Results of Self-Propulsion Experiments, 0.70 Block Coefficient

(All figures are for ship of 600-ft LBP)

Model No. LCB V	4212 0.50 per cent F			4221 0.55 per cent A			4222 1.54 per cent F			4223 2.55 per cent F			4230 2.05 per cent A		
	EHP	N	SHP	EHP	N	SHP	EHP	N	SHP	EHP	N	SHP	EHP	N	SHP
10	1660	41.1	2065	1625	40.0	1972	1618	40.2	1951	1596	40.3	1977	1729	40.2	2145
11	2207	45.3	2762	2172	44.0	2627	2173	44.5	2609	2131	44.2	2635	2305	44.4	2859
12	2867	49.6	3643	2842	48.5	3474	2835	48.9	3375	2790	48.9	3419	2995	48.6	3725
13	3652	54.0	4700	3652	52.8	4536	3607	53.1	4336	3593	53.1	4393	3821	52.7	4746
14	4597	58.4	5970	4594	57.0	5742	4542	57.5	5566	4553	57.5	5573	4814	57.1	6018
15	5788	63.2	7517	5690	61.5	7139	5754	62.4	7257	5729	62.2	7073	6010	61.7	7607
15.5	6454	65.4	8393	6322	63.5	7943	6428	64.8	8137	6419	64.7	8033	6673	64.1	8501
16	7117	67.5	9267	7026	66.1	8860	7127	67.1	9033	7208	67.4	9136	7378	66.5	9471
16.5	7827	69.7	10205	7770	68.5	9835	7895	69.5	10019	8113	70.3	10428	8145	69.0	10564
17	8603	71.8	11246	8581	70.8	10903	8754	72.0	11109	9137	72.9	11882	8954	71.3	11735
17.5	9545	74.4	12510	9468	73.4	12122	9733	74.7	12352	10275	76.1	13555	9831	73.7	12987
18	10634	77.2	13991	10452	76.1	13469	10894	77.2	13860	11567	79.1	15443	10781	76.3	14436
18.5	11934	80.0	15724	11597	78.9	15060	12306	80.3	15919	13127	82.4	17763	11827	79.0	15897
19	13470	83.1	17770	12892	81.5	16899	14067	83.7	18412	15038	86.3	20488	12983	81.6	17545
19.5	15097	86.4	20048	14317	84.5	18838	15980	87.2	21222	17400	90.5	23803	14285	84.5	19515
20	16775	89.3	22367	15912	87.3	21047	17985	90.8	24206	20027	94.9	27738	15697	87.2	21621
21	20756	95.3	28086	19583	93.1	26216	22619	98.3	31328	26381	103.9	37741	19187	93.3	26986
22	29724	107.5	41631	26948	102.7	37016	31477	109.9	45685	35065	114.2	52180	25803	103.8	37780

Table 30 - Results of Self-Propulsion Experiments, 0.75 Block Coefficient

(All figures are for ship of 600-ft LEP)

Model No. LCB V	4213 1.50 per cent F			4224 0.48 per cent F			4225 2.57 per cent F			4226 3.46 per cent F		
	BHP	N	SHP	BHP	N	SHP	BHP	N	SHP	BHP	N	SHP
10	1851	40.0	2193	1912	40.3	2192	1848	40.6	2222	1837	40.7	2159
11	2465	44.6	3002	2554	44.4	2902	2459	45.0	2991	2427	44.9	2939
12	3216	48.9	3961	3332	48.8	3875	3203	49.1	3864	3135	49.0	3823
13	4142	53.3	5126	4276	53.1	5072	4102	53.3	4930	4020	53.5	4944
14	5210	57.7	6489	5435	57.6	6548	5184	57.5	6238	5126	58.3	6399
14.5	5824	59.9	7279	6111	59.9	7425	5831	60.0	7051	5777	60.8	7249
15	6526	62.1	8178	6850	62.5	8374	6564	62.7	8015	6529	63.3	8233
15.5	7348	64.8	9278	7649	64.9	9431	7368	65.3	9096	7404	65.9	9360
16	8278	67.3	10508	8508	67.1	10542	8313	68.1	10430	8446	68.6	10691
16.5	9311	70.2	11937	9465	69.6	11757	9491	71.4	12215	9821	72.1	12479
17	10483	73.0	13527	10535	72.1	13136	10905	74.9	14330	11526	75.8	14834
17.5	11871	76.4	15538	11805	74.9	14793	12577	78.3	16690	13412	79.7	17601
18	13654	80.1	18206	13341	78.0	16887	14630	82.0	19455	15593	83.7	20791
19	18592	89.0	25858	18125	86.5	23880	20275	90.8	27399	21254	92.3	29235
20	25004	97.8	35669	24328	96.0	34120	27518	101.2	39367	28474	102.1	40620
21	32135	107.5	47749	30356	103.5	43804	33361	108.8	50318	37471	113.2	55595
22	40815	116.3	62504	39029	112.3	57396	42478	118.1	65250	47694	123.2	72705

Table 31 - Results of Self-Propulsion Experiments, 0.80 Block Coefficient

(All figures are for ship of 600-ft LBP)

Model No. LCB V	4214 2.50 per cent F			4227 0.76 per cent F			4228 1.45 per cent F			4229 3.51 per cent F		
	BHP	N	SHP	BHP	N	SHP	BHP	N	SHP	BHP	N	SHP
9	1531	37.8	1858	1751	42.2	2678	1599	38.9	1955	1530	37.5	1620
10	2096	42.2	2552	2403	47.0	3696	2187	43.2	2697	2089	42.1	2336
11	2791	46.6	3433	3212	51.8	4964	2914	47.7	3620	2800	46.5	3203
12	3639	51.2	4531	4197	56.6	6507	3786	52.0	4744	3680	51.1	4230
12.5	4127	53.3	5172	4772	59.0	7399	4305	54.3	5422	4187	54.2	4812
13	4666	55.6	5892	5405	61.7	8267	4878	56.9	6182	4756	55.7	5473
13.5	5274	58.2	6693	6096	64.1	9422	5505	59.5	7031	5405	58.0	6263
14	5970	60.6	7625	6855	66.7	10594	6208	62.1	7990	6190	60.7	7248
14.5	6796	63.3	8713	7693	69.3	11927	6993	64.9	9093	7162	63.7	8485
15	7792	66.2	10028	8635	72.1	13470	7896	67.7	10363	8327	67.5	9997
16	10315	72.9	13519	10876	78.2	17345	10222	73.9	13684	11456	74.4	14231
17	14099	81.0	18975	14117	85.5	22955	13546	81.3	18658	15580	82.4	20286
18	19249	90.5	27381	18642	93.4	30763	18102	90.0	26273	21280	92.0	29271
19	26847	101.3	40432	25823	103.1	42542	25703	101.2	38826	31410	104.0	45522

Table 32 — Comparison of DHP Results for *LCB* Series
(Speed and dhp are given for ship 600 ft long, between perpendiculars)

C_B	C_P	Position of <i>LCB</i> as Percent L_{BP} from Ⓢ	SERVICE SPEED (a)			TRIAL SPEED (a)			SEA SPEED (b)			TRIAL SPEED (b)		
			$\frac{V}{\sqrt{L_{BP}}}$	V knots	DHP	$\frac{V}{\sqrt{L_{BP}}}$	V knots	DHP	$\frac{V}{\sqrt{L_{BP}}}$	V knots	DHP	$\frac{V}{\sqrt{L_{BP}}}$	V knots	DHP
0.60	0.614	2.48A	0.90	22.04	22954	0.96	23.52	36197	0.869	21.26	18853	0.921	22.54	26372
		1.50A			22954			36353						26772
		0.51A			23328			37836						27688
		0.52F			24870			38382						29085
0.65	0.661	2.46A	0.80	19.60	16664	0.86	21.06	21950	0.792	19.40	16150	0.839	20.56	19676
		1.54A			15572			21204						18642
		0.50A			15602			21933						19120
		0.38F			16197			22390						19729
0.70	0.710	1.37F	0.70	17.15	17123	0.76	18.62	24473	0.714	17.49	12958	0.757	18.54	21319
		2.05A			12106			16282						16028
		0.55A			11263			15462						15180
		0.50F			11600			16205						15901
0.75	0.758	1.54F	0.60	14.70	11475	0.66	16.17	16482	0.637	15.60	9650	0.675	16.54	16111
		2.55F			12358			18400						17972
		0.48F			7807			10934						11855
		1.50F			7616			10993						12064
0.80	0.805	2.57F	0.50	12.25	7422	0.56	13.72	11000	0.562	13.77	10050	0.596	14.60	12390
		3.46F			7622			11242						12634
		0.76F			6948			9926						12230
		1.45F			5073			7447						9333
		2.50F			4843			7098						8972
		3.51F			4514			6672						8776

(a) From Equation 1

(b) From Equation 2

Figure 38 — Cross-Curves of DHP for *LCB* Series
(Speeds and dhp given for ship 600 ft long, between perpendiculars)

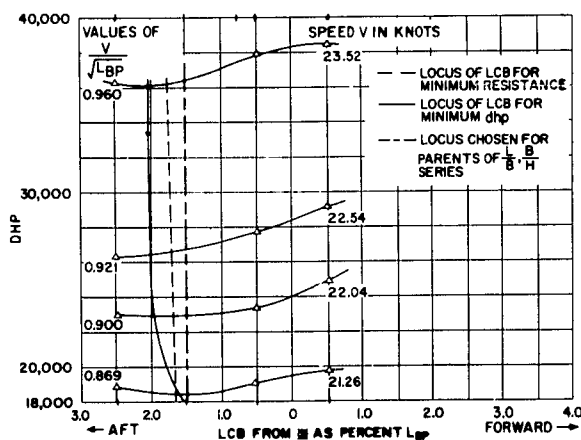


Figure 38a — $C_B = 0.60$.

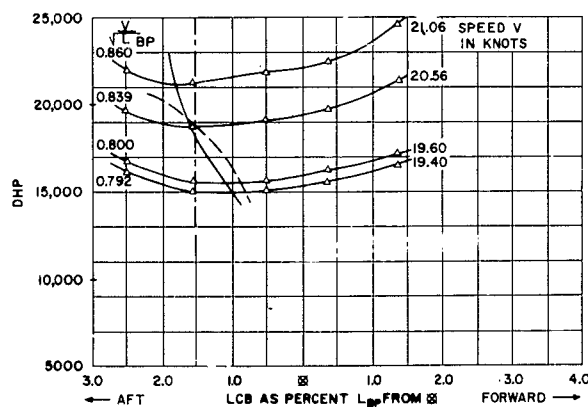


Figure 38b — $C_B = 0.65$

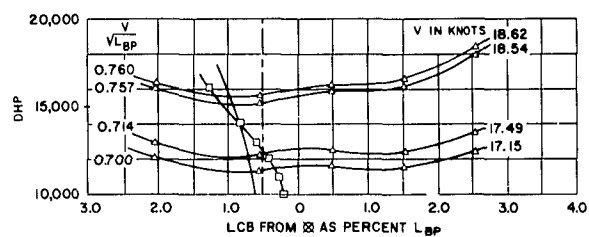


Figure 38c - $C_B = 0.70$

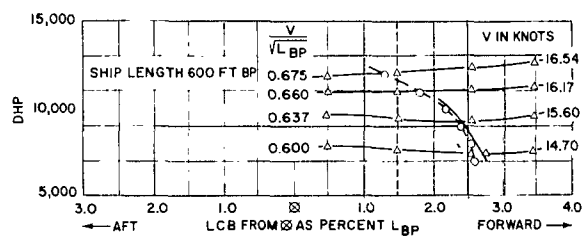


Figure 38d - $C_B = 0.75$

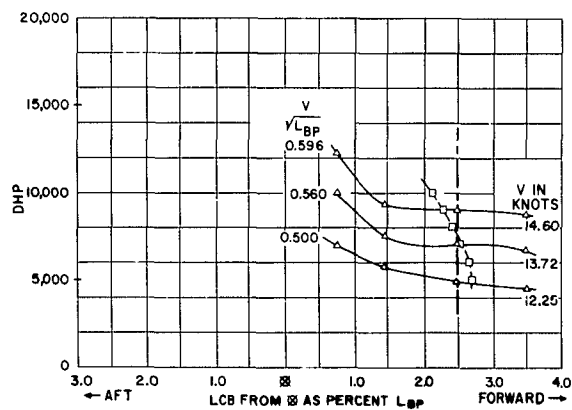


Figure 38e - $C_B = 0.80$

further movement forward would result in excessively full entrance waterlines and probably poor behavior and heavy speed loss in a seaway.

It can be concluded that if the *LCB* location is chosen to give minimum \textcircled{C} values and so minimum *ehp*, the *dhp* also will be practically a minimum except for the very fullest models of the series. The charts given in Figures 31 and 32 can thus be used by the designer with the knowledge that, within practical limits, they will lead to ship forms having both minimum *ehp* and *dhp* in smooth water.

The detailed results of the self-propelled experiments are given in Tables 27 to 31. Cross plots of these data show a general waviness of character, associated with changes in wake fraction w consequent upon changes in wave formation with speed, but for a given fullness, both wake fraction and thrust deduction fraction tend to decrease as the *LCB* moves forward, due to the progressive fining of the afterbody. As a result, the hull efficiency remains fairly constant, although showing considerable variation due to the interplay of the changes in w and t . The one exception to this pattern is the set of models of $0.80 C_B$, where the value of w remains fairly constant with *LCB* movement, but t decreases rapidly as the *LCB* moves forward. As a result, the hull efficiency increases continually, and the resultant increase in propulsive efficiency and decrease in *dhp* is the reason why this set shows no optimum *LCB* location for minimum *dhp* within the range tested.

CHAPTER VIII

EFFECT ON RESISTANCE AND DHP OF VARIATION IN SHIP PROPORTIONS

The experiments described in the last section showed that the original choice of LCB positions had not been too far from the optimum, although improvement could be obtained in certain areas. For the final series of experiments, in which the effect of variation in C_B , $\frac{L}{B}$, $\frac{B}{H}$, and $\frac{\Delta}{(\frac{L}{100})^3}$ upon resistance and propulsive efficiency were determined, the five models chosen as parents were those of the LCB series having the LCB in the position nearest to the optimum.

C_B	0.60	0.65	0.70	0.75	0.80
Model Number	4210	4218	4221	4213	4214
LCB as Percent L_{BP} from \bar{X}_{BP}	1.5 aft	1.54 aft	0.55 aft	1.5 fwd	2.5 fwd
LCB in Original Series 60 Parents	1.5 aft	0.5 aft	0.5 fwd	1.5 fwd	2.5 fwd

It will be seen that the change involves a movement of the LCB aft in the 0.65 and 0.70 C_B models. The models chosen for the final phase are also indicated in Figure 1. In developing this geometrical series, the assumption has been made that the optimum location of LCB for the model having the $\frac{L}{B}$ and $\frac{B}{H}$ ratios of any one parent will remain near-optimum with changes of $\frac{L}{B}$ and $\frac{B}{H}$ for the same block coefficient. This assumption has not been tested in the present research, but any other would have led to a great extension of the test program.

Having chosen the new parents, eight additional models were made for each block coefficient, making a total of 45 models in all, including the original parents.

C_B	VARIATION OF $\frac{L}{B}$ AND $\frac{B}{H}$ RATIOS		
	Range of Variation in		
	$\frac{L}{B}$	$\frac{B}{H}$	$\frac{\Delta}{(\frac{L}{100})^3}$
0.60	6.5-8.5	2.5-3.5	67.8-162.4
0.65	6.25-8.25	2.5-3.5	78.0-190.3
0.70	6.0-8.0	2.5-3.5	89.3-222.4
0.75	5.75-7.75	2.5-3.5	102.0-259.3
0.80	5.5-7.5	2.5-3.5	116.2-302.4

A typical pattern of the variation (for $C_B = 0.60$) is shown in Figure 2.

The eight new models of any one set were derived from the parents by a straightforward geometrical variation of beam and draft to give the required combinations of $\frac{L}{B}$ and $\frac{B}{H}$ values. The lines of the parents for C_B values of 0.60, 0.75, and 0.80 are shown in Figures 12, 15, and 16 and those for the new parents of 0.65 and 0.70 C_B are shown in Figures 39 and 40. Particulars of all 45 models are given in Tables 33 through 37.

The models were made in wax, 20 ft *LBP*, as before, but the turbulence stimulation was provided by a trip wire instead of studs; the 0.036-in. diameter wire was placed around a station 5 percent of the length from the forward perpendicular. This change was made for the reasons set out in Appendix A. The model results have been converted to apply to a ship 400 ft *LBP*, using the ATTC 1947 model-ship correlation line with an addition of +0.0004 for ship correlation allowance. The ship figures are given in Appendix B as values of C_T and C for a standard temperature of 59°F (15°C).

For the propulsion experiments, the models were fitted with a rudder and keelpiece and the experiments carried out as described in Chapter VII. The propeller diameter was in every case 0.7 of the draft. The propellers for the parent models were specially made for the Series 60 tests, and, as already described, were of the Troost B-type with four blades. As the draft was varied in this geometrical series, so also the propeller diameter had to be changed. To avoid making large numbers of new propellers, and since the principal objective of the propulsion tests was to obtain systematic data on the components of propulsive efficiency, such as wake and thrust-deduction fractions, stock model propellers were used whenever possible. These were chosen to have rake, blade-area ratio, sections, and other features as near to the Troost standard design as possible. Table 38 shows the propeller particulars.

The propulsion tests were run without bilge keels, and trip wires were used for turbulence stimulation. They were carried out at a propeller loading corresponding to the 600-ft ship self-propulsion point with a ship correlation allowance of +0.0004. The data extrapolated to apply to a ship 600 ft *LBP* are presented in detail in Appendix B.

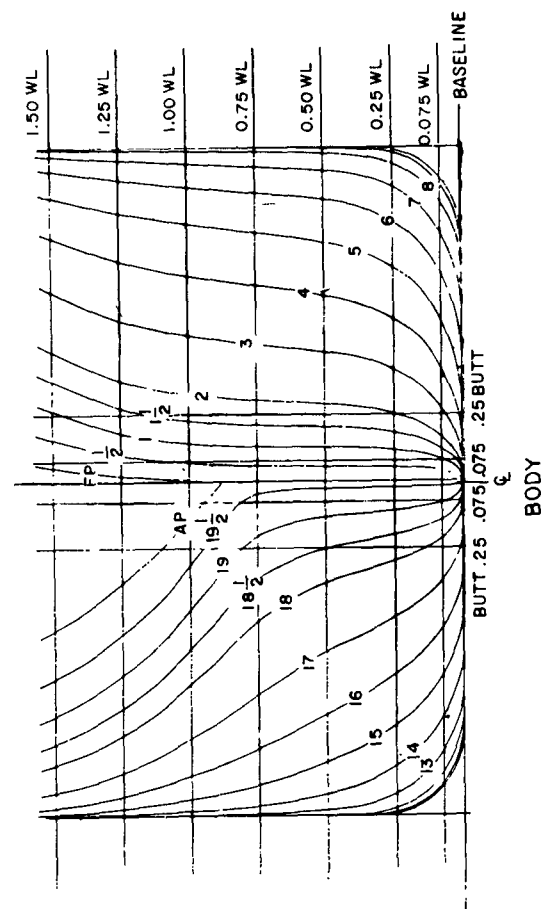
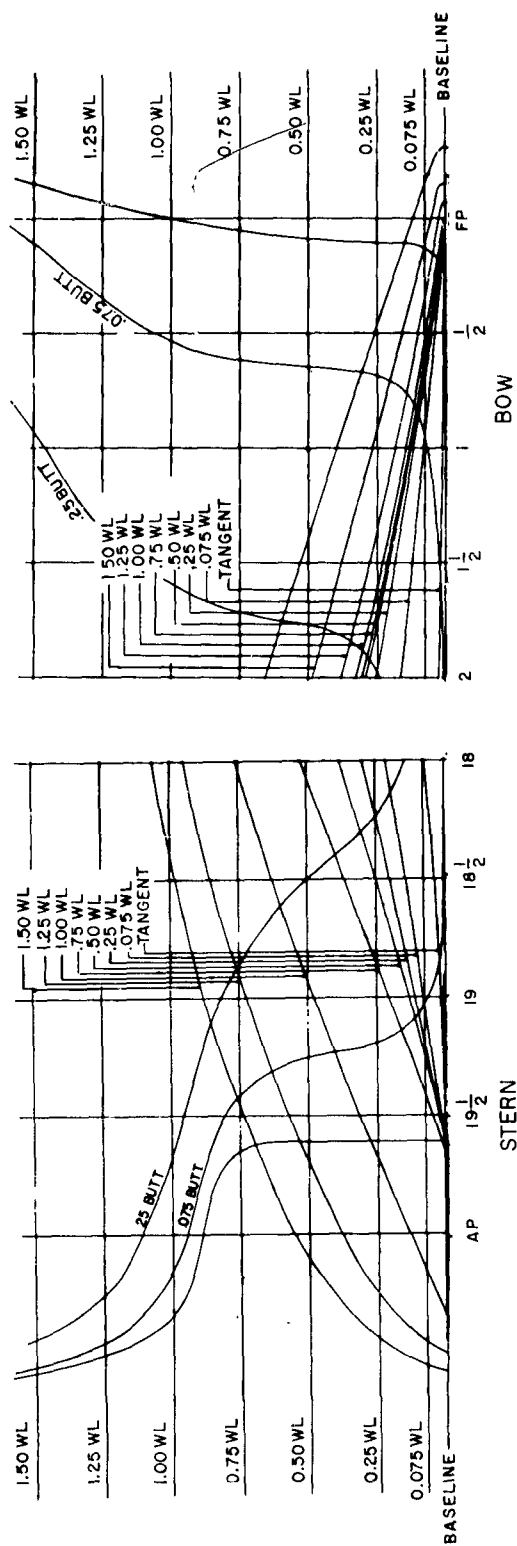


Figure 39 -- Lines of $0.65 C_B$ Parent for $\frac{L}{B}$ Series (Model 4218)

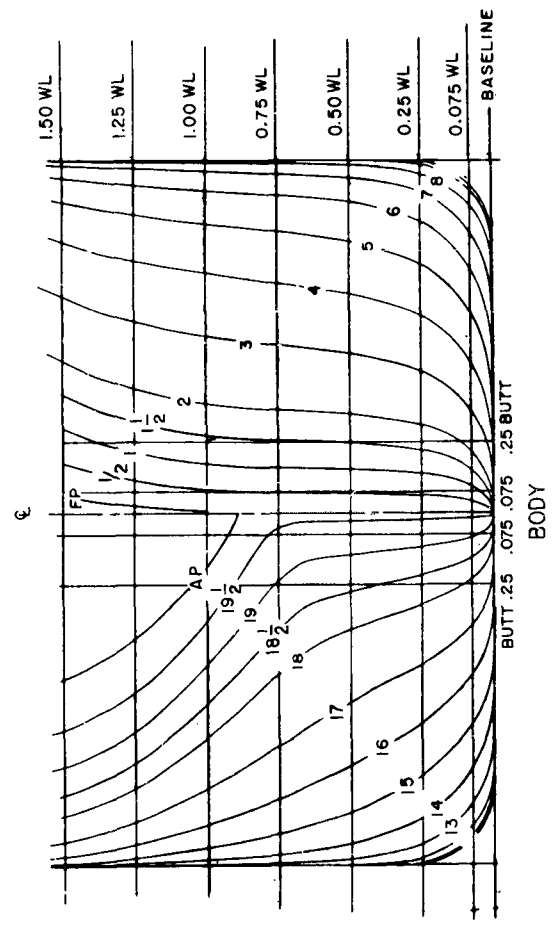
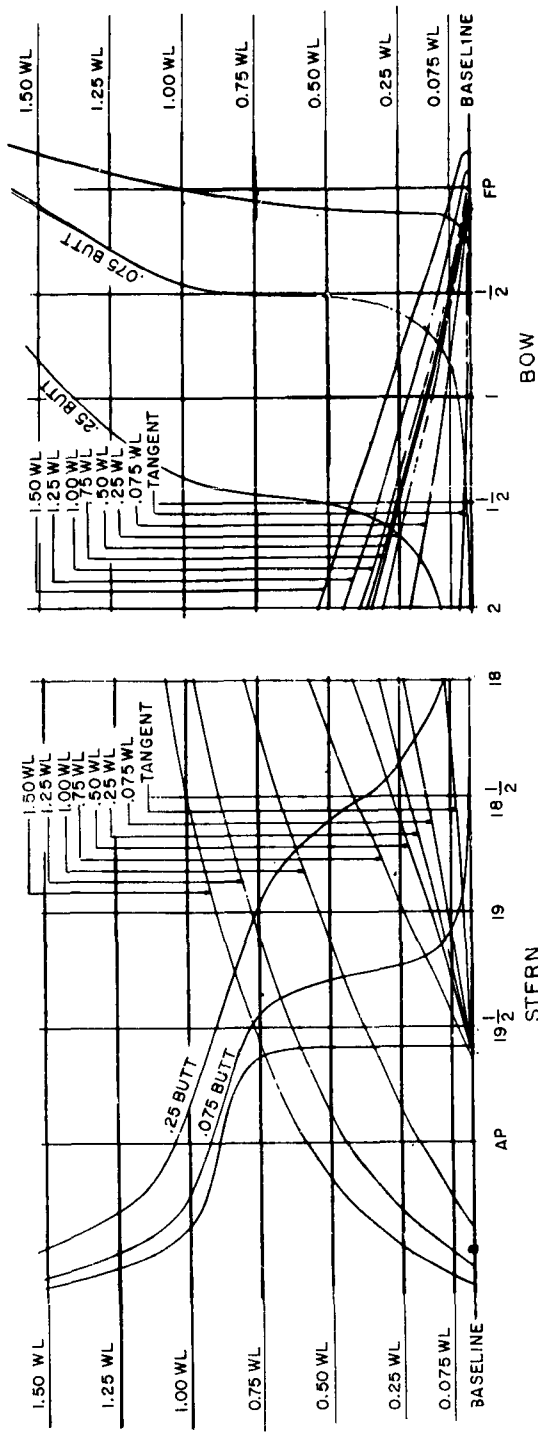


Figure 40 — Lines of 0.70 C_B Parent for $\frac{L}{B} \frac{B}{H}$ Series (Model 4221)

Table 33 — Principal Particulars of 0.60 Block Coefficient Models

Model Number	4210	4255	4253	4240	4252	4241	4243	4254	4242
L/B	7.50	7.5	7.5	6.5	6.5	6.5	8.5	8.5	8.5
B/H	2.50	3.0	3.5	2.5	3.0	3.5	2.5	3.0	3.5
B , ft	53.33	53.33	53.33	61.54	61.54	61.54	47.06	47.06	47.06
H , ft	21.33	17.78	15.24	24.62	20.51	17.58	18.82	15.69	13.44
Δ , tons	7807	6506	5577	10394	8661	7423	6077	5066	4340
$1/2 \alpha_E$, deg	7.0	7.0	7.0	8.7	8.7	8.7	6.2	6.2	6.2
$L/\nabla^{1/3}$	6.165	6.552	6.897	5.604	5.956	6.270	6.702	7.122	7.498
$\Delta/(L/100)^3$	122.0	101.6	87.14	162.4	135.3	116.0	94.95	79.16	67.81
WS , sq ft	27280	24906	23207	31590	28659	26893	24082	21941	20502
$S/\nabla^{2/3}$	6.481	6.682	6.900	6.202	6.354	6.608	6.762	6.955	7.205
L_{WL} , ft					406.7				
L_{BP} , ft					400.0				
L_E/L_{BP}					0.5				
L_X/L_{BP}					0				
L_R/L_{BP}					0.5				
C_B					0.60				
C_X					0.977				
C_P					0.614				
C_{PF}					0.581				
C_{PA}					0.646				
C_{PE}					0.581				
C_{PR}					0.646				
C_{PV}					0.850				
C_{PVF}					0.910				
C_{PVA}					0.802				
C_W					0.706				
C_{WF}					0.624				
C_{WA}					0.788				
C_{IT}					0.543				
LCB , % L_{BP} from ∇					1.5A				

Table 34 – Principal Particulars of 0.65 Block Coefficient Models

Model Number	4218	4275	4273	4264	4272	4265	4267	4274	4266
L/B	7.25	7.25	7.25	6.25	6.25	6.25	8.25	8.25	8.25
B/H	2.50	3.0	3.5	2.5	3.0	3.5	2.5	3.0	3.5
B , ft	55.17	55.17	55.17	64.00	64.00	64.00	48.48	48.48	48.48
H , ft	22.09	18.39	15.76	25.60	21.33	18.28	19.39	16.16	13.85
Δ , tons	9051	7542	6463	12179	10148	8696	6988	5824	4991
$1/2 \alpha_E$, deg	8.3	8.3	8.3	9.6	9.6	9.6	7.3	7.3	7.3
$L/\nabla^{1/3}$	5.869	6.236	6.566	5.316	5.649	5.948	6.398	6.798	7.157
$\Delta/(L/100)^3$	141.4	117.8	101.0	190.3	158.6	135.9	109.2	91.00	77.98
WS , sq ft	29380	26789	25042	34116	31082	29046	25822	23532	21989
$S/\nabla^{2/3}$	6.324	6.512	6.748	6.026	6.200	6.422	6.606	6.797	7.039
L_{WL} , ft					406.7				
L_{BP} , ft					400.0				
L_E/L_{BP}					0.475				
L_X/L_{BP}					0.035				
L_R/L_{BP}					0.490				
C_B					0.650				
C_X					0.982				
C_P					0.661				
C_{PF}					0.628				
C_{PA}					0.694				
C_{PE}					0.609				
C_{PR}					0.688				
C_{PV}					0.874				
C_{PVF}					0.924				
C_{PVA}					0.832				
C_W					0.744				
C_{WF}					0.668				
C_{WA}					0.819				
C_{IT}					0.593				
LCB , % LBP from \boxtimes					1.54A				

Table 35 – Principal Particulars of 0.70 Block Coefficient Models

Model Number	4221	4259	4257	4244	4256	4245	4247	4258	4246
L/B	7.00	7.0	7.0	6.0	6.0	6.0	8.0	8.0	8.0
B/H	2.50	3.0	3.5	2.5	3.0	3.5	2.5	3.0	3.5
B , ft	57.14	57.14	57.14	66.67	66.67	66.67	50.00	50.00	50.00
H , ft	22.86	19.05	16.32	26.67	22.22	19.05	20.00	16.67	14.28
Δ , tons	10456	8714	7465	14234	11859	10167	8005	6672	5716
$1/2 \alpha_E$, deg	11.6	11.6	11.6	12.9	12.9	12.9	9.7	9.7	9.7
$L/\nabla^{1/3}$	5.593	5.944	6.258	5.047	5.364	5.646	6.114	6.497	6.841
$\Delta/(L/100)^3$	163.4	136.2	116.6	222.4	185.3	158.8	125.1	104.2	89.31
WS , sq ft	31859	29183	27189	37070	33913	31882	27864	25436	23870
$S/\nabla^{2/3}$	6.230	6.444	6.656	5.901	6.097	6.352	6.510	6.710	6.981
L_{WL} , ft					406.7				
L_{BP} , ft					400.0				
L_B/L_{BP}					0.420				
L_X/L_{BP}					0.119				
L_R/L_{BP}					0.461				
C_B					0.700				
C_X					0.986				
C_P					0.710				
C_{PF}					0.700				
C_{PA}					0.721				
C_{PE}					0.642				
C_{PR}					0.698				
C_{PV}					0.890				
C_{PVF}					0.940				
C_{PVA}					0.846				
C_W					0.787				
C_{WF}					0.734				
C_{WA}					0.841				
C_{IT}					0.651				
LCB, % LBP from ∇					0.55A				

Table 36 – Principal Particulars of 0.75 Block Coefficient Models

Model Number	4213	4279	4277	4268	4276	4269	4271	4278	4270
L/B	6.75	6.75	6.75	5.75	5.75	5.75	7.75	7.75	7.75
B/H	2.50	3.0	3.5	2.5	3.0	3.5	2.5	3.0	3.5
B , ft	59.26	59.26	59.26	69.56	69.56	69.56	51.61	51.61	51.61
H , ft	23.70	19.75	16.93	27.82	23.19	19.87	20.64	17.20	14.74
Δ , tons	12048	10038	8606	16598	13836	11855	9136	7614	6525
$1/2 \alpha_E$, deg	22.5	22.5	22.5	25.9	25.9	25.9	19.8	19.8	19.8
$L/\nabla^{1/3}$	5.335	5.670	5.968	4.795	5.095	5.364	5.851	6.217	6.546
$\Delta/(L/100)^3$	188.2	156.8	134.4	259.3	216.2	185.2	142.8	119.0	102.0
WS , sq ft	34232	31459	29502	40252	36964	34659	29802	27400	25693
$S/\nabla^{2/3}$	6.090	6.322	6.569	5.784	5.997	6.233	6.376	6.620	6.880
L_{WL} , ft					406.7				
L_{BP} , ft					400.0				
L_E/L_{BP}					0.350				
L_X/L_{BP}					0.210				
L_R/L_{BP}					0.440				
C_B					0.750				
C_X					0.990				
C_P					0.758				
C_{PF}					0.792				
C_{PA}					0.724				
C_{PE}					0.704				
C_{PR}					0.686				
C_{PV}					0.907				
C_{PVF}					0.961				
C_{PVA}					0.856				
C_W					0.827				
C_{WF}					0.817				
C_{WA}					0.838				
C_{IT}					0.711				
LCB , % LBP from ∇					1.5F				

Table 37 – Principal Particulars of 0.80 Block Coefficient Models


Model Number	4214	4263	4261	4248	4260	4249	4251	4262	4250
L/B	6.50	6.5	6.5	5.5	5.5	5.5	7.5	7.5	7.5
B/H	2.50	3.0	3.5	2.5	3.0	3.5	2.5	3.0	3.5
B_1 , ft	61.54	61.54	61.54	72.73	72.73	72.73	53.33	53.33	53.33
H_1 , ft	24.59	20.51	17.58	29.09	24.24	20.78	21.33	17.78	15.24
Δ , tons	13859	11547	9898	19356	16129	13827	10407	8675	7436
$1/2 \alpha_E$, deg	43.0	43.0	43.0	47.8	47.8	47.8	38.9	38.9	38.9
$L/\nabla^{1/3}$	5.092	5.411	5.696	4.555	4.841	5.096	5.602	5.9542	6.266
$\Delta/(L/100)^3$	216.5	180.4	154.6	302.4	252.0	216.0	162.6	135.5	116.2
WS , sq ft	37200	34316	32149	44010	40512	38103	32230	29617	27868
$S/\nabla^{2/3}$	6.028	6.280	6.521	5.706	5.934	6.184	6.322	6.559	6.839
L_{WL} , ft					406.7				
L_{BP} , ft					400.0				
L_E/L_{BP}					0.290				
L_X/L_{BP}					0.300				
L_R/L_{BP}					0.410				
C_B					0.800				
C_X					0.994				
C_P					0.805				
C_{PF}					0.861				
C_{PA}					0.750				
C_{PE}					0.761				
C_{PR}					0.695				
C_{PV}					0.920				
C_{PVF}					0.971				
C_{PVA}					0.867				
C_W					0.871				
C_{WF}					0.881				
C_{WA}					0.860				
C_{IT}					0.776				
LCB, % LBP from 					2.5F				

Table 38 - Propellers Used on Series 60 Models

Propeller Number	D (ft)	P (ft)	P/D	MWR	EA/DA	BTF	Rake (deg)	Number of Blades
2452	27.66	30.88	1.116	0.237	0.503	0.047	8.78	4
2501	18.88	15.50	0.822	0.225	0.458	0.055	6.10	4
2502	20.00	23.81	1.190	0.203	0.415	0.042	15.00	4
2765	16.10	17.80	1.105	0.280	0.576	0.056	9.46	4
2813	16.90	19.65	1.162	0.280	0.582	0.056	9.46	4
2815	17.50	19.35	1.106	0.270	0.550	0.049	4.00	4
2828	26.82	27.08	1.010	0.220	0.456	0.042	5.014	4
2837	14.13	10.60	0.750	0.245	0.513	0.042	7.67	4
2944	22.00	18.70	0.850	0.279	0.588	0.047	4.761	4
3156	29.14	29.58	1.015	0.250	0.531	0.050	7.765	4
3375	21.36	20.30	0.950	0.255	0.536	0.045	6.00	4
3376	24.00	26.40	1.100	0.237	0.500	0.045	6.00	4
3377	25.82	23.75	0.920	0.213	0.450	0.045	6.00	4
3378	22.40	24.08	1.075	0.261	0.550	0.045	6.00	4
3379	24.89	25.51	1.025	0.225	0.475	0.045	6.00	4
3380	23.20	25.52	1.100	0.235	0.525	0.045	6.00	4
3446	24.60	25.07	1.019	0.204	0.428	0.048	4.35	4
3471	26.06	29.94	1.149	0.250	0.512	0.052	7.50	4
3488	17.52	18.33	1.046	0.229	0.477	0.048	6.33	4
3563	30.55	29.02	0.950	0.210	0.446	0.045	6.00	4
3564	15.00	14.25	0.950	0.261	0.554	0.045	6.00	4
3565	21.00	21.00	1.000	0.239	0.506	0.046	6.00	4
3645	19.25	19.25	1.000	0.259	0.549	0.045	6.00	4
3646	14.54	14.54	1.000	0.259	0.550	0.045	6.00	4
3647	15.48	12.77	0.825	0.258	0.548	0.045	6.00	4
3648	18.06	14.90	0.825	0.258	0.548	0.045	6.00	4

CHAPTER IX

DESIGN CHARTS

The resistance and propulsion results for ships exactly similar to each of the 45 models of the geometrical series have been given in Chapter VIII. This form of presentation is not very useful to the designer, however, since he will almost always have to do some interpolation to fit his particular problem of the moment. A great deal of thought was given to the most desirable method of plotting these data so as to make them of the greatest value and yet simple to use. It was finally decided to present the resistance information in the form of contour charts similar to those made so familiar by Taylor.

To reduce the data to this form presented a formidable proposition in fairing since there were 45 models in all and contours had to be drawn for a number of values of $\frac{V}{\sqrt{LWL}}$ and (K) . To expedite this phase of the work, the fairing was done on the UNIVAC computer in the Applied Mathematics Laboratory at Taylor Model Basin. The process is described in detail in Appendix C. The contours are given in Appendix B.

The first set shows contours of residuary resistance in pounds per ton of displacement

$\left(\frac{R_R}{\Delta}\right)$, each individual chart showing, for given values of $\frac{B}{H}$ and $\frac{V}{\sqrt{LWL}}$, the variation of $\frac{R_R}{\Delta}$ with block coefficient and $\frac{L}{B}$ ratio.

The second set is of the same kind but shows contours of (C) for a ship with LBP of 400 ft against C_B and $\frac{L}{B}$ for chosen values of (K) and $\frac{B}{H}$.

The third set gives contours of wake and thrust deduction fractions plotted against C_B and $\frac{L}{B}$ for chosen values of $\frac{V}{\sqrt{LWL}}$ and $\frac{B}{H}$.

Both the $\frac{R_R}{\Delta}$ and the (C) values have been derived on the basis of the Froude assumption that the total resistance can be divided into two parts, the skin friction of an "equivalent plank" and the residuary resistance, the latter obeying Froude's Law of Comparison. In the present work, the skin friction resistance for both model and ship has been calculated in accordance with the ATTC 1947 line, the appropriate values of C_F and Reynolds number being taken from previous Model Basin reports.^{59,60}

In using the first set of contours, the value of $\frac{R_R}{\Delta}$ is first determined for the desired speed-length ratio. To it must be added the frictional resistance, which can be expressed in the form $\frac{R_F}{S}$, where S is the wetted surface. The total resistance is then

$$R = \frac{R_R}{\Delta} \cdot \Delta + \frac{R_F}{S} \cdot S$$

To simplify the use of the contours, a nomograph is given in Appendix B from which the frictional resistance per square foot of wetted surface $\frac{R_F}{S}$ can be determined. Contours are also given for estimating the wetted surface for any combination of design parameters.

The \textcircled{C} - \textcircled{K} contours are for the total resistance, residuary plus frictional, and the \textcircled{C} values are those appropriate to a ship of 400 ft *LBP*. For any other length, a correction must be made which depends upon the actual length and the wetted surface coefficient $\frac{S}{\nabla^{2/3}}$.

For those who wish to compare the Series 60 \textcircled{C} values with those of other models in which the Froude values of O_m and O_s have been used in the analysis, a rapid method of making the conversion has been given by Gertler.⁴⁷ See also Appendix D.

In the \textcircled{C} charts and the nomograph for determining $\frac{R_F}{S}$, an allowance for ship correlation amounting to +0.0004 has been made in accordance with the ATTC 1947 recommendation. Calculation forms for finding the \textcircled{C} 400 ft and ehp values for any single-screw merchant ship having lines derived from the Series 60 contours and proportions within the range covered by the Series are also given in Appendix B. Methods are also described there for calculating \textcircled{C} for a ship of other than 400-ft length and for including a ship correlation allowance C_A having some value different from +0.0004. Although the calculation forms are largely self-explanatory, a numerical example is worked out in Appendix D to clear up any difficulties still remaining after reading the text.

As stated on page V-14 the ITTC agreed in 1957 to the use of a new "model-ship correlation line" in future published work. However, pending some agreement on a standard ship correlation allowance to be associated with the new line, it has not yet come into general use. The ITTC and ATTC lines differ both over the model and ship ranges of Reynolds number, and so affect the division of the model resistance into its "frictional" and "residuary" components, as well as the values of the corresponding ones for the ship. It is thus not merely a question of using different values of R_F ; all the values of residuary resistance $\frac{R_R}{\Delta}$ will be different also. Some notes and an additional nomograph are given in Appendices D and E for readers who may wish to make estimates using the ITTC line.

CHAPTER X

EFFECT OF VARIATIONS IN PROPELLER DIAMETER AND SHIP DRAFT AND TRIM

A propeller diameter equal to 0.70 of the designed load draft was adopted as a standard in the *LCB* and geometrical variation series. Although this is fairly representative of average practice, there will be many occasions on which a different diameter will be necessary because of the design of machinery used or for other reasons. In order to give some guidance on this matter, each of the five parent models of Series 60 was run with additional propellers having diameters smaller and larger than the standard.

Also, the main test program covered the models only at the full load draft and level trim. To get some information on the performance at other displacements and trims, additional experiments were made on three of the parent models, those with C_B of 0.60, 0.70, and 0.80.

The stern arrangement was identical with that already described in Chapter VII and shown in Figure 36. The vertical dimensions are given there as functions of the designed draft or propeller diameter, and all longitudinal dimensions are given as functions of *LBP*. The propeller position is so defined that the generating line at 0.70 radius is 0.94 percent of the *LBP* forward of the after perpendicular. The stern details are therefore defined completely regardless of the selection of design draft or propeller diameter, so that Figure 36 defines the arrangement for all the models. The clearances were rather larger than normal practice at the time, but this was considered desirable in view of the ever-increasing horsepower of single-screw ships, and their use has been justified by later developments.

One method of achieving larger clearances or, alternatively, of using a larger diameter propeller without sacrificing clearance is to fit a semi-balanced rudder and no rudder shoe. This arrangement was fitted to the MARINER ships, and has become known as a "clearwater stern," which is now used on many seagoing ships. In the course of the propulsion tests, the opportunity was taken to run the 0.60 C_B model with such a stern arrangement for comparison with the normal streamlined rudder results.

The standard propellers for the parent models had a diameter equal to 0.7 of the draft and have already been described in Chapter VII. For the experiments with larger and smaller diameters, propellers as similar as possible to the Troost type were selected from stock. The selection was made on a basis of general similarity, and the actual diameters of the propellers departed somewhat from the desired values.

The selection of propeller characteristics was based on the assumption that diameter was fixed and revolutions could be chosen to obtain maximum efficiency. The values of expanded-area ratio were selected on the basis of current design practice and checked for suitability as to cavitation by Lerb's data.⁴⁹

Table 39 - Particulars of 600-Ft Ships Corresponding to Series 60 Models

C_B	0.60			0.65			0.70			0.75			0.80		
LBP, ft	600.0			600.0			600.0			600.0			600.0		
B, ft	80.0			82.76			85.71			88.89			92.31		
H, ft	32.0	26.5**	20.6	33.14	----	----	34.29	28.0**	21.6†	35.55	----	----	36.93	30.0**	22.8†
Δ , tons	26349	21080	15810	30547	----	----	35289	28230	21170	40662	----	----	46774	37420	28060
$\frac{L}{B}$	7.5			7.25			7.0			6.75			6.50		
$\frac{B}{H}$	2.50	3.02	3.88	2.50	----	----	2.50	3.06	3.97	2.50	----	----	2.50	3.08	4.05
$\frac{LCB^*}{L}$	0.515	----	----	0.505	----	----	0.495	----	----	0.485	----	----	0.475	----	----
Propeller Number	2422	3378	3375	2852	3380	3375	2852	3376	2965	2828	3379	3066	3648†	1356	3377
D, ft	25.62	22.40	21.37	26.40	23.20	21.37	26.40	24.00	22.00	26.83	24.89	23.00	18.06	27.00	25.82
P, ft	25.62	24.08	20.30	26.61	25.52	20.30	26.61	26.40	20.75	28.23	25.51	22.24	14.90	24.52	23.75
P/D	1.00	1.075	0.95	1.008	1.100	0.95	1.008	1.100	0.943	1.052	1.025	0.967	0.825	0.908	0.929
BAR	0.456	0.550	0.536	0.454	0.525	0.537	0.454	0.500	0.519	0.456	0.475	0.515	0.548	0.448	0.450
BTF	0.044	0.045	0.045	0.047	0.045	0.045	0.047	0.045	0.056	0.042	0.045	0.055	0.045	0.044	0.045
Rake, deg	6.5	6.0	6.0	4.76	6.0	6.0	4.76	6.0	7.71	5.0	6.0	5.38	6.00	3.75	6.00
Number of Blades	4	4	4	4	4	4	4	4	4	4	4	4	4	4	4
Blade area sqft	235	216	192	248	222	192	248	226	197	258	231	214	140	257	236
Note: * $\frac{LCB}{L}$ Measured from forward perpendicular † Previously used on Model 4278 ** Trim by stern = 1 percent LBP ‡ Previously used on Models 4265, 4275 † Trim by stern = 2.5 percent LBP															

The details of the propellers and hulls referred to a ship length of 600 ft LBP are shown in Table 39. In fitting the different diameter propellers, the shaft centerline was altered vertically to maintain the same vertical position of the blade tips at their lowest point in the disk, and so also the same minimum clearance between blade tips and the rudder shoe. This was considered to be the more practical approach rather than fitting all propellers to the same shaft elevation. In the latter case, the hull lines would have to be adapted to the largest propeller, with excessive clearances for the smaller ones, and with these any advantage in resistance which might result from a lower and longer cruiser stern would be lost. The end lines from Station 18 aft were modified to suit the different apertures, and the rudder area was kept constant by narrowing the rudders associated with the larger diameter propellers.

The stern lines and aperture arrangements are shown in Figures 41 through 45, and the curves of power, wake, thrust deduction and other data in Figures 46 through 50. These figures all apply to ships of 600 ft LBP, as in the case of Chapters VII and VIII. The extrapolation used was the ATTC 1947 line, with a ship correlation allowance of +0.0004. During these tests, which chronologically were run before the LCB and geometrical variation series, turbulence was stimulated by studs and no bilge keels were fitted. The propulsion

(Text continued on page X-11.)

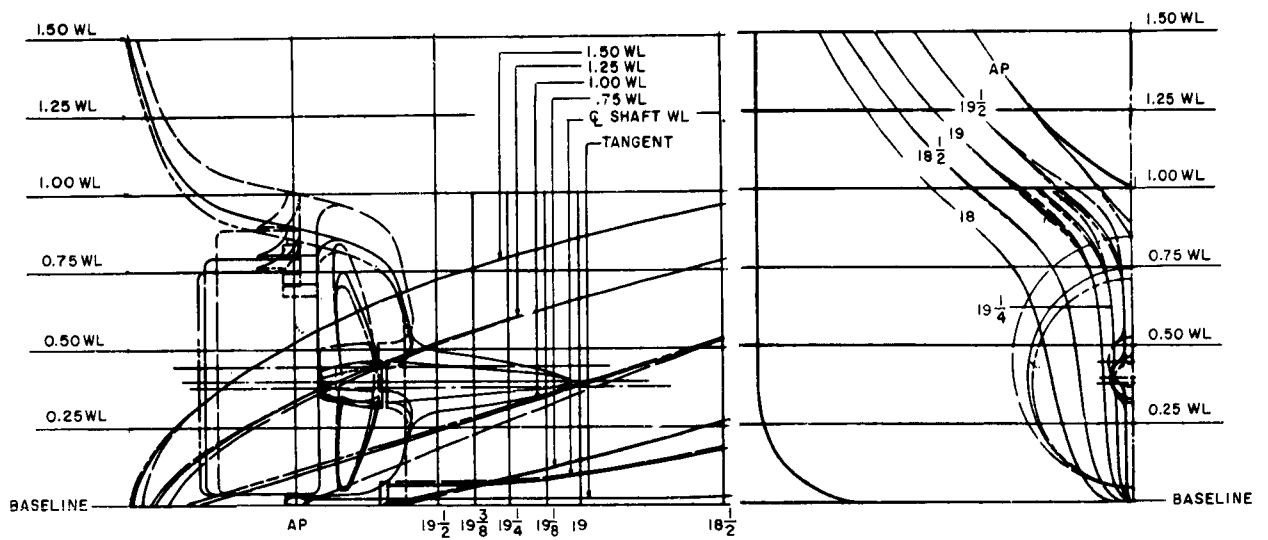


Figure 41 – Stern Lines for Propeller Diameter Variations, 0.60 Block Parent (Model 4210)

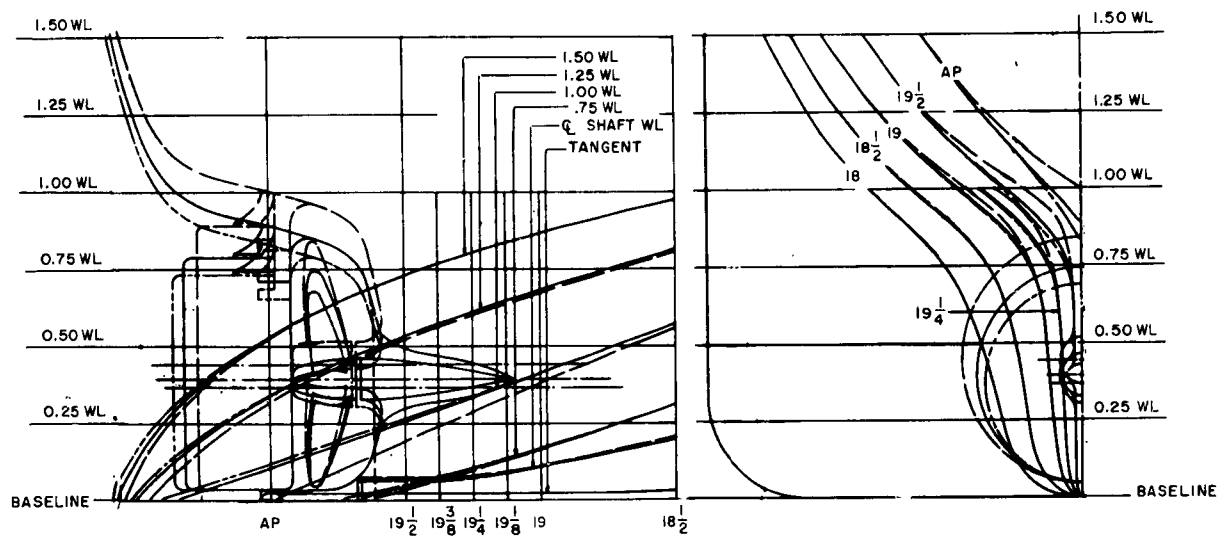


Figure 42 – Stern Lines for Propeller Diameter Variations, 0.65 Block Parent (Model 4211)

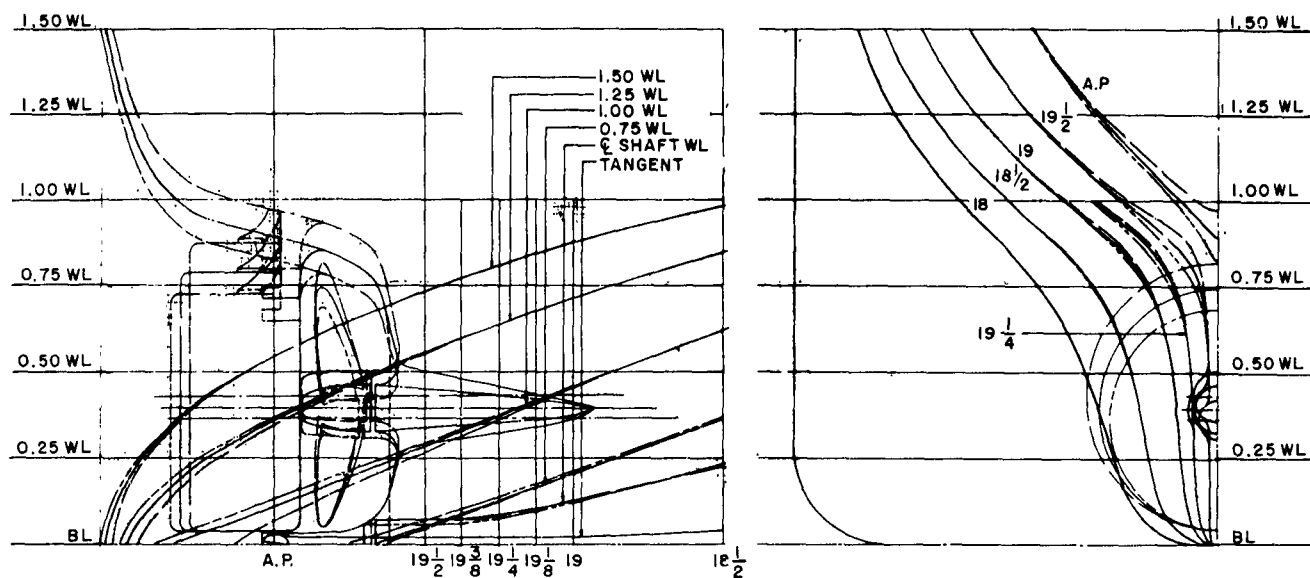


Figure 43 – Stern Lines for Propeller Diameter Variations, 0.70 Block Parent (Model 4212)

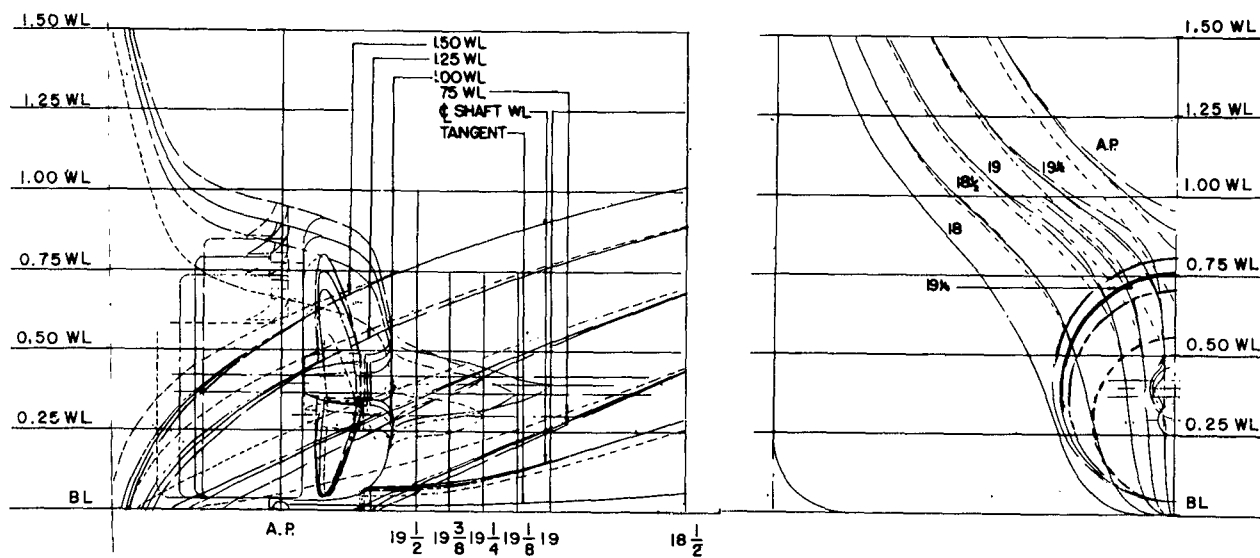


Figure 44 – Stern Lines for Propeller Diameter Variations, 0.75 Block Parent (Model 4213)

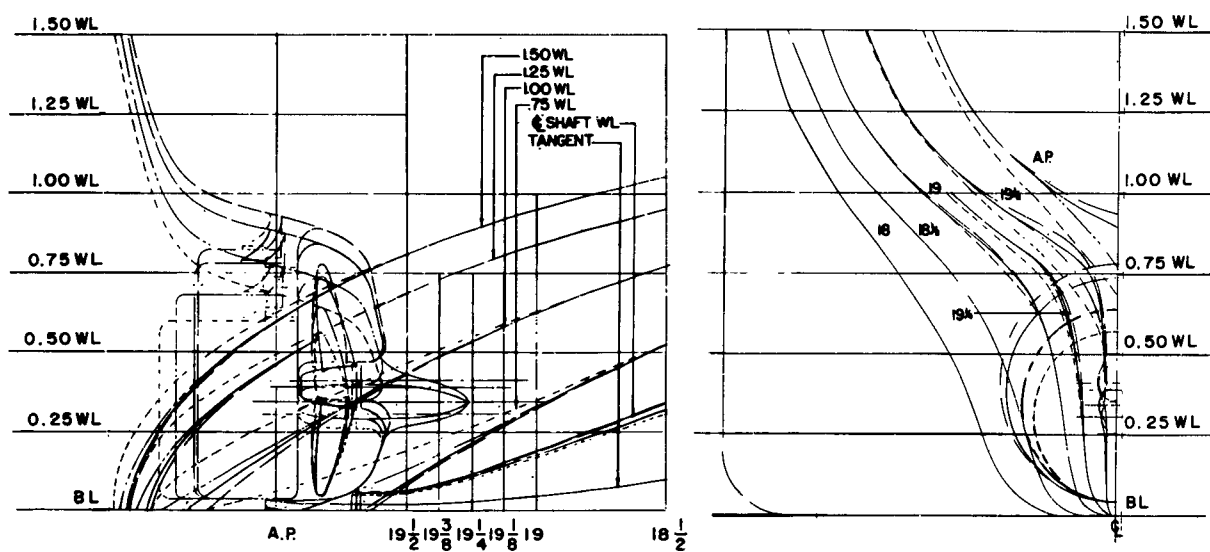


Figure 45 – Stern Lines for Propeller Diameter Variations, 0.80 Block Parent (Model 4214)

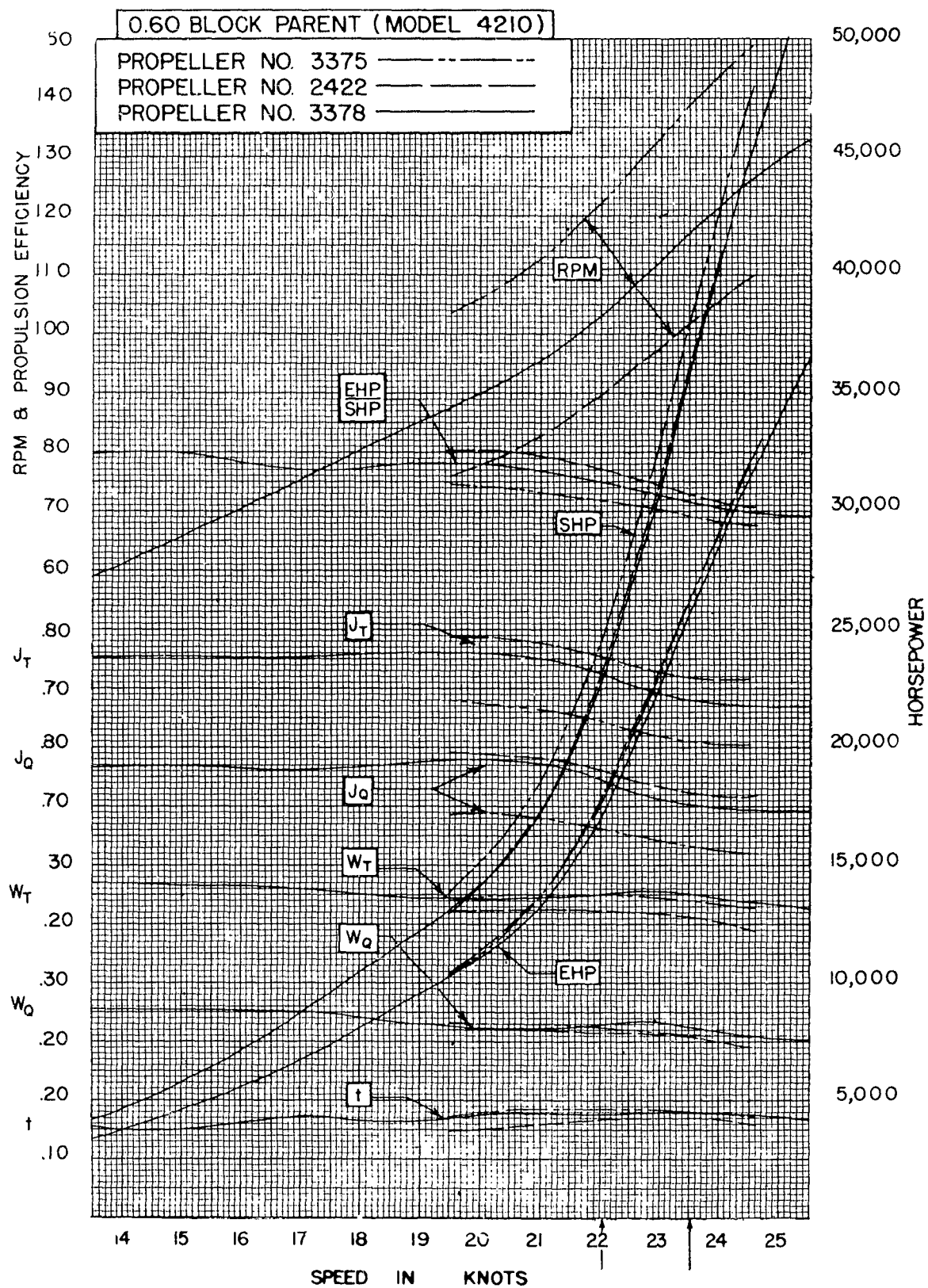


Figure 46 - Power, RPM, and Coefficient Curves for 0.60 Block Parent, at Even Keel and Designed Displacement-Model 4210

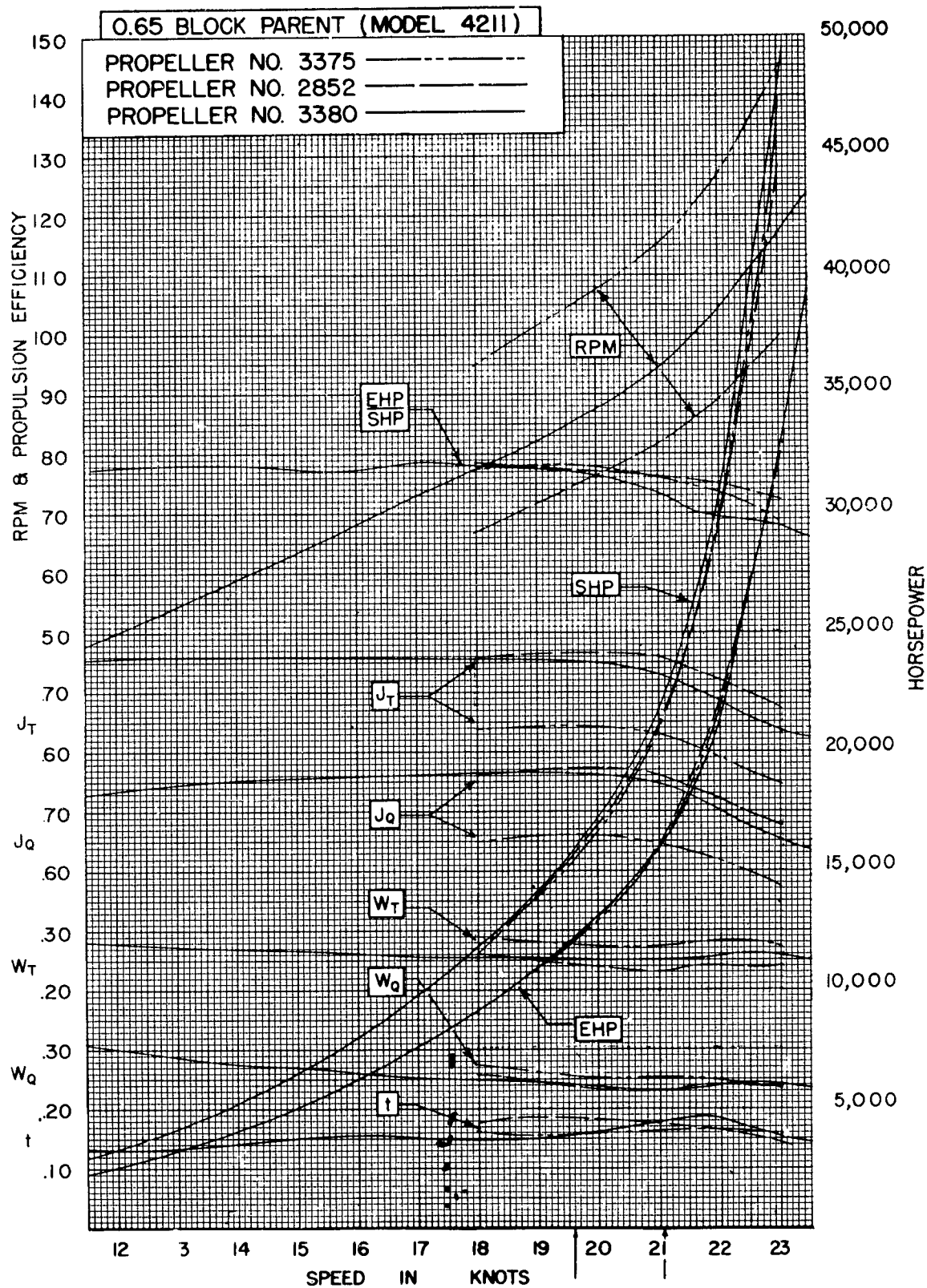


Figure 47 - Power, RPM, and Coefficient Curves for 0.65 Block Parent, at Even Keel and Designed Displacement—Model 4211

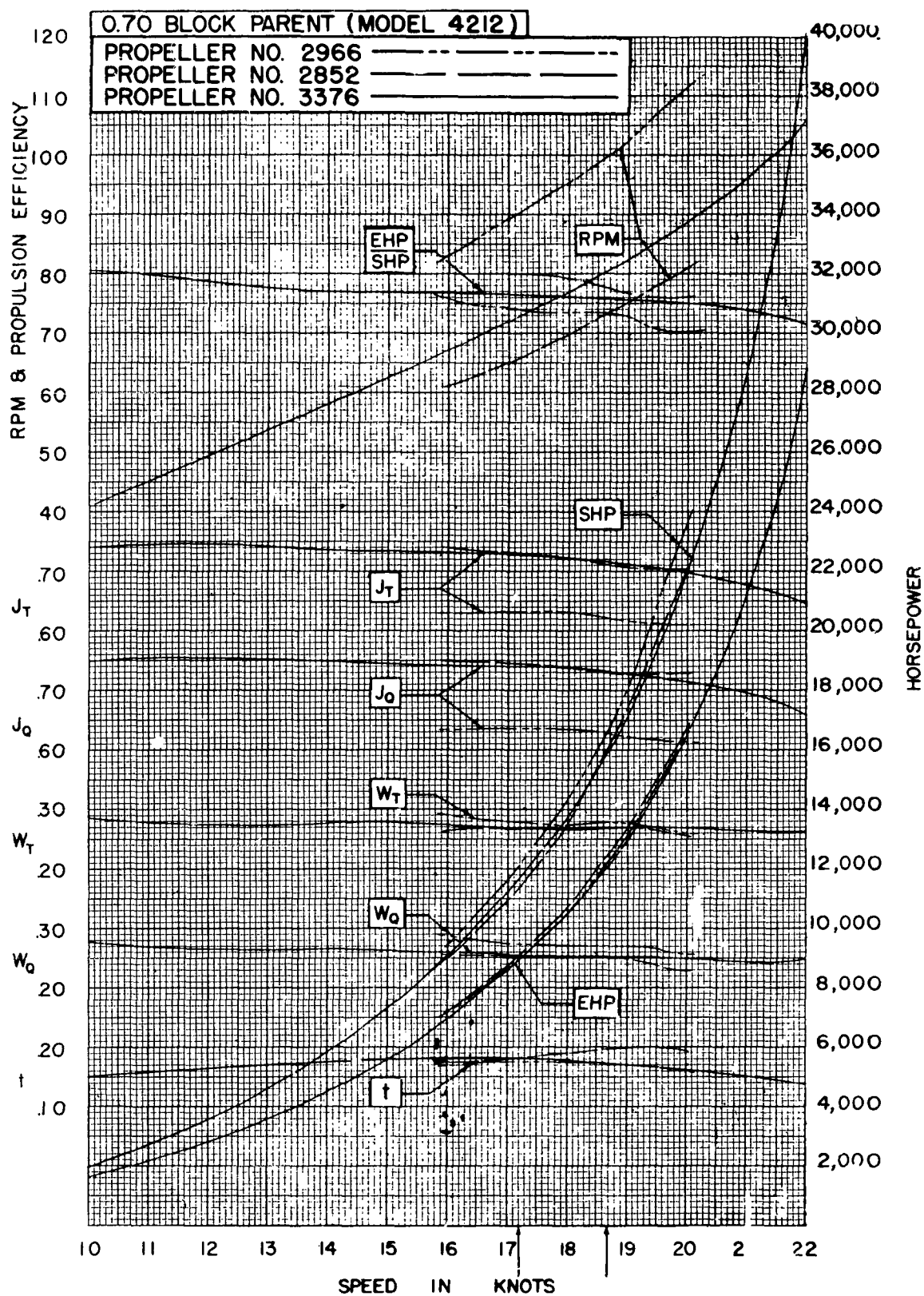


Figure 48 – Power, RPM, and Coefficient Curves for 0.70 Block Parent, at Even Keel and Designed Displacement—Model 4212

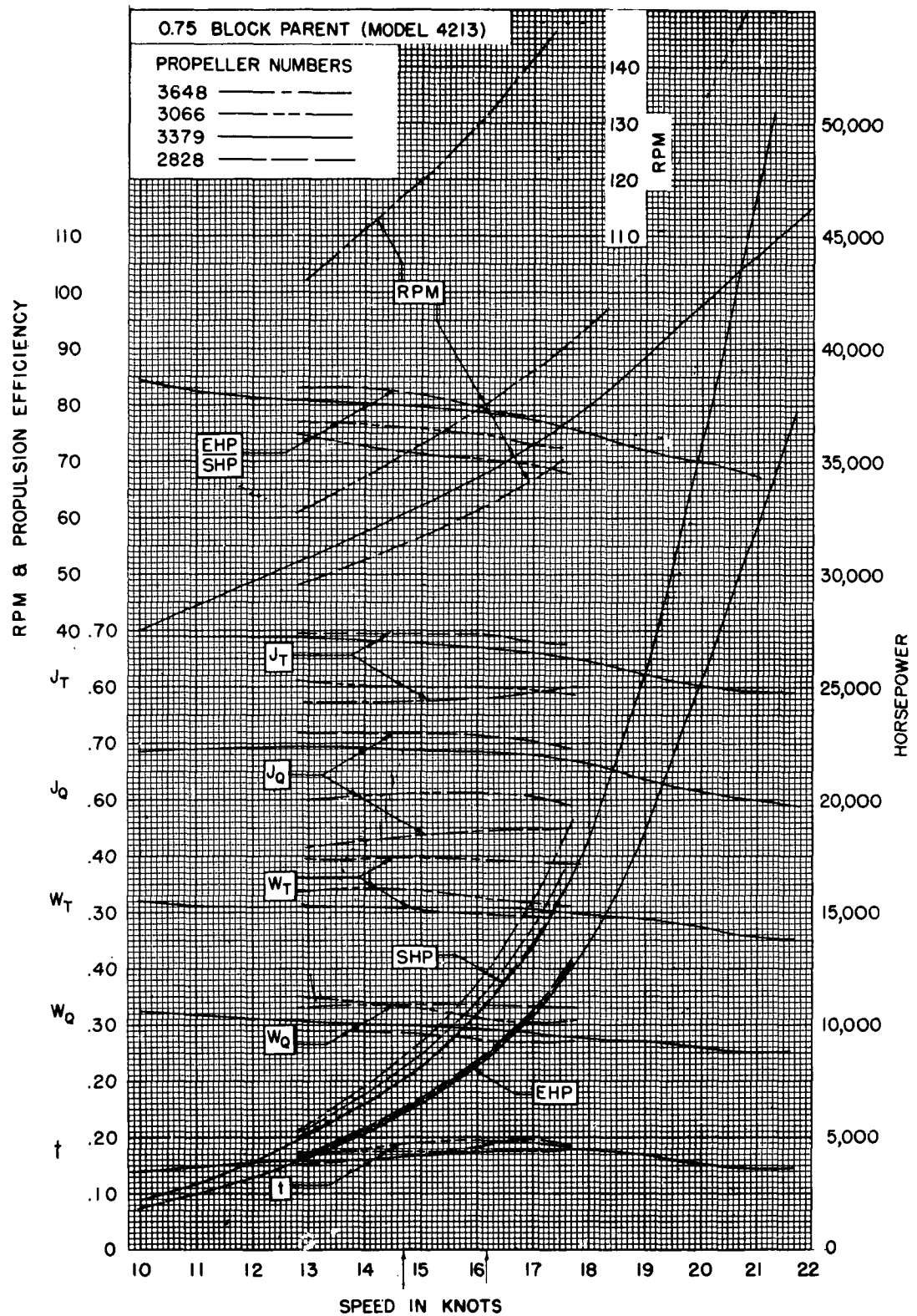
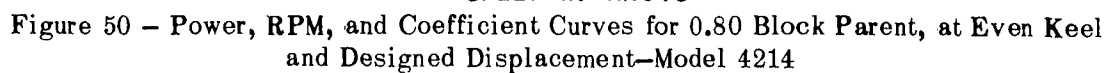


Figure 49 - Power, RPM, and Coefficient Curves for 0.75 Block Parent, at Even Keel and Designed Displacement—Model 4213



tests on the parent models with the propellers of standard diameter ($= 0.7H$) were run over a complete speed range, and those with the larger and smaller diameters were made only from speeds 10 percent below the service speed to 10 percent above the trial speed.

The three parent models of 0.60, 0.70, and 0.80 C_B were run at two lighter conditions, with the standard propellers of diameter equal to $0.7H$ only. The conditions chosen were 60 and 80 percent of the load displacement. With the models in the lighter of these conditions, the propellers were just submerged at a speed about 10 percent below the service speed; this was considered essential if reliable wake data were to be obtained. In addition to tests on even keel, the models were also run at 80 percent of load displacement with a trim of 1 percent of the *LBP* by the stern and at 60 percent of load displacement with a trim of 2.5 percent by the stern. These were chosen after reference to much data in the records of the Maritime Administration. The results of the propulsion tests in these conditions are shown in Figures 51 through 53.

Figure 54 shows the variation with diameter in the values of the propulsive coefficient and its various components for the five parent models. The trial and service speeds used throughout the presentation of these propulsion experiments are those derived on the Alexander basis given in Equation (1), page V-14. The wake fraction shown is the Taylor wake fraction calculated on the basis of thrust identity in open and behind the model. Having obtained actual wake fractions from these model experiments, estimates were made from the Troost design charts for Troost-type propellers for all the different conditions in which stock propellers had been used. These showed that any increase in propeller efficiency which would result from such a change was quite small—on the average less than 0.5 percent, the maximum being 1.1 percent.

Figure 55 shows the propulsive efficiency factors plotted against block coefficient. Figure 55b for the standard propellers represents actual test data. The results given in Figures 55a and 55c are for the smaller and larger diameter propellers, respectively, modified to suit the variation of diameter with block coefficient shown in Figure 56.

Similar curves for the 80- and 60-percent displacement conditions are shown in Figure 57. In the 60-percent condition for the 0.60 C_B model, even keel, there was some indication that air was being drawn into the propeller, and it is significant that the wake curve for this model appears to be inconsistent with the other data.

The principal reasons for running the experiments described in this section were to compare the propulsive performance of the parents with existing modern designs of ships and to give the practicing naval architect guidance on the general effects on propulsive efficiency of changes in propeller diameter, in ship displacement, and in trim.

As to the first of these, comparisons were made between models of the SCHUYLER OTIS BLAND and PENNSYLVANIA and their Series 60 counterparts. The corresponding pairs of models were run under as nearly similar conditions as possible. Thus the Series 60 sterns were modified to give the same aperture and rudder arrangements as in the actual

(Text continued on page X-18.)

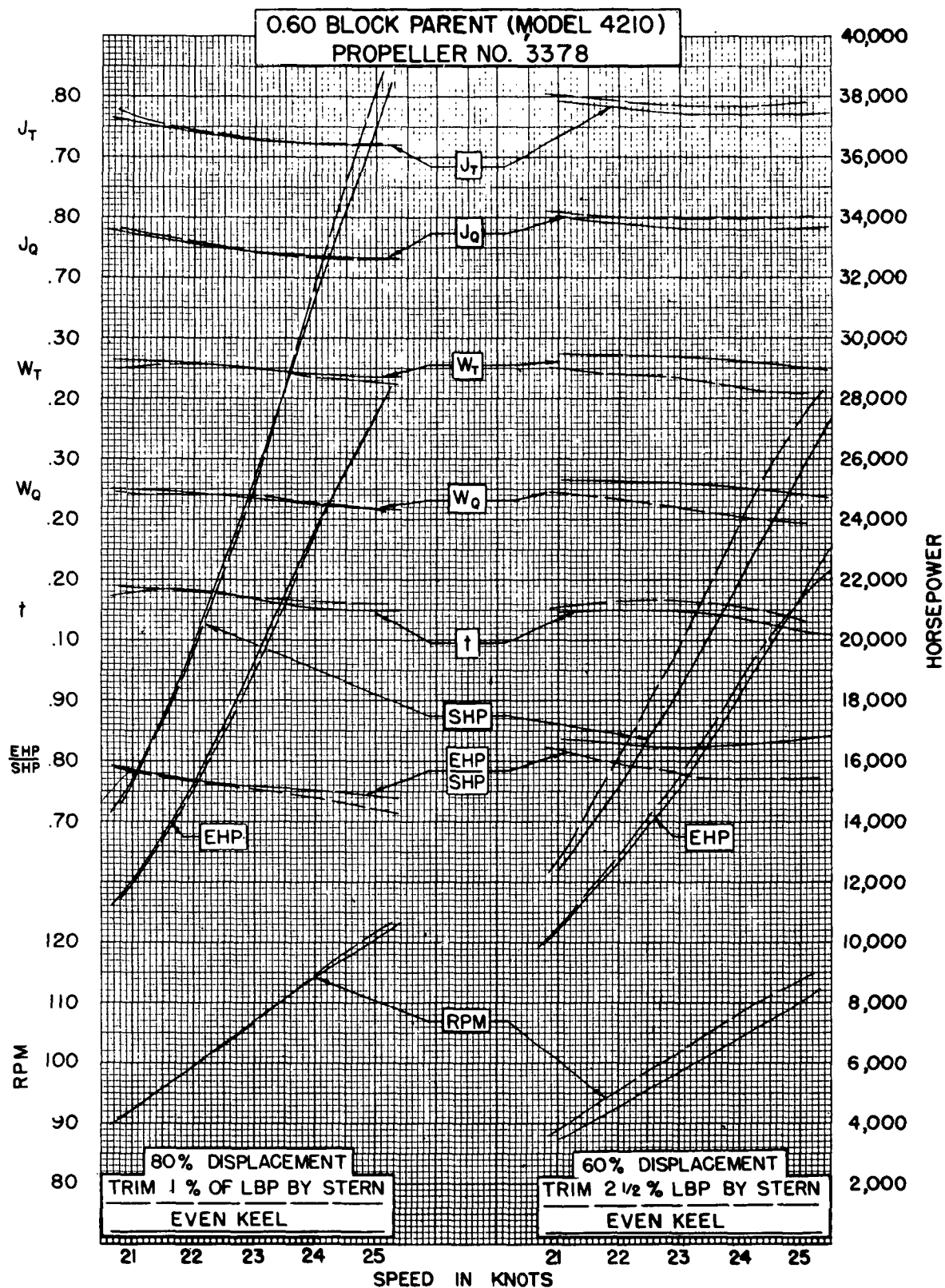


Figure 51 - Power, RPM, and Coefficient Curves for 0.60 Block Parent at Light Displacement Conditions

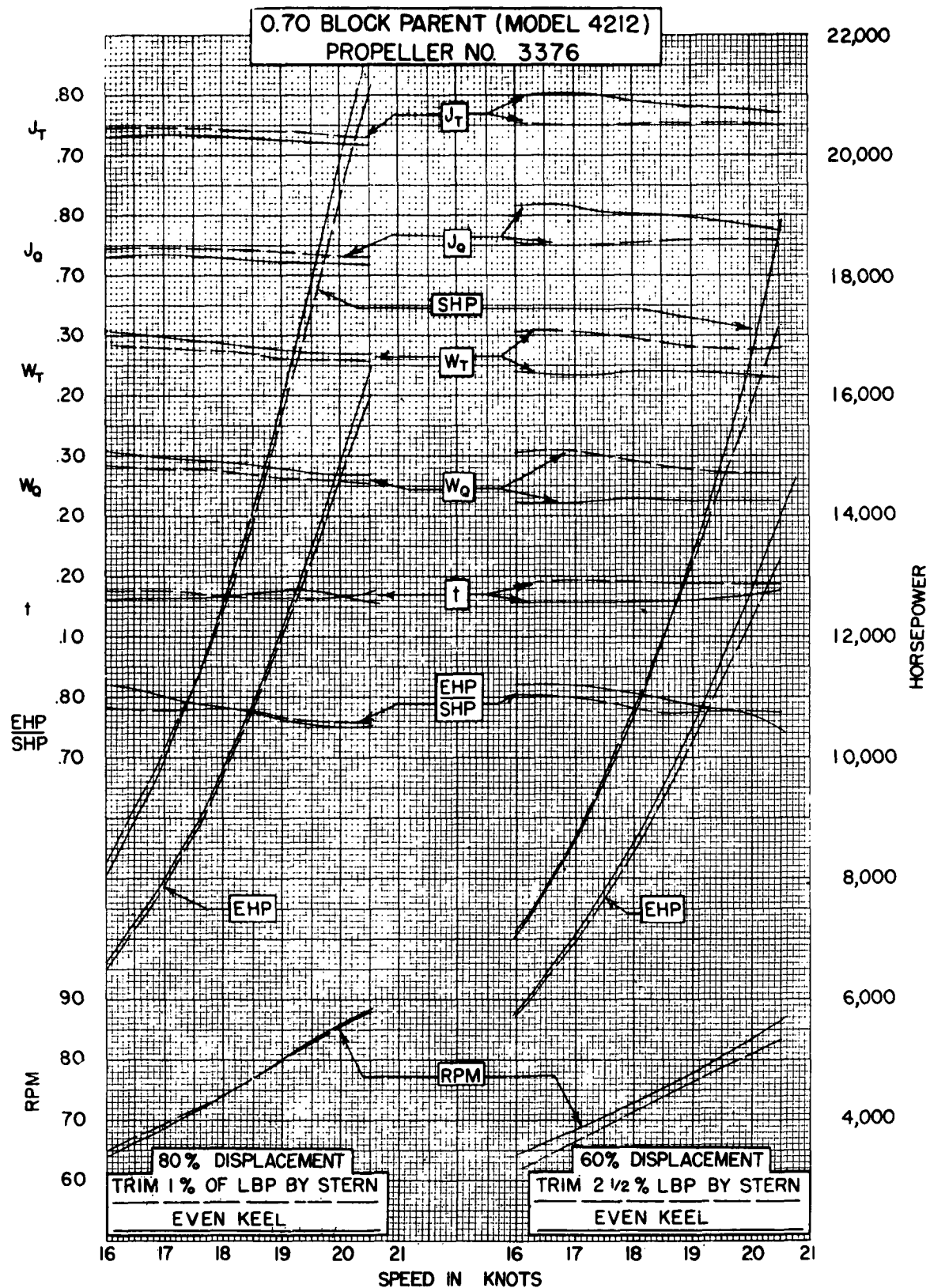


Figure 52 – Power, RPM, and Coefficient Curves for 0.70 Block Parent at Light Displacement Conditions

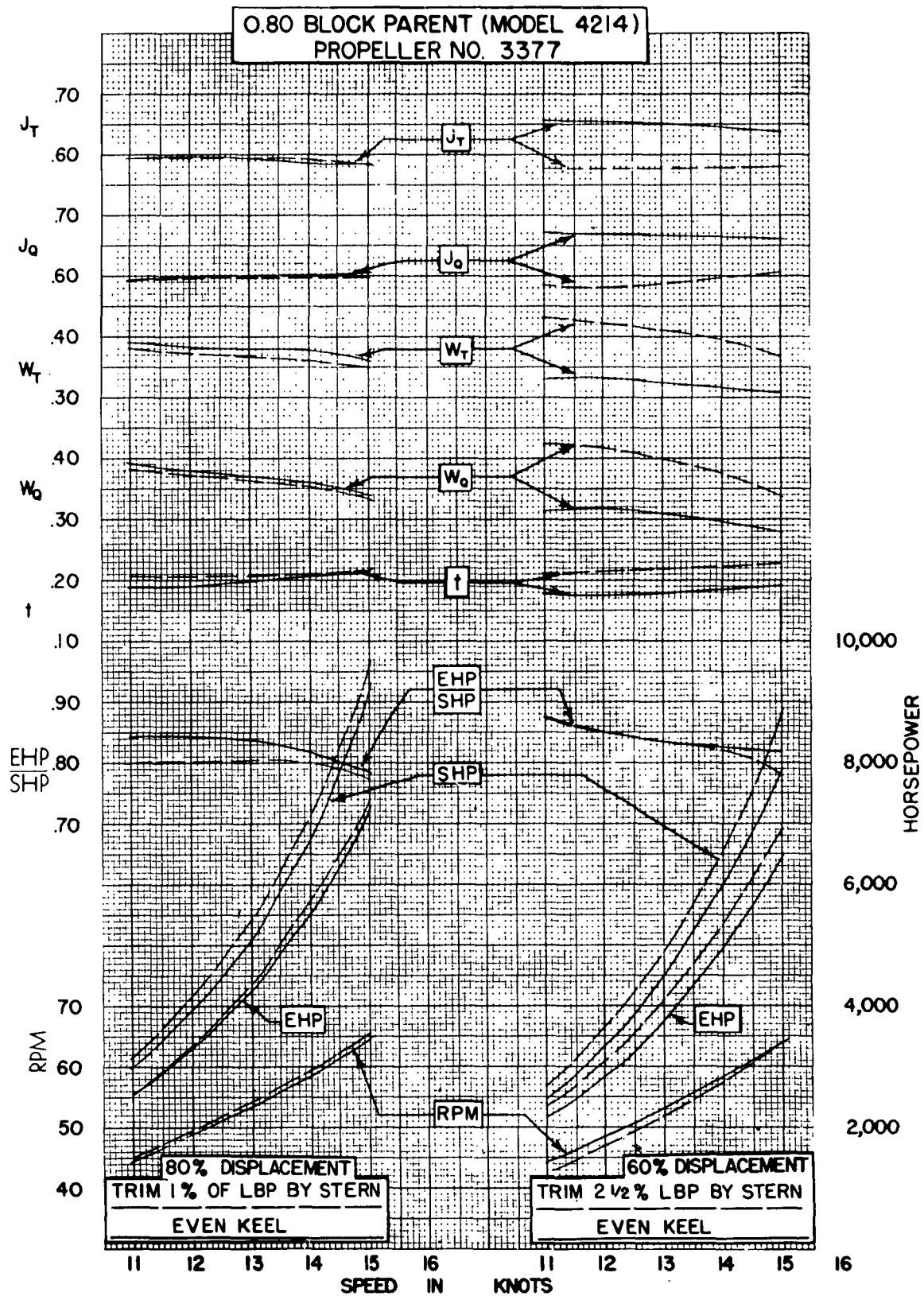


Figure 53 - Power, RPM, and Coefficient Curves for 0.80 Block Parent at Light Displacement Conditions

Figure 54 - Propulsive Efficiency Factors versus Diameter

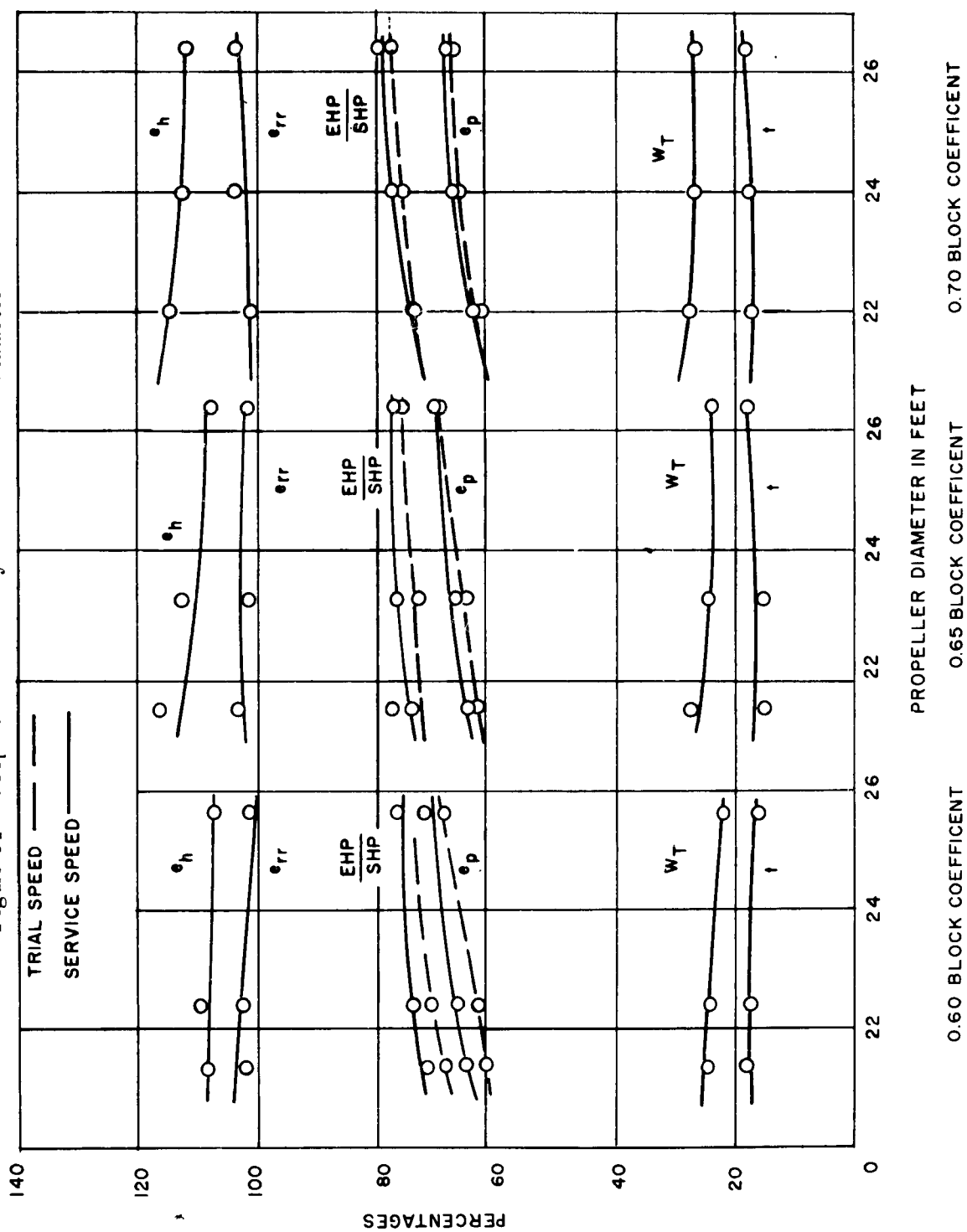


Figure 54a - 0.60, 0.65, and 0.70 Block Coefficients

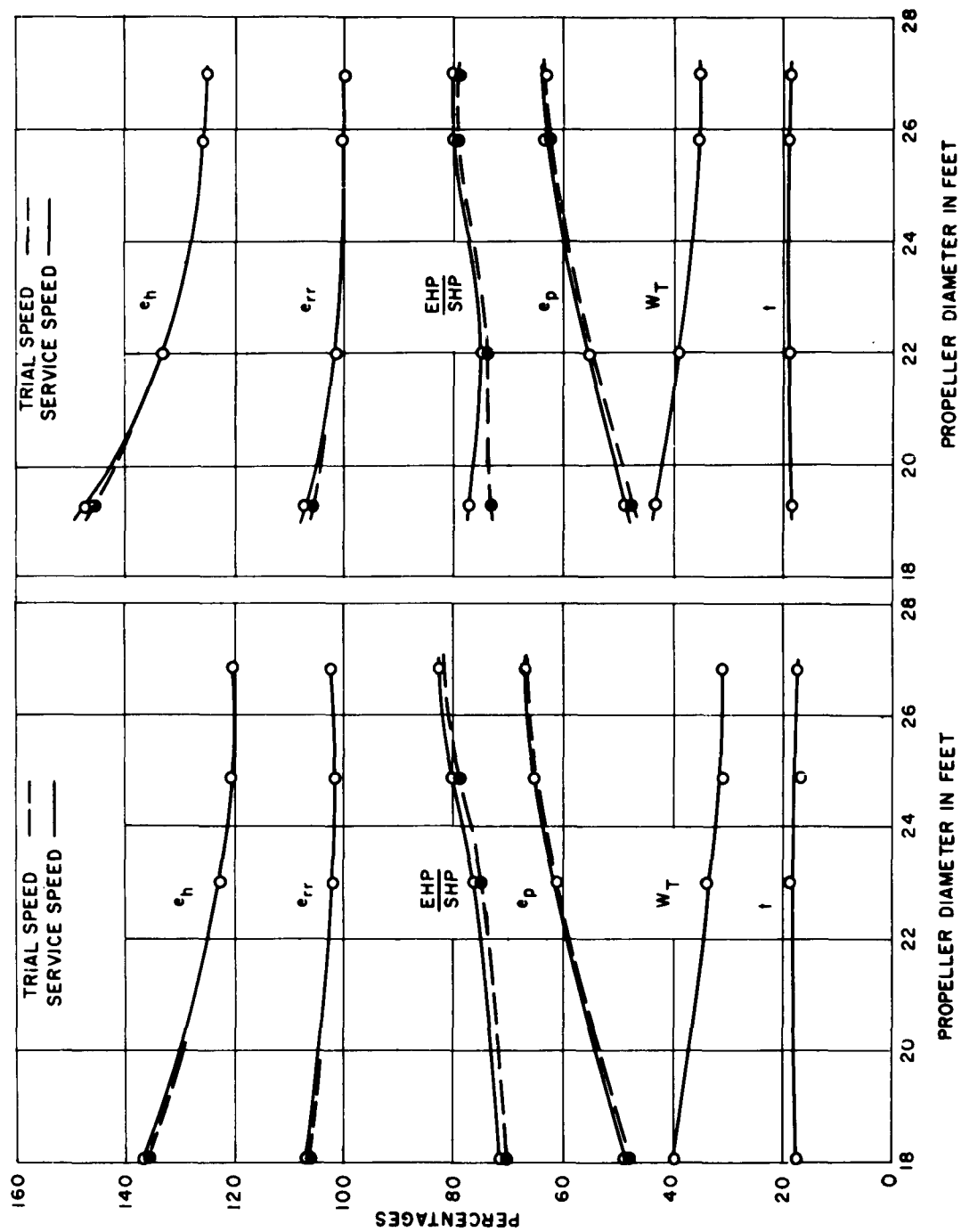


Figure 54b - 0.75 and 0.80 Block Coefficient

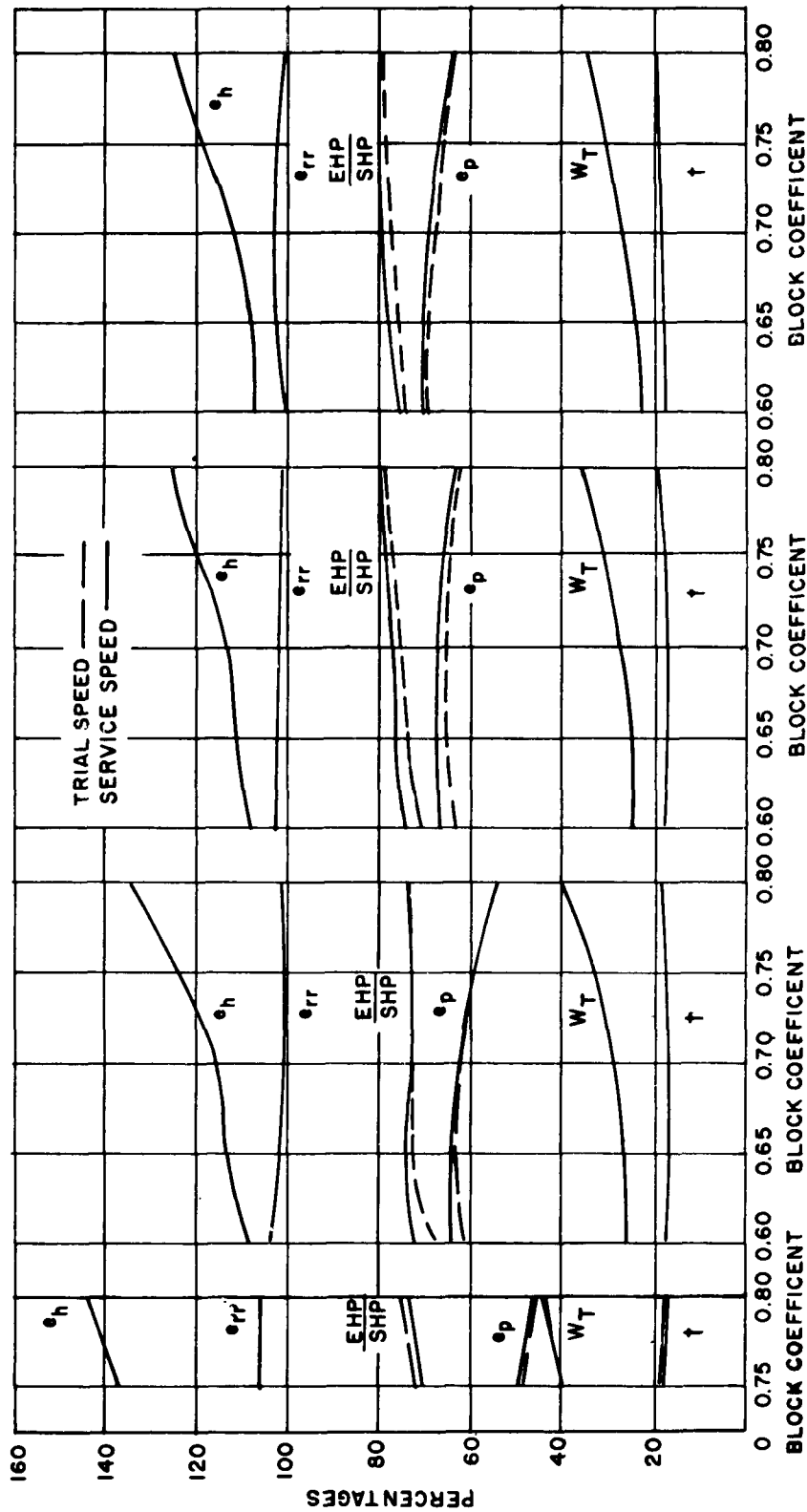


Figure 55a -- For Small Diameter

Figure 55b -- For Normal Diameter

Figure 55c -- For Large Diameter

Figure 55 -- Propulsive Efficiency Factors versus Block Coefficient

TABLE 40
Comparison of Series 60 Propulsion Results with Actual Ships

Model	4468-3	4057	4484-1	4133-2
Representing	Series 60 Equivalent of PENNSYLVANIA	PENNSYLVANIA as Built	Series 60 Equivalent of SCHUYLER OTIS BLAND	SCHUYLER OTIS BLAND as Built
V , knots	15.37	15.37	18.20	18.20
shp	9200	8850	8750	8900
ehp/shp	0.739	0.750	0.784	0.760
e_h	1.231	1.199	1.092	1.076
e_p	0.603	0.616	0.690	0.696
e_{rr}	0.995	1.016	1.040	1.015

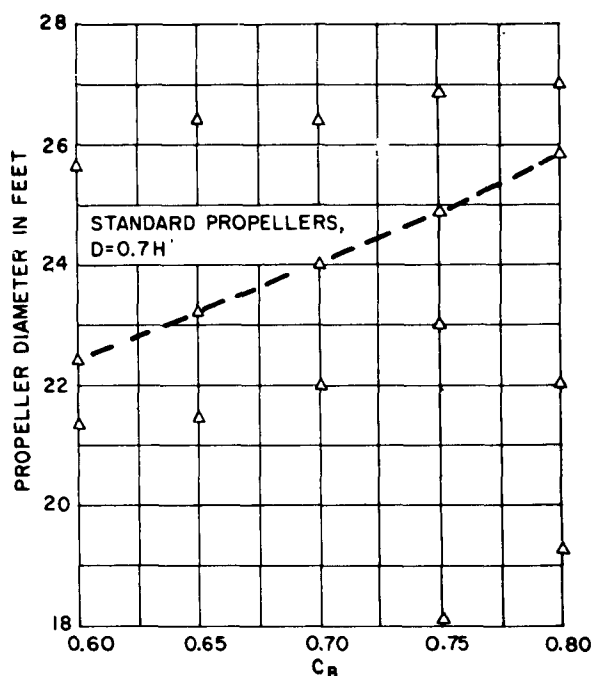


Figure 56 — Variation of Diameter with C_B

draw any overall conclusions regarding the variation of the propulsive factors. The data given can be applied to individual designs or used by the naval architect for his own research purposes to set up his own methods of estimating such coefficients for future use. Much additional information is included in Reference 61 for those who wish to study this part of the work in more detail.

ships, and the model propellers used were made to the designs fitted to the ships. The results given in Table 40 show that the performance of the Series 60 designs was very comparable with that of the two ships.

The designer can find the wake and thrust deduction fractions for any ship within the limits of the series and fitted with the standard diameter of propeller from the contours in Appendix B. The results given in this chapter will enable him to make estimates of the probable change in these and other factors when it is necessary or desirable to use larger or smaller propellers, and also for conditions of lighter displacement with or without trim.

It is not intended here to attempt to

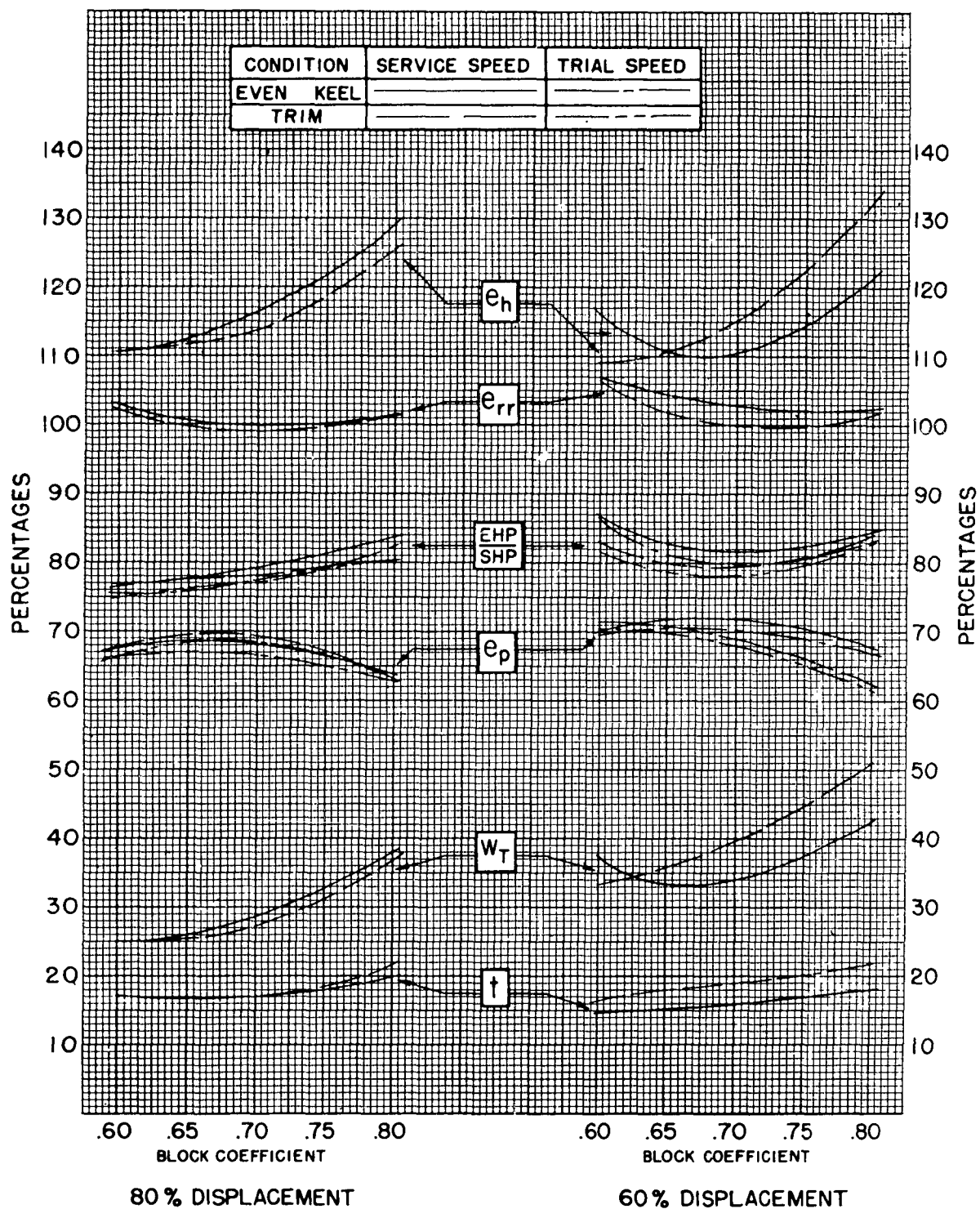


Figure 57 – Propulsive Efficiency Factors at Light Displacements

One other comparison made in the course of these tests is of general interest. A number of modern single-screw ships, including the MARINER class, have been fitted with a semi-balanced rudder and no rudder shoe. This arrangement enables a larger diameter propeller to be fitted without sacrifice of clearances or, conversely, larger clearances on the same diameter, both very desirable features in view of the large powers now being transmitted through a single shaft and the accompanying risk of propeller-excited vibration. In the endeavor to obtain such clearances with the normal single-screw aperture and rudder, the rudder shoe has become longer and more vulnerable, and a number of fractures have occurred, so that on this score also the new arrangement, generally known as a "clearwater stern," has something to offer.

The stern arrangements of the Series 60 parent of 0.60 C_B with the normal and clearwater sterns are shown in Figure 58, and the results of the model propulsion tests in Figure 59 and Table 41.

At a service speed of 22 knots, there is no noticeable difference in propeller performance.

The shp is higher for the conventional stern only because of its higher ehp, and this persists throughout the speed range.

TABLE 41
Comparison of Clearwater and Conventional Sterns
on 0.60 C_B Model 4210 of Series 60

(Principal dimensions: 600 ft \times 80 ft \times 32 ft \times 26,349 tons)

Stern Arrangement	Normal	Clearwater
Propeller Number	2422	1967
D , ft	25.62	25.33
P , ft	25.62	26.67
BAR	0.456	0.464
Rake, deg	6.5	6.0
Number of blades	4	4
V , knots	22.04	22.04
shp	23,250	22,530
ehp/shp	0.77	0.77
e_h	1.073	1.089
e_p	0.709	0.709
e_{rr}	1.012	0.997

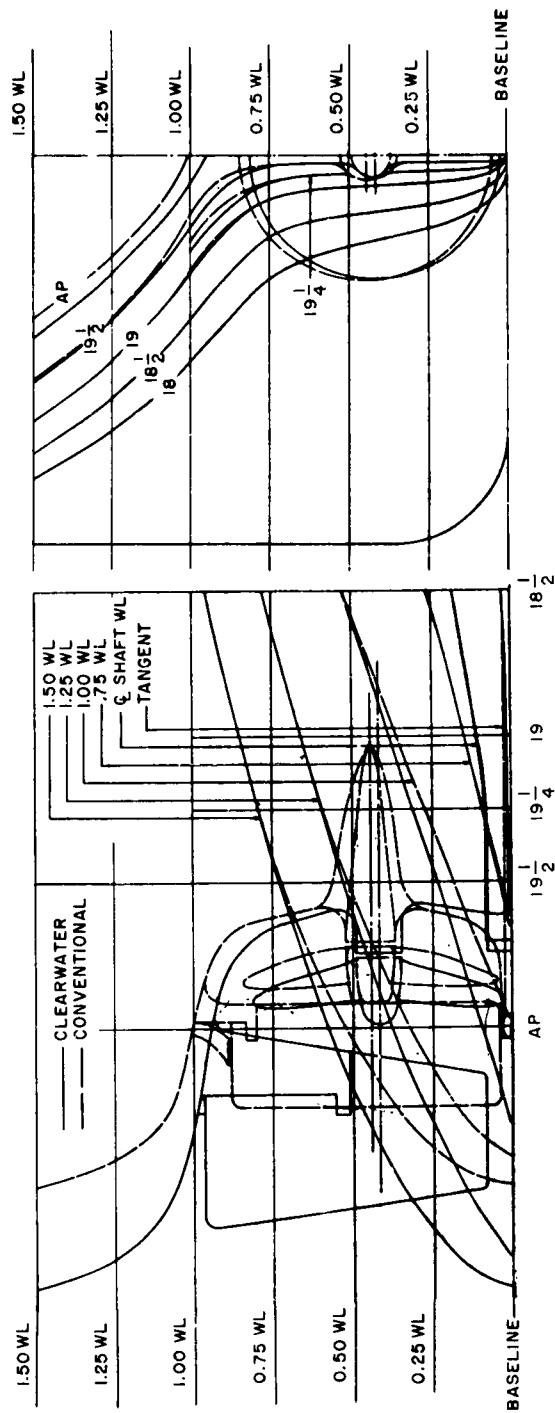


Figure 58 — Stern Arrangements for 0.60 Block Parent (Model 4210)

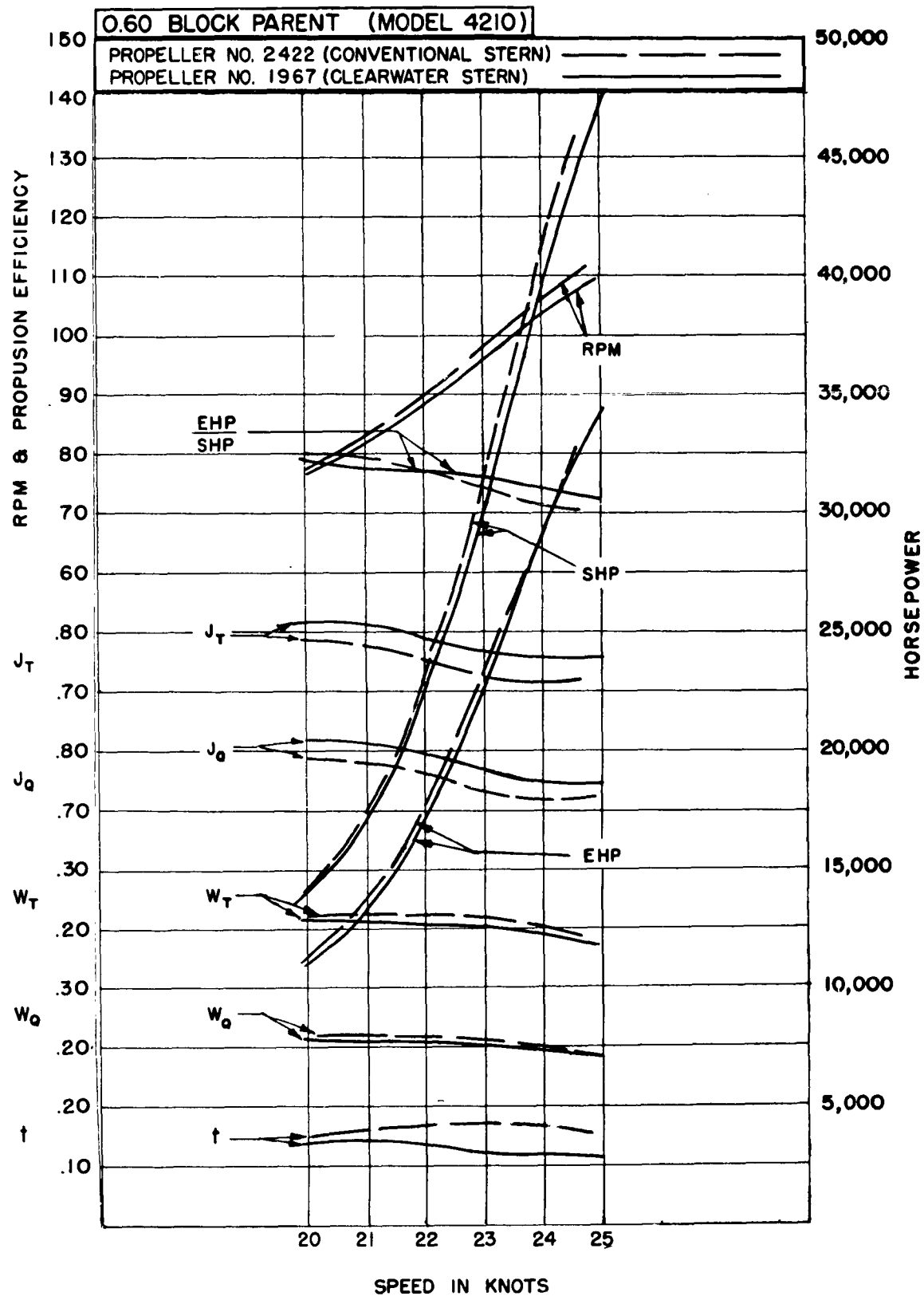


Figure 59 – Power, RPM, and Coefficient Curves of Clearwater and Conventional Sterns for 0.60 Block Parent–Model 4210

CHAPTER XI

EFFECT OF VARIATION IN AFTERBODY SHAPE UPON WAKE DISTRIBUTION AND POWER

The original conception of Series 60 was a set of related basic hull forms which, in terms of fullness and proportions, would cover the general field of single-screw merchant ships. The principal purpose was to indicate the trends which might be expected in resistance and power by changes in these basic parameters, but it was also realized that the results were likely to be used for making power estimates for new designs. It was therefore necessary that the resistance and power characteristics of the series models should be of reasonably good standard, and an effort was made to ensure this by the preliminary work with Series 57 and the later comparisons with models of existing ships of accepted good performance.^{62,63}

On the other hand, any effort to explore all the possible changes of shape in waterlines and sections before embarking on the series proper would have been prohibitive both in time and money. One of the objectives in setting up the Series 60 design contours has always been the hope that they would be used as a point of departure in future research so that there would always be a link with new work, and this hope has been in a large measure fulfilled.

The variation of hull shape as exemplified by changes in waterline and section shape is one such research which could well begin from Series 60 as a basis, and a start on this phase has been made at Taylor Model Basin. Since a great deal of interest has been generated in recent years in the effects of afterbody shape upon the wake distribution, propeller-excited forces on the hull, and horsepower, the first experiments covered the measurement of wake pattern behind the five parent models, together with the effect upon wake pattern and power of two additional models of 0.70 block coefficient having, respectively, more U- and more V-shaped afterbody sections than the parent. This work was sponsored by the Bureau of Ships, the Maritime Administration and SNAME, and carried out at the Taylor Model Basin. The results have been given in detail in Reference 64.

The parent 0.70 block coefficient model was No. 4280, made in wood, and identical as regards lines with the parent wax model No. 4221. Two additional wooden models, No. 4281 and No. 4282, were made with the same forebody, identical with that of No. 4280, but with more U- and more V-Type stern sections, respectively. The section area curve, load waterline (WL No. 1.00), deck waterline (WL No. 1.50), and stern profile remained unchanged. As a result, all coefficients of form and dimensions except those related to wetted surface and section shape are the same for all three models (Table 42). A comparison between the after end sections is shown in Figure 60. Table 42 also includes values of a coefficient τ to describe the slope of Station 18 at the level of the propeller shaft. This coefficient was first proposed by Harvald⁶⁵ and is measured as shown in Figure 61. Average values of τ

Table 42 - Principal Particulars of Models

	400-ft ship	600-ft ship
LWL, ft.....	406.7	610.0
LBP, ft.....	400.0	600.0
B, ft.....	57.14	85.71
H, ft.....	22.86	34.29
Δ , tons.....	10456	35289
$1/2\alpha_E$, deg.....	11.6	11.6
*WS, sq ft, (Model 4280).....	31859	71683
*WS, sq ft, (Model 4281).....	32008	72018
*WS, sq ft, (Model 4282).....	31759	71458

Hull Coefficients

L/B.....	7.00		
B/H.....	2.50		
$L/\nabla^{1/3}$	5.593	C_B	0.700
$\Delta/(L/100)^3$	163.4	C_X	0.986
$S/\nabla^{2/3}$ (4280).....	6.230	C_P	0.710
$S/\nabla^{2/3}$ (4281).....	6.260	C_{PF}	0.700
$S/\nabla^{2/3}$ (4282).....	6.210	C_{PA}	0.721
L_E/L_{BP}	0.420	C_{PE}	0.642
L_X/L_{BP}	0.119	C_{PR}	0.698
L_R/L_{BP}	0.461	LCB, per cent LBP from ∞	0.554

* Does not include rudder.

Section Coefficient τ

Series 60—Forms

Parent form.....	Model 4280:	$\tau = 0.359$
U-shaped form.....	Model 4281:	$\tau = 0.179$
V-shaped form.....	Model 4282:	$\tau = 0.543$

Average Values

Moderate stern sections.....	$\tau = 0.500$
Extreme U-shaped stern sections.....	$\tau = 0.20$
Extreme V-shaped stern sections.....	$\tau = 0.75$

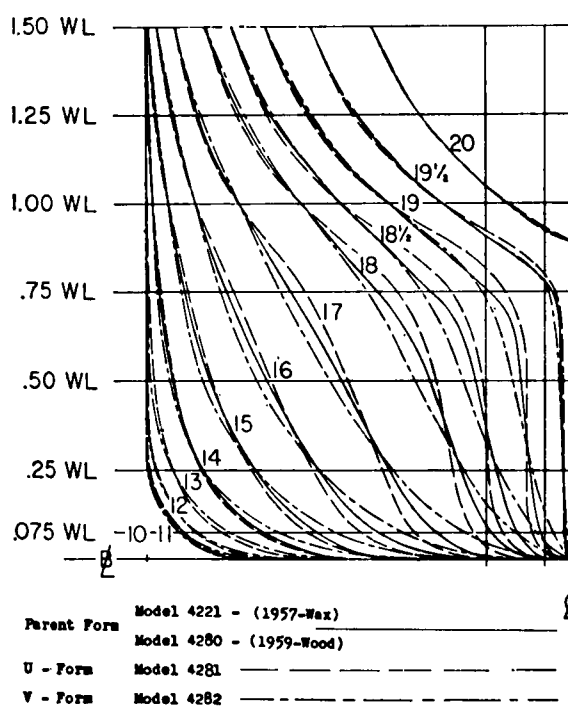


Figure 60 - Comparison of Afterbody Lines of 0.70 Block Parent Stern Variations

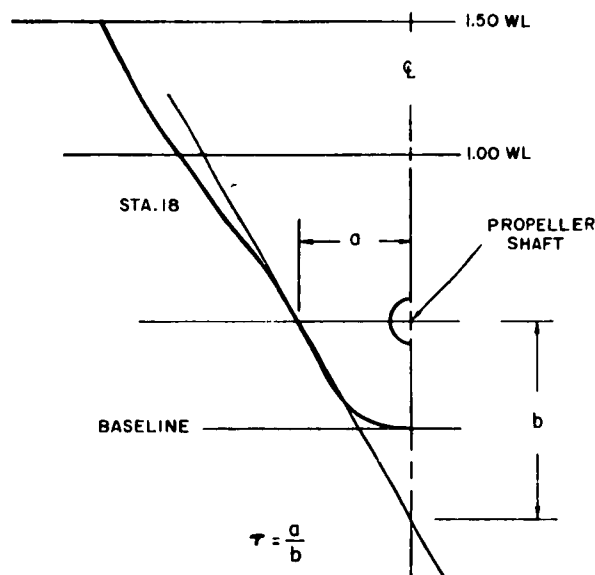


Figure 61 - Definition of Section Shape Coefficient

from a number of existing designs are also given in Table 42, and these show that the Series 60 parent of 0.70 C_B is somewhat U in character to start with, and the V-shaped variation is rather moderate in this respect. The models were fitted with rudder and propeller as previously described, the propeller used being TMB 3376 which was that fitted to the original 0.70 C_B parent, Model 4221. It represented a 24-ft diameter propeller on a 600-ft ship (or 16 ft on a 400-ft ship).

Models 4280, 4281, and 4282 were all made in wood, had an LBP of 20 ft, and a smooth enamel finish. They were fitted with a trip wire and run in the deep-water basin which is 51 ft wide and 22 ft deep. Experiments were made at the designed displacement, level trim, and at 60 percent of this displacement and a trim of 2.5 percent of LBP by the stern.

The results of the resistance and propulsion tests are given in Tables 43 through 48 and in Figures 62 through 70.

The change in resistance, as shown in Figures 62 to 65, is relatively small, the U-form being about 2 percent worse and the V-form 3 percent better than the parent at the Troost service speed. On the other hand, the U-form favors the propulsive efficiency, but this is insufficient to offset the superior resistance qualities of the V-stern, with the result that the latter has the lower dhp at all speeds in the full-load condition and over most of the speed range at 60-percent displacement. These changes in resistance and propulsive efficiency are of the kind to be expected as a result of such stern changes. In general, the increase in propulsive efficiency with the U-stern is usually sufficient to more than offset the increase in resistance, although not in this particular case.

Velocity surveys were also made in the plane of the propeller for all five of the Series 60 parents and for the two stern variations of the 0.70 C_B model. This plane was normal to the propeller shaft (and to the baseline) and 0.94 percent of the LBP forward of the after perpendicular. In accordance with the stern arrangement shown in Figure 36, it passed through the 0.7 radius point on the propeller generating line. The velocities were measured at 59 points over a rectangular grid extending from the baseline to a waterline at 0.85 of the load draft and on the port side from the centerline out to a vertical line distant 0.425 of the load draft. They were all made at the full-load displacement and at the Troost service speed, using a 5-hole spherical pitot tube, which determines the velocity vector at each point (for details, see Reference 64).

These velocities have been analysed into longitudinal (fore and aft), vertical and horizontal components V_x , V_v , and V_h , defined as shown in Figure 71. These can be converted to Taylor wake fractions

$$w_x = 1 - \frac{V_x}{V} \quad 100$$

$$w_v = 1 - \frac{V_v}{V} \quad 100$$

and
$$w_h = 1 - \frac{V_h}{V} \quad 100$$

Table 43 - Results of Resistance and Self-Propulsion Experiments for Parent Form-
Model 4280, 100-Percent Displacement

$V/\sqrt{L_{WL}}$	$C_f \times 10^3$	(K)	(C)	$V/\sqrt{L_{WL}}$	V	N	SHF	W_T	t	e_h	e_p	e_{rr}	EHP/SHF
0.30	2.826	0.766	0.706	0.394	8.0	32.7	1217	0.328	0.207	1.160	0.613	0.971	0.702
0.35	2.791	0.861	0.698	0.364	9.0	36.5	1696	0.330	0.204	1.158	0.631	0.972	0.752
0.40	2.762	1.006	0.690	0.405	10.0	40.5	2182	0.328	0.199	1.192	0.652	0.995	0.773
0.45	2.722	1.132	0.680	0.445	11.0	44.6	2753	0.330	0.197	1.181	0.657	1.004	0.779
0.50	2.712	1.258	0.678	0.486	12.0	48.6	3406	0.315	0.194	1.177	0.660	1.004	0.780
0.55	2.724	1.384	0.681	0.526	13.0	52.7	4145	0.313	0.192	1.176	0.662	0.998	0.777
0.60	2.787	1.510	0.697	0.566	14.0	57.3	5003	0.310	0.190	1.174	0.663	0.993	0.773
0.65	2.840	1.636	0.710	0.607	15.0	61.5	5886	0.307	0.192	1.165	0.663	0.993	0.767
0.70	2.890	1.781	0.722	0.628	15.5	63.7	6212	0.306	0.195	1.160	0.661	0.998	0.765
0.75	2.990	1.887	0.747	0.648	16.0	66.1	9092	0.305	0.196	1.154	0.659	1.003	0.763
0.800	3.216	2.013	0.804	0.668	16.5	68.5	10100	0.305	0.199	1.151	0.658	1.004	0.761
0.825	3.303	2.076	0.826	0.688	17.0	70.7	11180	0.303	0.200	1.148	0.657	1.006	0.759
0.85	3.412	2.139	0.853	0.706	17.5	73.2	12390	0.302	0.200	1.146	0.655	1.009	0.758
0.875	3.682	2.202	0.920	0.729	18.0	75.8	13740	0.301	0.200	1.144	0.653	1.010	0.756
0.90	4.267	2.265	1.066	0.749	18.5	78.3	15350	0.300	0.200	1.143	0.652	1.011	0.753
0.925	5.111	2.327	1.277	0.769	19.0	81.2	17150	0.300	0.201	1.141	0.649	1.013	0.750
0.950	6.028	2.390	1.506	0.790	19.5	84.0	19200	0.299	0.202	1.138	0.648	1.016	0.746
0.975	6.997	2.453	1.749	0.810	20.0	87.1	21380	0.298	0.203	1.135	0.642	1.016	0.740
1.000	7.857	2.516	1.964	0.830	20.5	90.4	23840	0.297	0.205	1.131	0.635	1.019	0.732
1.025	8.592	2.579	2.147	0.851	21.0	93.8	26890	0.296	0.207	1.126	0.628	1.018	0.730
1.050	9.088	2.642	2.271	0.871	21.5	96.0	31160	0.294	0.206	1.122	0.618	1.018	0.706
1.075	9.281	2.705	2.320	0.891	22.0	103.1	37530	0.293	0.208	1.120	0.602	1.024	0.691

(All numbers are for ship of 600-ft LBP)

(All numbers are for ship of
400-ft LBP)

Table 44 - Results of Resistance and Self-Propulsion Experiments for U-Shaped Form-
Model 4281, 100-Percent Displacement

$V/\sqrt{L_{WL}}$	$C_f \times 10^3$	(K)	(C)	$V/\sqrt{L_{WL}}$	V	N	SHF	W_T	t	e_h	e_p	e_{rr}	EHP/SHF
0.30	2.868	0.755	0.720	0.324	8.0	32.1	1178	0.358	0.198	1.257	0.635	0.932	0.744
0.35	2.821	0.881	0.708	0.364	9.0	36.0	1575	0.367	0.190	1.280	0.631	0.987	0.797
0.40	2.783	1.006	0.699	0.405	10.0	39.8	2078	0.366	0.188	1.281	0.633	1.009	0.818
0.45	2.757	1.132	0.692	0.445	11.0	43.8	2692	0.351	0.185	1.266	0.645	1.015	0.822
0.50	2.734	1.258	0.686	0.486	12.0	47.8	3467	0.343	0.181	1.247	0.650	1.014	0.822
0.55	2.754	1.384	0.692	0.526	13.0	51.8	4428	0.343	0.178	1.251	0.649	1.011	0.821
0.60	2.835	1.510	0.712	0.566	14.0	56.0	5611	0.343	0.179	1.250	0.648	1.012	0.820
0.65	2.890	1.636	0.726	0.607	15.0	60.4	7072	0.343	0.181	1.247	0.644	1.019	0.819
0.70	2.955	1.761	0.742	0.628	15.5	62.8	7913	0.343	0.184	1.242	0.643	1.023	0.817
0.75	3.082	1.887	0.774	0.648	16.0	65.0	8609	0.343	0.187	1.237	0.642	1.026	0.815
0.80	3.281	2.013	0.824	0.668	16.5	67.4	9744	0.341	0.188	1.232	0.641	1.029	0.813
0.825	3.371	2.076	0.846	0.688	17.0	69.7	10790	0.341	0.188	1.230	0.640	1.030	0.811
0.850	3.472	2.139	0.872	0.706	17.5	72.1	11880	0.339	0.188	1.228	0.638	1.037	0.810
0.875	3.750	2.202	0.949	0.729	18.0	74.5	13220	0.338	0.188	1.227	0.635	1.036	0.807
0.900	4.387	2.265	1.097	0.749	18.5	77.1	14810	0.337	0.189	1.223	0.633	1.038	0.804
0.925	5.261	2.327	1.321	0.769	19.0	79.8	16540	0.336	0.189	1.221	0.628	1.043	0.800
0.950	6.156	2.390	1.546	0.790	19.5	82.5	18430	0.335	0.190	1.218	0.625	1.044	0.795
0.975	7.191	2.453	1.806	0.810	20.0	85.6	20880	0.334	0.191	1.215	0.620	1.046	0.788
1.000	8.017	2.516	2.013	0.830	20.5	88.7	22740	0.332	0.193	1.208	0.618	1.041	0.777
1.025	8.762	2.579	2.200	0.851	21.0	92.4	25910	0.330	0.195	1.201	0.609	1.046	0.765
1.050	9.163	2.642	2.301	0.871	21.5	96.8	30450	0.328	0.195	1.189	0.600	1.051	0.750
1.075	9.323	2.705	2.341	0.891	22.0	102.1	36700	0.326	0.195	1.194	0.588	1.045	0.734

(All numbers are for ship of 600-ft LBP)

(All numbers are for ship of
400-ft LBP)

Table 45 - Results of Resistance and Self-Propulsion Experiments for V-Shaped Form-Model 4282, 100-Percent Displacement

$V/\sqrt{L_{WL}}$	$C_t \times 10^3$	(K)	(C)	$V/\sqrt{L_{WL}}$	V	N	SHP	W_T	t	ϕ_h	ϕ_p	ϕ_{rr}	EHP/SHP
0.30	2.746	0.755	0.684	0.324	8.0	32.7	1184	0.323	0.229	1.189	0.652	0.945	0.702
0.35	2.736	0.881	0.679	0.364	9.0	36.7	1590	0.334	0.228	1.159	0.648	1.001	0.752
0.40	2.697	1.006	0.672	0.405	10.0	40.5	2083	0.334	0.226	1.162	0.649	1.025	0.773
0.45	2.657	1.123	0.663	0.445	11.0	44.8	2691	0.320	0.222	1.144	0.660	1.032	0.779
0.50	2.614	1.258	0.651	0.486	12.0	48.6	3480	0.314	0.220	1.137	0.663	1.035	0.780
0.55	2.635	1.394	0.657	0.526	13.0	52.6	4475	0.315	0.219	1.140	0.662	1.029	0.777
0.60	2.702	1.510	0.673	0.566	14.0	57.1	5717	0.314	0.219	1.138	0.660	1.029	0.773
0.65	2.758	1.626	0.687	0.607	15.0	61.5	7175	0.311	0.220	1.132	0.660	1.025	0.766
0.70	2.788	1.761	0.695	0.628	15.5	63.7	7976	0.308	0.220	1.127	0.660	1.027	0.764
0.75	2.874	1.887	0.716	0.648	16.0	66.1	8871	0.306	0.221	1.122	0.660	1.026	0.760
0.80	2.119	2.013	0.777	0.668	16.5	68.5	9797	0.304	0.224	1.114	0.659	1.031	0.757
0.825	2.208	2.076	0.798	0.688	17.0	70.8	10600	0.304	0.227	1.111	0.658	1.033	0.755
0.850	2.212	2.138	0.825	0.708	17.5	73.2	12000	0.303	0.229	1.106	0.657	1.033	0.751
0.875	2.599	2.202	0.895	0.729	18.0	75.8	13800	0.301	0.232	1.099	0.653	1.040	0.747
0.900	4.127	2.265	1.028	0.749	18.5	78.3	14800	0.301	0.234	1.096	0.651	1.043	0.744
0.925	4.969	2.327	1.238	0.769	19.0	81.2	16620	0.302	0.237	1.093	0.648	1.044	0.739
0.950	5.876	2.390	1.464	0.790	19.5	84.0	18600	0.303	0.238	1.093	0.642	1.047	0.735
0.975	6.851	2.453	1.707	0.810	20.0	87.1	20900	0.304	0.239	1.093	0.635	1.050	0.729
1.000	7.697	2.516	1.918	0.830	20.5	90.4	23450	0.304	0.240	1.092	0.628	1.051	0.721
1.025	8.472	2.579	2.111	0.851	21.0	93.8	26530	0.304	0.240	1.092	0.620	1.050	0.711
1.050	9.006	2.642	2.244	0.871	21.5	98.0	30820	0.305	0.241	1.092	0.610	1.046	0.697
1.075	9.203	2.705	2.293	0.891	22.0	103.0	37040	0.305	0.241	1.092	0.597	1.043	0.680
1.100	9.161	2.768	2.288	(All numbers are for ship of 600-ft LBP)									
1.125	9.047	2.831	2.292										
1.150	8.831	2.894	2.200										
1.175	8.647	2.957	2.154										
1.200	8.553	3.019	2.131										
1.225	8.579	3.082	2.138										

(All numbers are for ship of 400-ft LBP)

Table 46 - Results of Resistance and Self-Propulsion Experiments for Parent Form-Model 4280, 60-Percent Displacement, Trim $2\frac{1}{2}$ Percent L_{BP} by Stern

$V/\sqrt{L_{WL}}$	$C_t \times 10^3$	(K)	(C)	$V/\sqrt{L_{WL}}$	V	N	SHP	W_T	t	ϕ_h	ϕ_p	ϕ_{rr}	EHP/SHP
0.30	2.886	0.822	0.794	0.324	8.0	29.2	851	0.393	0.210	1.302	0.654	0.975	0.830
0.35	2.837	0.959	0.781	0.364	9.0	32.9	1201	0.393	0.207	1.306	0.653	0.979	0.835
0.40	2.810	1.096	0.774	0.405	10.0	36.6	1605	0.390	0.205	1.303	0.654	0.984	0.839
0.45	2.795	1.233	0.769	0.445	11.0	40.2	2061	0.384	0.204	1.292	0.661	0.984	0.840
0.50	2.774	1.370	0.764	0.486	12.0	44.2	2703	0.376	0.202	1.278	0.663	0.995	0.843
0.55	2.809	1.507	0.773	0.526	13.0	48.0	3438	0.366	0.200	1.262	0.669	0.998	0.843
0.60	2.857	1.644	0.786	0.566	14.0	52.2	4338	0.356	0.200	1.242	0.671	1.008	0.840
0.65	2.902	1.781	0.799	0.607	15.0	56.6	5462	0.347	0.201	1.224	0.672	1.011	0.832
0.70	2.967	1.918	0.817	0.628	15.5	58.8	6121	0.343	0.203	1.213	0.672	1.014	0.827
0.75	3.029	2.055	0.834	0.648	16.0	61.0	6839	0.339	0.204	1.204	0.672	1.014	0.821
0.80	3.089	2.192	0.850	0.668	16.5	63.2	7645	0.337	0.207	1.196	0.672	1.016	0.817
0.825	3.153	2.260	0.868	0.688	17.0	65.4	8473	0.334	0.210	1.186	0.672	1.017	0.811
0.850	3.272	2.329	0.901	0.708	17.5	67.6	9338	0.331	0.212	1.178	0.672	1.019	0.807
0.875	3.492	2.397	0.961	0.729	18.0	69.8	10250	0.328	0.218	1.171	0.672	1.023	0.805
0.900	3.847	2.466	1.059	0.749	18.5	72.1	11330	0.326	0.215	1.165	0.672	1.022	0.800
0.925	4.261	2.534	1.173	0.769	19.0	74.5	12470	0.323	0.217	1.156	0.671	1.026	0.796
0.950	4.681	2.603	1.289	0.790	19.5	76.9	13680	0.321	0.220	1.149	0.669	1.029	0.791
0.975	5.121	2.672	1.410	0.810	20.0	79.2	15060	0.321	0.222	1.146	0.668	1.028	0.787
1.000	5.539	2.740	1.525	0.830	20.5	81.8	16650	0.320	0.223	1.143	0.667	1.027	0.782
1.025	5.852	2.808	1.611	0.851	21.0	84.7	18660	0.319	0.223	1.141	0.662	1.028	0.776
1.050	5.966	2.877	1.642	0.871	21.5	88.0	21290	0.318	0.222	1.141	0.654	1.029	0.768
1.075	6.038	2.945	1.663	0.891	22.0	92.2	24960	0.317	0.220	1.143	0.643	1.026	0.754
1.100	6.100	3.014	1.679	0.911	22.5	97.0	29740	0.314	0.216	1.143	0.632	1.020	0.737
1.125	6.157	3.082	1.695	0.932	23.0	102.4	35360	0.310	0.212	1.142	0.619	1.017	0.719
1.150	6.210	3.151	1.710	(All numbers are for ship of 600-ft LBP)									
1.175	6.300	3.219	1.734										
1.200	6.450	3.288	1.776										
1.225	6.669	3.356	1.836										

(All numbers are for ship of 400-ft LBP)

Table 47 — Results of Resistance and Self-Propulsion Experiments for U-Shaped Form—
Model 4281, 60-Percent Displacement, Trim $2\frac{1}{2}$ Percent L_{BP} by Stern

$V/\sqrt{L_{WL}}$	$C_f \times 10^3$	(K)	(C)	$V/\sqrt{L_{WL}}$	V	N	SHP	W_T	t	ϵ_h	ϵ_p	ϵ_m	ELP/SHP
0.30	2.996	0.822	0.822	0.324	8.0	29.1	832	0.396	0.150	1.407	0.653	0.958	0.880
0.35	2.932	0.959	0.807	0.364	9.0	32.7	1185	0.399	0.155	1.406	0.652	0.963	0.883
0.40	2.923	1.096	0.805	0.405	10.0	36.3	594	0.396	0.159	1.397	0.653	0.970	0.885
0.45	2.917	1.233	0.803	0.445	11.0	40.0	4048	0.394	0.164	1.379	0.655	0.983	0.888
0.50	2.894	1.370	0.797	0.486	12.0	43.4	2678	0.390	0.168	1.364	0.655	0.992	0.891
0.55	2.913	1.507	0.802	0.526	13.0	47.4	2434	0.388	0.173	1.347	0.657	1.006	0.890
0.60	2.962	1.644	0.815	0.566	14.0	51.7	4329	0.382	0.177	1.323	0.656	1.017	0.889
0.65	3.002	1.781	0.829	0.607	15.0	55.9	5430	0.377	0.181	1.315	0.657	1.021	0.882
0.70	3.070	1.918	0.845	0.648	15.5	58.1	6038	0.374	0.184	1.304	0.657	1.025	0.878
0.75	3.142	2.055	0.865	0.688	16.0	60.3	6736	0.370	0.187	1.290	0.656	1.030	0.872
0.80	3.213	2.192	0.884	0.688	16.5	62.4	7495	0.367	0.189	1.281	0.656	1.032	0.867
0.825	3.258	2.260	0.897	0.688	17.0	64.3	8273	0.364	0.192	1.270	0.656	1.035	0.862
0.850	3.385	2.329	0.926	0.708	17.5	66.8	9122	0.360	0.195	1.258	0.657	1.039	0.859
0.875	3.632	2.397	1.000	0.729	18.0	69.0	10060	0.357	0.197	1.249	0.658	1.040	0.855
0.900	4.017	2.466	1.106	0.749	18.5	71.2	11040	0.354	0.199	1.240	0.658	1.044	0.852
0.925	4.451	2.534	1.225	0.769	19.0	73.6	12110	0.351	0.202	1.230	0.657	1.048	0.850
0.950	4.904	2.603	1.350	0.790	19.5	76.0	13220	0.349	0.205	1.221	0.657	1.054	0.846
0.975	5.356	2.672	1.474	0.810	20.0	78.5	14630	0.347	0.208	1.213	0.653	1.060	0.840
1.000	5.759	2.740	1.585	0.830	20.5	81.0	16200	0.346	0.210	1.208	0.652	1.056	0.832
1.025	6.025	2.808	1.658	0.851	21.0	84.0	18210	0.346	0.210	1.206	0.647	1.052	0.823
1.050	6.158	2.877	1.695	0.871	21.5	87.4	20870	0.347	0.211	1.208	0.638	1.053	0.812
1.075	6.242	2.945	1.718	0.891	22.0	91.5	24510	0.347	0.210	1.210	0.627	1.054	0.800
1.100	6.287	3.014	1.730	0.911	22.5	96.2	29210	0.346	0.207	1.212	0.610	1.058	0.789
1.125	6.317	3.082	1.739	0.932	23.0	101.3	35050	0.343	0.203	1.213	0.599	1.044	0.780

(All numbers are for ship of 600-ft LBP)

(All numbers are for ship of
400-ft LBP)

Table 48 — Results of Resistance and Self-Propulsion Experiments for V-Shaped Form—
Model 4282, 60-Percent Displacement, Trim $2\frac{1}{2}$ Percent L_{BP} by Stern

$V/\sqrt{L_{WL}}$	$C_f \times 10^3$	(K)	(C)	$V/\sqrt{L_{WL}}$	V	N	SHP	W_T	t	ϵ_h	ϵ_p	ϵ_m	ELP/SHP
0.30	2.754	0.822	0.759	0.324	8.0	29.9	818	0.347	0.246	1.155	0.678	1.013	0.793
0.35	2.711	0.959	0.747	0.364	9.0	34.0	1183	0.346	0.246	1.153	0.672	1.023	0.800
0.40	2.668	1.096	0.755	0.405	10.0	37.6	1560	0.343	0.246	1.158	0.672	1.032	0.804
0.45	2.643	1.233	0.728	0.445	11.0	41.6	2030	0.338	0.246	1.139	0.678	1.044	0.806
0.50	2.651	1.370	0.790	0.486	12.0	45.3	2673	0.334	0.246	1.122	0.681	1.047	0.807
0.55	2.675	1.507	0.787	0.526	13.0	49.2	3424	0.329	0.246	1.114	0.682	1.062	0.807
0.60	2.717	1.644	0.748	0.566	14.0	53.3	4305	0.325	0.246	1.117	0.682	1.055	0.804
0.65	2.763	1.781	0.761	0.607	15.0	57.3	5458	0.320	0.245	1.110	0.685	1.044	0.794
0.70	2.827	1.918	0.779	0.648	15.5	59.5	6119	0.317	0.244	1.107	0.685	1.035	0.785
0.75	2.896	2.055	0.798	0.688	16.0	61.7	6851	0.315	0.243	1.105	0.683	1.031	0.778
0.80	2.966	2.192	0.817	0.688	16.5	63.9	7630	0.312	0.243	1.100	0.684	1.027	0.773
0.825	3.039	2.260	0.837	0.688	17.0	66.3	8506	0.306	0.243	1.094	0.683	1.029	0.769
0.850	3.137	2.329	0.864	0.708	17.5	68.5	9410	0.307	0.244	1.091	0.681	1.031	0.766
0.875	3.320	2.397	0.915	0.729	18.0	70.7	10370	0.306	0.245	1.088	0.680	1.031	0.762
0.900	3.632	2.466	1.000	0.749	18.5	73.0	11460	0.305	0.246	1.085	0.679	1.032	0.760
0.925	4.041	2.534	1.113	0.769	19.0	75.3	12590	0.304	0.246	1.080	0.678	1.032	0.756
0.950	4.444	2.603	1.224	0.790	19.5	77.6	13880	0.305	0.250	1.079	0.678	1.027	0.751
0.975	4.851	2.672	1.336	0.810	20.0	80.0	15280	0.306	0.253	1.076	0.675	1.027	0.746
1.000	5.227	2.740	1.440	0.830	20.5	82.5	16810	0.306	0.254	1.075	0.671	1.031	0.744
1.025	5.532	2.808	1.524	0.851	21.0	85.3	18720	0.307	0.254	1.076	0.668	1.028	0.739
1.050	5.718	2.877	1.575	0.871	21.5	88.6	21260	0.307	0.254	1.076	0.658	1.035	0.733
1.075	5.801	2.945	1.598	0.891	22.0	92.4	24690	0.306	0.253	1.076	0.650	1.037	0.726
1.100	5.834	3.014	1.607	0.911	22.5	97.0	28980	0.305	0.250	1.079	0.640	1.041	0.719
1.125	5.873	3.082	1.618	0.932	23.0	102.0	34410	0.302	0.245	1.082	0.625	1.044	0.706

(All numbers are for ship of 600-ft LBP)

(All numbers are for ship of
400-ft LBP)

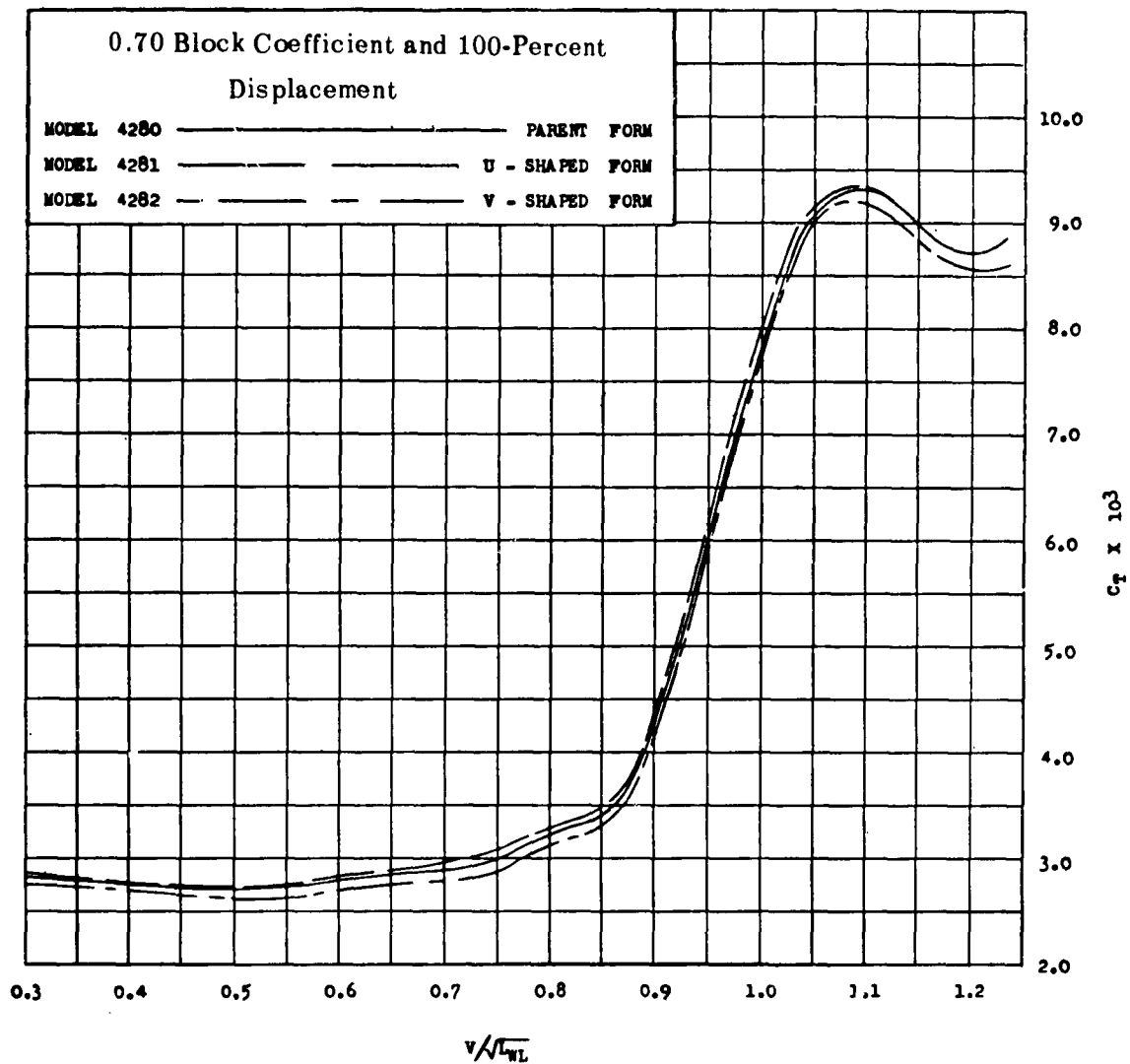


Figure 62 - Curves of Resistance Coefficient C_T to a Base of

$$\frac{V}{\sqrt{L_{WL}}} \text{ for Series 60, } 0.70 C_B \text{ Models}$$

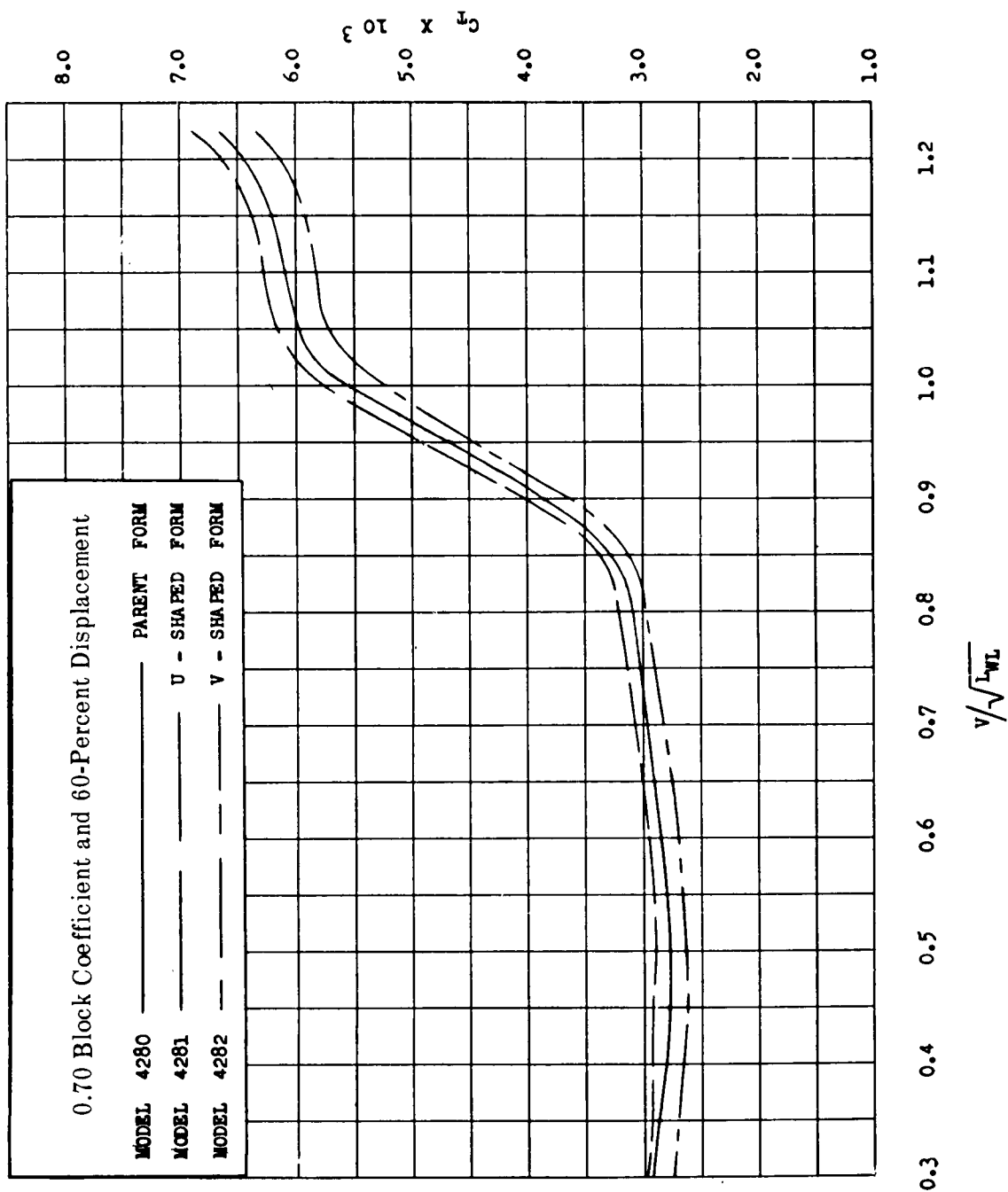


Figure 63 — Curves of Resistance Coefficient C_T to a Base of $\frac{V}{\sqrt{L WL}}$ for Series 60, 0.70 C_B Models

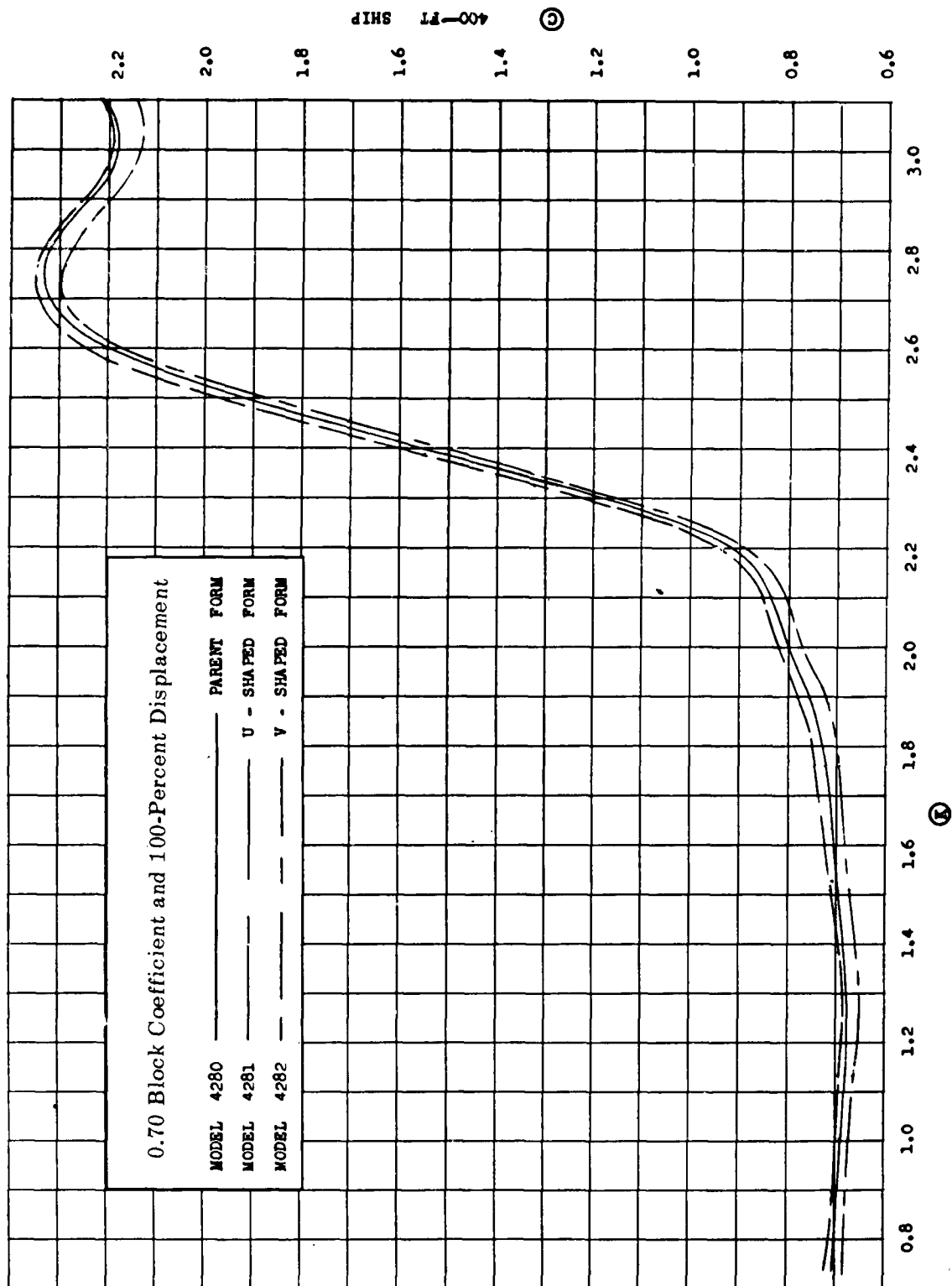


Figure 64 — Curves of Resistance Coefficient C to a Base of K for Series 60, 0.70 C_B Models

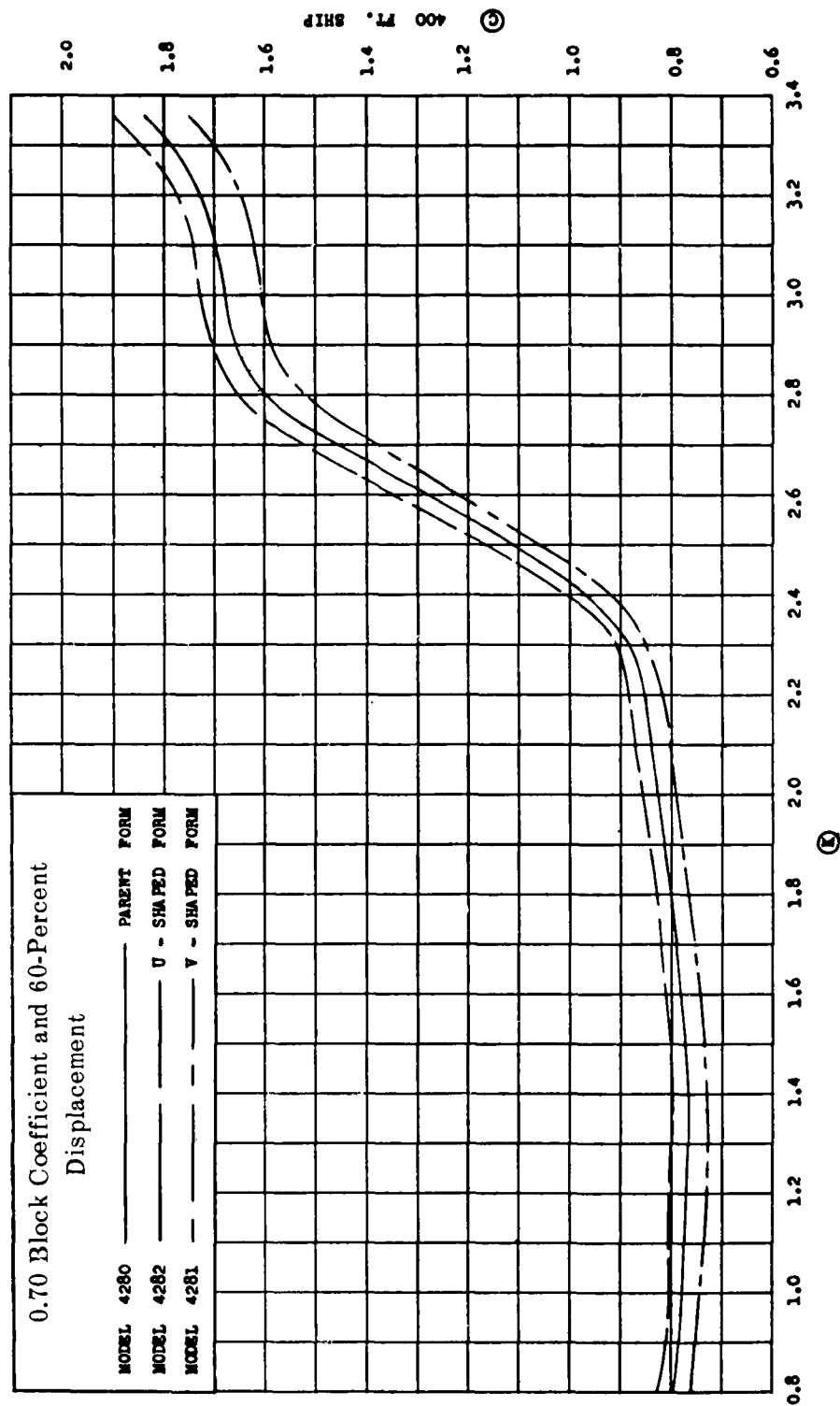


Figure 65 — Curves of Resistance Coefficient C to a Base of K for Series 60, 0.70 C_B Models

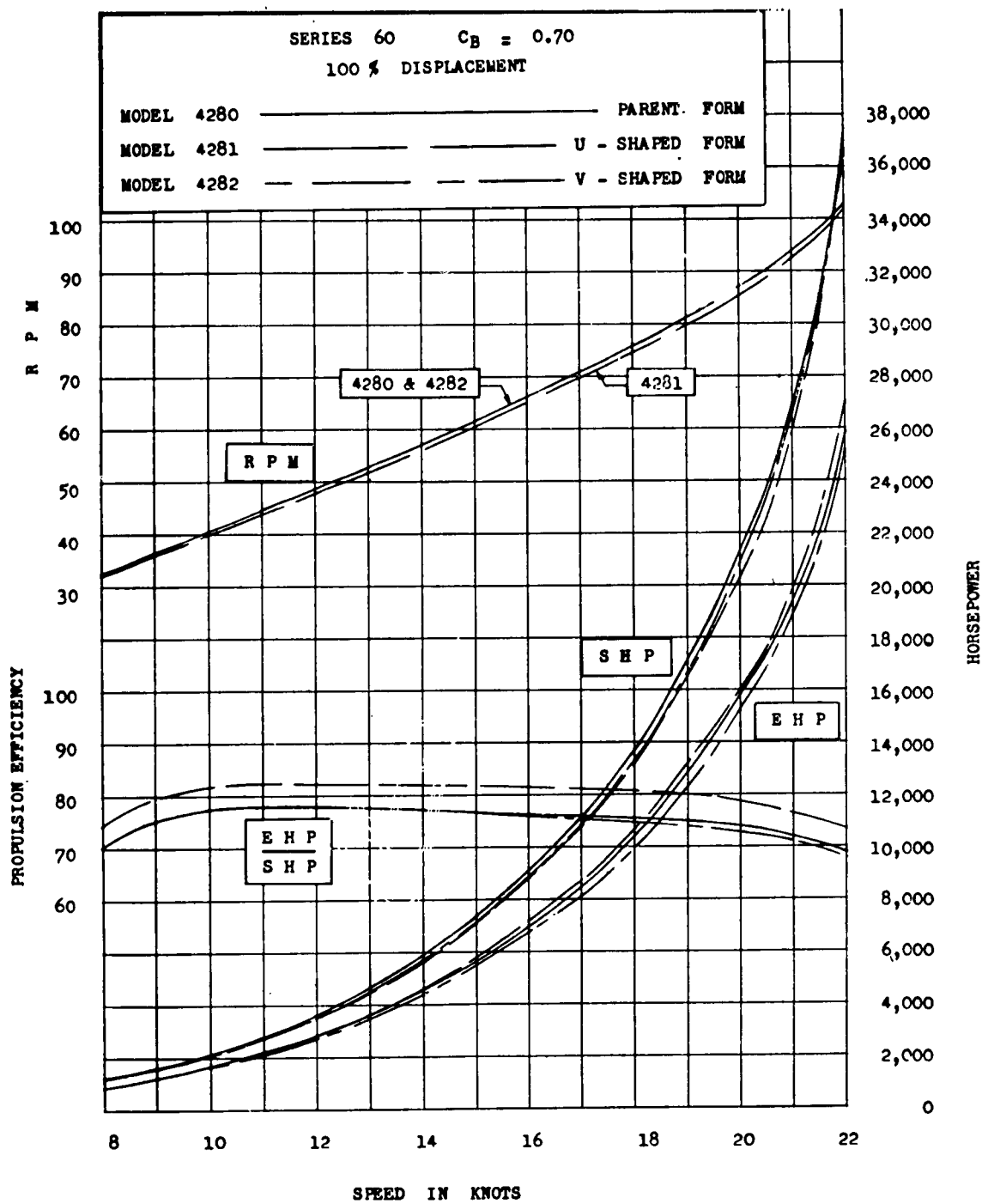


Figure 66 – Comparison of Power, RPM, and Efficiency Curves

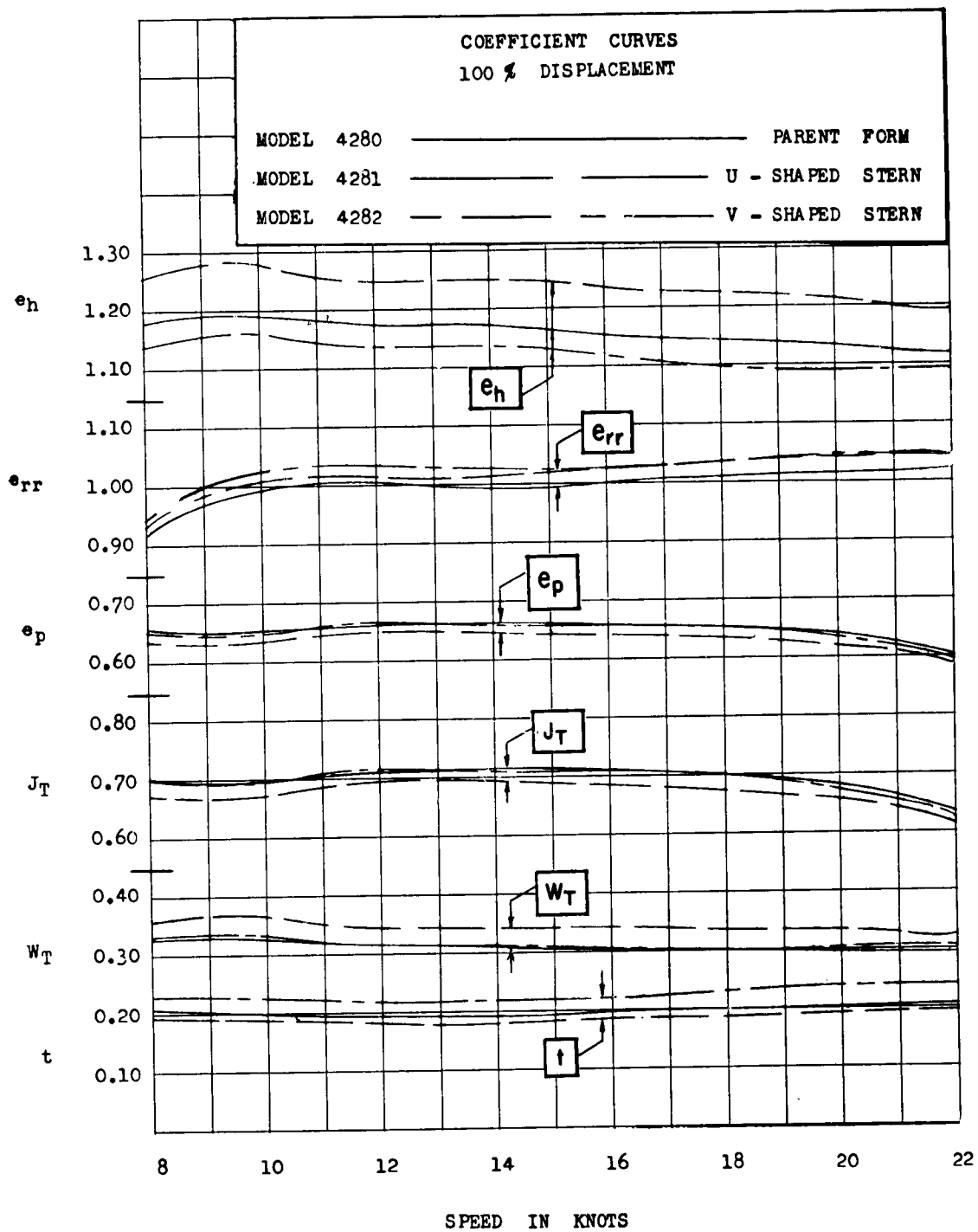


Figure 67 - Comparison of Coefficient Curves

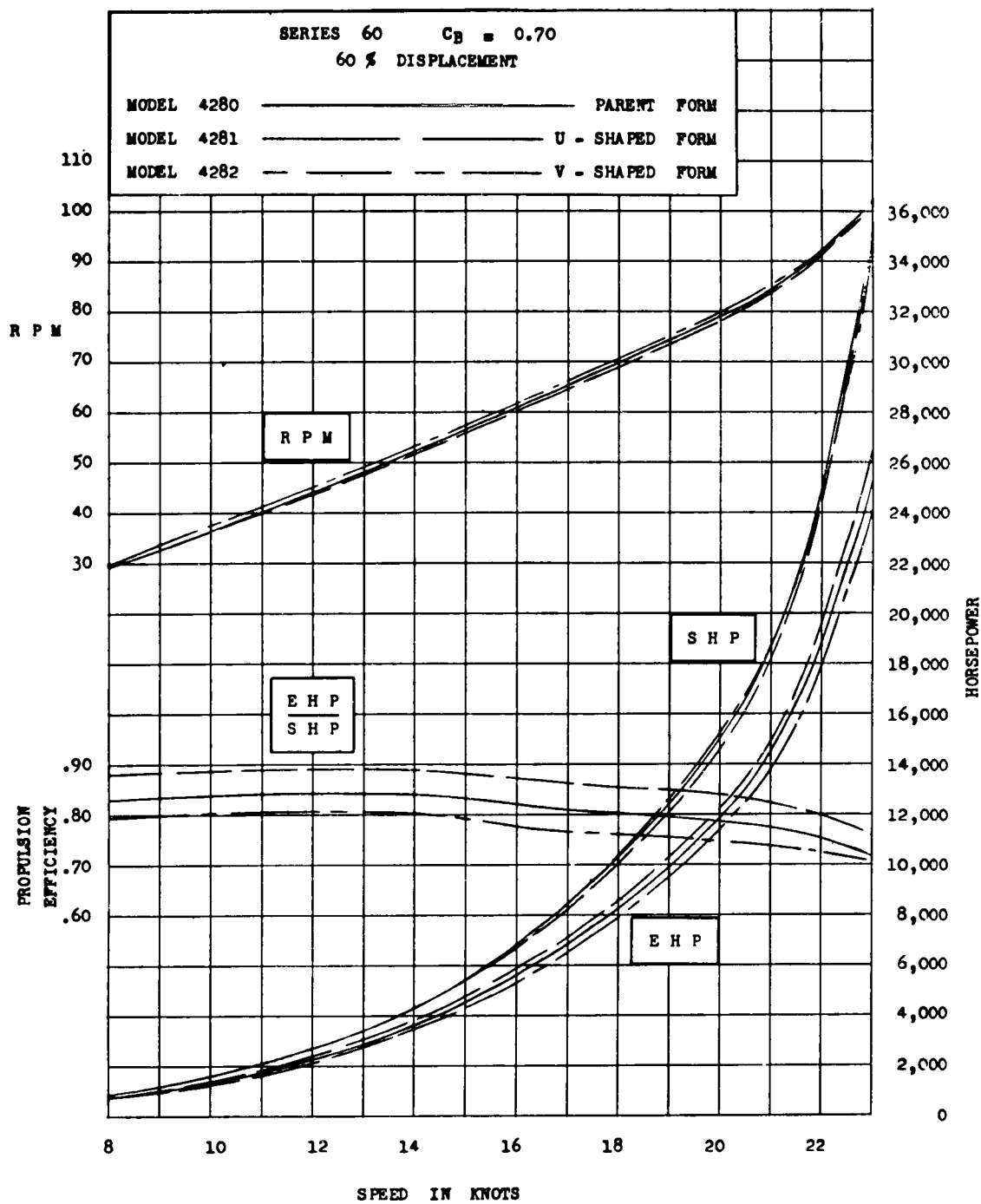


Figure 68 - Comparison of Power, RPM, and Efficiency Curves

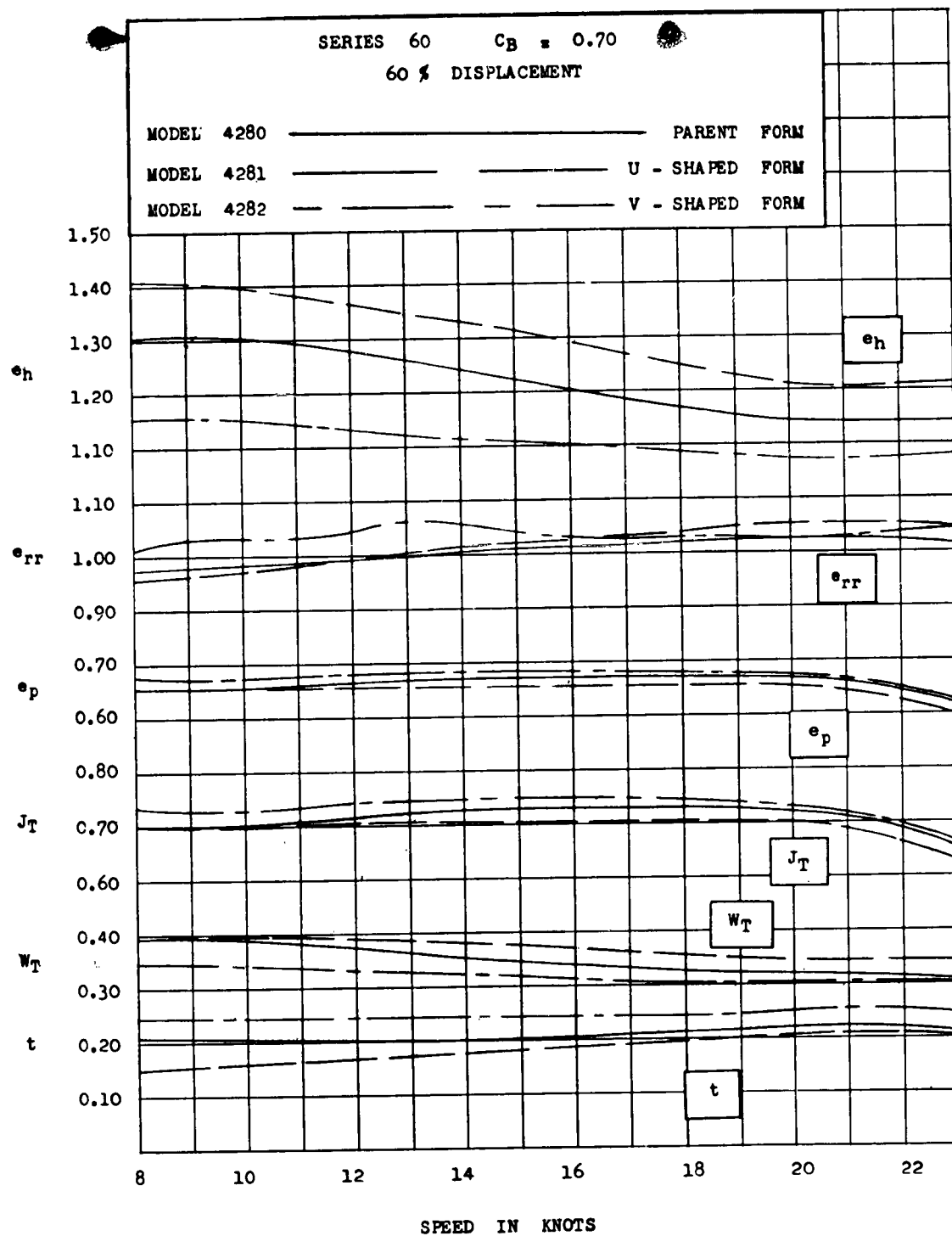


Figure 69 — Comparison of Coefficient Curves

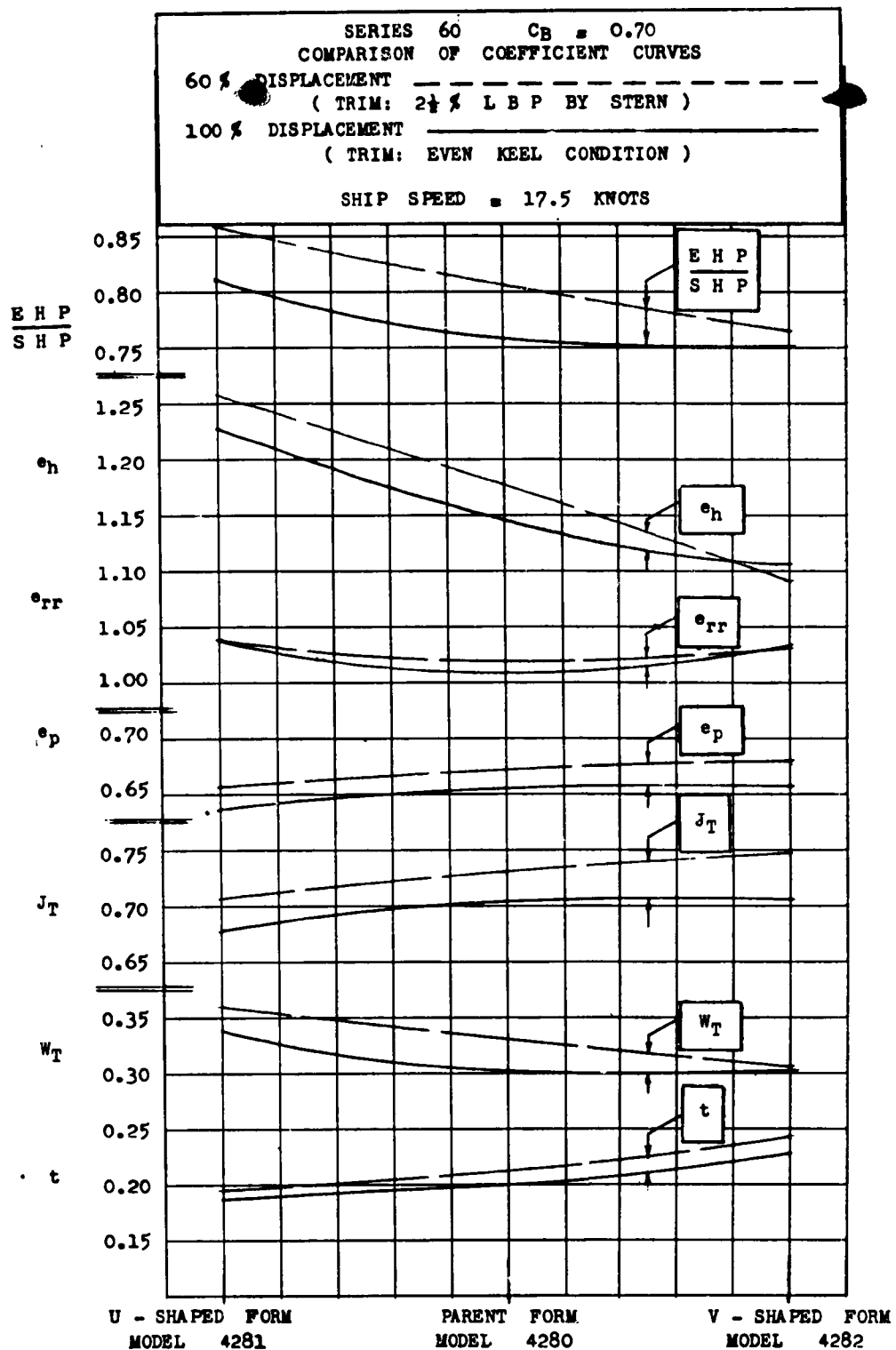


Figure 70 - Comparison of Coefficient Curves

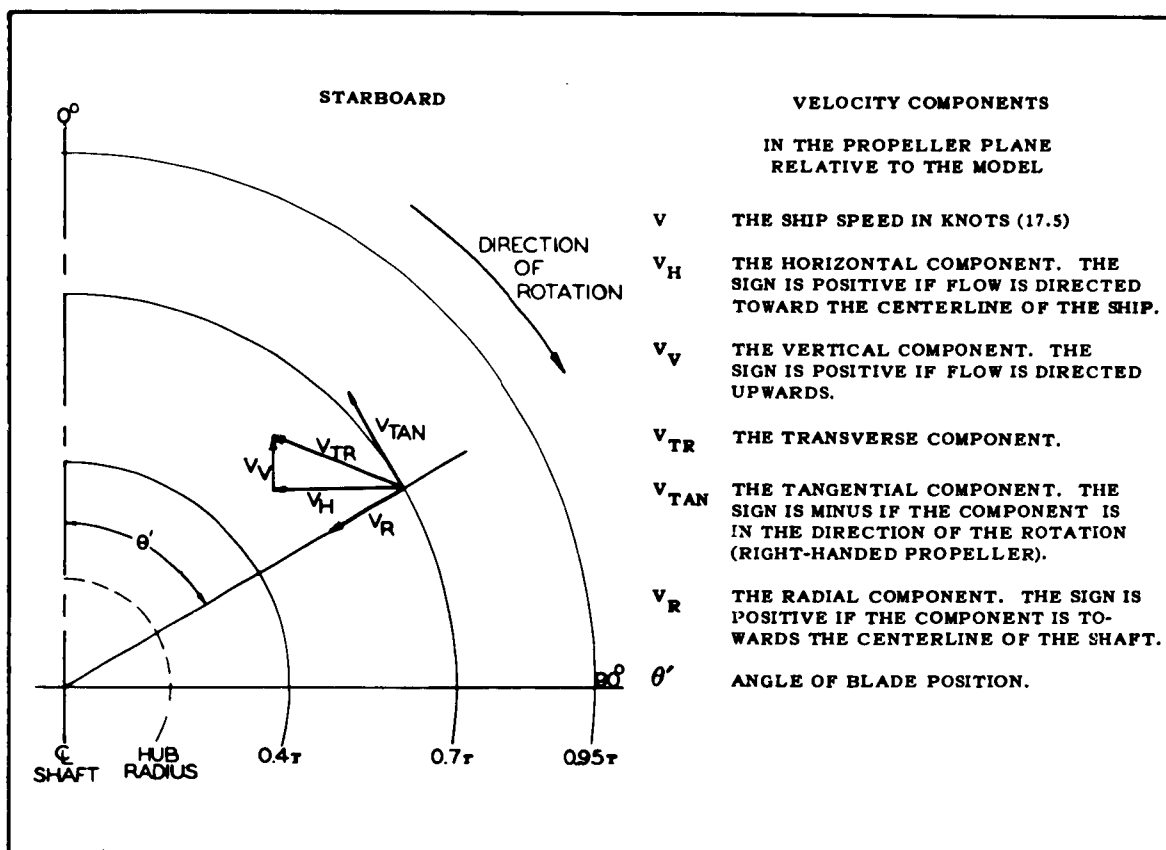


Figure 71 – Velocity-Component Vectors in Propeller Plane

Contours of constant values of w_x , w_v , and w_h are shown in Figures 72 through 77 for the five parent models and the two stern variations of the 0.70 C_B design.

In designing a propeller for a ship, we are interested in the fore and aft and transverse components of the wake. The total transverse wake w_{tr} , compounded of the values of w_v and w_h , is shown for the seven models in Figures 78 through 84.

Figure 75 shows that the wake in the fore and aft direction has the same general pattern for all block coefficients; there is a steady increase in the wake values with increase in block coefficient, and the same is generally true for the transverse wakes in Figures 81 through 84.

One rather important feature of the transverse wake pattern for the three different stern designs for the 0.70 C_B model should be noted in Figures 78, 79, and 80. In the V-stern model, there is a strong upward component over most of the disk except for an inward and downward component near the centerline immediately above the propeller. For the parent form, intermediate between V and U, there is an indication of a definite rotation in the wake below the propeller centerline (Figure 78) and with the more pronounced U-stern, this rotation seems to be definitely established (Figure 79). Flow tests carried out in the circulating water channel at the Taylor Model Basin have shown that when a model has excessively U stern sections, a definite vortex may leave the bilge line some distance ahead of the propeller and extend aft right through the disk. In such cases, this downward flow ahead of and into the propeller may cause cavitation with consequent noise and vibration. It is therefore wise to avoid a very hard bilge radius aft when using U sections, and it would be good practice to carry out flow tests before deciding on the final shape of the aft end sections of fuller ships.

The principal uses of the wake data are in the design of the propeller and the calculation of the variation in thrust and torque on the blades.

The average circumferential wake around a circle of any particular radius within the propeller disk can be found from such diagrams, and from this the appropriate pitch and blade section can be determined. However, in actual operation, the propeller section at that radius will meet constantly changing velocity conditions in the course of a revolution and so experience constantly changing thrust and torque forces. Integrating such forces over the blade will give the variation of thrust and torque on that blade during a complete revolution, and summing these forces for all blades will give the variation in total thrust and torque on the whole propeller. While the forces on a single blade will vary over 360 deg, the pattern for the whole propeller will repeat itself as the blades successively reach the same position. Thus for a 4-bladed propeller, the pattern of thrust and torque variation will repeat every 90 deg; in other words, at blade frequency. The importance of these variations in thrust and torque is that they are one of the causes of hull and machinery vibration; the varying pressures around the blades cause varying pressures on the neighboring hull structure, and the varying force and torque are also transmitted through the shaft and stern bearings to the hull and

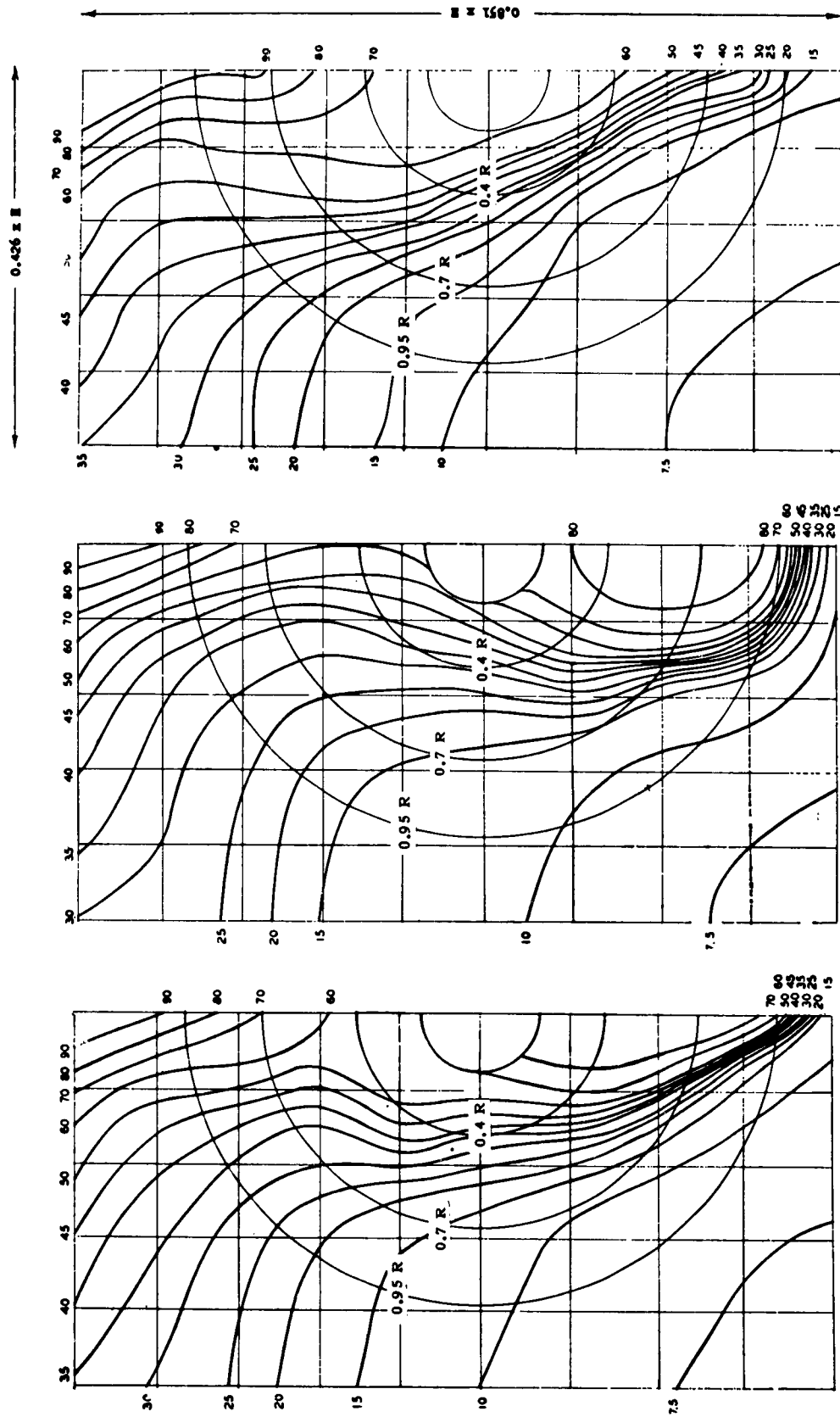


Figure 72a - Parent Form, Model 4280

Figure 72b - U-Shaped Stern, Model 4281

Figure 72c - V-Shaped Stern, Model 4282

Figure 72 - Lines of Equal Longitudinal Wake Components $w_x = (1 - V_x/V)100$

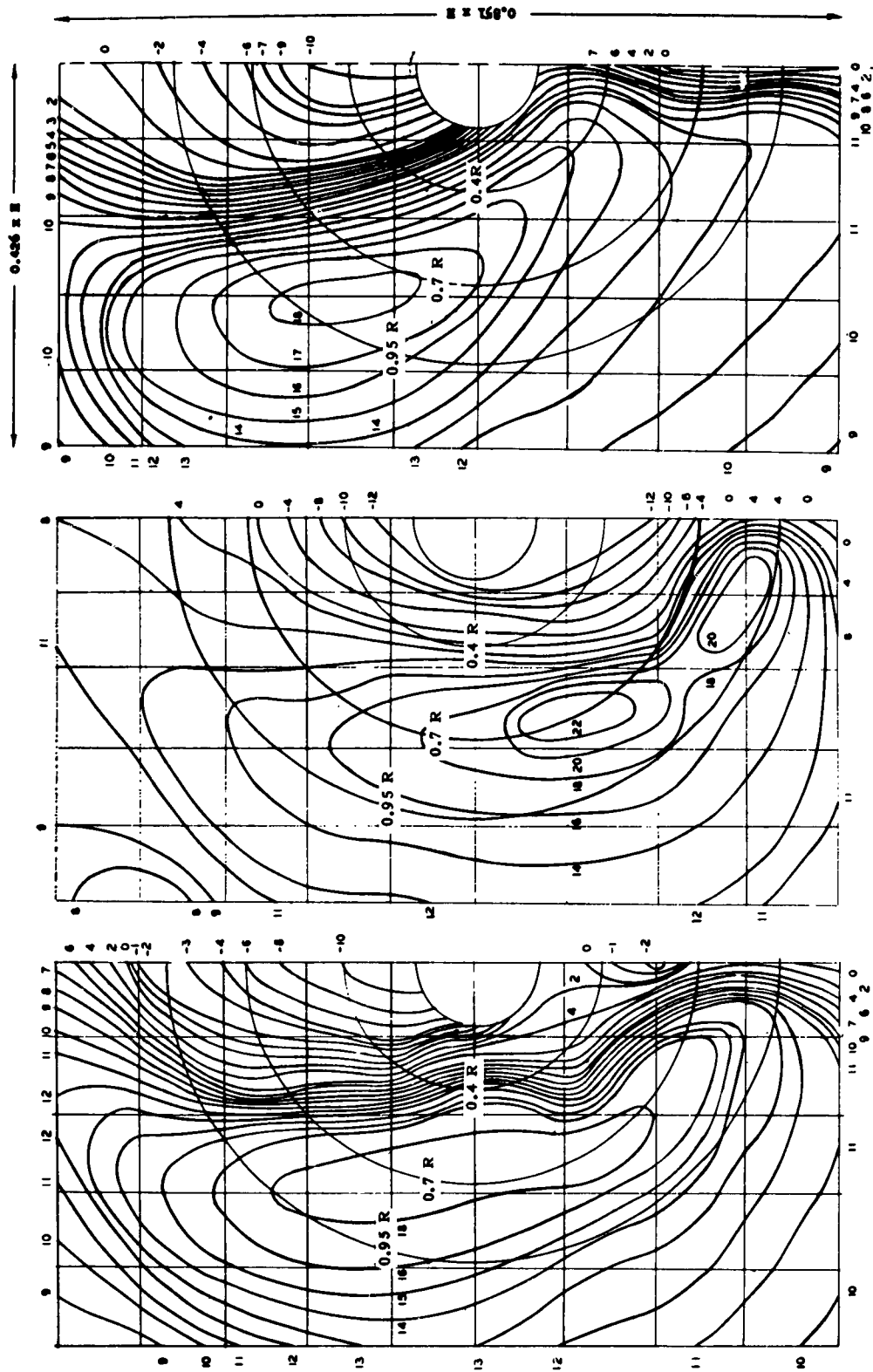
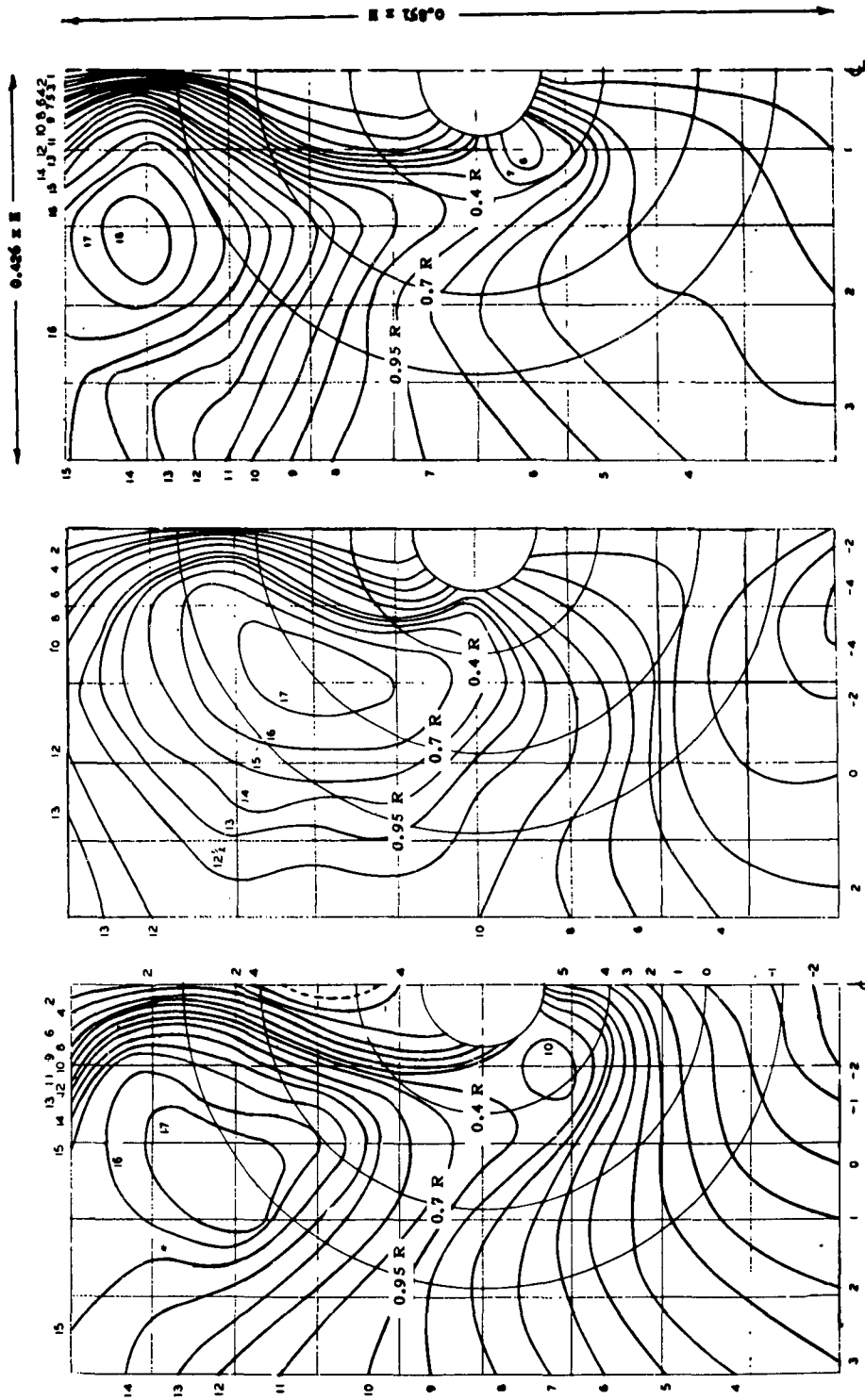


Figure 73a — Parent Form, Model 4280

Figure 73b — U-Shaped Stern, Model 4281

Figure 73c — V-Shaped Stern, Model 4282

Figure 73 — Lines of Equal Vertical Wake Components $w_v = (V_v/V) \cdot 100$



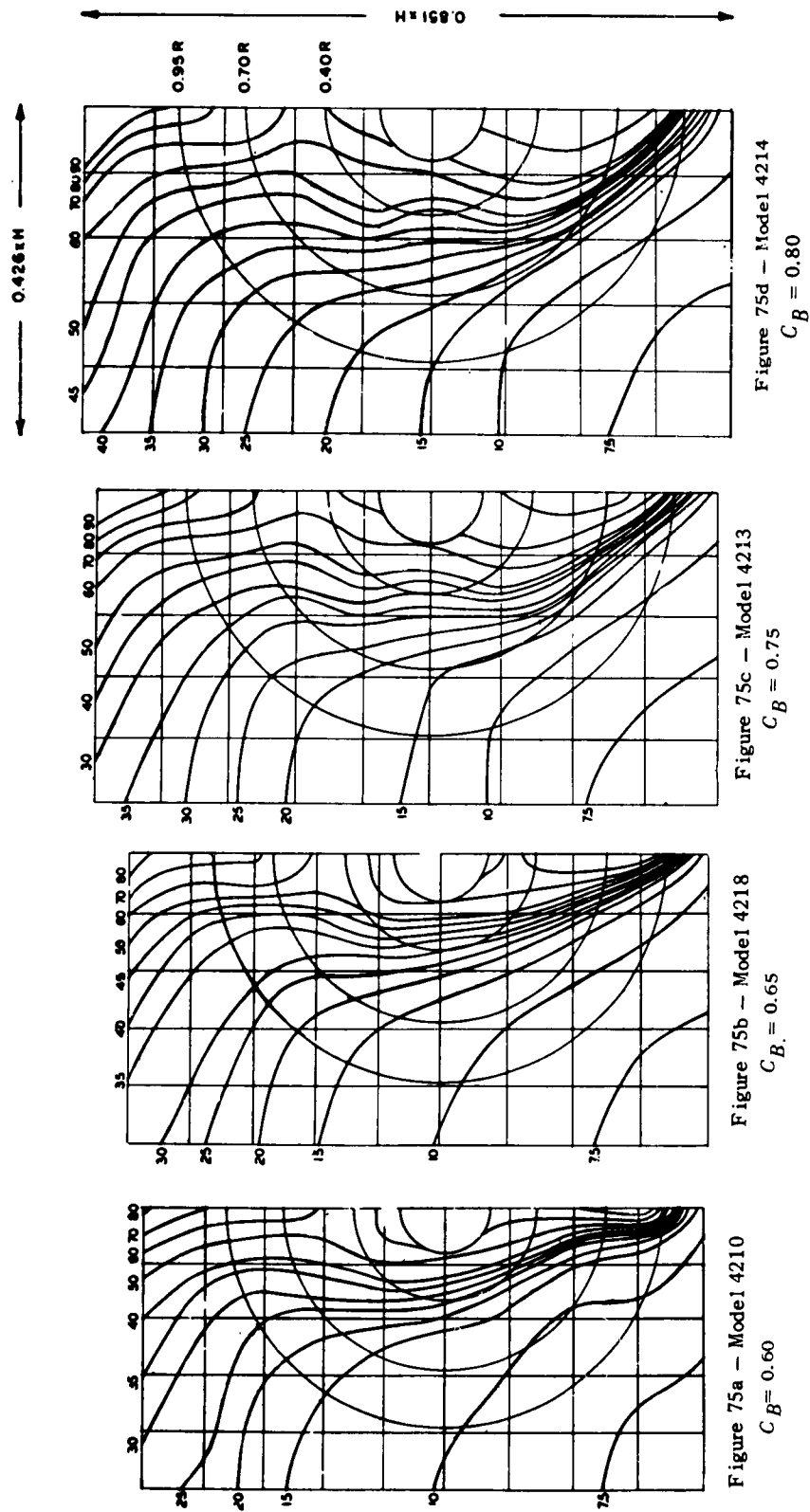


Figure 75 - Lines of Equal Longitudinal Wake Components $w_x = [1 - (V_x/V)]100$

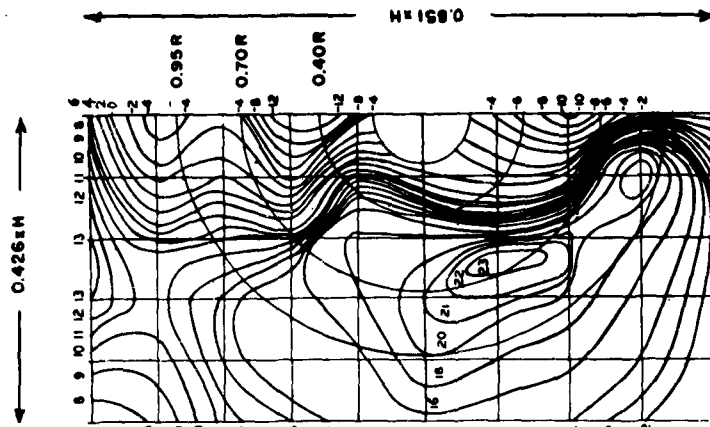


Figure 76d — Model 4214
 $C_B = 0.80$

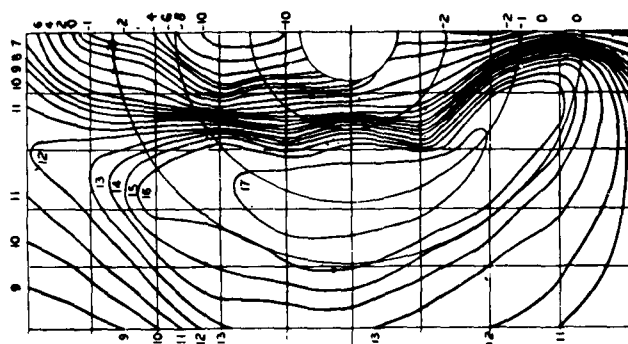


Figure 76c — Model 4213
 $C_B = 0.75$

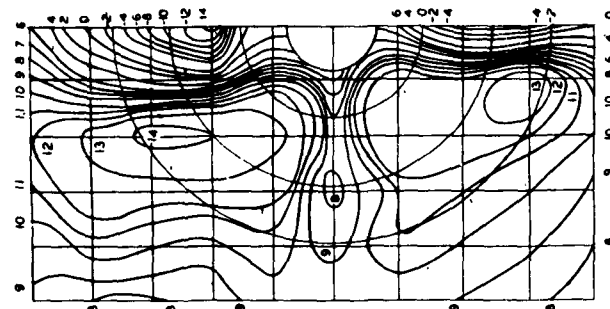


Figure 76b — Model 4218
 $C_B = 0.65$

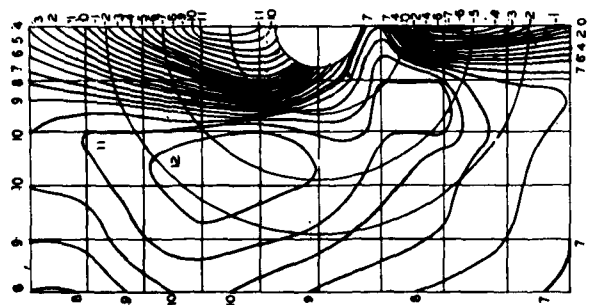


Figure 76a — Model 4210
 $C_B = 0.60$

Figure 76 — Lines of Equal Vertical Wake Components $w_v = [(V_v/V)]100$

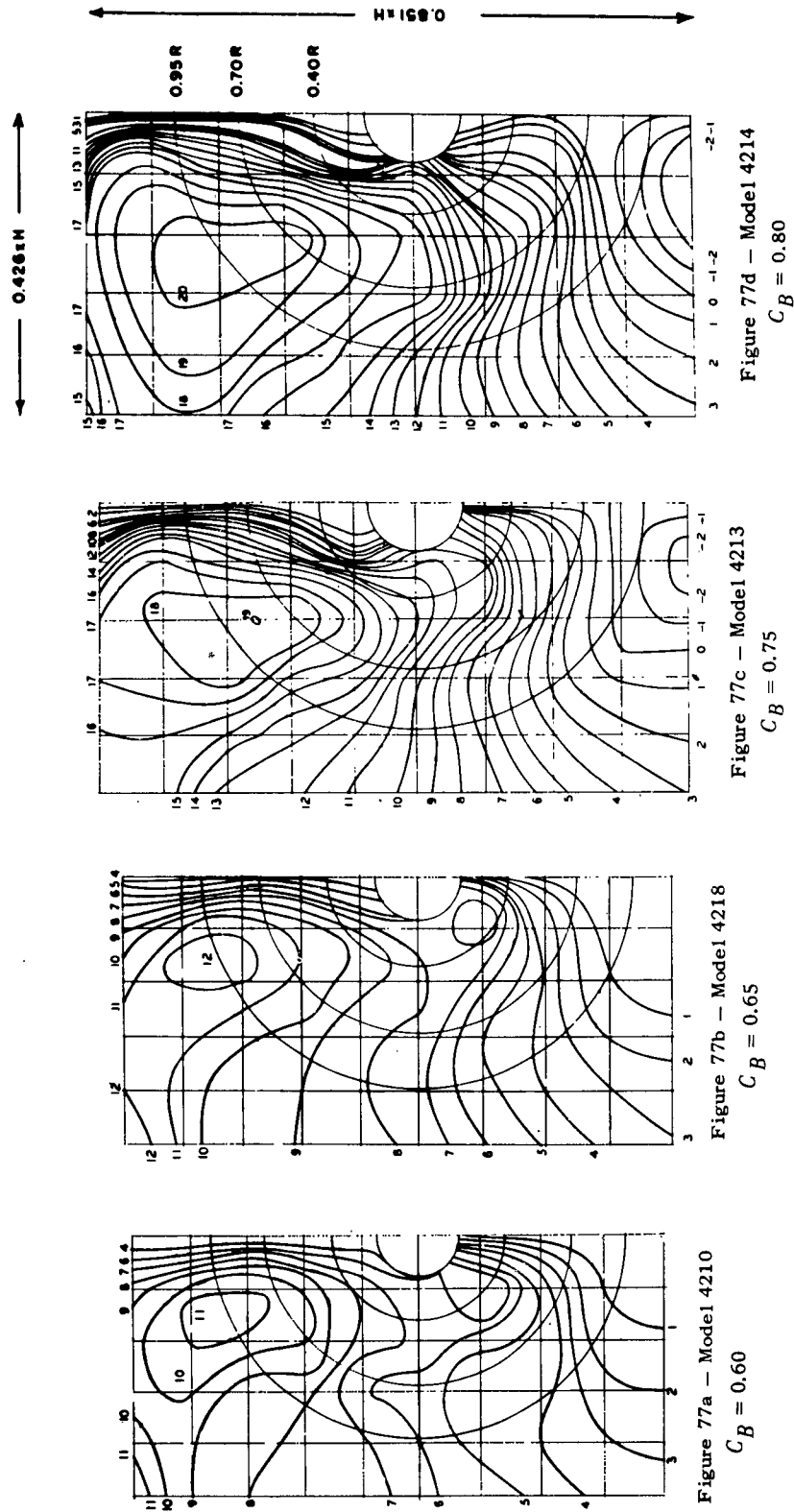


Figure 77 — Lines of Equal Horizontal Wake Components $w_h = [(V_h/V)]100$

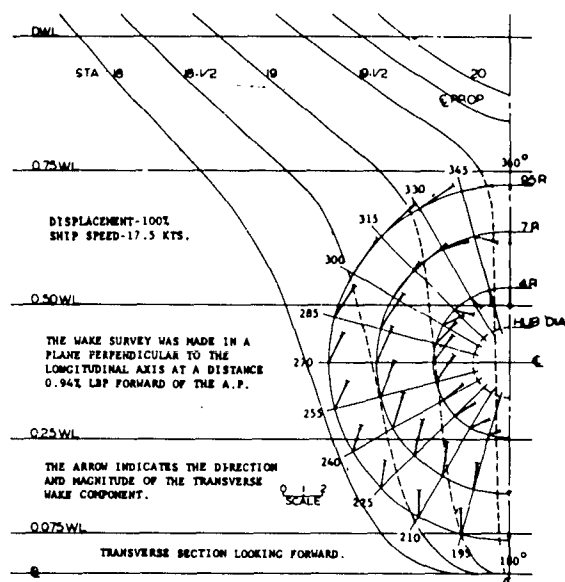


Figure 78 -- Wake Diagram for Parent Form, Model 4280, $C_B = 0.70$

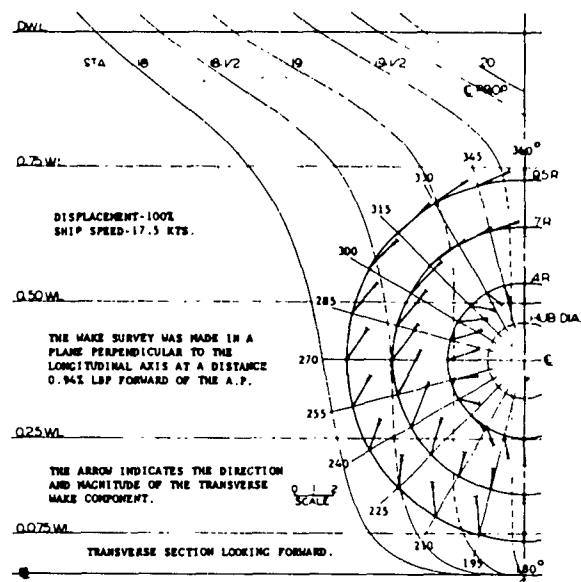


Figure 79 -- Wake Diagram for U-Shaped Form, Model 4281, $C_B = 0.70$

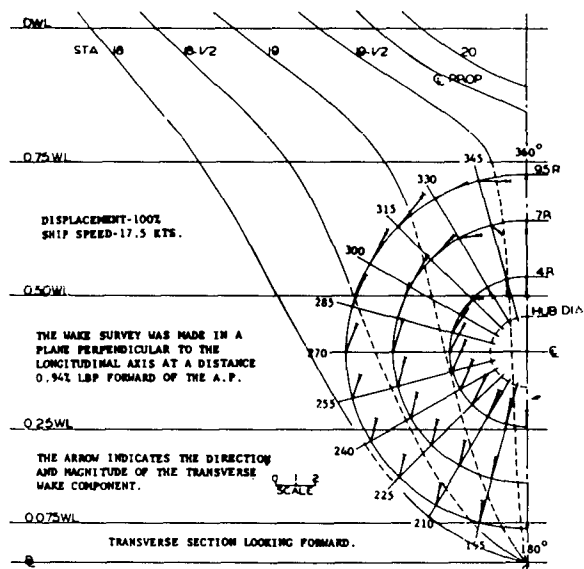


Figure 80 -- Wake Diagram for V-Shaped Form, Model 4282, $C_B = 0.70$

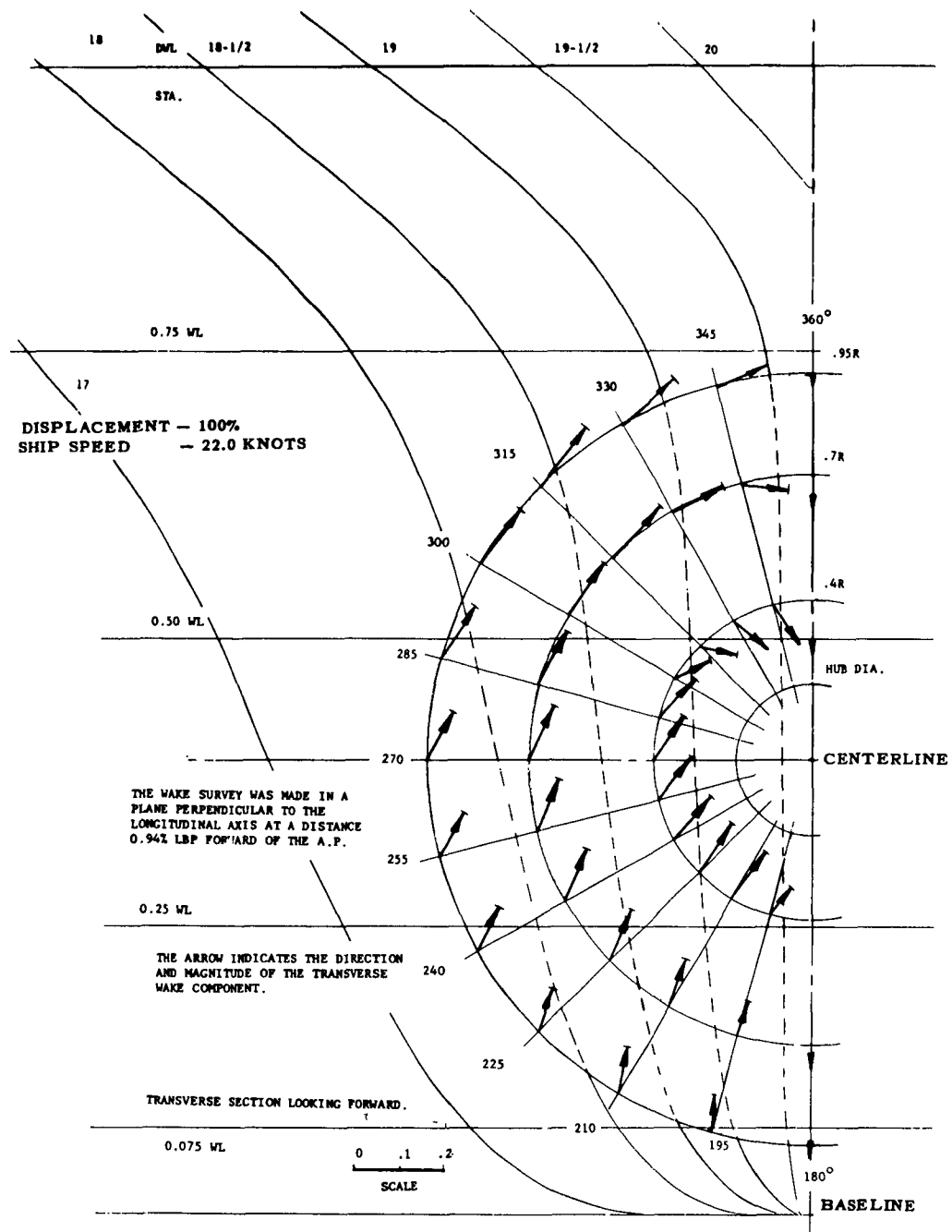


Figure 81 - Wake Diagram for Model 4210- $C_B = 0.60$

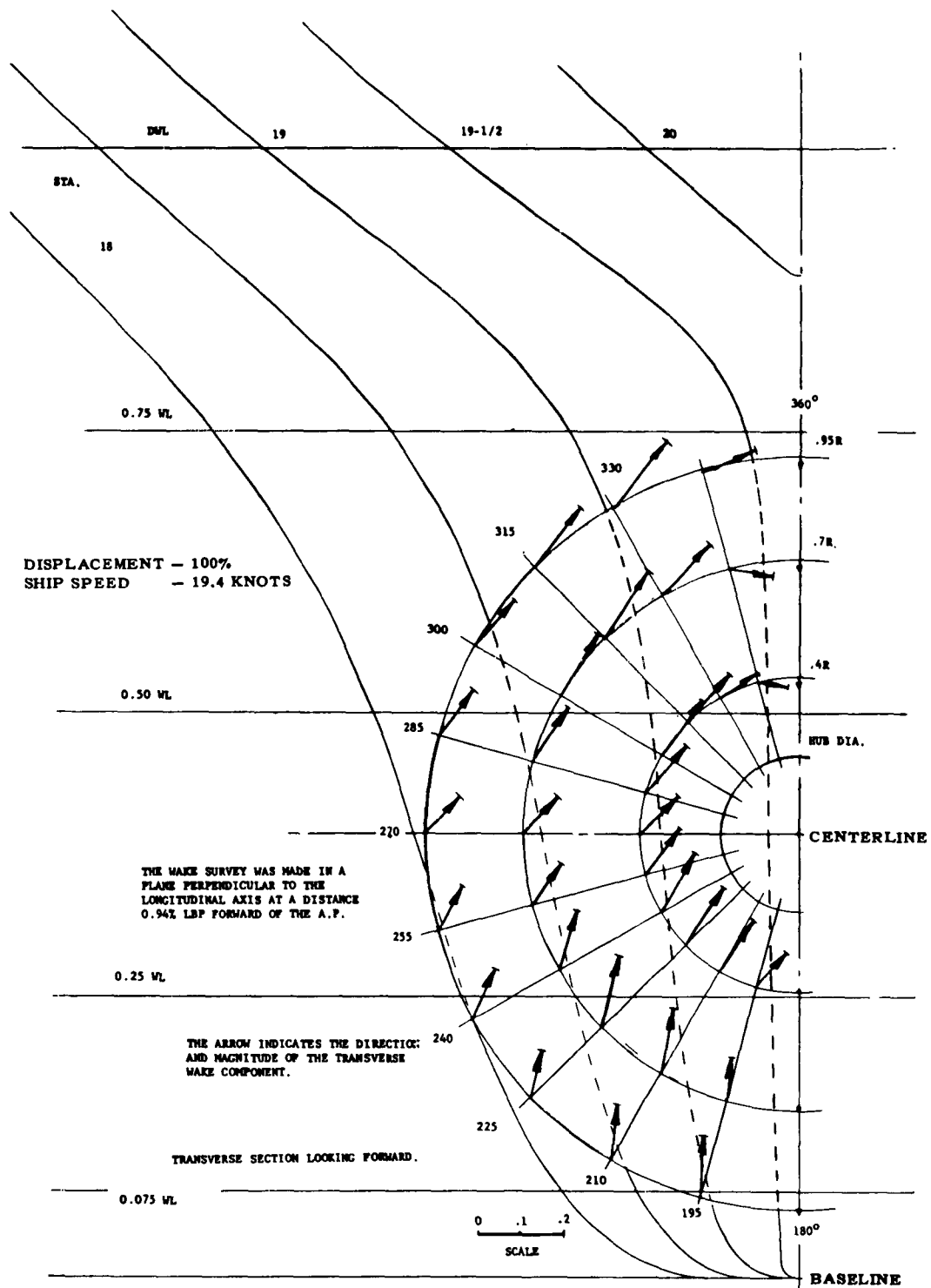


Figure 82 - Wake Diagram for Model 4218- $C_B = 0.65$

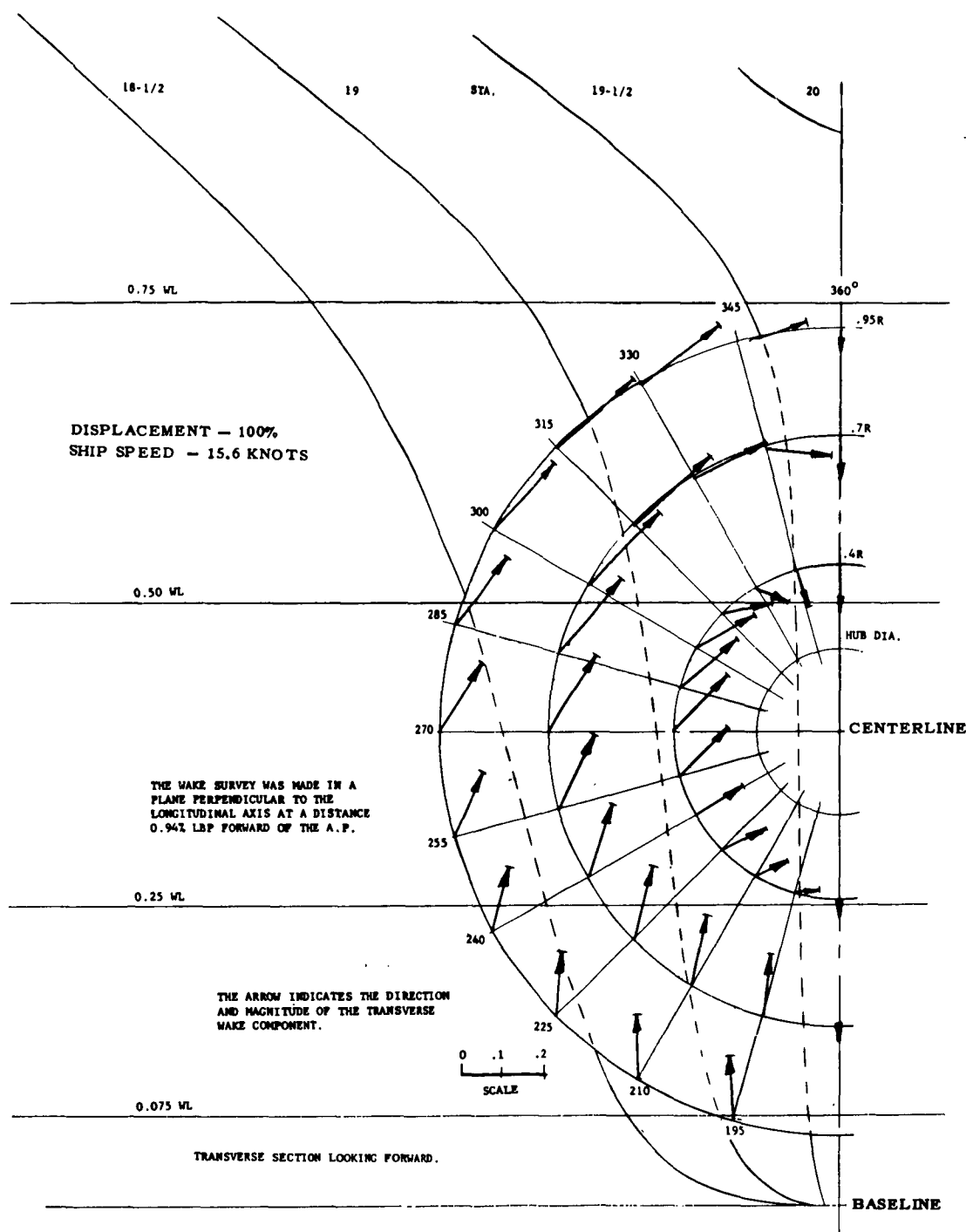


Figure 83 — Wake Diagram for Model 4213— $C_B = 0.75$

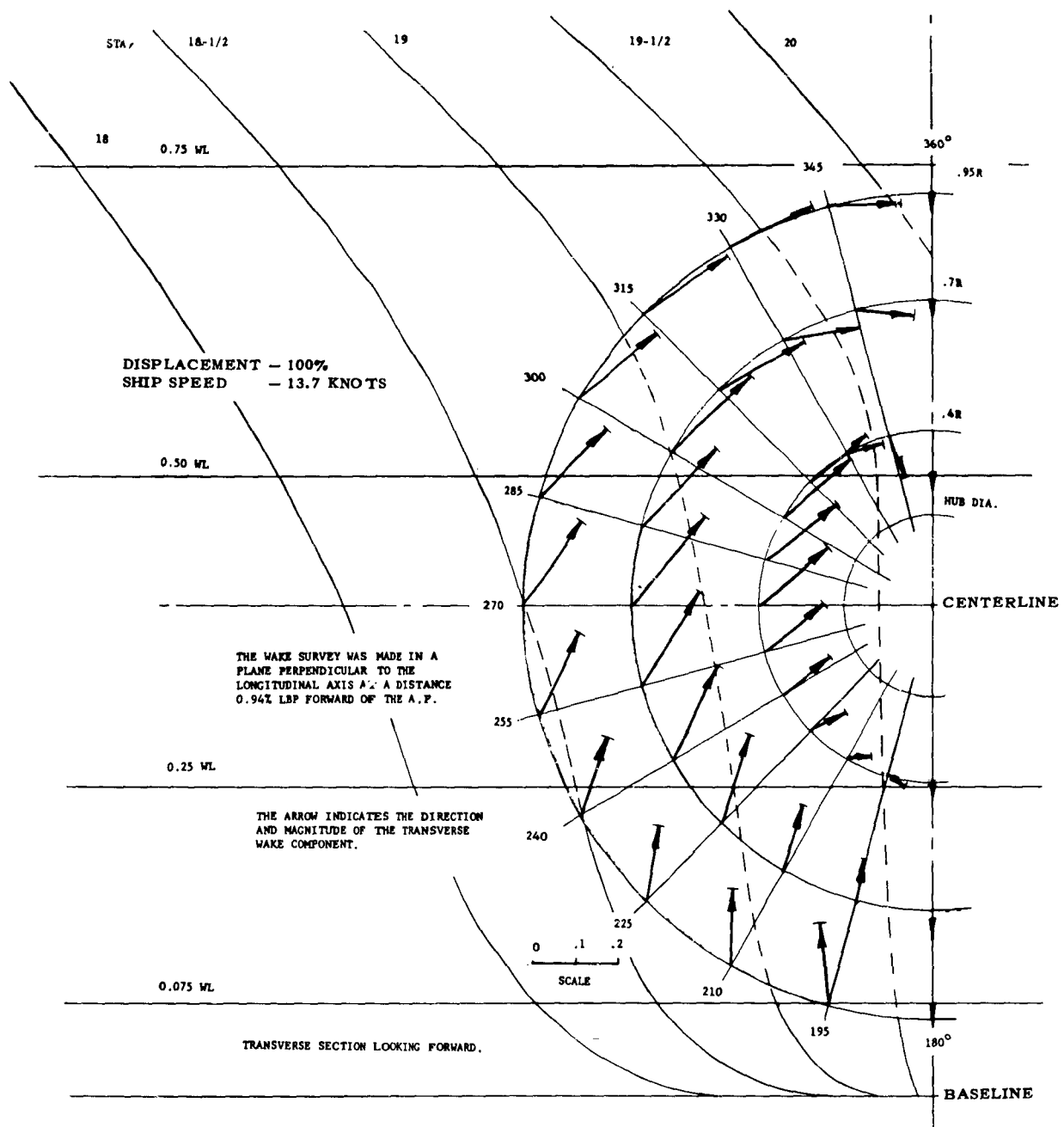


Figure 84 - Wake Diagram for Model 4214- $C_B = 0.80$

thrust block. Any smoothing of the wake will therefore not only improve the hydrodynamic performance of the propeller but also reduce one of the causes of hull vibration.

Knowing the wake components at any point, it is possible to calculate the forces on the section of the propeller blade at that point on the assumption that they will be the same as those it would encounter in a steady flow of the same pattern and, by summation, the total force and moment on the whole propeller. This method of analysis is called the "quasi-steady" method, and Figure 85 shows the variation in total thrust for a 4-bladed propeller behind the three $0.70 C_B$ models calculated in this way. Much theoretical work is in progress directed towards taking into account the dynamic effects of variations in wake velocity—the so-called "unsteady" method—but in the meantime the "quasi-steady" method is commonly used for comparative qualitative calculations when considering the effects of possible changes in propeller design. Wake diagrams of the type given will be useful in this respect. The longitudinal and tangential velocity components around any circumferential line in the propeller disk can be analysed into harmonic components, and the relative magnitudes of these will have an important influence on the vibratory thrust and torque forces. The wake pattern should therefore be considered as one factor whenever any decision is to be made in the choice of number of propeller blades.

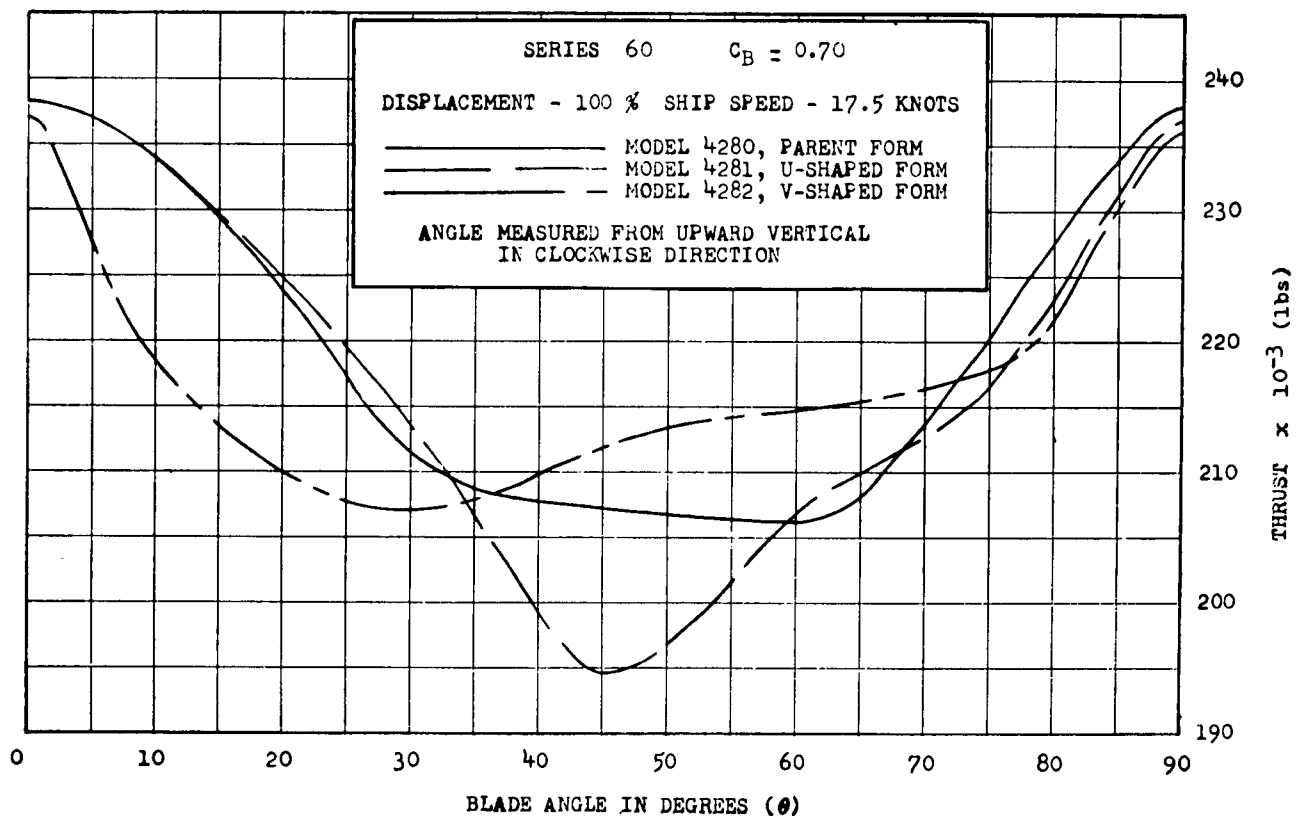


Figure 85 — Thrust Fluctuation

CHAPTER XII

REVIEW OF SERIES 60 PROJECT

In the design of any given ship the naval architect has always to meet a number of conflicting demands which, to a greater or lesser extent, limit his choice of dimensions, proportions, fullness, and other features. An increase in length is generally favorable from the points of view of low resistance in smooth water and maintenance of speed in rough weather, but it is expensive structurally, carries penalties in crew numbers, and, in specific cases, may be limited by dimensions of locks, piers, drydocks, etc, which may also restrict beam and draft. The depth of water in the world's harbors today is also a definite limitation on draft, particularly for large tankers and other bulk carriers. On the other hand, beam is limited on the minimum side by the need for adequate stability, and questions of trim and weight distribution, especially in bulk carriers, may exercise some control over the necessary longitudinal distribution of displacement and so on the *LCB* position.

In practice, therefore, the naval architect has usually to design a ship within dimensions already defined to a large extent by such considerations, but there is generally some latitude available for adjustment to suit the demands of good resistance and propulsion qualities.

The results of the Series 60 experiments can be of material help to the designer in any single-screw ship design which in its proportions and other features falls within the area of variables covered. If the designer adopts the lines of Series 60, the position of *LCB* as used in the parent forms, and a propeller having the standard ratio of diameter to draft of 0.7, he can make a very accurate estimate of both the ehp and shp of a ship for any particular selection of length, beam, draft, and displacement:

If for trim or other reasons, the *LCB* has to be placed in some other position, allowance for this can be made using the data given in Chapter VII or in Tables 49 through 53, and for departures from the standard propeller diameter the values of w , t , and relative rotative efficiency (e_{rr}) from the contours can be corrected by using the results of the experiments with different diameter propellers detailed in Chapter X. The w and t data can also be used for assessing the propulsive efficiency to be expected for power plant conditions different from those assumed in the propeller designs used with the series models.

In addition to estimating the required power for a particular ship design having agreed characteristics, the data are also useful in assessing the penalties which must be paid or the advantages to be gained by changing such characteristics. This is a problem which occurs at some time or other in almost every design study, and this use of the data may well be as important as estimates of actual power.

Table 49 – Effect of Change in *LCB* Position – 0.60 C_B

Figures show increase or decrease in resistance for movement of *LCB* from position in parent model, in percentage of \textcircled{C}

$\frac{V}{\sqrt{L_{WL}}}$	\textcircled{K}	$\frac{V}{\sqrt{L_{BP}}}$	<i>LCB</i> Position			
			2.48A	1.50A Parent	0.51A	0.52F
0.40	1.057	0.403	-0.4	----	-0.3	-1.0
0.45	1.189	0.454	-0.9	----	-0.3	-2.2
0.50	1.321	0.504	-0.2	----	-0.3	-2.2
0.55	1.453	0.555	---	----	-0.3	-1.3
0.60	1.585	0.605	---	----	-0.2	-1.2
0.65	1.717	0.655	+0.6	----	+0.4	+0.7
0.70	1.849	0.706	+0.3	----	+1.0	+0.9
0.75	1.981	0.756	+1.3	----	+1.0	+1.2
0.80	2.113	0.807	+2.0	----	+0.3	+1.7
0.85	2.245	0.857	+2.4	----	+3.2	+6.5
0.90	2.378	0.908	+1.2	----	+2.0	+6.9
0.95	2.510	0.958	+0.5	----	+4.7	+5.4
1.00	2.642	1.008	-0.6	----	+3.2	+5.7
1.05	2.774	1.059	-0.9	----	+3.6	+6.0
1.10	2.906	1.109	-1.3	----	+3.6	+5.6
1.15	3.038	1.160	-1.5	----	+3.1	+6.1
1.20	3.170	1.210	-0.5	----	-0.3	+3.6

Table 50 – Effect of Change in *LCB* Position – 0.65 C_B

Figures show increase or decrease in resistance for movement of
LCB from position in parent model, in percentage of (C)

$\frac{V}{\sqrt{L_{WL}}}$	(K)	$\frac{V}{\sqrt{L_{BP}}}$	<i>LCB</i> Position				
			2.46A	1.54A Parent	0.50A	0.38F	1.37F
0.40	1.031	0.403	+4.8	----	+1.7	-1.5	- 1.6
0.45	1.160	0.454	+4.2	----	+0.6	-1.8	- 1.2
0.50	1.289	0.504	+3.3	----	-0.3	-1.1	- 0.5
0.55	1.418	0.555	+2.7	----	-0.7	-0.3	+ 0.3
0.60	1.546	0.605	+2.4	----	+0.3	+0.4	+ 1.2
0.65	1.675	0.655	+1.4	----	-0.5	---	+ 1.1
0.70	1.804	0.706	+2.7	----	-1.4	+0.7	+ 2.2
0.75	1.933	0.756	+2.4	----	-0.4	+1.7	+ 5.6
0.80	2.062	0.807	+0.7	----	+0.2	+3.3	+10.4
0.85	2.191	0.857	-0.4	----	+1.3	+7.2	+16.2
0.90	2.320	0.908	-5.3	----	+0.4	+5.2	+10.2
0.95	2.448	0.958	-5.0	----	+2.0	+5.5	+10.6
1.00	2.577	1.008	-2.9	----	+4.5	+6.0	+ 9.8
1.05	2.706	1.059	-2.4	----	+3.6	+4.1	+ 8.6
1.10	2.835	1.109	-1.9	----	+3.6	+6.2	+ 8.6
1.15	2.964	1.160	-1.7	----	+2.6	+4.6	+ 9.1

Table 51 – Effect of Change in *LCB* Position – 0.70 C_B

Figures show increase or decrease in resistance for movement of
LCB from position in parent model, in percentage of (C)

$\frac{V}{\sqrt{L_{WL}}}$	(K)	$\frac{V}{\sqrt{L_{BP}}}$	<i>LCB</i> Position				
			2.05A	0.55A Parent	0.50F	1.54F	2.55F
0.40	1.006	0.403	+6.0	----	+1.9	- 0.6	- 1.9
0.45	1.132	0.454	+5.8	----	+1.6	+ 0.2	- 1.6
0.50	1.258	0.504	+4.8	----	+0.7	- 0.4	- 1.6
0.55	1.384	0.555	+4.9	----	-0.4	- 1.4	- 1.3
0.60	1.510	0.605	+5.5	----	+1.6	+ 0.9	+ 0.4
0.65	1.636	0.655	+4.3	----	+0.9	+ 1.4	+ 2.6
0.70	1.761	0.706	+4.0	----	+0.4	+ 2.3	+ 7.4
0.75	1.887	0.756	+2.0	----	+3.1	+ 6.1	+13.0
0.80	2.013	0.807	-0.9	----	+5.4	+12.0	+23.0
0.85	2.139	0.857	-2.0	----	+5.6	+15.0	+33.6
0.90	2.264	0.908	-5.6	----	+3.9	+15.5	+26.6
0.95	2.390	0.958	-5.0	----	+6.5	+12.7	+21.4
1.00	2.516	1.008	-4.7	----	+7.8	+10.9	+20.2
1.05	2.642	1.059	-5.5	----	+7.6	+11.2	+21.3
1.10	2.768	1.109	-4.8	----	+7.4	+13.2	+22.4
1.15	2.894	1.160	-6.9	----	+4.6	+11.1	+20.5

Table 52 – Effect of Change in *LCB* Position – 0.75 C_B

Figures show increase or decrease in resistance for movement of *LCB* from position in parent model, in percentage of (C)

$\frac{V}{\sqrt{L_{WL}}}$	(K)	$\frac{V}{\sqrt{L_{BP}}}$	<i>LCB</i> Position			
			0.48F	1.50F Parent	2.57F	3.46F
0.40	0.983	0.403	+2.2	-----	- 0.3	- 0.6
0.45	1.106	0.454	+2.3	-----	- 0.1	- 1.3
0.50	1.229	0.504	+2.4	-----	- 0.6	- 2.7
0.55	1.352	0.555	+2.7	-----	- 2.1	- 1.9
0.60	1.474	0.605	+4.1	-----	- 2.6	+ 0.1
0.65	1.597	0.655	+1.7	-----	+ 0.5	+ 2.5
0.70	1.720	0.706	-1.1	-----	+ 4.9	+11.7
0.75	1.843	0.756	-4.0	-----	+ 7.2	+14.3
0.80	1.966	0.807	-3.1	-----	+10.2	+13.7
0.85	2.089	0.857	-6.1	-----	+ 7.4	+16.6
0.90	2.212	0.908	-4.5	-----	+ 7.7	+16.2

Table 53 – Effect of Change in *LCB* Position – 0.80 C_B

Figures show increase or decrease in resistance for movement of *LCB* from position in parent model, in percentage of (C)

$\frac{V}{\sqrt{L_{WL}}}$	(K)	$\frac{V}{\sqrt{L_{BP}}}$	<i>LCB</i> Position			
			0.76F	1.45F	2.50F Parent	3.51F
0.40	0.960	0.403	+14.2	+4.3	-----	- 0.1
0.45	1.080	0.454	+14.4	+4.2	-----	+ 0.7
0.50	1.200	0.504	+14.9	+4.1	-----	+ 1.5
0.55	1.320	0.555	+14.8	+4.1	-----	+ 2.7
0.60	1.440	0.605	+11.2	+1.7	-----	+ 6.2
0.65	1.561	0.655	+ 5.0	-0.9	-----	+11.0
0.70	1.681	0.706	- 1.3	-5.0	-----	+ 9.7
0.75	1.801	0.756	- 3.7	-4.8	-----	+14.2
0.80	1.921	0.807	- 2.7	-7.2	-----	+12.8
0.85	2.041	0.857	- 7.0	-3.4	-----	+13.0

The number of models run had to be limited both on the score of time and expense. In view of the wide field covered, the question may be asked as to how well the contours of residuary resistance, C , wake fraction, thrust deduction fraction, and relative rotative efficiency represent the probable values of these quantities at points not directly supported by test results—in other words, how reliable would be estimates made of these quantities from the interpolated contours? One such comparison is given in Appendix C (see Figure C-3) where it is shown that the particular set of contours chosen represents extremely well the results of the nine models on which they were based.

A more general method of answering this question is available, however. In the process of assessing the merits of the Series 60 parents, actual models of Series 60 equivalents of the SCHUYLER OTIS BLAND, C.2., and PENNSYLVANIA were made and tested. These models had the corresponding dimensions, displacement, and LCB position of the actual ship but Series 60 lines. It is now possible to estimate the ehp for these three forms from the contours and to compare the results with the ehp actually measured on the models. Such comparisons are shown in Figures 86, 87, and 88. Two estimated curves are shown in each

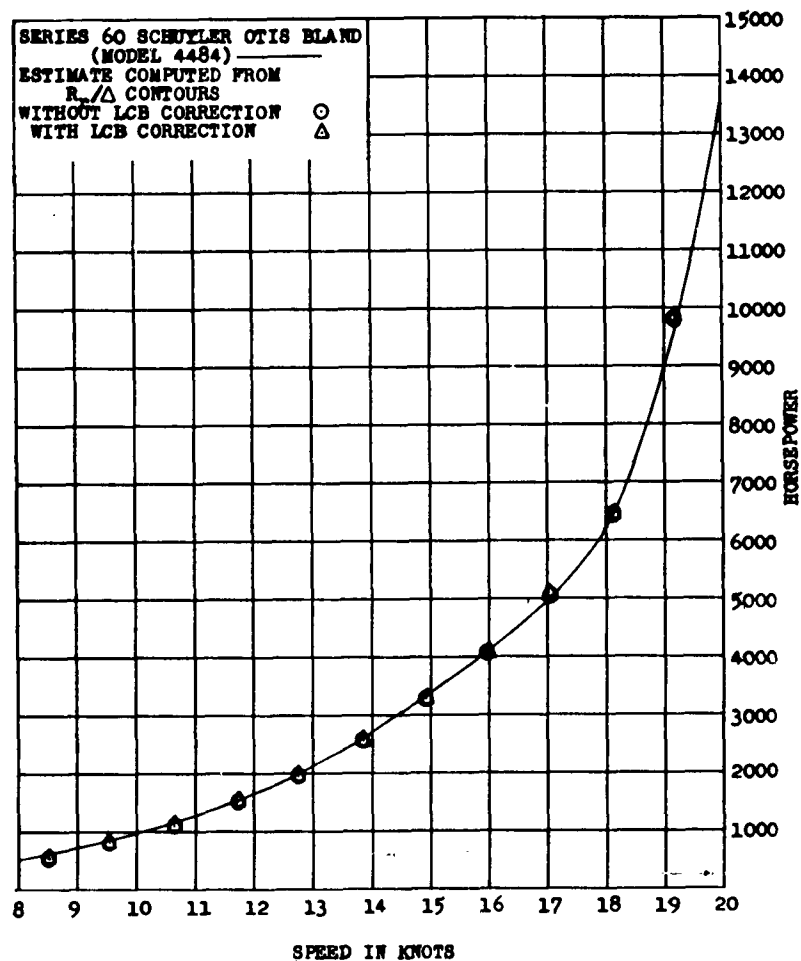


Figure 86 — Comparison of EHP obtained by testing a Model having Series 60 Lines and Proportions of SCHUYLER OTIS BLAND with Corresponding Estimate from Series 60 Contours

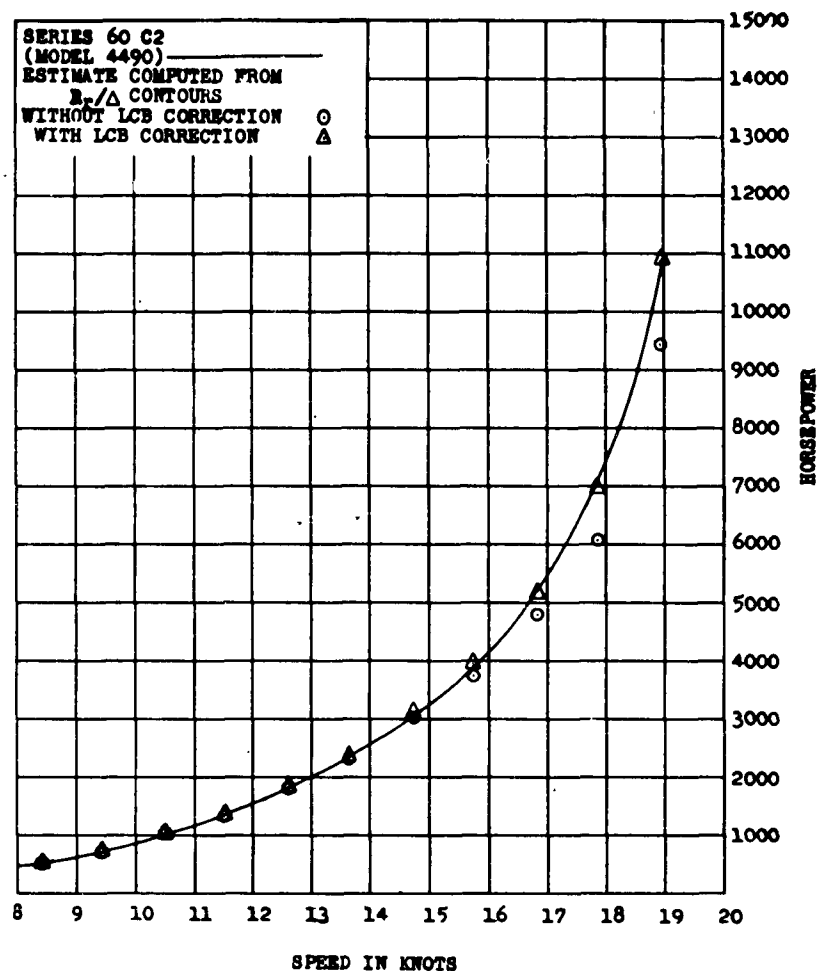


Figure 87 – Comparison of EHP obtained by testing a Model having Series 60 Lines and Proportions of C.2. Class with Corresponding Estimate from Series 60 Contours

case, one for a ship having the *LCB* in the position used in the Series 60 models on which the contours are based, the other for a ship having the *LCB* in the same position as the actual ship in question. The change in ehp for the shift in *LCB* was estimated from the data in Chapter VII and Tables 49 to 53.

For the SCHUYLER OTIS BLAND and PENNSYLVANIA, the actual *LCB* positions were within 0.5 percent *LBP* of those used in the Series 60 models from which the contours were developed, and the effects on ehp were extremely small (Figures 86 and 88). In the case of the C.2. design, the actual ship had the *LCB* 1.4 percent forward of midships, and the position corresponding to the Series 60 contours was 1 percent aft. The actual and estimated ehp did not differ materially below 15 knots, but above this speed, the estimated ehp from the Series 60 contours was lower than that of the C.2. Series 60 equivalent, the reduction at 18 knots being some 12 percent (Figure 87). This illustrates the advantage of the finer entrance at these higher speeds. The estimated curve for the Series 60 equivalent with the *LCB* in the actual ship position (1.4 percent forward), corrected by the data in

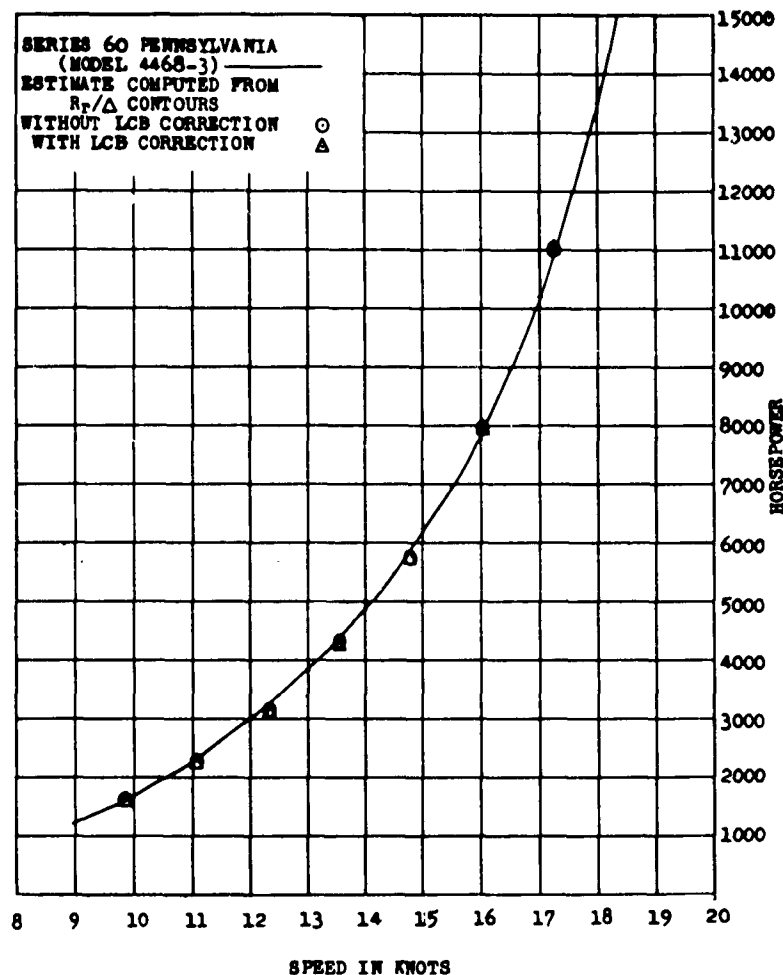


Figure 88 — Comparison of EHP obtained by testing a Model having Series 60 Lines and Proportions of SS PENNSYLVANIA with Corresponding Estimate from Series 60 Contours

Chapter VII, shows excellent agreement with the ehp measured on the model. Thus when allowance is made for differences in *LCB* position, the ehp estimated from the contours is in very good agreement with that measured on these three models. This fact should give confidence in the use of the contours throughout the range, for of course the results of the tests on these three Series 60 equivalent models were not used in any way in the process of deriving contours.

Self-propulsion tests were also carried out on the Series 60 equivalents of the SCHUYLER OTIS BLAND and the PENNSYLVANIA. The values of w , t , and e_{rr} measured in the tests are compared in Figures 89 and 90 with the corresponding values estimated from the appropriate contours, and the agreement is again very satisfactory.

Although estimates of power made from the contours apply strictly only to ships having lines derived from the Series 60 charts, they can, with proper exercise of caution, be used as guides over a somewhat wider field. For example, in developing the original Series 60 lines, Bethlehem Steel Company provided a set of lines equivalent to the MARINER class of fast

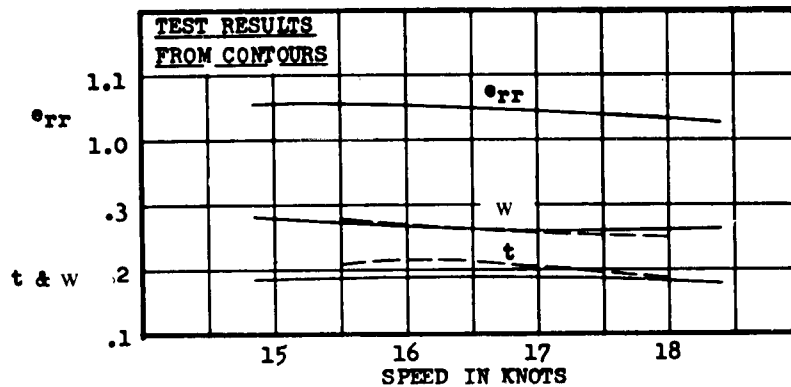


Figure 89 – Comparison of w , t , and e_{rr} for Series 60 SCHUYLER OTIS BLAND from Contours and Test Results

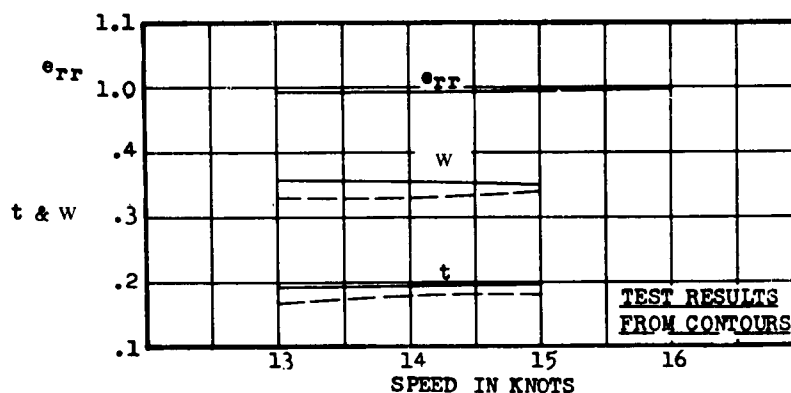


Figure 90 – Comparison of w , t , and e_{rr} for Series 60 PENNSYLVANIA from Contours and Test Results

cargo ships but without a bulbous bow (Model 4440). A comparison of this model with the Series 60, 0.60 C_B parent (Model 4210) showed the latter to have appreciably lower \textcircled{C} values at the service and trial speeds (Figure 6 of Reference 45). Although the lines were rather similar, the hull form coefficients were different—for example, the block coefficient of Model 4440 was 0.611—and a comparison of the ehp for Model 4440 with that derived from the contours for a Series 60 equivalent form of C_B 0.611 (Figure 91) indicates that again the agreement is good.

The contours can also be used for comparative purposes in much the same way as is done with the Taylor Standard Series. If a new design has secondary characteristics which differ from those of its Series 60 equivalent but model results are available for some other ship which more closely resembles it in these respects, the latter may be used as a “basic” ship. Calculations of ehp can be made from the contours for the “Series 60 equivalents” of both the new design and the basic ship. Then the approximate ehp for the new ship will be

$$\text{ehp of Series 60 equivalent} \times \frac{\text{ehp for basic ship}}{\text{ehp of Series 60 equivalent of basic ship}}$$

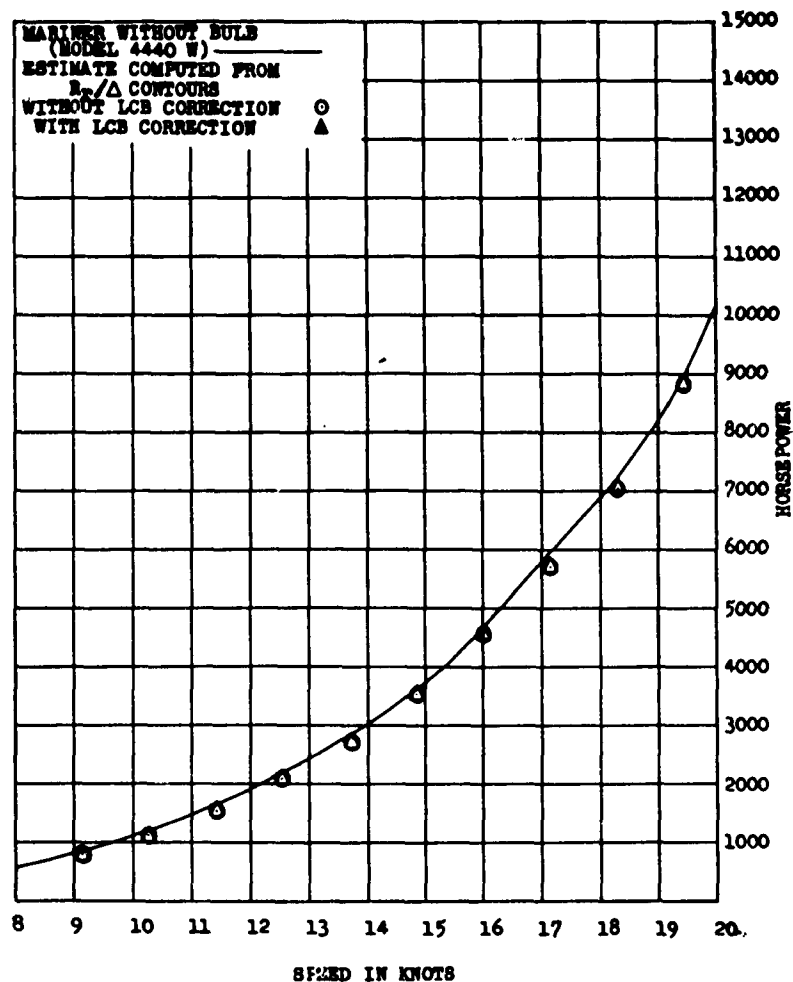


Figure 91 — Comparison of EHP obtained by testing a Model having Proportions of MARINER Class, but without Bulbous Bow, with Corresponding Estimate from Series 60 Contours

Figure 92 shows the predicted ehp for an ocean-going ore carrier of $0.78 C_B$ compared with actual model test results; the estimate was made as outlined above, using the PENNSYLVANIA as the "basic" ship.

Even more extreme uses can be made of the Series with some success, as shown by Professor Baier's adoption of the series bow and stern lines with parallel body in the design of lake ships (page V-22). The demonstration of the qualitative uses of Series 60 is easy, but the establishment of their absolute quantitative value is more difficult. In discussing the very first paper in the series (Reference 44), Mr. V. L. Russo made the following observations: "The real value of the contours proposed in the paper could be established best by determining what results these contours would give by comparison with acceptable results exemplified not by the standard of a phantom form but by actual successful ship designs . . . This way of comparison . . . would have the advantage of being conclusive as it would furnish a true comparison under practical conditions and be devoid of imponderable

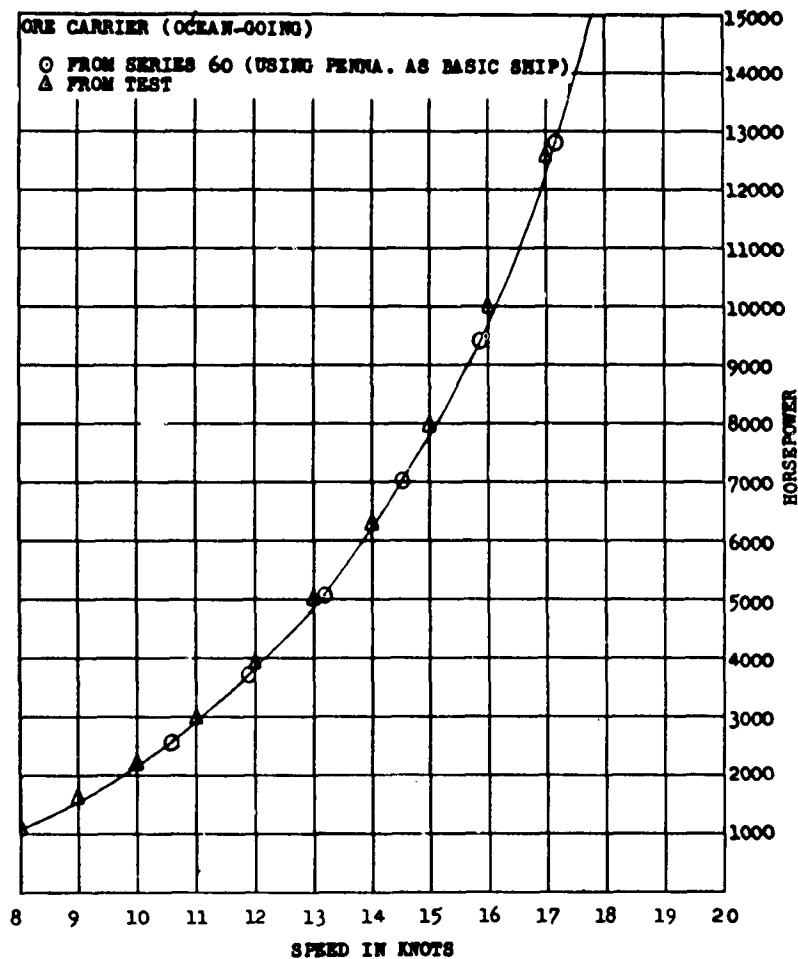


Figure 92 - Comparison of EHP obtained by testing a Model of an Ocean-going Ore Carrier with Corresponding Estimate from Series 60 Contours using SS PENNSYLVANIA as Basic Ship

discrepancies." This suggestion was taken up by the SNAME Panel (of which Mr. Russo was a member), and the subsequent Series 60 parents were developed using just this method, as described earlier in this report. It is believed that these parents now compare very well in performance with the successful ship designs on which they were based.

Comparisons with results of similar work at the Netherlands tank have already been mentioned in Chapter VI, and in this connection, it is of interest to quote the remarks of Professor L. Troost, one-time Director of that establishment, with a vast experience in the model testing field: "The writer has applied the computations as presented in the paper to the results of some high-quality hulls and propellers of foreign (European) design. He is satisfied that the optimum Series 60 data are indicative of very high performance and that it will require great skill and experience to improve on them for an amount of 2 percent in total ehp and shp in regular designs. He also found that an extrapolation to 0.82 block, which will often be necessary in the field of super-tankers and comparable ships, not too hazardous." (Discussion on Reference 64).

Although no claim can possibly be made that Series 60—or indeed any other Series—represents optimum resistance qualities, the above remarks and other evidence do suggest that the contours will be of help in preliminary design work and can be used with some confidence in the estimation of ship performance, both in the absolute sense and also in the investigation of various alternative choices which may face the naval architect.

In using the Series 60 results, it is worth recalling that the hull forms are all related to one another in a clear and unambiguous way by means of graphical methods. As has been pointed out before, this has the advantage over geometrical variation of one parent form in that the characteristics can be varied with fullness to suit the corresponding changes in speed-length ratio. The alternative use of a single parent form to cover such a wide range of variables as used in Series 60 would have led inevitably to unrealistic designs towards the limits of the area covered. Another point to remember is that all models were of the same length and run in the same tank with the same instrumentation, thus eliminating other possible sources of difference.

In the course of the discussions on the many Series 60 papers, much has been said about various methods of presenting the data. The two most commonly used are to give values of residuary resistance per ton of displacement $\frac{R_R}{\Delta}$, in terms of speed-length ratio $\frac{V}{\sqrt{L_{WL}}}$, almost universally used in the United States, or values of $C_{400 \text{ ft}}$ in terms of K , as used in Great Britain. Both systems have merits and demerits, as one might expect, but they are well-entrenched in their respective homes. The Series 60 results have therefore been given in both ways as contours of $\frac{R_R}{\Delta}$ and of C to their respective bases. There is a vast amount of model data expressed in one or other of these forms, with which the Series 60 results can be compared directly. The SNAME Model Resistance Data sheets also give the information in both these forms.

The presentation of $\frac{R_R}{\Delta}$ in terms of $\frac{V}{\sqrt{L_{WL}}}$ has the advantage of simplicity but suffers from two drawbacks. In the first place, a true merit comparison has to be made on the basis of total resistance per ton of displacement, and comparisons on the basis of $\frac{R_R}{\Delta}$ can be quite misleading. Skin friction resistance is the major component of total resistance in most if not all single-screw merchant ships, and this depends on wetted surface, not directly on displacement. To make a merit comparison from data presented in this way, it is therefore necessary to estimate the frictional resistance in each case and so obtain total resistance or ehp.

The true merit comparison of interest to the naval architect and ship owner is the total resistance per ton of displacement $\frac{R_T}{\Delta}$. To present this properly in curve form it is

necessary to have the abscissa and ordinate values compatible. For abscissa, the speed-length ratio $\frac{V}{\sqrt{L}}$ is preferred by many naval architects for its simplicity. In order to keep the values of $\frac{R_T}{\Delta}$ within a reasonable numerical range, it is usual to divide them by some function of (speed)² since this makes the ordinates almost constant over the lower speed range. If it is desired to use $\frac{V}{\sqrt{L}}$ as the speed parameter, then the ordinates should be

$$\frac{\frac{R_T}{\Delta}}{\left(\frac{V}{\sqrt{L}}\right)^2} \quad \text{or} \quad \frac{R_T \cdot L}{\Delta \cdot V^2}$$

If the comparison is to be made on a power basis, then the ordinate becomes $\frac{R_T \cdot L \cdot V}{\Delta \cdot V^3}$

$$\text{or} \quad \frac{\text{EHP} \cdot L}{\Delta \cdot V^3} \quad \text{or} \quad \frac{\text{SHP} \cdot L}{\Delta \cdot V^3}$$

Dr. Telfer has made this point very clearly in discussing the Series 60 papers. "... the designer's problem is usually to find the model having the lowest resistance per ton displacement on a given length, length being usually approximately fixed by conditions other than resistance" (discussion on Reference 44). And again, "Figure 16 gives us an incompatible presentation of a power-displacement function $\frac{\text{SHP}}{\Delta^{2/3} V^3}$ presented in terms of a speed-length function $\frac{V}{\sqrt{L}}$. From this diagram a designer is led to infer that the finest ships are always the most economical. Such a conclusion from the basic data would be completely erroneous. To review the data correctly they must be presented in a compatible form. As the speed-length ratio $\frac{V}{\sqrt{L}}$ is preferred by most practical ship designers it must be retained and the requisite change for compatibility made in the power-displacement function. This must be converted to a power-length basis, still using, however, power per ton displacement. The conversion produces the function $\frac{\text{SHP} \cdot L}{\Delta \cdot V^3}$ which correctly grades the power per ton of all vessels having the same length and speed" (discussion of Reference 61).

The basic resistance and dhp data for the Series 60 parents are presented in this form in Figures 93 and 94. To again quote Dr. Telfer: "A designer now sees that if his speed is low the most economical ships have the fuller and not the finer forms. Certainly as the speed is increased the finer form becomes the more economical, and by drawing a tentative envelope to the individual curves a mean scale of optimum block coefficient and optimum power constant for given speed-length ratio is at once available."⁶¹

Dr. Telfer has recently converted the results of the resistance experiments on the Series 60 models to this method of presentation, and compared them with other available data. ("The Design Presentation of Ship Model Resistance Data." E.V. Telfer, Trans NECI, Vol. 79 (1962-63).)

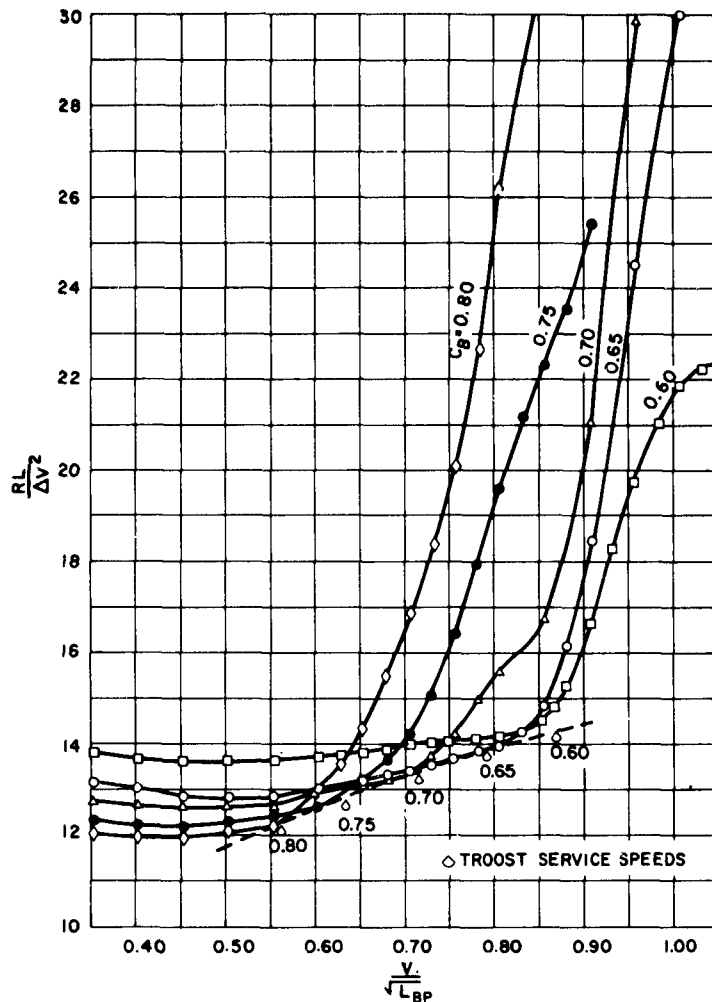


Figure 93 - $\frac{RL}{\Delta V^2}$ on $\frac{V}{\sqrt{L}}$ for Series 60 Parents

The \textcircled{C} and \textcircled{K} constants were introduced by R.E. Froude. At corresponding speeds for model and ship, $\frac{V}{\sqrt{L}}$ is the same, ∇ (volume of displacement) is proportional to L^3 , and so $\frac{V}{\nabla^{1/6}}$ is the same. This ratio has different values in different systems of units, and Froude therefore related the ship speed to the speed of a wave having a length equal to $\frac{\nabla^{1/3}}{2}$.

$$\text{Wave speed} = \sqrt{\frac{g\lambda}{2\pi}} = \sqrt{\frac{g}{2\pi} \cdot \frac{\nabla^{1/3}}{2}} = \nabla^{1/6} \sqrt{\frac{g}{4\pi}}.$$

Hence $\textcircled{K} = \frac{\text{ship speed}}{\text{wave speed}} = \frac{V}{\nabla^{1/6}} \cdot \sqrt{\frac{4\pi}{g}}$, which is nondimensional. The resistance is expressed in terms of $\frac{R_T}{\Delta}$ which is also nondimensional in a consistent system of units. If this is to be presented to a base of \textcircled{K} , we must divide by \textcircled{K}^2 , and Froude added 1000

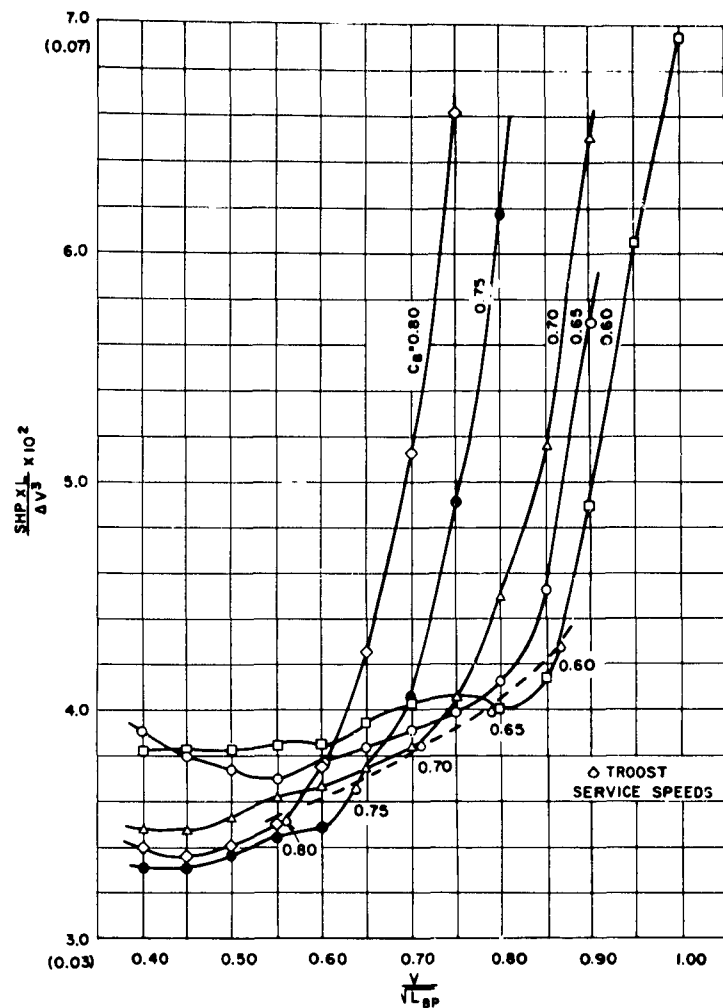


Figure 94 - $\frac{SHP \cdot L}{\Delta V^3}$ on $\frac{V}{\sqrt{L}}$ for Series 60 Parents

to the numerator to avoid unnecessarily small numerical quantities. Thus he defined his resistance constant \textcircled{C} as

$$\textcircled{C} = \frac{R_T}{\Delta \cdot \textcircled{K}^2} \times 1000$$

and speed constant

$$\textcircled{K} = \frac{V}{V^{1/6}} \cdot \sqrt{\frac{4\pi}{g}}$$

both being nondimensional.

For use in usual ship units of V in knots and displacement Δ in tons, these assume the well-known forms

$$\textcircled{K} = 0.5834 \cdot \frac{V}{\Delta^{1/6}}$$

and
$$\textcircled{C} = \frac{R_T}{\Delta} \cdot \frac{\Delta^{1/3}}{(0.5834 \cdot V)^2} \times 1000 = \frac{R_T}{\Delta^{2/3} \cdot V^2} \times 2938$$

where R and Δ are both in tons or, in terms of horsepower,

$$\textcircled{C} = \frac{\text{EHP}}{\Delta^{2/3} V^3} \times 427.1$$

A presentation of resistance data in the \textcircled{C} - \textcircled{K} system is therefore compatible and places models or ships in a correct merit order. In the design of a merchant ship, the two principal basic design factors are the speed and displacement--how much displacement (and therefore deadweight) has the ship to carry at a given speed? The \textcircled{C} - \textcircled{K} system involves only V and Δ and leaves length along with other dimensions and coefficients among the variables which are at the designer's disposal in attempting to find that combination which will result in the most economical overall design.

From the various charts and tables presented in this report, the designer can extract the data he desires in either form, according to his needs and in keeping with the method with which he is most familiar or in which his own data are recorded. The conversion of the \textcircled{C} data using the ATTC line, as given in this paper, to the equivalent \textcircled{C} data using Froude, or vice versa, can also be quickly made by the use of the chart given in Appendix D (Figure D-4), thus giving a connecting link with the large quantity of \textcircled{C} data in existence in this form.

CHAPTER XIII

POSSIBLE EXTENSION OF SERIES 60 AND FUTURE RESEARCH

Although at the time the original series was planned, the numerical ranges adopted for the variables seemed adequate for future designs of single-screw ships, developments over the last 15 years have already overtaken the choice made in 1948.

The single-screw arrangement is preferred by most ship owners because it results in higher propulsive coefficients, cheaper machinery installations and lower running costs than equivalent twin-screw machinery, and in recent years single-screw ships have been built of greater and greater size, with more and more power, higher speeds, and larger propellers. For the dry-cargo or refrigerated ship there has been a demand for increasing speed which, with these other factors, has resulted in many single-screw ships having block coefficients less than the smallest one of 0.60 used in Series 60. Coefficients of 0.55 have been used, and to take care of the future and have adequate design information, it would be useful to extend the series down to a block coefficient of at least 0.55 and perhaps 0.50.

At the other end of the scale, the economics of carrying bulk cargoes, whether oil, ore or grain, have resulted in the mammoth supertankers of today with block coefficients in the neighborhood of 0.825 to 0.85. An extension of Series 60 to 0.85 block coefficient would therefore be of great interest to designers in this field.

The range of $\frac{B}{H}$ for the Series is from 2.5 to 3.5. The former figure is rather too high (many cargo ships have ratios around 2.25), and an extension to a value of $\frac{B}{H}$ equal to 2.0 would be of interest. The upper limit of 3.5 is probably adequate for most ships in fully loaded condition, but with draft restrictions in many ports and canals, it is reasonable to suppose that supertankers and similar ships may well spend appreciable time in a partially loaded condition when $\frac{B}{H}$ may quite likely exceed 3.5. As a first step, a few models having $\frac{B}{H}$ values of 2.0 and 4.0 could be run to see how reliable an extrapolation outside the present limits might prove to be before embarking on an extensive program.

Studies of seakeeping characteristics have shown the advantages of longer ships in maintaining sea speed, and an extension of the series at the finer block coefficients to higher values of $\frac{L}{B}$ would be of interest in this respect; at the full end, a similar increase in $\frac{L}{B}$ would cover ships designed for the Great Lakes trade.

The extension of Series 60 to cover any or all of these areas would be a worthwhile research project. In addition, there remain the planning and running of additional series to cover twin-screw ships, trawlers, tugs, and high displacement-length craft of all kinds. In

the latter types, the effect of shallow water on performance would also be a matter of special interest. The availability of such systematic information would provide the naval architect with much basic and background information and greatly reduce the need for routine model testing.

The results presented in this report are for models tested for resistance and propulsion in smooth water only. They cover the major features of single-screw merchant ships such as proportions, fullness, *LCB* position, and variation in propeller diameter. They enable a designer to obtain very quickly from contours a lines plan having the correct dimensions, displacement and *LCB*. Moreover, because of the graphical relationship between the models, he can also associate with these lines a close estimate of resistance and shaft horsepower. As pointed out earlier, although no claim can be made that such a design is an optimum one, the comparisons made between Series 60 and new successful ships indicates that it will be of a reasonably high standard.

When the series was begun, the hope was expressed that it would provide an acceptable starting point for additional series planned to investigate many other facets of the hull design problem. This hope has been realized to a very considerable extent—models of Series 60 have been used for a number of comparisons of models in waves, sponsored by the ATTC and the ITTC, for a methodical investigation into launching, and for calculations of the forces on ships in a seaway and their responses to such forces. They have also been used in studies of wavemaking resistance and of the effects of adding different sizes of bulb at the bow upon resistance and ship motions. As described in this report, the Series 60 parent models have also been used for the measurement of wake patterns and the resultant propeller forces, and for the median model of $0.70 C_B$, the effects on these and upon resistance and propulsion of changes in shape of stern sections from U to V have also been evaluated.

Probably the most urgent need for extension of this methodical series work lies in the realm of seagoing qualities. It by no means follows that the hull form chosen for good performance in smooth water will be equally successful in waves, either as regards maintenance of speed or minimum ship motions. This applies particularly to the fuller, slower ships, where the absence of any significant wavemaking calls for full bows and slender sterns to achieve good smooth-water performance. A methodical program should be carried out first, to test key models of the series in waves, and this should include experiments to find the effect of *LCB* position upon maintenance of sea speed. The next step would be to evaluate the effects of changes in section and waterline shapes, both below and above water. These would include, for example, an examination of the relative merits of U- and V-sections, and the best type of above-water form at the bow to ensure a clean, dry ship by the provision of adequate freeboard and flare. An extensive program of experiments of this kind, based on Series 60 models as parents, has been designed at the NSMB. The results of some tests have already been published, but much yet remains to be done.

In order to keep the original program at the Taylor Model Basin within reasonable bounds, a graphical method of delineating the models was adopted, and except for the fact that comparisons were made with existing "good" ships, no attempt was made at that time to explore the vast field of possible changes in the shapes of area curves, sections or waterlines. At the time of publication of the earlier papers, this adoption of certain area curve and section shapes was subject to some criticism as having been done too arbitrarily and accepted too easily. But the fact that it has taken 15 years to reach the present position is sufficient indication of how long it might have taken had we been led astray in the early days by the temptation to explore all the delectable byways, opening up vistas of attractive changes in area curves, waterline and section shapes. Now that the main framework has been finished, such exploration is undoubtedly necessary; it could well form the subject of a number of research projects in different tanks.

There are a number of possible approaches to this type of research. One would be the trial and error method of trying different shapes of area curves, waterlines and sections, being guided in successive choices by the results of each step in turn. A second would be to apply statistical methods to the results of previous model tests—both Series 60 and others—to determine the influence of the different design parameters, and so approach closer to an optimum combination to suit any given design conditions. Considerable success has been achieved in this way in the particular field of trawler design.⁶⁶

Thirdly, one may seek guidance from the mathematical work being carried out in the field of wavemaking resistance. As a matter of history, it is perhaps worth recording that much thought was given to this aspect of ship resistance research when the original series was being planned. At that time, Dr. Weinblum was a consultant at the Taylor Model Basin, and he took an active part in the planning and in the early phases of the project. The question of using mathematically defined lines was seriously considered, and it is perhaps of interest to record some of Dr. Weinblum's views as set out in his discussion on the first series paper (discussion on Reference 44, pp 722-4).

"For a considerable time attempts have been made to establish a rational theory of ship resistance as the function of its form by using analytical methods and pertinent basic experiments. Although this approach is developing successfully, if slowly, the choice of proper ship forms for practice has still to rely widely upon experimental data, obtained by testing methodical series or single models. Clearly, the latter procedure is the most wasteful way of getting results which are capable of appropriate generalization. Therefore, from a practical point of view, the need for Series work cannot be denied at present. On the contrary, the substitution of methodical experimenting for single testing promises within plausible limits decisive advantages in various respects . . . when the present series was being planned the authors received proposals to base the work on algebraically defined lines . . . There is no magic in mathematical lines. Their use in research work is desirable essentially

1. to obtain well-defined expressions for the ship forms, which admit especially of clearly defined variations in these forms . . .

2. to enable us to perform resistance, seaworthiness and similar calculations in a simple and systematical manner.

. . . in the writer's opinion a reasonable evaluation of the existing theories (of wave resistance and sea-going qualities) could be reached by using graphically-defined parent hulls, by approximating these forms mathematically and using the latter for the calculations involved. . . . This reasoning together with some difficulties . . . in representing full sections justifies the use of empirical lines at present . . . The idea of the proposed wave resistance calculations is essentially two-fold: we intend to make a contribution to the analysis of the experimentally-obtained resistance curves and to indicate what improvements in the parent forms are suggested by theory. Especially the latter purpose can become rather interesting. On the other hand, since we are dealing with a first order theory, valuable checks of its validity may be obtained from systematic experiments.

. . . Finally, the series work may make use of other procedures applied in hydrodynamics and thus stimulate the whole field of model research. It does not give credit to theoretical naval architecture and to general hydrodynamics that in text books on the latter subject the ship has nearly disappeared."

In view of such opinions, the basic lines of Series 60 were developed empirically and defined graphically, and Dr. Weinblum showed in his discussion how the waterlines and sections could be closely represented by polynomial expressions.

Today much effort is being applied to the problem of representing a ship form mathematically, either by means of sections and waterlines or as a three-dimensional surface, for use on a digital computer.^{67,68,69} Such an approach would enable calculations of wave-making resistance, velocity distribution, and motions in waves to be made very quickly and permit examination of many alternative ideas. In the particular case of calculations of wave-making resistance, these will still suffer in the absolute sense from limitations in the theory, particularly as regards the inclusion of viscosity effects, but they should furnish a guide to the experimenter in the choice of hull changes likely to reduce wavemaking resistance. It must be remembered, however, that in the type of ship with which this research is concerned, the wavemaking resistance is, in general, only a small part of the total. By fining the entrance, for example, it may well be that the reduction in wavemaking resistance will be equalled or even exceeded by an increase in viscous form drag and eddymaking occasioned by the correspondingly fuller stern. On the other hand, the wavemaking resistance is the part over which we have most control since it depends essentially on the hull shape, and every use should be made of any guidance that mathematical work can provide as to the type and character of changes likely to reduce it. This approach will be most fruitful in high-speed ships, but at present it seems that for low-speed cargo ships we must in the final analysis still have resort to experiments.

Finally, it is believed that much of the value of ship model research in the past has not been realized because of the lack of a common point of departure. Indeed, as a result of this lack, there has been much duplication of effort. It is suggested that Series 60 provides such a common starting point. Used in this way, it would have the effect, in its own limited field, of unifying research everywhere. Much more research, both fundamental and applied, remains to be done; there are staff shortages in most places, but with such a link these problems could be shared among towing tanks everywhere and the rate of progress much enhanced.

APPENDIX A

EFFECTS OF TURBULENCE STIMULATORS

The need for artificial stimulation of turbulence on ship models in order to avoid the spurious results obtained in ship predictions based upon model experiments in which some laminar flow persisted was recognised in some tanks, including Hamburg and Wageningen, before 1930. Its importance was not generally appreciated, however, until around 1948 when it was realised that on some hull forms, notably those with a full forebody and raked stem, laminar flow could persist to an alarming extent. Thus experiments with LIBERTY ship models showed that the effect of stimulation over the lower speed range could amount to 15 or even 20 percent.

A number of methods of stimulating turbulence have been devised from time to time. Kempf early proposed a "comb" which made a pattern of grooves in the wax hull around a station about 5 percent of the length aft of the stem, while a "trip-wire" placed around the hull at the same place was adopted very early in the work and has maintained its place as one accepted method to the present time. Sand strips down the stem and along the LWL for a short distance from the fore end are also used. All these devices add some parasitic drag to the hull, and to avoid this use has been made of struts ahead of the model attached to the towing carriage. Some experiments of this kind made with fine models in which no laminar flow effects could be detected suggested that the wake from the strut could actually reduce the measured resistance of the hull. In order to avoid some of these effects, studs similar to those developed on aircraft models were tried; they have the stimulating effect of trip wires or sand strips but a very low parasitic drag. These were described by Hughes and Allan in 1951.⁴⁶

The original Series 57 models were run with and without turbulence stimulation. The standard method used on all models was a sand strip $\frac{1}{2}$ in. wide down each side of stem and along the LWL for a distance of 4 ft or one-fifth of the length of the model. In addition, some models were run with a trip wire, 0.04 in. in diameter placed around a station at $\frac{L}{20}$ from the stem. Others were fitted with studs, as described in Reference 46; these have a diameter of $\frac{1}{8}$ in., were $\frac{1}{10}$ in. high and spaced 1 in. apart along a line parallel to the stem profile. The distance of the line from the stem depends on the half angle of entrance on the LWL ($\frac{1}{2} \alpha_E$). For the three Series 57 models of 0.70, 0.75, and 0.80 C_B , the $\frac{1}{2} \alpha_E$ values were 13.3, 27.1, and 44.0 deg, the distance of the studs from the stem being, respectively, 2.13, 2.70, and 3.25 in.

The effects upon resistance were somewhat erratic but never very serious.

Model	Sand Strips	Trip Wire	Studs
4200 (0.60 C_B)	Slight increase over lower speeds	No change	—
4201 (0.65 C_B)	No change except at very lowest speed, C_T rising slightly with decreasing speed	No change except at very lowest speed, C_T level with decreasing speed	—
4202 (0.70 C_B)	No change	—	No change
4203 (0.75 C_B)	Below $\frac{V}{\sqrt{L}} = 0.4$, large increase in resistance—some 60 percent on C_R . At service speed, increase in C_R was 4 percent and in C_T about 1 ½ percent	—	Same as sand strips
4204 (0.80 C_B)	Slight increase at all speeds— C_T up 1 ½ percent at service speed	—	Somewhat larger increase— C_T up 3 percent at service speed

(The percentage increases are for a 400-ft ship)

In view of the small effects of stimulation, it was decided to use results with sand strips without deduction for any parasitic drag.

The first step in developing the new Series 60 was a comparison between the results of certain good ships and the Series 57 equivalents. Studs were used for these tests because they were easy to fit, were positive in location, had some theoretical backing as a means of stimulation, and had very small parasitic drag. The only peculiar results found were with the models of the PENNSYLVANIA series. The PENNSYLVANIA was a tanker of 0.76 C_B and a number of variations were tested. The models are listed in the order in which the tests were carried out. For the first five, the increases in resistance were quite substantial, averaging 10 and 7.5 percent at the service and trial speeds respectively. For the last four, the corresponding figures were 0.8 and 1.2 percent. It should be noted that Models 4435W and 4435W.A are built to identical lines, both of wax, and yet they fall into the two groups as regards stimulation effects. The $C_{400 \text{ ft}}$ values listed are those derived from the model results with stimulation; they show no serious change in the resistance picture, indicating that the differences occurred in the tests in the unstimulated conditions. The only division one can make is a chronological one, and no explanation has been found for this peculiar behaviour.

Model	Details	Percentage Increase in C_B with Studs		C_B 400 ft with Stimulation	
		Service Speed	Trial Speed	Service Speed	Trial Speed
4435W	PENNSYLVANIA (as built)	11.8	9.0	0.715	0.735
4420W	Series 57 equivalent	10.4	8.2	0.735	0.765
4420W-1	PENNSYLVANIA forebody-Series 57 aft body	10.7	7.0	0.710	0.730
4468W	Series 60 equivalent	9.0	7.0	0.727	0.760
4468WA-1	PENNSYLVANIA forebody with Series 60 stem profile-Series 60 stern aft body	9.0	6.6	0.736	0.763
4435WA-1	PENNSYLVANIA with Series 60 stem and stern contours	0.3	2.0	0.735	0.760
4435WA-2	PENNSYLVANIA with Series 60 stern and PENNSYLVANIA bow contours	2.0	0	0.730	0.753
4435W.A.	PENNSYLVANIA (new casting of 4435W)	0.0	2.8	0.725	0.772
4468W-2	Series 60 equivalent with PENNSYL- VANIA stem contour	0.8	0	0.747	0.772

For the actual Series 60 parent models, studs were used throughout and the following effects were measured:

$$C_B = 0.60 \text{ and } 0.65$$

Resistance unaffected

$$C_B = 0.70$$

C_B 400 ft values increased 0 to 3 percent

$$C_B = 0.75 \text{ and } 0.80$$

C_B 400 ft values increased 0 to 12 percent

The propulsion tests on the Series 60 parents were all carried out with models fitted with studs.

The LCB series were all run in the first place with studs. For comparison, 14 of the 22 models were also run with trip wires.

The results for the models *without stimulation and with studs* were as follows:

C_B	LCB from $\frac{L}{B}$	Effect of Studs = $\frac{C_T \text{ Studs}}{C_T \text{ Bare}}$	
0.60 0.65 0.70	All Models	No measurable effect	
0.75	0.48F 1.50F 2.57F 3.46F	Sea Speed 1.037 1.030 Mean 1.090 1.050 1.068	Trial Speed 1.022 1.028 Mean 1.098 1.050 1.075
0.80	0.76F 1.45F 2.50F 3.51F	1.050 1.079 Mean 1.035 1.055 1.074	1.054 1.081 Mean 1.037 1.060 1.070

The average increase with the two fuller block coefficients is 5 to 6 percent. For the 0.75 C_B , there appears to be some tendency for the increase in resistance with stimulation to be higher the further forward the LCB, and therefore the fuller the forebody and entrance. The 0.80 C_B does not show such a definite trend, however, and no generalization can be made on this point.

When trip wires were used in place of studs, there was no difference in the results except for two of the 0.80 C_B models, when the service and trial speed \odot values were about 2 percent higher with wires than with studs.

For the models used in the main series to explore the effects of changes in $\frac{L}{B}$ and $\frac{B}{H}$ ratios, turbulence was stimulated by trip wires, 0.036 in. in diameter, placed around a section of the model 5 percent of the length from the stem. This choice was made basically on two grounds. Although in general there was no difference in the results using studs or trip wires, the latter did give the higher results on some fuller models, as described above, and, secondly, a review of practices in other model basins indicated a more general acceptance of the trip-wire technique rather than studs.

The results of the main series of models, from which all the contours of C_R and \odot have been derived, were therefore consistent in that they were all measured on models fitted with trip wires.

APPENDIX B

USE OF CONTOURS AND CHARTS

In order to make the data derived from the very extensive Series 60 research project readily available and useful to naval architects, they have been presented wherever possible as design charts and contours. From these the designer can very quickly make an estimate of performance for any normal single-screw merchant ship whose proportions fall within the area covered by the series.

The essential data are shown in the following figures and tables:

Figure 3	Variation of C_X , C_P , and Bilge Radius with C_B
Figure 4	Variation of Angle of Entrance, Position, and Amount of Parallel Body for Series 60 Parents
Figure 5	Contours of Cross-Sectional Area Coefficients
Figure 6	Contours of Waterline Half-Breadth Coefficients
Figure 9	Ratio of $\frac{L_E}{L_{BP}}$ for Different Values of C_B and Positions of LCB
Figure 10	Ratio of $\frac{C_{PE}}{C_{PR}}$ for Different Values of C_B and Positions of LCB
Figure 11	Bow and Stern Contours
Figures 26-30	Cross Curves of \textcircled{C} to Base of LCB Position
Figure 31	Minimum Values of \textcircled{C} and Corresponding Optimum LCB Locations
Figure 38	Cross Curves of DHP on LCB Position
Figures 54-57	Variation of Propulsive Factors with Propeller Diameter and Draft
Figures B1-B39	Contours of Residuary Resistance in Pounds per Ton of Displacement
Figures B40-B78	Contours of \textcircled{C} for Ship with 400-Ft LBP
Figures B79-B120	Contours of Wake Fraction and Thrust Deduction
Figures B121-B123	Contours of Relative Rotative Efficiency e_{rr}
Figures B124-B126	Contours of Wetted Surface Coefficient
Figure B127	Nomograph for Calculating Frictional Component of Resistance R_F on Basis of ATTC Line
Figure D4	Chart for Conversion of \textcircled{C} Values from Froude to ATTC Basis
Tables 16-26	Resistance Data for LCB Series
Tables 27-32	Propulsion Data for LCB Series
Tables 49-53	Corrections to $\textcircled{C}_{400 \text{ ft}}$ for Change in LCB Position
Tables B1-B45	Results of Resistance and Self-Propulsion Experiments on $\frac{L}{B}$, $\frac{B}{H}$ Series

To assist in the use of the data, calculation forms for the prediction of c_{hp} and $C_{400\text{ ft}}$ are given in Tables B46 and B47. The tables are largely self-explanatory, but a few points call for a little comment.

The contours give $\frac{R_R}{\Lambda}$ and C for three values of $\frac{B}{H} = 2.5, 3.0, \text{ and } 3.5$. For any particular ship, therefore, it is necessary to interpolate between these to obtain the correct value for the actual $\frac{B}{H}$ of the ship in question. This could be done by plotting the three values and lifting off the ordinate at the correct $\frac{B}{H}$ value. In Table B46, it is suggested that this interpolation be done by assuming a parabola to pass through the three points. This, in effect, means that all users will obtain the same value of $\frac{R_R}{\Lambda}$ or C for the desired $\frac{B}{H}$, i.e., it removes personal interpretation of the data; moreover, experience has shown that the data can thereby be extended to $\frac{B}{H}$ values of 2.0 and 4.0.

For comparison purposes, it is sometimes desirable to compute C and K for the actual ship under consideration, and this can be done by completing columns O, P, and Q in Table B46. This value of C will be different from that for the equivalent 400-ft ship, of course, since frictional resistance is a function of length. The value of C for lengths other than 400 ft can be estimated approximately from the differences shown in Table B48, due to Professor L.A. Baier (discussion on Reference 63, page 571). Much of the resistance data published elsewhere refer to a standard ship length of 400 ft and the C contours given in this report are for such a standard length, and for $\frac{B}{H}$ values of 2.5, 3.0, and 3.5. Table B47 will enable the value of $C_{400\text{ ft}}$ to be interpolated for any other desired value of $\frac{B}{H}$.

The $\frac{R_F}{S}$ nomograph in Figure B127 gives a rapid graphical method of finding the frictional resistance per square foot of wetted surface for ships of different lengths operating at various speeds. The results apply to a ship in sea water at a temperature of 59°F (15°C), which has been adopted as a standard figure by the ITTC. A standard ship correlation allowance of +0.0004 has been included. $\frac{R_F}{S}$ is obtained by passing a straight line through appropriate values of VL and V and reading the answer at the intersection of this line with the $\frac{R_F}{S}$ scale which is connected to the V -scale used. Estimates for other than standard correlation allowance of +0.0004 can be made by taking the above $\frac{R_F}{S}$ values and increasing them in the ratio of the total C_F values for the desired allowance and +0.0004, respectively.

In computing the frictional resistance for estimating power for a proposed vessel, it is recommended that the wetted surface for the proposed vessel be used. If this figure is not known, the wetted surface for the equivalent Series 60 hull can be obtained from the contours in Figures B124 to B126.

The models used in the $\frac{L}{B}$, $\frac{B}{H}$ series had, for any given block coefficient, a fixed position of *LCB*, determined from the earlier series of models in which the *LCB* position was varied. In making an estimate of power for a new ship using the Series 60 resistance contours, the result will apply to a ship having the *LCB* in the position chosen for the parent series. If for one reason or another, the new design must have the *LCB* in some other fore and aft position, then a correction must be made for this difference. If it is assumed that the effect of movement of *LCB* on the parent model of given C_B and values of $\frac{L}{B}$ and $\frac{B}{H}$ applies also to a model of the same C_B but different values of $\frac{L}{B}$ and $\frac{B}{H}$, appropriate to the design in question, then the correction can be made from the data given in Chapter VI of this report; see Tables 49-53.

In applying results of the kind given in this report, there are often a number of points which at first are somewhat obscure to the new user and may create difficulties or even errors in making estimates. For this reason, a numerical example has been worked in some detail in Appendix D in the hope that it will obviate any such problems arising in the present work.

Figures B1 through B39

Contours of Residuary Resistance in Pounds per Ton of Displacement

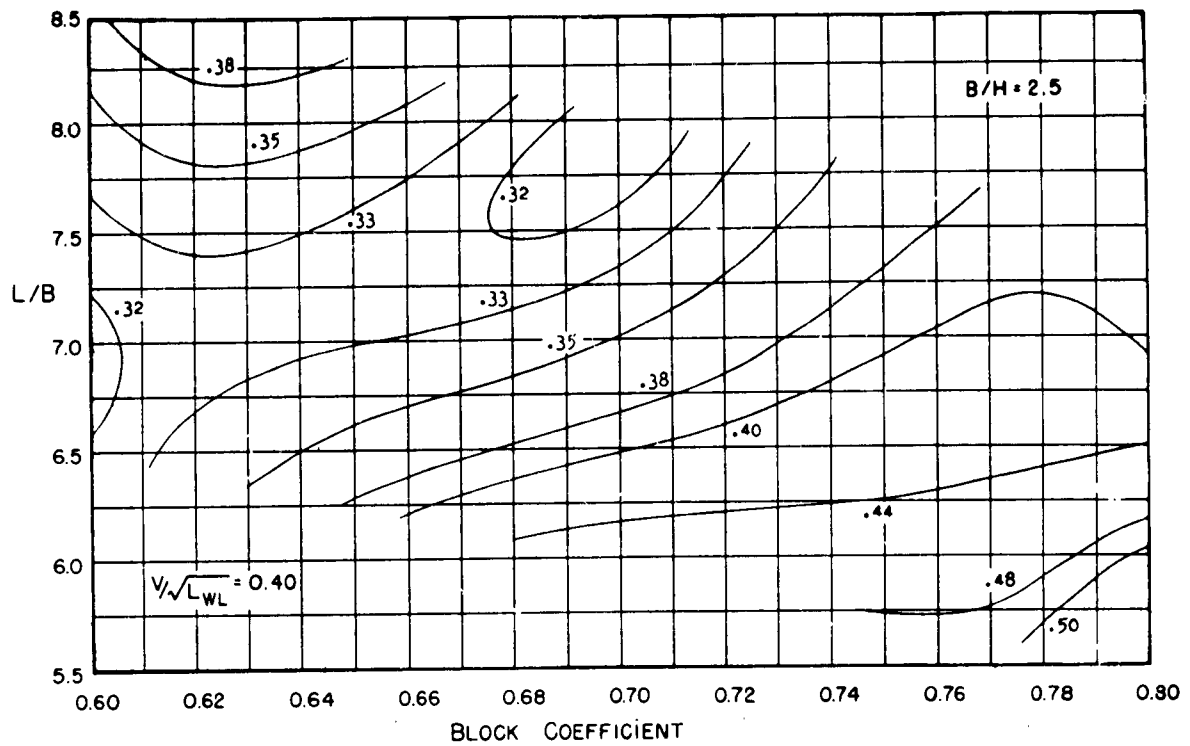


Figure B1

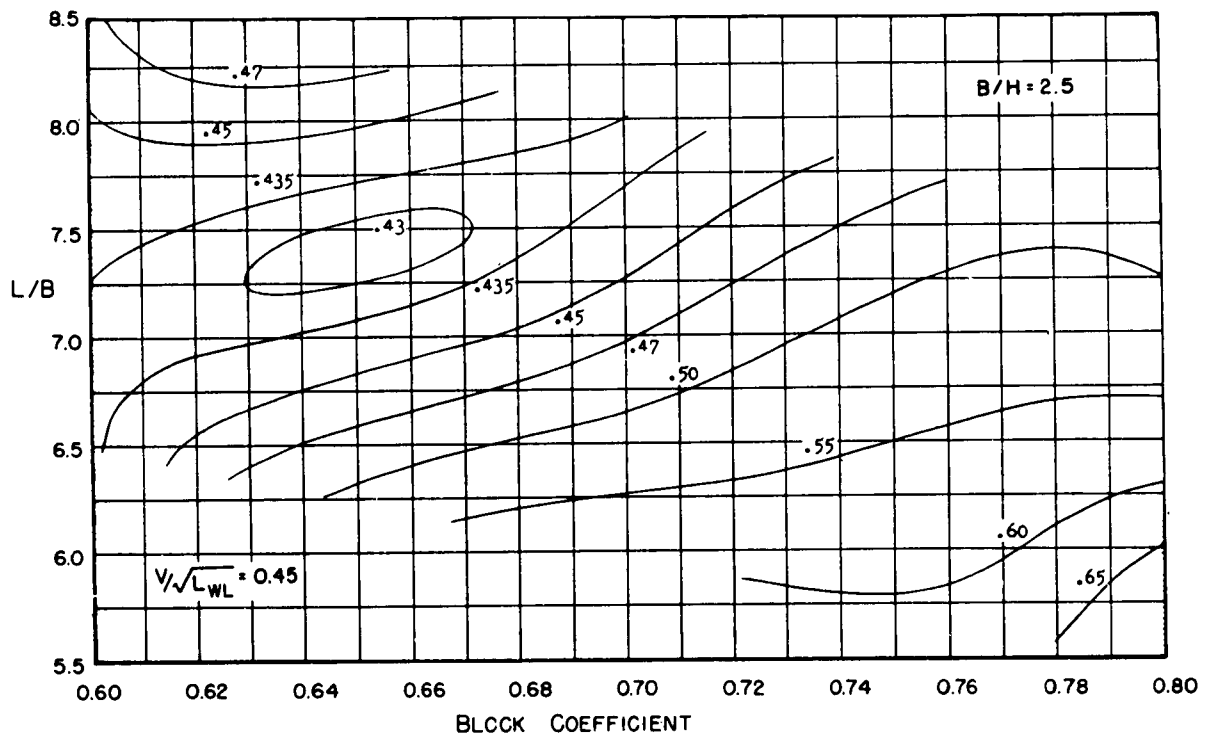


Figure B2

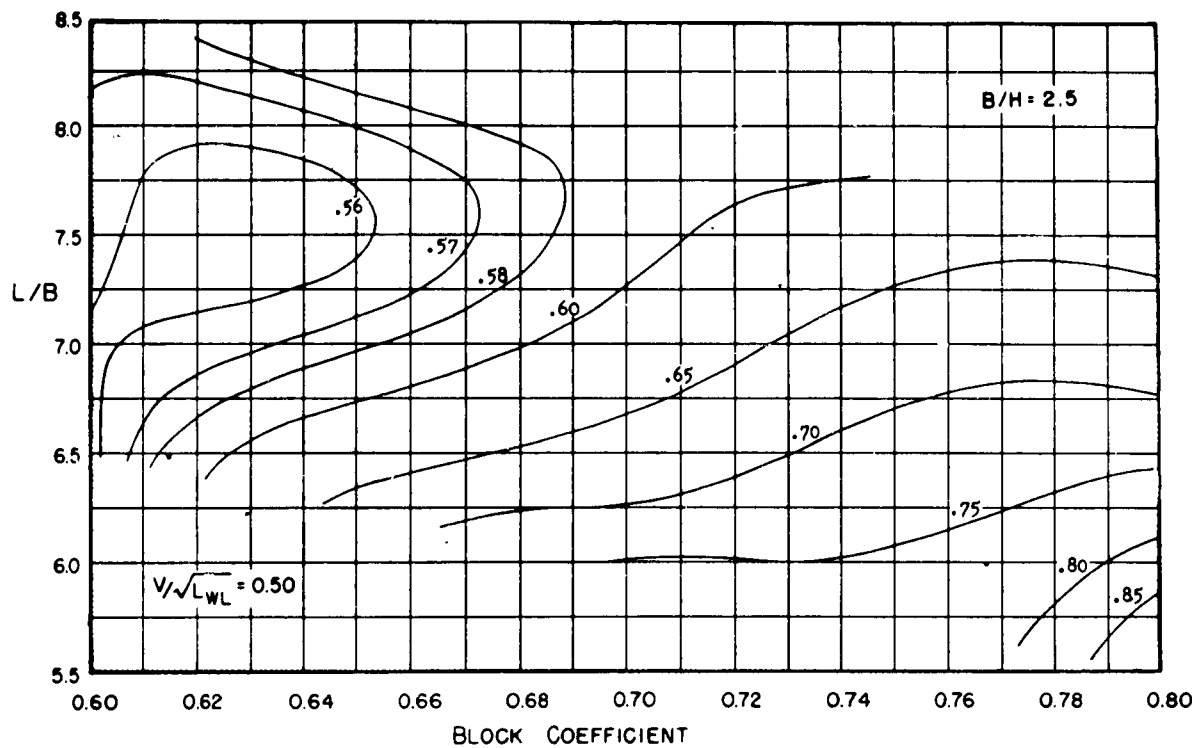


Figure B3

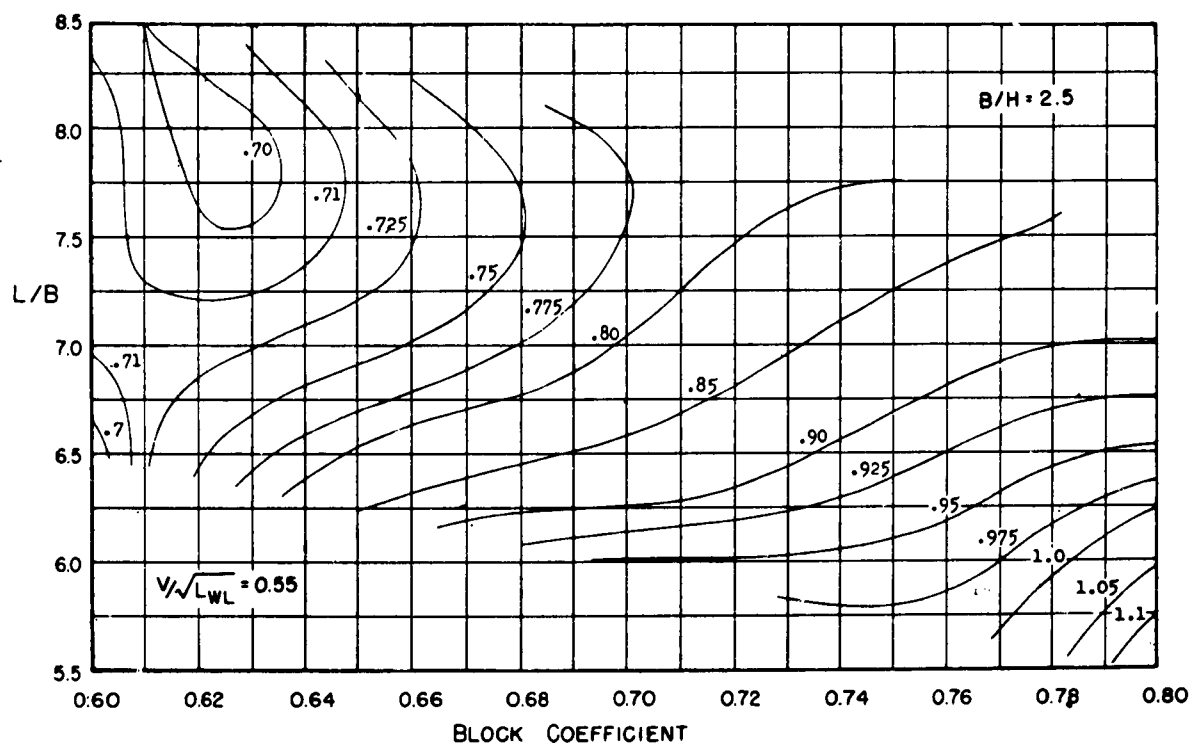


Figure B4

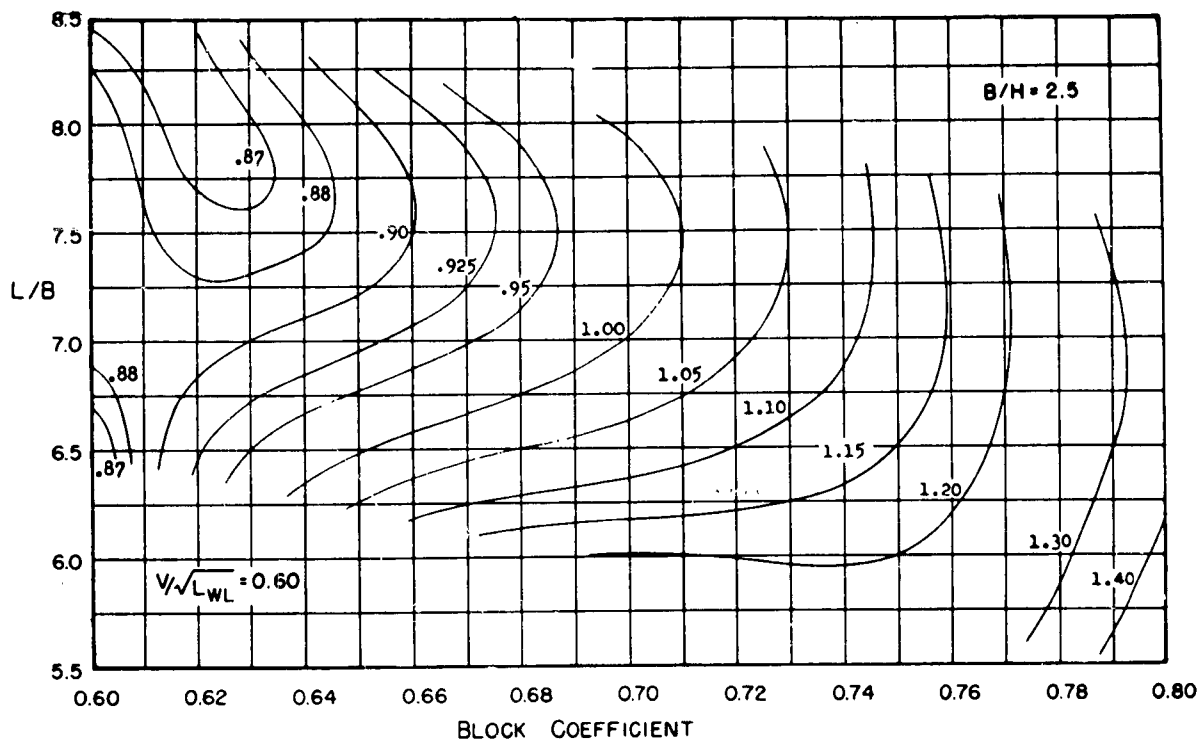


Figure B5

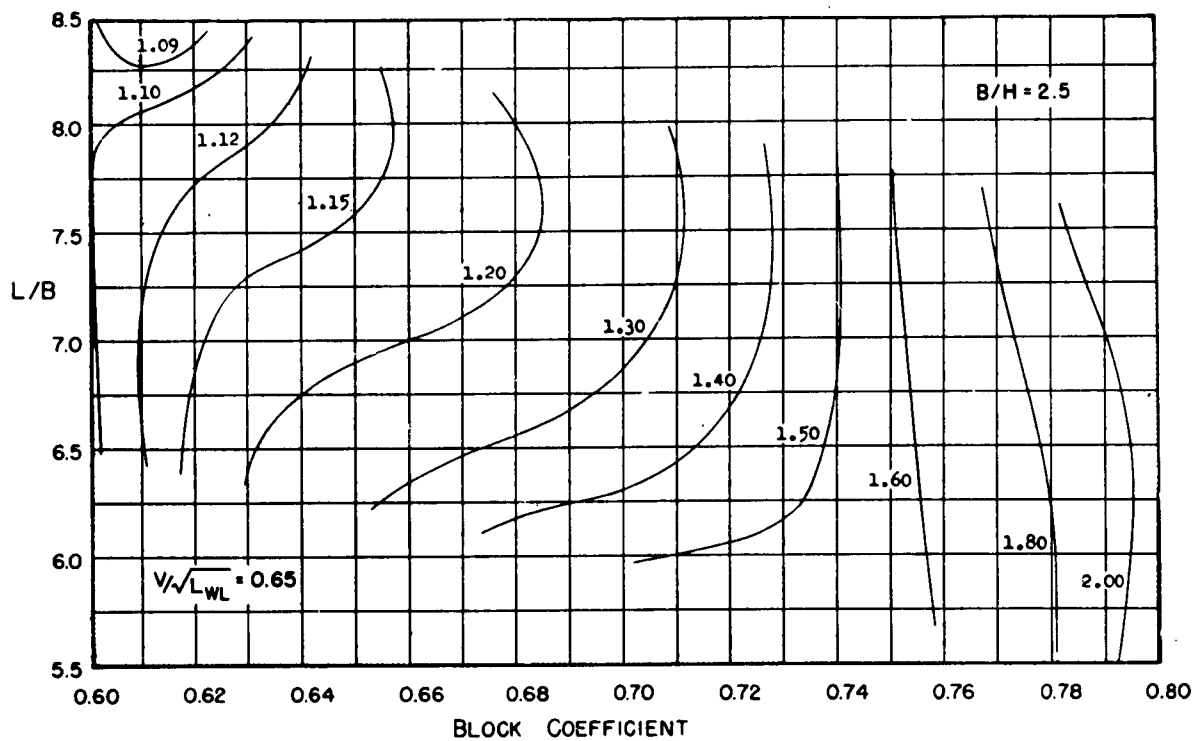


Figure B6

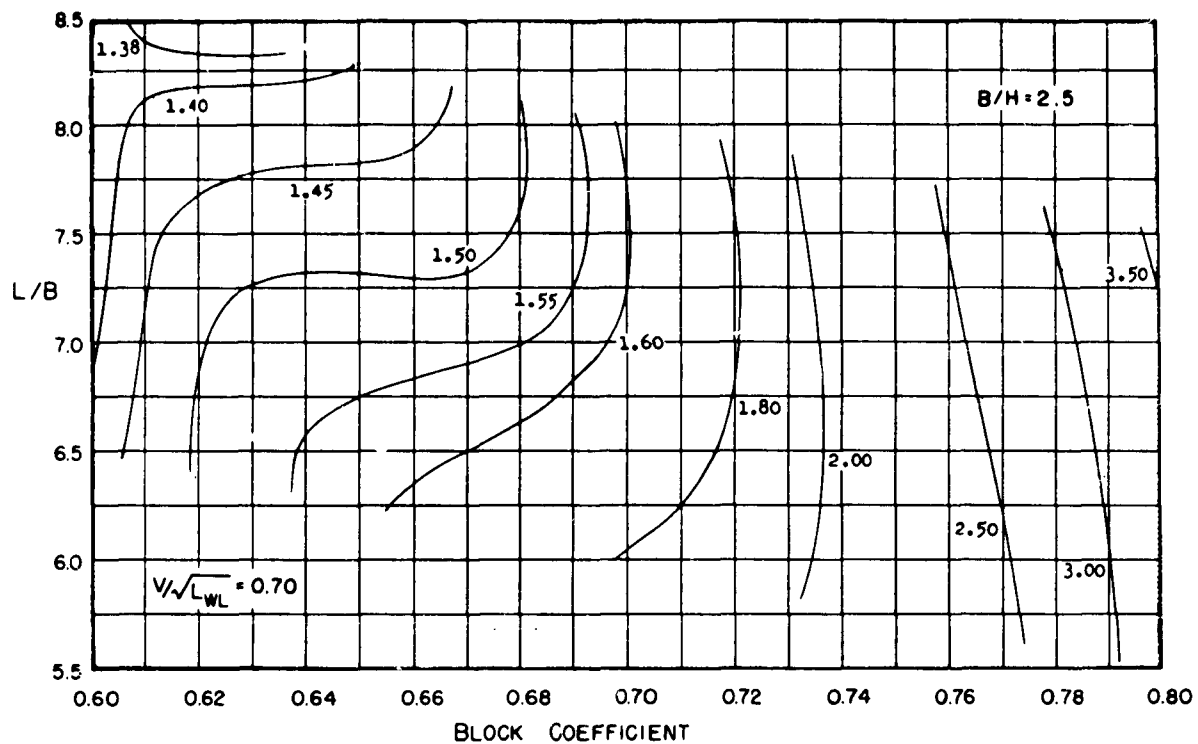


Figure B7

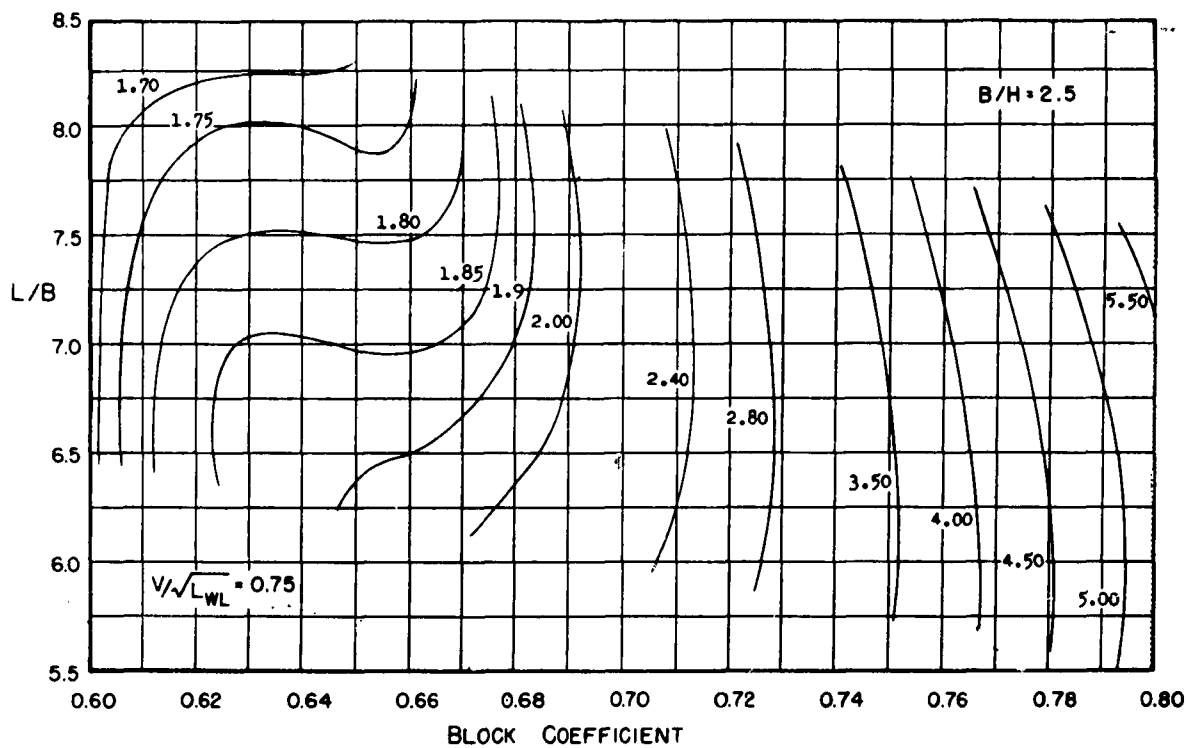


Figure B8

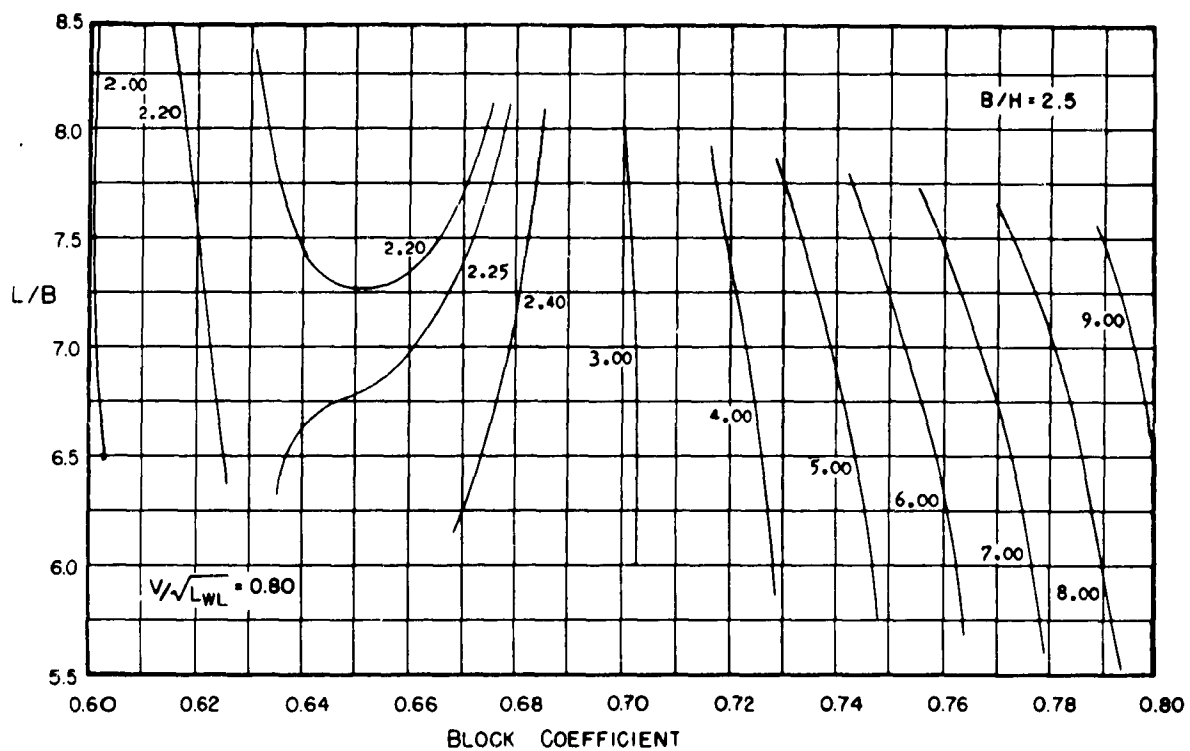


Figure B9

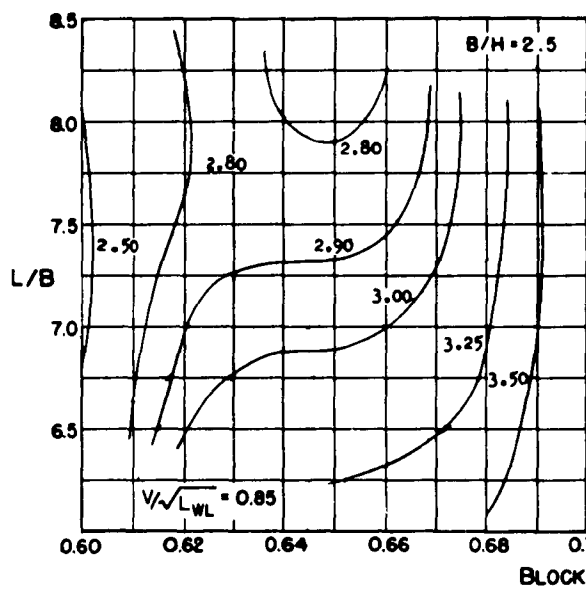


Figure B10

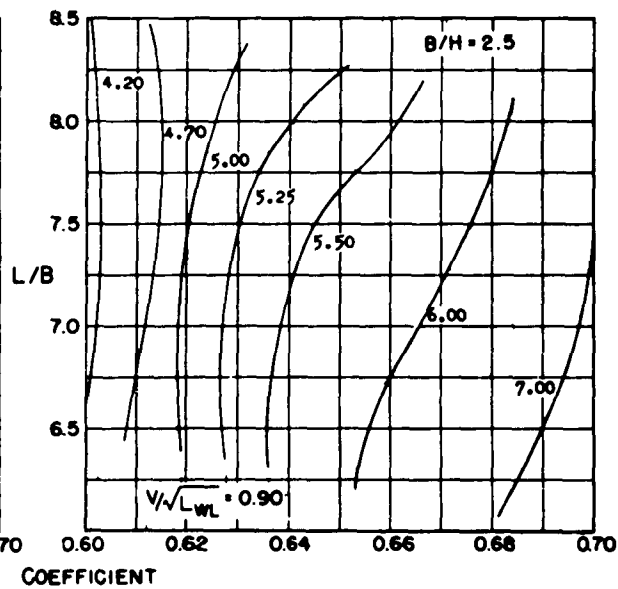


Figure B11

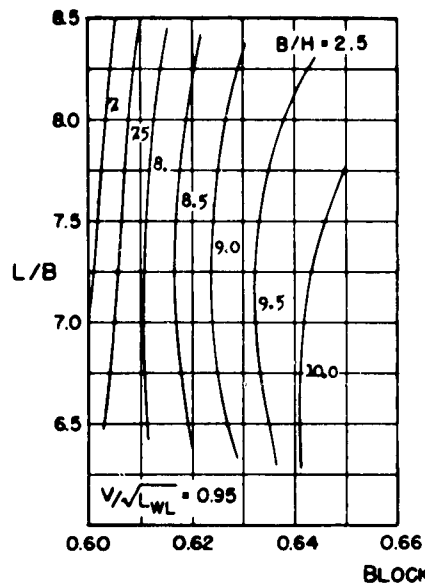


Figure B12

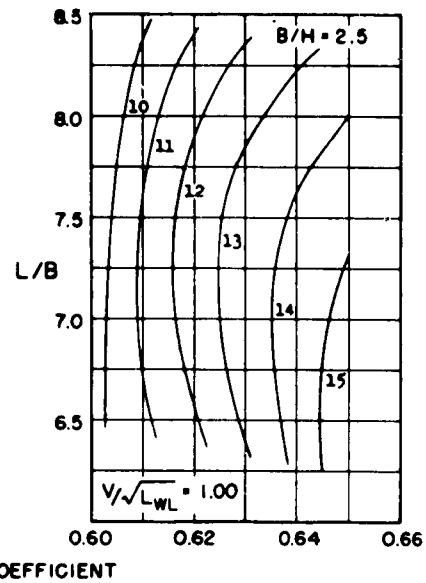


Figure B13

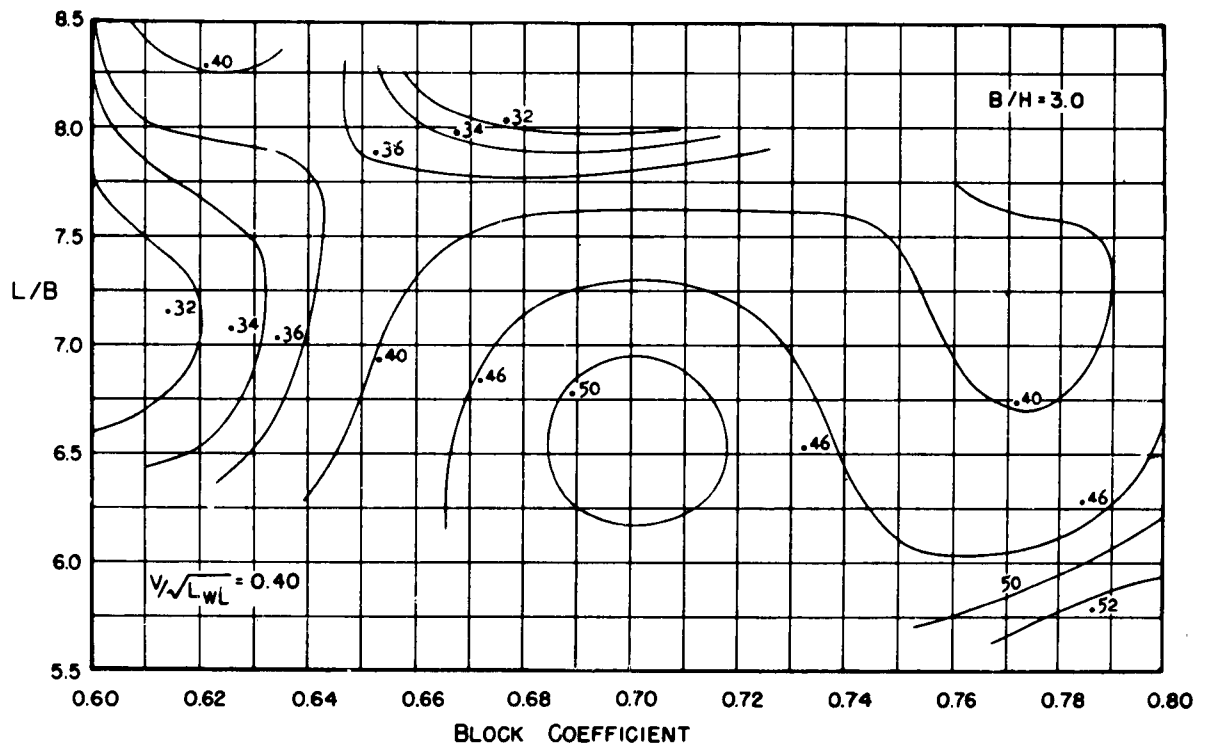


Figure B14

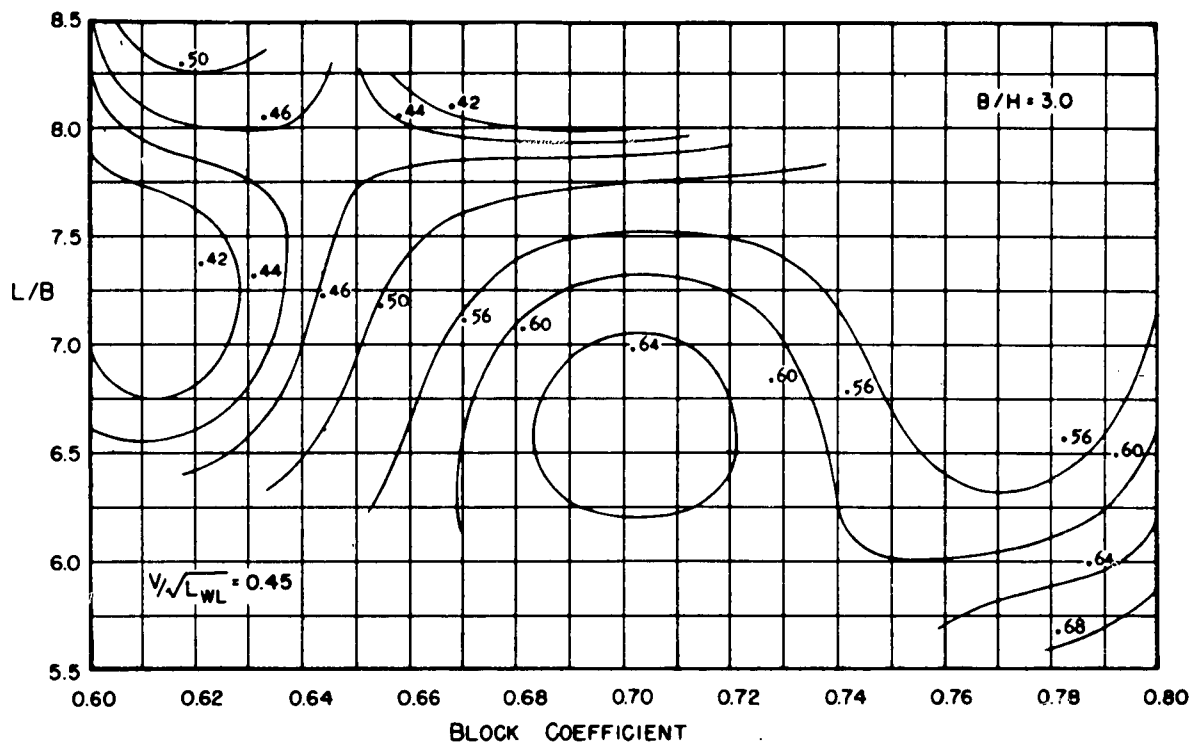


Figure B15

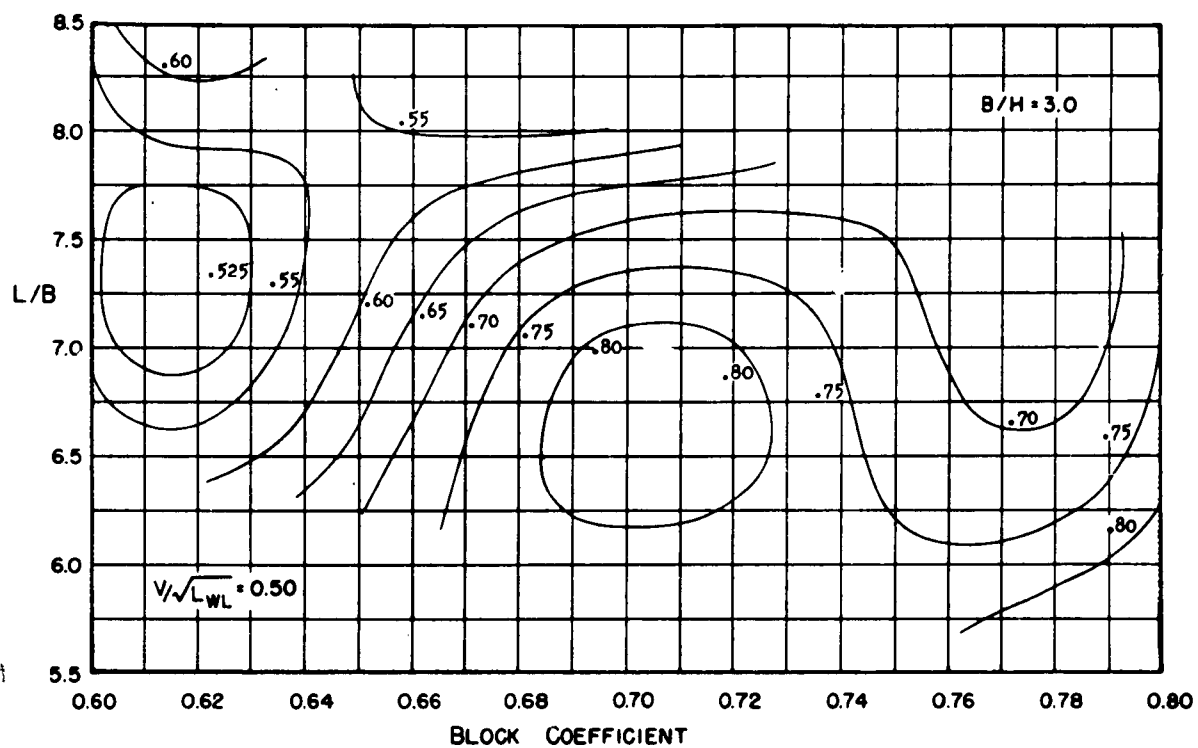


Figure B16

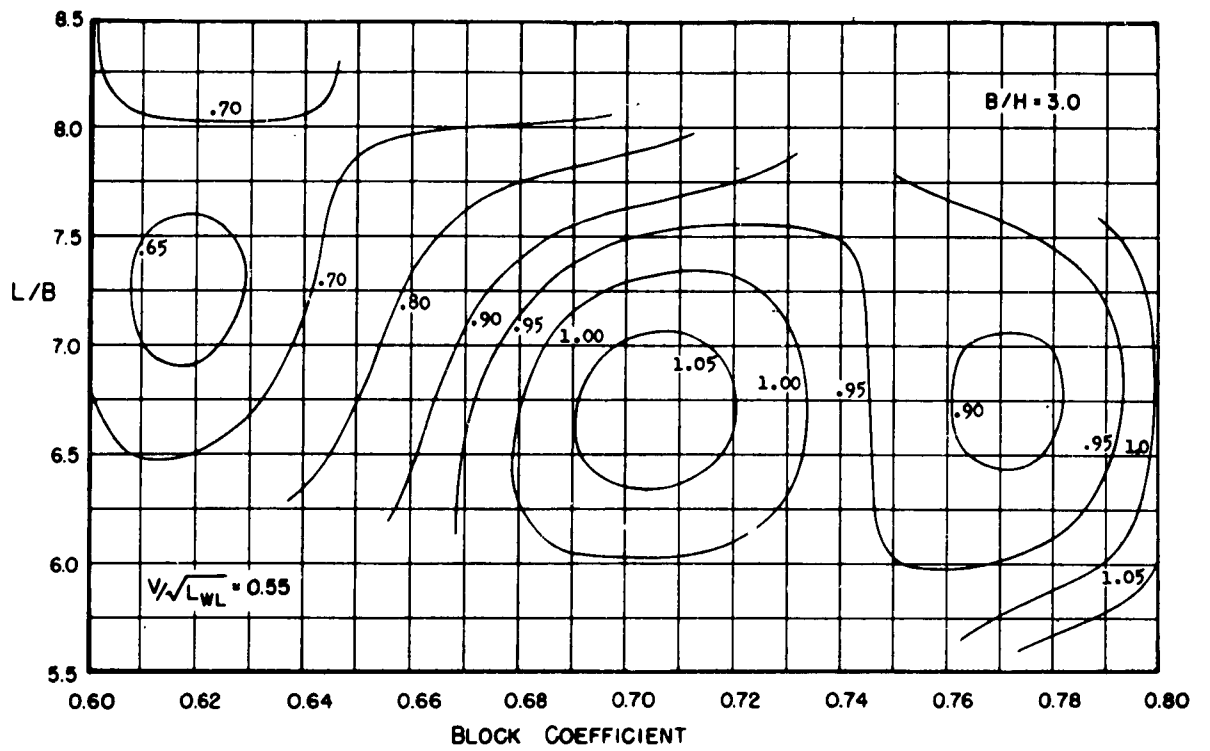


Figure B17

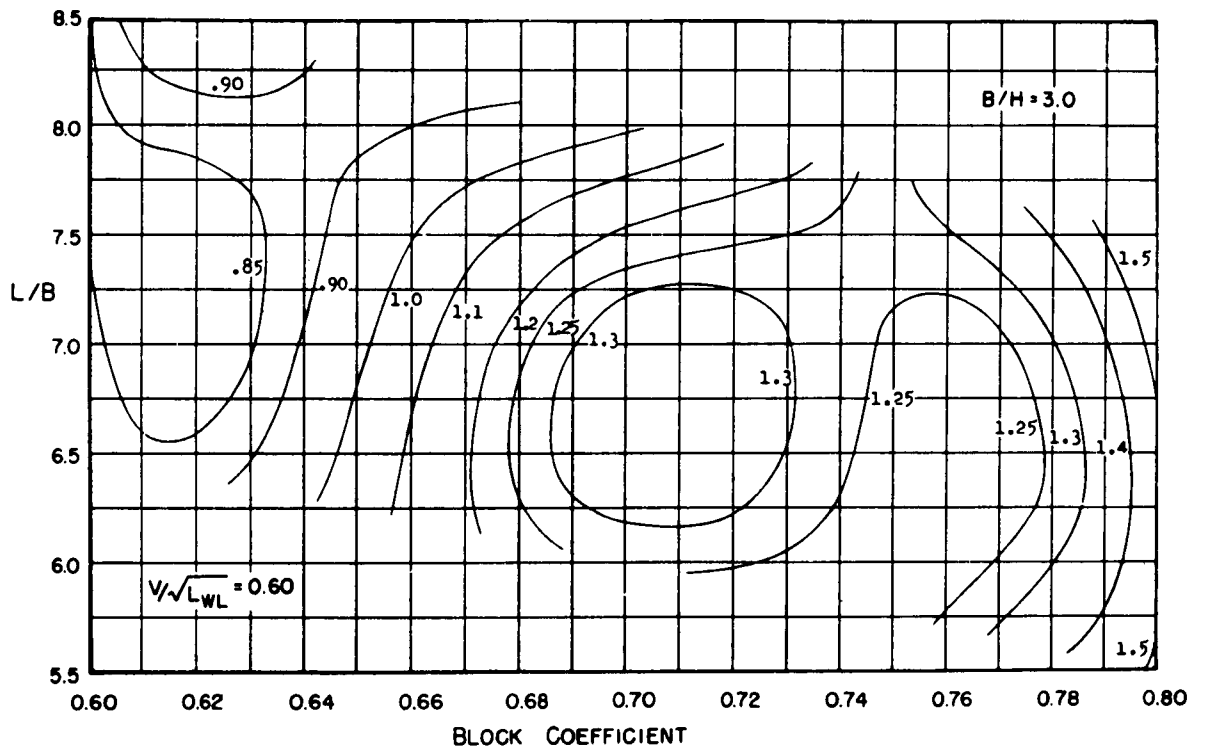


Figure B18

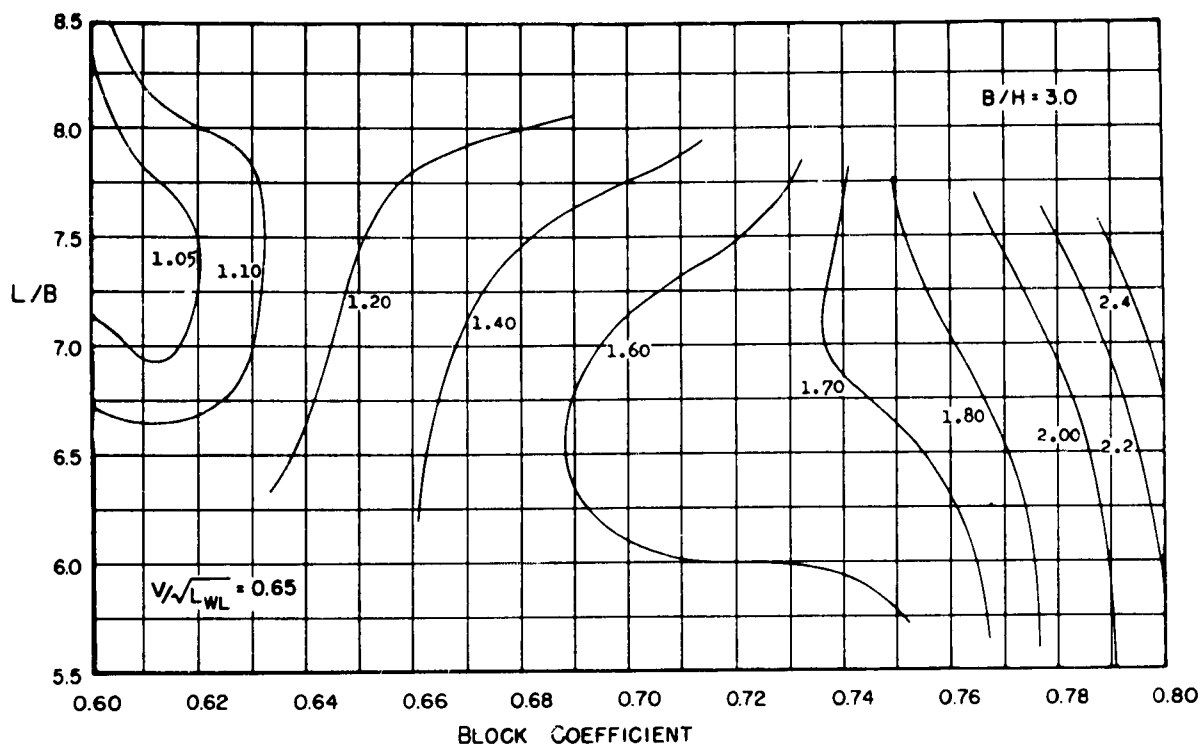


Figure B19

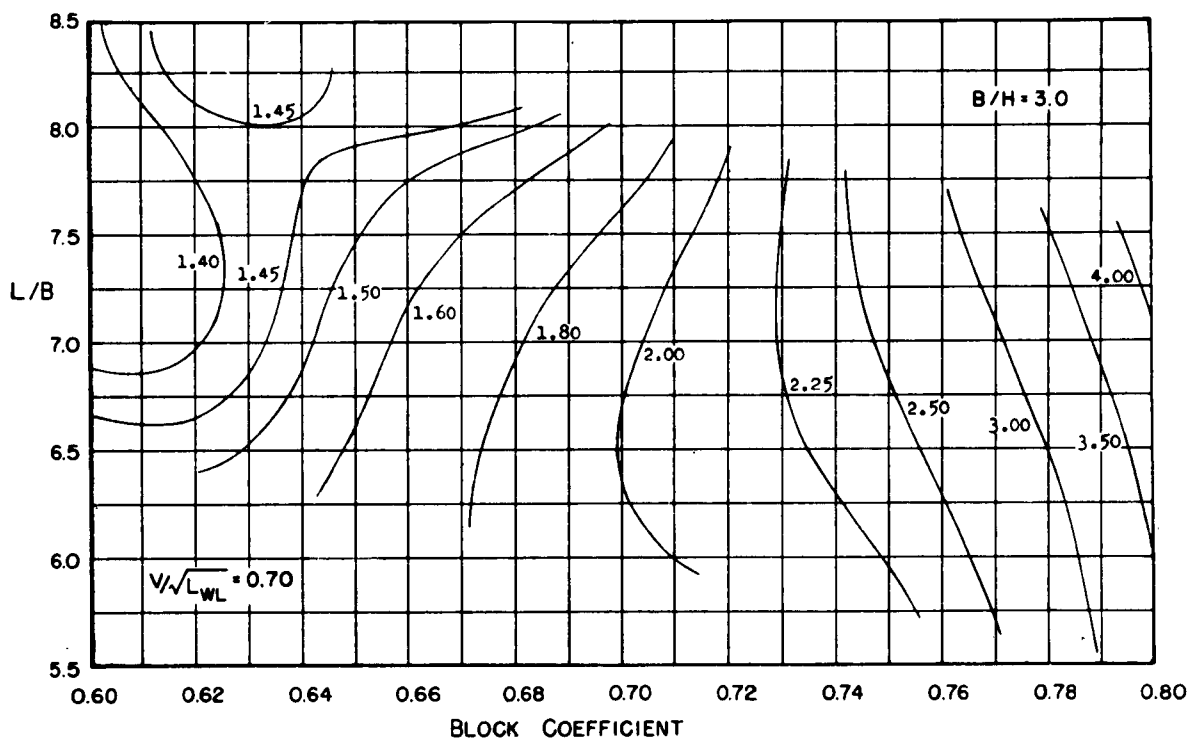


Figure B20

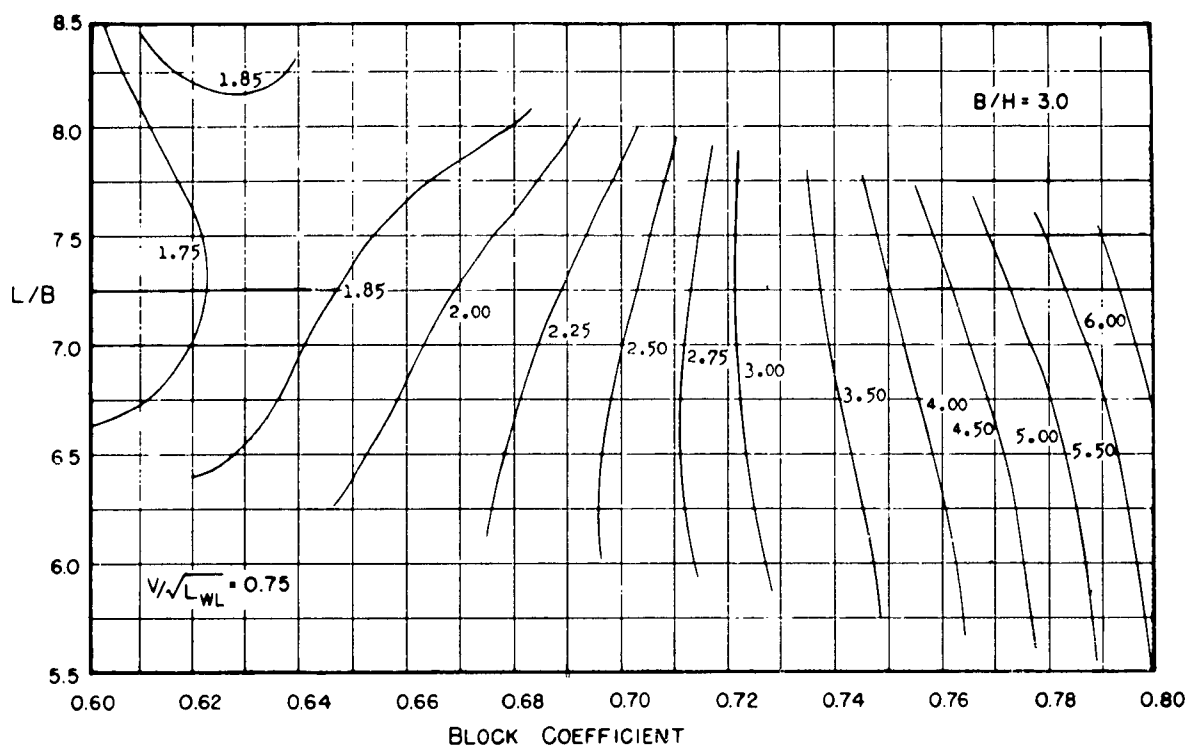


Figure B21

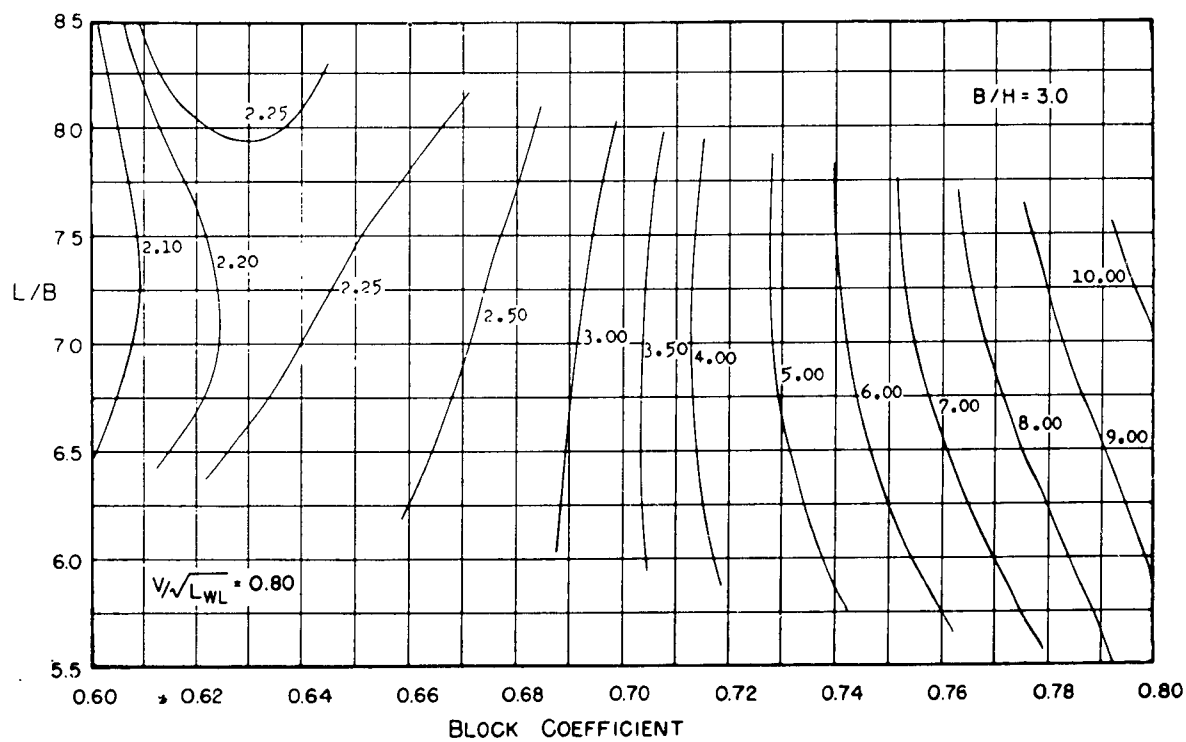


Figure B22

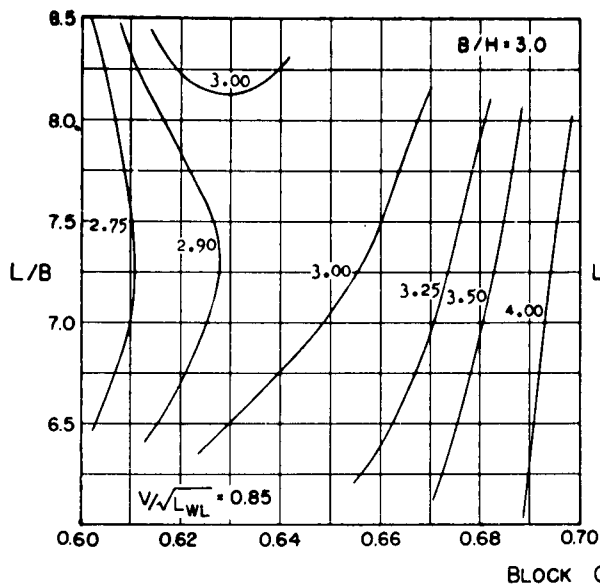


Figure B23

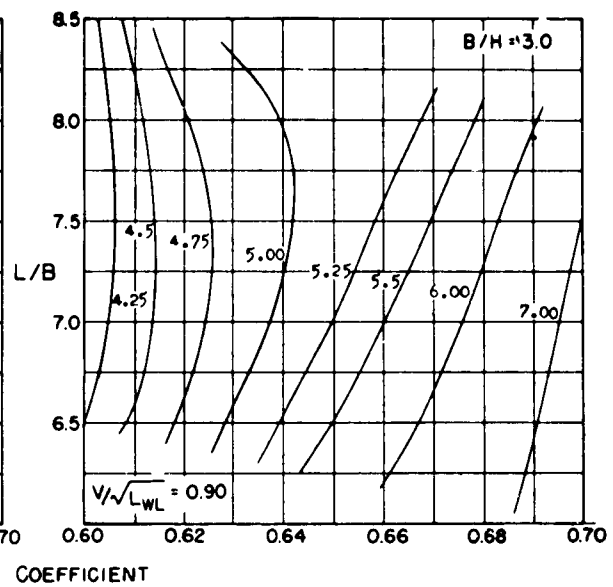


Figure B24

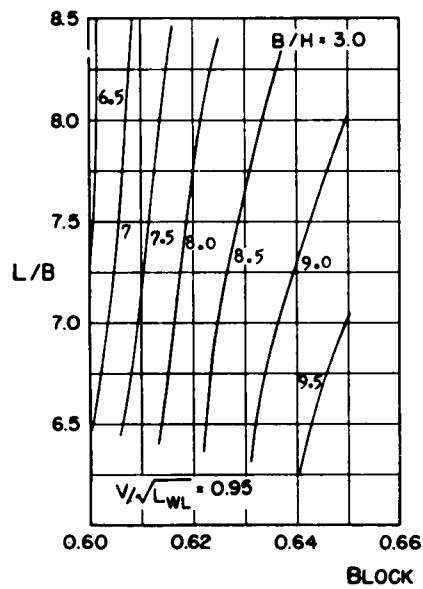


Figure B25

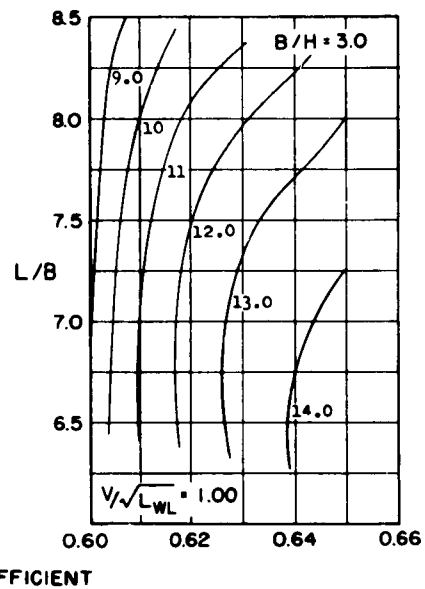


Figure B26

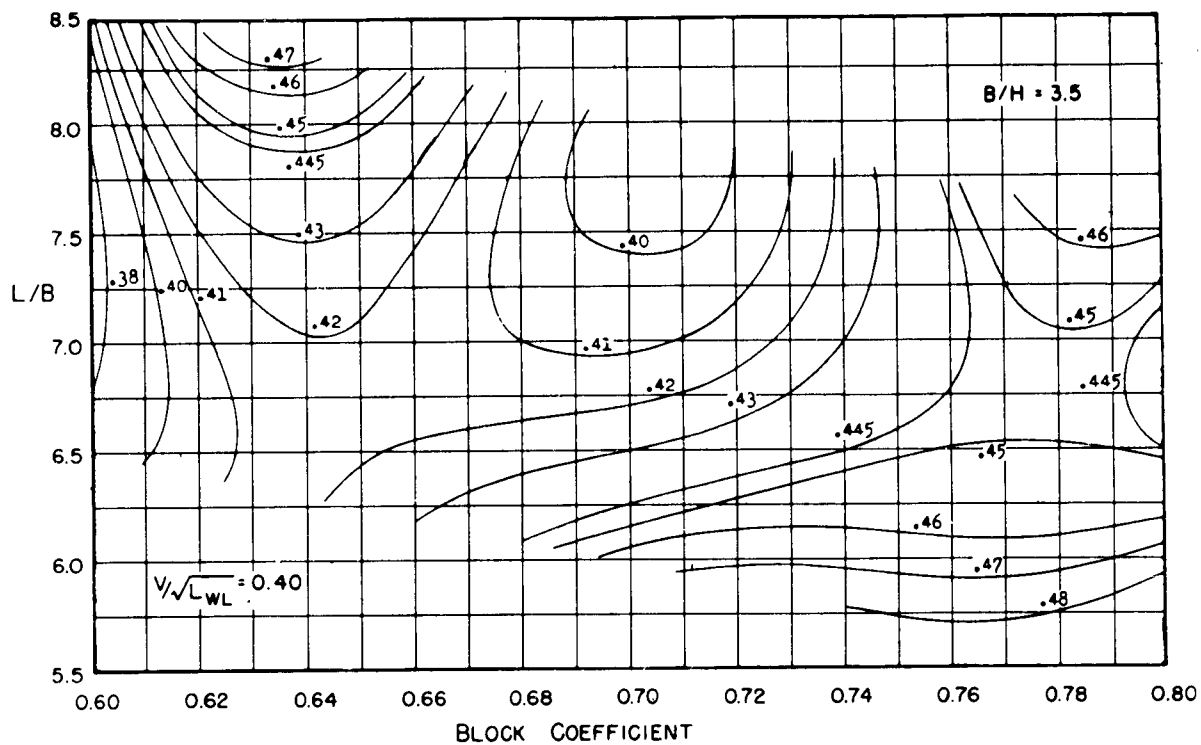


Figure B27

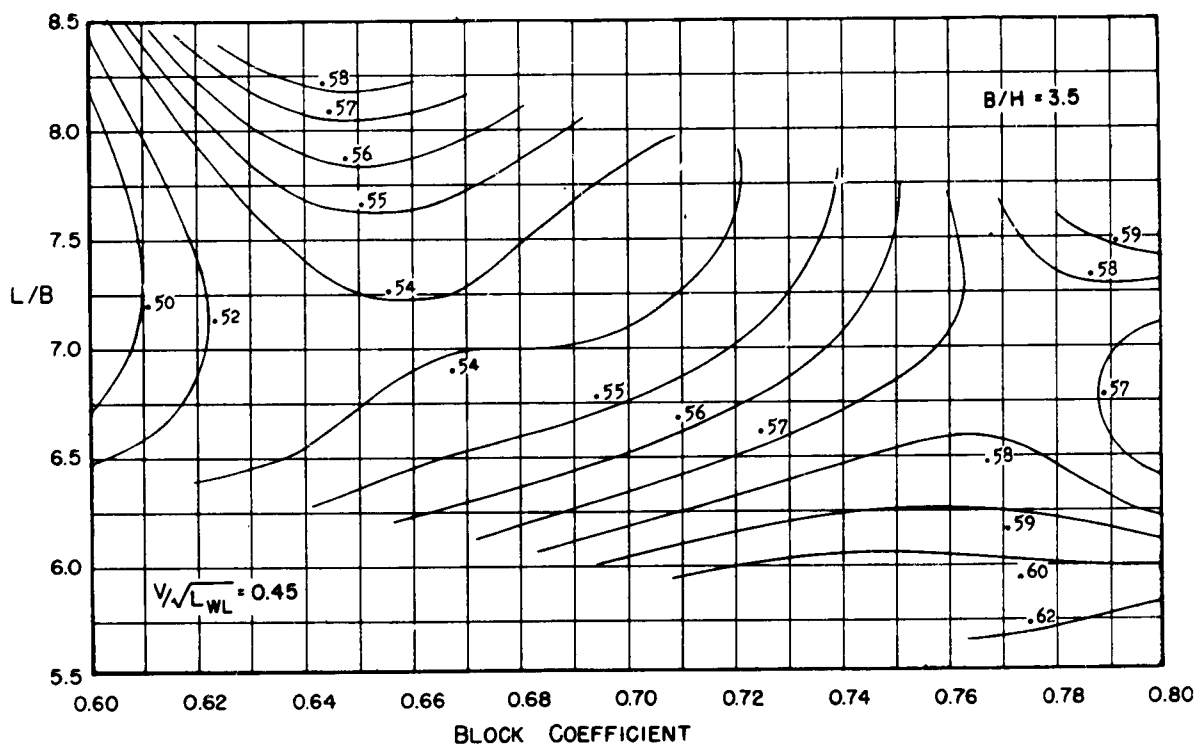


Figure B28

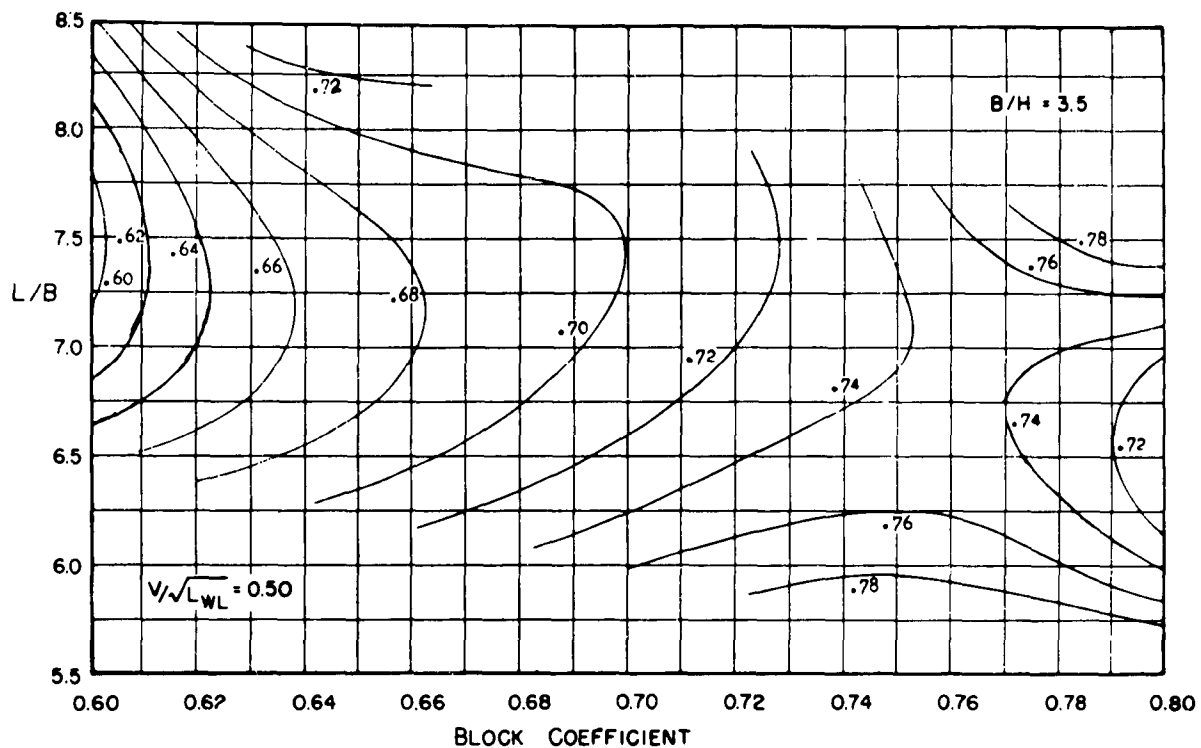


Figure B29

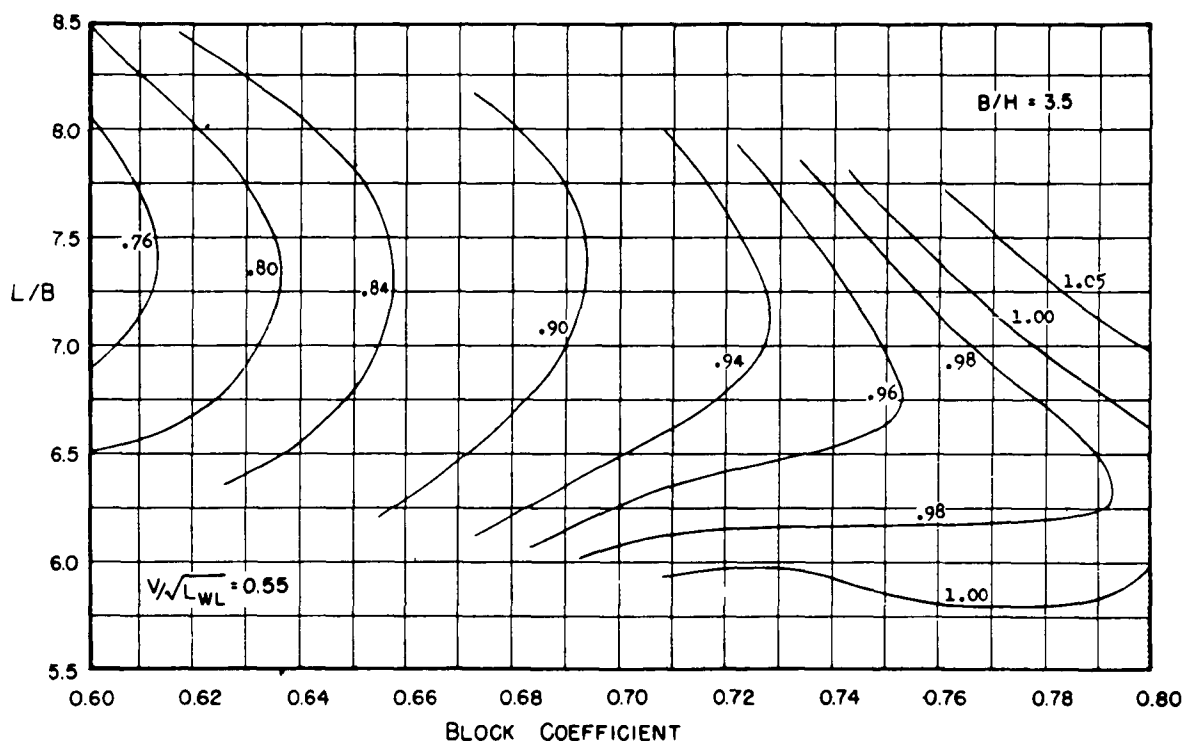


Figure B30

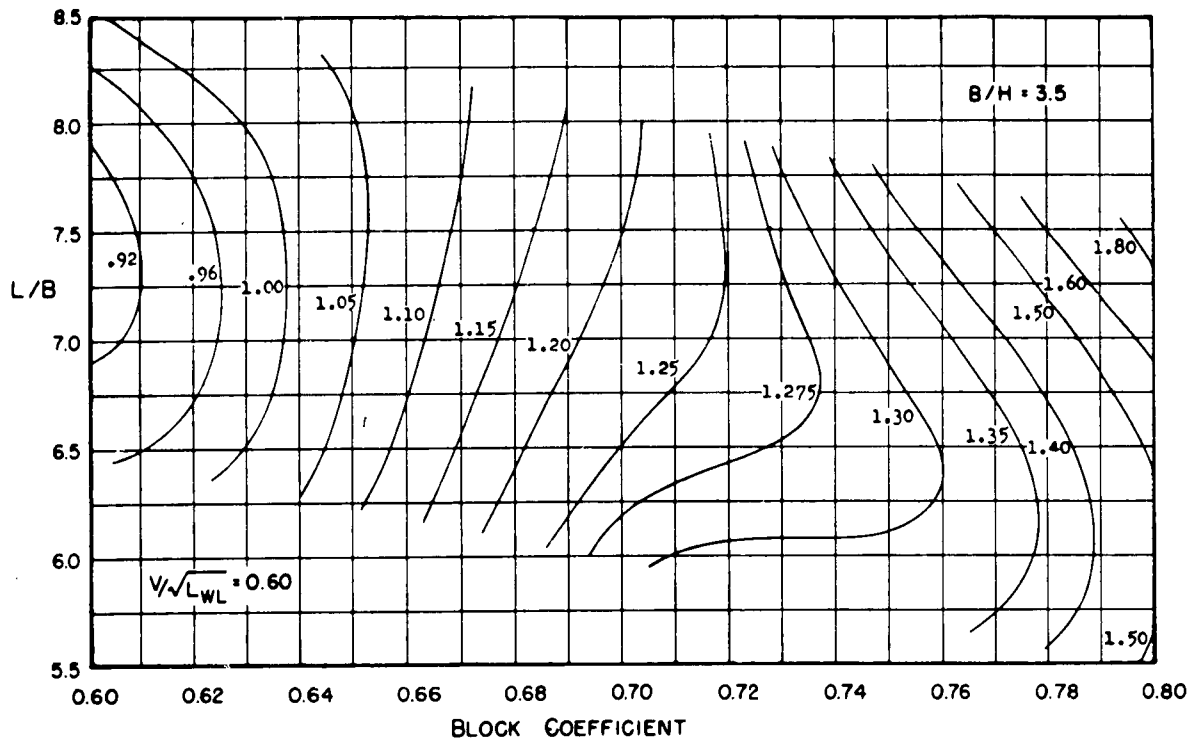


Figure B31

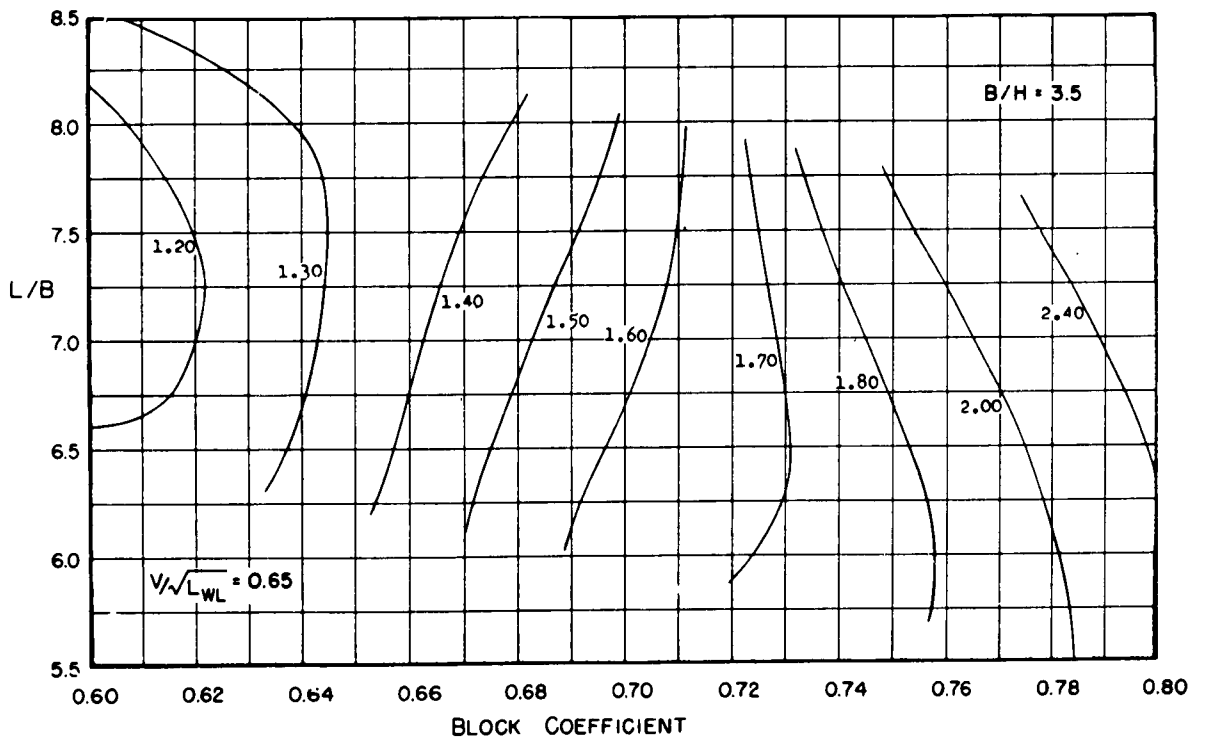


Figure B32

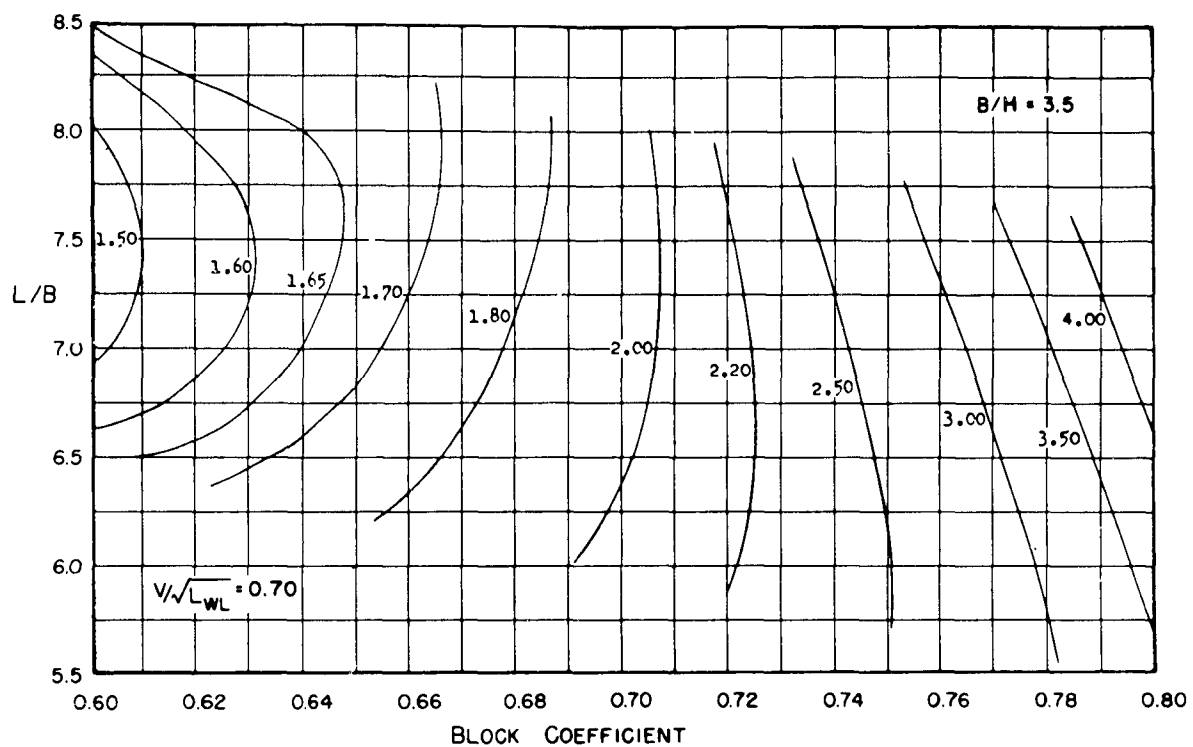


Figure B33

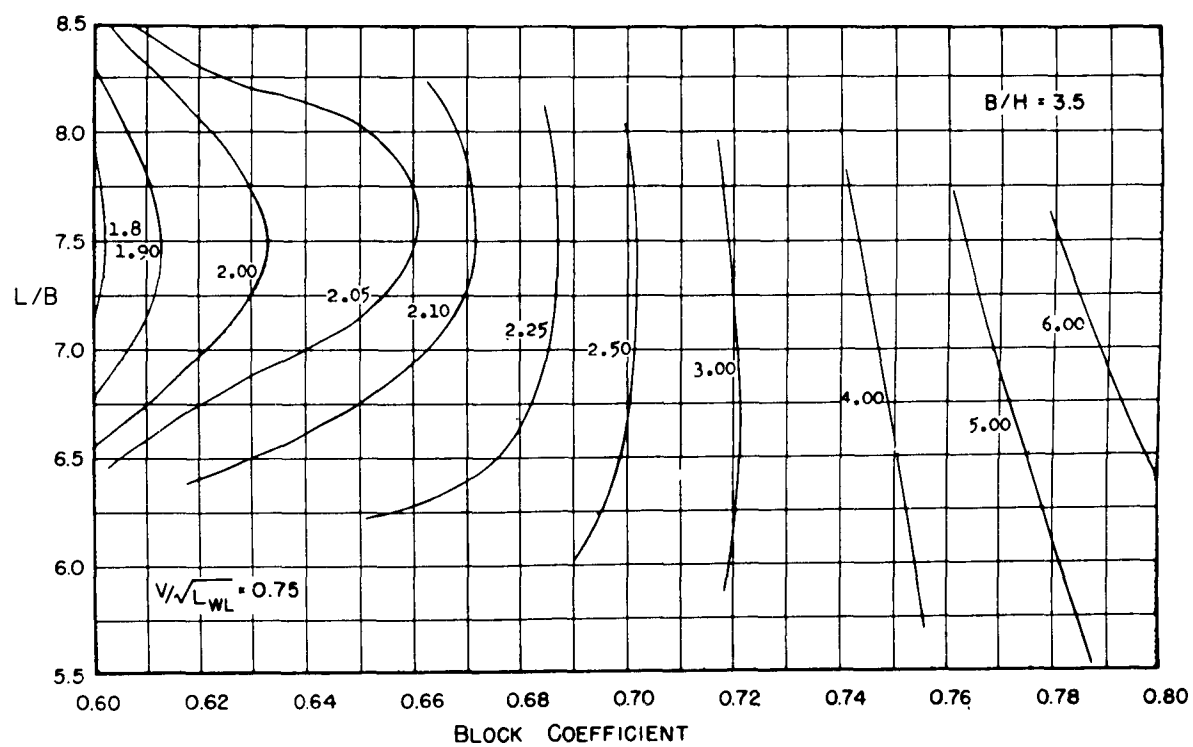


Figure B34

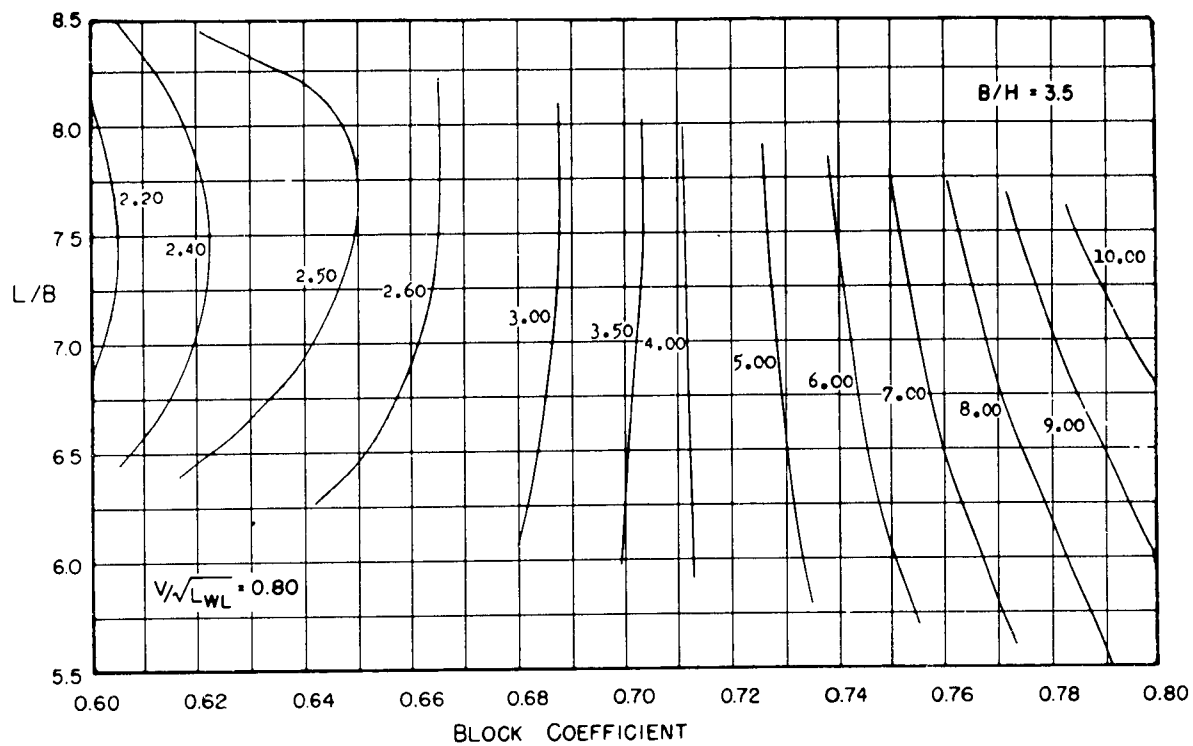


Figure B35

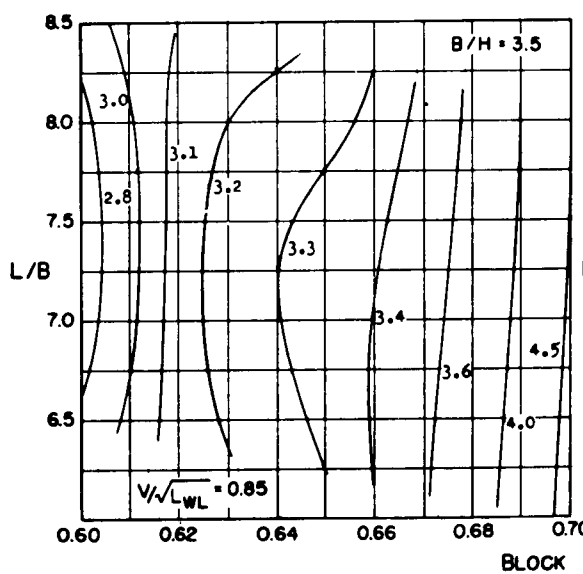


Figure B36

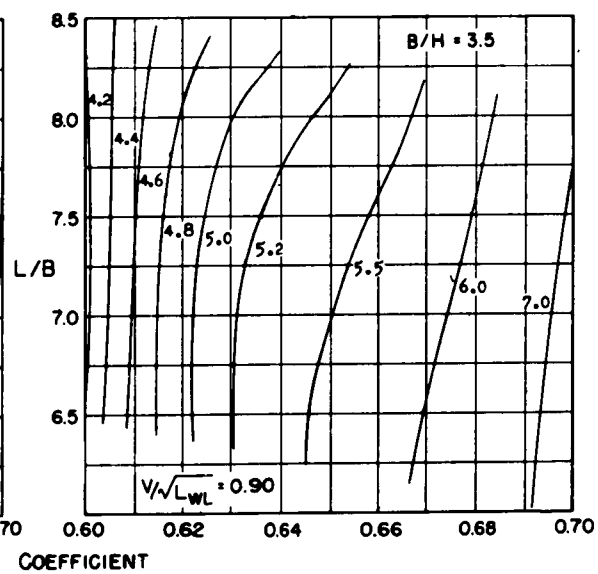


Figure B37

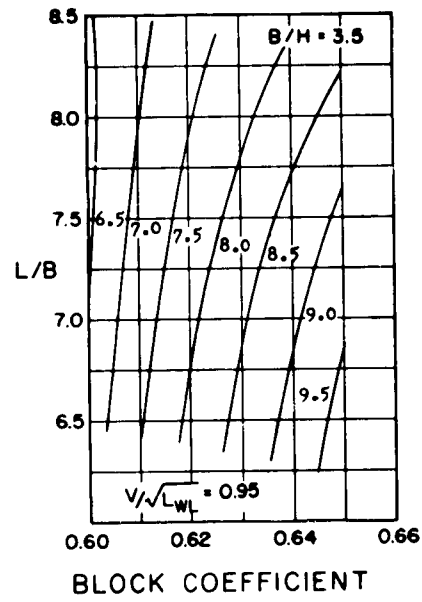


Figure B38

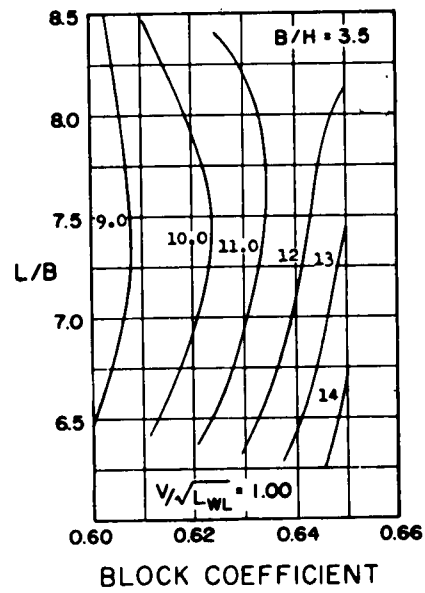


Figure B39

Figures B40 through B78
Contours of ©, 400 Ft Ship *LBP*

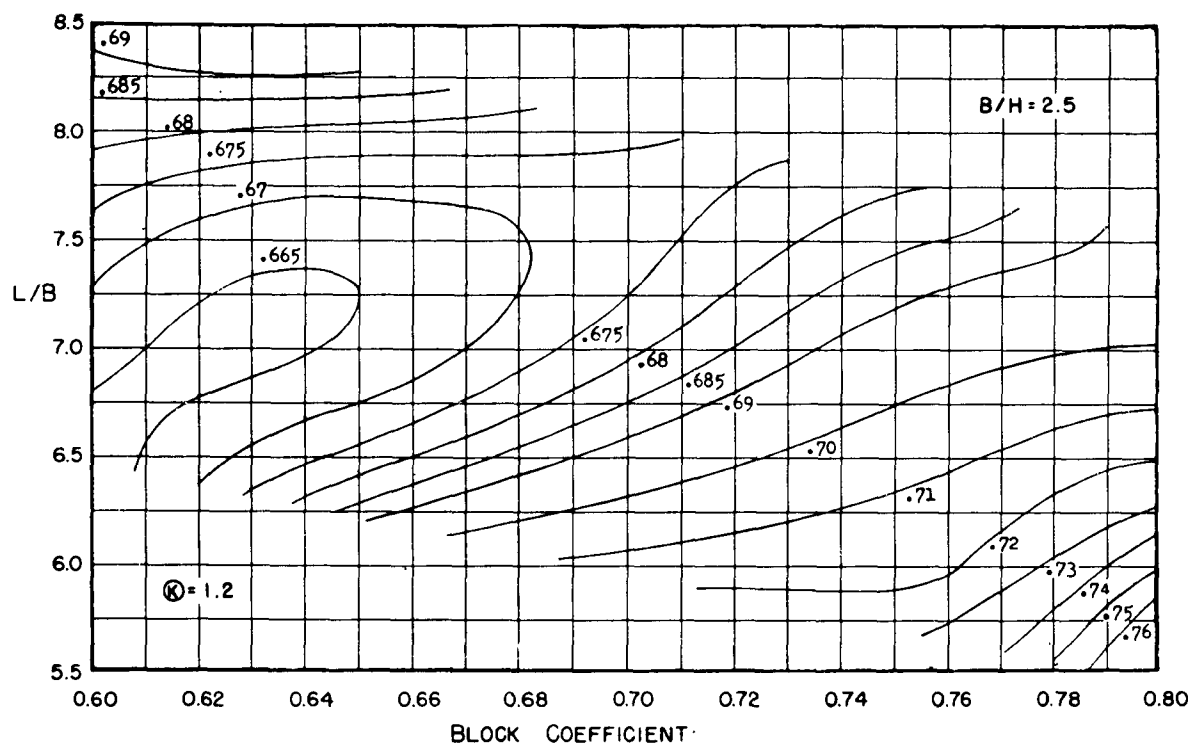


Figure B40

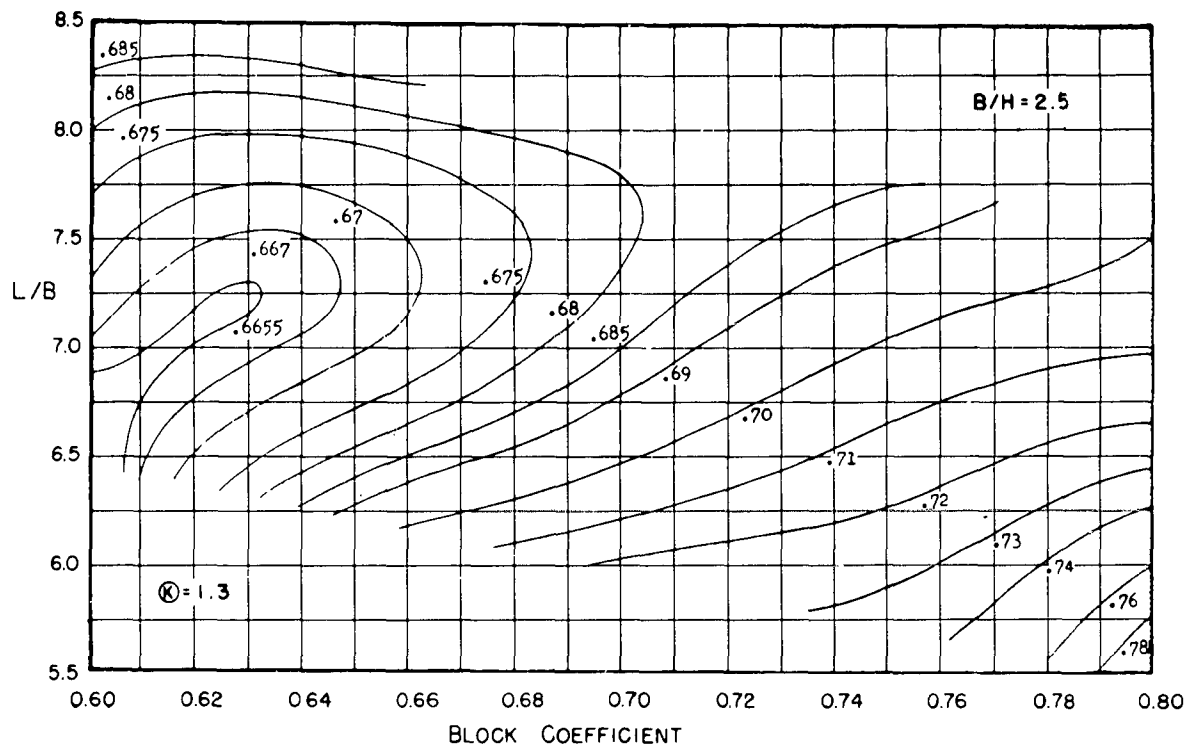


Figure B41

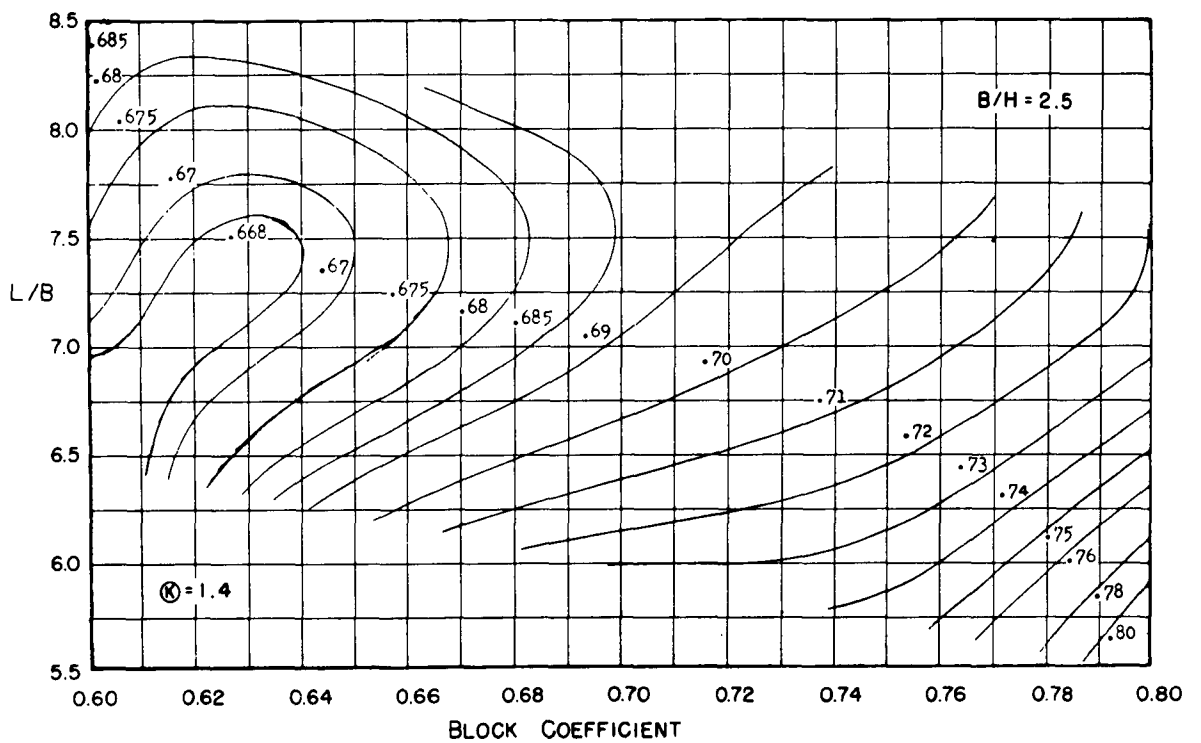


Figure B42

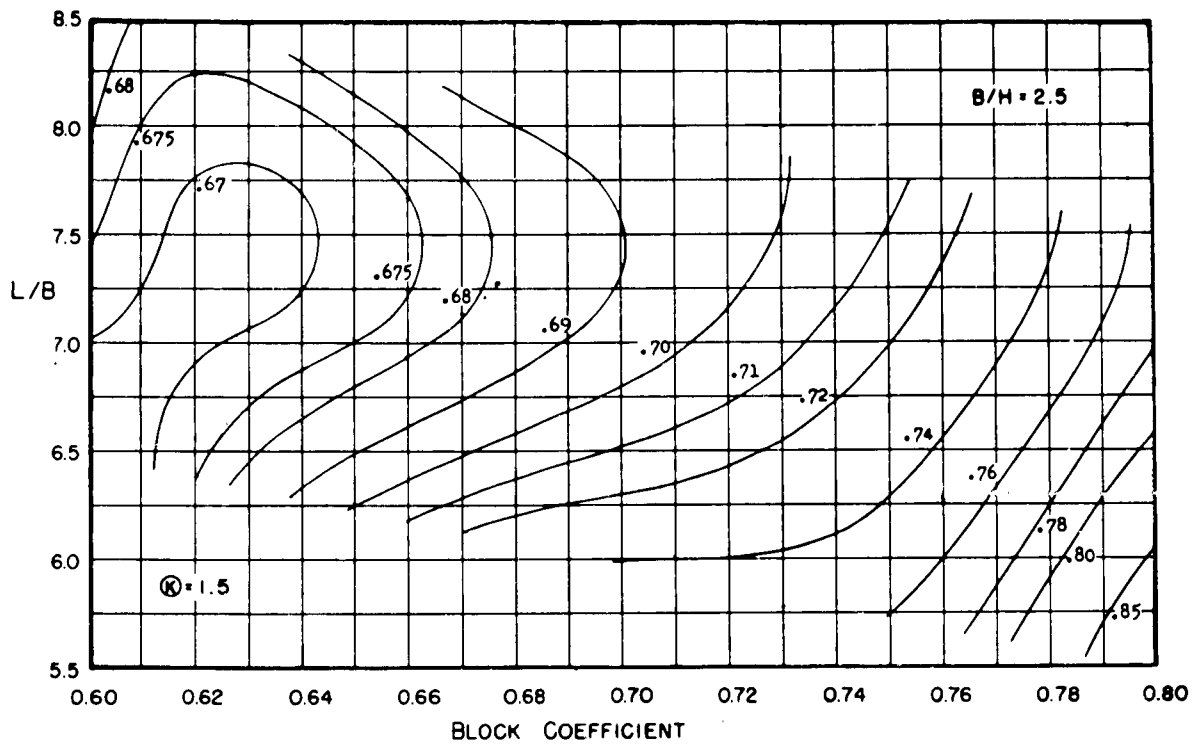


Figure B43

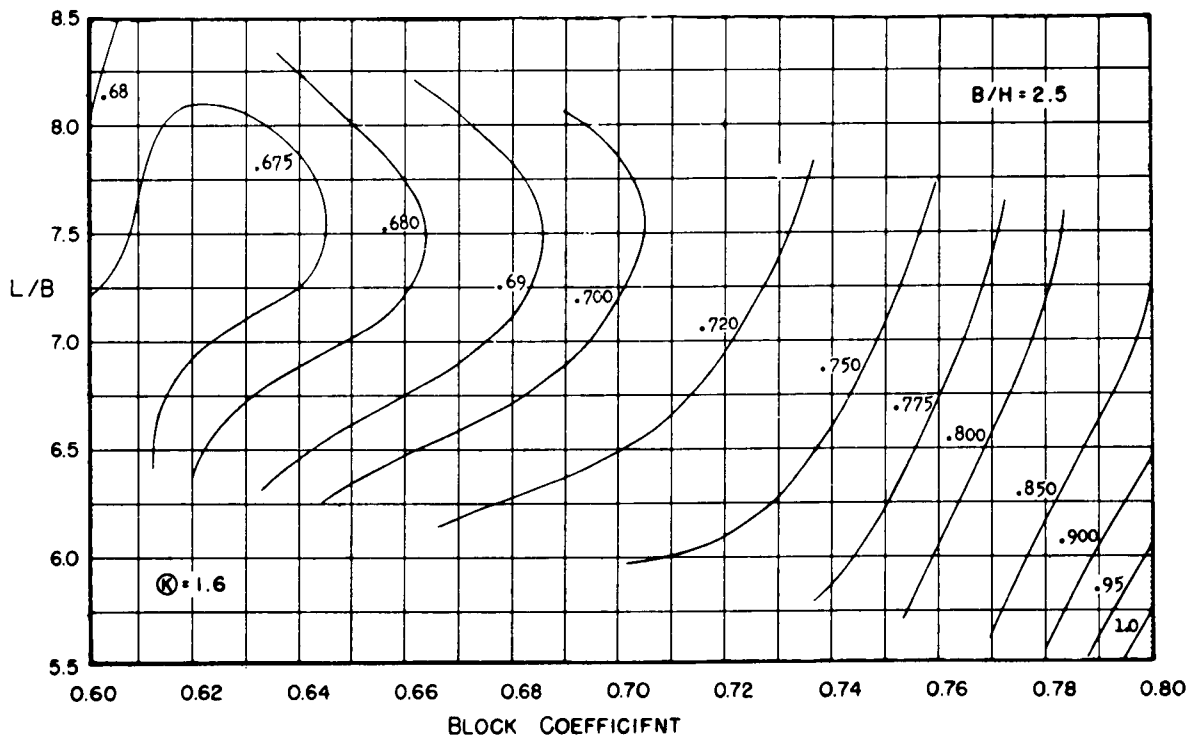


Figure B44

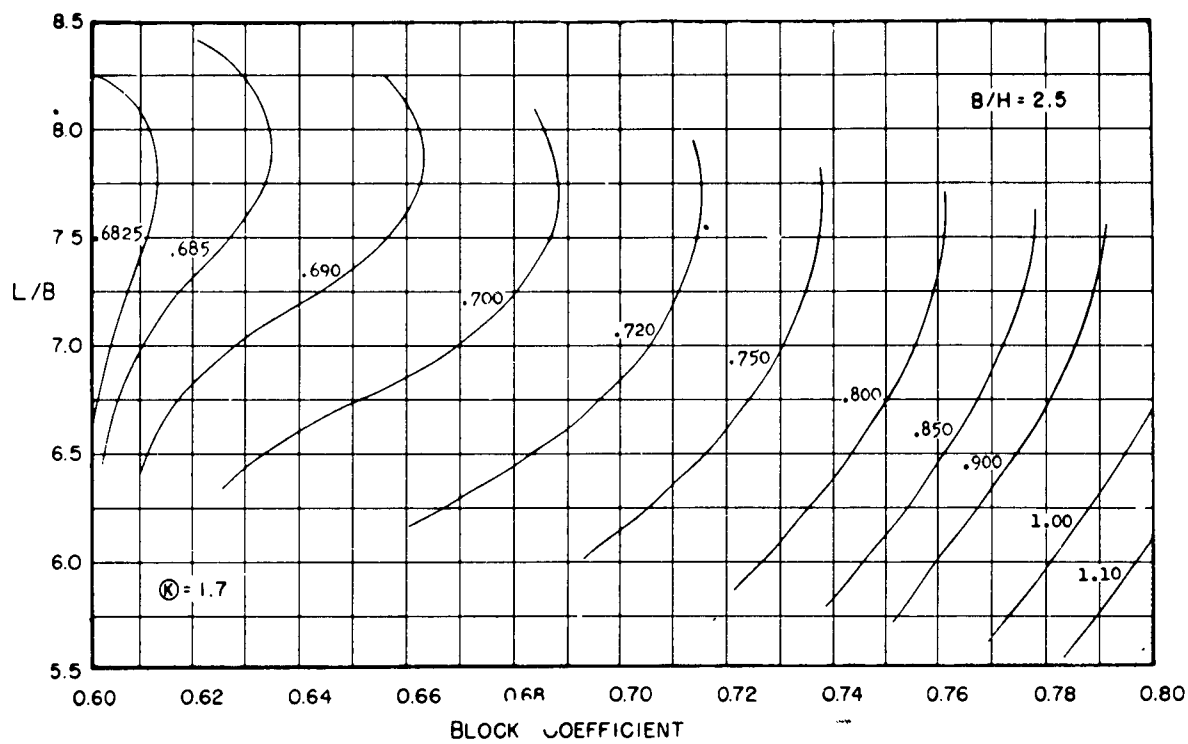


Figure B45

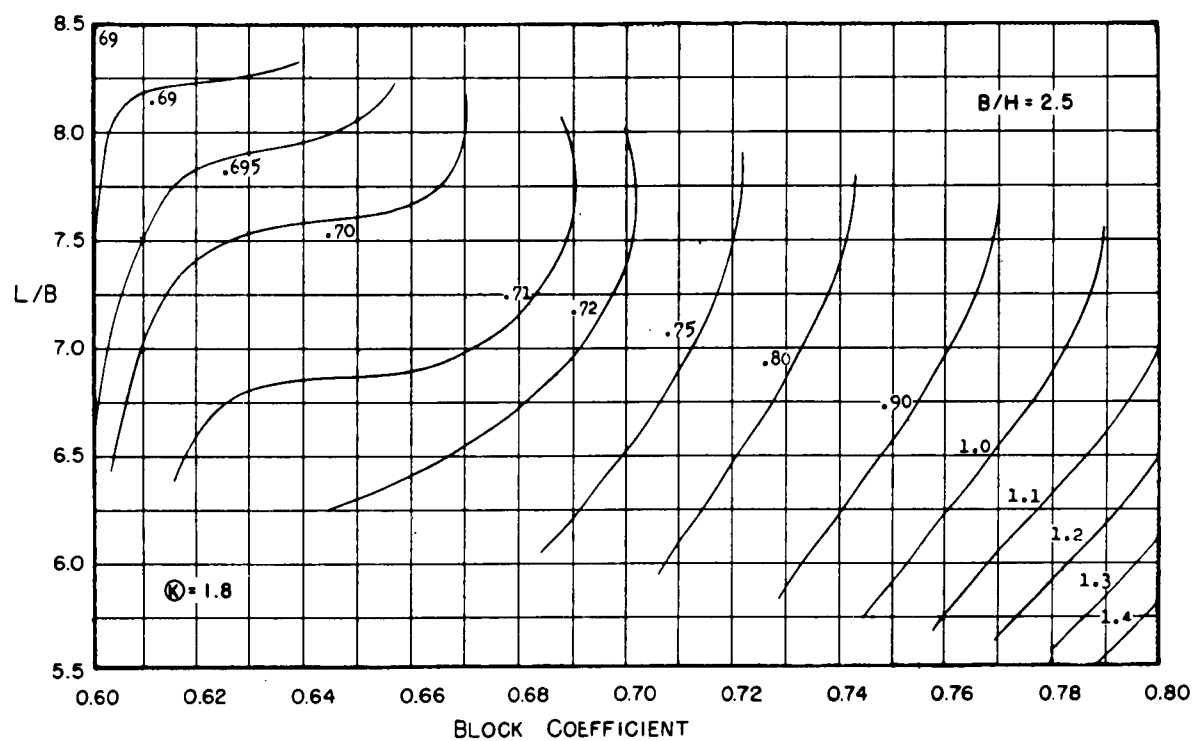


Figure B46

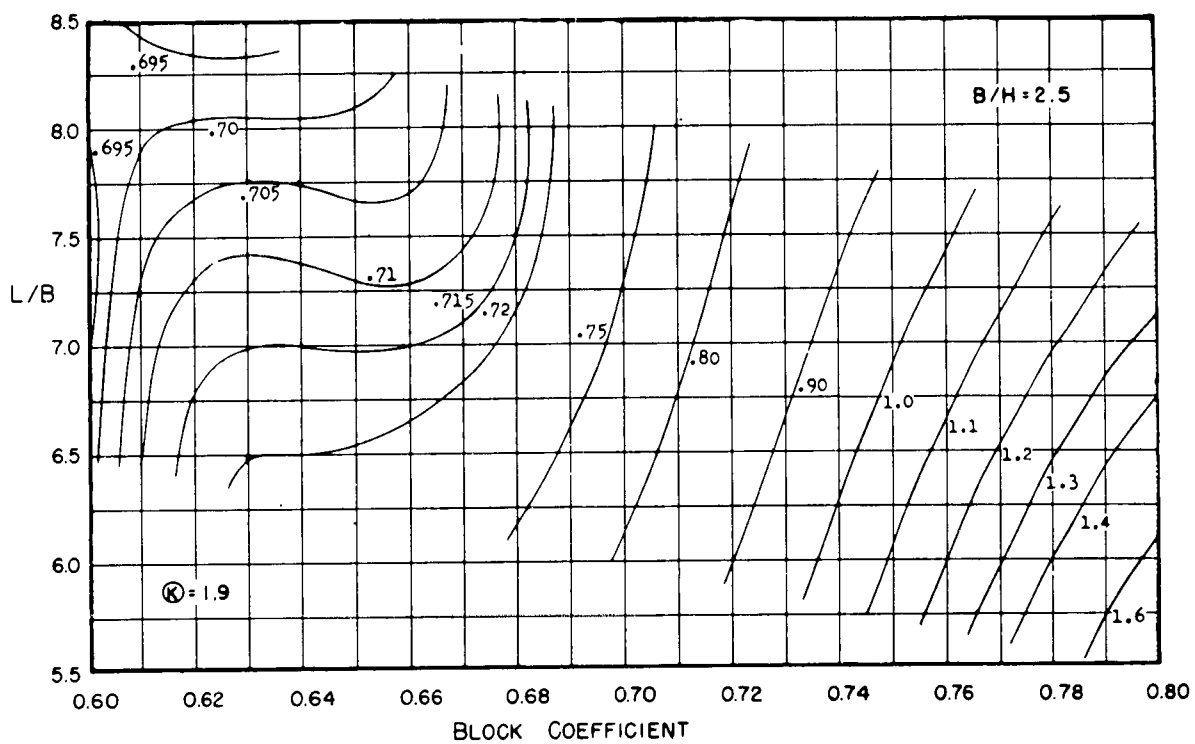


Figure B47

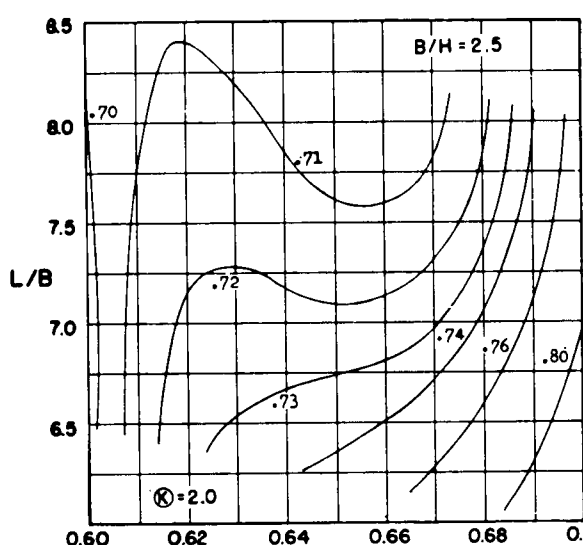


Figure B48

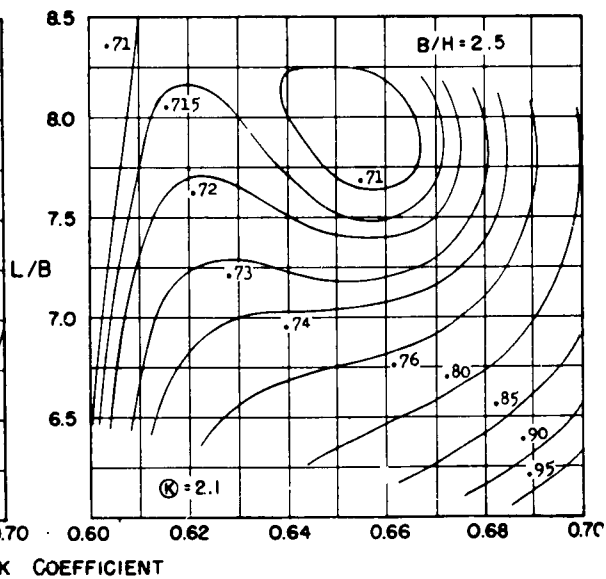


Figure B49

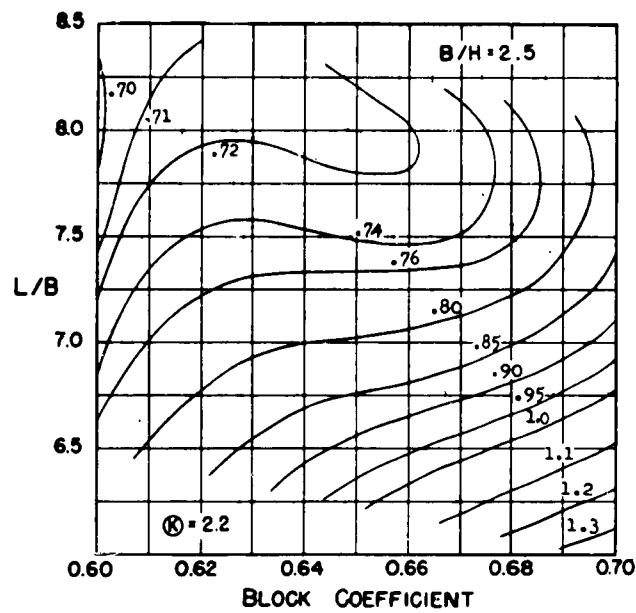


Figure B50

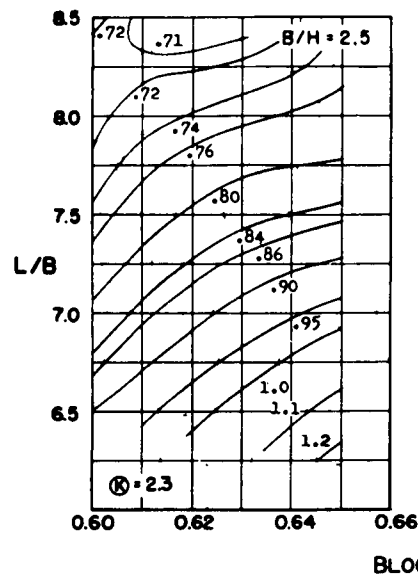


Figure B51

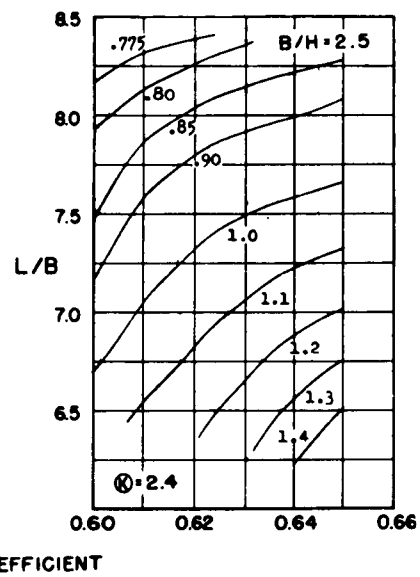


Figure B52

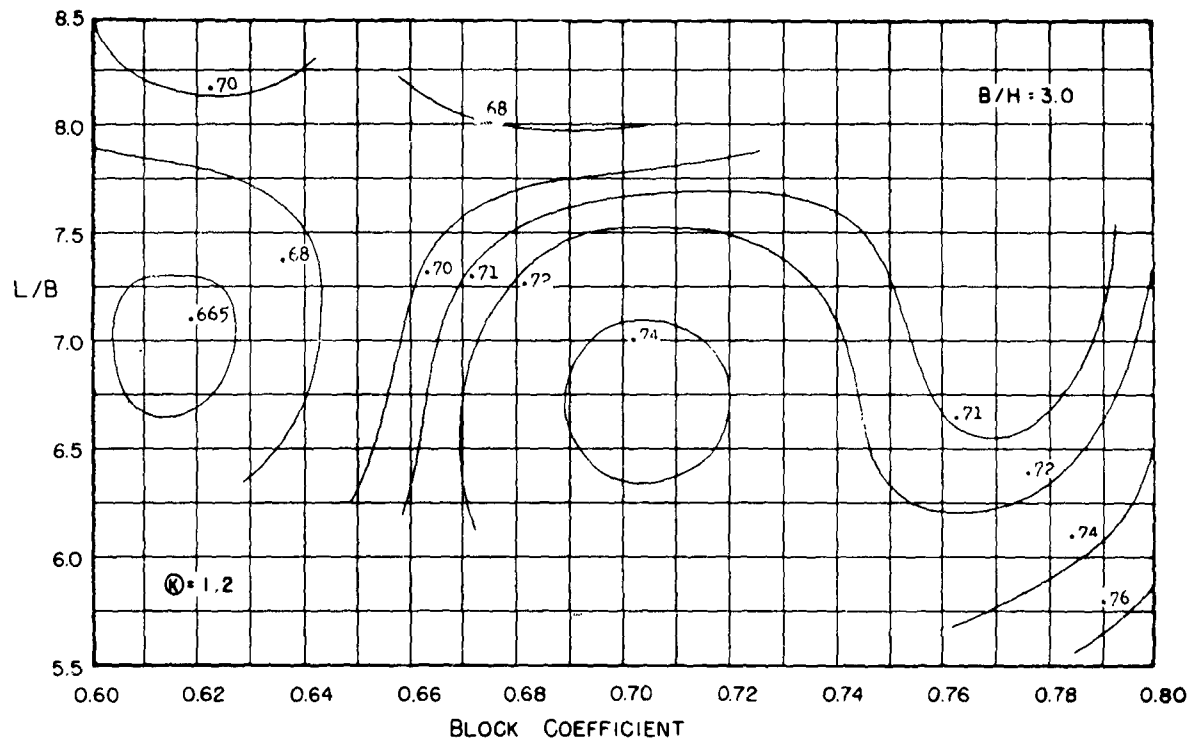


Figure B53

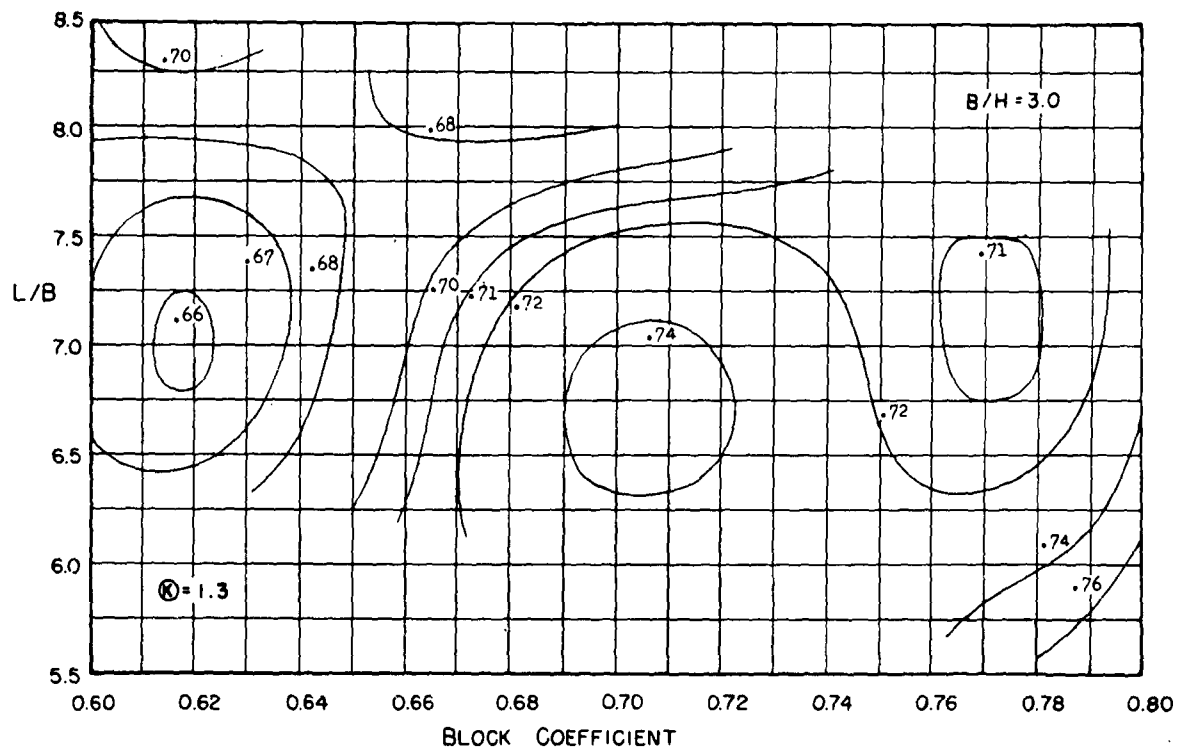


Figure B54

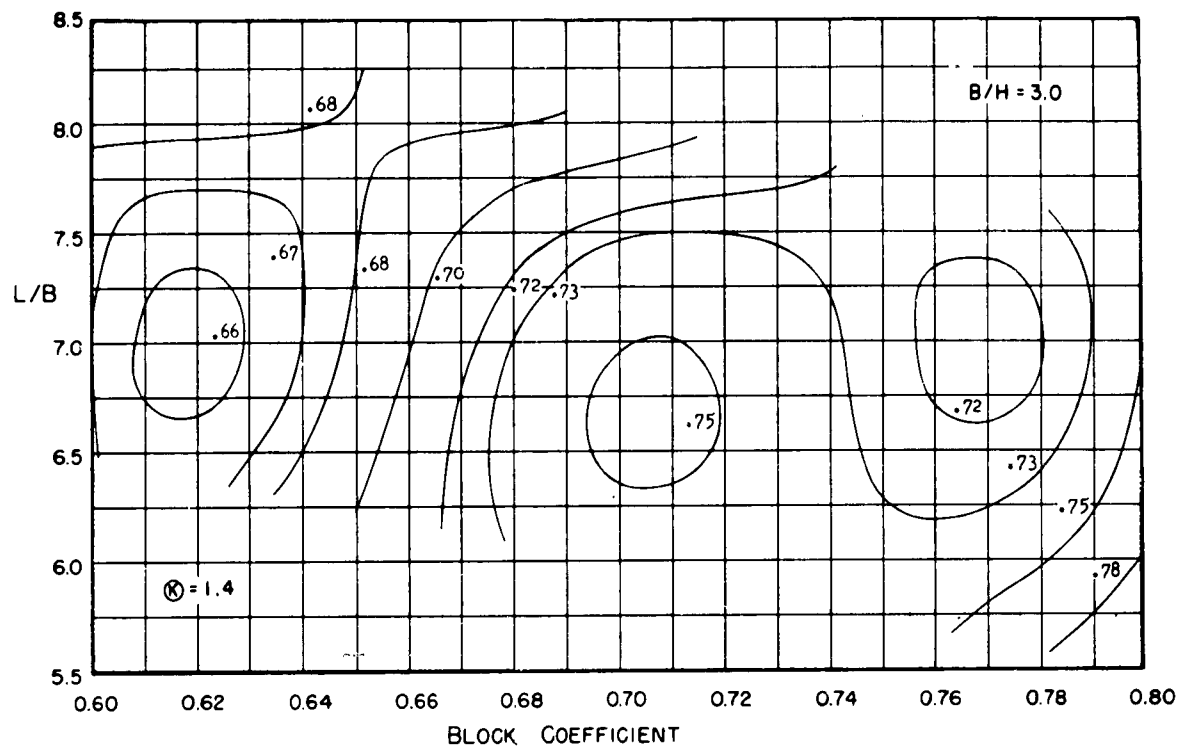


Figure B55

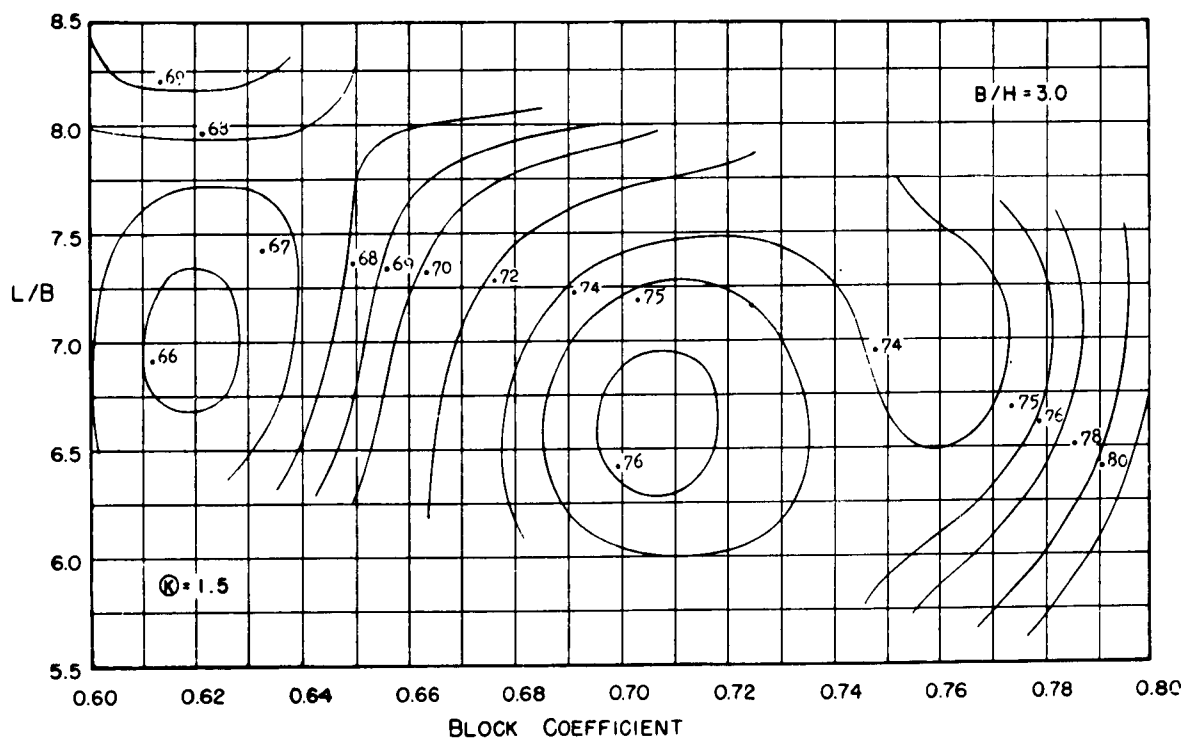


Figure B56

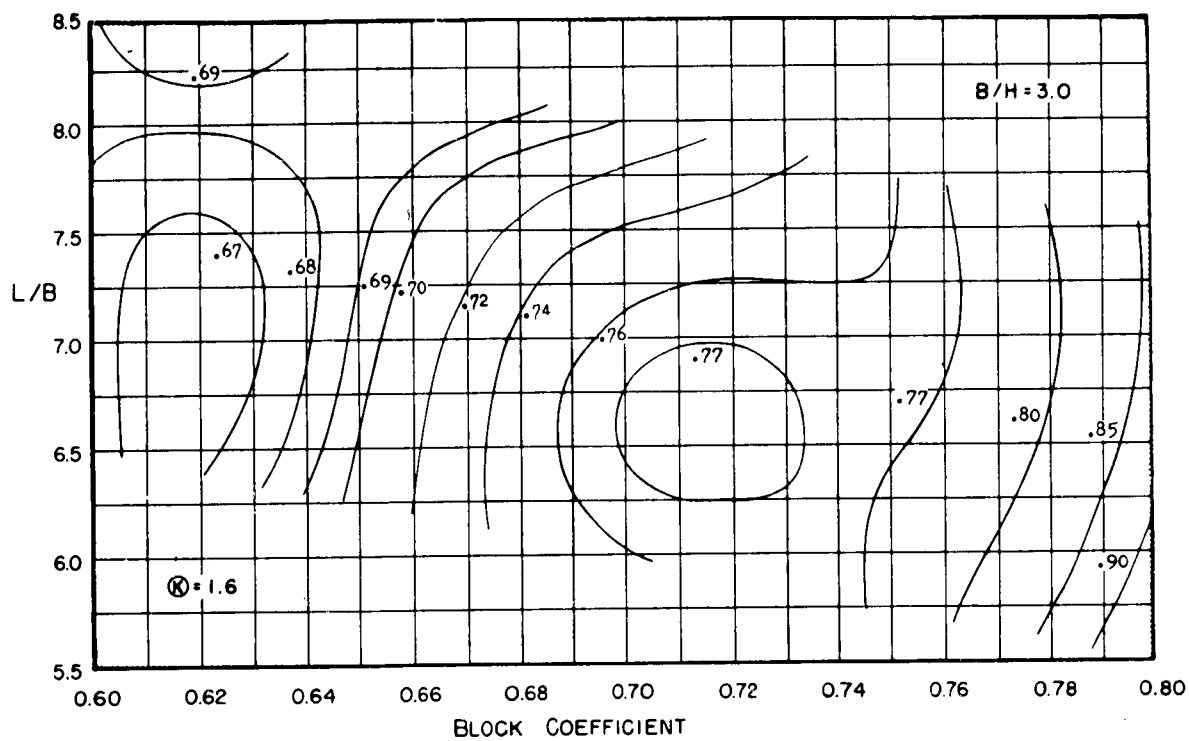


Figure B57

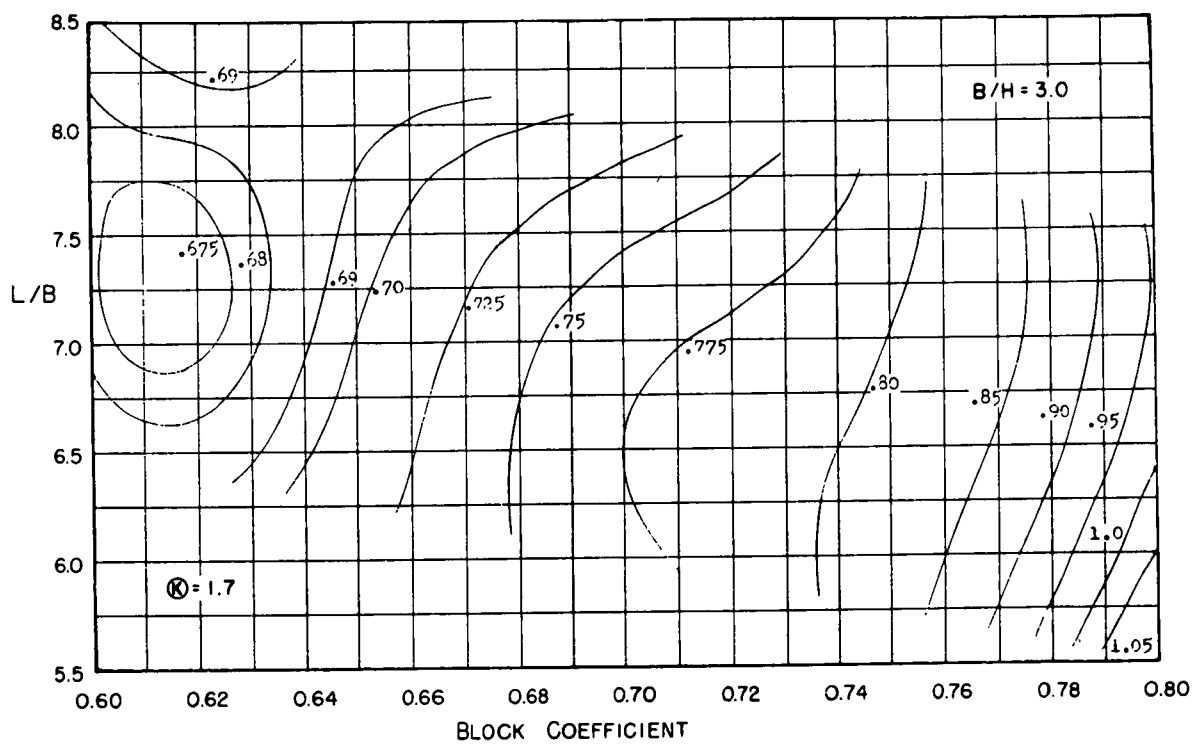


Figure B58

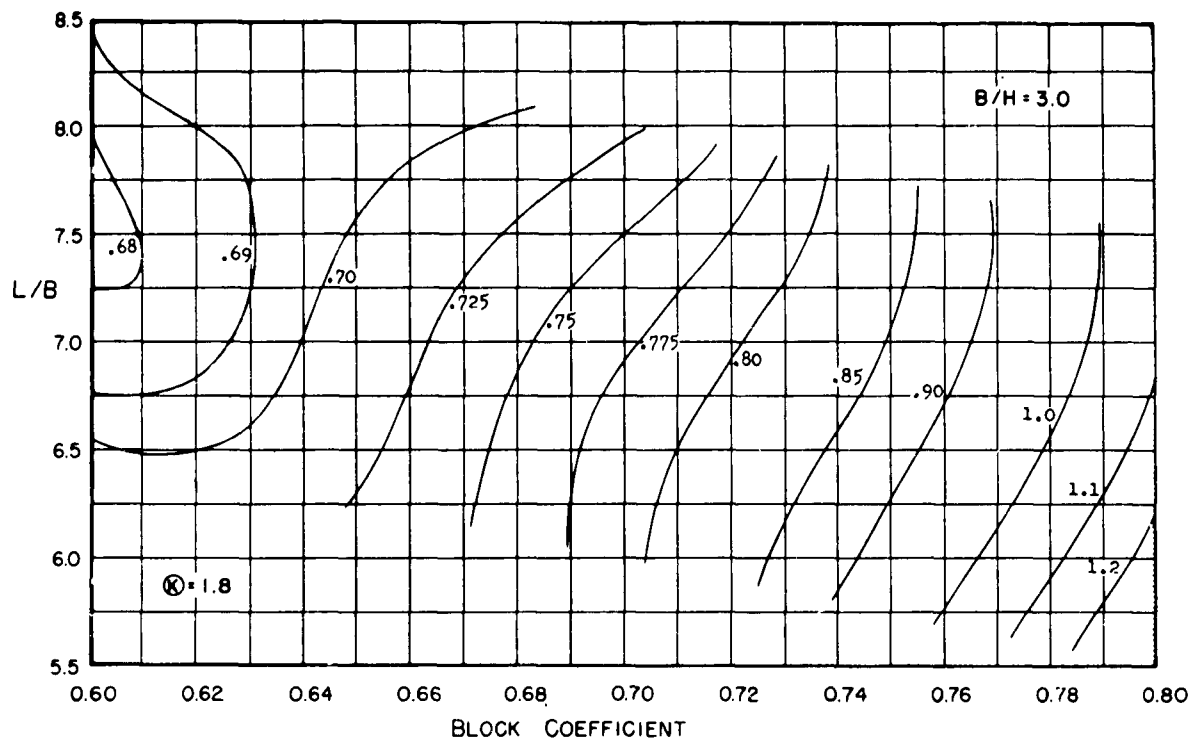


Figure B59

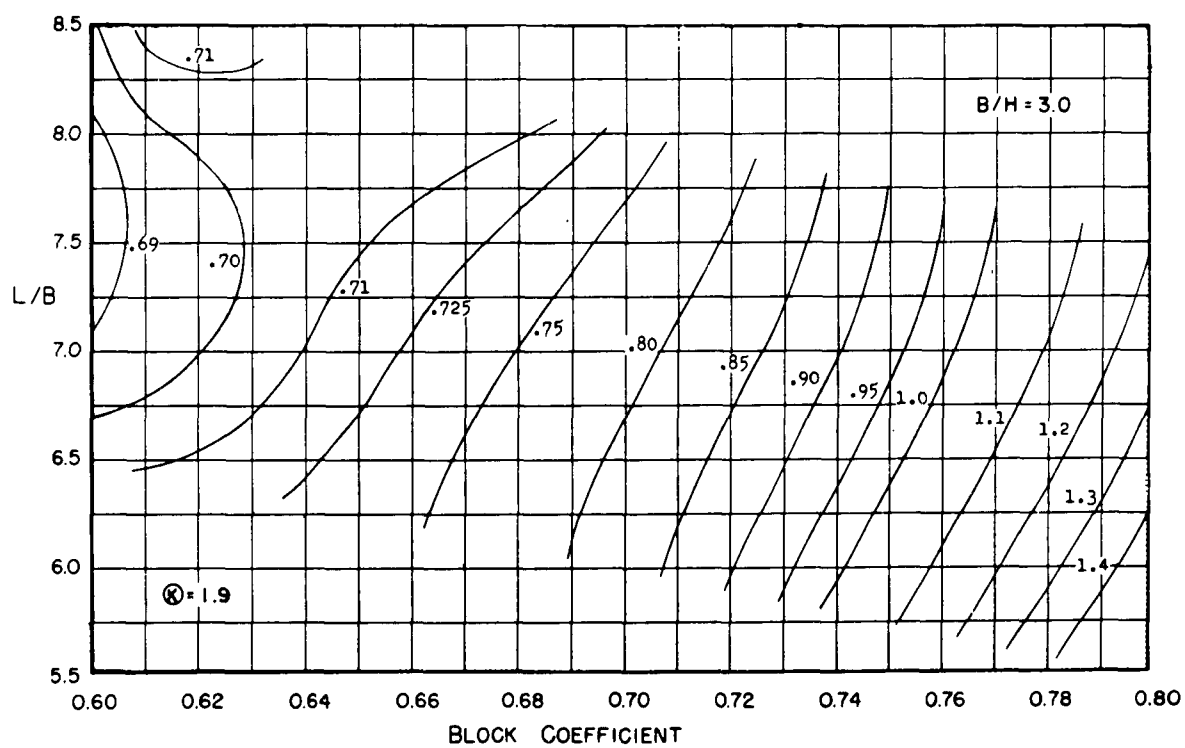


Figure B60

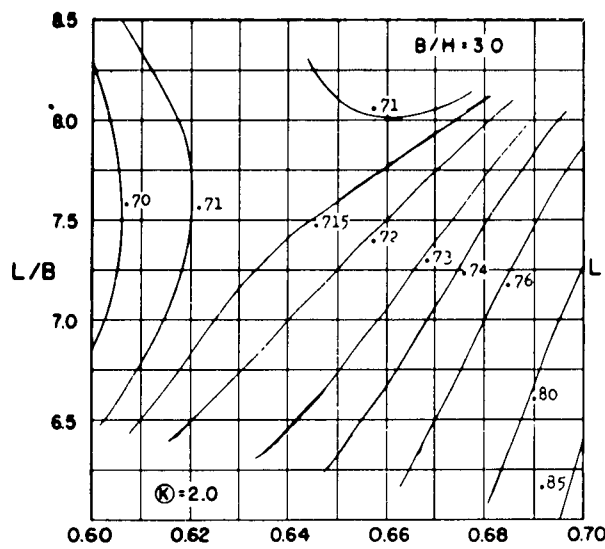


Figure B61

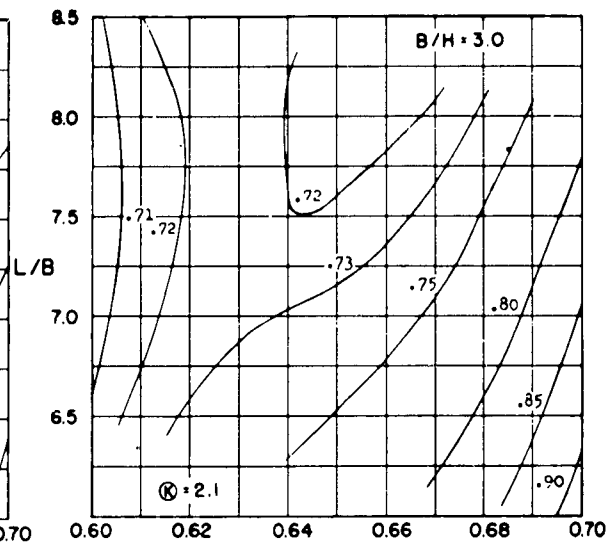


Figure B62

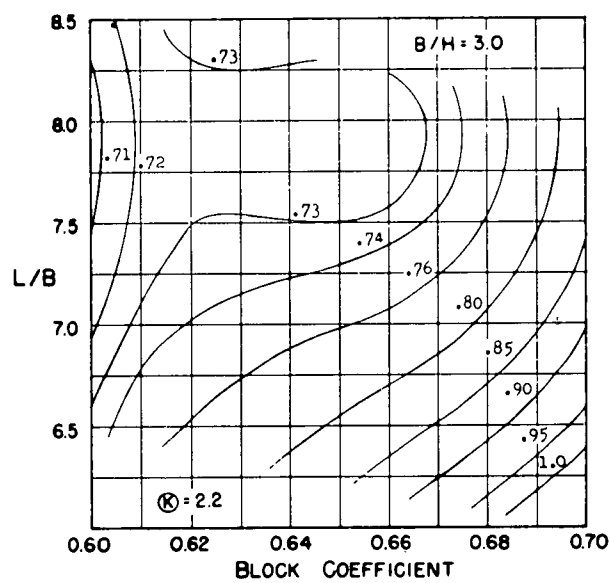


Figure B63

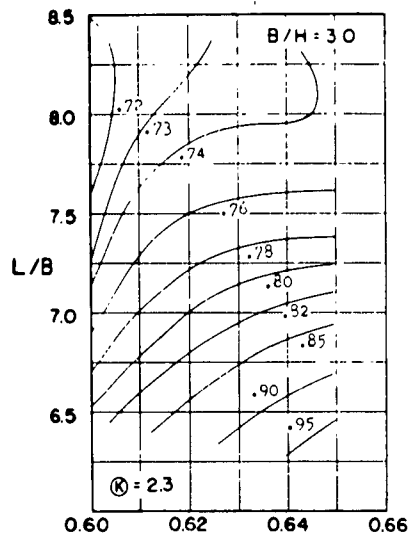


Figure B64

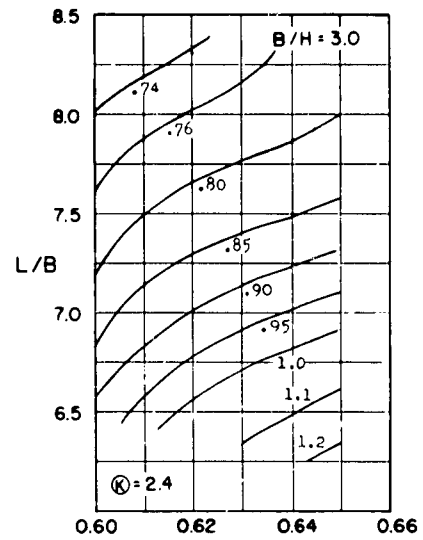


Figure B65

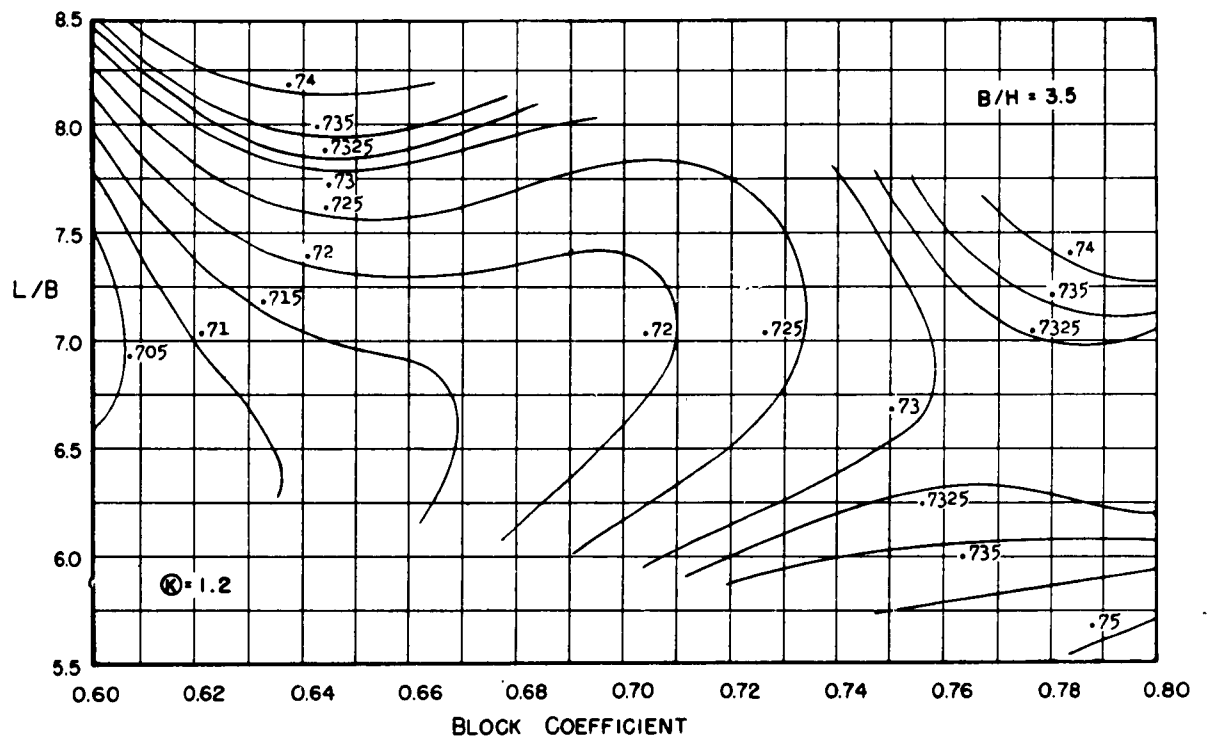


Figure B66

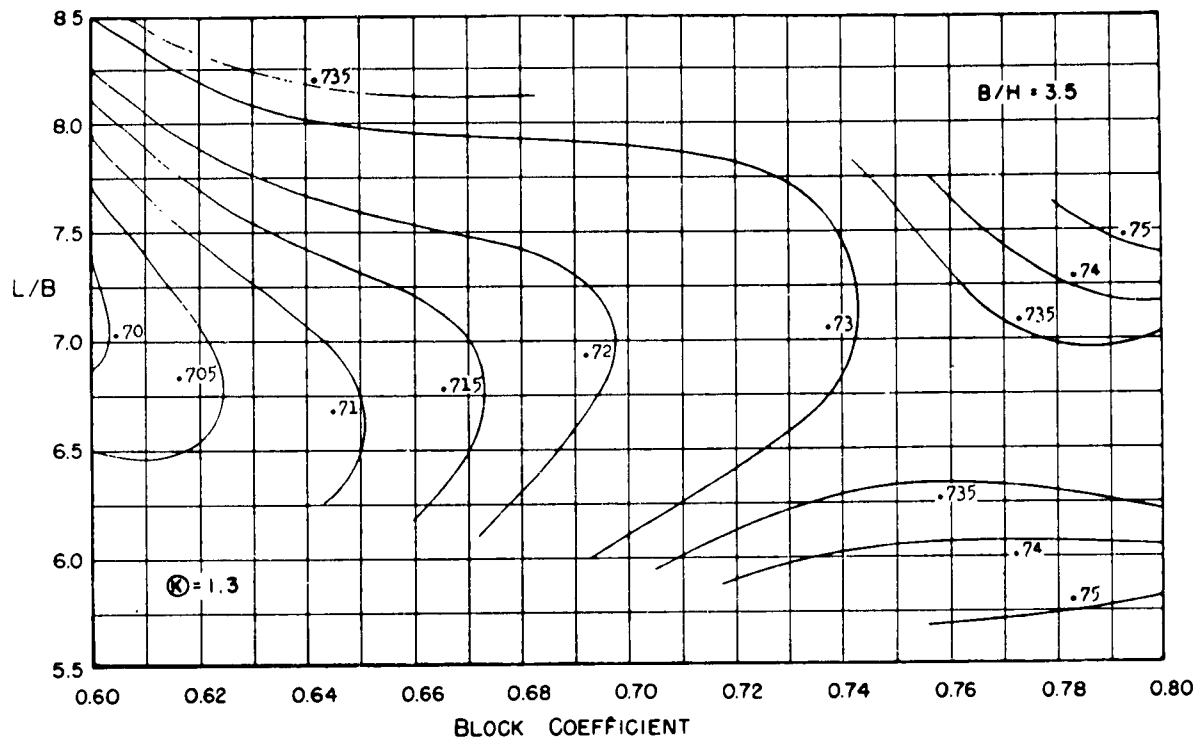


Figure B67

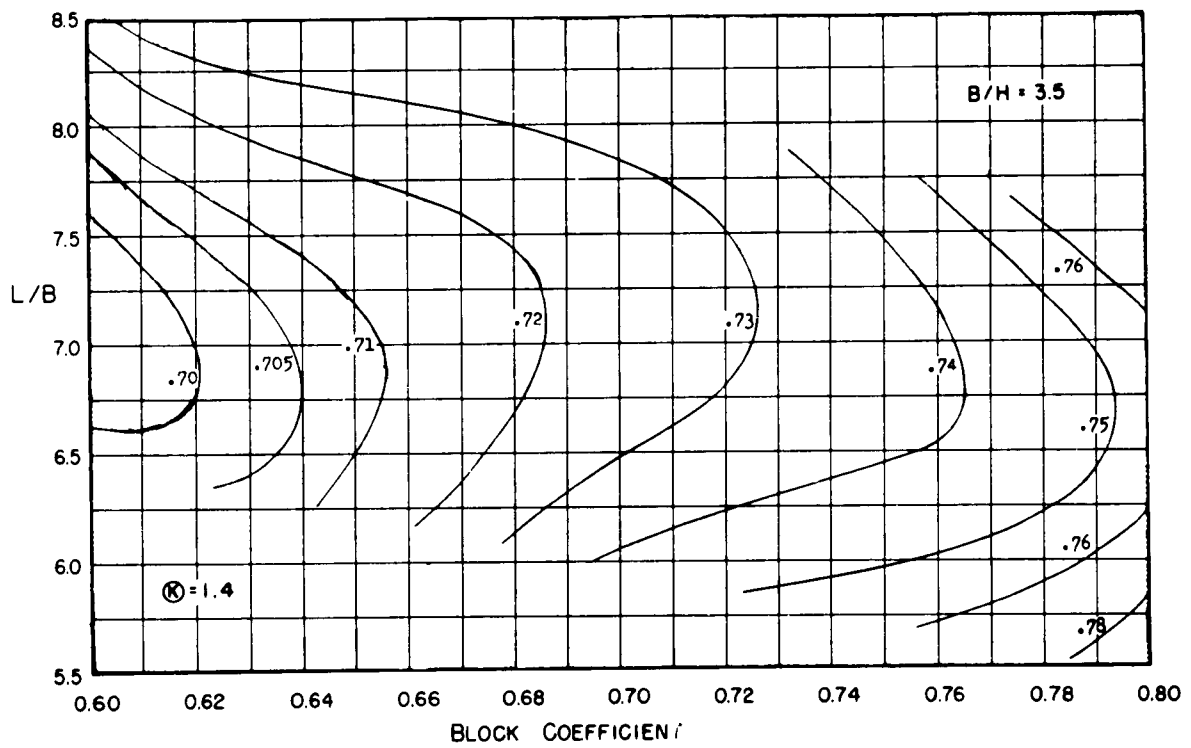


Figure B68

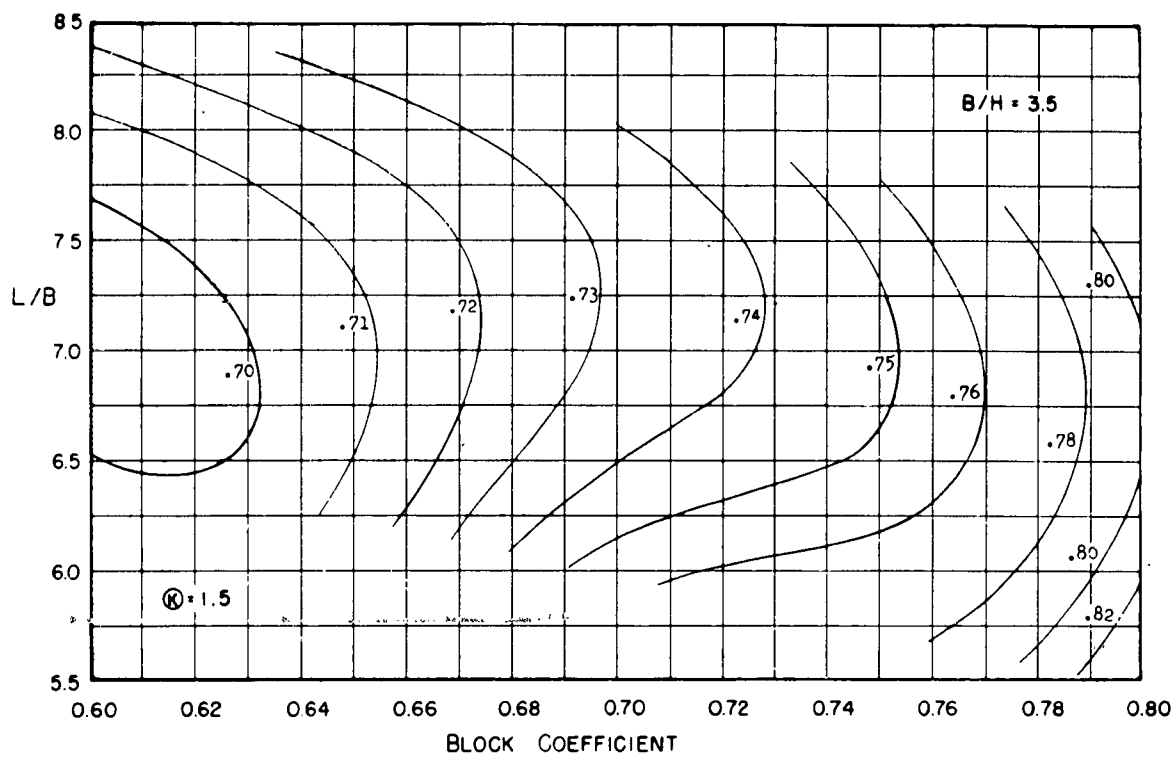


Figure B69

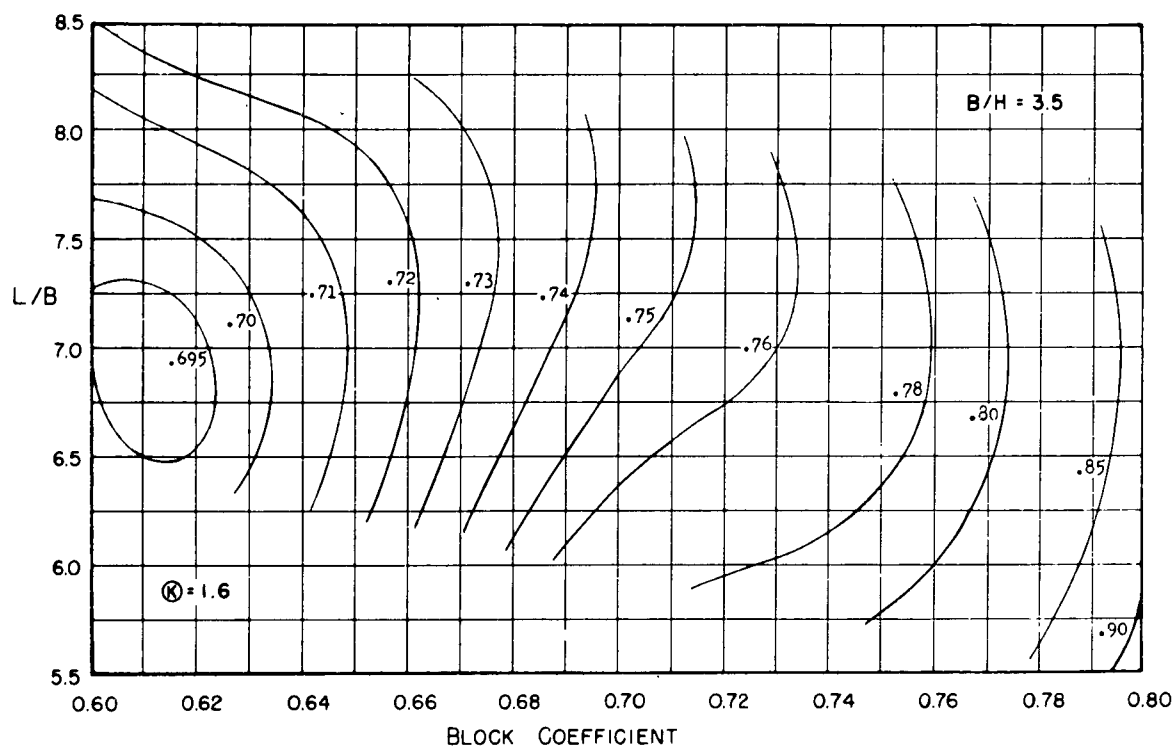


Figure B70

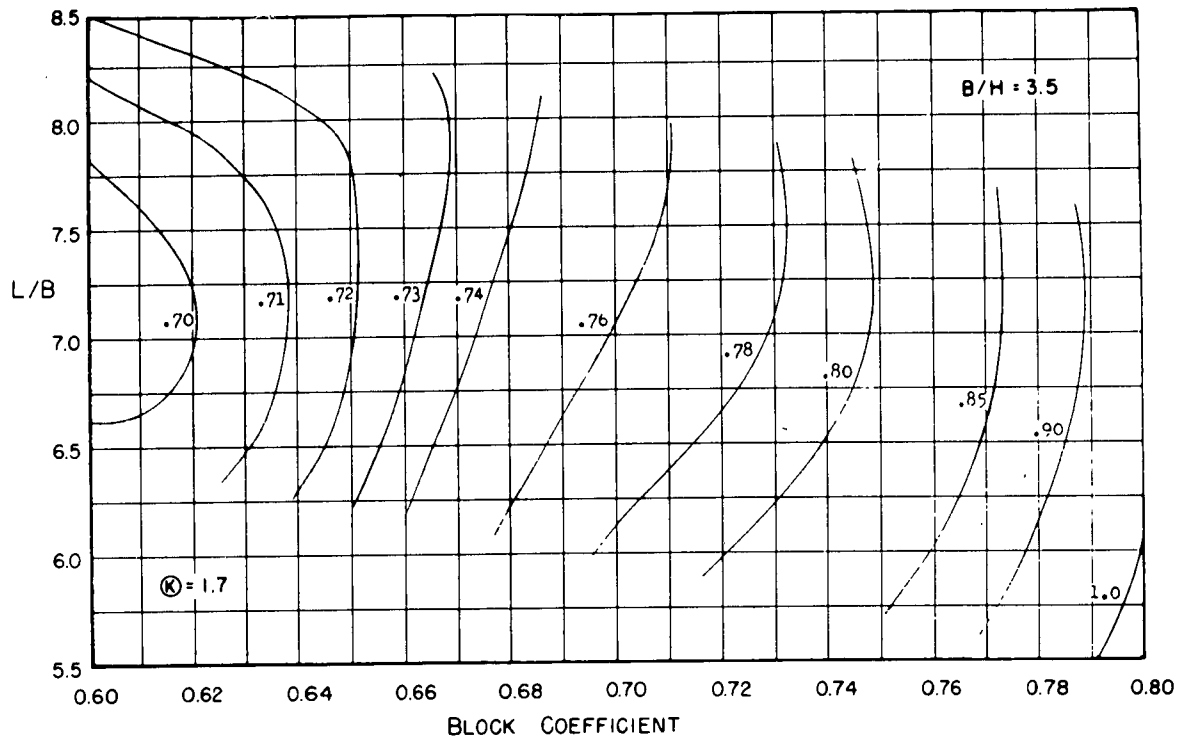


Figure B71

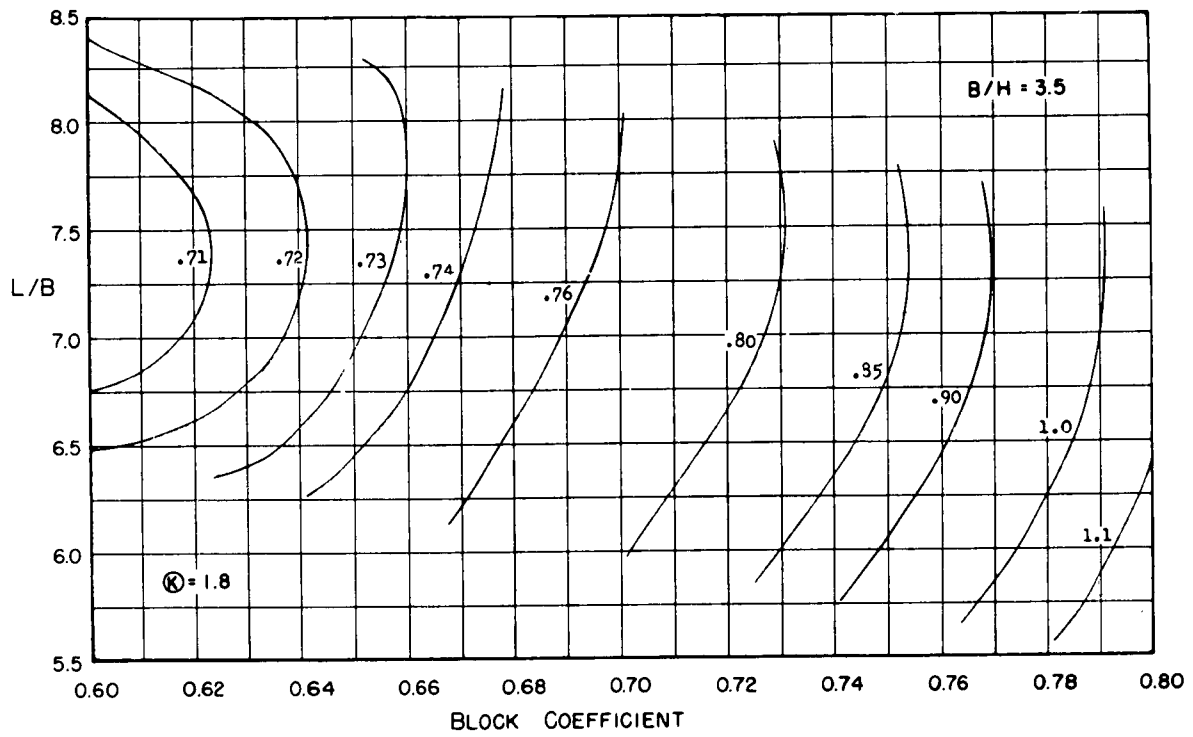


Figure B72

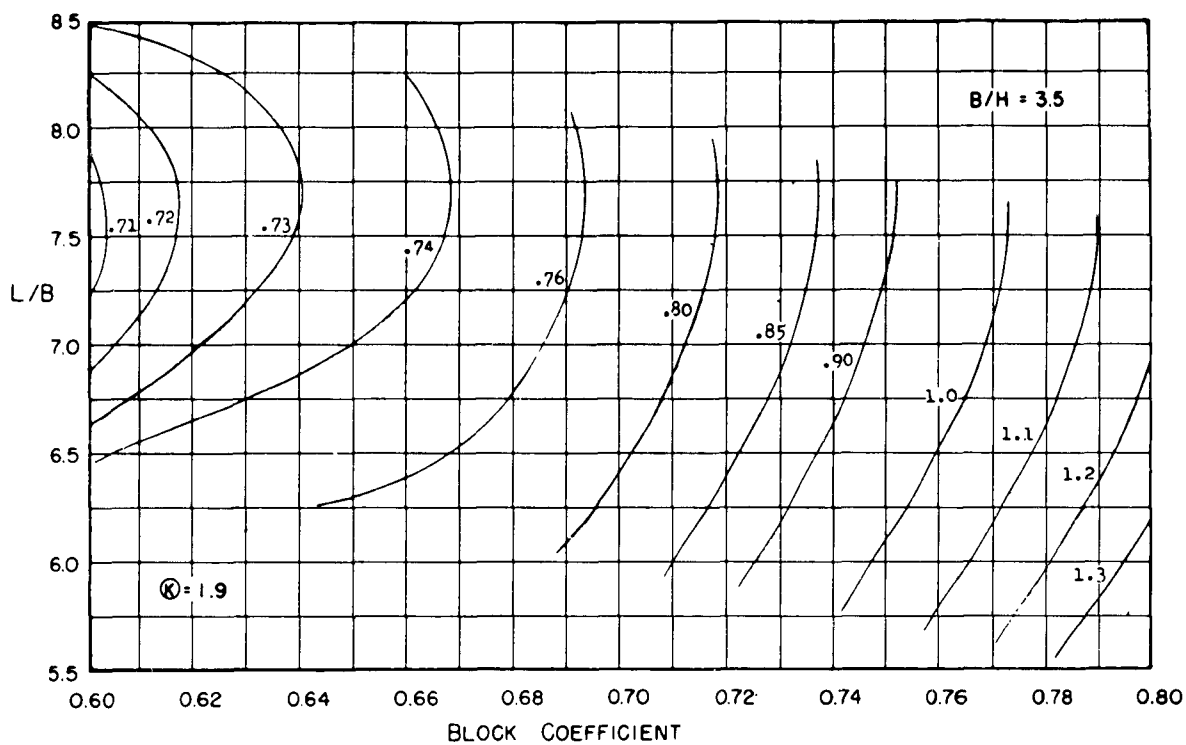


Figure B73

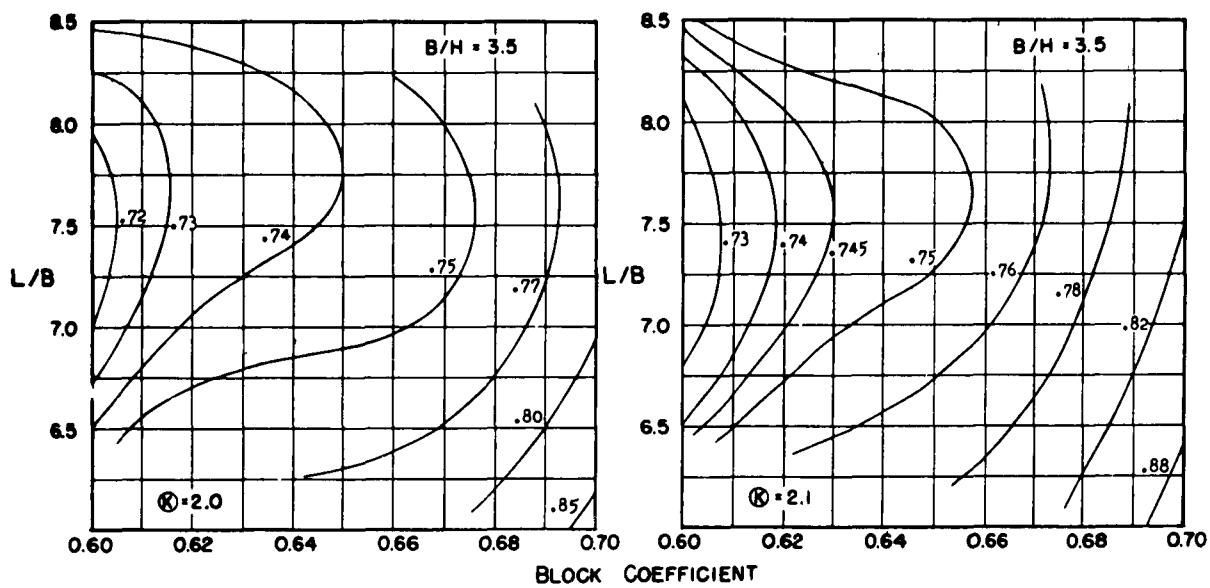


Figure B74

Figure B75

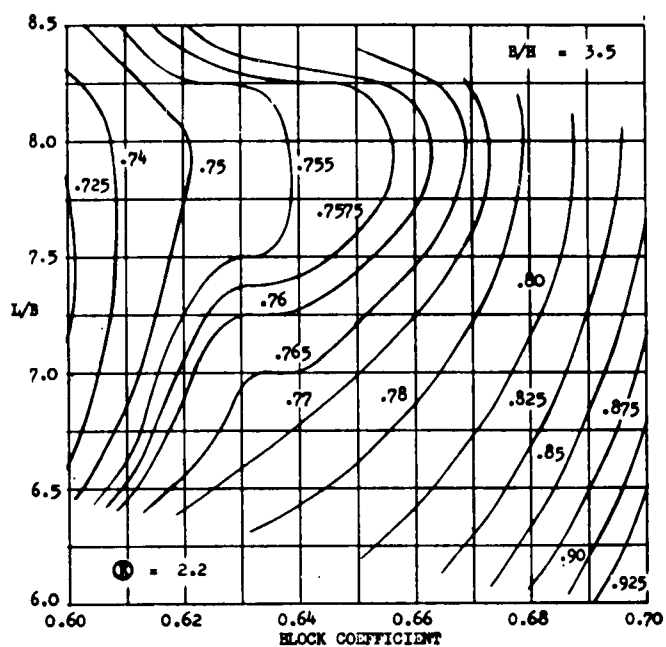


Figure B76

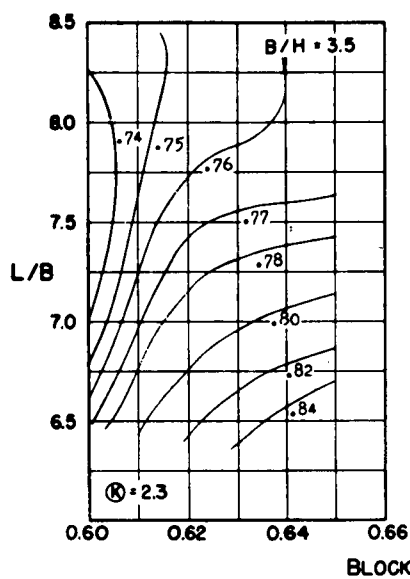


Figure B77

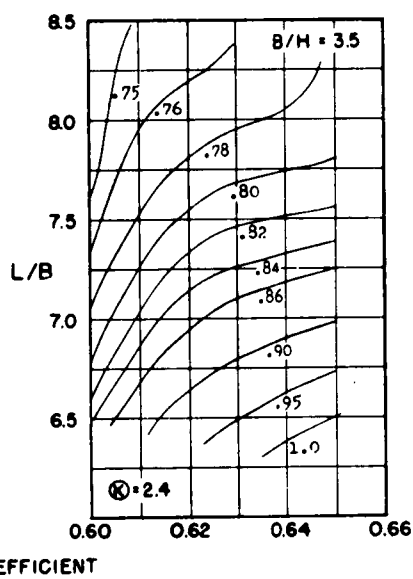


Figure B78

Figures B79 through B120
Contours of Wake Fraction and Thrust Deduction

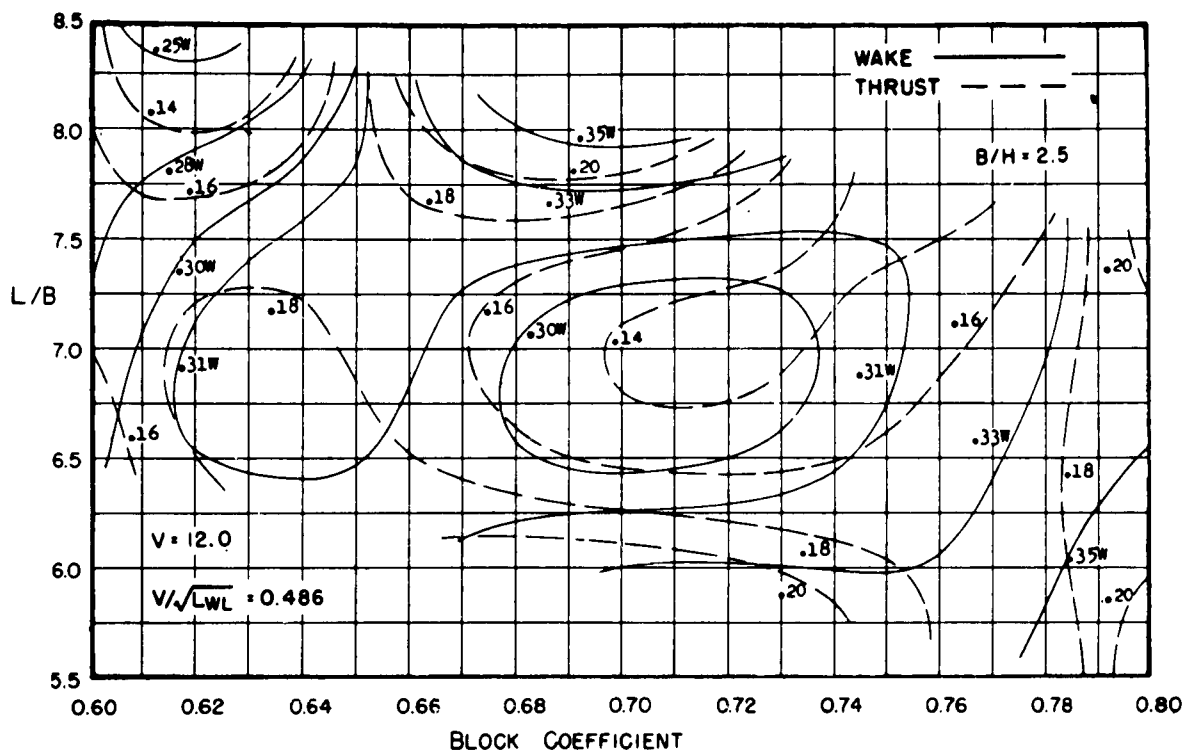


Figure B79

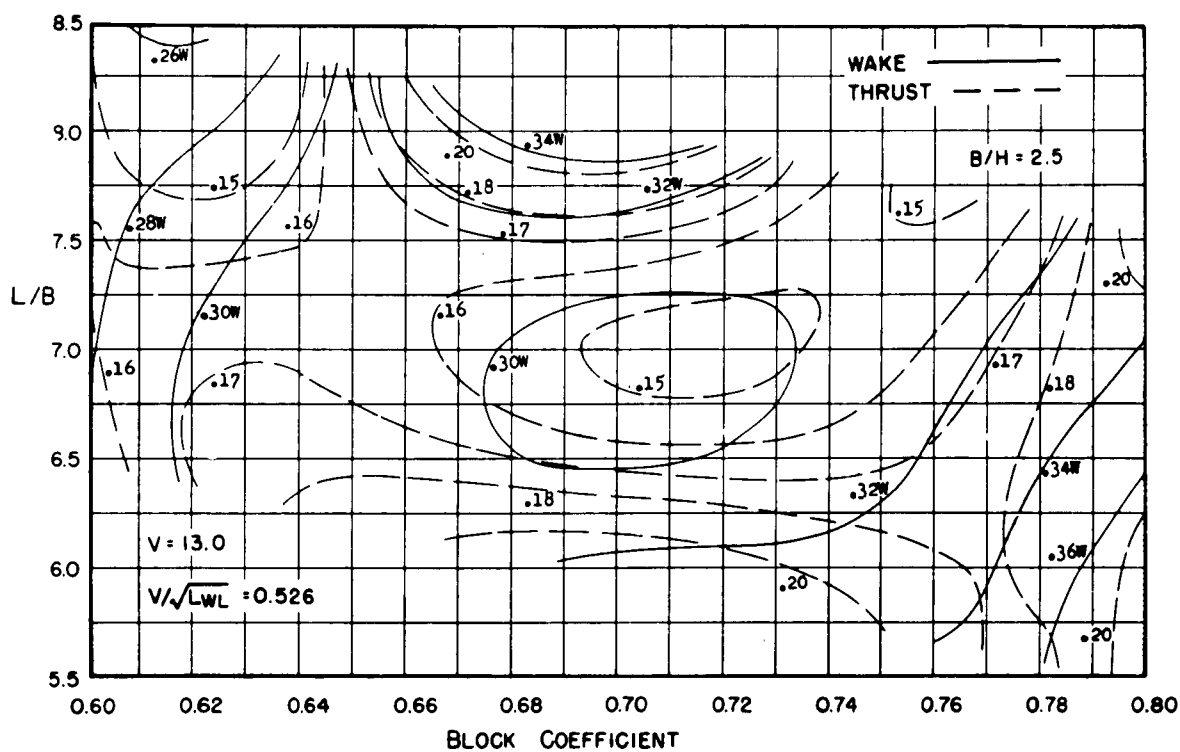


Figure B80

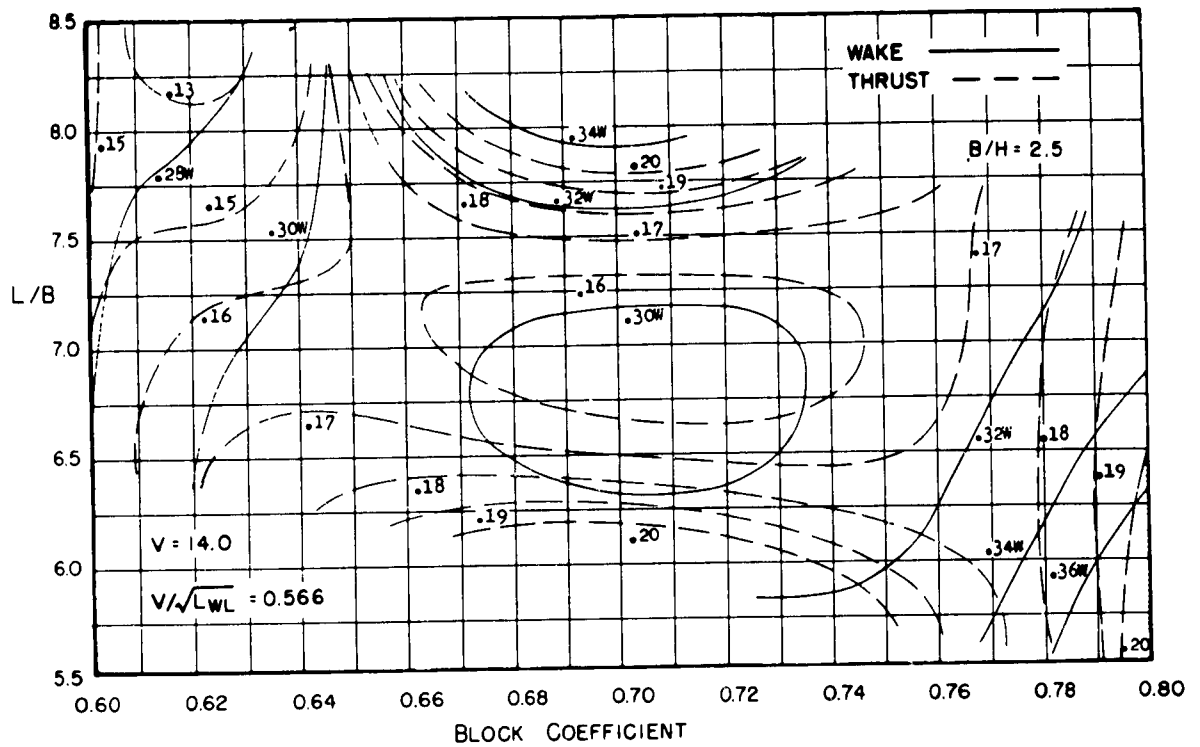


Figure B81

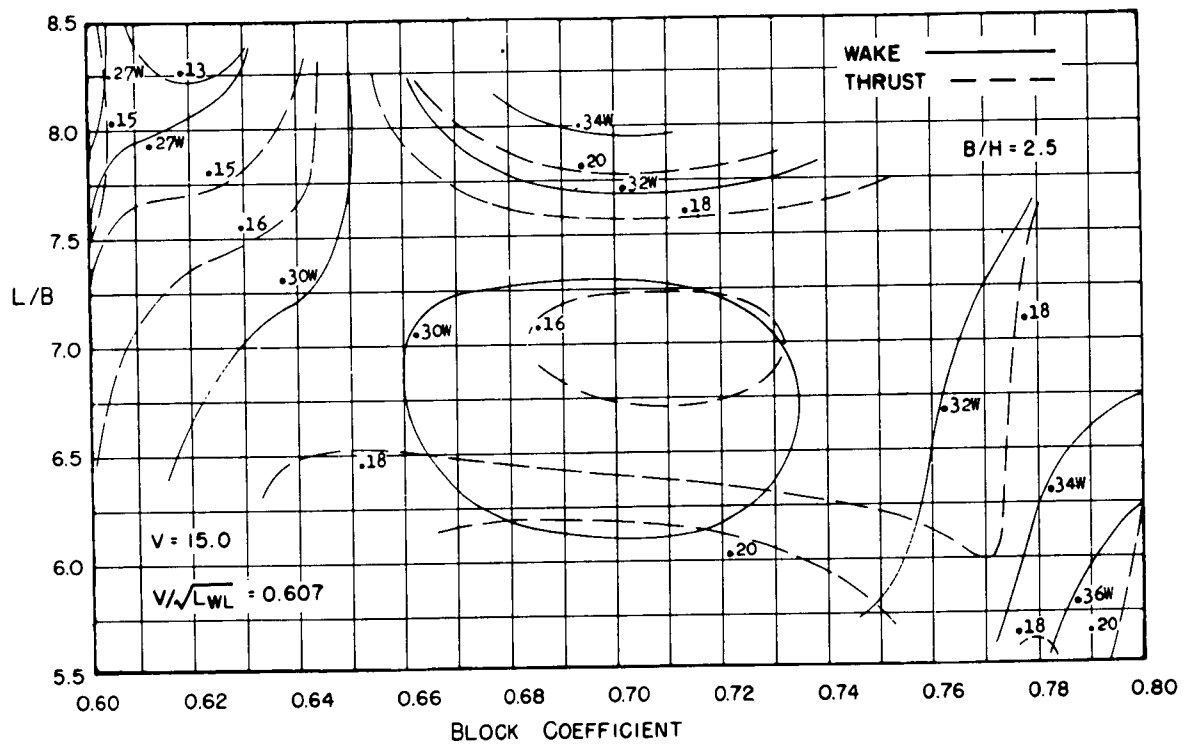


Figure B82

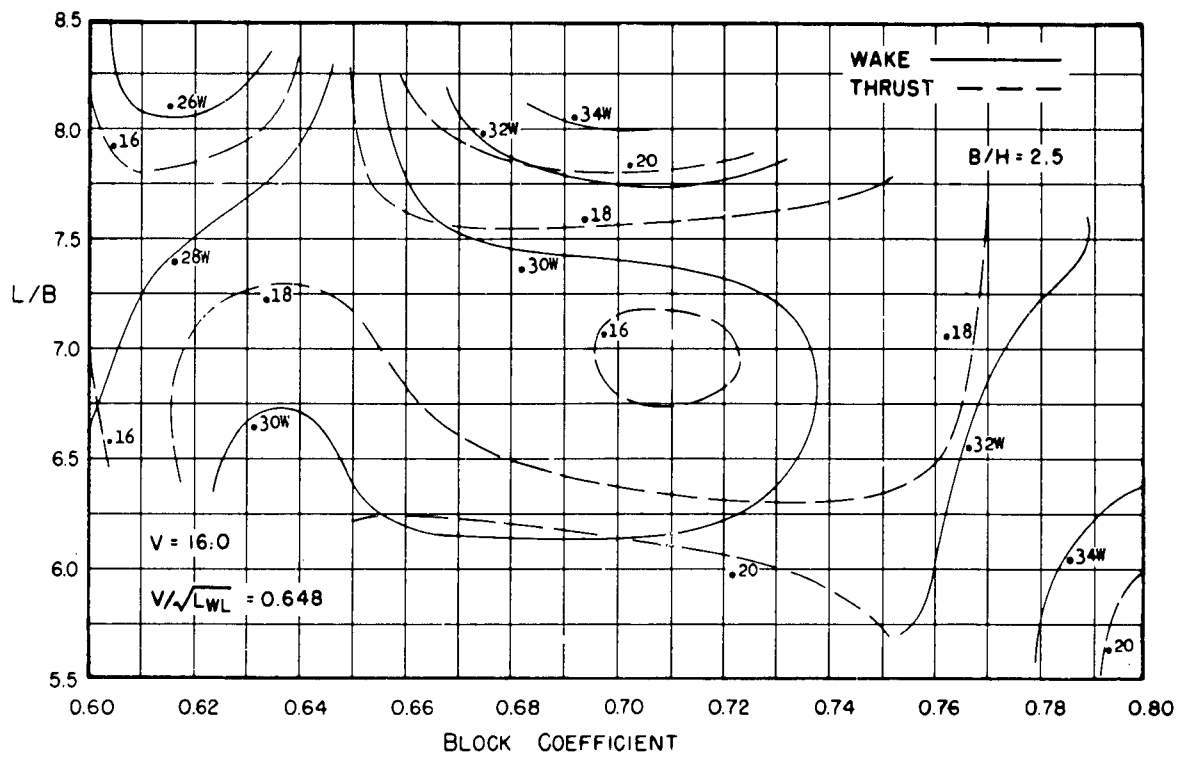


Figure B83

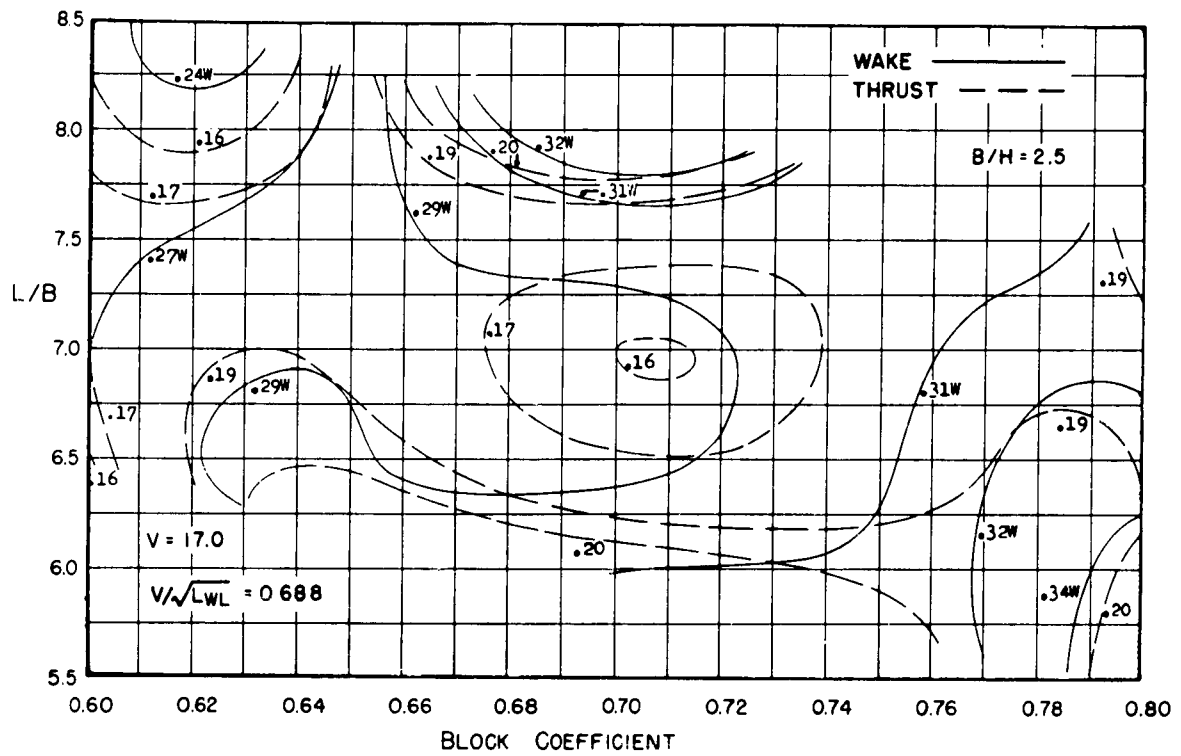


Figure B84

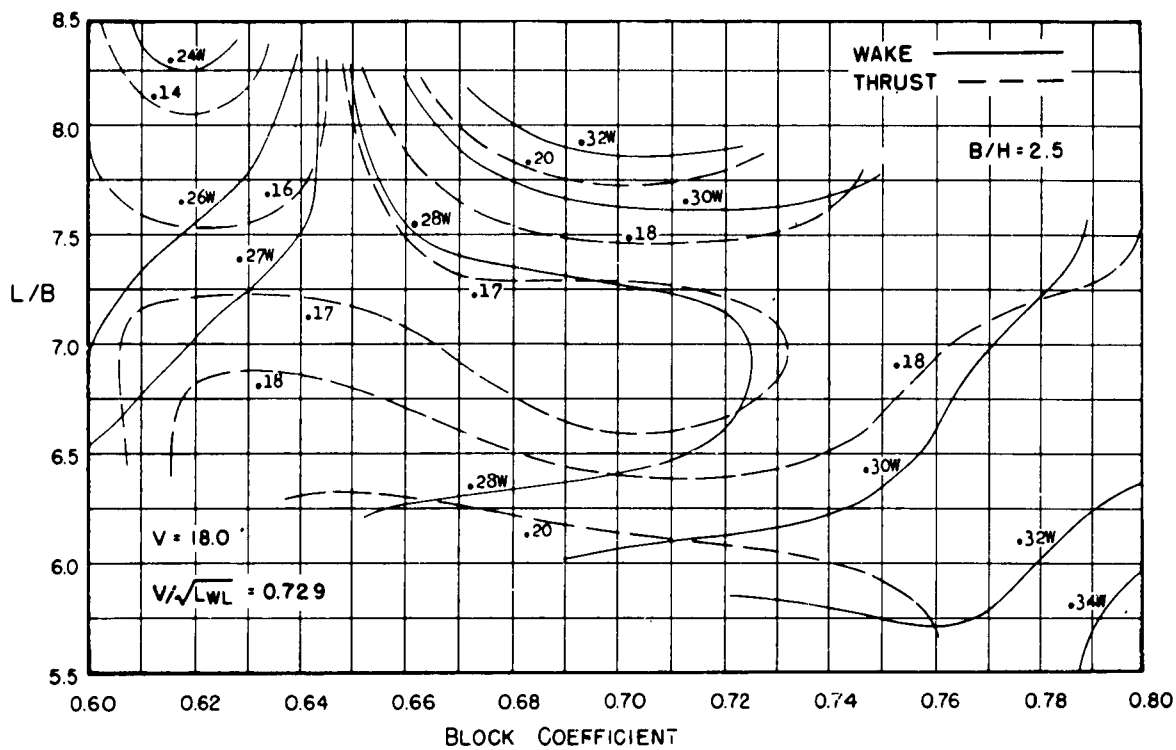


Figure B85

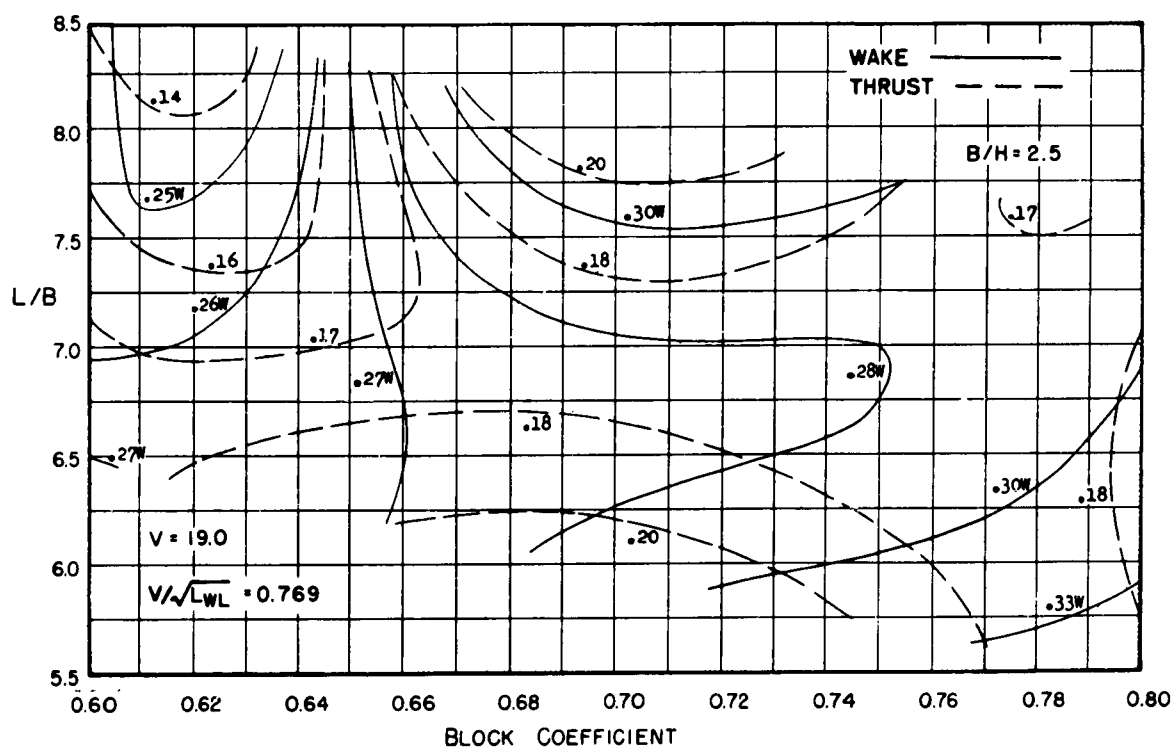


Figure B86

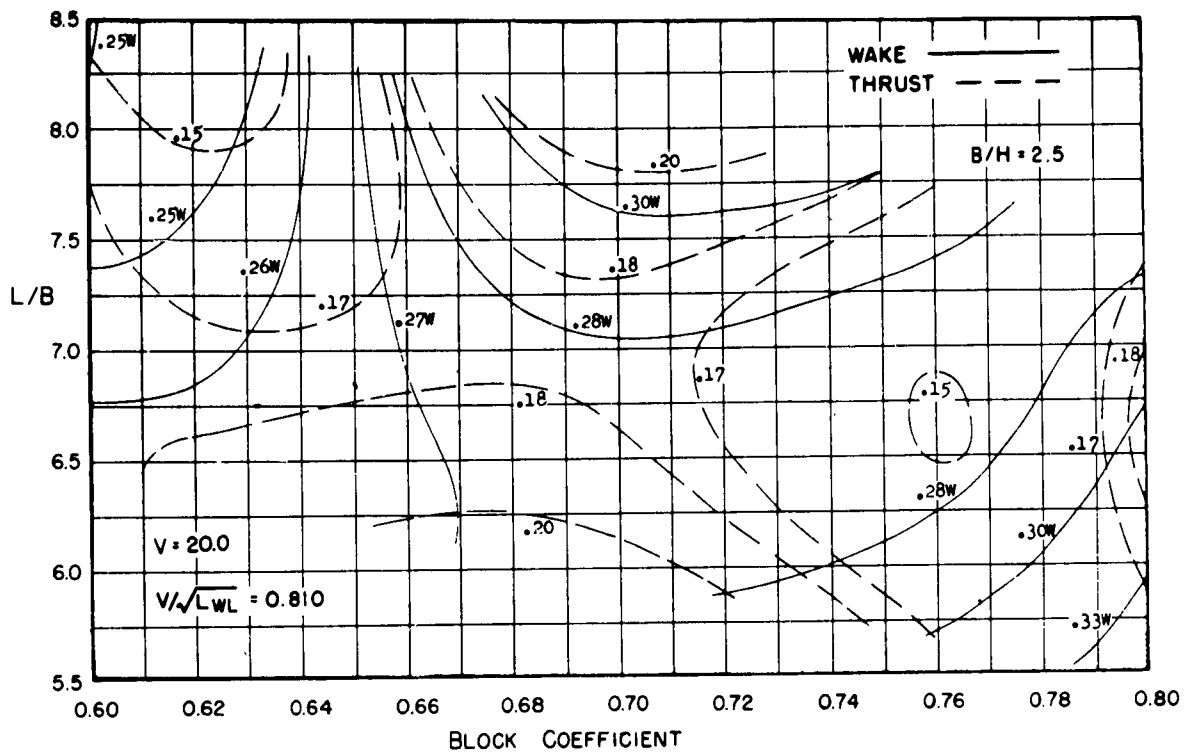


Figure B87

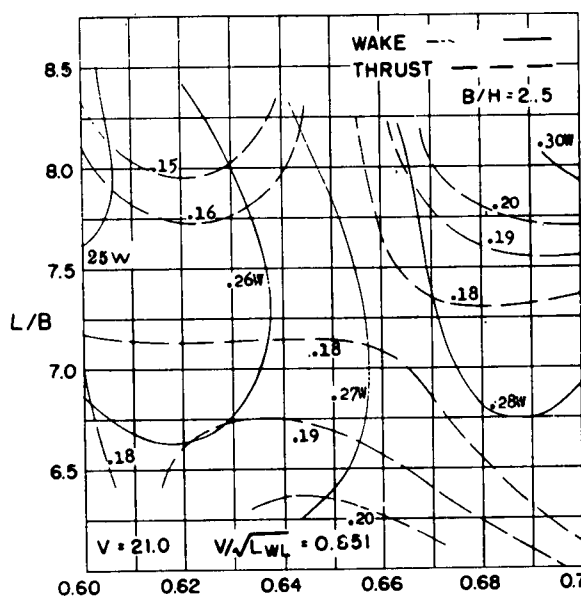


Figure B88

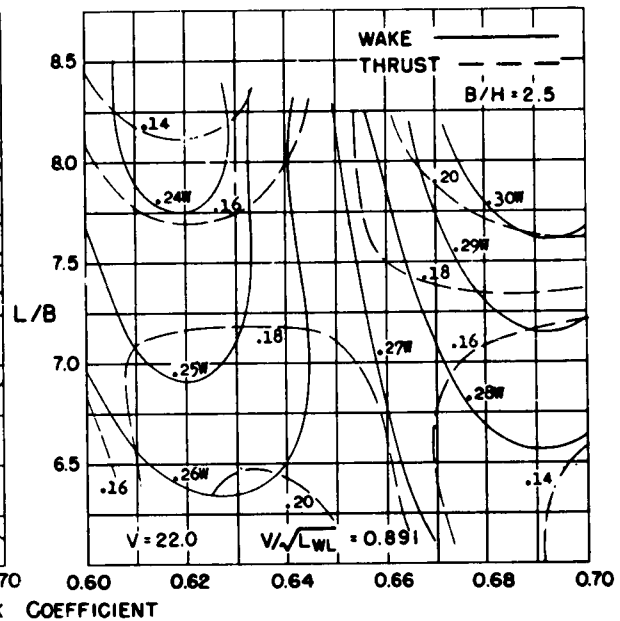


Figure B89

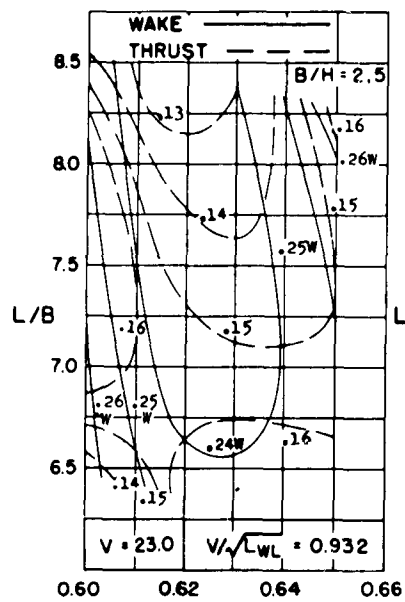


Figure B90

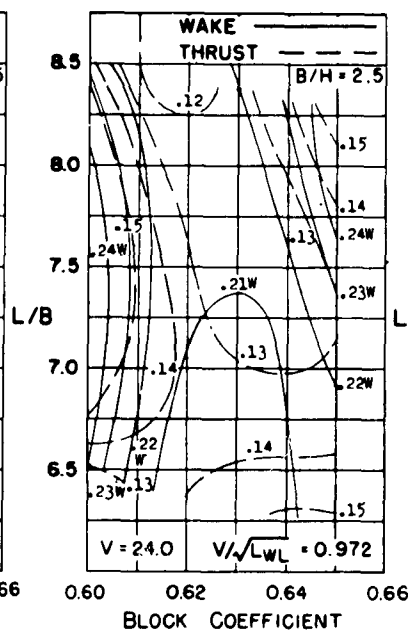


Figure B91

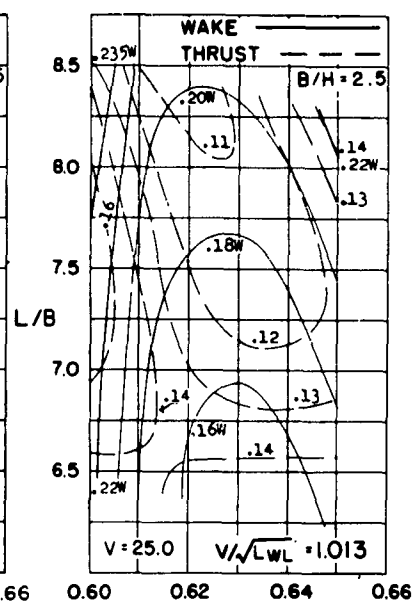


Figure B92

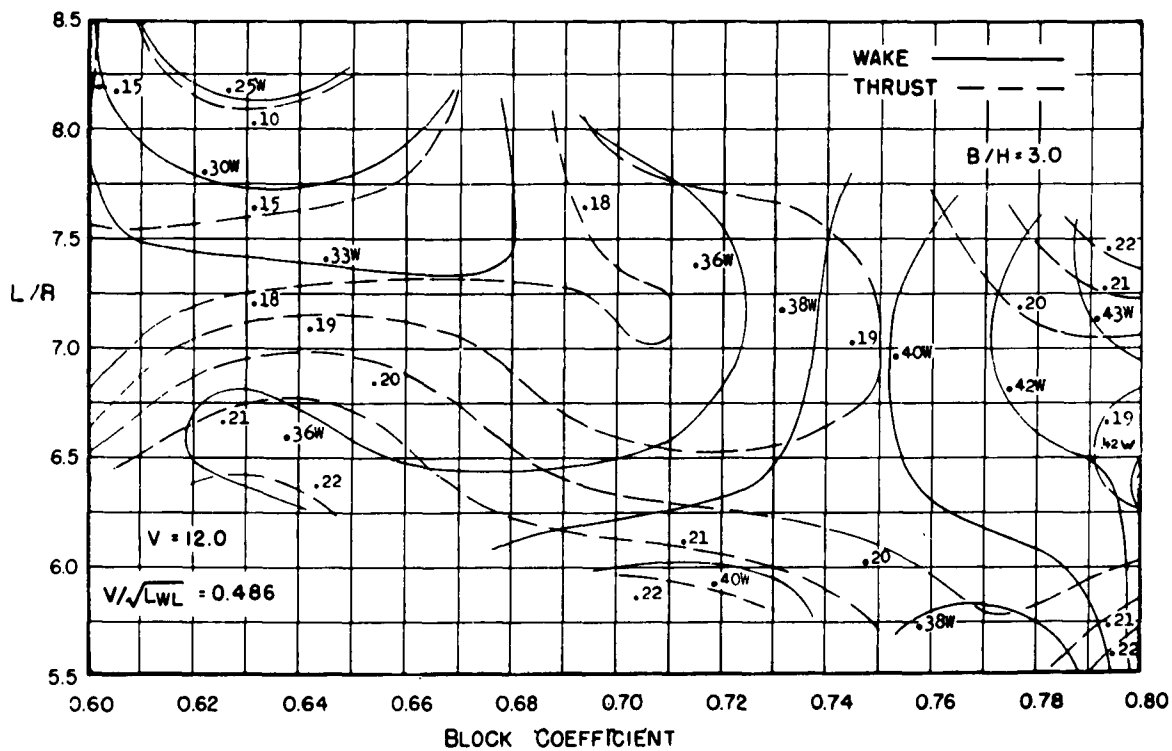
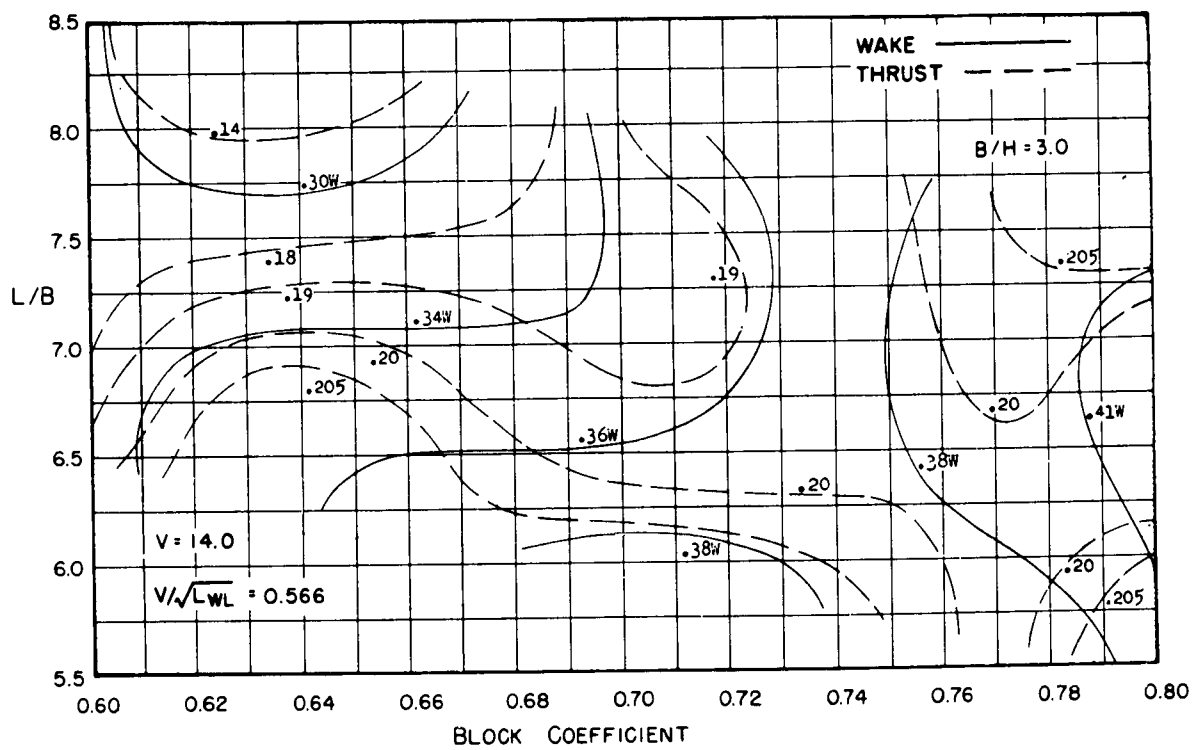
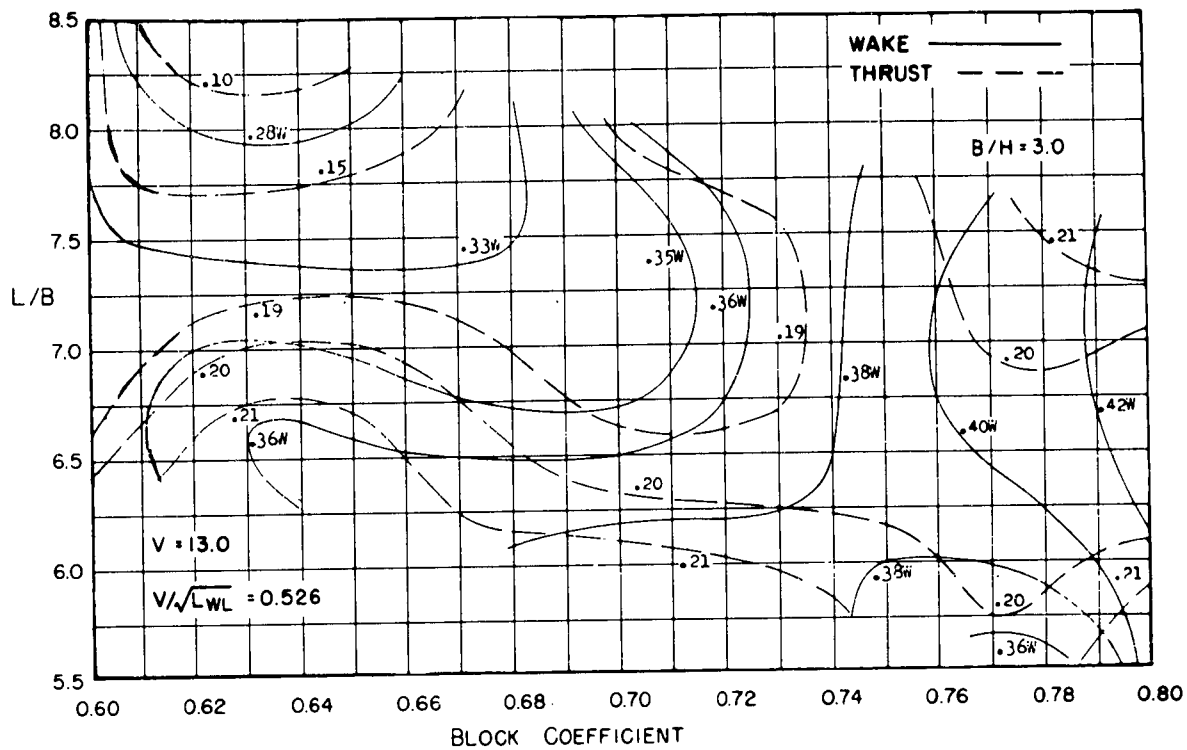


Figure B93



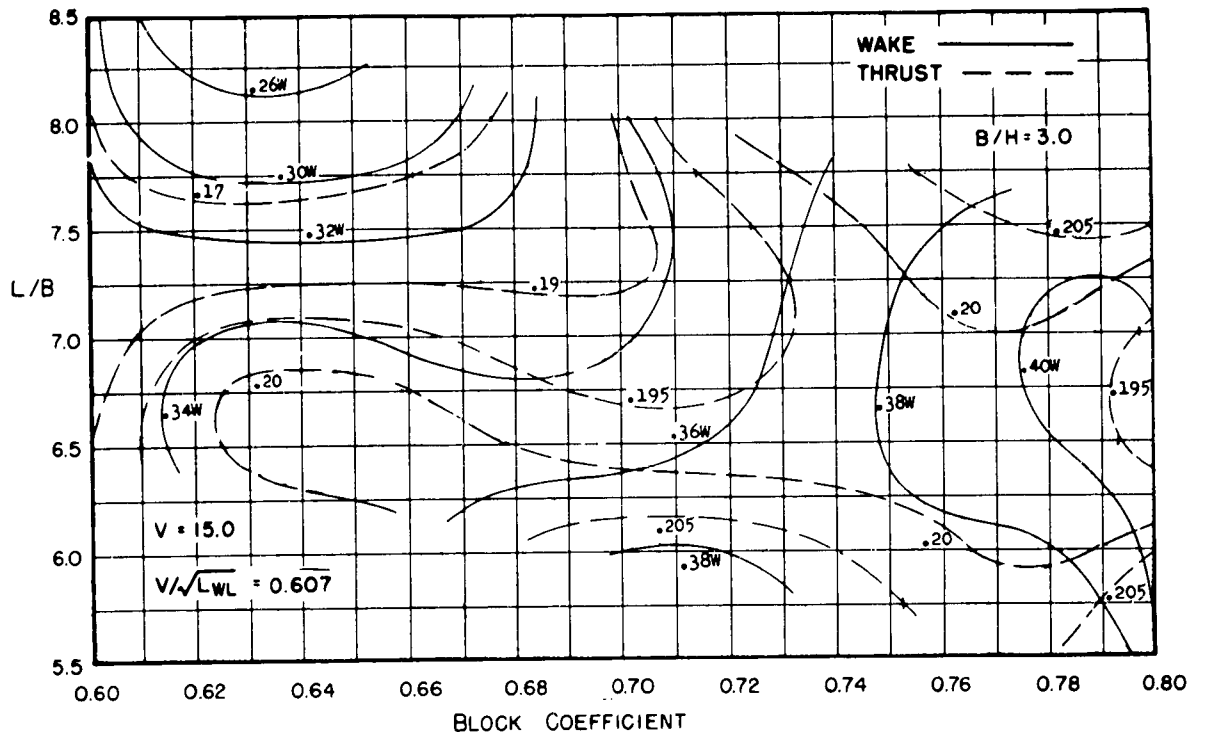


Figure B96

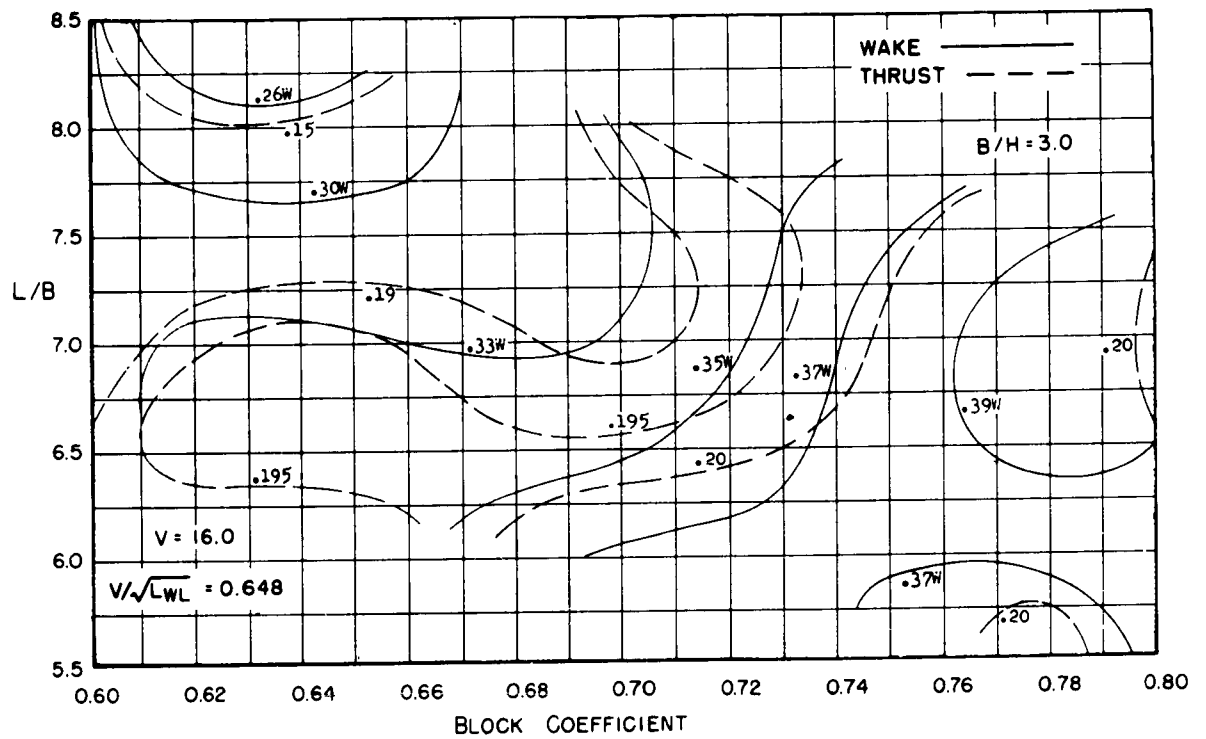


Figure B97

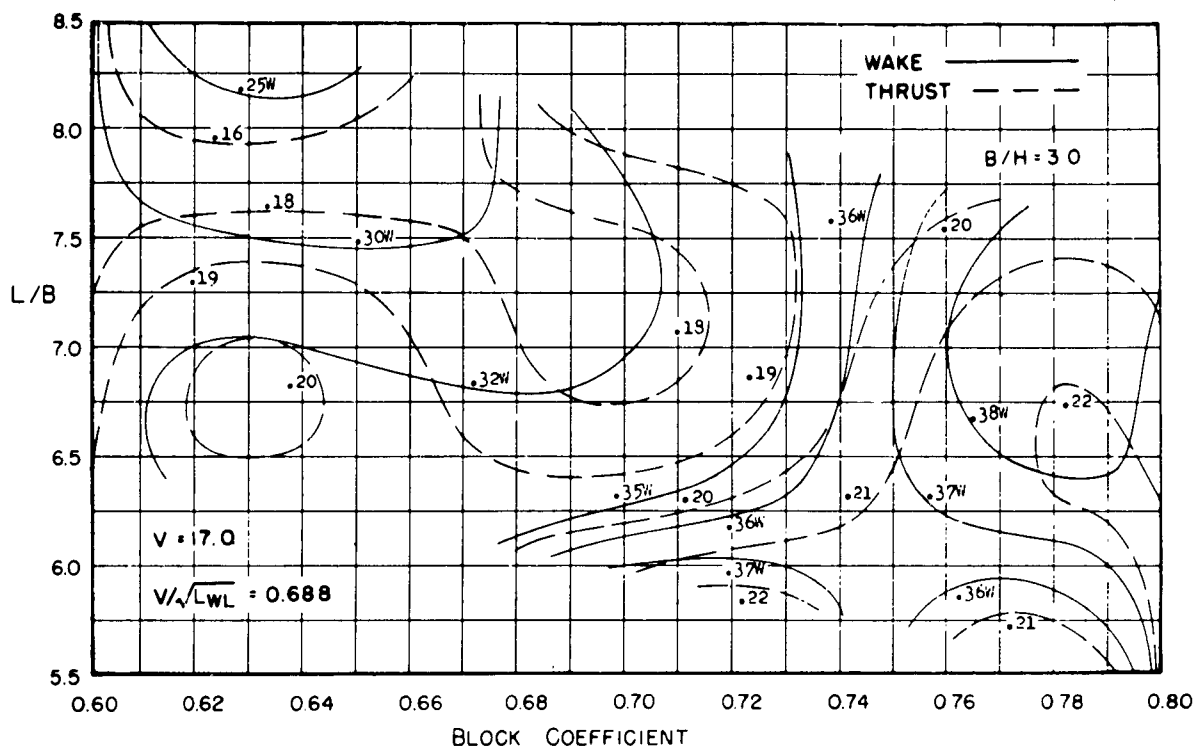


Figure B98

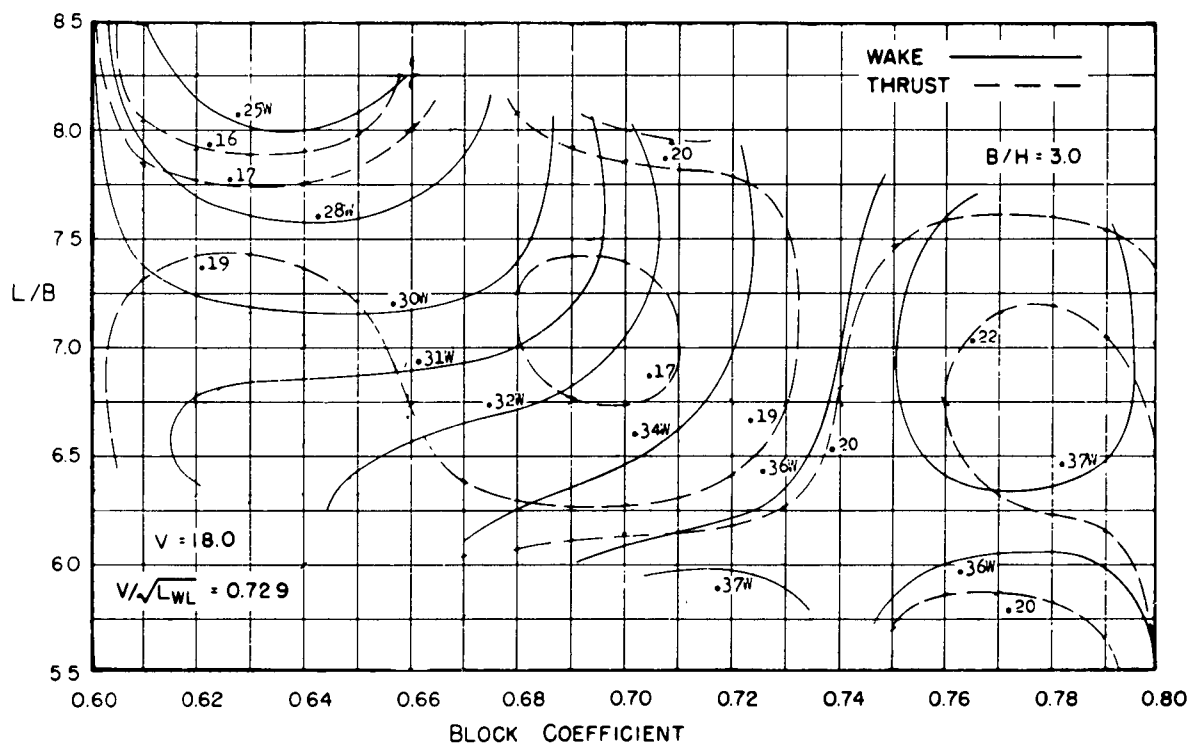


Figure B99

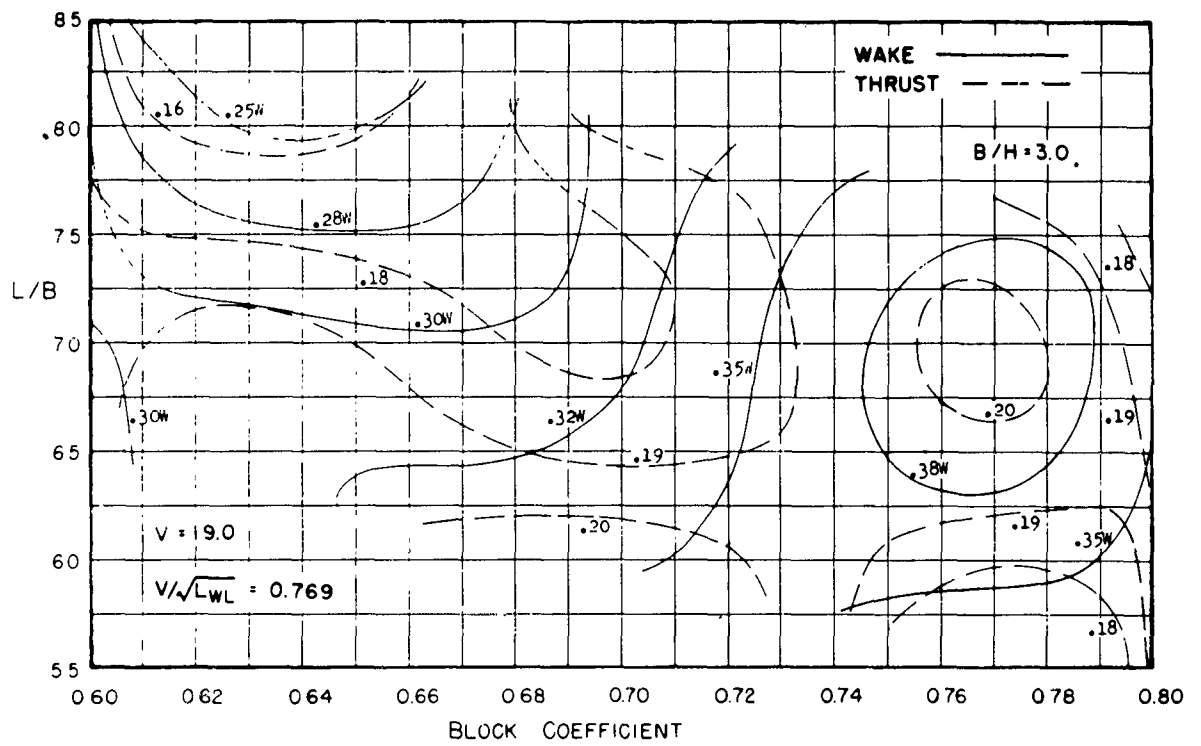


Figure B100

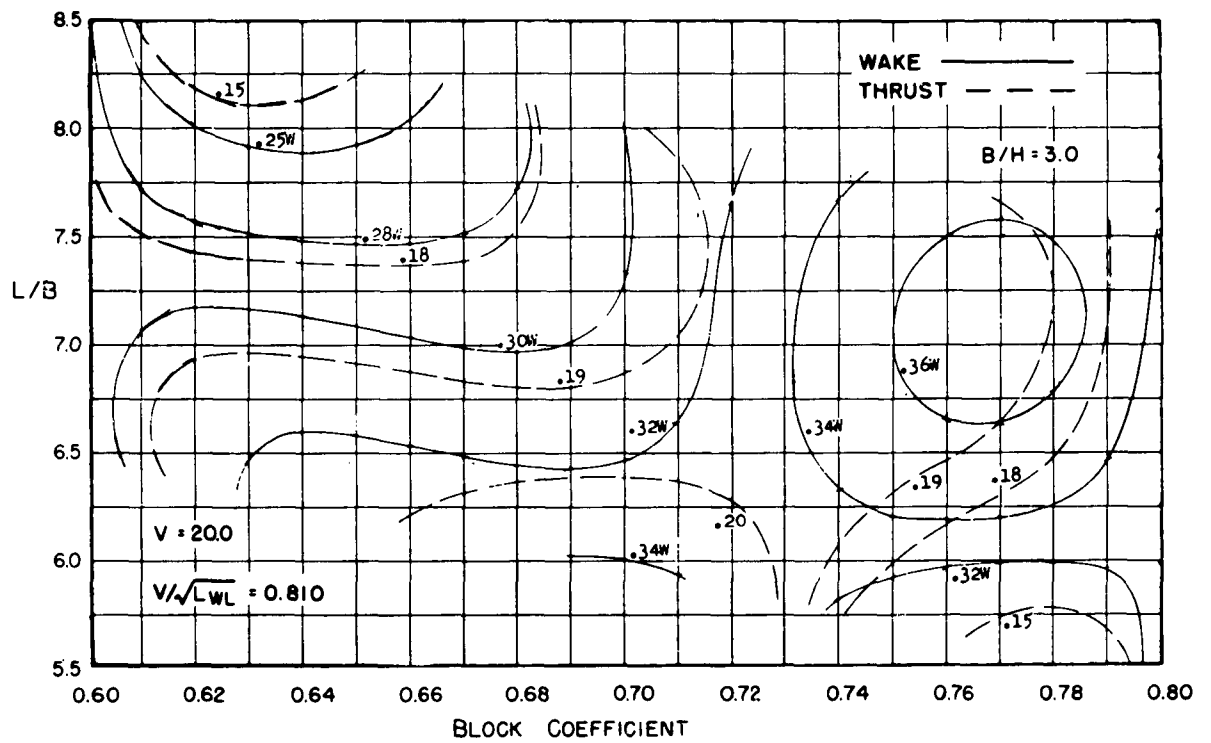


Figure B101

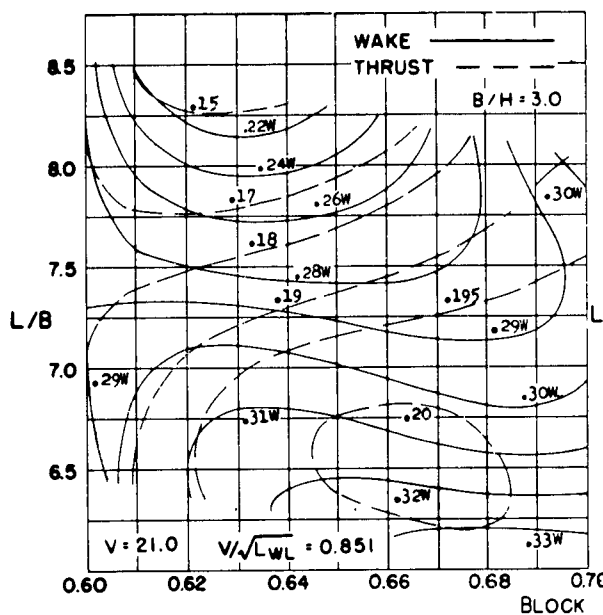


Figure B102

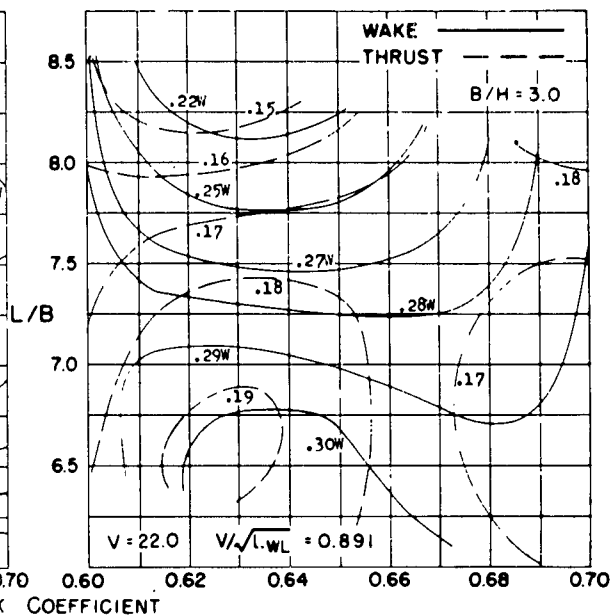


Figure B103

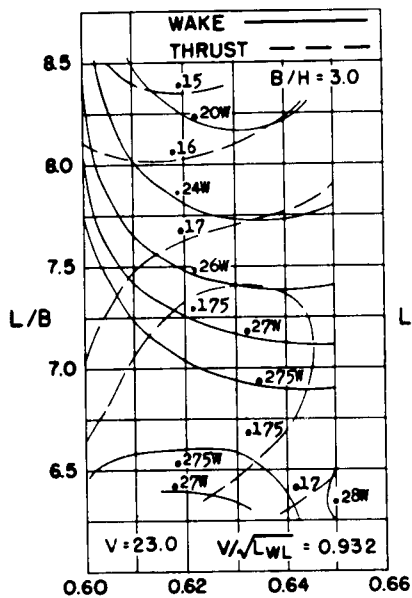


Figure B104

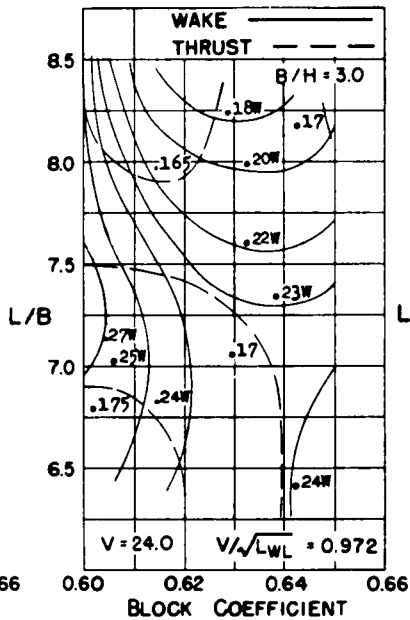


Figure B105

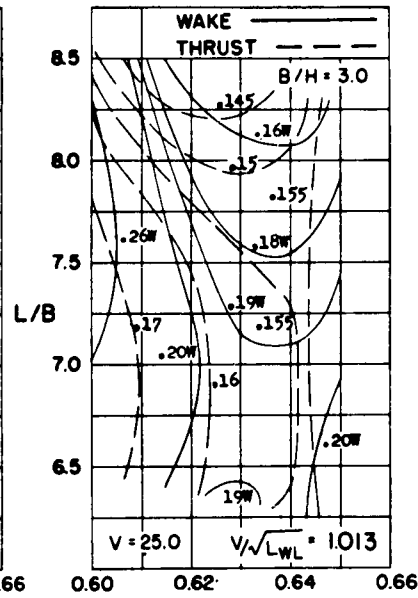


Figure B106

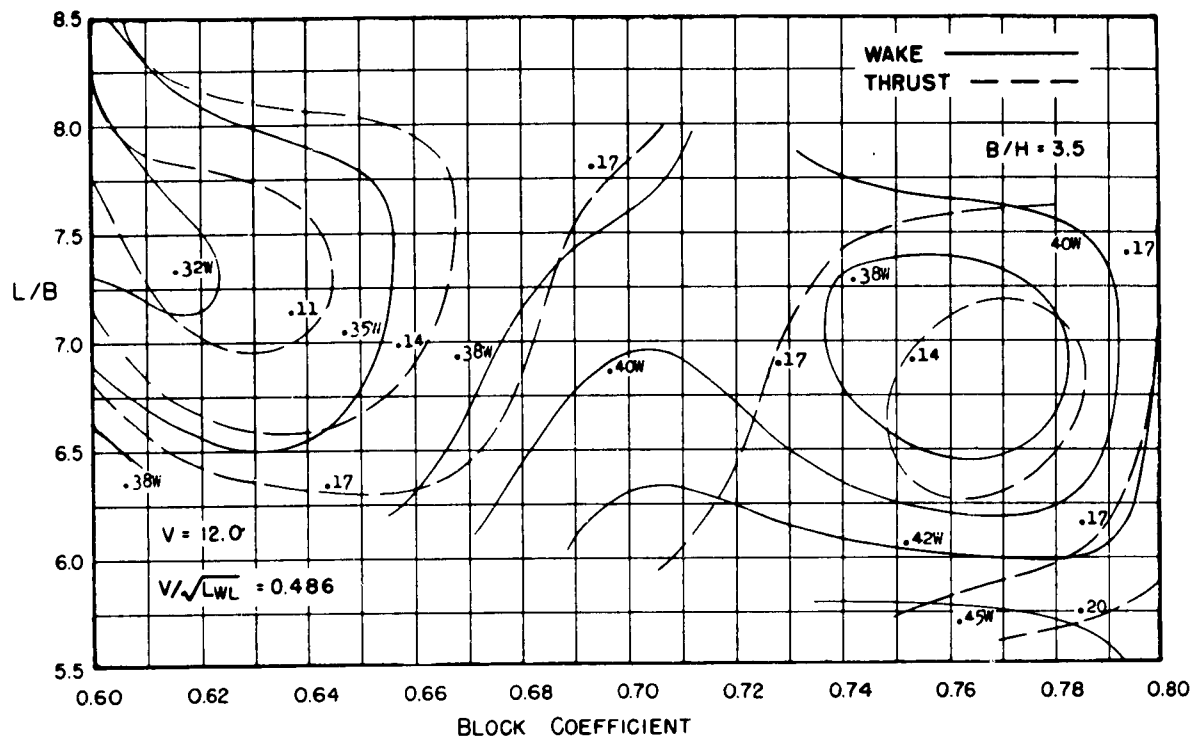


Figure B107

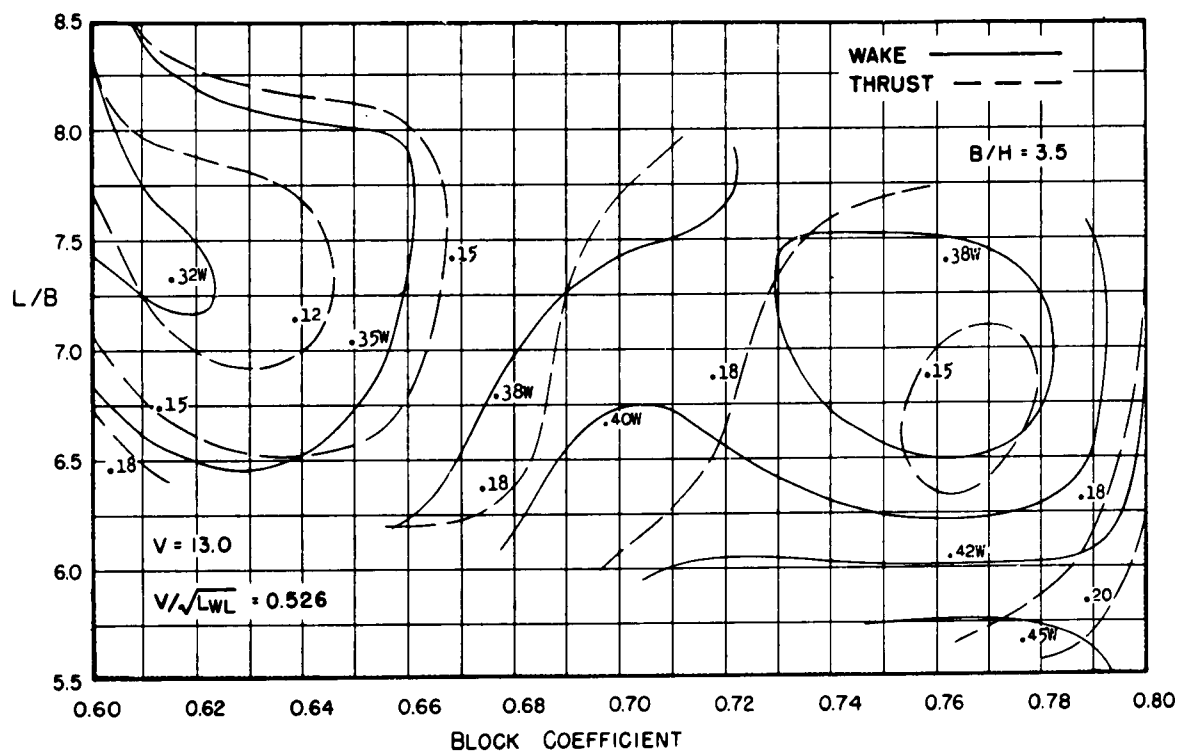


Figure B108

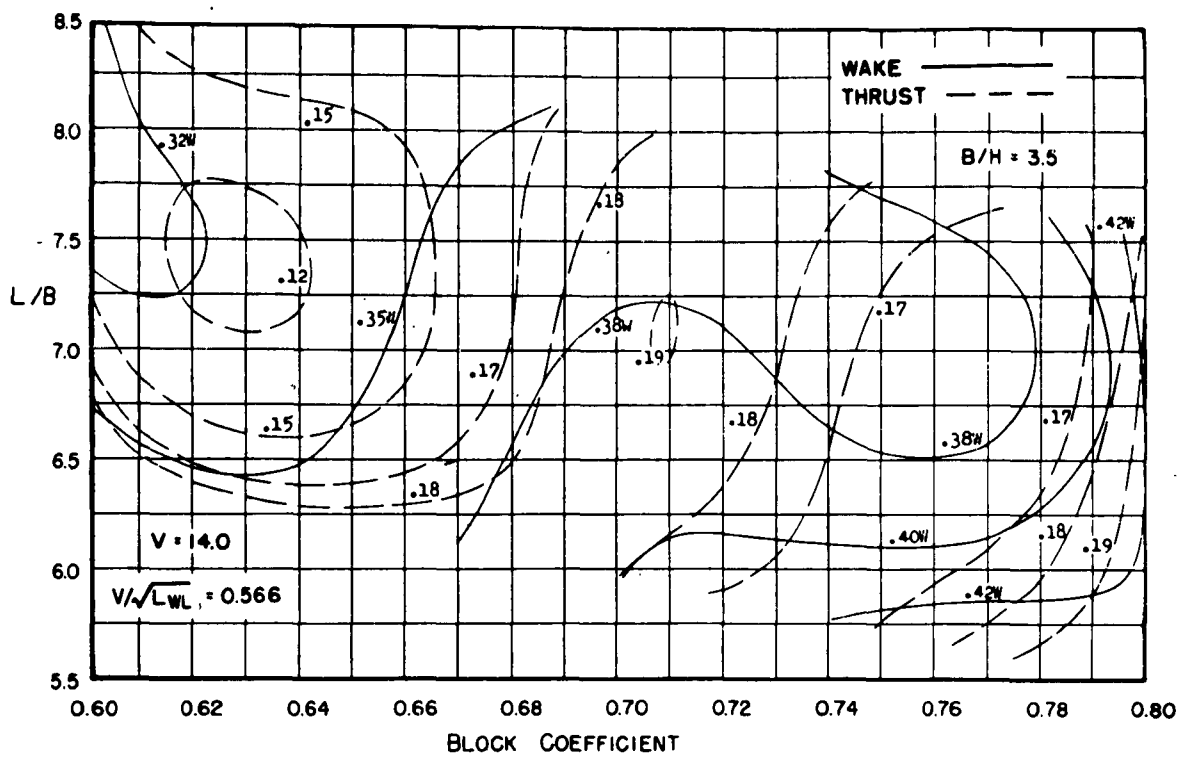


Figure B109

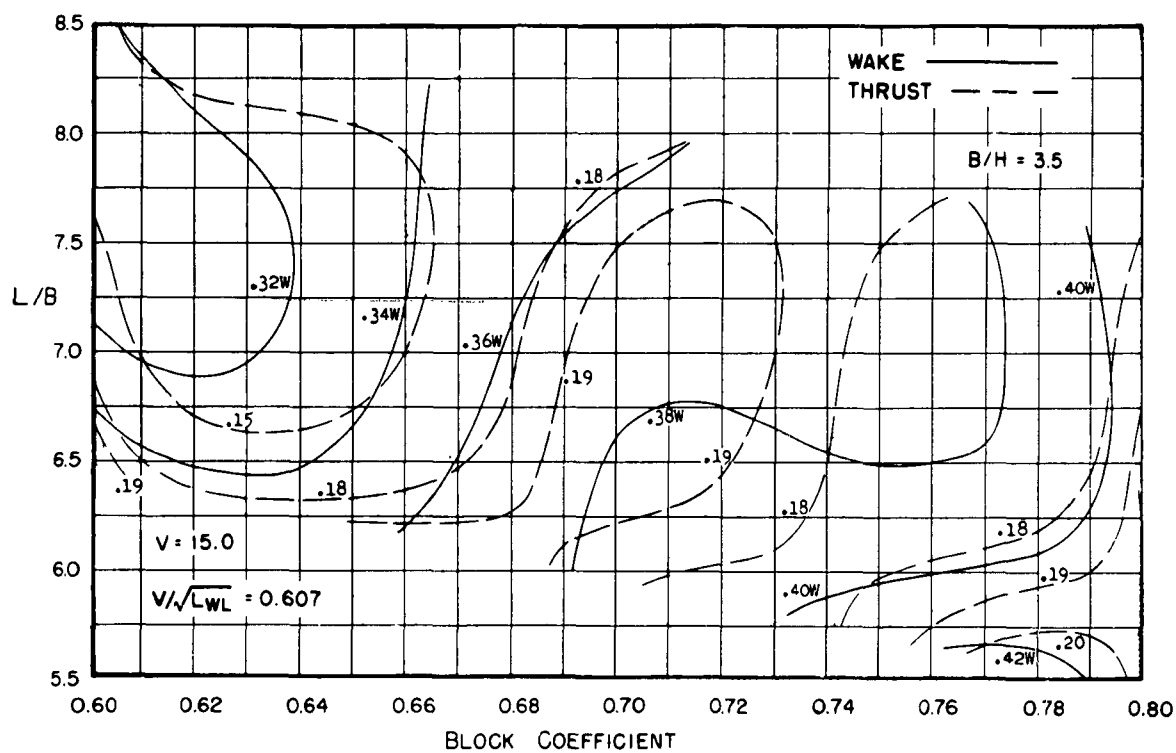


Figure B110

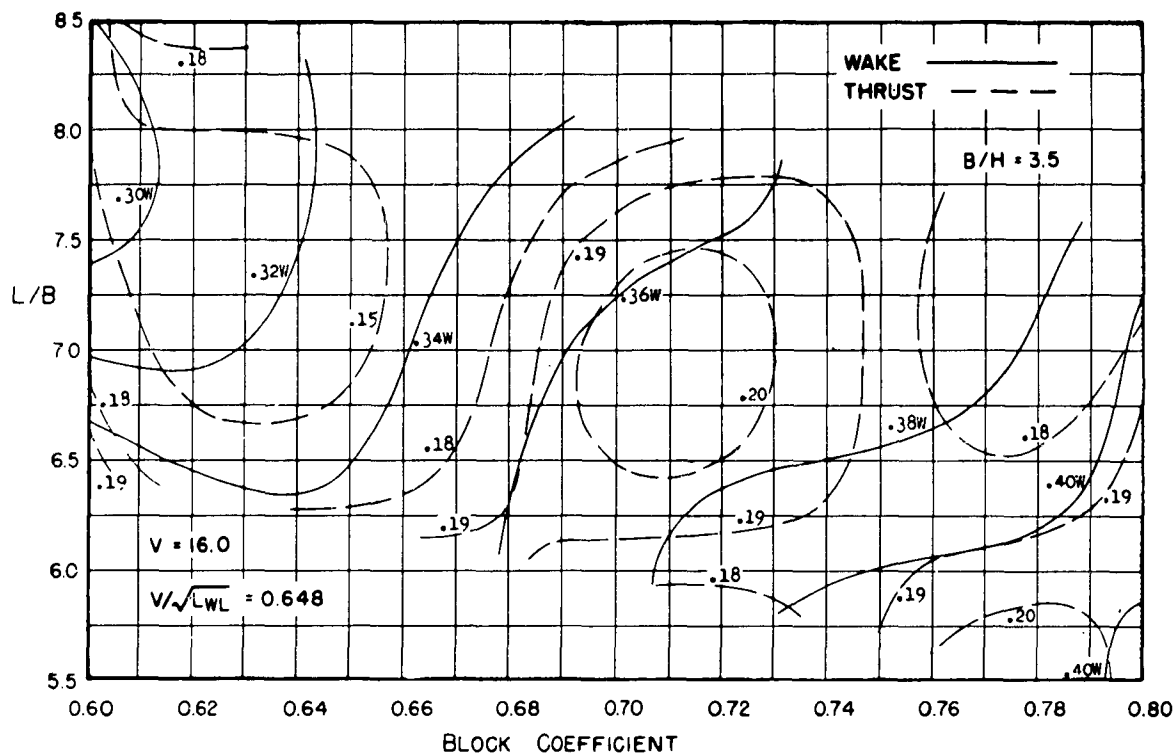


Figure B111

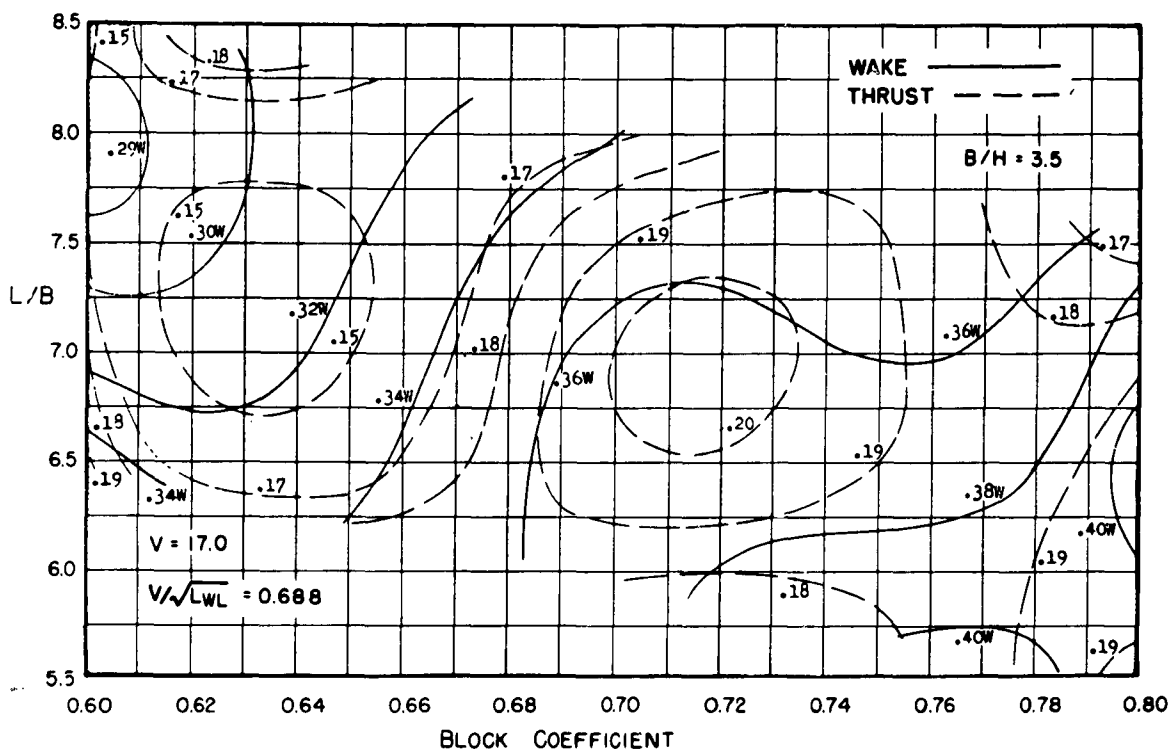


Figure B112

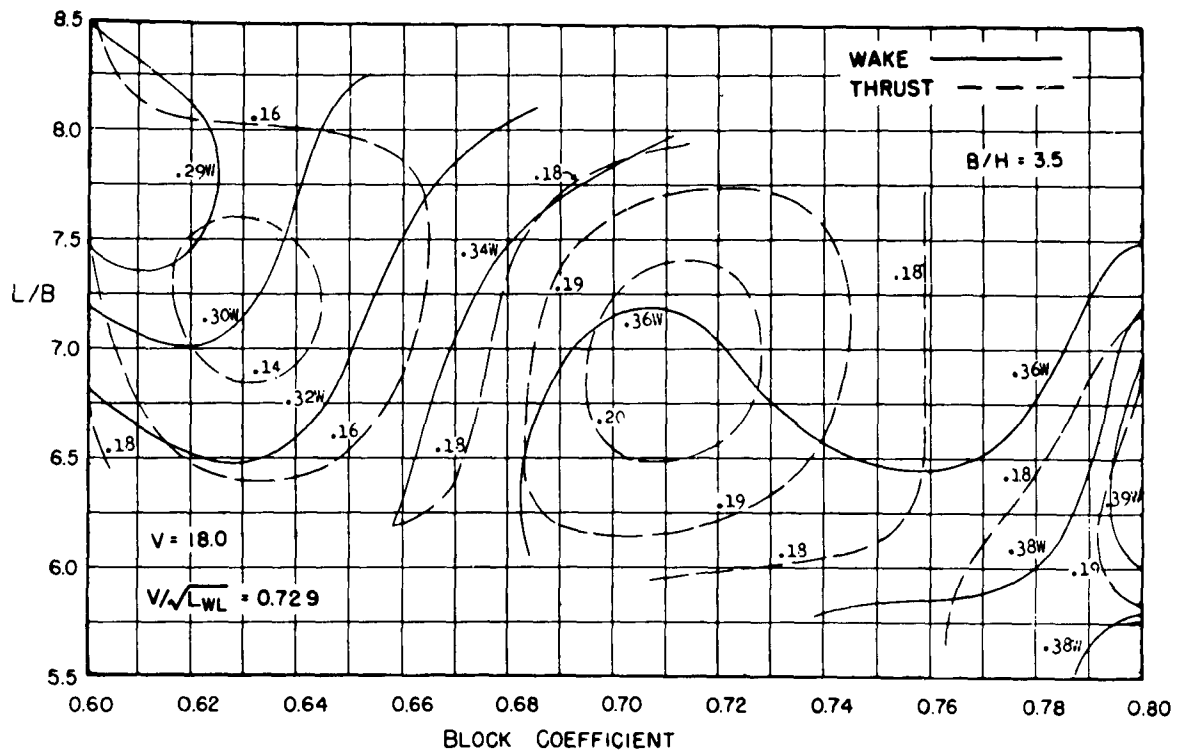


Figure B113

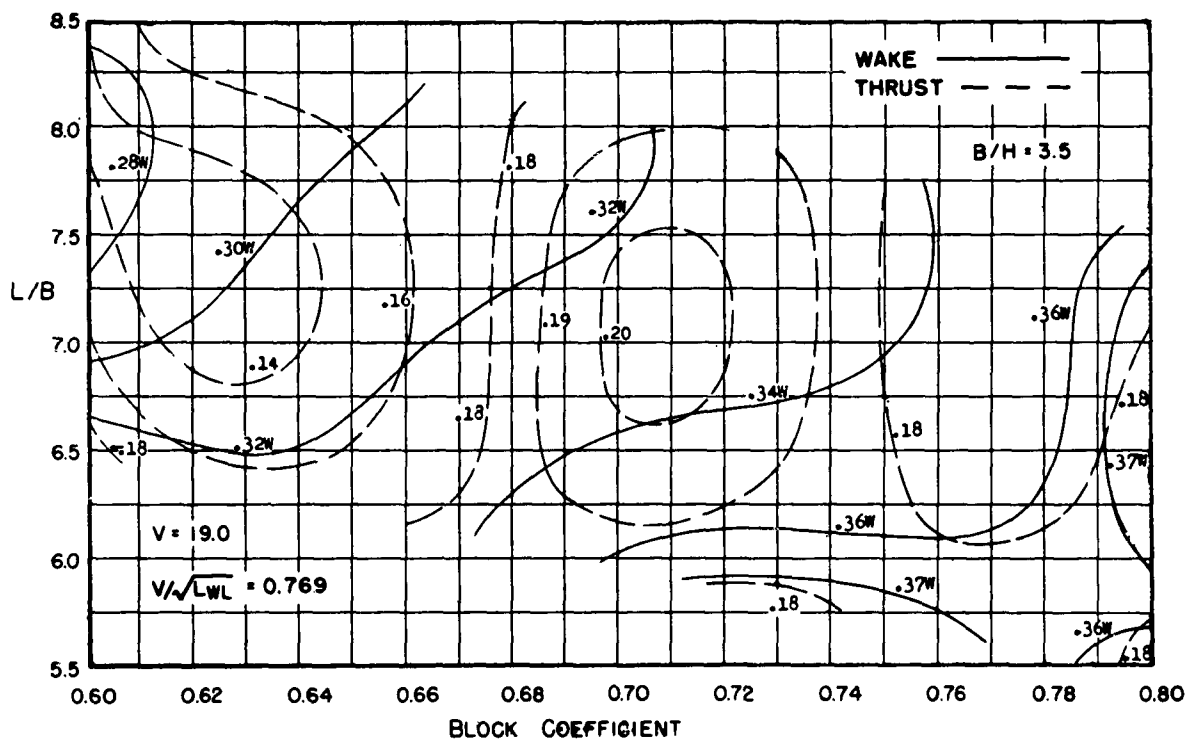


Figure B114

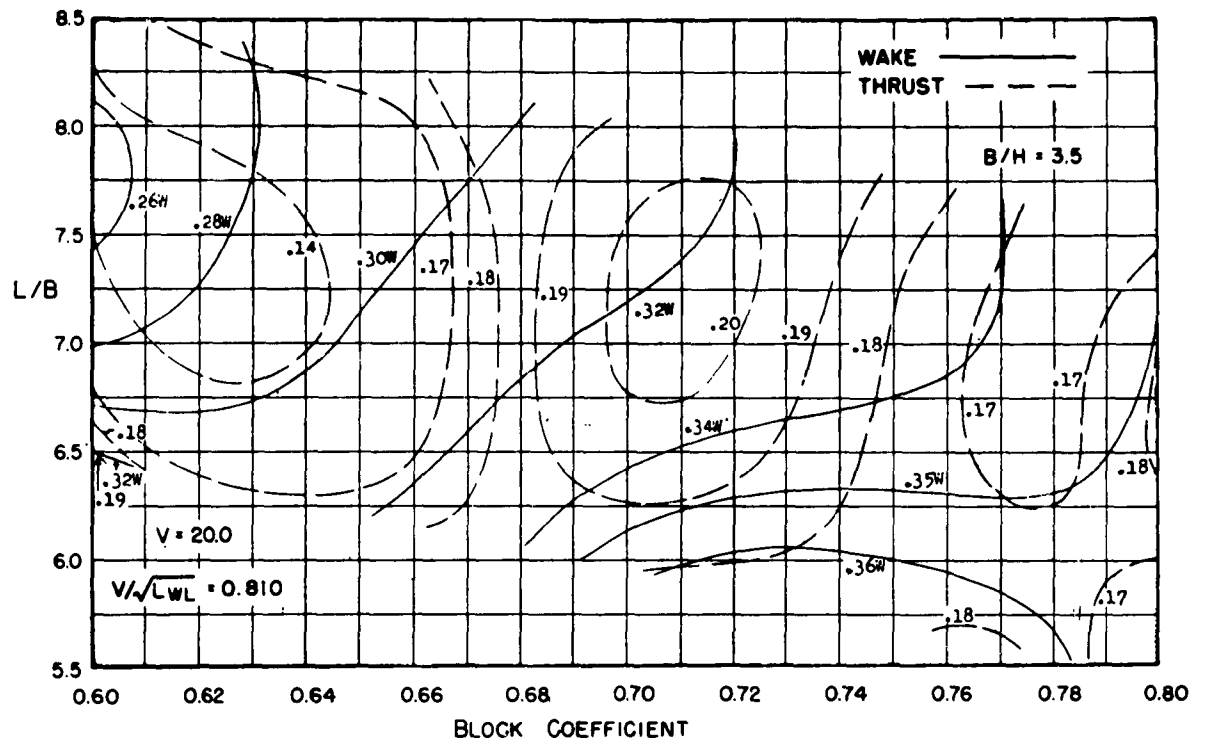


Figure B115

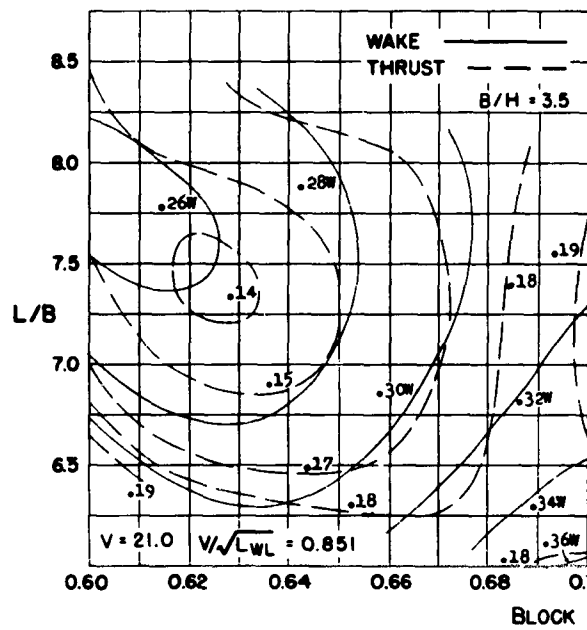


Figure B116

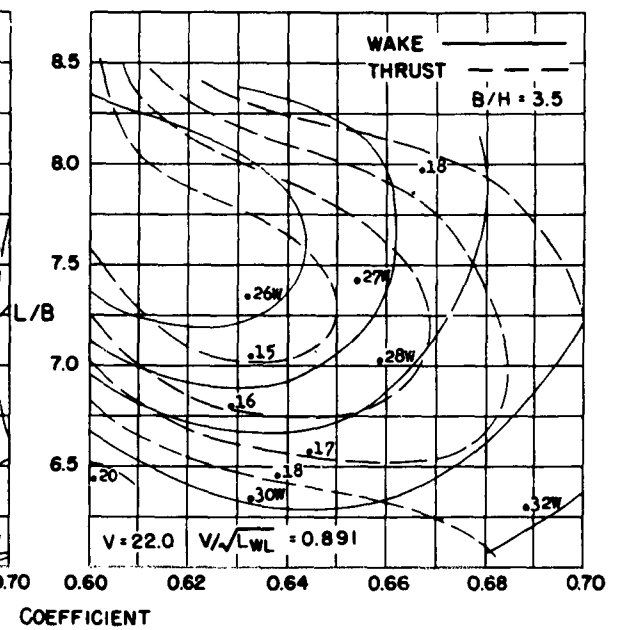


Figure B117

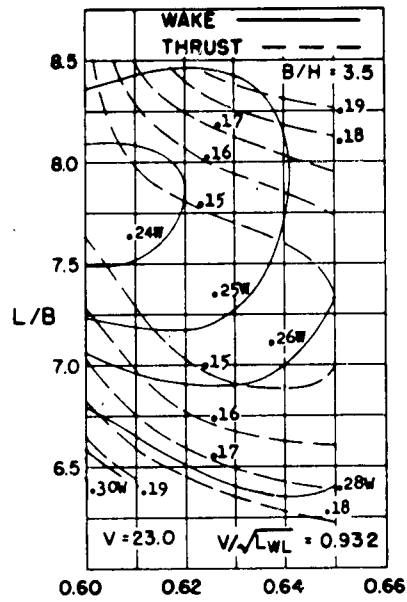


Figure B118

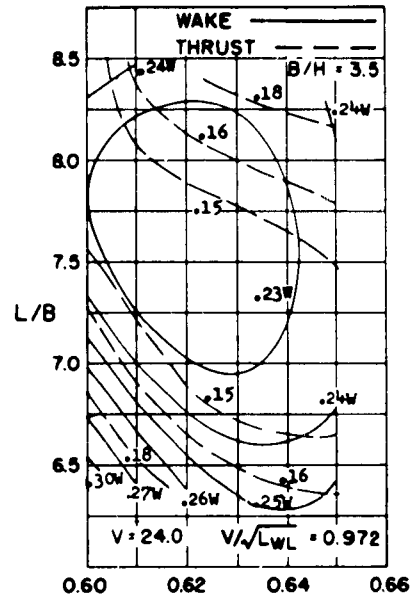


Figure B119

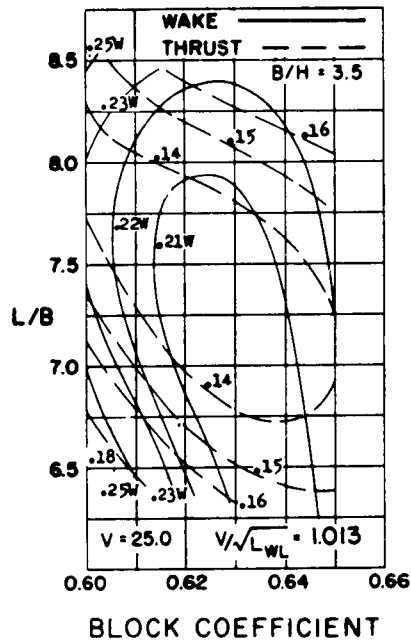


Figure B120

Figures B121 through B123

Contours of Relative Rotative Efficiency, e_{rr}

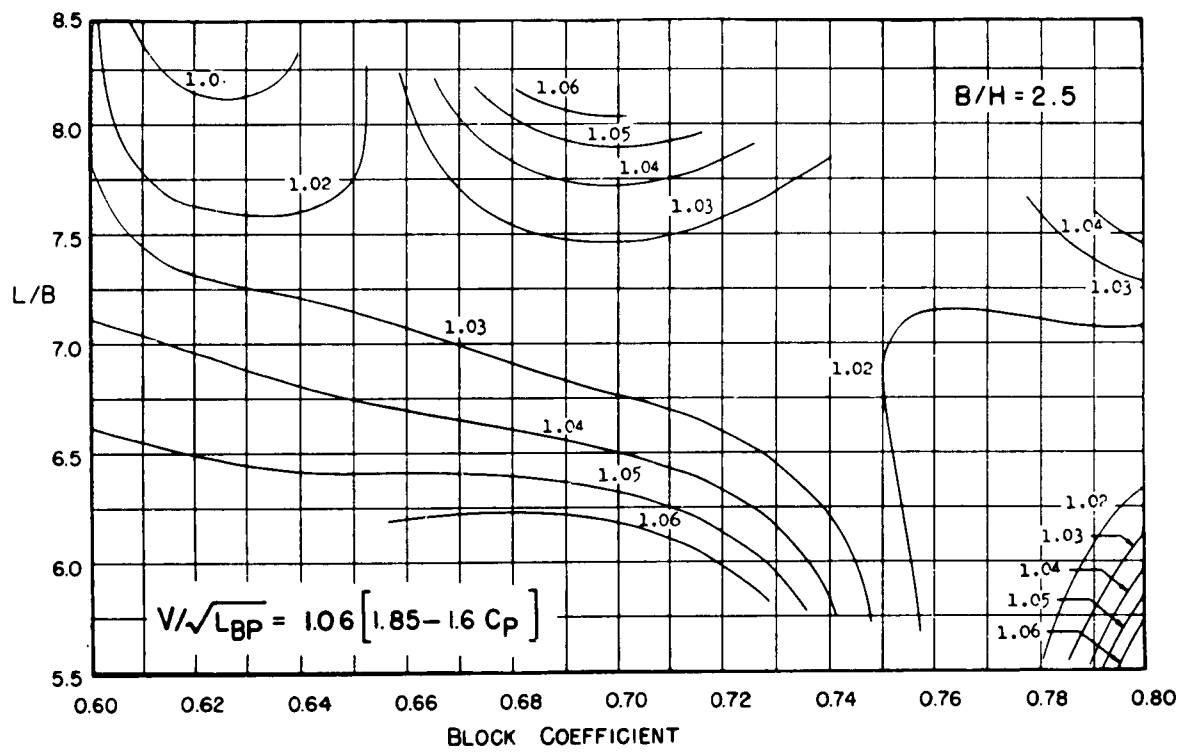


Figure B121

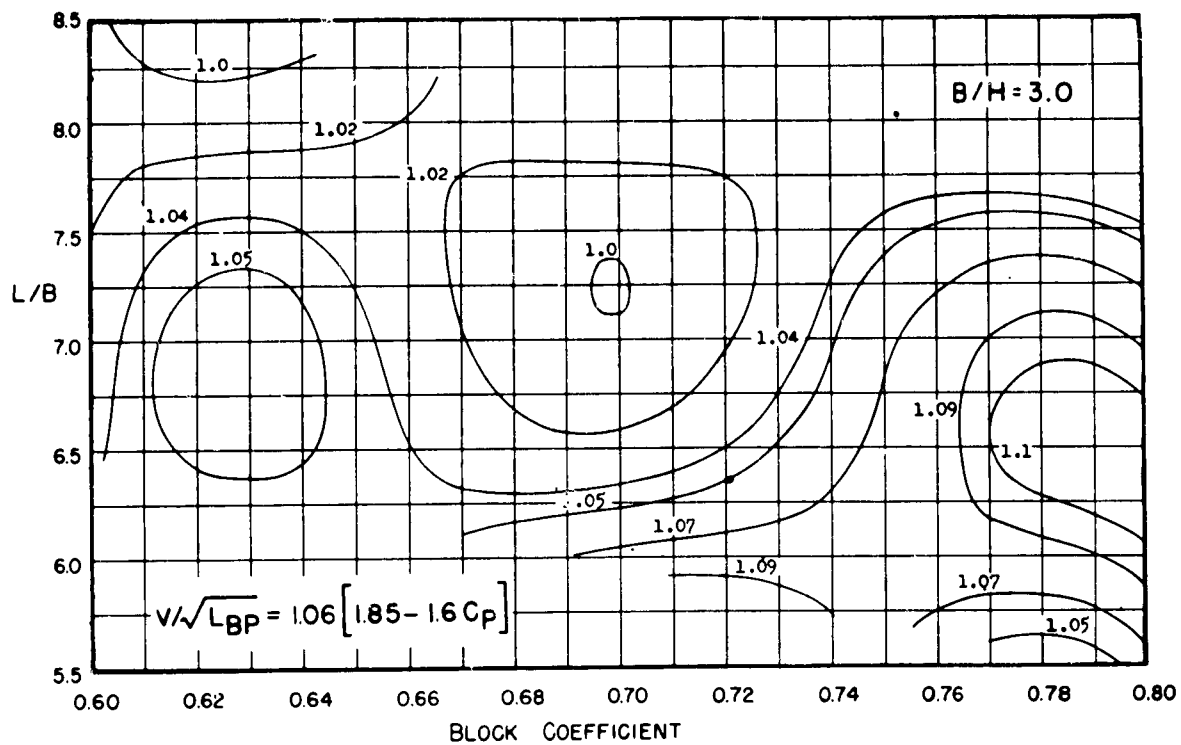


Figure B122

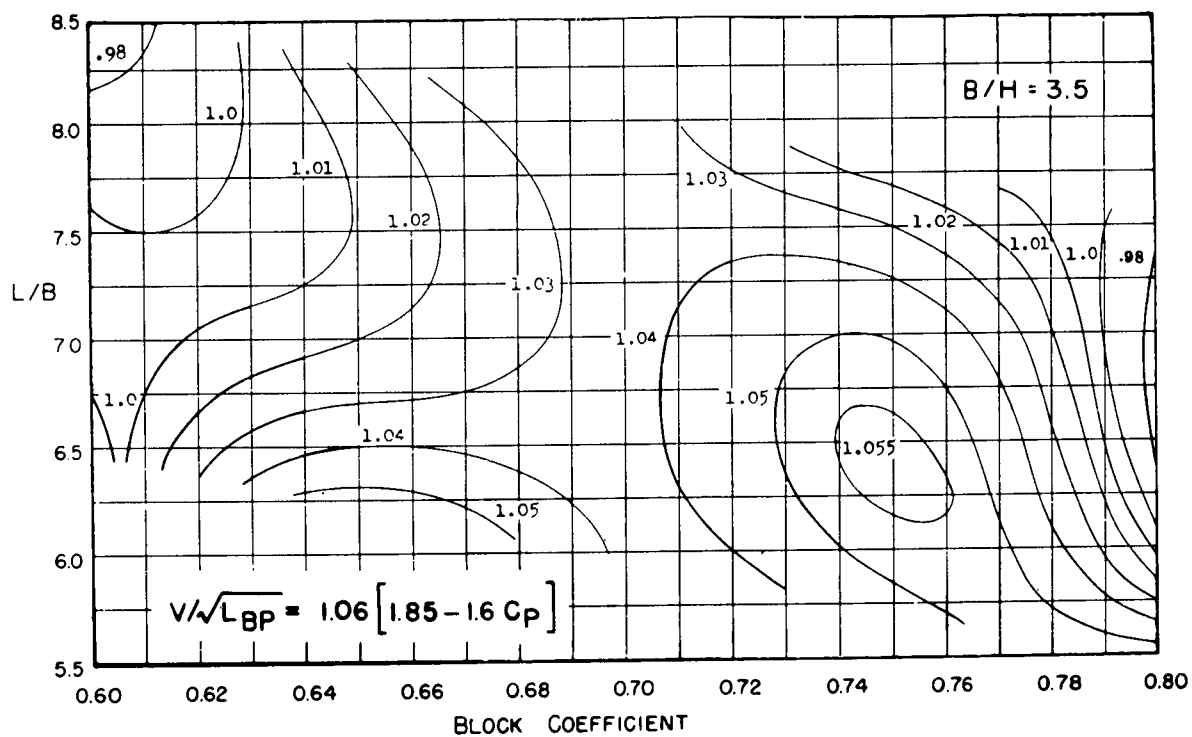


Figure 123

Figures B124 through B126
Contours of Wetted Surface Coefficient

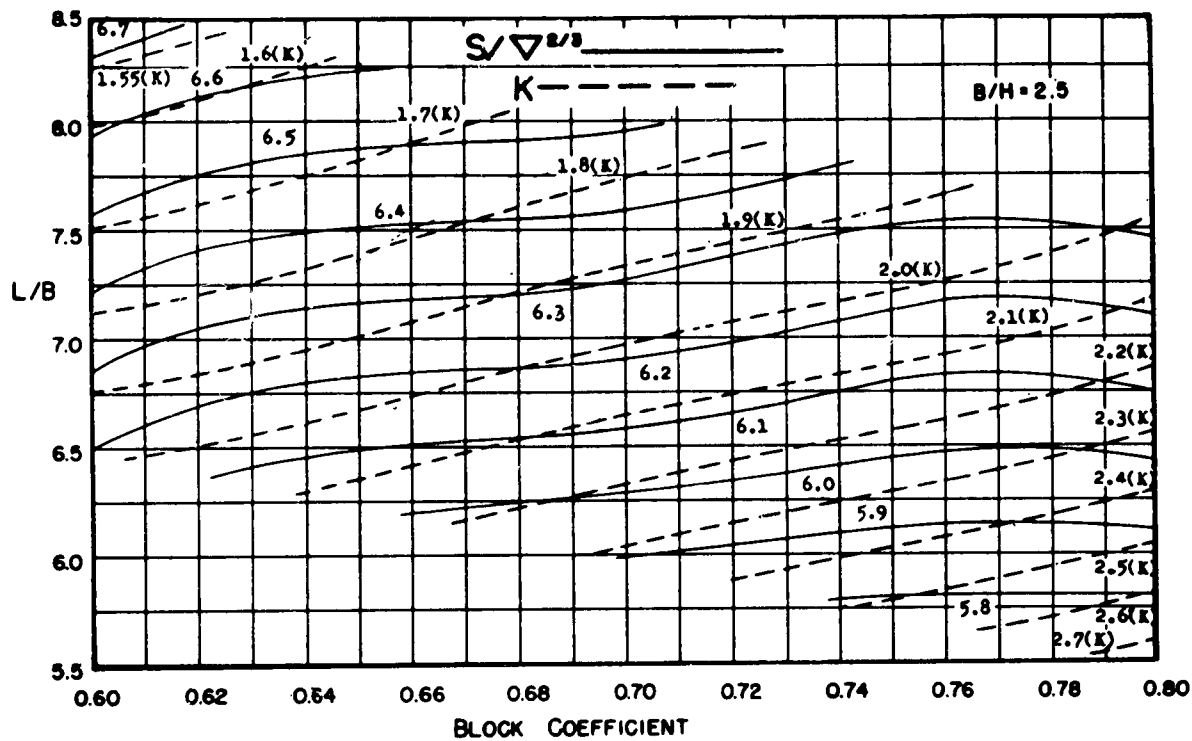


Figure B124

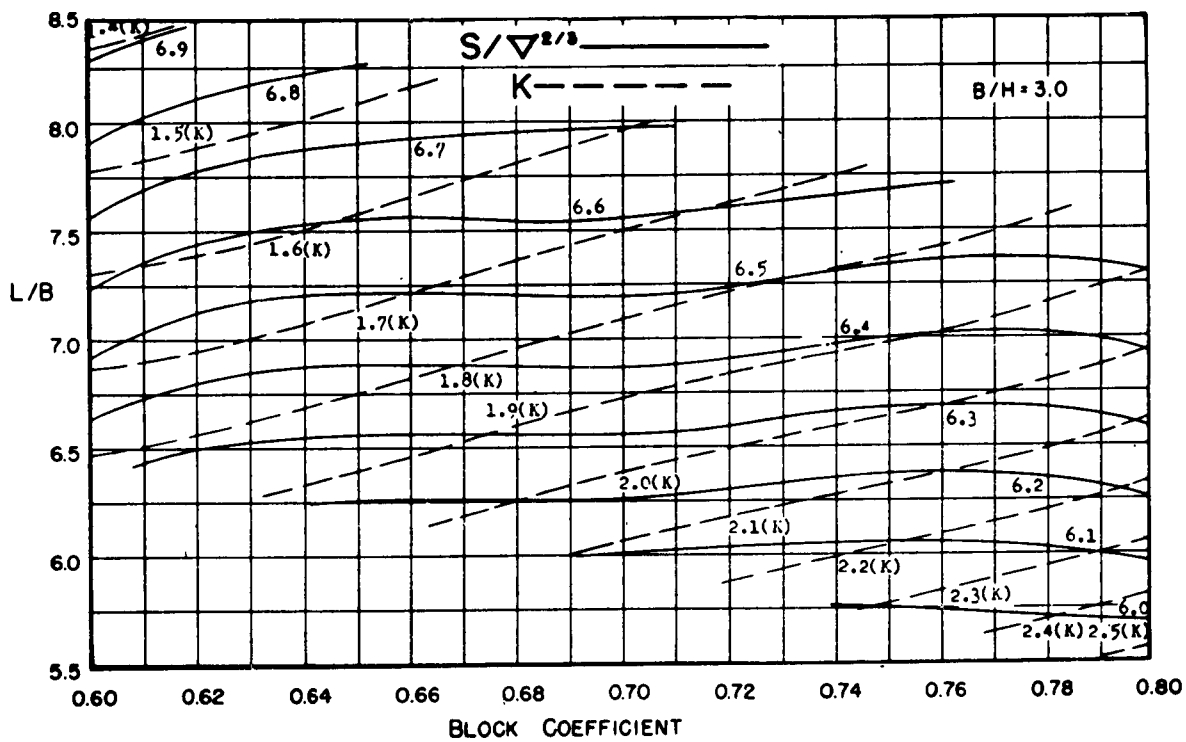


Figure B125

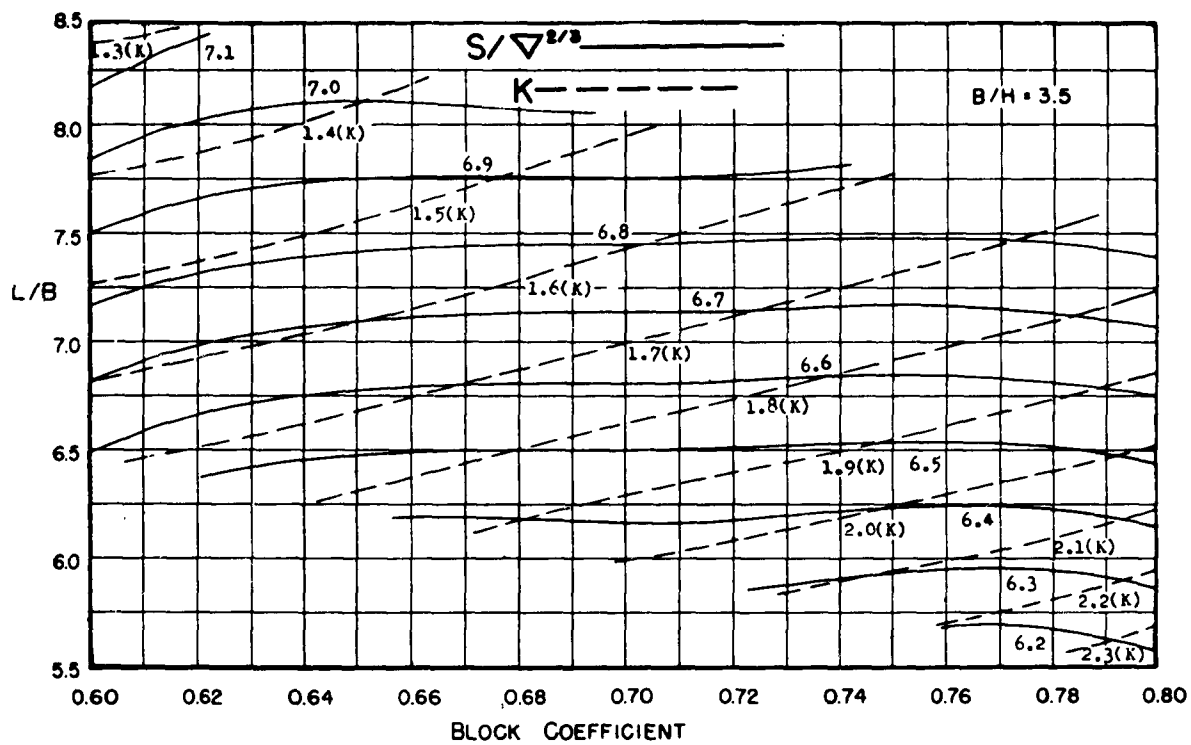


Figure B126

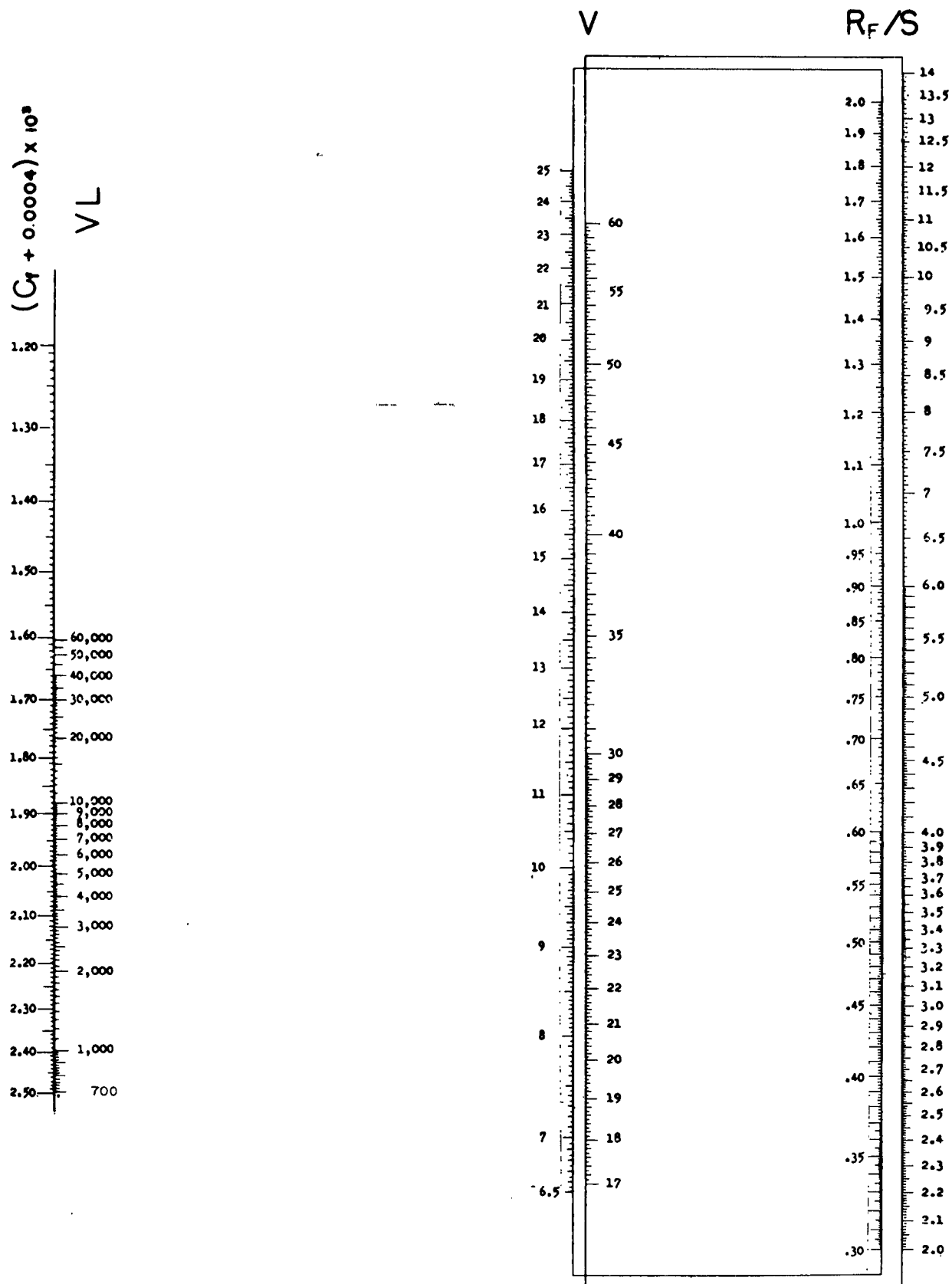


Figure B127 - Nomograph for Calculating Frictional Component of Resistance R_F on Basis of ATTC Line

TABLES B-1 through B-45

**Results of Resistance and Self-Propulsion Experiment for
45 Models of Series 60**

TABLE B-1

Results of Resistance and Self-Propulsion Experiments

Model Number 4240, $C_B = 0.60$, $L/B = 6.5$, $B/H = 2.5$, Propeller Number 3471

All Figures are for Ship of 400 Ft Length BP				All Figures are for Ship of 600 Ft Length BP									
V/\sqrt{gL}	$C_t \times 10^3$	\textcircled{R}	\textcircled{C}	V	N	SHP	W_T	t	e_h	e_p	e_{rr}	EHP/SHP	
0.45	2.685	1.134	0.662	0.445	11.0	36.7	2632	0.304	0.140	1.236	0.642	1.065	0.845
0.50	2.688	1.260	0.662	0.486	12.0	40.1	3371	0.294	0.146	1.210	0.647	1.069	0.837
0.55	2.685	1.386	0.662	0.526	13.0	43.7	4322	0.285	0.152	1.186	0.650	1.069	0.824
0.60	2.689	1.512	0.663	0.566	14.0	47.3	4503	0.280	0.152	1.178	0.650	1.065	0.815
0.65	2.723	1.638	0.671	0.607	15.0	51.0	6893	0.280	0.154	1.174	0.650	1.065	0.810
0.70	2.810	1.764	0.692	0.628	15.5	52.7	7682	0.281	0.154	1.174	0.648	1.062	0.808
0.75	2.825	1.890	0.696	0.648	16.0	54.5	8565	0.283	0.155	1.178	0.646	1.060	0.806
0.80	2.825	2.016	0.696	0.668	16.5	56.4	9496	0.280	0.157	1.171	0.646	1.059	0.801
0.825	2.855	2.079	0.704	0.688	17.0	58.3	10490	0.278	0.158	1.166	0.646	1.058	0.797
0.85	2.955	2.143	0.728	0.708	17.5	60.3	11570	0.273	0.161	1.155	0.647	1.060	0.792
0.875	3.160	2.205	0.779	0.729	18.0	62.2	12630	0.271	0.163	1.147	0.647	1.065	0.791
0.90	3.468	2.268	0.855	0.749	18.5	63.8	13730	0.270	0.169	1.138	0.647	1.066	0.785
0.925	3.856	2.331	0.950	0.769	19.0	65.7	14830	0.270	0.175	1.130	0.647	1.068	0.781
0.95	4.238	2.394	1.044	0.790	19.5	67.5	16020	0.268	0.176	1.126	0.648	1.070	0.780
0.975	4.526	2.457	1.116	0.810	20.0	69.3	17310	0.267	0.179	1.120	0.648	1.072	0.778
1.000	4.686	2.520	1.155	0.830	20.5	71.2	19040	0.267	0.178	1.122	0.645	1.070	0.774
1.025	4.751	2.583	1.171	0.850	21.0	73.6	21130	0.267	0.173	1.128	0.643	1.065	0.773
1.05	4.757	2.646	1.172	0.871	21.5	76.3	24020	0.268	0.166	1.140	0.637	1.060	0.770
1.075	4.755	2.709	1.171	0.891	22.0	79.4	27700	0.269	0.154	1.155	0.629	1.058	0.769
1.1	4.799	2.772	1.183	0.911	22.5	82.7	32230	0.273	0.145	1.177	0.619	1.054	0.767
				0.932	23.0	86.7	37860	0.266	0.134	1.180	0.612	1.050	0.758
				0.952	23.5	91.0	44480	0.256	0.128	1.173	0.606	1.046	0.743
				0.972	24.0	95.4	51810	0.240	0.129	1.146	0.604	1.039	0.720
				0.992	24.5	99.0	58610	0.230	0.131	1.128	0.603	1.033	0.703
				1.013	25.0	102.1	64100	0.226	0.133	1.120	0.600	1.039	0.698
				1.033	25.5	104.4	67760	0.222	0.131	1.117	0.601	1.049	0.704
				1.053	26.0	106.7	70720	0.212	0.124	1.112	0.606	1.061	0.715
				1.074	26.5	109.1	73920	0.196	0.111	1.106	0.613	1.069	0.725
				1.094	27.0	111.4	77420	0.184	0.098	1.105	0.619	1.072	0.733

TABLE B-2

Results of Resistance and Self-Propulsion Experiments

Model Number 4210, $C_B = 0.60$, $L/B = 7.5$, $B/H = 2.5$, Propeller Number 3378

All Figures are for Ship of 400 Ft Length BP										All Figures are for Ship of 600 Ft Length BP									
$V/\sqrt{L_{WL}}$	$C_t \times 10^3$	ζ	ζ	$V/\sqrt{L_{WL}}$	V	N	SHP	W_T	t	e_h	e_p	e_r	EHP/SHP						
0.45	2.612	1.190	0.673	0.486	12.0	52.3	2920	0.277	0.165	1.156	0.677	1.004	0.786						
0.50	2.612	1.322	0.673	0.526	13.0	56.9	3719	0.273	0.160	1.155	0.679	1.010	0.792						
0.55	2.623	1.454	0.676	0.566	14.0	61.1	4850	0.277	0.150	1.175	0.677	1.005	0.800						
0.60	2.634	1.586	0.678	0.607	15.0	66.9	5752	0.268	0.150	1.162	0.680	1.011	0.799						
0.65	2.643	1.718	0.681	0.628	15.5	68.2	6413	0.269	0.162	1.147	0.679	1.007	0.784						
0.70	2.684	1.850	0.691	0.648	16.0	70.5	7108	0.268	0.162	1.145	0.678	1.006	0.782						
0.75	2.702	1.983	0.696	0.668	16.5	73.0	7894	0.266	0.170	1.130	0.678	1.009	0.773						
0.80	2.722	2.115	0.701	0.688	17.0	75.5	8698	0.264	0.173	1.123	0.678	1.012	0.770						
0.825	2.739	2.181	0.705	0.708	17.5	78.0	9524	0.258	0.168	1.121	0.680	1.013	0.772						
0.85	2.767	2.247	0.718	0.729	18.0	80.5	10420	0.253	0.166	1.116	0.682	1.015	0.772						
0.875	2.928	2.313	0.754	0.749	18.5	82.9	11330	0.251	0.169	1.110	0.682	1.019	0.771						
0.90	3.192	2.379	0.822	0.769	19.0	85.1	12190	0.253	0.185	1.118	0.681	1.026	0.781						
0.925	3.492	2.445	0.899	0.790	19.5	87.7	13100	0.246	0.169	1.103	0.683	1.041	0.764						
0.95	3.782	2.511	0.974	0.810	20.0	90.0	14160	0.249	0.176	1.097	0.681	1.044	0.780						
0.975	4.032	2.577	1.039	0.830	20.5	92.6	15440	0.246	0.178	1.090	0.681	1.044	0.775						
1.00	4.192	2.643	1.080	0.851	21.0	95.4	17250	0.251	0.177	1.098	0.675	1.036	0.768						
1.025	4.263	2.710	1.098	0.871	21.5	99.0	19590	0.249	0.176	1.097	0.669	1.035	0.759						
1.05	4.267	2.776	1.099	0.891	22.0	103.0	22850	0.252	0.177	1.101	0.658	1.036	0.750						
1.075	4.253	2.842	1.095	0.911	22.5	107.5	26620	0.256	0.178	1.106	0.644	1.034	0.738						
1.10	4.268	2.908	1.099	0.932	23.0	112.3	30940	0.257	0.179	1.105	0.634	1.037	0.721						
				0.952	23.5	117.1	35800	0.256	0.179	1.104	0.625	1.037	0.716						
				0.972	24.0	121.7	40500	0.249	0.178	1.095	0.621	1.038	0.706						
				0.992	24.5	125.9	44940	0.240	0.174	1.088	0.620	1.037	0.700						
				1.013	25.0	129.6	49090	0.233	0.172	1.079	0.621	1.034	0.693						
				1.033	25.5	132.9	52730	0.226	0.168	1.075	0.623	1.034	0.692						
				1.053	26.0	135.4	55990	0.227	0.162	1.085	0.622	1.031	0.686						
				1.074	26.5	138.0	59030	0.222	0.154	1.087	0.626	1.028	0.699						
				1.094	27.0	140.1	61760	0.219	0.141	1.101	0.629	1.022	0.707						

TABLE B-3

Results of Resistance and Self-Propulsion Experiments

Model Number 4267, $C_B = 0.65$, $L/B = 8.25$, $B/H = 2.5$, Propeller Number 2502

All Figures are for Ship of 400 Ft Length BP				All Figures are for Ship of 600 Ft Length BP									
$V/\sqrt{L_{WL}}$	$C_t \times 10^3$	\textcircled{K}	\textcircled{C}	$V/\sqrt{L_{WL}}$	V	N	SHP	W_T	t	e_h	e_p	e_π	EHP/SHP
0.40	2.651	1.077	0.696	0.405	10.0	50.1	1845	0.286	0.178	1.151	0.606	1.005	0.701
0.45	2.626	1.212	0.689	0.445	11.0	54.5	2362	0.289	0.181	1.151	0.609	1.005	0.705
0.50	2.605	1.346	0.684	0.486	12.0	58.7	2985	0.302	0.177	1.179	0.606	0.998	0.714
0.55	2.600	1.481	0.683	0.526	13.0	63.2	3754	0.310	0.173	1.199	0.604	0.996	0.721
0.60	2.611	1.616	0.685	0.566	14.0	68.2	4694	0.309	0.169	1.202	0.604	1.000	0.726
0.625	2.620	1.683	0.688	0.587	14.5	71.0	5270	0.301	0.168	1.191	0.607	1.000	0.722
0.65	2.631	1.750	0.690	0.607	15.0	73.6	5885	0.300	0.170	1.186	0.606	0.998	0.718
0.675	2.643	1.818	0.694	0.628	15.5	76.4	6568	0.293	0.173	1.169	0.609	0.999	0.711
0.70	2.656	1.885	0.697	0.648	16.0	79.3	7300	0.289	0.182	1.150	0.609	1.002	0.702
0.725	2.668	1.952	0.700	0.668	16.5	82.3	8079	0.278	0.180	1.136	0.613	1.006	0.701
0.75	2.683	2.020	0.704	0.688	17.0	85.1	8894	0.275	0.181	1.130	0.614	1.009	0.700
0.775	2.698	2.087	0.708	0.708	17.5	87.6	9727	0.280	0.180	1.139	0.610	1.012	0.704
0.80	2.726	2.154	0.715	0.729	18.0	90.1	10610	0.281	0.175	1.148	0.609	1.011	0.707
0.825	2.769	2.222	0.727	0.749	18.5	92.9	11620	0.278	0.171	1.148	0.610	1.010	0.708
0.85	2.847	2.289	0.747	0.769	19.0	95.9	12700	0.270	0.167	1.142	0.613	1.013	0.709
0.875	3.041	2.356	0.798	0.790	19.5	98.8	13870	0.268	0.166	1.140	0.612	1.016	0.709
0.90	3.454	2.424	0.907	0.810	20.0	101.6	15140	0.269	0.164	1.142	0.611	1.014	0.708
0.925	3.963	2.491	1.040	0.830	20.5	104.6	16530	0.270	0.165	1.143	0.608	1.018	0.707
0.95	4.446	2.558	1.167	0.851	21.0	108.1	18430	0.273	0.171	1.140	0.601	1.018	0.698
0.975	4.846	2.625	1.272	0.871	21.5	112.8	21190	0.271	0.171	1.138	0.593	1.022	0.690
1.00	5.106	2.693	1.340	0.891	22.0	118.5	25050	0.271	0.174	1.133	0.577	1.031	0.674
1.025	5.201	2.760	1.366	0.911	22.5	125.8	30260	0.268	0.168	1.136	0.565	1.028	0.658
				0.932	23.0	133.4	37040	0.264	0.165	1.134	0.550	1.021	0.637
				0.952	23.5	141.3	44980	0.258	0.162	1.129	0.538	1.014	0.616
				0.972	24.0	149.1	53620	0.247	0.157	1.119	0.529	1.010	0.596
				0.992	24.5	156.1	61950	0.238	0.152	1.113	0.523	1.010	0.588
				1.013	25.0	162.2	70150	0.227	0.149	1.101	0.522	1.002	0.576
				1.033	25.5	166.5	76300	0.225	0.146	1.102	0.520	0.998	0.572

TABLE B-4

Results of Resistance and Self-Propulsion Experiments
Model Number 4264, $C_B = 0.65$, $L/B = 6.25$, $B/H = 2.5$, Propeller Number 2828

All Figures are for Ship of 400 Ft Length BP				All Figures are for Ship of 600 Ft Length BP									
$V/\sqrt{L_{WL}}$	$C_t \times 10^3$	(K)	(C)	$V/\sqrt{L_{WL}}$	V	N	SHP	W_T	t	e_h	e_p	e_{rr}	EHP/SHP
0.400	2.841	0.982	0.680	0.405	10.0	37.6	2412	0.295	0.195	1.141	0.674	0.999	0.769
0.450	2.856	1.105	0.684	0.445	11.0	41.0	3073	0.300	0.192	1.154	0.675	1.012	0.789
0.500	2.874	1.227	0.688	0.486	12.0	44.5	3882	0.306	0.190	1.166	0.673	1.034	0.812
0.550	2.898	1.350	0.694	0.526	13.0	48.3	4905	0.306	0.186	1.173	0.672	1.046	0.825
0.600	2.919	1.473	0.699	0.566	14.0	52.0	6120	0.309	0.184	1.182	0.670	1.055	0.836
0.625	2.928	1.534	0.701	0.587	14.5	54.0	6859	0.308	0.185	1.177	0.670	1.055	0.832
0.650	2.940	1.596	0.704	0.607	15.0	56.0	7646	0.307	0.188	1.172	0.669	1.057	0.829
0.675	2.962	1.657	0.709	0.628	15.5	58.0	8534	0.306	0.192	1.164	0.667	1.058	0.821
0.700	2.985	1.718	0.715	0.648	16.0	60.3	9540	0.302	0.199	1.147	0.669	1.057	0.811
0.725	3.008	1.780	0.720	0.668	16.5	62.5	10610	0.296	0.205	1.129	0.670	1.057	0.800
0.750	3.022	1.841	0.724	0.688	17.0	64.7	11760	0.291	0.206	1.120	0.671	1.053	0.792
0.775	3.030	1.902	0.726	0.708	17.5	67.0	13030	0.283	0.206	1.107	0.673	1.050	0.783
0.800	3.069	1.964	0.735	0.729	18.0	69.1	14290	0.279	0.204	1.104	0.675	1.045	0.778
0.825	3.150	2.025	0.754	0.749	18.5	71.2	15610	0.275	0.199	1.104	0.676	1.043	0.778
0.850	3.334	2.086	0.798	0.769	19.0	73.3	16900	0.270	0.196	1.101	0.678	1.043	0.783
0.875	3.663	2.148	0.877	0.790	19.5	75.5	18290	0.267	0.195	1.098	0.678	1.058	0.787
0.900	4.189	2.209	1.003	0.810	20.0	77.7	20000	0.268	0.197	1.097	0.676	1.058	0.785
0.925	4.816	2.270	1.153	0.830	20.5	80.0	22080	0.269	0.199	1.095	0.673	1.057	0.779
0.950	5.591	2.332	1.339	0.851	21.0	83.0	25240	0.271	0.203	1.094	0.666	1.051	0.766
0.975	6.251	2.393	1.497	0.871	21.5	87.0	29910	0.268	0.201	1.091	0.659	1.040	0.750
1.000	6.816	2.455	1.632	0.891	22.0	92.0	36500	0.265	0.198	1.092	0.649	1.033	0.732
1.025	7.226	2.516	1.731	0.911	22.5	97.5	45140	0.262	0.188	1.100	0.632	1.022	0.711
				0.932	23.0	103.5	56250	0.250	0.175	1.100	0.622	1.008	0.690
				0.952	23.5	110.0	70160	0.236	0.161	1.099	0.613	0.987	0.665
				0.972	24.0	117.6	86350	0.216	0.152	1.081	0.606	0.976	0.640
				0.992	24.5	124.1	103800	0.189	0.152	1.047	0.604	0.972	0.615
				1.013	25.0	131.0	123000	0.164	0.159	1.005	0.603	0.967	0.586
				1.033	25.5	137.6	142000	0.132	0.173	0.952	0.607	0.965	0.557

TABLE B-5

Results of Resistance and Self-Propulsion Experiments

Model Number 4218, $C_B = 0.65$, $L/B = 7.25$, $B/H = 2.5$, Propeller Number 3380

All Figures are for Ship of 400 Ft Length BP				All Figures are for 600 Ft Length BP									
V/L_{WL}	$C_t \times 10^3$	K	C	V/L_{WL}	V	M	SRP	\dot{W}_T	t	ϕ_h	ϕ_p	ϕ_{TP}	KRP/SPR
0.40	2.643	1.032	0.664	0.405	10.0	41.3	1895	0.330	0.195	1.202	0.638	1.023	0.784
0.45	2.643	1.161	0.664	0.445	11.0	45.3	2467	0.319	0.187	1.194	0.647	1.021	0.783
0.50	2.656	1.290	0.668	0.486	12.0	49.7	3232	0.316	0.174	1.204	0.647	1.022	0.797
0.55	2.671	1.419	0.672	0.526	13.0	53.9	4102	0.309	0.163	1.212	0.651	1.017	0.803
0.575	2.671	1.483	0.672	0.566	14.0	58.3	5144	0.302	0.161	1.203	0.654	1.020	0.802
0.60	2.681	1.548	0.674	0.587	14.5	60.5	5765	0.302	0.163	1.198	0.652	1.019	0.798
0.625	2.700	1.612	0.678	0.607	15.0	62.9	6501	0.301	0.167	1.191	0.652	1.018	0.791
0.65	2.738	1.676	0.688	0.628	15.5	65.2	7246	0.298	0.173	1.178	0.652	1.016	0.781
0.675	2.772	1.741	0.697	0.648	16.0	67.5	8010	0.295	0.179	1.164	0.653	1.019	0.775
0.70	2.805	1.805	0.705	0.668	16.5	69.9	8852	0.289	0.180	1.153	0.655	1.019	0.770
0.725	2.820	1.870	0.709	0.688	17.0	72.2	9725	0.287	0.180	1.149	0.655	1.021	0.769
0.75	2.836	1.934	0.713	0.708	17.5	74.6	10710	0.280	0.174	1.148	0.658	1.020	0.770
0.775	2.859	1.999	0.718	0.729	18.0	77.1	11750	0.274	0.169	1.145	0.660	1.018	0.770
0.80	2.878	2.063	0.723	0.749	18.5	79.6	12860	0.269	0.166	1.141	0.661	1.021	0.770
0.825	2.908	2.128	0.731	0.769	19.0	82.0	14050	0.268	0.166	1.139	0.661	1.023	0.770
0.85	3.022	2.192	0.760	0.790	19.5	84.5	15400	0.268	0.167	1.138	0.659	1.026	0.769
0.875	3.282	2.256	0.825	0.810	20.0	87.2	16970	0.267	0.169	1.134	0.656	1.030	0.766
0.90	3.794	2.321	0.954	0.830	20.5	89.7	18730	0.270	0.172	1.133	0.652	1.028	0.760
0.925	4.341	2.385	1.091	0.851	21.0	93.1	21070	0.268	0.178	1.122	0.647	1.030	0.748
0.95	4.966	2.450	1.248	0.871	21.5	97.0	24260	0.264	0.180	1.114	0.641	1.027	0.733
0.975	5.521	2.515	1.388	0.891	22.0	102.0	29100	0.264	0.178	1.117	0.627	1.025	0.718
1.00	5.936	2.579	1.492	0.911	22.5	108.0	35850	0.262	0.165	1.131	0.612	1.018	0.704
1.025	6.221	2.644	1.564	0.932	23.0	116.0	46010	0.250	0.150	1.134	0.595	1.015	0.685
1.05	6.308	2.708	1.586	0.952	23.5	123.0	56200	0.244	0.141	1.137	0.581	1.015	0.671
1.10	6.219	2.837	1.563	0.972	24.0	130.0	67600	0.228	0.131	1.126	0.575	1.007	0.652
1.15	6.156	2.966	1.548	0.992	24.5	136.0	78010	0.211	0.127	1.106	0.574	1.002	0.636
				1.013	25.0	141.0	87310	0.193	0.123	1.087	0.577	0.992	0.622
				1.033	25.5	146.3	97970	0.174	0.122	1.062	0.580	0.982	0.605

TABLE B-6

Results of Resistance and Self-Propulsion Experiments

Model Number 4243, $C_B = 0.60$, $L/B = 8.5$, $B/H = 2.5$, Propeller Number 2502

All Figures are for Ship of 400 Ft length BP				All Figures are for Ship of 600 Ft Length BP									
$V/\sqrt{L_{WL}}$	$C_t \times 10^3$	(K)	(C)	$V/\sqrt{L_{WL}}$	V	N	SHP	W_T	t	e_h	e_p	e_{π}	EHP/SHP
0.45	2.575	1.240	0.692	0.486	12.0	57.1	2531	0.272	0.147	1.172	0.637	1.022	0.763
0.50	2.556	1.378	0.687	0.526	13.0	61.6	3186	0.279	0.152	1.175	0.634	1.025	0.764
0.55	2.542	1.516	0.683	0.566	14.0	66.4	3996	0.280	0.156	1.172	0.633	1.026	0.761
0.60	2.542	1.654	0.683	0.607	15.0	71.4	4979	0.278	0.160	1.164	0.633	1.029	0.758
0.65	2.565	1.792	0.689	0.628	15.5	74.1	5561	0.276	0.160	1.161	0.632	1.027	0.754
0.70	2.608	1.929	0.701	0.648	16.0	76.8	6188	0.273	0.158	1.159	0.633	1.027	0.751
0.75	2.613	2.067	0.702	0.668	16.5	79.5	6863	0.268	0.152	1.158	0.634	1.023	0.751
0.80	2.630	2.205	0.707	0.688	17.0	82.2	7606	0.265	0.152	1.154	0.634	1.021	0.746
0.825	2.664	2.274	0.716	0.708	17.5	84.8	8352	0.262	0.147	1.157	0.634	1.019	0.748
0.85	2.731	2.343	0.734	0.729	18.0	87.3	9101	0.261	0.145	1.157	0.634	1.020	0.748
0.875	2.855	2.412	0.767	0.749	18.5	89.9	9933	0.260	0.144	1.156	0.635	1.020	0.749
0.90	3.063	2.480	0.823	0.769	19.0	92.5	10830	0.258	0.140	1.159	0.635	1.018	0.749
0.925	3.301	2.550	0.887	0.790	19.5	95.1	11750	0.255	0.139	1.156	0.636	1.020	0.750
0.95	3.536	2.616	0.950	0.810	20.0	97.7	12720	0.252	0.143	1.147	0.636	1.023	0.746
0.975	3.706	2.687	0.999	0.830	20.5	100.8	13870	0.248	0.144	1.140	0.636	1.027	0.744
1.00	3.833	2.756	1.030	0.851	21.0	103.9	15270	0.247	0.141	1.141	0.634	1.025	0.742
1.025	3.893	2.825	1.046	0.871	21.5	107.5	17210	0.245	0.138	1.142	0.628	1.024	0.735
1.05	3.879	2.894	1.042	0.891	22.0	112.0	19630	0.244	0.136	1.144	0.623	1.022	0.728
1.075	3.860	2.963	1.037	0.911	22.5	116.8	22610	0.246	0.137	1.144	0.613	1.024	0.719
1.10	3.858	3.032	1.037	0.932	23.0	122.2	26080	0.245	0.143	1.134	0.603	1.026	0.702
				0.952	23.5	127.6	29980	0.235	0.146	1.116	0.599	1.032	0.690
				0.972	24.0	132.5	33790	0.228	0.143	1.111	0.595	1.031	0.682
				0.992	24.5	136.3	37390	0.235	0.136	1.129	0.588	1.026	0.682
				1.013	25.0	139.5	40380	0.239	0.132	1.141	0.584	1.025	0.683
				1.033	25.5	142.3	43090	0.238	0.126	1.147	0.582	1.023	0.687
				1.053	26.0	145.1	45360	0.232	0.121	1.144	0.586	1.020	0.687
				1.074	26.5	147.9	47520	0.223	0.120	1.132	0.594	1.023	0.686
				1.094	27.0	150.9	50170	0.217	0.115	1.131	0.596	1.025	0.691

TABLE B-7

Results of Resistance and Self-Propulsion Experiments

Model Number 4244, $C_B = 0.70$, $L/B = 6.0$, $B/H = 2.5$, Propeller Number 2452

All Figures are for Ship of 400 Ft Length BP				All Figures are for Ship of 600 Ft Length BP									
$V/\sqrt{L_{WL}}$	$C_t \times 10^3$	(K)	(C)	$V/\sqrt{L_{WL}}$	V	N	SHP	W_T	t	e_h	e_p	e_{π}	EHP/SHP
0.40	3.068	0.957	0.720	0.364	9.0	31.1	1895	0.324	0.214	1.164	0.657	1.081	0.827
0.45	3.048	1.076	0.715	0.405	10.0	34.5	2541	0.316	0.218	1.144	0.664	1.084	0.824
0.50	3.052	1.196	0.716	0.445	11.0	37.8	3339	0.324	0.219	1.156	0.661	1.088	0.831
0.55	3.081	1.315	0.723	0.486	12.0	41.2	4354	0.330	0.218	1.168	0.657	1.085	0.833
0.60	3.128	1.435	0.734	0.526	13.0	44.9	5635	0.325	0.221	1.154	0.658	1.087	0.825
0.625	3.150	1.495	0.739	0.566	14.0	48.9	7254	0.313	0.225	1.129	0.661	1.084	0.809
0.65	3.173	1.555	0.744	0.607	15.0	52.8	9166	0.304	0.222	1.117	0.663	1.079	0.799
0.675	3.191	1.614	0.748	0.628	15.5	54.6	10220	0.305	0.218	1.125	0.662	1.072	0.798
0.70	3.217	1.674	0.754	0.648	16.0	56.4	11280	0.307	0.216	1.130	0.661	1.070	0.800
0.725	3.266	1.734	0.766	0.668	16.5	58.1	12370	0.310	0.213	1.141	0.659	1.072	0.806
0.75	3.332	1.794	0.781	0.688	17.0	60.0	13560	0.309	0.213	1.140	0.659	1.076	0.808
0.775	3.395	1.854	0.796	0.708	17.5	62.0	14940	0.308	0.214	1.135	0.658	1.077	0.806
0.80	3.477	1.913	0.815	0.729	18.0	64.0	16480	0.305	0.214	1.131	0.658	1.077	0.801
0.825	3.589	1.973	0.842	0.749	18.5	66.3	18270	0.297	0.214	1.118	0.660	1.076	0.794
0.85	3.777	2.033	0.866	0.769	19.0	68.8	20330	0.288	0.214	1.105	0.661	1.076	0.785
0.875	4.249	2.093	0.996	0.790	19.5	71.2	22740	0.284	0.212	1.100	0.660	1.071	0.777
0.90	5.076	2.153	1.190	0.810	20.0	73.9	25520	0.275	0.202	1.093	0.660	1.067	0.770
				0.830	20.5	76.6	28810	0.270	0.198	1.099	0.657	1.060	0.766
				0.851	21.0	79.5	32760	0.271	0.187	1.115	0.651	1.054	0.765
				0.891	22.0	87.8	47450	0.272	0.189	1.181	0.624	1.037	0.765

TABLE B-8

Results of Resistance and Self-Propulsion Experiments

Model Number 4221, $C_B = 0.70$, $L/B = 7.00$, $B/H = 2.5$, Propeller Number 3376

All Figures are for Ship of 400 Ft Length BP				All Figures are for Ship of 600 Ft Length BP									
$V/\sqrt{L_{WL}}$	$C_t \times 10^3$	(K)	(C)	$V/\sqrt{L_{WL}}$	V	N	SHP	W_T	t	ϕ_h	ϕ_p	ϕ_π	EHP/SHP
0.40	2.723	1.007	0.674	0.364	9.0	36.4	1520	0.314	0.146	1.245	0.661	0.995	0.819
0.45	2.732	1.133	0.676	0.406	10.0	40.4	2039	0.297	0.128	1.240	0.673	0.986	0.824
0.50	2.757	1.259	0.682	0.445	11.0	44.5	2717	0.299	0.130	1.241	0.671	0.992	0.827
0.55	2.788	1.385	0.690	0.486	12.0	48.7	3517	0.291	0.138	1.216	0.675	0.996	0.818
0.60	2.806	1.511	0.695	0.526	13.0	52.9	4558	0.294	0.148	1.207	0.672	0.993	0.805
0.625	2.830	1.574	0.700	0.566	14.0	57.3	5842	0.296	0.152	1.205	0.668	0.994	0.800
0.65	2.862	1.637	0.708	0.607	15.0	61.9	7307	0.291	0.156	1.191	0.667	1.003	0.797
0.675	2.891	1.700	0.716	0.628	15.5	64.2	8206	0.294	0.157	1.194	0.663	1.005	0.796
0.70	2.926	1.762	0.724	0.648	16.0	66.5	9036	0.287	0.158	1.181	0.666	1.007	0.793
0.725	2.971	1.826	0.736	0.668	16.5	69.0	10050	0.283	0.160	1.172	0.666	1.012	0.790
0.75	3.045	1.888	0.754	0.688	17.0	71.2	11100	0.284	0.160	1.172	0.665	1.009	0.787
0.775	3.143	1.951	0.778	0.708	17.5	73.8	12320	0.277	0.161	1.160	0.666	1.010	0.781
0.80	3.250	2.014	0.804	0.729	18.0	76.4	13630	0.272	0.164	1.149	0.666	1.014	0.776
0.825	3.359	2.077	0.832	0.749	18.5	79.2	15250	0.277	0.171	1.146	0.659	1.025	0.774
0.85	3.490	2.140	0.864	0.769	19.0	81.9	17030	0.279	0.176	1.143	0.654	1.025	0.767
0.875	3.784	2.203	0.937	0.790	19.5	84.8	19010	0.276	0.177	1.137	0.652	1.025	0.760
0.90	4.452	2.266	1.102	0.810	20.0	87.8	21390	0.279	0.176	1.143	0.645	1.024	0.756
0.95	6.167	2.392	1.527	0.830	20.5	90.6	23900	0.281	0.176	1.147	0.641	1.016	0.747
1.00	7.997	2.518	1.980	0.851	21.0	93.8	26810	0.281	0.168	1.157	0.636	1.015	0.747
1.05	9.175	2.644	2.272	0.871	21.5	98.2	31550	0.275	0.151	1.171	0.629	1.002	0.738
1.10	9.307	2.770	2.304	0.891	22.0	104.0	38430	0.286	0.157	1.181	0.605	1.019	0.728
1.15	9.121	2.896	2.258										

TABLE B-9
Results of Resistance and Self-Propulsion Experiments
Model Number 4247, $C_B = 0.70$, $L/B = 8.0$, $B/H = 2.5$, Propeller Number 3565

All Figures are for Ship of 400 Ft Length BP				All Figures are for Ship of 600 Ft Length BP									
$V/\sqrt{L_{WL}}$	$C_t \times 10^3$	(K)	(C)	$V/\sqrt{L_{WL}}$	V	N	SHP	W_T	t	e_h	e_p	e_r	EHP/SHP
0.40	2.593	1.053	0.611	0.364	9.0	45.6	1472	0.411	0.279	1.225	0.556	1.010	0.688
0.45	2.611	1.185	0.676	0.405	10.0	50.8	1949	0.382	0.261	1.195	0.576	1.020	0.703
0.50	2.639	1.316	0.683	0.445	11.0	56.0	2548	0.368	0.248	1.189	0.536	1.025	0.714
0.55	2.674	1.448	0.692	0.486	12.0	61.2	3277	0.360	0.234	1.196	0.590	1.034	0.730
0.60	2.711	1.580	0.701	0.526	13.0	66.6	4159	0.354	0.228	1.194	0.593	1.041	0.737
0.625	2.727	1.645	0.706	0.566	14.0	72.1	5215	0.348	0.229	1.182	0.594	1.051	0.738
0.65	2.745	1.711	0.710	0.607	15.0	77.6	6464	0.344	0.228	1.176	0.595	1.057	0.739
0.675	2.772	1.777	0.717	0.628	15.5	80.3	7153	0.344	0.226	1.180	0.594	1.058	0.742
0.70	2.807	1.843	0.726	0.648	16.0	83.1	7922	0.341	0.224	1.177	0.595	1.058	0.741
0.725	2.863	1.909	0.741	0.668	16.5	86.0	8765	0.339	0.223	1.175	0.595	1.059	0.740
0.75	2.948	1.974	0.763	0.688	17.0	88.9	9686	0.336	0.225	1.168	0.595	1.060	0.736
0.775	3.032	2.040	0.784	0.708	17.5	91.8	10710	0.338	0.226	1.167	0.592	1.060	0.732
0.80	3.119	2.106	0.807	0.729	18.0	95.0	11890	0.335	0.228	1.159	0.592	1.060	0.727
0.825	3.195	2.172	0.827	0.749	18.5	98.6	13320	0.329	0.225	1.156	0.591	1.060	0.726
0.85	3.330	2.238	0.862	0.769	19.0	102.3	14990	0.329	0.216	1.167	0.587	1.058	0.725
0.875	3.579	2.303	0.926	0.790	19.5	106.3	16840	0.322	0.210	1.166	0.586	1.060	0.724
0.90	4.046	2.369	1.047	0.810	20.0	110.1	18740	0.318	0.212	1.155	0.584	1.062	0.716
				0.830	20.5	115.1	20940	0.310	0.219	1.132	0.584	1.060	0.700
				0.851	21.0	118.7	23490	0.302	0.225	1.110	0.583	1.064	0.688
				0.891	22.0	130.7	31810	0.308	0.236	1.103	0.570	1.065	0.669

TABLE B-10
Results of Resistance and Self-Propulsion Experiments
Model Number 4268, $C_B = 0.75$, $L/B = 5.75$, $B/H = 2.5$, Propeller Number 3156

All Figures are for Ship of 400 Ft Length BP				All Figures are for Ship of 600 Ft Length BP									
$V/\sqrt{L_{WL}}$	$C_t \times 10^3$	(K)	(C)	$V/\sqrt{L_{WL}}$	V	N	SHP	W_T	t	e_h	e_p	e_{rr}	EHP/SHP
0.35	3.193	0.816	0.734	0.405	10.0	34.8	3055	0.323	0.174	1.219	0.650	1.011	0.801
0.40	3.166	0.932	0.728	0.445	11.0	38.0	3970	0.330	0.186	1.215	0.648	1.016	0.801
0.45	3.144	1.049	0.723	0.486	12.0	41.2	5103	0.340	0.192	1.225	0.645	1.018	0.803
0.50	3.154	1.166	0.725	0.526	13.0	44.9	6587	0.337	0.199	1.209	0.644	1.021	0.795
0.55	3.186	1.282	0.732	0.566	14.0	48.9	8416	0.326	0.202	1.184	0.646	1.027	0.786
0.575	3.206	1.340	0.737	0.587	14.5	50.9	9463	0.323	0.202	1.178	0.646	1.030	0.784
0.60	3.238	1.399	0.744	0.607	15.0	52.8	10620	0.321	0.201	1.176	0.646	1.029	0.781
0.625	3.275	1.457	0.753	0.628	15.5	54.8	11890	0.322	0.203	1.175	0.644	1.029	0.778
0.65	3.330	1.515	0.765	0.648	16.0	56.8	13320	0.319	0.199	1.177	0.643	1.027	0.778
0.675	3.407	1.574	0.783	0.668	16.5	59.1	15010	0.316	0.201	1.169	0.642	1.028	0.771
0.70	3.545	1.632	0.815	0.688	17.0	61.5	16980	0.316	0.206	1.160	0.638	1.033	0.764
0.725	3.815	1.690	0.877	0.708	17.5	64.2	19500	0.316	0.208	1.158	0.631	1.038	0.758
0.75	4.177	1.748	0.960	0.729	18.0	67.1	22760	0.320	0.206	1.168	0.621	1.040	0.754
0.775	4.525	1.807	1.040	0.749	18.5	70.4	26840	0.324	0.204	1.177	0.609	1.039	0.745
0.80	4.824	1.865	1.109	0.769	19.0	74.0	31780	0.317	0.194	1.181	0.603	1.031	0.734
0.825	5.063	1.923	1.164	0.790	19.5	77.8	37330	0.303	0.183	1.171	0.602	1.022	0.721
0.85	5.277	1.982	1.213	0.810	20.0	81.2	42980	0.293	0.175	1.168	0.600	1.014	0.710
0.875	5.491	2.040	1.262	0.830	20.5	84.7	48720	0.278	0.168	1.152	0.602	1.011	0.701
				0.851	21.0	87.6	54240	0.276	0.163	1.155	0.599	1.010	0.699
				0.871	21.5	90.7	59880	0.276	0.156	1.164	0.594	1.012	0.700
				0.891	22.0	93.4	66280	0.276	0.152	1.170	0.591	1.016	0.702

TABLE B-11

Results of Resistance and Self-Propulsion Experiments

Model Number 4213, $C_B = 0.75$, $L/B = 6.75$, $B/H = 2.5$, Propeller Number 3379

All Figures are for Ship of 400 Ft Length BP				All Figures are for Ship of 600 Ft Length BP									
$V/\sqrt{L_{WL}}$	$C_t \times 10^3$	(K)	(C)	$V/\sqrt{L_{WL}}$	V	N	SHP	W_T	t	e_h	e_p	e_π	SHP/EHP
0.35	2.911	0.861	0.705	0.364	9.0	36.1	1638	0.337	0.140	1.295	0.650	0.998	0.840
0.40	2.881	0.984	0.697	0.405	10.0	40.1	2204	0.329	0.139	1.282	0.656	1.004	0.844
0.45	2.876	1.107	0.696	0.445	11.0	44.4	2955	0.313	0.149	1.239	0.663	0.998	0.821
0.50	2.902	1.230	0.702	0.486	12.0	48.7	3895	0.310	0.154	1.224	0.663	1.001	0.812
0.55	2.934	1.352	0.710	0.526	13.0	53.1	5064	0.311	0.161	1.218	0.659	1.006	0.808
0.575	2.947	1.414	0.713	0.566	14.0	57.5	6408	0.307	0.164	1.206	0.659	1.010	0.803
0.60	2.977	1.475	0.720	0.587	14.5	59.8	7223	0.307	0.166	1.203	0.658	1.011	0.800
0.625	3.046	1.537	0.737	0.607	15.0	62.1	8172	0.311	0.168	1.208	0.652	1.013	0.798
0.65	3.135	1.598	0.759	0.628	15.5	64.5	9143	0.307	0.171	1.196	0.653	1.014	0.792
0.675	3.222	1.660	0.780	0.648	16.0	67.0	10340	0.309	0.173	1.197	0.648	1.016	0.788
0.70	3.357	1.721	0.812	0.668	16.5	70.0	11820	0.305	0.176	1.186	0.644	1.020	0.780
0.725	3.563	1.783	0.862	0.688	17.0	72.9	13470	0.306	0.178	1.185	0.638	1.024	0.775
0.75	3.871	1.844	0.937	0.708	17.5	76.2	15410	0.298	0.180	1.169	0.636	1.027	0.764
0.775	4.230	1.906	1.024	0.729	18.0	80.0	18100	0.293	0.179	1.162	0.630	1.025	0.750
0.80	4.623	1.967	1.119	0.749	18.5	84.1	21380	0.287	0.178	1.153	0.623	1.020	0.733
0.825	4.983	2.029	1.206	0.769	19.0	88.5	25410	0.280	0.171	1.152	0.616	1.013	0.719
0.85	5.272	2.090	1.276	0.790	19.5	93.3	30630	0.280	0.158	1.170	0.604	1.007	0.711
0.875	5.562	2.152	1.346	0.810	20.0	98.2	36110	0.271	0.151	1.164	0.597	1.008	0.701
				0.830	20.5	102.5	41200	0.258	0.146	1.152	0.596	1.005	0.691
				0.851	21.0	106.9	46890	0.242	0.147	1.126	0.598	0.999	0.673
				0.871	21.5	111.0	53090	0.238	0.148	1.119	0.594	0.995	0.662
				0.891	22.0	115.0	60290	0.244	0.147	1.129	0.584	0.990	0.653

TABLE B-12

Results of Resistance and Self-Propulsion Experiments

Model Number 4271, $C_B = 0.75$, $L/B = 7.75$, $B/H = 2.5$, Propeller Number 3375

All Figures are for Ship of 400 Ft Length BP				All Figures are for Ship of 600 Ft Length BP									
$V/\sqrt{L_{WL}}$	$C_t \times 10^3$	(B)	(C)	$V/\sqrt{L_{WL}}$	V	N	SHP	W_T	t	θ_h	θ_p	θ_{rr}	SHP/SHP
0.35	2.731	0.901	0.692	0.364	9.0	46.4	1499	0.300	0.110	1.272	0.633	0.937	0.755
0.40	2.701	1.030	0.684	0.405	10.0	51.0	1995	0.310	0.118	1.278	0.634	0.935	0.758
0.45	2.680	1.159	0.679	0.445	11.0	55.9	2632	0.316	0.124	1.280	0.633	0.938	0.761
0.50	2.695	1.288	0.683	0.486	12.0	61.3	3428	0.315	0.133	1.266	0.632	0.955	0.765
0.525	2.713	1.352	0.688	0.526	13.0	67.4	4417	0.308	0.151	1.226	0.632	0.986	0.764
0.55	2.738	1.416	0.694	0.566	14.0	73.4	5658	0.311	0.174	1.198	0.625	1.011	0.757
0.575	2.779	1.481	0.704	0.587	14.5	76.3	6363	0.315	0.182	1.194	0.621	1.021	0.756
0.60	2.840	1.545	0.720	0.607	15.0	79.1	7222	0.315	0.181	1.196	0.616	1.023	0.754
0.625	2.917	1.610	0.739	0.628	15.5	82.2	8130	0.314	0.180	1.194	0.613	1.028	0.753
0.65	3.005	1.674	0.761	0.648	16.0	85.6	9200	0.311	0.180	1.190	0.613	1.030	0.752
0.675	3.114	1.738	0.789	0.668	16.5	89.4	10380	0.306	0.179	1.183	0.618	1.024	0.748
0.70	3.253	1.803	0.824	0.688	17.0	93.4	12000	0.302	0.178	1.177	0.610	1.022	0.733
0.725	3.453	1.867	0.875	0.708	17.5	97.8	14090	0.302	0.179	1.175	0.606	1.020	0.726
0.75	3.792	1.931	0.961	0.729	18.0	102.3	16330	0.299	0.177	1.174	0.597	1.019	0.714
0.775	4.265	1.996	1.081	0.749	18.5	107.9	19530	0.299	0.181	1.168	0.586	1.013	0.699
0.80	4.699	2.060	1.191	0.769	19.0	113.9	23720	0.302	0.182	1.172	0.573	1.006	0.676
0.825	4.986	2.124	1.264	0.790	19.5	120.2	28600	0.304	0.184	1.173	0.560	1.005	0.660
0.85	5.197	2.189	1.317	0.810	20.0	126.3	33430	0.298	0.178	1.171	0.554	1.007	0.653
0.875	5.341	2.253	1.354	0.830	20.5	131.5	38150	0.294	0.172	1.173	0.549	1.004	0.647
				0.851	21.0	136.3	42510	0.291	0.170	1.170	0.546	1.008	0.644
				0.871	21.5	141.9	47510	0.278	0.176	1.140	0.547	1.016	0.634
				0.891	22.0	149.2	53390	0.231	0.172	1.076	0.562	1.026	0.620

TABLE B-13

Results of Resistance and Self-Propulsion Experiments

Model Number 4248, $C_B = 0.80$, $L/B = 5.5$, $B/H = 2.5$, Propeller Number 3563

All Figures are for Ship of 400 Ft Length BP				All Figures are for Ship of 600 Ft Length BP									
$V/\sqrt{L_{WL}}$	$C_t \times 10^3$	(X)	(C)	$V/\sqrt{L_{WL}}$	V	N	SHP	W_T	t	σ_h	σ_p	σ_{rr}	KRP/SHF
0.35	3.563	0.795	0.808	0.364	9.0	31.8	2788	0.429	0.238	1.334	0.548	1.061	0.775
0.40	3.533	0.909	0.802	0.405	10.0	35.0	3665	0.428	0.238	1.331	0.552	1.073	0.789
0.45	3.508	1.022	0.796	0.445	11.0	38.4	4774	0.428	0.233	1.342	0.553	1.084	0.804
0.50	3.489	1.136	0.791	0.465	11.5	40.1	5440	0.426	0.232	1.339	0.555	1.085	0.806
0.525	3.485	1.193	0.791	0.486	12.0	41.8	6151	0.426	0.228	1.345	0.556	1.084	0.810
0.55	3.508	1.250	0.796	0.506	12.5	43.6	6950	0.421	0.223	1.342	0.559	1.084	0.813
0.575	3.566	1.306	0.809	0.526	13.0	45.5	7829	0.417	0.219	1.339	0.562	1.084	0.815
0.60	3.664	1.363	0.831	0.546	13.5	47.3	8843	0.417	0.216	1.346	0.560	1.082	0.816
0.625	3.793	1.420	0.860	0.566	14.0	49.3	10010	0.415	0.215	1.344	0.559	1.085	0.815
0.65	3.982	1.477	0.903	0.587	14.5	51.4	11390	0.413	0.215	1.336	0.558	1.086	0.810
0.675	4.237	1.534	0.961	0.607	15.0	53.7	12980	0.414	0.216	1.340	0.552	1.092	0.808
0.70	4.585	1.590	1.040	0.628	15.5	56.1	14940	0.412	0.220	1.327	0.548	1.092	0.794
0.75	5.567	1.704	1.263	0.648	16.0	58.8	17290	0.404	0.220	1.309	0.548	1.090	0.781
0.80	7.029	1.818	1.594	0.688	17.0	64.9	23580	0.393	0.216	1.293	0.539	1.084	0.755
				0.729	18.0	72.4	33870	0.375	0.199	1.283	0.529	1.062	0.721
				0.769	19.0	82.4	51360	0.349	0.175	1.268	0.514	1.056	0.688
				0.810	20.0	93.8	80720	0.349	0.155	1.298	0.488	1.055	0.668

TABLE B-14

Results of Resistance and Self-Propulsion Experiments

Model Number 4214, $C_B = 0.80$, $L/B = 6.5$, $B/H = 2.5$, Propeller Number 3377

All Figures are for Ship of 400 Ft Length BP				All Figures are for Ship of 600 Ft Length BP									
$V/\sqrt{L_{WL}}$	$C_t \times 10^3$	ζ	ζ	$V/\sqrt{L_{WL}}$	V	N	SHP	W_T	t	e_h	e_p	e_{rr}	RHP/SHP
0.35	3.006	0.841	0.719	0.364	9.0	38.4	1959	0.363	0.164	1.313	0.624	1.005	0.824
0.40	2.991	0.961	0.715	0.405	10.0	42.6	2640	0.359	0.171	1.293	0.628	1.011	0.821
0.45	2.992	1.081	0.716	0.445	11.0	46.8	3491	0.356	0.177	1.279	0.630	1.008	0.813
0.50	3.009	1.201	0.720	0.466	11.5	48.9	3983	0.357	0.182	1.272	0.630	1.009	0.809
0.525	3.025	1.261	0.724	0.486	12.0	51.2	4543	0.352	0.186	1.256	0.632	1.011	0.802
0.55	3.056	1.321	0.731	0.506	12.5	53.4	5193	0.355	0.191	1.255	0.629	1.010	0.798
0.575	3.116	1.381	0.745	0.526	13.0	55.8	5951	0.357	0.197	1.250	0.626	1.013	0.792
0.60	3.236	1.441	0.774	0.546	13.5	58.2	6692	0.350	0.199	1.233	0.628	1.016	0.788
0.625	3.387	1.502	0.810	0.566	14.0	60.7	7671	0.352	0.200	1.235	0.624	1.014	0.783
0.65	3.585	1.562	0.857	0.587	14.5	63.4	8767	0.350	0.198	1.234	0.622	1.015	0.780
0.675	3.857	1.622	0.922	0.607	15.0	66.5	10170	0.348	0.196	1.233	0.618	1.020	0.777
0.70	4.210	1.682	1.007	0.628	15.5	69.7	11800	0.341	0.191	1.228	0.616	1.018	0.770
0.75	5.003	1.802	1.196	0.648	16.0	73.3	13750	0.336	0.190	1.219	0.611	1.024	0.763
0.80	6.538	1.922	1.564	0.688	17.0	81.2	19110	0.329	0.188	1.211	0.596	1.029	0.743
				0.729	18.0	90.8	27650	0.315	0.184	1.192	0.581	1.022	0.708
				0.769	19.0	102.4	41790	0.309	0.183	1.183	0.555	1.011	0.664

TABLE B-15
Results of Resistance and Self-Propulsion Experiments
Model Number 4215, $C_B = 0.80$, $L/B = 7.5$, $B/H = 2.5$, Propeller Number 3378

All Figures are for Ship of 400 Ft Length BP				All Figures are for Ship of 600 Ft Length BP									
$V/\sqrt{L_{WL}}$	$C_t \times 10^3$	Ⓐ	Ⓑ	$V/\sqrt{L_{WL}}$	V	N	SRP	W_T	t	θ_h	θ_p	θ_{TP}	SRP/SRP
0.35	2.782	0.882	0.699	0.364	9.0	40.9	1624	0.378	0.199	1.287	0.585	1.056	0.795
0.40	2.759	1.008	0.693	0.405	10.0	45.1	2149	0.372	0.208	1.260	0.593	1.053	0.787
0.45	2.750	1.134	0.691	0.445	11.0	49.7	2866	0.363	0.213	1.235	0.602	1.049	0.780
0.50	2.767	1.260	0.695	0.466	11.5	52.4	3295	0.353	0.214	1.215	0.607	1.049	0.774
0.525	2.799	1.323	0.703	0.486	12.0	54.7	3754	0.348	0.213	1.208	0.607	1.050	0.770
0.55	2.851	1.386	0.716	0.506	12.5	57.4	4304	0.337	0.210	1.192	0.608	1.049	0.765
0.575	2.942	1.449	0.739	0.526	13.0	60.0	4916	0.334	0.204	1.195	0.608	1.049	0.762
0.60	3.093	1.512	0.777	0.546	13.5	62.7	5628	0.331	0.198	1.199	0.607	1.050	0.765
0.625	3.290	1.575	0.826	0.566	14.0	65.5	6439	0.331	0.194	1.206	0.604	1.050	0.765
0.65	3.502	1.638	0.880	0.587	14.5	68.3	7440	0.336	0.194	1.212	0.598	1.046	0.758
0.675	3.752	1.701	0.943	0.607	15.0	71.6	8684	0.334	0.194	1.210	0.594	1.040	0.747
0.70	4.040	1.764	1.015	0.628	15.5	75.0	10170	0.333	0.198	1.202	0.588	1.035	0.732
0.75	4.824	1.890	1.211	0.648	16.0	78.9	11980	0.328	0.199	1.192	0.583	1.029	0.715
0.80	6.069	2.016	1.525	0.688	17.0	87.4	16780	0.317	0.195	1.177	0.572	1.022	0.689
				0.729	18.0	97.4	23730	0.304	0.182	1.176	0.552	1.025	0.666
				0.769	19.0	109.4	34910	0.293	0.174	1.168	0.538	1.020	0.641
				0.810	20.0	123.6	52840	0.274	0.166	1.149	0.519	1.001	0.597

TABLE B-16

Results of Resistance and Self-Propulsion Experiments

Model Number 4252, $C_B = 0.60$, $L/B = 6.5$, $B/H = 3.0$, Propeller Number 3375

All Figures are for Ship of 400 Ft Length BP				All Figures are for Ship of 600 Ft Length BP									
$V/\sqrt{L_{WL}}$	$C_t \times 10^3$	(K)	(C)	$V/\sqrt{L_{WL}}$	V	N	SHIP	W_P	t	θ_h	θ_p	θ_{PT}	SHIP/SHIP
0.45	2.659	1.169	0.671	0.445	11.0	55.5	2606	0.361	0.205	1.244	0.609	0.986	0.746
0.50	2.662	1.299	0.672	0.486	12.0	60.5	3289	0.349	0.201	1.229	0.617	0.995	0.754
0.55	2.658	1.429	0.671	0.526	13.0	65.8	4111	0.339	0.195	1.217	0.624	1.008	0.765
0.60	2.668	1.559	0.674	0.566	14.0	71.2	5127	0.331	0.194	1.205	0.626	1.018	0.768
0.65	2.714	1.689	0.685	0.607	15.0	76.6	6314	0.326	0.190	1.201	0.628	1.027	0.775
0.70	2.787	1.819	0.704	0.628	15.5	79.6	7039	0.322	0.192	1.190	0.629	1.031	0.771
0.75	2.800	1.949	0.707	0.648	16.0	82.4	7775	0.320	0.192	1.189	0.628	1.036	0.774
0.80	2.812	2.078	0.710	0.668	16.5	85.4	8620	0.314	0.188	1.185	0.630	1.036	0.773
0.825	2.843	2.144	0.718	0.688	17.0	88.3	9506	0.311	0.188	1.179	0.631	1.036	0.771
0.85	2.925	2.208	0.739	0.708	17.5	91.3	10460	0.306	0.189	1.169	0.632	1.039	0.767
0.875	3.075	2.273	0.776	0.729	18.0	94.2	11490	0.304	0.188	1.167	0.634	1.038	0.764
0.90	3.308	2.338	0.835	0.749	18.5	97.0	12510	0.299	0.187	1.160	0.634	1.035	0.762
0.925	3.636	2.403	0.918	0.769	19.0	100.0	13640	0.293	0.184	1.153	0.637	1.033	0.759
0.95	3.951	2.468	0.998	0.790	19.5	102.8	14810	0.291	0.186	1.148	0.637	1.033	0.756
0.975	4.173	2.533	1.054	0.810	20.0	106.0	16110	0.287	0.187	1.142	0.638	1.041	0.757
1.000	4.341	2.598	1.096	0.830	20.5	109.2	17740	0.287	0.186	1.144	0.635	1.041	0.755
1.025	4.461	2.663	1.127	0.851	21.0	112.7	19690	0.286	0.185	1.141	0.632	1.037	0.748
1.05	4.547	2.728	1.148	0.871	21.5	117.0	22260	0.282	0.184	1.136	0.628	1.036	0.739
1.075	4.603	2.793	1.162	0.891	22.0	121.5	25390	0.281	0.178	1.143	0.621	1.034	0.734
1.10	4.629	2.858	1.169	0.911	22.5	127.2	29830	0.277	0.177	1.138	0.611	1.036	0.721
				0.932	23.0	133.3	34910	0.276	0.177	1.136	0.602	1.036	0.708
				0.952	23.5	139.6	40940	0.270	0.179	1.124	0.594	1.029	0.687
				0.972	24.0	145.4	46880	0.262	0.179	1.112	0.590	1.025	0.673
				0.992	24.5	150.8	52410	0.252	0.178	1.098	0.589	1.025	0.663
				1.013	25.0	155.4	57610	0.245	0.176	1.091	0.587	1.024	0.656
				1.033	25.5	159.8	62510	0.240	0.175	1.085	0.588	1.022	0.652
				1.053	26.0	163.1	66600	0.239	0.167	1.094	0.588	1.022	0.658
				1.074	26.5	166.5	70730	0.238	0.162	1.100	0.588	1.023	0.662
				1.094	27.0	169.6	74850	0.238	0.156	1.107	0.588	1.020	0.665

TABLE B-17

Results of Resistance and Self-Propulsion Experiments

Model Number 4255, $C_B = 0.60$, $L/B = 7.5$, $B/H = 3.0$, Propeller Number 2501

All Figures are for Ship of 400 Ft Length BP													All Figures are for Ship of 600 Ft Length BP												
V/\sqrt{gL}	$C_t \times 10^3$	(K)	(C)	V/\sqrt{gL}	V	N	SHP	W_T	t	e_h	e_p	e_{rr}	EHP/SHp												
0.45	2.535	1.226	0.673	0.445	11.0	71.2	2207	0.335	0.132	1.304	0.620	0.945	0.764												
0.50	2.534	1.362	0.673	0.486	12.0	77.4	2772	0.334	0.151	1.274	0.622	0.959	0.761												
0.55	2.543	1.499	0.675	0.526	13.0	83.8	3444	0.332	0.159	1.259	0.624	0.978	0.768												
0.60	2.550	1.635	0.677	0.566	14.0	90.8	4272	0.323	0.169	1.229	0.626	0.995	0.766												
0.65	2.548	1.771	0.676	0.607	15.0	97.5	5241	0.324	0.179	1.215	0.623	1.012	0.771												
0.70	2.585	1.908	0.686	0.628	15.5	101.3	5806	0.320	0.177	1.209	0.625	1.017	0.770												
0.75	2.622	2.044	0.696	0.648	16.0	104.8	6438	0.319	0.175	1.211	0.625	1.019	0.771												
0.80	2.659	2.180	0.706	0.668	16.5	108.7	7116	0.315	0.178	1.199	0.626	1.025	0.769												
0.825	2.685	2.248	0.713	0.688	17.0	112.5	7849	0.310	0.177	1.193	0.626	1.031	0.770												
0.85	2.734	2.316	0.726	0.708	17.5	116.3	8636	0.306	0.181	1.179	0.626	1.033	0.768												
0.875	2.860	2.384	0.759	0.729	18.0	119.8	9462	0.305	0.180	1.181	0.627	1.031	0.763												
0.90	3.048	2.452	0.809	0.749	18.5	123.5	10300	0.302	0.180	1.175	0.627	1.035	0.764												
0.925	3.301	2.521	0.876	0.769	19.0	127.0	11250	0.302	0.181	1.173	0.627	1.033	0.755												
0.95	3.536	2.589	0.939	0.790	19.5	130.8	12250	0.296	0.182	1.163	0.629	1.031	0.753												
0.975	3.746	2.657	0.995	0.810	20.0	134.5	13350	0.294	0.183	1.157	0.629	1.029	0.749												
1.000	3.884	2.725	1.022	0.830	20.5	138.7	14670	0.291	0.180	1.157	0.628	1.024	0.744												
1.025	3.956	2.793	1.051	0.851	21.0	142.7	16180	0.289	0.176	1.159	0.627	1.018	0.740												
1.050	3.982	2.861	1.058	0.871	21.5	147.8	18090	0.285	0.175	1.153	0.625	1.018	0.734												
1.075	3.968	2.929	1.059	0.891	22.0	153.5	20390	0.282	0.166	1.160	0.620	1.018	0.732												
1.100	4.019	2.998	1.067	0.911	22.5	160.2	23600	0.280	0.165	1.161	0.614	1.018	0.726												
				0.932	23.0	167.2	27290	0.278	0.165	1.156	0.607	1.021	0.717												
				0.952	23.5	174.2	31180	0.275	0.167	1.148	0.601	1.022	0.706												
				0.972	24.0	180.9	35140	0.271	0.169	1.139	0.596	1.026	0.697												
				0.992	24.5	187.3	39290	0.264	0.171	1.126	0.594	1.023	0.684												
				1.013	25.0	192.5	42860	0.266	0.175	1.124	0.591	1.025	0.681												
				1.033	25.5	197.0	46150	0.266	0.176	1.123	0.589	1.023	0.677												
				1.053	26.0	201.3	49070	0.263	0.172	1.123	0.590	1.024	0.678												
				1.074	26.5	205.0	51730	0.262	0.171	1.123	0.591	1.025	0.680												
				1.094	27.0	209.0	54710	0.266	0.170	1.130	0.588	1.032	0.686												

TABLE B-18

Results of Resistance and Self-Propulsion Experiments

Model Number 4254, $C_B = 0.60$, $L/B = 8.5$, $B/H = 3.0$, Propeller Number 2765

All Figures are for Ship of 400 Ft Length BP				All Figures are for Ship of 600 Ft Length BP									
$V/\sqrt{g_L}$	$C_t \times 10^3$	(K)	(C)	$V/\sqrt{g_L}$	V	M	SHP	W_T	t	σ_h	σ_p	σ_{rr}	EHP/SHP
0.45	2.526	1.278	0.698	0.445	11.0	71.5	2000	0.321	0.147	1.256	0.609	0.901	0.689
0.50	2.505	1.420	0.692	0.486	12.0	77.7	2516	0.325	0.162	1.242	0.609	0.919	0.695
0.55	2.488	1.563	0.688	0.526	13.0	84.0	3130	0.326	0.167	1.235	0.610	0.931	0.701
0.60	2.484	1.705	0.686	0.566	14.0	91.0	3905	0.319	0.170	1.219	0.612	0.945	0.704
0.65	2.507	1.847	0.693	0.607	15.0	98.0	4810	0.316	0.168	1.217	0.611	0.958	0.713
0.70	2.541	1.989	0.702	0.628	15.5	102.0	5361	0.308	0.169	1.201	0.613	0.966	0.712
0.75	2.567	2.131	0.709	0.648	16.0	105.5	5919	0.307	0.169	1.199	0.612	0.970	0.712
0.80	2.601	2.273	0.719	0.668	16.5	109.5	6583	0.305	0.172	1.192	0.612	0.978	0.712
0.825	2.632	2.344	0.727	0.688	17.0	113.2	7238	0.307	0.174	1.192	0.610	0.985	0.714
0.850	2.687	2.415	0.743	0.708	17.5	116.8	7948	0.309	0.177	1.190	0.607	0.991	0.716
0.875	2.789	2.486	0.771	0.729	18.0	120.8	8730	0.301	0.178	1.176	0.610	0.993	0.712
0.90	2.939	2.556	0.812	0.749	18.5	124.4	9540	0.299	0.178	1.173	0.610	0.994	0.710
0.925	3.144	2.628	0.869	0.769	19.0	128.0	10370	0.296	0.177	1.169	0.612	0.994	0.711
0.95	3.329	2.699	0.920	0.790	19.5	131.5	11190	0.293	0.177	1.165	0.612	0.994	0.709
0.975	3.481	2.770	0.962	0.810	20.0	135.3	12130	0.286	0.176	1.153	0.615	0.993	0.704
1.000	3.598	2.841	0.995	0.830	20.5	139.4	13130	0.278	0.172	1.147	0.618	0.998	0.707
1.025	3.671	2.912	1.015	0.851	21.0	144.3	14350	0.274	0.166	1.149	0.618	1.001	0.710
1.050	3.689	2.983	1.020	0.871	21.5	148.6	15930	0.273	0.164	1.151	0.614	1.005	0.709
1.075	3.678	3.054	1.017	0.891	22.0	154.2	17940	0.271	0.154	1.161	0.609	1.005	0.711
1.100	3.681	3.125	1.017	0.911	22.5	159.6	20520	0.265	0.158	1.145	0.605	1.005	0.697
				0.932	23.0	168.0	23650	0.257	0.158	1.133	0.599	1.005	0.683
				0.952	23.5	175.2	27200	0.249	0.164	1.113	0.596	1.005	0.666
				0.972	24.0	181.2	30170	0.249	0.164	1.113	0.590	1.005	0.660
				0.992	24.5	186.6	33290	0.247	0.158	1.118	0.587	0.999	0.656
				1.013	25.0	190.9	35950	0.252	0.152	1.133	0.583	0.998	0.659
				1.033	25.5	195.4	38470	0.252	0.150	1.136	0.582	0.997	0.659
				1.053	26.0	199.3	40820	0.251	0.148	1.137	0.582	1.002	0.663
				1.074	26.5	203.4	43290	0.252	0.152	1.134	0.581	1.006	0.663
				1.094	27.0	207.5	45970	0.249	0.152	1.129	0.582	1.009	0.663

TABLE B-19

Results of Resistance and Self-Propulsion Experiments

Model Number 4272, $C_B = 0.65$, $L/B = 6.25$, $B/H = 3.0$, Propeller Number 3378

All Figures are for Ship of 400 Ft Length BP				All Figures are for Ship of 600 Ft Length BP									
$V/\sqrt{L_{WL}}$	$C_t \times 10^3$	(K)	(C)	$V/\sqrt{L_{WL}}$	V	N	SNP	W_T	t	θ_h	θ_p	θ_{rr}	EXP/SNP
0.40	2.854	1.012	0.703	0.405	10.0	46.1	2072	0.341	0.214	1.190	0.600	1.146	0.819
0.45	2.847	1.139	0.702	0.445	11.0	49.7	2660	0.355	0.220	1.211	0.600	1.121	0.815
0.50	2.844	1.265	0.701	0.486	12.0	53.7	3427	0.362	0.218	1.226	0.601	1.093	0.805
0.55	2.841	1.392	0.700	0.526	13.0	58.0	4396	0.363	0.214	1.233	0.602	1.073	0.796
0.60	2.844	1.518	0.701	0.566	14.0	62.5	5605	0.362	0.207	1.242	0.603	1.050	0.786
0.625	2.860	1.582	0.705	0.587	14.5	64.9	6323	0.357	0.202	1.241	0.605	1.040	0.781
0.65	2.882	1.645	0.710	0.607	15.0	67.4	7126	0.353	0.200	1.237	0.605	1.033	0.774
0.675	2.912	1.708	0.718	0.628	15.5	70.1	7987	0.346	0.197	1.227	0.608	1.031	0.769
0.70	2.935	1.771	0.723	0.648	16.0	72.8	8935	0.341	0.194	1.222	0.609	1.028	0.765
0.725	2.963	1.835	0.730	0.668	16.5	75.5	9978	0.336	0.194	1.213	0.610	1.026	0.759
0.75	2.992	1.898	0.737	0.688	17.0	78.3	11030	0.332	0.194	1.205	0.610	1.033	0.760
0.775	3.000	1.961	0.739	0.708	17.5	81.0	12190	0.327	0.196	1.194	0.611	1.036	0.755
0.80	3.024	2.024	0.745	0.729	18.0	83.7	13370	0.323	0.197	1.185	0.611	1.040	0.753
0.825	3.076	2.088	0.758	0.749	18.5	86.2	14610	0.322	0.198	1.182	0.611	1.040	0.751
0.85	3.197	2.151	0.788	0.769	19.0	88.6	15900	0.322	0.198	1.183	0.610	1.042	0.752
0.875	3.482	2.214	0.858	0.790	19.5	90.9	17140	0.324	0.198	1.187	0.609	1.044	0.755
0.90	3.916	2.277	0.965	0.810	20.0	93.2	18620	0.329	0.197	1.197	0.605	1.045	0.757
0.925	4.481	2.341	1.104	0.830	20.5	96.3	20570	0.327	0.197	1.193	0.604	1.044	0.752
0.95	5.061	2.404	1.247	0.851	21.0	100.1	23300	0.325	0.199	1.187	0.597	1.045	0.740
0.975	5.631	2.467	1.388	0.871	21.5	105.0	27170	0.313	0.194	1.174	0.594	1.040	0.725
1.000	6.146	2.530	1.514	0.891	22.0	110.8	32600	0.304	0.183	1.173	0.586	1.036	0.713
1.025	6.531	2.594	1.610	0.911	22.5	117.8	40170	0.293	0.176	1.164	0.576	1.027	0.689
				0.932	23.0	125.3	49860	0.280	0.167	1.156	0.568	1.016	0.667
				0.952	23.5	133.2	61450	0.264	0.163	1.138	0.561	1.003	0.640
				0.972	24.0	140.7	73760	0.248	0.163	1.112	0.557	0.994	0.616
				0.992	24.5	148.2	87180	0.230	0.160	1.092	0.556	0.988	0.600
				1.013	25.0	155.1	101400	0.212	0.154	1.075	0.555	0.979	0.584
				1.033	25.5	162.1	118200	0.197	0.153	1.057	0.554	0.977	0.572
				1.053	26.0	169.5	134700	0.194	0.148	1.057	0.547	0.978	0.566

TABLE B-20

Results of Resistance and Self-Propulsion Experiments
 Model Number 4275, $C_B = 0.65$, $L/B = 7.25$, $B/H = 3.0$, Propeller Number 3645

All Figures are for Ship of 400 Ft Length BP					All Figures are for Ship of 600 Ft Length BP									
$V/\sqrt{L_{WL}}$	$C_t \times 10^3$	(K)	(C)		$V/\sqrt{L_{WL}}$	V	N	SHP	Wt	t	σ_h	σ_p	σ_{TP}	EHP/SHP
0.40	2.681	1.064	0.694		0.486	12.0	68.1	2951	0.337	0.184	1.231	0.595	1.065	0.780
0.45	2.656	1.196	0.687		0.526	13.0	73.9	3837	0.337	0.189	1.224	0.595	1.045	0.761
0.50	2.634	1.329	0.682		0.566	14.0	80.0	4906	0.332	0.192	1.210	0.596	1.035	0.747
0.55	2.635	1.462	0.682		0.587	14.5	82.9	5489	0.332	0.192	1.210	0.596	1.033	0.745
0.60	2.664	1.595	0.689		0.607	15.0	86.0	6148	0.330	0.190	1.209	0.596	1.031	0.742
0.625	2.685	1.662	0.695		0.628	15.5	89.2	6866	0.329	0.190	1.206	0.595	1.031	0.740
0.65	2.703	1.728	0.700		0.648	16.0	92.6	7632	0.323	0.191	1.194	0.596	1.033	0.736
0.675	2.723	1.795	0.705		0.668	16.5	96.0	8477	0.317	0.191	1.183	0.598	1.035	0.731
0.70	2.743	1.861	0.710		0.688	17.0	99.4	9346	0.309	0.191	1.171	0.600	1.037	0.729
0.725	2.763	1.928	0.715		0.708	17.5	102.8	10290	0.304	0.190	1.164	0.601	1.038	0.726
0.75	2.782	1.994	0.720		0.729	18.0	106.2	11260	0.296	0.189	1.153	0.604	1.041	0.725
0.775	2.797	2.060	0.724		0.749	18.5	109.5	12330	0.293	0.186	1.152	0.604	1.040	0.724
0.80	2.821	2.127	0.730		0.769	19.0	112.6	13420	0.293	0.184	1.154	0.604	1.040	0.725
0.825	2.858	2.194	0.740		0.790	19.5	115.8	14620	0.293	0.182	1.157	0.604	1.039	0.726
0.85	2.950	2.260	0.764		0.810	20.0	119.2	15940	0.292	0.183	1.154	0.605	1.038	0.724
0.875	3.162	2.326	0.818		0.830	20.5	122.9	17580	0.290	0.189	1.141	0.603	1.038	0.714
0.90	3.491	2.393	0.904		0.851	21.0	127.3	19630	0.289	0.193	1.134	0.598	1.040	0.705
0.925	3.956	2.459	1.024		0.871	21.5	132.8	22630	0.285	0.188	1.135	0.590	1.040	0.696
0.95	4.456	2.526	1.153		0.891	22.0	139.6	26820	0.280	0.181	1.137	0.581	1.036	0.685
0.975	4.956	2.592	1.283		0.911	22.5	147.4	32230	0.275	0.176	1.137	0.571	1.034	0.672
1.000	5.331	2.659	1.380		0.932	23.0	155.0	39060	0.265	0.174	1.124	0.562	1.030	0.651
1.025	5.531	2.725	1.432		0.952	23.5	165.4	47190	0.250	0.170	1.107	0.556	1.025	0.631
					0.972	24.0	174.7	56460	0.234	0.167	1.088	0.551	1.018	0.610
					0.992	24.5	183.4	66530	0.215	0.160	1.070	0.549	1.003	0.589
					1.013	25.0	190.6	76360	0.194	0.154	1.050	0.550	0.981	0.566
					1.033	25.5	196.9	85870	0.171	0.147	1.029	0.555	0.953	0.544

TABLE B-21
Results of Resistance and Self-Propulsion Experiments
Model Number 4274, $C_B = 0.65$, $L/B = 8.25$, $B/H = 3.0$, Propeller Number 2813

All Figures are for Ship of 400 Ft Length BP					All Figures are for Ship of 600 Ft Length BP									
$V/\sqrt{L_{WL}}$	$C_t \times 10^3$	(K)	(C)		$V/\sqrt{L_{WL}}$	V	M	ESP	W_T	t	η_h	η_p	η_{TP}	ESP/HP
0.40	2.571	1.110	0.695		0.486	12.0	72.1	2807	0.255	0.087	1.226	0.626	0.893	0.685
0.45	2.546	1.249	0.688		0.526	13.0	78.1	3511	0.257	0.103	1.208	0.625	0.911	0.688
0.50	2.524	1.388	0.682		0.566	14.0	84.7	4383	0.255	0.118	1.184	0.624	0.931	0.687
0.55	2.519	1.527	0.681		0.587	14.5	87.9	4879	0.256	0.123	1.180	0.622	0.939	0.689
0.60	2.536	1.666	0.685		0.607	15.0	91.2	5423	0.257	0.128	1.173	0.620	0.947	0.689
0.625	2.550	1.735	0.689		0.628	15.5	94.6	6021	0.256	0.135	1.164	0.619	0.956	0.689
0.65	2.568	1.804	0.694		0.648	16.0	98.1	6666	0.256	0.141	1.156	0.617	0.966	0.689
0.675	2.585	1.874	0.698		0.668	16.5	101.8	7400	0.253	0.145	1.145	0.617	0.972	0.686
0.70	2.606	1.943	0.704		0.688	17.0	105.3	8171	0.251	0.146	1.141	0.616	0.978	0.688
0.725	2.628	2.012	0.710		0.708	17.5	109.1	9035	0.245	0.145	1.133	0.617	0.982	0.686
0.75	2.650	2.082	0.716		0.729	18.0	112.9	9954	0.238	0.145	1.123	0.618	0.985	0.683
0.775	2.672	2.151	0.722		0.749	18.5	116.6	10920	0.233	0.144	1.117	0.619	0.986	0.682
0.80	2.704	2.221	0.730		0.769	19.0	120.2	11920	0.230	0.145	1.109	0.619	0.990	0.680
0.825	2.748	2.290	0.742		0.790	19.5	123.8	12950	0.226	0.148	1.100	0.619	0.995	0.678
0.85	2.822	2.359	0.762		0.810	20.0	127.4	14050	0.224	0.149	1.097	0.619	1.000	0.679
0.875	2.987	2.429	0.807		0.830	20.5	131.2	15330	0.225	0.150	1.096	0.617	1.004	0.679
0.90	3.281	2.498	0.886		0.851	21.0	135.7	17010	0.225	0.154	1.091	0.615	1.009	0.677
0.925	3.664	2.568	0.990		0.871	21.5	141.3	19380	0.224	0.156	1.088	0.611	1.010	0.671
0.950	4.041	2.637	1.092		0.891	22.0	148.6	22750	0.220	0.157	1.081	0.604	1.015	0.662
0.975	4.376	2.706	1.182		0.911	22.5	156.6	27250	0.214	0.159	1.070	0.590	1.017	0.642
1.000	4.621	2.776	1.248		0.932	23.0	165.2	33000	0.210	0.165	1.057	0.574	1.020	0.618
1.025	4.751	2.845	1.284		0.952	23.5	174.4	39250	0.204	0.171	1.042	0.564	1.020	0.599
					0.972	24.0	182.6	45370	0.197	0.171	1.033	0.559	1.021	0.590
					0.992	24.5	189.6	51040	0.191	0.164	1.033	0.555	1.022	0.586
					1.013	25.0	196.6	56780	0.172	0.155	1.021	0.558	1.020	0.581
					1.033	25.5	203.0	62460	0.156	0.149	1.008	0.561	1.016	0.574

TABLE B-22

Results of Resistance and Self-Propulsion Experiments

Model Number 4256, $C_B = 0.70$, $L/B = 6.0$, $B/H = 3.0$, Propeller Number 3380

All Figures are for Ship of 400 Ft Length BP				All Figures are for Ship of 600 Ft Length BP									
$V/\sqrt{L_{WL}}$	$C_t \times 10^3$	(K)	(C)	$V/\sqrt{L_{WL}}$	V	N	SEP	W_T	t	ϕ_h	ϕ_p	ϕ_{rr}	KSP/SBP
0.40	3.013	0.986	0.730	0.364	9.0	39.8	1918	0.397	0.211	1.308	0.555	1.094	0.766
0.45	2.993	1.110	0.725	0.405	10.0	43.6	2491	0.402	0.219	1.307	0.557	1.068	0.777
0.50	2.991	1.233	0.725	0.445	11.0	47.8	3255	0.400	0.222	1.298	0.561	1.068	0.777
0.55	3.024	1.356	0.733	0.486	12.0	52.1	4204	0.401	0.218	1.306	0.560	1.070	0.783
0.60	3.076	1.479	0.745	0.526	13.0	56.8	5410	0.395	0.215	1.298	0.562	1.074	0.784
0.625	3.106	1.541	0.752	0.566	14.0	61.6	6916	0.388	0.211	1.289	0.564	1.073	0.779
0.65	3.136	1.603	0.760	0.607	15.0	66.7	8712	0.380	0.210	1.272	0.566	1.073	0.773
0.675	3.157	1.664	0.765	0.628	15.5	69.1	9751	0.377	0.208	1.272	0.566	1.069	0.770
0.70	3.195	1.726	0.774	0.648	16.0	71.6	10810	0.374	0.210	1.262	0.566	1.071	0.766
0.725	3.259	1.788	0.790	0.668	16.5	74.1	11940	0.373	0.210	1.260	0.566	1.071	0.764
0.75	3.344	1.849	0.810	0.688	17.0	76.6	13240	0.370	0.211	1.254	0.566	1.072	0.761
0.775	3.433	1.911	0.832	0.708	17.5	79.3	14690	0.369	0.211	1.251	0.565	1.073	0.757
0.80	3.544	1.972	0.859	0.729	18.0	82.1	16290	0.366	0.210	1.246	0.564	1.075	0.755
0.825	3.655	2.034	0.886	0.749	18.5	85.2	18110	0.357	0.210	1.227	0.566	1.076	0.748
0.85	3.800	2.096	0.921	0.769	19.0	88.4	20250	0.347	0.209	1.212	0.568	1.073	0.739
0.875	4.097	2.157	0.993	0.790	19.5	91.7	22550	0.342	0.211	1.199	0.567	1.076	0.731
0.90	4.771	2.219	1.156	0.810	20.0	94.9	25180	0.340	0.213	1.192	0.565	1.073	0.722
				0.830	20.5	98.0	28200	0.343	0.206	1.208	0.559	1.065	0.719
				0.851	21.0	101.8	32010	0.341	0.198	1.216	0.554	1.060	0.714
				0.891	22.0	113.5	44610	0.298	0.169	1.183	0.554	1.054	0.691

TABLE B-23

Results of Resistance and Self-Propulsion Experiments

Model Number 4259, $C_B = 0.70$, $L/B = 7.0$, $B/H = 3.0$, Propeller Number 2502

All Figures are for Ship of 400 Ft Length BP					All Figures are for Ship of 600 Ft Length BP								
$V/\sqrt{L_{WL}}$	$C_t \times 10^3$	(K)	(C)	$V/\sqrt{L_{WL}}$	V	M	SHP	W_T	t	θ_h	θ_p	θ_{rr}	ESP/SHP
0.40	2.903	1.038	0.744	0.364	9.0	48.3	1858	0.319	0.193	1.185	0.547	0.983	0.638
0.45	2.901	1.168	0.743	0.405	10.0	52.9	2407	0.330	0.189	1.210	0.547	0.991	0.656
0.50	2.896	1.298	0.742	0.445	11.0	57.9	3140	0.337	0.184	1.230	0.552	0.980	0.665
0.55	2.933	1.428	0.751	0.486	12.0	63.2	4074	0.340	0.181	1.242	0.552	0.980	0.672
0.60	2.975	1.557	0.762	0.526	13.0	68.8	5209	0.342	0.183	1.242	0.550	0.989	0.675
0.625	2.990	1.622	0.766	0.566	14.0	74.3	6525	0.346	0.188	1.241	0.541	1.012	0.679
0.65	2.996	1.687	0.767	0.607	15.0	80.1	8170	0.339	0.191	1.224	0.541	1.015	0.671
0.675	3.004	1.752	0.769	0.628	15.5	82.9	9061	0.340	0.191	1.225	0.539	1.016	0.671
0.70	3.023	1.817	0.774	0.648	16.0	85.8	10030	0.332	0.189	1.215	0.543	1.017	0.670
0.725	3.059	1.882	0.783	0.668	16.5	88.7	11020	0.328	0.184	1.211	0.546	1.017	0.672
0.75	3.121	1.947	0.799	0.688	17.0	91.4	12000	0.319	0.176	1.211	0.551	1.015	0.678
0.775	3.207	2.012	0.821	0.708	17.5	94.2	13160	0.315	0.169	1.213	0.553	1.010	0.678
0.80	3.307	2.076	0.847	0.729	18.0	96.9	14510	0.321	0.166	1.228	0.549	1.003	0.677
0.825	3.398	2.141	0.870	0.749	18.5	100.2	16120	0.322	0.169	1.226	0.546	1.001	0.670
0.85	3.517	2.206	0.901	0.769	19.0	104.4	18150	0.315	0.178	1.200	0.545	1.005	0.657
0.875	3.737	2.271	0.957	0.790	19.5	108.8	20470	0.310	0.184	1.183	0.542	1.009	0.647
0.90	4.276	2.336	1.095	0.810	20.0	113.2	23140	0.305	0.188	1.169	0.539	1.008	0.635
				0.830	20.5	117.3	25890	0.301	0.191	1.156	0.536	1.010	0.625
				0.851	21.0	121.7	28950	0.298	0.196	1.143	0.531	1.017	0.617
				0.891	22.0	132.8	38460	0.294	0.164	1.183	0.516	1.012	0.617

TABLE B-24
Results of Resistance and Self-Propulsion Experiments
Model Number 4258, $C_B = 0.70$, $L/B = 8.0$, $B/H = 3.0$, Propeller Number 3488

All Figures are for Ship of 400 Ft Length BP

All Figures are for Ship of 600 Ft Length BP

$V/\sqrt{L_{WL}}$	$C_t \times 10^3$	(K)	(C)	$V/\sqrt{L_{WL}}$	V	N	SHP	W_T	t	e_h	e_p	e_π	EHP/SHP
0.40	2.539	1.086	0.677	0.364	9.0	55.7	1336	0.386	0.168	1.355	0.549	0.973	0.724
0.45	2.545	1.221	0.679	0.405	10.0	61.2	1747	0.388	0.184	1.333	0.553	0.982	0.723
0.50	2.562	1.357	0.683	0.445	11.0	67.1	2266	0.379	0.188	1.308	0.560	0.993	0.727
0.55	2.592	1.492	0.691	0.486	12.0	73.7	2940	0.365	0.194	1.271	0.567	1.001	0.720
0.60	2.636	1.628	0.703	0.526	13.0	80.3	3757	0.357	0.191	1.258	0.570	1.012	0.725
0.625	2.661	1.696	0.710	0.566	14.0	87.3	4755	0.346	0.189	1.240	0.573	1.022	0.725
0.65	2.689	1.764	0.717	0.607	15.0	94.4	5936	0.338	0.191	1.221	0.574	1.034	0.725
0.675	2.713	1.832	0.724	0.628	15.5	98.0	6575	0.334	0.191	1.215	0.575	1.042	0.727
0.70	2.742	1.900	0.731	0.648	16.0	101.5	7275	0.331	0.194	1.205	0.575	1.046	0.725
0.725	2.781	1.967	0.742	0.668	16.5	104.8	8049	0.330	0.193	1.205	0.575	1.041	0.721
0.75	2.851	2.035	0.760	0.688	17.0	108.3	8925	0.328	0.195	1.198	0.575	1.036	0.713
0.775	2.953	2.103	0.788	0.708	17.5	112.2	9939	0.324	0.200	1.183	0.575	1.034	0.704
0.80	3.051	2.171	0.814	0.729	18.0	116.3	11060	0.318	0.200	1.173	0.575	1.035	0.698
0.825	3.140	2.239	0.837	0.749	18.5	120.6	12340	0.312	0.197	1.167	0.575	1.036	0.695
0.85	3.242	2.307	0.865	0.769	19.0	125.2	13750	0.306	0.191	1.165	0.574	1.039	0.698
0.875	3.432	2.374	0.915	0.790	19.5	129.9	15400	0.301	0.186	1.165	0.573	1.040	0.693
0.90	3.781	2.442	1.008	0.810	20.0	134.6	17190	0.300	0.189	1.159	0.569	1.041	0.686
				0.830	20.5	139.4	19210	0.297	0.190	1.153	0.566	1.039	0.678
				0.851	21.0	144.2	21510	0.303	0.191	1.161	0.559	1.037	0.673
				0.891	22.0	157.8	28560	0.286	0.181	1.148	0.550	1.035	0.653

TABLE B-25
Results of Resistance and Self-Propulsion Experiments
Model Number 4276, $C_B = 0.75$, $L/B = 5.75$, $B/H = 3.0$, Propeller Number 3446

All Figures are for Ship of 400 Ft Length BP				All Figures are for Ship of 600 Ft Length BP									
V/\sqrt{L}	$C_t \times 10^3$	ζ	ζ	V/\sqrt{L}	V	R	C_{DP}	W_T	t	e_h	e_p	e_{tr}	EHP/SHIP
0.35	3.121	0.841	0.744	0.364	9.0	38.6	2014	0.403	0.219	1.309	0.569	1.056	0.786
0.40	3.091	0.961	0.737	0.405	10.0	42.4	2685	0.408	0.210	1.335	0.570	1.049	0.798
0.45	3.066	1.081	0.731	0.445	11.0	46.6	3520	0.401	0.205	1.326	0.576	1.052	0.803
0.50	3.049	1.202	0.726	0.486	12.0	51.1	4579	0.386	0.209	1.288	0.584	1.057	0.795
0.525	3.053	1.262	0.728	0.526	13.0	55.8	5879	0.375	0.207	1.269	0.587	1.063	0.793
0.55	3.063	1.322	0.730	0.566	14.0	60.5	7500	0.370	0.208	1.263	0.595	1.068	0.789
0.575	3.084	1.382	0.735	0.587	14.5	63.0	8401	0.370	0.206	1.262	0.585	1.072	0.792
0.60	3.121	1.442	0.744	0.607	15.0	65.6	9456	0.368	0.205	1.256	0.583	1.080	0.792
0.625	3.168	1.502	0.755	0.628	15.5	68.1	10680	0.367	0.207	1.246	0.582	1.080	0.783
0.65	3.222	1.562	0.768	0.648	16.0	70.6	11880	0.365	0.207	1.250	0.580	1.080	0.782
0.675	3.292	1.622	0.784	0.668	16.5	73.5	13500	0.365	0.211	1.237	0.577	1.079	0.770
0.70	3.432	1.682	0.818	0.688	17.0	76.6	15400	0.362	0.216	1.229	0.575	1.071	0.757
0.725	3.668	1.742	0.874	0.708	17.5	80.0	17780	0.360	0.214	1.228	0.571	1.063	0.746
0.75	4.007	1.802	0.955	0.729	18.0	83.6	20580	0.358	0.201	1.245	0.566	1.059	0.746
0.775	4.365	1.862	1.040	0.749	18.5	87.9	24040	0.355	0.191	1.254	0.559	1.062	0.744
0.80	4.704	1.922	1.121	0.769	19.0	92.5	28190	0.345	0.178	1.256	0.553	1.066	0.741
0.825	4.973	1.982	1.185	0.790	19.5	97.7	33470	0.336	0.172	1.246	0.547	1.064	0.725
0.85	5.192	2.043	1.237	0.810	20.0	103.0	40190	0.307	0.170	1.198	0.543	1.060	0.690
0.875	5.402	2.103	1.287	0.830	20.5	108.0	45680	0.291	0.170	1.171	0.551	1.054	0.650
				0.851	21.0	112.4	51220	0.284	0.169	1.160	0.553	1.048	0.672
				0.871	21.5	116.1	57550	0.285	0.170	1.160	0.547	1.041	0.660
				0.891	22.0	119.7	64220	0.287	0.170	1.164	0.543	1.028	0.649

TABLE B-26

Results of Resistance and Self-Propulsion Experiments
 Model Number 4279, $C_B = 0.75$, $L/B = 6.75$, $B/H = 3.0$, Propeller Number 3565

All Figures are for Ship of 400 Ft Length BP				All Figures are for Ship of 600 Ft Length BP									
V/\sqrt{L}	$C_t \times 10^3$	ζ	\odot	V/\sqrt{L}	V	N	SHP	W_T	t	θ_h	θ_p	θ_{rr}	EHP/SHP
0.35	2.866	0.887	0.720	0.364	9.0	47.2	1653	0.405	0.180	1.379	0.544	1.017	0.763
0.40	2.836	1.014	0.712	0.405	10.0	52.0	2158	0.408	0.183	1.382	0.546	1.033	0.780
0.45	2.836	1.141	0.712	0.445	11.0	57.3	2829	0.404	0.188	1.362	0.548	1.051	0.785
0.50	2.859	1.268	0.718	0.486	12.0	63.0	3701	0.397	0.191	1.342	0.549	1.066	0.786
0.525	2.868	1.331	0.720	0.526	13.0	68.9	4807	0.389	0.195	1.316	0.551	1.073	0.778
0.55	2.886	1.394	0.725	0.566	14.0	75.0	5823	0.380	0.198	1.294	0.554	1.078	0.773
0.575	2.916	1.458	0.733	0.587	14.5	77.9	6936	0.381	0.198	1.295	0.551	1.076	0.768
0.60	2.964	1.521	0.744	0.607	15.0	81.0	7866	0.382	0.198	1.296	0.549	1.070	0.761
0.625	3.030	1.584	0.761	0.628	15.5	84.2	8874	0.382	0.198	1.297	0.547	1.068	0.758
0.65	3.120	1.648	0.784	0.648	16.0	87.6	9984	0.381	0.202	1.287	0.544	1.072	0.751
0.675	3.232	1.711	0.812	0.668	16.5	91.3	11380	0.379	0.206	1.278	0.540	1.073	0.740
0.70	3.385	1.774	0.850	0.688	17.0	95.6	13070	0.370	0.207	1.259	0.538	1.074	0.728
0.725	3.560	1.838	0.894	0.708	17.5	100.2	15130	0.366	0.211	1.244	0.534	1.076	0.714
0.750	3.837	1.901	0.944	0.729	18.0	104.8	17490	0.369	0.211	1.251	0.524	1.080	0.708
0.775	4.267	1.965	1.072	0.749	18.5	109.9	20600	0.380	0.210	1.275	0.508	1.082	0.701
0.80	4.749	2.028	1.193	0.769	19.0	115.9	24510	0.384	0.198	1.301	0.496	1.085	0.700
0.825	5.098	2.091	1.281	0.790	19.5	123.2	29610	0.368	0.196	1.273	0.491	1.085	0.678
0.850	5.324	2.155	1.338	0.810	20.0	130.2	35290	0.357	0.198	1.246	0.487	1.081	0.655
0.875	5.522	2.218	1.387	0.830	20.5	136.3	40960	0.351	0.202	1.230	0.482	1.074	0.637
				0.851	21.0	141.9	46520	0.346	0.196	1.229	0.479	1.071	0.630
				0.871	21.5	147.2	52440	0.348	0.192	1.238	0.473	1.068	0.625
				0.891	22.0	152.3	58790	0.354	0.183	1.264	0.465	1.065	0.626

TABLE B-27

Results of Resistance and Self-Propulsion Experiments
Model Number 4278, $C_B = 0.75$, $L/B = 7.75$, $B/H = 3.0$, Propeller Number 3648

All Figures are for Ship of 400 Ft Length BP				All Figures are for Ship of 600 Ft Length BP									
$V/\sqrt{L_{WL}}$	$C_t \times 10^3$	(K)	(C)	$V/\sqrt{L_{WL}}$	V	N	SHP	W_T	t	θ_h	θ_p	θ_{TP}	EHP/SHP
0.35	2.726	0.929	0.717	0.364	9.0	64.6	1285	0.387	0.194	1.312	0.546	1.098	0.787
0.40	2.696	1.062	0.709	0.405	10.0	71.1	1734	0.392	0.197	1.322	0.547	1.084	0.783
0.45	2.683	1.195	0.706	0.445	11.0	78.2	2339	0.394	0.197	1.324	0.546	1.069	0.773
0.50	2.719	1.327	0.715	0.486	12.0	86.0	3152	0.386	0.196	1.310	0.548	1.051	0.755
0.525	2.751	1.394	0.724	0.526	13.0	94.1	4204	0.383	0.198	1.301	0.546	1.036	0.736
0.550	2.786	1.460	0.734	0.566	14.0	102.8	5564	0.376	0.199	1.282	0.545	1.024	0.715
0.575	2.828	1.526	0.744	0.587	14.5	107.4	6352	0.371	0.202	1.269	0.544	1.024	0.707
0.60	2.874	1.593	0.756	0.607	15.0	112.0	7214	0.366	0.204	1.254	0.544	1.024	0.699
0.625	2.938	1.659	0.773	0.628	15.5	116.6	8129	0.362	0.200	1.254	0.543	1.025	0.699
0.65	3.028	1.725	0.796	0.648	16.0	121.4	9186	0.358	0.198	1.250	0.542	1.026	0.696
0.675	3.152	1.792	0.829	0.668	16.5	126.4	10390	0.358	0.197	1.257	0.538	1.030	0.697
0.70	3.312	1.858	0.871	0.688	17.0	131.8	11850	0.363	0.195	1.264	0.529	1.038	0.694
0.725	3.500	1.925	0.921	0.708	17.5	137.7	13660	0.362	0.193	1.264	0.523	1.040	0.688
0.75	3.772	1.991	0.992	0.729	18.0	144.4	15770	0.362	0.192	1.266	0.513	1.055	0.686
0.775	4.122	2.057	1.084	0.749	18.5	152.0	18480	0.358	0.192	1.259	0.505	1.063	0.677
0.80	4.551	2.124	1.197	0.769	19.0	160.3	22030	0.355	0.192	1.253	0.496	1.061	0.660
0.825	4.878	2.190	1.283	0.790	19.5	169.1	26380	0.349	0.192	1.240	0.489	1.051	0.638
0.85	5.127	2.256	1.349	0.810	20.0	177.8	31070	0.345	0.192	1.234	0.481	1.050	0.623
0.875	5.292	2.323	1.392	0.830	20.5	186.2	35940	0.333	0.188	1.217	0.479	1.045	0.609
				0.851	21.0	194.1	40770	0.323	0.185	1.203	0.479	1.043	0.601
				0.891	22.0	209.0	50880	0.300	0.177	1.175	0.441	1.040	0.588

TABLE B-28

Results of Resistance and Self-Propulsion Experiments

Model Number 4260, $C_B = 0.80$, $L/B = 5.5$, $B/H = 3.0$, Propeller Number 3377

All Figures are for Ship of 400 Ft Length BP				All Figures are for Ship of 600 Ft Length BP									
$V/\sqrt{g L}$	$C_t \times 10^3$	ζ	\odot	$V/\sqrt{g L}$	V	N	SHP	W_T	t	e_h	e_p	e_{rr}	ERP/SHP
0.35	3.343	0.820	0.788	0.364	9.0	40.1	2346	0.420	0.238	1.314	0.558	1.078	0.789
0.40	3.313	0.937	0.781	0.405	10.0	44.2	3178	0.429	0.240	1.332	0.557	1.065	0.790
0.45	3.288	1.054	0.775	0.445	11.0	48.3	4195	0.436	0.244	1.340	0.554	1.060	0.788
0.50	3.276	1.171	0.772	0.466	11.5	50.6	4798	0.435	0.245	1.335	0.555	1.062	0.786
0.525	3.281	1.230	0.774	0.486	12.0	52.8	5451	0.430	0.244	1.325	0.558	1.061	0.785
0.55	3.311	1.288	0.781	0.506	12.5	55.2	6189	0.424	0.242	1.320	0.560	1.061	0.785
0.575	3.369	1.347	0.795	0.526	13.0	57.8	7012	0.415	0.237	1.305	0.566	1.064	0.784
0.60	3.464	1.405	0.817	0.547	13.5	60.3	7963	0.410	0.235	1.296	0.567	1.064	0.782
0.625	3.600	1.464	0.849	0.566	14.0	62.9	8980	0.406	0.233	1.291	0.568	1.070	0.784
0.65	3.785	1.522	0.892	0.587	14.5	65.6	10240	0.402	0.229	1.290	0.567	1.066	0.780
0.675	4.032	1.581	0.951	0.607	15.0	68.5	11730	0.398	0.226	1.285	0.566	1.063	0.774
0.70	4.395	1.640	1.036	0.628	15.5	71.6	13450	0.394	0.220	1.287	0.564	1.061	0.770
0.75	5.402	1.757	1.274	0.648	16.0	75.1	15550	0.389	0.220	1.277	0.561	1.063	0.762
0.80	6.659	1.874	1.570	0.688	17.0	83.4	21830	0.378	0.225	1.246	0.549	1.056	0.722
				0.729	18.0	93.8	32080	0.360	0.229	1.205	0.534	1.046	0.673
				0.769	19.0	105.5	46660	0.340	0.191	1.226	0.520	1.042	0.664
				0.810	20.0	117.8	65780	0.326	0.164	1.240	0.504	1.049	0.656

TABLE B-29

Results of Resistance and Self-Propulsion Experiments

Model Number 4263, $C_B = 0.80$, $L/B = 6.5$, $B/H = 3.0$, Propeller Number 3375

All Figures are for Ship of 400 Ft Length BP

All Figures are for Ship of 600 Ft Length BP

$v/\sqrt{L_{WL}}$	$C_t \times 10^3$	(K)	(C)	$v/\sqrt{L_{WL}}$	V	N	SHP	W_T	t	e_h	e_p	e_{rr}	EHP/SHP
0.35	2.983	0.867	0.745	0.364	9.0	48.0	1763	0.422	0.170	1.435	0.539	1.071	0.828
0.40	2.961	0.991	0.739	0.405	10.0	52.8	2328	0.432	0.175	1.453	0.535	1.083	0.842
0.450	2.956	1.114	0.738	0.445	11.0	58.0	3050	0.426	0.183	1.423	0.539	1.095	0.840
0.50	2.972	1.238	0.742	0.466	11.5	60.8	3482	0.423	0.185	1.413	0.540	1.101	0.840
0.525	2.985	1.300	0.745	0.486	12.0	63.5	3959	0.420	0.186	1.405	0.541	1.103	0.839
0.55	3.014	1.362	0.752	0.506	12.5	66.4	4497	0.419	0.190	1.396	0.541	1.107	0.835
0.575	3.089	1.424	0.771	0.526	13.0	69.2	5125	0.422	0.191	1.398	0.538	1.106	0.832
0.60	3.216	1.486	0.803	0.547	13.5	72.2	5850	0.422	0.191	1.400	0.537	1.105	0.828
0.625	3.388	1.548	0.846	0.566	14.0	75.4	6696	0.422	0.193	1.396	0.533	1.104	0.821
0.650	3.602	1.610	0.899	0.587	14.5	79.2	7746	0.416	0.192	1.382	0.532	1.105	0.812
0.675	3.872	1.672	0.966	0.607	15.0	83.3	9048	0.406	0.193	1.359	0.531	1.106	0.798
0.70	4.190	1.734	1.046	0.628	15.5	87.8	10660	0.397	0.195	1.335	0.530	1.101	0.778
0.75	5.022	1.857	1.253	0.648	16.0	92.8	12720	0.390	0.201	1.310	0.525	1.093	0.752
0.80	6.309	1.981	1.575	0.688	17.0	103.6	18270	0.378	0.218	1.257	0.515	1.076	0.696
				0.729	18.0	116.2	26920	0.365	0.220	1.229	0.502	1.050	0.648
				0.769	19.0	131.1	39870	0.349	0.188	1.247	0.486	1.033	0.627
				0.810	20.0	147.5	58810	0.325	0.162	1.241	0.474	1.013	0.596

TABLE B-30

Results of Resistance and Self-Propulsion Experiments
Model Number 4262, $C_B = 0.80$, $L/B = 7.5$, $B/H = 3.0$, Propeller Number 2501

All Figures are for Ship of 400 Ft Length BP				All Figures are for Ship of 600 Ft Length BP									
$V/\sqrt{L_{WL}}$	$C_t \times 10^3$	\odot	\odot	$V/\sqrt{L_{WL}}$	V	N	SHP	W_T	t	e_h	e_p	e_{rr}	EHP/SHP
0.35	2.791	0.909	0.728	0.364	9.0	61.3	1483	0.463	0.242	1.412	0.510	1.091	0.785
0.40	2.761	1.039	0.720	0.405	10.0	67.5	1959	0.458	0.242	1.399	0.518	1.091	0.790
0.45	2.748	1.169	0.716	0.445	11.0	74.2	2571	0.449	0.240	1.379	0.525	1.092	0.791
0.50	2.784	1.299	0.726	0.466	11.5	77.9	2954	0.440	0.236	1.365	0.530	1.089	0.788
0.525	2.831	1.364	0.738	0.486	12.0	81.4	3397	0.439	0.234	1.366	0.531	1.083	0.785
0.55	2.905	1.429	0.757	0.506	12.5	85.4	3931	0.428	0.230	1.348	0.535	1.073	0.775
0.575	3.022	1.494	0.788	0.526	13.0	89.5	4560	0.423	0.225	1.345	0.536	1.061	0.765
0.60	3.181	1.558	0.829	0.546	13.5	94.3	5316	0.405	0.220	1.311	0.544	1.055	0.751
0.625	3.388	1.624	0.883	0.566	14.0	98.6	6161	0.404	0.213	1.320	0.541	1.044	0.745
0.65	3.630	1.688	0.946	0.587	14.5	103.7	7172	0.395	0.207	1.310	0.541	1.044	0.739
0.675	3.892	1.753	1.015	0.607	15.0	109.0	8439	0.390	0.205	1.304	0.537	1.036	0.726
0.70	4.185	1.818	1.091	0.628	15.5	114.4	9925	0.391	0.203	1.308	0.530	1.028	0.713
0.75	4.942	1.948	1.288	0.648	16.0	120.1	11710	0.392	0.201	1.313	0.523	1.019	0.700
0.80	6.079	2.078	1.585	0.688	17.0	133.5	16460	0.381	0.204	1.287	0.511	1.013	0.666
				0.729	18.0	149.2	23280	0.363	0.194	1.265	0.501	1.011	0.641
				0.769	19.0	166.1	32890	0.356	0.175	1.281	0.483	1.011	0.626
				0.810	20.0	187.7	47580	0.334	0.170	1.246	0.468	1.025	0.598

TABLE B-31

Distance and Self-Propulsion Experiments

 $\eta = 0.60$, $L/B = 6.5$, $B/H = 3.5$, Propeller Number 2501

All Figures are for Ship of 400 Ft Length BP				All Figures are for Ship of 600 Ft Length BP									
Model Number				Result									
V/\sqrt{Lg}	$C_t \times 10^3$	(A)	(C)	V/\sqrt{Lg}	V	N	SRP	V_T	t	η_h	η_p	η_{TP}	SRP/BRP
0.45	2.687	1.200	0.706	0.486	12.0	80.3	3943	0.396	0.209	1.309	0.568	0.941	0.699
0.50	2.680	1.333	0.704	0.526	13.0	86.4	4240	0.377	0.207	1.273	0.584	0.949	0.705
0.55	2.669	1.466	0.701	0.566	14.0	93.6	5313	0.367	0.206	1.255	0.587	0.957	0.705
0.60	2.662	1.599	0.700	0.607	15.0	101.0	6582	0.358	0.201	1.244	0.590	0.963	0.708
0.65	2.690	1.733	0.706	0.628	15.5	104.5	7297	0.358	0.197	1.251	0.590	0.964	0.711
0.70	2.790	1.866	0.733	0.648	16.0	108.5	8108	0.356	0.196	1.248	0.591	0.962	0.710
0.75	2.824	1.999	0.741	0.668	16.5	112.0	8949	0.354	0.195	1.246	0.590	0.968	0.711
0.80	2.824	2.133	0.742	0.688	17.0	115.5	9807	0.352	0.192	1.247	0.589	0.974	0.716
0.825	2.841	2.199	0.746	0.708	17.5	119.5	10780	0.346	0.188	1.242	0.592	0.971	0.714
0.85	2.885	2.266	0.758	0.729	18.0	123.2	11770	0.344	0.189	1.237	0.592	0.975	0.714
0.875	2.989	2.333	0.785	0.749	18.5	127.0	12790	0.340	0.188	1.229	0.594	0.980	0.715
0.90	3.179	2.399	0.835	0.769	19.0	130.8	13840	0.334	0.190	1.216	0.596	0.984	0.713
0.925	3.449	2.466	0.906	0.790	19.5	134.5	14930	0.328	0.189	1.207	0.599	0.986	0.713
0.95	3.709	2.532	0.974	0.810	20.0	138.6	16190	0.320	0.191	1.190	0.602	0.989	0.708
0.975	3.921	2.599	1.030	0.830	20.5	142.5	17610	0.320	0.195	1.183	0.601	0.991	0.704
1.00	4.066	2.666	1.068	0.851	21.0	147.2	19480	0.319	0.200	1.175	0.599	0.988	0.695
1.025	4.188	2.732	1.100	0.871	21.5	152.0	21830	0.317	0.201	1.170	0.594	0.989	0.687
1.05	4.270	2.799	1.122	0.891	22.0	158.6	24880	0.315	0.201	1.167	0.589	0.991	0.681
1.075	4.333	2.866	1.138	0.911	22.5	166.0	28600	0.313	0.200	1.164	0.583	0.993	0.674
1.10	4.399	2.932	1.155	0.932	23.0	173.0	32600	0.309	0.199	1.159	0.577	0.999	0.668
				0.952	23.5	180.2	37430	0.305	0.200	1.151	0.570	1.001	0.656
				0.972	24.0	187.0	42340	0.303	0.202	1.145	0.564	0.998	0.645
				0.992	24.5	193.8	47480	0.295	0.202	1.133	0.564	0.990	0.633
				1.013	25.0	199.8	52430	0.293	0.202	1.129	0.561	0.989	0.626
				1.033	25.5	205.5	57230	0.289	0.200	1.125	0.560	0.984	0.620
				1.053	26.0	210.5	61680	0.289	0.200	1.125	0.557	0.990	0.620
				1.074	26.5	215.5	66130	0.288	0.196	1.129	0.556	0.992	0.622
				1.094	27.0	220.5	70890	0.284	0.187	1.135	0.556	0.991	0.626

TABLE B-32

Results of Resistance and Self-Propulsion Experiments

Model Number 4253, $C_B = 0.60$, $L/B = 7.5$, $B/H = 3.5$, Propeller Number 2765

All Figures are for Ship of 400 Ft Length BP				All Figures are for Ship of 600 Ft Length BP									
$V/\sqrt{L_{WL}}$	$C_t \times 10^3$	ζ	\odot	$V/\sqrt{L_{WL}}$	V	N	SHP	W_T	t	θ_h	θ_p	θ_{Pr}	EHP/SHP
0.45	2.563	1.258	0.703	0.486	12.0	79.7	2429	0.312	0.119	1.281	0.607	1.029	0.800
0.50	2.546	1.398	0.598	0.526	13.0	86.1	3070	0.319	0.128	1.280	0.604	1.033	0.799
0.55	2.540	1.538	0.697	0.566	14.0	93.2	3900	0.316	0.141	1.256	0.605	1.039	0.790
0.60	2.536	1.678	0.695	0.607	15.0	100.8	4858	0.307	0.155	1.219	0.605	1.045	0.771
0.65	2.551	1.817	0.699	0.628	15.5	104.8	5427	0.301	0.160	1.202	0.606	1.050	0.765
0.70	2.590	1.957	0.710	0.648	16.0	108.7	6034	0.296	0.164	1.189	0.607	1.053	0.760
0.75	2.624	2.097	0.719	0.668	16.5	112.5	6704	0.293	0.167	1.178	0.607	1.050	0.751
0.80	2.640	2.237	0.724	0.688	17.0	116.2	7381	0.293	0.17	1.175	0.606	1.052	0.749
0.825	2.661	2.307	0.730	0.708	17.5	119.5	8129	0.297	0.169	1.182	0.604	1.043	0.745
0.85	2.710	2.376	0.743	0.729	18.0	123.5	8972	0.290	0.165	1.176	0.607	1.038	0.741
0.875	2.830	2.446	0.776	0.749	18.5	127.3	9871	0.284	0.160	1.173	0.609	1.029	0.735
0.90	2.998	2.516	0.822	0.769	19.0	131.5	10820	0.273	0.147	1.172	0.614	1.018	0.732
0.925	3.187	2.586	0.874	0.790	19.5	135.0	11830	0.266	0.141	1.170	0.617	1.008	0.728
0.95	3.408	2.656	0.934	0.810	20.0	139.2	12940	0.258	0.140	1.159	0.619	1.005	0.721
0.975	3.579	2.726	0.981	0.830	20.5	143.5	14200	0.254	0.146	1.145	0.619	1.005	0.712
1.000	3.701	2.796	1.015	0.850	21.0	147.5	15600	0.261	0.151	1.149	0.614	1.004	0.708
1.025	3.781	2.866	1.037	0.871	21.5	152.7	17440	0.262	0.153	1.148	0.609	1.007	0.703
1.050	3.815	2.936	1.046	0.891	22.0	159.0	19850	0.256	0.152	1.139	0.605	1.005	0.692
1.075	3.833	3.006	1.051	0.911	22.5	165.0	22680	0.248	0.152	1.127	0.604	1.004	0.684
1.100	3.879	3.076	1.064	0.932	23.0	172.5	26360	0.240	0.153	1.115	0.595	1.001	0.664
				0.952	23.5	180.8	30220	0.238	0.153	1.111	0.588	1.000	0.653
				0.972	24.0	186.9	33590	0.234	0.152	1.108	0.585	1.000	0.648
				0.992	24.5	192.4	36730	0.234	0.146	1.114	0.582	1.003	0.650
				1.013	25.0	197.0	39680	0.228	0.145	1.108	0.581	1.002	0.647
				3	25.5	202.5	42940	0.225	0.144	1.105	0.582	0.999	0.642
				53	26.0	207.2	46270	0.222	0.142	1.104	0.582	0.994	0.638
				74	26.5	212.5	49500	0.222	0.142	1.103	0.580	0.993	0.635
				94	27.0	216.5	53230	0.224	0.142	1.106	0.578	0.992	0.634

TABLE B-33

Results of Resistance and Self-Propulsion Experiments

Model Number 4242, $C_B = 0.60$, $L/B = 8.5$, $B/H = 3.5$, Propeller Number 2837

All Figures are for Ship of 400 Ft Length BP				All Figures are for Ship of 600 Ft Length BP									
$V/\sqrt{g_L}$	$C_t \times 10^3$	R	C	$V/\sqrt{g_L}$	V	N	SHP	W_T	t	θ_h	θ_p	θ_{rr}	RHP/SEHP
0.45	2.551	1.312	0.730	0.445	11.0	109.8	2062	0.338	0.106	1.350	0.566	0.851	0.650
0.50	2.533	1.458	0.725	0.486	12.0	119.2	2603	0.331	0.118	1.318	0.560	0.882	0.651
0.55	2.519	1.603	0.721	0.526	13.0	130.3	3295	0.323	0.122	1.298	0.574	0.875	0.652
0.60	2.520	1.749	0.722	0.566	14.0	141.2	4125	0.316	0.122	1.282	0.577	0.884	0.654
0.65	2.552	1.895	0.731	0.607	15.0	152.5	5122	0.307	0.127	1.258	0.579	0.894	0.651
0.70	2.606	2.041	0.746	0.628	15.5	158.3	5693	0.302	0.131	1.245	0.580	0.898	0.648
0.75	2.615	2.186	0.748	0.648	16.0	164.2	6315	0.299	0.138	1.230	0.580	0.901	0.643
0.80	2.629	2.332	0.753	0.668	16.5	170.0	6968	0.294	0.139	1.220	0.581	0.904	0.641
0.825	2.648	2.405	0.758	0.688	17.0	175.5	7633	0.294	0.143	1.215	0.581	0.909	0.641
0.85	2.687	2.478	0.769	0.708	17.5	181.1	8307	0.293	0.144	1.211	0.581	0.918	0.646
0.875	2.764	2.551	0.791	0.729	18.0	186.7	9015	0.290	0.143	1.207	0.581	0.927	0.651
0.90	2.894	2.623	0.829	0.749	18.5	192.2	9764	0.288	0.140	1.208	0.581	0.933	0.655
0.925	3.071	2.697	0.879	0.769	19.0	197.9	10550	0.287	0.138	1.209	0.582	0.941	0.662
0.950	3.236	2.770	0.926	0.790	19.5	203.9	11440	0.281	0.142	1.194	0.584	0.946	0.659
0.975	3.361	2.842	0.962	0.810	20.0	209.9	12440	0.277	0.146	1.182	0.584	0.948	0.654
1.00	3.456	2.915	0.990	0.830	20.5	216.5	13610	0.273	0.149	1.171	0.584	0.952	0.651
1.025	3.508	2.988	1.005	0.851	21.0	223.5	14960	0.269	0.151	1.161	0.583	0.953	0.646
1.05	3.542	3.061	1.014	0.871	21.5	230.4	16650	0.273	0.150	1.169	0.579	0.950	0.642
1.075	3.548	3.134	1.016	0.891	22.0	239.0	18620	0.266	0.145	1.164	0.577	0.950	0.638
1.10	3.544	3.207	1.015	0.911	22.5	247.9	20800	0.262	0.144	1.160	0.574	0.958	0.637
				0.932	23.0	257.4	23320	0.258	0.145	1.152	0.570	0.963	0.633
				0.952	23.5	266.9	26080	0.253	0.143	1.147	0.567	0.971	0.632
				0.972	24.0	276.0	28840	0.250	0.141	1.146	0.564	0.974	0.629
				0.992	24.5	284.1	31600	0.251	0.142	1.145	0.560	0.976	0.626
				1.013	25.0	290.5	34210	0.254	0.144	1.146	0.556	0.977	0.623
				1.033	25.5	297.0	36470	0.256	0.145	1.149	0.556	0.976	0.623
				1.053	26.0	302.5	38660	0.259	0.145	1.155	0.554	0.975	0.624
				1.074	26.5	308.0	40910	0.260	0.144	1.157	0.553	0.976	0.625
				1.094	27.0	315.0	43510	0.259	0.143	1.156	0.554	0.979	0.626

TABLE B-34

Results of Resistance and Self-Propulsion Experiments

Model Number 4265, $C_B = 0.65$, $L/B = 6.25$, $B/H = 3.5$, Propeller Number 3645

All Figures are for Ship of 400 Ft Length BP				All Figures are for Ship of 600 Ft Length BP									
$V/\sqrt{L\pi}$	$C_t \times 10^3$	①	②	$V/\sqrt{L\pi}$	V	N	SRP	W_t	t	θ_h	θ_p	θ_{FF}	KHP/SHIP
0.40	2.786	1.039	0.711	0.486	12.0	70.0	3438	0.373	0.176	1.314	0.561	1.039	0.781
0.45	2.786	1.168	0.711	0.526	13.0	76.0	4448	0.371	0.175	1.312	0.562	1.045	0.771
0.50	2.787	1.298	0.712	0.566	14.0	82.2	5641	0.364	0.183	1.285	0.565	1.037	0.754
0.55	2.793	1.428	0.713	0.587	14.5	85.5	6328	0.357	0.185	1.267	0.568	1.037	0.746
0.60	2.801	1.558	0.715	0.607	15.0	88.6	7043	0.353	0.187	1.256	0.567	1.039	0.740
0.625	2.820	1.623	0.720	0.628	15.5	92.0	7874	0.347	0.186	1.246	0.572	1.031	0.735
0.65	2.848	1.688	0.727	0.648	16.0	95.2	8696	0.344	0.183	1.246	0.572	1.034	0.737
0.675	2.889	1.753	0.737	0.668	16.5	98.6	9628	0.344	0.185	1.244	0.570	1.040	0.738
0.70	2.930	1.818	0.747	0.688	17.0	102.0	10610	0.340	0.178	1.245	0.571	1.044	0.733
0.725	2.973	1.882	0.759	0.708	17.5	105.5	11690	0.338	0.177	1.243	0.572	1.049	0.744
0.75	3.007	1.947	0.767	0.729	18.0	108.9	12820	0.334	0.174	1.240	0.572	1.051	0.745
0.775	3.023	2.012	0.772	0.749	18.5	112.1	14050	0.330	0.172	1.236	0.574	1.047	0.743
0.80	3.027	2.077	0.772	0.769	19.0	115.8	15410	0.326	0.173	1.226	0.574	1.048	0.737
0.825	3.058	2.142	0.780	0.790	19.5	119.3	16840	0.323	0.172	1.222	0.574	1.048	0.735
0.85	3.132	2.207	0.799	0.810	20.0	123.2	18470	0.318	0.174	1.211	0.574	1.052	0.731
0.875	3.351	2.272	0.855	0.830	20.5	127.8	20510	0.313	0.177	1.198	0.570	1.054	0.720
0.90	3.726	2.337	0.951	0.851	21.0	132.9	23060	0.308	0.181	1.183	0.566	1.055	0.706
0.925	4.206	2.402	1.074	0.871	21.5	138.2	26300	0.304	0.184	1.169	0.565	1.047	0.692
0.95	4.736	2.467	1.209	0.891	22.0	144.4	30910	0.302	0.187	1.163	0.557	1.041	0.675
0.975	5.256	2.532	1.342	0.911	22.5	153.0	37630	0.298	0.185	1.161	0.545	1.037	0.656
1.00	5.691	2.596	1.453	0.932	23.0	163.4	46780	0.285	0.178	1.149	0.532	1.034	0.632
1.025	5.976	2.661	1.526	0.952	23.5	172.8	56300	0.272	0.177	1.131	0.525	1.026	0.609
1.05	6.267	2.726	1.600	0.972	24.0	182.0	66650	0.255	0.164	1.122	0.522	1.018	0.596
				0.992	24.5	191.1	78320	0.235	0.154	1.106	0.520	1.008	0.580
				1.013	25.0	200.3	91220	0.215	0.154	1.078	0.519	0.999	0.559
				1.033	25.5	209.5	105100	0.195	0.160	1.043	0.520	0.990	0.537

TABLE B-35
Results of Resistance and Self-Propulsion Experiments
Model Number 4273, $C_B = 0.65$, $L/B = 7.25$, $B/H = 3.5$, Propeller Number 2765

All Figures are for Ship of 400 Ft Length BP				All Figures are for Ship of 600 Ft Length BP									
$V/\sqrt{L_{WL}}$	$C_t \times 10^3$	ϕ	ϕ_c	$V/\sqrt{L_{WL}}$	V	M	SRP	V_T	t	ϕ_h	ϕ_p	ϕ_{TT}	KSP/SHP
0.40	2.691	1.091	0.722	0.486	12.0	81.0	2734	0.343	0.117	1.345	0.580	1.009	0.768
0.45	2.672	1.228	0.716	0.526	13.0	88.0	3495	0.340	0.125	1.327	0.582	1.007	0.777
0.50	2.654	1.364	0.712	0.566	14.0	95.0	4418	0.340	0.128	1.321	0.581	1.005	0.771
0.55	2.643	1.500	0.709	0.587	14.5	98.9	4968	0.332	0.130	1.303	0.584	1.004	0.763
0.60	2.663	1.637	0.714	0.607	15.0	102.7	5555	0.330	0.132	1.294	0.584	1.005	0.759
0.625	2.681	1.705	0.719	0.628	15.5	106.5	6196	0.329	0.140	1.282	0.582	1.008	0.752
0.65	2.702	1.773	0.724	0.648	16.0	110.3	6865	0.329	0.141	1.279	0.581	1.012	0.752
0.675	2.723	1.841	0.730	0.668	16.5	114.3	7637	0.327	0.147	1.268	0.580	1.014	0.746
0.70	2.745	1.910	0.736	0.688	17.0	118.3	8458	0.322	0.147	1.258	0.582	1.013	0.741
0.725	2.762	1.978	0.741	0.708	17.5	122.5	9390	0.317	0.147	1.248	0.582	1.012	0.735
0.75	2.781	2.046	0.746	0.729	18.0	126.5	10360	0.315	0.145	1.249	0.581	1.011	0.734
0.775	2.805	2.114	0.752	0.749	18.5	130.4	11380	0.314	0.145	1.246	0.581	1.009	0.730
0.80	2.837	2.182	0.761	0.769	19.0	134.5	12490	0.311	0.146	1.240	0.581	1.010	0.727
0.825	2.888	2.251	0.774	0.790	19.5	139.0	13770	0.305	0.146	1.229	0.582	1.009	0.721
0.85	2.979	2.319	0.790	0.810	20.0	143.4	15030	0.298	0.147	1.216	0.583	1.012	0.713
0.875	3.159	2.387	0.847	0.830	20.5	148.1	16550	0.293	0.148	1.206	0.583	1.014	0.712
0.90	3.438	2.455	0.922	0.851	21.0	153.9	18470	0.278	0.150	1.178	0.586	1.014	0.700
0.925	3.826	2.523	1.026	0.871	21.5	160.0	20960	0.271	0.150	1.167	0.583	1.009	0.687
0.95	4.226	2.592	1.133	0.891	22.0	168.2	24790	0.266	0.150	1.159	0.574	1.005	0.668
0.975	4.591	2.660	1.231	0.911	22.5	177.4	30030	0.265	0.150	1.156	0.558	1.005	0.649
1.00	4.891	2.728	1.312	0.932	23.0	188.1	36450	0.261	0.149	1.151	0.547	0.999	0.627
1.025	5.056	2.796	1.356	0.952	23.5	198.2	43440	0.248	0.148	1.132	0.542	0.981	0.602
				0.972	24.0	207.7	50690	0.238	0.146	1.120	0.536	0.976	0.586
				0.992	24.5	217.5	58270	0.228	0.142	1.113	0.536	0.964	0.574
				1.013	25.0	227.0	66760	0.220	0.140	1.102	0.525	0.967	0.559
				1.033	25.5	235.5	75460	0.201	0.135	1.083	0.528	0.962	0.550

TABLE B-36

Results of Resistance and Self-Propulsion Experiments
Model Number 4266, $C_B = 0.65$, $L/B = 8.25$, $B/H = 3.5$, Propeller Number 3646

All Figures are for Ship of 400 Ft Length BP														All Figures are for Ship of 600 Ft Length BP													
$V/\sqrt{L_{WL}}$	$C_t \times 10^3$	Ⓐ	Ⓑ	$V/\sqrt{L_{WL}}$	V	N	SHP	W_T	t	e_h	e_p	e_{rr}	EHP/SHP														
0.400	2.669	1.139	0.747	0.445	11.00	9.02	1936	0.365	0.159	1.325	0.533	1.068	0.754														
0.450	2.644	1.282	0.740	0.486	12.00	98.2	2496	0.369	0.158	1.335	0.534	1.042	0.744														
0.500	2.622	1.424	0.733	0.526	13.00	106.7	3216	0.359	0.160	1.312	0.540	1.025	0.727														
0.550	2.601	1.566	0.728	0.566	14.00	115.9	4137	0.345	0.164	1.276	0.546	1.012	0.705														
0.575	2.594	1.638	0.726	0.587	14.50	120.2	4650	0.346	0.163	1.281	0.545	1.006	0.702														
0.600	2.593	1.709	0.725	0.607	15.00	125.0	5245	0.338	0.163	1.264	0.548	0.999	0.692														
0.625	2.600	1.780	0.727	0.628	15.50	130.1	5927	0.329	0.163	1.247	0.551	0.991	0.681														
0.650	2.618	1.851	0.732	0.648	16.00	135.1	6650	0.322	0.168	1.228	0.553	0.986	0.669														
0.675	2.637	1.922	0.738	0.668	16.50	140.1	7416	0.315	0.170	1.214	0.554	0.983	0.661														
0.700	2.659	1.994	0.744	0.688	17.00	145.4	8245	0.307	0.173	1.193	0.557	0.983	0.654														
0.725	2.680	2.065	0.750	0.708	17.50	150.2	9044	0.303	0.174	1.186	0.559	0.987	0.653														
0.750	2.700	2.136	0.755	0.729	18.00	155.1	9903	0.299	0.174	1.179	0.559	0.990	0.652														
0.775	2.715	2.207	0.760	0.749	18.50	160.0	10820	0.295	0.174	1.171	0.559	0.995	0.652														
0.800	2.732	2.278	0.764	0.769	19.00	165.0	11770	0.293	0.175	1.168	0.559	1.003	0.655														
0.825	2.766	2.350	0.774	0.790	19.50	170.2	12810	0.290	0.176	1.161	0.559	1.012	0.657														
0.850	2.827	2.421	0.791	0.810	20.00	175.5	13930	0.286	0.175	1.156	0.558	1.021	0.659														
0.875	2.964	2.492	0.829	0.830	20.50	180.7	15240	0.285	0.174	1.155	0.557	1.021	0.657														
0.900	3.186	2.563	0.891	0.851	21.00	186.1	16830	0.287	0.175	1.157	0.554	1.016	0.651														
0.925	3.471	2.634	0.971	0.871	21.50	193.5	19090	0.281	0.178	1.144	0.550	1.013	0.638														
0.950	3.776	2.706	1.056	0.891	22.00	202.5	22100	0.270	0.185	1.118	0.547	1.010	0.617														
0.975	4.036	2.777	1.129	0.911	22.50	213.0	25920	0.264	0.190	1.101	0.541	1.011	0.602														
1.000	4.256	2.848	1.191	0.932	23.00	223.5	30180	0.256	0.189	1.091	0.532	1.020	0.592														
1.025	4.456	2.919	1.247	0.952	23.50	233.8	35020	0.250	0.188	1.082	0.526	1.026	0.584														
1.050	4.697	2.991	1.314	0.972	24.00	244.0	40150	0.242	0.186	1.074	0.521	1.028	0.576														
				0.992	24.50	254.0	45330	0.236	0.180	1.073	0.516	1.030	0.570														
				1.013	25.00	263.5	50240	0.228	0.171	1.075	0.512	1.036	0.570														
				1.033	25.50	271.5	54590	0.220	0.170	1.065	0.512	1.043	0.569														

TABLE B-37
Results of Resistance and Self-Propulsion Experiments
Model Number 4245, $C_B = 0.70$, $L/B = 6.0$, $B/H = 3.5$, Propeller Number 2502

All Figures are for Ship of 400 Ft Length BP				All Figures are for Ship of 600 Ft Length BP									
$V/\sqrt{L_{WL}}$	$C_t \times 10^3$	③	④	$V/\sqrt{L_{WL}}$	V	R	SRP	W_T	t	η_h	η_p	η_{TP}	SRP/BRP
0.40	2.901	1.012	0.732	0.364	9.0	47.5	1795	0.436	0.197	1.425	0.476	1.034	0.702
0.45	2.886	1.138	0.728	0.405	10.0	52.3	2378	0.442	0.189	1.455	0.475	1.041	0.720
0.50	2.892	1.265	0.730	0.445	11.0	57.6	3143	0.435	0.182	1.448	0.480	1.049	0.730
0.55	2.936	1.391	0.741	0.486	12.0	63.0	4110	0.430	0.174	1.451	0.483	1.045	0.733
0.60	3.005	1.518	0.758	0.526	13.0	68.8	5343	0.417	0.178	1.410	0.490	1.041	0.718
0.625	3.040	1.581	0.767	0.566	14.0	75.1	6925	0.399	0.181	1.362	0.497	1.038	0.702
0.65	3.077	1.644	0.777	0.607	15.0	81.6	8831	0.384	0.184	1.326	0.501	1.039	0.690
0.675	3.110	1.708	0.785	0.628	15.5	85.0	9915	0.374	0.183	1.307	0.504	1.042	0.687
0.70	3.143	1.771	0.793	0.648	16.0	88.1	11050	0.376	0.184	1.306	0.502	1.044	0.684
0.725	3.190	1.834	0.805	0.668	16.5	91.3	12340	0.371	0.184	1.296	0.503	1.040	0.678
0.75	3.264	1.897	0.824	0.688	17.0	94.4	13630	0.372	0.182	1.302	0.500	1.042	0.679
0.775	3.370	1.960	0.851	0.708	17.5	97.4	15030	0.372	0.182	1.304	0.499	1.040	0.677
0.80	3.481	2.024	0.879	0.729	18.0	100.6	16580	0.369	0.184	1.293	0.500	1.038	0.671
0.825	3.593	2.087	0.907	0.749	18.5	104.2	18430	0.362	0.184	1.280	0.504	1.037	0.665
0.85	3.725	2.150	0.940	0.769	19.0	108.5	20830	0.361	0.185	1.276	0.496	1.041	0.659
0.875	3.940	2.213	0.994	0.790	19.5	113.0	23590	0.356	0.183	1.269	0.493	1.042	0.652
0.90	4.481	2.277	1.131	0.810	20.0	116.5	26040	0.355	0.182	1.267	0.494	1.035	0.648
				0.830	20.5	120.2	28910	0.358	0.176	1.283	0.486	1.030	0.643
				0.851	21.0	124.9	32510	0.362	0.178	1.288	0.478	1.036	0.638
				0.891	22.0	139.5	46460	0.332	0.173	1.237	0.471	1.017	0.592

TABLE B-38

Results of Resistance and Self-Propulsion Experiments
 Model Number 4257, $C_B = 0.70$, $L/B = 7.0$, $B/H = 3.5$, Propeller Number 2815

All Figures are for Ship of 400 Ft Length BP				All Figures are for Ship of 600 Ft Length BP									
$V/\sqrt{L_{WL}}$	$C_t \times 10^3$	ζ	ζ	$V/\sqrt{L_{WL}}$	V	N	SHP	W_T	t	θ_h	θ_p	θ_{rr}	KHP/SHP
0.40	2.706	1.066	0.716	0.364	9.0	54.0	1430	0.405	0.152	1.425	0.538	0.939	0.720
0.45	2.712	1.199	0.718	0.405	10.0	59.8	1879	0.404	0.174	1.386	0.541	0.962	0.721
0.50	2.724	1.332	0.721	0.445	11.0	65.8	2462	0.399	0.178	1.368	0.544	0.975	0.725
0.55	2.750	1.465	0.728	0.486	12.0	72.1	3199	0.398	0.185	1.355	0.542	0.992	0.729
0.60	2.821	1.598	0.747	0.526	13.0	78.9	4131	0.393	0.189	1.337	0.542	1.008	0.730
0.625	2.858	1.665	0.756	0.566	14.0	86.1	5309	0.384	0.189	1.317	0.542	1.017	0.726
0.65	2.888	1.732	0.764	0.607	15.0	93.6	6745	0.375	0.197	1.284	0.543	1.026	0.715
0.675	2.910	1.798	0.770	0.628	15.5	97.5	7554	0.368	0.197	1.272	0.544	1.034	0.715
0.70	2.926	1.865	0.774	0.648	16.0	101.2	8413	0.364	0.204	1.253	0.544	1.039	0.708
0.725	2.959	1.931	0.783	0.668	16.5	104.7	9302	0.364	0.204	1.250	0.543	1.043	0.708
0.75	3.014	1.998	0.798	0.688	17.0	108.0	10260	0.364	0.200	1.258	0.542	1.037	0.708
0.775	3.125	2.064	0.827	0.708	17.5	111.4	11320	0.364	0.202	1.255	0.541	1.034	0.702
0.80	3.237	2.131	0.857	0.729	18.0	115.2	12550	0.363	0.203	1.251	0.540	1.033	0.698
0.825	3.345	2.198	0.885	0.749	18.5	120.3	14150	0.345	0.204	1.216	0.545	1.036	0.686
0.85	3.450	2.264	0.913	0.769	19.0	125.7	16080	0.329	0.202	1.190	0.548	1.035	0.675
0.875	3.669	2.331	0.971	0.790	19.5	130.6	18090	0.324	0.206	1.176	0.546	1.036	0.664
0.90	4.081	2.398	1.080	0.810	20.0	135.1	20180	0.324	0.202	1.180	0.542	1.033	0.661
				0.830	20.5	139.6	22470	0.325	0.199	1.188	0.538	1.031	0.658
				0.851	21.0	144.5	25170	0.326	0.193	1.197	0.533	1.028	0.656
				0.891	22.0	158.3	33470	0.304	0.179	1.180	0.527	1.025	0.638

TABLE B-39
Results of Resistance and Self-Propulsion Experiments
Model Number 4246, $C_B = 0.70$, $L/B = 8.0$, $B/H = 3.5$, Propeller Number 3564

All Figures are for Ship of 400 Ft Length BP				All Figures are for Ship of 600 Ft Length BP									
V/\sqrt{LWL}	$C_t \times 10^3$	①	②	V/\sqrt{LWL}	V	R	SRP	W_T	t	ϕ_h	ϕ_p	σ_{rr}	SRP/SRP
0.40	2.613	1.114	0.725	0.364	9.0	74.2	1082	0.375	0.163	1.340	0.528	1.132	0.800
0.45	2.633	1.253	0.730	0.405	10.0	81.8	1444	0.371	0.164	1.331	0.534	1.126	0.800
0.50	2.643	1.392	0.733	0.445	11.0	89.9	1926	0.368	0.163	1.324	0.537	1.115	0.793
0.55	2.669	1.532	0.741	0.486	12.0	98.2	2544	0.368	0.164	1.323	0.536	1.101	0.781
0.60	2.698	1.671	0.748	0.526	13.0	107.2	3321	0.361	0.172	1.295	0.538	1.093	0.762
0.625	2.719	1.740	0.754	0.566	14.0	116.2	4296	0.359	0.177	1.284	0.537	1.080	0.744
0.65	2.741	1.810	0.760	0.607	15.0	125.4	5441	0.353	0.173	1.278	0.538	1.067	0.734
0.675	2.769	1.880	0.768	0.628	15.5	130.3	6124	0.347	0.175	1.264	0.540	1.061	0.724
0.70	2.803	1.949	0.778	0.648	16.0	134.9	6867	0.345	0.172	1.263	0.540	1.050	0.717
0.725	2.846	2.019	0.790	0.668	16.5	139.9	7689	0.342	0.173	1.260	0.539	1.048	0.712
0.75	2.897	2.088	0.804	0.688	17.0	144.7	8593	0.340	0.168	1.262	0.539	1.037	0.706
0.775	2.975	2.158	0.825	0.708	17.5	149.9	9595	0.336	0.167	1.256	0.539	1.033	0.699
0.80	3.072	2.228	0.852	0.729	18.0	155.4	10720	0.333	0.172	1.242	0.538	1.033	0.690
0.825	3.153	2.297	0.875	0.749	18.5	161.4	12000	0.326	0.180	1.218	0.538	1.033	0.676
0.85	3.237	2.367	0.898	0.769	19.0	168.1	13500	0.317	0.188	1.188	0.538	1.038	0.663
0.875	3.397	2.436	0.942	0.790	19.5	174.8	15160	0.310	0.192	1.170	0.536	1.042	0.654
0.90	3.699	2.506	1.026	0.810	20.0	181.0	16870	0.309	0.192	1.170	0.532	1.046	0.651
				0.830	20.5	186.9	18750	0.311	0.186	1.181	0.528	1.045	0.651
				0.851	21.0	193.3	20950	0.314	0.186	1.187	0.522	1.044	0.647
				0.891	22.0	212.1	28260	0.291	0.186	1.149	0.516	1.032	0.612

TABLE B-40
Results of Resistance and Self-Propulsion Experiments
Model Number 4269, $C_B = 0.75$, $L/B = 5.75$, $B/H = 3.5$, Propeller Number 3565

All Figures are for Ship of 400 Ft Length BP				All Figures are for Ship of 600 Ft Length BP									
$V/\sqrt{L_{WL}}$	$C_t \times 10^3$	(K)	(C)	$V/\sqrt{L_{WL}}$	V	N	SHP	W_T	t.	ϕ_h	ϕ_p	ϕ_π	EHP/SHP
0.35	3.014	0.863	0.747	0.364	9.0	49.1	2075	0.441	0.191	1.448	0.501	0.966	0.701
0.40	2.989	0.986	0.741	0.405	10.0	53.8	2662	0.447	0.188	1.469	0.503	0.991	0.732
0.45	2.976	1.110	0.737	0.445	11.0	58.8	3392	0.448	0.178	1.490	0.505	1.010	0.760
0.50	2.994	1.233	0.741	0.486	12.0	64.0	4326	0.456	0.169	1.527	0.500	1.029	0.785
0.525	3.013	1.294	0.746	0.526	13.0	69.8	5567	0.450	0.166	1.517	0.501	1.035	0.787
0.55	3.036	1.356	0.752	0.566	14.0	76.6	7219	0.425	0.169	1.444	0.512	1.043	0.771
0.575	3.067	1.418	0.760	0.587	14.5	80.2	8218	0.412	0.175	1.404	0.517	1.044	0.758
0.60	3.108	1.479	0.770	0.607	15.0	83.5	9264	0.410	0.186	1.380	0.516	1.044	0.743
0.625	3.169	1.541	0.785	0.628	15.5	86.9	10490	0.409	0.192	1.368	0.513	1.043	0.733
0.65	3.243	1.603	0.803	0.648	16.0	90.0	11780	0.412	0.190	1.378	0.508	1.044	0.730
0.675	3.344	1.664	0.828	0.668	16.5	94.5	13400	0.401	0.184	1.363	0.509	1.047	0.727
0.70	3.491	1.726	0.865	0.688	17.0	98.4	15220	0.397	0.178	1.364	0.508	1.045	0.724
0.725	3.713	1.788	0.920	0.708	17.5	103.0	17470	0.386	0.170	1.351	0.509	1.043	0.717
0.75	3.987	1.849	0.988	0.729	18.0	107.4	20190	0.383	0.175	1.337	0.498	1.050	0.700
0.775	4.305	1.911	1.066	0.749	18.5	114.3	23920	0.377	0.179	1.318	0.494	1.058	0.688
0.80	4.634	1.972	1.148	0.769	19.0	120.9	28640	0.374	0.182	1.306	0.484	1.058	0.668
0.825	4.933	2.034	1.222	0.790	19.5	126.8	33780	0.377	0.180	1.315	0.472	1.053	0.654
0.85	5.242	2.096	1.299	0.810	20.0	133.2	39190	0.370	0.177	1.307	0.467	1.055	0.644
0.875	5.542	2.158	1.373	0.830	20.5	138.6	44800	0.365	0.176	1.297	0.464	1.053	0.634
				0.851	21.0	145.2	51440	0.353	0.178	1.271	0.463	1.055	0.621
				0.871	21.5	151.7	58950	0.346	0.177	1.258	0.459	1.054	0.609
				0.891	22.0	158.3	67710	0.338	0.186	1.268	0.444	1.060	0.597

TABLE B-41
Results of Resistance and Self-Propulsion Experiments
Model Number 4277, $C_B = 0.75$, $L/B = 6.75$, $B/H = 3.5$, Propeller Number 3488

All Figures are for Ship of 400 Ft Length BP														All Figures are for Ship of 600 Ft Length BP													
$V/\sqrt{L_{WL}}$	$C_t \times 10^3$	⊗	⊙	$V/\sqrt{L_{WL}}$	V	N	SHP	W_T	t	e_h	e_p	e_r	EHP/SHP														
0.35	2.824	0.910	0.737	0.364	9.0	58.5	1421	0.384	0.157	1.368	0.528	1.088	0.786														
0.40	2.798	1.040	0.730	0.405	10.0	64.6	1932	0.387	0.144	1.398	0.529	1.075	0.795														
0.45	2.791	1.170	0.729	0.445	11.0	71.2	2558	0.382	0.138	1.395	0.531	1.086	0.805														
0.50	2.804	1.300	0.732	0.486	12.0	78.3	3374	0.373	0.139	1.372	0.534	1.093	0.801														
0.525	2.815	1.365	0.735	0.526	13.0	85.6	4420	0.373	0.153	1.350	0.530	1.095	0.784														
0.55	2.833	1.430	0.740	0.566	14.0	93.2	5786	0.374	0.165	1.334	0.525	1.088	0.761														
0.575	2.864	1.496	0.748	0.587	14.5	97.4	6808	0.373	0.171	1.323	0.522	1.087	0.750														
0.60	2.924	1.560	0.763	0.607	15.0	101.5	7577	0.374	0.174	1.318	0.518	1.078	0.737														
0.625	2.994	1.626	0.781	0.628	15.5	105.8	8698	0.376	0.180	1.313	0.514	1.070	0.721														
0.65	3.080	1.691	0.804	0.648	16.0	110.4	9998	0.375	0.186	1.300	0.512	1.060	0.705														
0.675	3.182	1.756	0.831	0.668	16.5	115.3	11520	0.373	0.191	1.290	0.506	1.054	0.688														
0.70	3.315	1.821	0.865	0.688	17.0	120.8	13250	0.364	0.192	1.271	0.505	1.055	0.677														
0.725	3.521	1.886	0.919	0.708	17.5	126.7	15300	0.357	0.187	1.265	0.501	1.058	0.671														
0.75	3.790	1.951	0.989	0.729	18.0	133.0	17750	0.352	0.185	1.258	0.496	1.060	0.662														
0.775	4.130	2.016	1.078	0.749	18.5	139.9	20760	0.345	0.184	1.246	0.491	1.061	0.649														
0.80	4.512	2.081	1.178	0.769	19.0	147.4	24540	0.343	0.180	1.248	0.482	1.060	0.637														
0.825	4.873	2.146	1.272	0.790	19.5	155.4	29130	0.341	0.178	1.247	0.473	1.056	0.623														
0.85	5.147	2.211	1.344	0.810	20.0	163.6	34640	0.340	0.177	1.247	0.462	1.052	0.607														
0.875	5.392	2.276	1.408	0.830	20.5	172.0	40760	0.335	0.181	1.232	0.456	1.047	0.589														
				0.851	21.0	180.3	47250	0.334	0.187	1.221	0.448	1.040	0.569														
				0.871	21.5	188.2	53500	0.311	0.188	1.179	0.453	1.041	0.556														
				0.891	22.0	195.5	59460	0.289	0.192	1.136	0.460	1.044	0.545														

TABLE B-42
Results of Resistance and Self-Propulsion Experiments
Model Number 4270, $C_B = 0.75$, $L/B = 7.75$, $B/H = 3.5$, Propeller Number 3647

All Figures are for Ship of 400 Ft Length BP					All Figures are for Ship of 600 Ft Length BP									
$V/\sqrt{L_{WL}}$	$C_t \times 10^3$	(K)	(C)	$V/\sqrt{L_{WL}}$	N	SHP	W_T	t	e_b	e_p	e_π	EHP/SHP		
0.35	2.729	0.953	0.746	0.364	80.9	1155	0.438	0.201	1.423	0.476	1.251	0.848		
0.40	2.699	1.090	0.738	0.406	88.9	1561	0.431	0.199	1.409	0.488	1.208	0.830		
0.45	2.684	1.226	0.734	0.445	97.8	2118	0.418	0.191	1.391	0.500	1.166	0.810		
0.50	2.714	1.362	0.742	0.486	107.5	2872	0.406	0.188	1.366	0.507	1.129	0.782		
0.525	2.741	1.430	0.749	0.526	117.9	3885	0.393	0.183	1.346	0.512	1.090	0.751		
0.55	2.770	1.498	0.758	0.566	128.7	5218	0.382	0.179	1.329	0.515	1.052	0.720		
0.576	2.816	1.566	0.770	0.587	134.5	6038	0.378	0.179	1.319	0.515	1.029	0.705		
0.60	2.878	1.634	0.787	0.607	140.1	6934	0.374	0.185	1.302	0.511	1.034	0.689		
0.625	2.958	1.702	0.809	0.628	146.6	7955	0.370	0.185	1.294	0.512	1.021	0.677		
0.65	3.050	1.770	0.834	0.648	152.5	9071	0.365	0.186	1.282	0.512	1.016	0.667		
0.676	3.154	1.839	0.862	0.668	159.7	10360	0.360	0.187	1.270	0.509	1.017	0.657		
0.70	3.290	1.907	0.900	0.688	166.8	11860	0.353	0.188	1.256	0.508	1.017	0.648		
0.725	3.470	1.975	0.949	0.708	174.2	13590	0.350	0.187	1.256	0.502	1.022	0.644		
0.75	3.702	2.043	1.012	0.729	182.9	15700	0.346	0.184	1.248	0.497	1.026	0.637		
0.775	4.015	2.111	1.098	0.749	185	18160	0.341	0.181	1.242	0.490	1.043	0.636		
0.80	4.359	2.179	1.192	0.769	190	21190	0.337	0.180	1.237	0.483	1.052	0.628		
0.825	4.606	2.247	1.276	0.790	195	25150	0.336	0.181	1.233	0.469	1.044	0.605		
0.85	4.802	2.315	1.329	0.810	200	29820	0.334	0.188	1.219	0.466	1.033	0.587		
0.875	5.021	2.383	1.362	0.830	205	34250	0.325	0.188	1.204	0.464	1.031	0.576		
				0.851	210	38810	0.322	0.182	1.206	0.461	1.033	0.574		
				0.871	215	43270	0.315	0.169	1.213	0.460	1.023	0.570		
				0.891	220	48730	0.318	0.166	1.222	0.453	1.018	0.564		

TABLE B-43
Results of Resistance and Self-Propulsion Experiments
 Model Number 4249, $C_B = 0.80$, $L/B = 5.5$, $B/H = 3.5$, Propeller Number 2944

All Figures are for Ship of 400 Ft Length BP				All Figures are for Ship of 600 Ft Length BP									
$V/\sqrt{L_{WL}}$	$C_t \times 10^3$	ζ	\odot	$V/\sqrt{L_{WL}}$	V	N	SHP	W_T	t	e_h	e_p	e_{rr}	EEP/SHP
0.35	3.171	0.841	0.779	0.364	9.0	51.9	2017	0.466	0.234	1.431	0.496	1.162	0.824
0.40	3.143	0.961	0.773	0.405	10.0	57.7	2776	0.448	0.211	1.430	0.510	1.129	0.824
0.45	3.119	1.081	0.766	0.445	11.0	63.5	3766	0.437	0.210	1.403	0.519	1.097	0.798
0.50	3.101	1.202	0.762	0.466	11.5	66.6	4356	0.432	0.214	1.385	0.521	1.085	0.784
0.525	3.115	1.262	0.766	0.486	12.0	69.6	5022	0.428	0.215	1.372	0.523	1.075	0.772
0.55	3.158	1.322	0.776	0.506	12.5	72.5	5730	0.429	0.211	1.382	0.523	1.061	0.767
0.575	3.242	1.382	0.797	0.526	13.0	75.5	6493	0.430	0.213	1.381	0.522	1.062	0.765
0.60	3.346	1.442	0.822	0.546	13.5	78.7	7348	0.425	0.205	1.383	0.524	1.058	0.767
0.625	3.481	1.502	0.855	0.566	14.0	81.9	8286	0.422	0.197	1.391	0.524	1.057	0.771
0.65	3.640	1.562	0.894	0.587	14.5	85.6	9497	0.417	0.192	1.386	0.524	1.055	0.766
0.675	3.865	1.622	0.950	0.607	15.0	90.0	10980	0.405	0.194	1.355	0.526	1.056	0.753
0.70	4.175	1.682	1.026	0.628	15.5	94.7	12830	0.396	0.195	1.334	0.525	1.054	0.738
0.75	5.037	1.802	1.238	0.648	16.0	99.9	15020	0.388	0.189	1.325	0.522	1.052	0.728
0.80	6.209	1.923	1.526	0.688	17.0	110.4	20970	0.379	0.184	1.314	0.511	1.046	0.702
				0.729	18.0	123.5	30160	0.361	0.178	1.285	0.500	1.038	0.667
				0.769	19.0	138.4	43980	0.351	0.172	1.276	0.482	1.030	0.633
				0.810	20.0	155.2	64600	0.349	0.144	1.314	0.457	1.024	0.615

TABLE B-44
Results of Resistance and Self-Propulsion Experiments
Model Number 4261, $C_B = 0.80$, $L/B = 6.5$, $B/H = 3.5$, Propeller Number 2501

All Figures are for Ship of 400 Ft Length BP				All Figures are for Ship of 600 Ft Length BP									
$V/\sqrt{L_{WL}}$	$C_t \times 10^3$	①	②	$V/\sqrt{L_{WL}}$	V	R	SHP	W_T	t	ϕ_h	ϕ_p	σ_{rr}	$\Sigma HP / SHP$
0.35	2.873	0.889	0.744	0.364	9.0	62.9	1930	0.397	0.140	1.427	0.544	0.859	0.667
0.40	2.843	1.016	0.737	0.405	10.0	69.1	2542	0.417	0.157	1.445	0.536	0.876	0.679
0.45	2.818	1.144	0.730	0.445	11.0	75.8	3297	0.425	0.167	1.450	0.532	0.896	0.691
0.50	2.802	1.270	0.726	0.466	11.5	79.2	3739	0.431	0.176	1.447	0.528	0.908	0.694
0.525	2.836	1.334	0.735	0.486	12.0	83.0	4256	0.429	0.184	1.429	0.528	0.920	0.694
0.55	2.906	1.398	0.753	0.506	12.5	86.9	4832	0.430	0.193	1.417	0.525	0.932	0.694
0.575	3.011	1.461	0.780	0.526	13.0	91.2	5498	0.425	0.196	1.398	0.526	0.946	0.695
0.60	3.143	1.525	0.814	0.546	13.5	95.5	6255	0.424	0.200	1.391	0.523	0.958	0.696
0.625	3.328	1.588	0.862	0.566	14.0	100.4	7185	0.420	0.198	1.381	0.525	0.967	0.693
0.65	3.550	1.652	0.920	0.587	14.5	105.1	8233	0.416	0.195	1.378	0.517	0.976	0.696
0.675	3.810	1.715	0.987	0.607	15.0	110.3	9482	0.412	0.192	1.374	0.516	0.982	0.697
0.70	4.125	1.779	1.069	0.628	15.5	115.7	11040	0.412	0.190	1.377	0.510	0.984	0.691
0.75	4.882	1.906	1.265	0.648	16.0	121.9	13000	0.409	0.194	1.365	0.503	0.987	0.678
0.80	5.969	2.033	1.547	0.688	17.0	135.8	18260	0.404	0.198	1.347	0.487	0.991	0.650
				0.729	18.0	152.1	26140	0.399	0.197	1.337	0.468	0.994	0.623
				0.769	19.0	171.2	37630	0.381	0.190	1.308	0.455	1.001	0.596
				0.810	20.0	193.2	53870	0.353	0.182	1.265	0.445	1.014	0.571

TABLE B-45

Results of Resistance and Self-Propulsion Experiments

Model Number 4250, $C_B = 0.8$, $L/B = 7.5$, $B/H = 3.5$, Propeller Number 2765

All Figures are for Ship of 400 Ft Length BP				All Figures are for Ship of 600 Ft Length BP								
$V/\sqrt{L_{WL}}$	$C_t \times 10^3$	ζ	ζ	V	R	SEP	W_T	t	η_h	η_p	η_{TP}	SEP/SEP
0.35	2.799	0.933	0.761	9.0	62.8	1616	0.435	0.147	1.510	0.497	0.890	0.668
0.40	2.769	1.066	0.753	10.0	69.3	2135	0.433	0.152	1.496	0.502	0.898	0.674
0.45	2.759	1.199	0.750	11.0	76.8	2848	0.419	0.161	1.444	0.510	0.908	0.668
0.50	2.804	1.332	0.762	11.5	80.8	3276	0.418	0.166	1.433	0.508	0.913	0.664
0.525	2.855	1.399	0.776	12.0	84.8	3776	0.417	0.173	1.418	0.506	0.921	0.660
0.55	2.945	1.466	0.801	12.5	94.6	4597	0.414	0.176	1.406	0.504	0.936	0.663
0.575	3.066	1.532	0.834	13.0	93.6	4973	0.414	0.179	1.402	0.500	0.955	0.670
0.60	3.216	1.599	0.874	13.5	98.2	5701	0.420	0.182	1.409	0.492	0.971	0.673
0.625	3.398	1.666	0.924	14.0	102.9	6531	0.422	0.183	1.412	0.486	0.980	0.673
0.65	3.620	1.732	0.984	14.5	108.1	7551	0.420	0.182	1.409	0.482	0.987	0.670
0.675	3.870	1.799	1.052	15.0	113.8	8857	0.418	0.181	1.406	0.476	0.986	0.660
0.70	4.155	1.866	1.129	15.5	120.0	10460	0.405	0.172	1.391	0.476	0.981	0.650
0.75	4.915	1.999	1.335	16.0	126.7	12410	0.392	0.166	1.372	0.476	0.974	0.635
0.80	6.049	2.132	1.644	17.0	141.6	17400	0.370	0.165	1.326	0.470	0.975	0.607
				18.0	158.4	24590	0.359	0.162	1.308	0.454	0.982	0.583
				19.0	177.0	35160	0.366	0.162	1.322	0.427	0.985	0.556
				20.0	199.9	51570	0.349	0.168	1.273	0.411	0.982	0.514

Table B-46 — Effective Horsepower Estimate from Series 60 $\frac{R_R}{\Delta}$ Contours

Ship SS PENNSYLVANIA Model No. 4051

Ship Dimensions

English or Metric Units	English Units	Metric Units
LWL	668.03	CB (LBP) 0.765
LBP	595.00	LBP/B 7.083
B	84.00	B/H 2.545
H	33.00	$\Delta^{2/3}$ 1082.3
Δ	36100	$\Delta^{1/6}$ 5.7489
S	72531	X -0.9100
\sqrt{LWL}	24.858	X ² 0.8281

Formulae and Constants

English Units	Metric Units
$R_r/\Delta = R_r/\Delta$ (for $B/H = 3.0$) $+ QX + bX^2$	R_r in kg. = $0.4464(R_r/\Delta)\Delta$ (met. tons)
$X = 2 \left[\frac{B}{H} \text{ (of prototype)} - 3.0 \right]$	R_r in kg. = $4.882(R_r/S) S$ (sq. m)
$Q = \frac{R_r/\Delta (3.5) - R_r/\Delta (2.5)}{2}$	V in knots = $1.811(V/\sqrt{LWL}) \sqrt{LWL}$ (m)
$b = \frac{R_r/\Delta (3.5) + R_r/\Delta (2.5) - 2 R_r/\Delta (3.0)}{2}$	EHP in Metric HP = $\frac{V \cdot R}{145.7}$
$\odot = Y \cdot \frac{EHP}{V^3}$	$V L = 3.281 \cdot V \cdot LWL$ (m)
$\ominus = Z \cdot V$	$Y = 425.7/\Delta^{2/3}$ (met. tons)
	$Z = 0.5850/\Delta^{1/6}$ (met. tons)

A	B	C	D	E	F	G	H	I	J	K	L	M	N	O	P	Q
V/\sqrt{LWL}	R_r/Δ from contours			Q	b	R_r/Δ	R_r	$V L$	R_r/S	R_r	R	EHP	V	V^3	\odot	\ominus
	$B/H=2.5$	$B/H=3.0$	$B/H=3.5$	$\frac{D-B}{2}$	$\frac{D+B-2C}{2}$	$C \cdot E \cdot X \cdot F \cdot X^2$	$G \cdot \Delta$	$N \cdot LWL$	from Nomograph	$J \cdot S$	$H \cdot K$	$\frac{N \cdot L}{325.6}$	$A \cdot \sqrt{LWL}$	N^3	$\frac{Y \cdot M}{O}$	$Z \cdot N$
0.40																
.45																
.50																
.55																
.60																
.65	1.725	1.882	2.028	0.1515	0.0145	1.736	82670	9147	1.372	99510	162100	7984	16.03	4119	0.758	1.827
.70																
.75																
.80																
.85																
.90																
.95																
1.00																

Table B-47 - (C) Estimate from Series 60 (C) Contours

Ship SS PENNSYLVANIA Model No. 4057

Ship Dimensions				Formulae	
LWL	<u>608.03</u>	C _B (L _{BP})	<u>0.765</u>	Ⓒ 400 =	Ⓒ 400 (for B/H = 3.0) + a X + b X ²
LBP	<u>595.00</u>	L _{BP} /B	<u>7.083</u>	X =	2 [B/H (of prototype) - 3.0]
B	<u>84.00</u>	B/H	<u>2.545</u>	a =	$\frac{\text{Ⓒ 400 (3.5)} - \text{Ⓒ 400 (2.5)}}{2}$
H	<u>33.00</u>	X	<u>-0.9100</u>	b =	$\frac{\text{Ⓒ 400 (3.5)} + \text{Ⓒ 400 (2.5)} - 2 \text{Ⓒ 400 (3.0)}}{2}$
∇	<u>1262670</u>	X ²	<u>0.8281</u>		
S/∇ ^{2/3}	<u>6.209</u>				

A	B	C	D	E	F	G
(K)	(C) 400 from contours			a	b	(C) 400
	B/H = 2.5	B/H = 3.0	B/H = 3.5	$\frac{D-B}{2}$	$\frac{D+B-2C}{2}$	C+EX+FX ²
1.2						
1.3						
1.4						
1.5						
1.6	0.7735	0.7730	0.7883	0.0074	0.0079	0.7728
1.7						
1.8						
1.9						
2.0						
2.1						
2.2						
2.3						
2.4						

Table B48 - Approximate Corrections to $C_{400 \text{ Ft}}$ for Other Ship Lengths

Wetted Surface Coefficient $S/\Delta^{2/3}$	65			75			85		
Speed Length Ratio V/\sqrt{L}	0.60	0.80	1.00	0.60	0.80	1.00	0.60	0.80	1.00
Length L in Ft	Additions to Basic $C_{400 \text{ ft}}$								
100	0.086	0.082	0.079	0.100	0.095	0.091	0.113	0.107	0.103
125	0.070	0.066	0.063	0.081	0.077	0.073	0.091	0.087	0.083
150	0.058	0.055	0.053	0.066	0.063	0.061	0.075	0.072	0.069
175	0.048	0.046	0.044	0.055	0.053	0.051	0.063	0.060	0.057
200	0.040	0.038	0.036	0.046	0.044	0.042	0.052	0.050	0.048
225	0.033	0.031	0.030	0.038	0.036	0.035	0.043	0.041	0.040
250	0.027	0.025	0.024	0.031	0.030	0.029	0.035	0.034	0.033
275	0.021	0.020	0.019	0.025	0.024	0.023	0.028	0.027	0.026
300	0.017	0.016	0.015	0.019	0.018	0.017	0.022	0.021	0.020
325	0.012	0.011	0.011	0.014	0.013	0.013	0.016	0.015	0.014
350	0.008	0.007	0.007	0.009	0.008	0.008	0.010	0.009	0.009
400	---	---	---	---	---	---	---	---	---
Deductions from Basic $C_{400 \text{ ft}}$									
450	0.007	0.006	0.006	0.008	0.007	0.007	0.009	0.008	0.008
500	0.013	0.012	0.011	0.015	0.014	0.013	0.016	0.015	0.015
550	0.018	0.017	0.016	0.021	0.020	0.019	0.023	0.022	0.022
600	0.023	0.022	0.021	0.026	0.025	0.024	0.030	0.028	0.027
650	0.027	0.026	0.025	0.032	0.030	0.029	0.035	0.034	0.033
700	0.032	0.030	0.029	0.037	0.035	0.033	0.041	0.039	0.038
750	0.036	0.034	0.032	0.041	0.039	0.038	0.046	0.044	0.043
800	0.039	0.037	0.036	0.045	0.043	0.041	0.051	0.049	0.047
850	0.043	0.041	0.039	0.049	0.047	0.045	0.056	0.053	0.051
900	0.046	0.044	0.042	0.053	0.050	0.048	0.060	0.056	0.055
950	0.048	0.046	0.044	0.056	0.053	0.051	0.063	0.060	0.058
1000	0.051	0.048	0.046	0.058	0.056	0.053	0.066	0.063	0.060

APPENDIX C

METHODS OF ANALYSIS AND FAIRING OF RESULTS

For each $\frac{B}{H}$ value, 15 models were built and tested, the three models at each block coefficient covering a range of $\frac{L}{B}$ values. It is desirable to have sets of contours to facilitate the interpolation of the results given in this paper. The contours also will give ship designers a visual picture to guide them in choosing the principal proportions and coefficients of the ship.

Consider the contours of $\frac{R_R}{\Delta}$. A two-way interpolation is involved—first between $\frac{L}{B}$ values at each block coefficient and then across the block coefficient at each $\frac{L}{B}$ value. Such interpolation could be done by drawing curves through the test points as shown in Figures C1 and C2. Then Figure C2 would be replotted by using constant $\frac{R_R}{\Delta}$ values as parameter, C_B as abscissa and $\frac{L}{B}$ as ordinate to obtain the final contours. However, it is not easy to follow this procedure. In general, the points taken along any horizontal line in Figure C2 will be quite scattered in the final plot. A tedious cross fairing is then necessary among these three plots. This process has to be done for many values of $\frac{V}{\sqrt{L}}$. At the end, a plot of $\frac{R_R}{\Delta}$ against $\frac{V}{\sqrt{L}}$ as lifted from the contours for fixed values of C_B and $\frac{L}{B}$ may not be a fair curve. Further refairing among the four plots is necessary. With the experience of fairing a set of ship lines between two plots, body plan and waterlines, it is quite evident that it would be extremely tedious and frustrating to obtain a set of consistent $\frac{R_R}{\Delta}$ contours by manual fairing. Accordingly, it was decided to interpolate between $\frac{L}{B}$ and across the block coefficients mathematically and to program the computation work into a UNIVAC computer, by the method devised by Dr. P.C. Pien.

For interpolating between $\frac{L}{B}$ values, three values of $\frac{R_R}{\Delta}$ corresponding to three $\frac{L}{B}$ values at each block coefficient and a fixed value of $\frac{B}{H}$, are known from the model tests. It was rather difficult to decide how the interpolation should be done since an infinite number of curves can be drawn to pass through three given points. Without any definite knowledge as to how such a curve should look, a simple curve expressed as follows was chosen

$$\frac{R_R}{\Delta} = a + b \left(\frac{L}{B} \right) + c \left(\frac{L}{B} \right)^2$$

With this equation, $\frac{R_R}{\Delta}$ values for $\frac{L}{B}$ values between 5.5 and 8.5 at intervals of 0.25 were computed for each block coefficient at constant values of $\frac{V}{\sqrt{L}}$.

For interpolation between block coefficients, there are five points, one for each block coefficient for given values $\frac{L}{B}$ and $\frac{V}{\sqrt{L}}$. The polynomial

$$\frac{R_R}{\Delta} = A + B \cdot C_B + C \cdot C_B^2 + D \cdot C_B^3 + E \cdot C_B^4$$

could be used for this interpolation. However, it was felt that the interpolation near one end of the curve might be influenced unduly by the values near the other end. It was decided to use two equations of the following type, one for each end of the curve:

$$\frac{R_R}{\Delta} = A + B \cdot C_B + C \cdot C_B^2 + D \cdot C_B^3$$

The coefficients of the equations were so determined that each equation would pass through three points and have equal ordinates and first and second derivatives where they joined at the midpoint. Values of $\frac{R_R}{\Delta}$ at intervals of 0.01 in C_B values were computed by using these two equations. Figures C1 and C2 show the interpolating curves between the $\frac{L}{B}$ values and across block coefficient, respectively, as obtained by using the foregoing equations.

If we consider a three-dimensional surface plot with C_B as x , $\frac{L}{B}$ as y , and $\frac{R_R}{\Delta}$ as z , then Figure C1 indicates the cuts of this surface by a series of planes with constant z -values, and Figure C2 indicates the cuts of this surface by a series of planes with constant y -values. The cuts of this surface by a series of planes with constant z -values are the required contours of $\frac{R_R}{\Delta}$.

Figure C3 shows the contours of $\frac{R_R}{\Delta}$ obtained in this way for a $\frac{V}{\sqrt{L}}$ of 0.60 and a $\frac{B}{H}$ value of 3.0. Also shown are the actual values of $\frac{R_R}{\Delta}$ for the 15 models (having three values of $\frac{L}{B}$ at each of five block coefficients) from which the contours were derived. It will be agreed that the contours show an excellent interpolation among these 15 points and give confidence in their use for power estimates.

The three-dimensional surface mentioned is determined by 15 points from model testing. Each of the points follows a faired curve as $\frac{V}{\sqrt{L}}$ changes. Any spot at fixed values of x and y , therefore, will follow a faired curve of its own as $\frac{V}{\sqrt{L}}$ changes. That is to say, the $\frac{R_R}{\Delta}$ values of any particular model lifted from the contours at various $\frac{V}{\sqrt{L}}$ values will give a faired curve when they are plotted against $\frac{V}{\sqrt{L}}$.

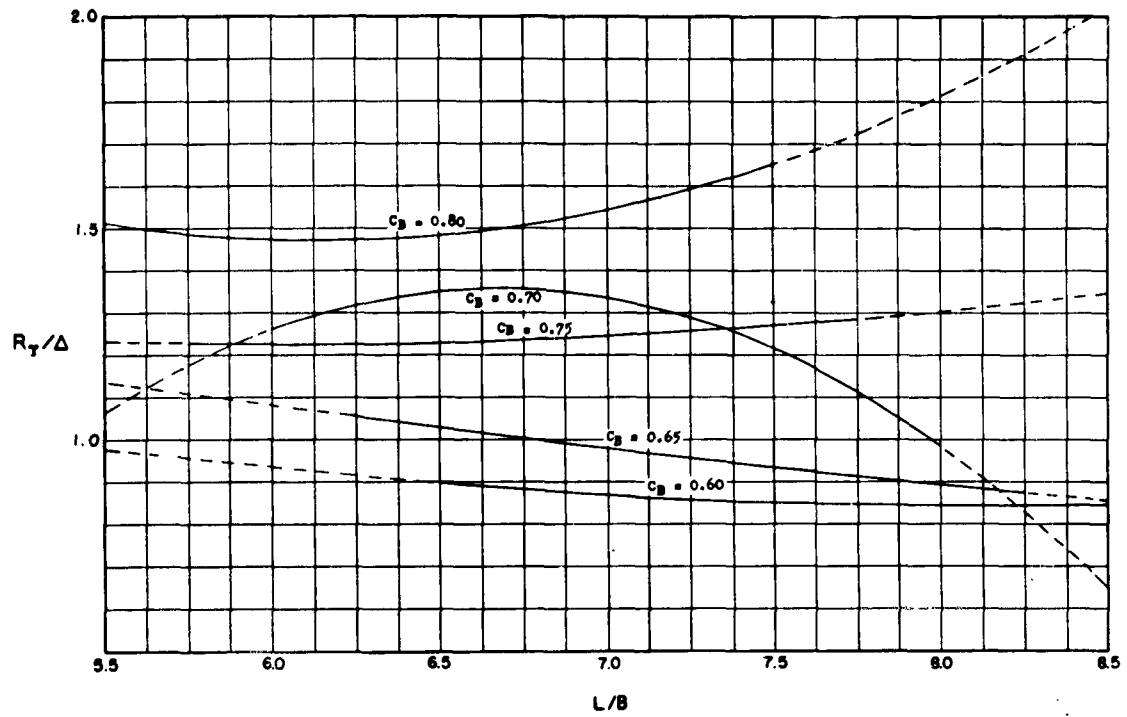


Figure C1 – Interpolation Curves of $\frac{R_r}{\Delta}$ between $\frac{L}{B}$ Values

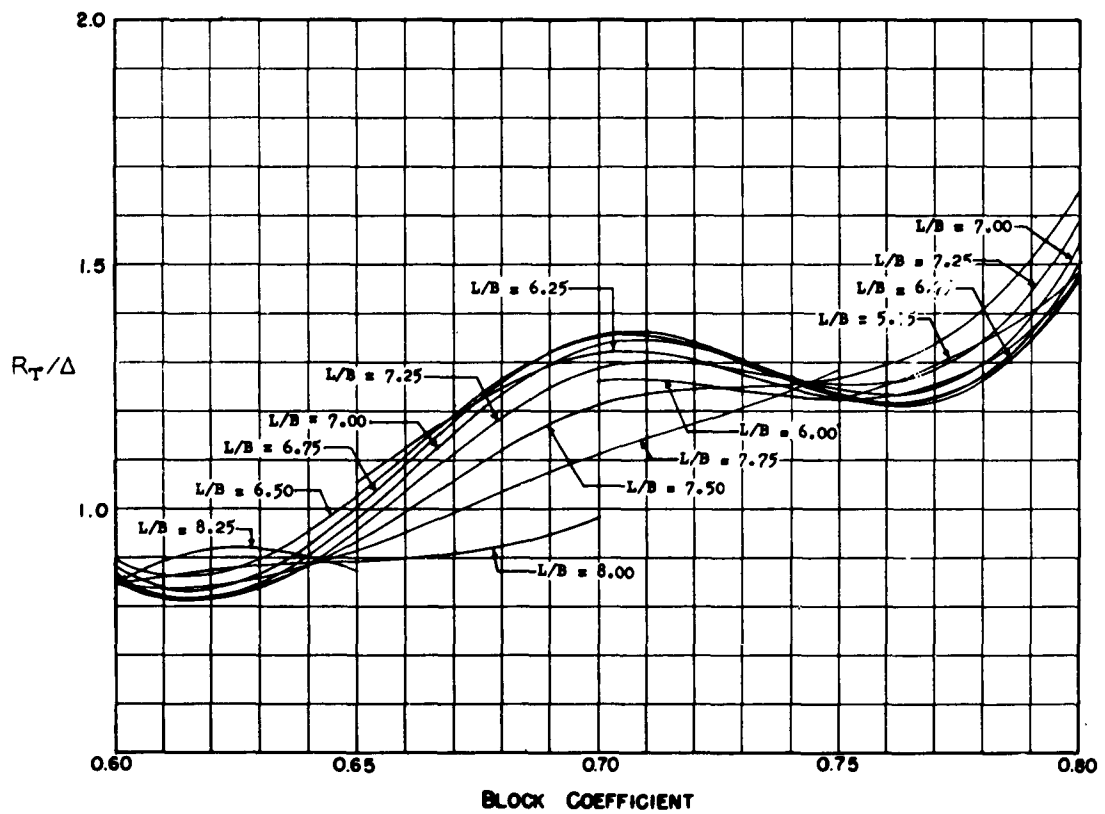


Figure C2 – Interpolation Curves of $\frac{R_r}{\Delta}$ between C_B Values

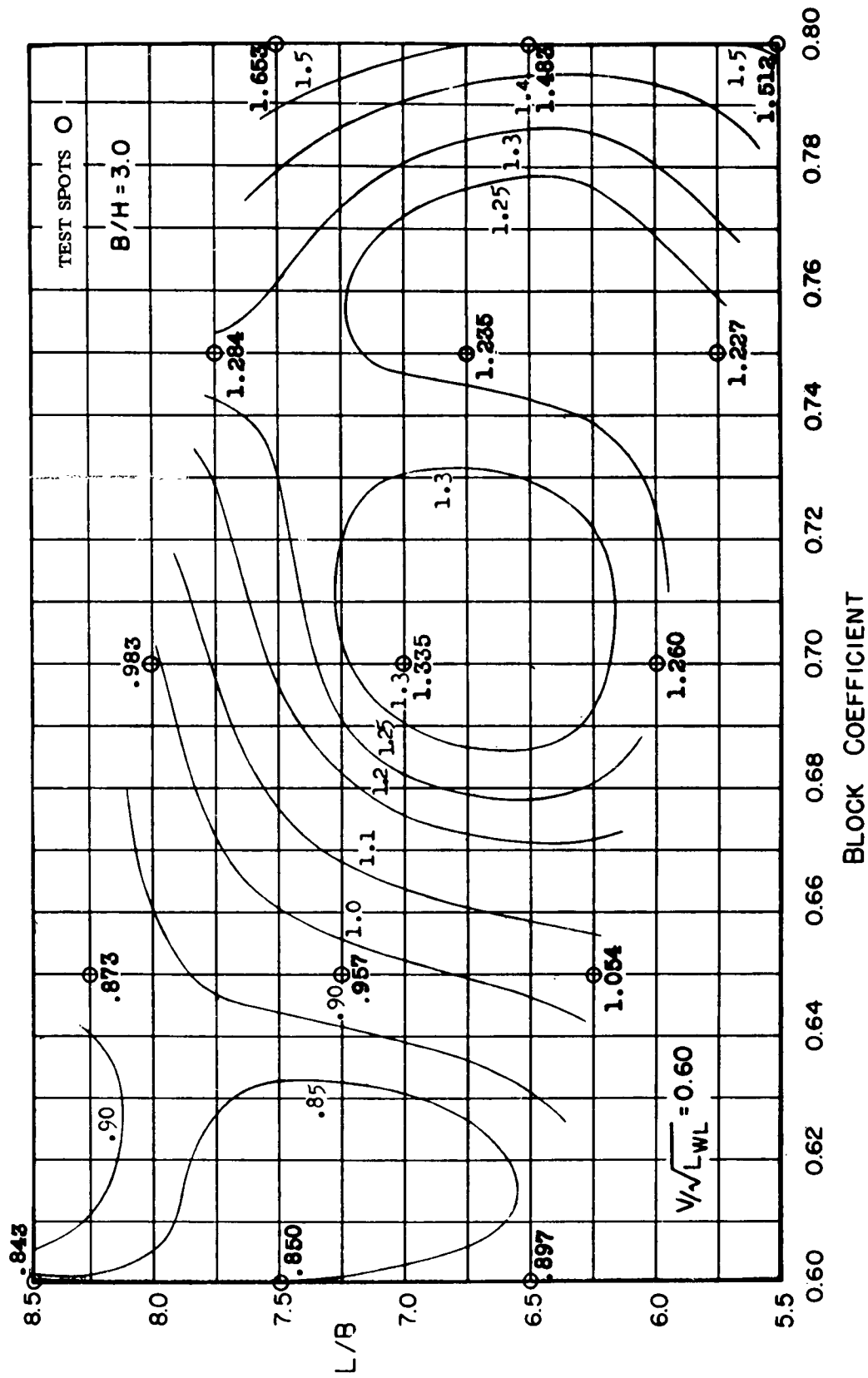


Figure C3 - Interpolation Curves of $\frac{R_r}{\Delta}$ between C_B Values

All the $\frac{R_R}{\Delta}$ contours show only the portion covered by the range of model tests. The tests were not conducted to as high a speed range for models of higher block coefficients, as for those of lower block coefficient. Hence the contours at higher $\frac{V}{\sqrt{L}}$ values cover only the lower block coefficient range.

The contours of \textcircled{C} , thrust deduction t , and wake fraction w , were obtained in the same manner as those of $\frac{R_R}{\Delta}$ except that the original 15 points were taken at constant \textcircled{K} and constant ship speed, respectively.

All the computation work was done by the Applied Mathematics Laboratory on a UNIVAC computer; this not only saved a great deal of time and money but also greatly reduced the chance of errors. The choice of the interpolation equations was somewhat arbitrary, but the comparison made in Figure C3 suggests that they do give a very good presentation of the data. However, the original results are all included in Appendix B and may be used to carry out any other form of plotting or interpolation desired.

APPENDIX D

NUMERICAL EXAMPLE OF USE OF SERIES 60 CHARTS

In order to illustrate the use of the Series 60 Charts in preparing lines plans and power estimates, a numerical example is worked out in this appendix.

The design chosen is that of a ship corresponding in main dimensions with SCHUYLER OTIS BLAND. It was selected because a model of the resultant Series 60 equivalent of this ship had been made and run, as described in the report, so that actual model data are available for comparison with the Series 60 estimates.

The principal particulars of SCHUYLER OTIS BLAND as built are given in the first column of Table D1.

Table D1 – Principal Design Data of SCHUYLER OTIS BLAND

	SCHUYLER OTIS BLAND	SERIES 60 EQUIVALENT
L_{WL} , ft	453.0	457.6
L_{BP} , ft	450.0	450.0
Beam, ft	66.0	66.0
Draft, ft	27.0	27.0
Displacement, tons	14,920	14,920
C_B	0.651	0.651
C_X	0.980	0.982
C_P	0.664	0.663
$\frac{1}{2} \alpha_E$, deg	9.5	9.3
x/L	0.510	0.510
L_E/L	0.503	0.472
L_X/L	0	0.036
L_R/L	0.497	0.492
K_R		0.204
LCB	4.5 ft aft \square = 1 percent L_{BP} aft	4.5 ft aft \square = 1 percent L_{BP} aft

Knowing the value of the block coefficient (0.651), the midship area coefficient, prismatic coefficient and bilge radius coefficient can be obtained from Figure 3. The values are 0.982, 0.663 and 0.204 respectively as given in the second column of the table. They correspond to the characteristics chosen for Series 60, and so differ a little from those of the type ship.

From Figures 4 and 9 the half-angle of entrance on the load waterline $\frac{1}{2} \alpha_E$ is found to be 9.3 deg, the parallel body is 3.6 percent of the LBP . $\left(\frac{L_X}{L_{BP}} = 0.036 \right)$ and the length of entrance L_E is given by the ratio $\frac{L_E}{L_{BP}} = 0.472$. Hence the length of run is determined by the ratio $\frac{L_R}{L_{BP}} = 0.492$.

The LCB is required to be at 1.0 percent LBP aft of amidships, between perpendiculars. For this position and a block coefficient of 0.651, Figure 10 shows that the ratio of prismatics of entrance and run must be 0.916.

We then have two conditions to determine C_{PE} and C_{PR} :

$$\frac{C_{PE}}{C_{PR}} = 0.916$$

$$C_P \times L = C_{PE} \times L_E + L_X + C_{PR} \times L_R$$

i.e., $0.663 = C_{PE} \times 0.472 + 0.036 + C_{PR} \times 0.492$

Substituting for C_{PR}

$$0.663 - 0.036 = (0.472 + 0.537) C_{PE}$$

and $C_{PE} = 0.621$

and $C_{PR} = 0.678$

The form particulars are now

$$L_E = 0.472 \times 450 = 212.4 \quad C_{PE} = 0.621$$

$$L_P = 0.036 \times 450 = 16.2 \quad C_{PX} = 1.000$$

$$L_R = 0.492 \times 450 = \underline{221.4} \quad C_{PR} = 0.678$$

$$L_{BP} = 450.0$$

The offsets for the area curve can now be obtained from Figures 5a and 5b. The charts must be entered with the correct coefficient, C_{PE} or C_{PR} , as necessary, and the area ordinates obtained are to be equally spaced along the lengths of entrance and run respectively.

In this particular case, the ordinates are:

RUN											
Station	1 (AP)	2	3	4	5	6	7	8	9	10	11
Dist. from AP, ft	0	22.14	44.28	66.42	88.56	110.70	132.84	154.98	177.12	199.26	221.40
Area Coefficient	0.006	0.129	0.313	0.505	0.672	0.803	0.900	0.960	0.988	0.998	1.000

ENTRANCE											
Station	21 (FP)	20	19	18	17	16	15	14	13	12	11
Dist. from FP, ft	0	21.24	42.48	63.72	84.96	106.20	127.44	148.68	169.92	191.16	212.40
Area Coefficient	0	0.102	0.233	0.385	0.551	0.707	0.830	0.920	0.970	0.995	1.000

The parallel middle body is inserted between the entrance and run. An area curve is now plotted, area coefficients lifted at equally spaced stations, and a calculation made to check that the right prismatic coefficient and LCB position have been obtained. (Figure D1).

This calculation is shown in Table D2.

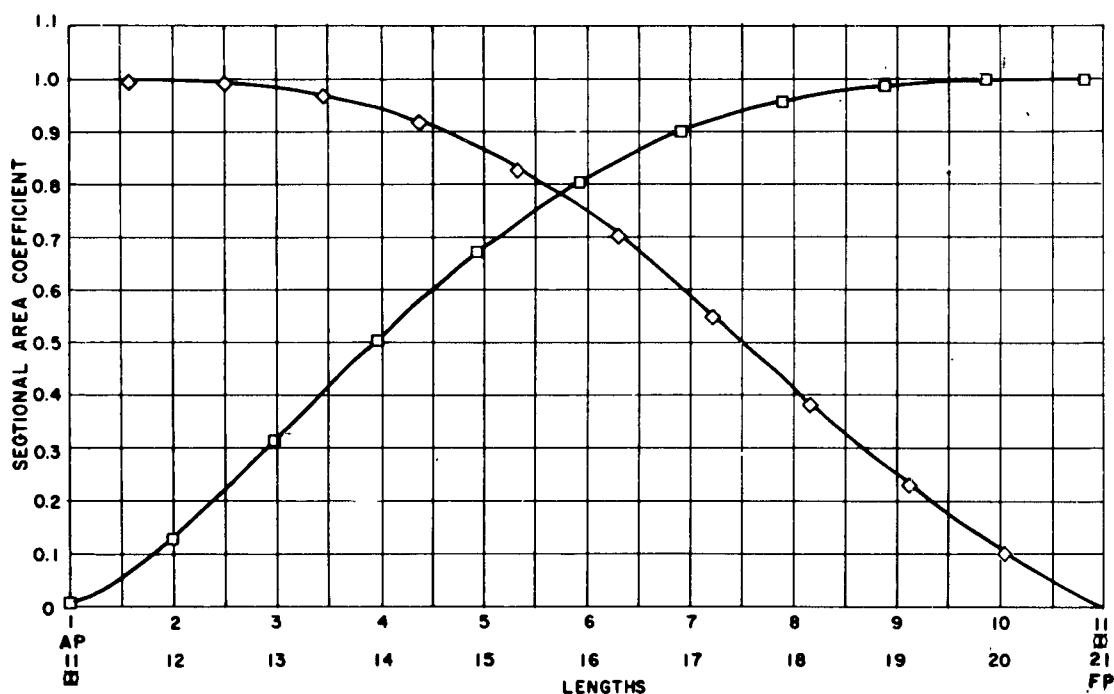


Figure D1 – Area Curves for Series 60 Equivalent of SCHUYLER OTIS BLAND

Table D2 – Check on C_p and LCB Position

(New ordinates at equal spacing, 22.5 ft)

Station	Ordinates	SM.	f (vol)	lever	f (moment)
1 AP	0.006	1	0.006	10	0.060
2	0.135	4	0.540	9	4.860
3	0.322	2	0.644	8	5.152
4	0.514	4	2.056	7	14.392
5	0.683	2	1.366	6	8.196
6	0.815	4	3.260	5	16.300
7	0.910	2	1.820	4	7.280
8	0.965	4	3.860	3	11.580
9	0.990	2	1.980	2	3.960
10	0.999	4	3.996	1	3.996
11 ☒	1.000	2	2.000	0	75.776
12	0.999	4	3.996	1	3.996
13	0.985	2	1.970	2	3.940
14	0.947	4	3.788	3	11.364
15	0.868	2	1.736	4	6.944
16	0.750	4	3.000	5	15.000
17	0.590	2	1.180	6	7.080
18	0.416	4	1.664	7	11.648
19	0.250	2	0.500	8	4.000
20	0.110	4	0.440	9	3.960
21 FP	–	1	0	10	–
			60)39.802		67.932
			<u>$C_p = 0.663$</u>		<u>75.776</u>
					7.844
$LCB = \frac{7.844}{39.802} \times 22.5 = 4.434 \text{ ft aft } \text{☒}$					
$= 0.985 \text{ percent } L \text{ aft } \text{☒ } B_p$					

The resultant prismatic coefficient is 0.663, as desired, and the LCB is 0.985 percent L_{BP} aft of midships, as compared with 1.00 percent required, which is sufficiently close for practical purposes. It is significant that this close agreement was obtained immediately from the contours without any adjustment or personal factor being involved. This shows the usefulness of the Series to the designer for obtaining a set of lines which will fulfill the design requirements at a very early stage and from which stability, capacities and similar quantities can be obtained.

A similar procedure can now be used to draw the lines plan; half-breadths on different waterlines and stations can be obtained from Figures 6a to 6p and the bow and stern contours from Figure 11. The half-breadths must be set off at stations equally spaced along the entrance and run.

An estimate of the resistance and ehp can now be made from the contour charts, using the format given in Tables B46 and B47.

The information required to complete the tables is as follows:

L_{WL} ft	= 457.6	$\sqrt{L_{WL}}$	= 21.39
L_{BP} ft	= 450.0	$\sqrt{L_{BP}}$	= 21.21
B ft	= 66.0	L_M ft	= 20.338 on WL
H ft	= 27.0	λ	= 22.5
Δ , tons	= 14,920	$\Delta^{2/3}$	= 606.19
S , sq ft	= 39,994	$\Delta^{1/3}$	= 24.621
C_B	= 0.651	$\Delta^{1/6}$	= 4.962
$\frac{L_{BP}}{B}$	= $\frac{450}{66} = 6.82$	∇	= 522,200 cu ft
$\frac{B}{H}$	= $\frac{66}{27} = 2.444$	$\nabla^{2/3}$	= 648.35
		$\nabla^{1/3}$	= 80.52
		$\frac{S}{\nabla^{2/3}}$	= $\frac{39994}{648.35} = 6.168$

For the interpolation process, we need the values of X and X^2 , where

$$X = 2\left(\frac{B}{H} - 3.0\right) = 2(2.444 - 3.0) = -1.112$$

and

$$X^2 = + 1.2365$$

The value of the wetted surface S used above was calculated from the lines drawing. An approximate value can be obtained from the contours shown in Figures B124 to B126 for use in the first ehp estimates, which will probably be made for a number of forms before any lines are drawn.

COLUMN					
B	C	D	E	F	G
$\frac{S}{\nabla^{2/3}}$ from contours for $\frac{B}{H}$ of			$\frac{D-B}{2}$	$\frac{D+B-2C}{2}$	$\frac{S}{\nabla^{2/3}}$ for $\frac{B}{H} = 2.444$ $= C + E \cdot X + F \cdot X^2$ $= 6.38 - 0.228 + 0.031$
2.5	3.0	3.5			
6.20	6.38	6.61	+ 0.205	+ 0.025	6.183

This compares with a value of $\frac{S}{\nabla^{2/3}}$ of 6.168 from the calculated wetted surface, a difference of only 0.24 percent.

Table D3 shows the calculation of ehp and ship \textcircled{C} values from the $\frac{R_R}{\Delta}$ contours given in Figures B1 to B39. The table is largely self-explanatory. Columns B, C, and D give the values of $\frac{R_R}{\Delta}$ lifted from the contours for different values of $\frac{V}{\sqrt{L_{\psi L}}}$ and $\frac{B}{H}$. These are corrected to the desired $\frac{B}{H}$ for the ship in columns E, F, and G by the interpolation process described in the text and illustrated above in its application to the $\frac{S}{\nabla^{2/3}}$ contours.

Column J shows the values of $\frac{R_F}{S}$ obtained from the nomograph in Figure B127.

The final ehp in column M is for the bare hull, without bilge keels, rudder, or other appendages.

For comparison with other models, the values of \textcircled{C} and \textcircled{K} for the actual ship are given in columns P and Q.

Estimates of the \textcircled{C} value for a 400-ft standard ship ($\textcircled{C}_{400 \text{ ft}}$) can be made directly from $\textcircled{C}_{400 \text{ ft}}$ contours given in Figures B40 through B78. These are useful for estimates and comparisons with other data when considering various alternative choices of length, beam, draft, fullness, etc., before the design is finalized and an actual ehp for the ship is required.

The calculation is shown in Table D4; it follows the same method of interpolation as used in Table D3 but is much shorter for the purpose in view.

The \textcircled{C} and ehp estimates made up to this point are for a ship having the LCB in the position chosen for the parents of the $\frac{L}{B}$, $\frac{B}{H}$ series. For a block coefficient of 0.65, this position was 1.54 percent L_{BP} aft of midships, whereas for this particular ship SCHUYLER

Table D3 — Effective Horsepower Estimate from Series 60 $\frac{R_R}{\Delta}$ Contours

SERIES 60 MODEL NO. 4484W
Ship Equivalent of SCHUYLER OTIS BLAND

Formulae and Constants

Ship Dimensions
English or Metric Units

English Units

Metric Units

$$\begin{aligned}
 L_{WL} & \quad .457.6 & C_B (L_{BP}) & \quad 0.651 \\
 L_{BP} & \quad 450.0 & \frac{L_{BP}}{B} & \quad 6.82 \\
 B & \quad 66.0 & \frac{B}{H} & \quad 2.444 \\
 H & \quad 27.0 & \Delta^{2/3} & \quad 606.19 \\
 \lambda & \quad 14.920 & \Delta^{1/6} & \quad 4.962 \\
 S & \quad 33.994 & X & \quad -1.112 \\
 \sqrt{L_{WL}} & \quad 21.39 & X^2 & \quad +1.2365
 \end{aligned}$$

$$\begin{aligned}
 \frac{R_R}{\Delta} &= \frac{R_R}{\Delta} \left(\text{for } \frac{B}{H} = 3.0 \right) + aX + bX^2 \\
 X &= 2 \left[\frac{B}{H} - \frac{R_R}{\Delta} \right]_{H(\text{of prototype})} - 3.0 \\
 a &= \frac{R_R}{\Delta(3.5)} - \frac{\Delta(2.5)}{2} \\
 b &= \frac{R_R}{\Delta(3.5)} + \frac{R_R}{\Delta(2.5)} - 2 \frac{R_R}{\Delta(3.0)} \\
 \odot &= Y \cdot \frac{EHP}{V^3} \\
 \otimes &= Z \cdot V
 \end{aligned}$$

$$\begin{aligned}
 R_R \text{ in kg.} &= 0.4464 \left(\frac{R_R}{\Delta} \right) \Delta \text{ (met. tons)} \\
 R_F \text{ in kg.} &= 4.882 \left(\frac{R_F}{S} \right) S \text{ (sq.m)} \\
 V \text{ in knots} &= 1.811 \left(\frac{V}{\sqrt{L_{WL}}} \right) \sqrt{L_{WL}} \text{ (m)} \\
 EHP \text{ in Metric HP} &= \frac{V \cdot R \text{ (kg)}}{145.7} \\
 VL &= 3.281 \cdot V \cdot L_{WL} \text{ (m)} \\
 Y &= \frac{425.7}{\Delta^{2/3}} \text{ (met. tons)} \\
 Z &= \frac{0.5850}{\Delta^{1/6}} \text{ (met. tons)}
 \end{aligned}$$

A	B	C	D	E	F	G	H	I	J	K	L	M	N	O	P	Q
$\frac{V}{\sqrt{L_{WL}}}$	$\frac{R_R}{\Delta}$ from contours			$\frac{a}{D-B}$	$\frac{b}{D+B-2C}$	$\frac{R_R}{\Delta}$	$\frac{R_R}{\Delta}$	$\frac{VL}{N \cdot L_{WL}}$	$\frac{R_F}{S}$	$\frac{R_F}{J \cdot S}$	$\frac{R}{H+K}$	$\frac{EHP}{N \cdot L}$	$\frac{V}{\Delta \cdot \sqrt{L_{WL}}}$	$\frac{V^3}{N^3}$	$\frac{Y \cdot M}{O}$	$\frac{\otimes}{Z \cdot N}$
	$\frac{R}{H}$	$\frac{B}{H} = 3.0$	$\frac{B}{H} = 3.5$													
0.40	0.340	0.400	0.415	+0.0375	-0.022	0.3311	4940	3915	0.428	17.117	22.057	580	8.556	626	0.653	1.006
0.45	0.451	0.510	0.538	+0.0435	-0.015	0.4431	6611	4404	0.534	21.357	27.968	827	9.625	892	0.653	1.132
0.50	0.595	0.640	0.676	+0.0405	-0.005	0.5888	8785	4894	0.652	26.076	34.861	1145	10.695	1223	0.660	1.257
0.55	0.762	0.800	0.840	+0.0390	+0.001	0.7579	11,308	5383	0.779	31.115	42.463	1534	11.764	1628	0.664	1.383
0.60	0.940	1.010	1.060	+0.060	-0.010	0.9310	13,890	5873	0.922	36.874	50.764	2001	12.834	2114	0.667	1.509
0.65	1.215	1.270	1.340	+0.062	+0.007	1.2079	18,022	6562	1.070	42.794	60.816	2597	13.903	2687	0.681	1.635
0.70	1.542	1.580	1.700	+0.079	+0.041	1.5429	23,020	6852	1.235	49.393	72.413	3330	14.973	3357	0.699	1.760
0.75	1.930	1.930	2.090	+0.080	+0.080	1.9399	28,943	7341	1.407	56.272	85.215	4198	16.042	4128	0.716	1.886
0.80	2.245	2.360	2.570	+0.162	+0.048	2.2392	33,409	7830	1.600	63.990	97.399	5119	17.112	5011	0.720	2.012
0.85	3.030	3.070	3.350	+0.160	+0.120	3.0404	45,363	8320	1.780	71.190	116.553	6508	18.181	6010	0.763	2.138
0.90	5.000	5.380	5.560	-0.120	+0.300	5.8843	87,794	8609	1.985	79.388	167,182	9885	19.251	7134	0.976	2.263

Table D4 – (C) Estimate from Series 60 (C) Contours

Ship SERIES 60 MODEL NO. 4484W
Equivalent of SCHUYLER OTIS BLAND

Ship Dimensions				Formulae	
L_{WL}	<u>457.6</u>	$C_B(L_{BP})$	<u>0.651</u>	$\textcircled{C}_{400} = \textcircled{C}_{400 \text{ (for } B/H = 3.0)} + aX + bX^2$	
L_{BP}	<u>450.0</u>	L_{BP}/B	<u>6.82</u>	$X = 2[B/H \text{ (of prototype)} - 3.0]$	
B	<u>66.0</u>	B/H	<u>2.444</u>	$a = \frac{\textcircled{C}_{400 \text{ (3.5)}} - \textcircled{C}_{400 \text{ (2.5)}}}{2}$	
H	<u>27.0</u>	X	<u>-1.112</u>	$b = \frac{\textcircled{C}_{400 \text{ (3.5)}} + \textcircled{C}_{400 \text{ (2.5)}} - 2\textcircled{C}_{400 \text{ (3.0)}}}{2}$	
∇	<u>522,200</u>	X^2	<u>+1.2365</u>		
$S/\nabla^{2/3}$	<u>6.168</u>				

A	B	C	D	E	F	G
K	C ₄₀₀ from contours			a	b	C ₄₀₀
	B/H = 2.5	B/H = 3.0	B/H = 3.5	$\frac{D-B}{2}$	$\frac{D+B-2C}{2}$	C+EX+FX ²
1.2	0.669	0.692	0.713	+0.022	-0.001	0.667
1.3	0.673	0.690	0.711	+0.019	+0.002	0.671
1.4	0.677	0.689	0.708	+0.015	+0.003	0.676
1.5	0.680	0.691	0.709	+0.015	+0.003	0.678
1.6	0.685	0.697	0.713	+0.014	+0.002	0.683
1.7	0.695	0.706	0.722	+0.013	+0.002	0.694
1.8	0.711	0.716	0.733	+0.011	+0.006	0.711
1.9	0.717	0.724	0.745	+0.014	+0.007	0.716
2.0	0.728	0.729	0.752	+0.012	+0.011	0.730
2.1	0.756	0.742	0.758	+0.001	+0.015	0.759
2.2	0.835	0.778	0.776	-0.030	+0.027	0.844
2.3	1.030	0.875	0.825	-0.102	+0.052	1.052
2.4	1.280	1.030	0.930	-0.175	+0.075	1.318

OTIS BLAND, the required position is 1.00 percent L_{BP} aft. The correction can be made from the data given in Tables 49–53, and the resultant ehp and \textcircled{C} values are shown in Table D5. The parent model of 0.65 C_B had the LCB 1.54 percent L_{BP} aft of midships, whereas the position required in the Series 60 equivalent of SCHUYLER OTIS BLAND is 1.00 percent L_{BP} aft.

The corrections given in Tables 49–53 were cross plotted to a base of LCB position and the values lifted off at the desired point are shown in Table D5. Because of the erratic variation of \textcircled{C} with LCB position, linear interpolation is not possible.

These values are plotted in Figures D2 and D3. The two \textcircled{C} curves in Figure D2 are in very good agreement, remembering that the one for the 450-ft ship should be lower than that for the 400-ft ship because of the difference in skin friction coefficient. This agreement is of considerable interest because one \textcircled{C} curve is derived from the $\frac{R_R}{\Delta}$ contours, the other from the $\textcircled{C}_{400 \text{ ft}}$ contours, and although both sets of contours are based ultimately on the same model experiment results, the subsequent fairing to obtain the contours was done quite independently. The agreement indicates that both sets represent the results very closely.

In the course of the analysis of the Series 60 original parents, a comparison was made between the model of the actual SCHUYLER OTIS BLAND and a model of the Series 60 equivalent. It is thus possible to make a direct comparison between these model results and the estimates made from the Series 60 contours. The actual model results are shown in Table D6 and plotted in Figures D2 and D3. They give considerable confidence in estimates made from the Series 60 contours.

For propulsion data, the wake and thrust deduction fractions and the relative rotative efficiencies can be obtained from the respective contours in Figures B79 through B123, using the same method of interpolation as with the $\frac{R_R}{\Delta}$ and \textcircled{C} contours. With this information and suitable propeller design charts, estimates can easily be made of propulsive efficiencies for different engine conditions, provided the propeller diameter is about 0.7 of the draft. For any other diameter/draft ratio, corrections can be made from the data given in Chapter X of this report.

Much of the model data in the world is published in the form of $\textcircled{C}_{400 \text{ ft}}$ using the Froude O_M and O_S frictional coefficients in the extrapolation from model to ship. As stated in the text, Gertler has given a quick method of converting $\textcircled{C}_{400 \text{ ft}}$ from the Froude values to the ATTC values, or vice versa,⁴⁷ and his chart is reproduced in Figure D4.

As an example, take the case of the Series 60 equivalent of SCHUYLER OTIS BLAND at a \textcircled{K} value of 2.0.

$$l_m = 20.338 \text{ ft}$$

$$\Delta = 14,920 \text{ tons for 450-ft ship and } \Delta = 14,920 \times \left(\frac{400}{450}\right)^3 \text{ for 400-ft ship}$$

$$\textcircled{S} = 6.168 \qquad \qquad \qquad = 10,473 \text{ tons.}$$

Table D5a – Correction to Actual Ship \textcircled{C} and EHP for Shift in *LCB* Position

$\frac{V}{\sqrt{L_{WL}}}$	Percent Correction from Series 60 LCB Position	Uncorrected \textcircled{C} Ship from Table D3	\textcircled{C} Ship Corrected	Uncorrected EHP from Table D3	EHP Corrected
0.40	+1.0	0.653	0.659	580	586
0.45	+0.4	0.653	0.655	827	830
0.50	-0.2	0.660	0.659	1145	1143
0.55	-0.5	0.664	0.661	1534	1526
0.60	---	0.667	0.667	2001	2001
0.65	-0.3	0.681	0.679	2597	2589
0.70	-1.0	0.699	0.692	3330	3297
0.75	-0.4	0.716	0.713	4198	4181
0.80	+0.1	0.720	0.721	5119	5124
0.85	+0.5	0.763	0.767	6508	6540
0.90	+0.7	0.976	0.983	9885	9954

Table D5b – Correction to $\textcircled{C}_{400 \text{ ft}}$ Ship and EHP for Shift in *LCB* Position

\textcircled{K}	$\frac{V}{\sqrt{L_{WL}}}$	Percent Correction from Series 60 LCB Position	$\textcircled{C}_{400 \text{ ft}}$ Uncorrected from Table D4	$\textcircled{C}_{400 \text{ ft}}$ Corrected
1.2	0.477	+0.1	0.667	0.668
1.3	0.517	-0.3	0.671	0.669
1.4	0.557	-0.5	0.676	0.673
1.5	0.596	---	0.678	0.678
1.6	0.636	-0.2	0.683	0.682
1.7	0.676	-0.7	0.694	0.689
1.8	0.716	-0.9	0.711	0.705
1.9	0.755	-0.4	0.716	0.713
2.0	0.795	---	0.730	0.730
2.1	0.835	+0.4	0.759	0.762
2.2	0.875	+0.6	0.844	0.849
2.3	0.915	+0.8	1.052	1.060
2.4	0.954	+1.0	1.318	1.331

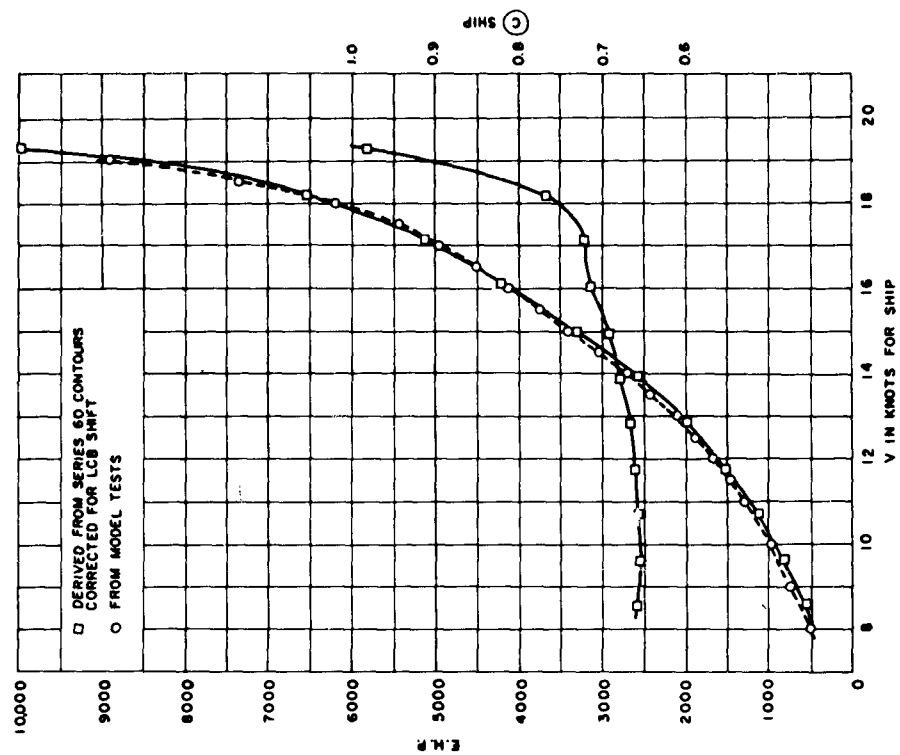


Figure D3 - Comparison of Ship C and EHP for SCHUYLER OTIS BLAND as Estimated with Those from Model Tests

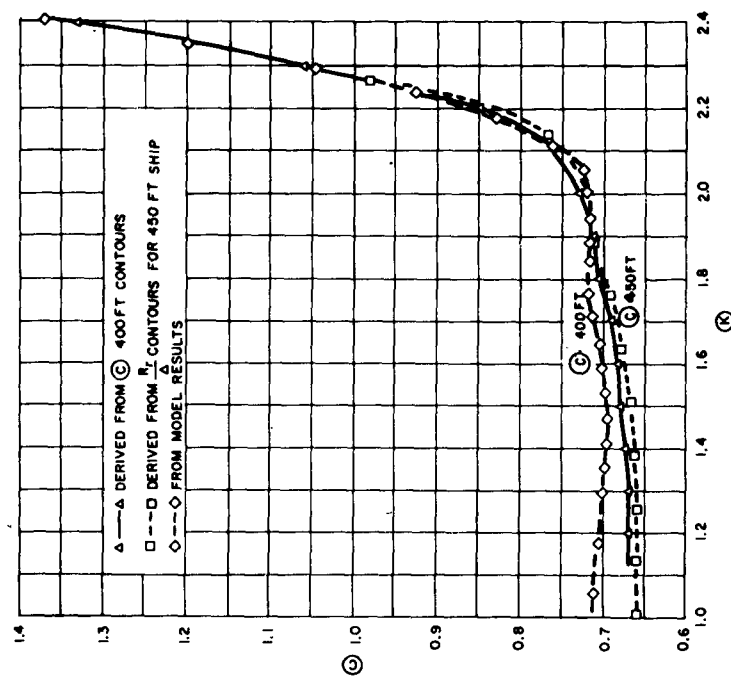


Figure D2 - Comparison of C Curves from C and $\frac{R_R}{\Delta}$ Contours for SCHUYLER OTIS BLAND

Table D6 – Model Results for Series 60
Equivalent of SCHUYLER OTIS BLAND

V, Knots	EHP for Ship	(K)	(C) _{400 ft Ship}
8	514	1.058	0.711
9	725	1.176	0.706
10	987	1.293	0.701
11	1305	1.352	0.698
11.5	1486	1.411	0.696
12	1683	1.470	0.695
12.5	1899	1.528	0.698
13	2144	1.587	0.702
13.5	2415	1.646	0.704
14	2691	1.705	0.713
14.5	3044	1.764	0.720
15	3403	1.822	0.719
15.5	3749	1.881	0.717
16	4115	1.940	0.716
16.5	4505	1.999	0.718
17	4943	2.058	0.724
17.5	5433	2.116	0.763
18	6213	2.175	0.830
18.5	7372	2.234	0.925
19	8906	2.293	1.046
19.5	10908	2.352	1.200
20.0	13517	2.410	1.373

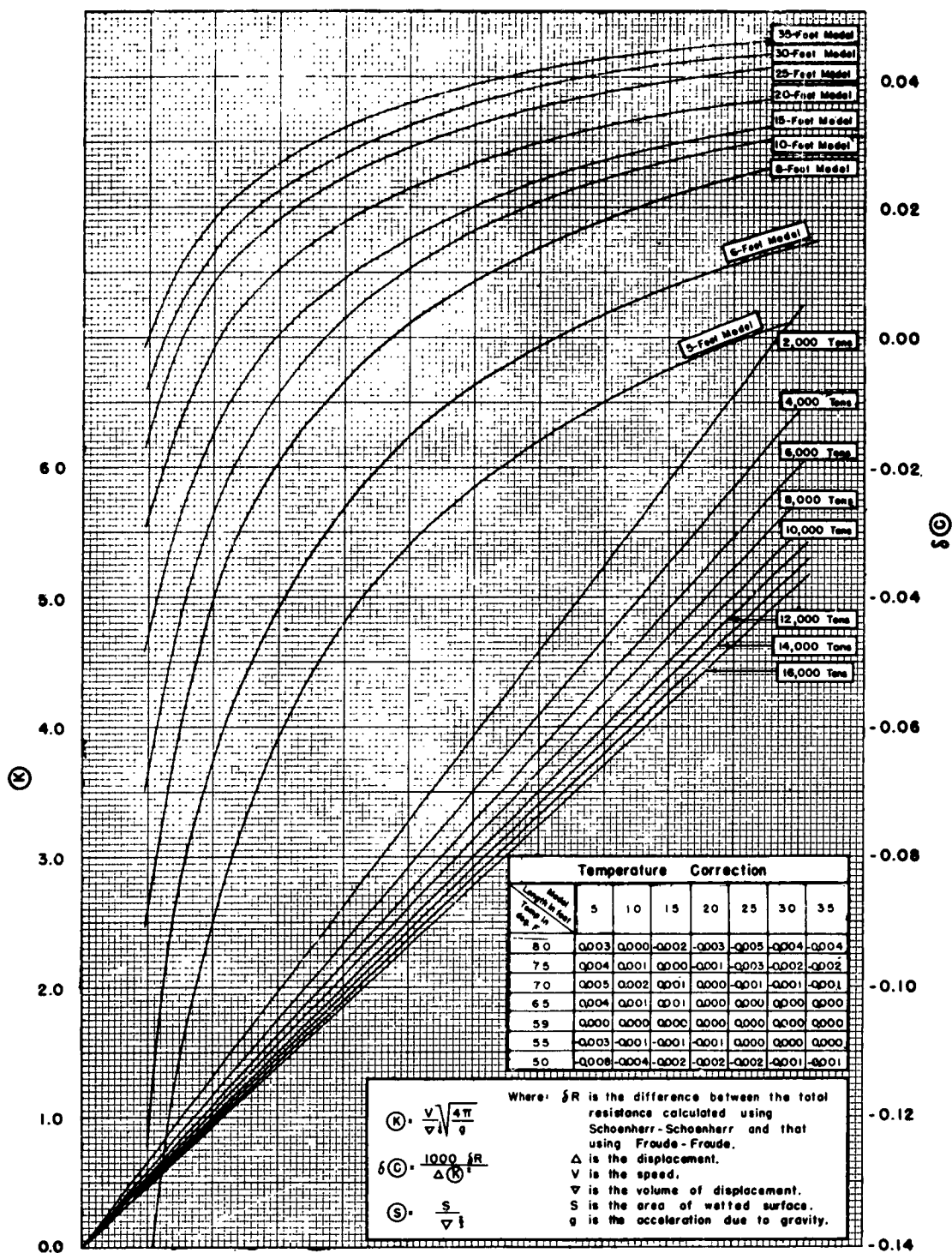


Figure D4 - The Difference δC between the Froude C and the Schoenerr C with a Roughness Allowance of 0.0004

The values given in the contours are for a 400-foot ship having a S of 6.00 and operating in salt water of 59°F. A positive δC indicates that the Schoenerr C is higher than the Froude C .

The chart is drawn for 59°F and a ship correlation allowance of +0.0004 on the ATTC C_F values.

Entering the chart at $(K) = 2.0$, going across to a displacement of 10,473 tons, up to the model length of 20.338 ft and across to the scale of $\delta(C)$, we find $\delta(C)$ has a value of 0.017, to be subtracted from the ATTC value to obtain the Froude value. This is for a standard (S) of 6.0; for the actual (S) of 6.168, the correction will be

$$\delta(C) = \frac{6.168}{6.000} \times 0.017 = 0.0175$$

$$\begin{aligned} \text{Hence the Froude value of } (C)_{400 \text{ ft}} &= 0.730 - 0.017 \\ &= 0.713 \end{aligned}$$

or 2.3 percent less than the ATTC value with +0.0004 correlation allowance. One other calculation may be necessary—the conversion from ATTC to ITTC correlation lines. The procedure for doing this is set out in full in Appendix E, to which reference may be made for details.

The calculation for the SCHUYLER OTIS BLAND Series 60 equivalent is given below to illustrate the difference between the final ehp obtained by the two methods.

At a speed defined by $\frac{V}{\sqrt{L_{WL}}} = 0.70$, we have from Table D3

$$\frac{R_R}{\Delta} = 1.5429 \text{ and } R_R = 23,020 \text{ lbs}$$

For the ship, $VL = 14.973 \times 457.6 = 6852$, and entering the nomograph in Figure E1 with this value, the corresponding value of $C'_{F \text{ ship}} + 0.0004 = 0.001950$ for the ITTC line.

The model length is 20.338 ft, so that the scale is 22.5, and the model speed corresponding to a ship speed of 14.973 knots is

$$\frac{14.973}{\sqrt{22.5}} = 3.16 \text{ knots}$$

Hence for the model, $VL = 3.16 \times 20.338 = 64.3$. Entering the same chart at this value of VL gives a value for the ITTC line of $C'_{F \text{ model}} + 0.0004 = 0.003490$.

For the same value of VL , but using the line at the extreme left of Figure E1, the corresponding value for the ATTC line is

$$C_{F \text{ model}} + 0.0004 = 0.003415$$

It is shown in Appendix E that the value of $(C'_{FS} + 0.0004)$ for the ship for use with this chart when making a conversion of this kind is

$$\begin{array}{ccc} C'_{F \text{ ship}} + C_{F \text{ model}} - C'_{F \text{ model}} \\ \text{(ITTC)} & \text{(ATTC)} & \text{(ITTC)} \end{array}$$

$$\text{or} \quad 0.001950 + 0.003415 - 0.003490$$

$$\text{or} \quad 0.001950 - 0.000075$$

$$\text{or} \quad 0.001875$$

Entering Figure E1 with this value for $(C'_{FS} + 0.0004)$ and a speed of 14.973 knots, the

value of $\frac{R_F}{S}$ is 1.197, whence $R_F = 1.197 \times 39994 = 47873$ lb. Hence $R_T = R_R + R_F$

$$= 23020 + 47873 = 70893 \text{ lb}$$

$$\text{Then ehp} = \frac{70893 \times 14.973}{325.6}$$

$$= 3260$$

The corresponding ehp using the ATTC line is 3330 (Table D3), so that using the ITTC line gives about 2 percent less ehp in this particular case.

APPENDIX E

INTERNATIONAL TOWING TANK CONFERENCE 1957

MODEL-SHIP CORRELATION LINE

Meeting in London in 1948, the ITTC* agreed that in future published work the extrapolation of model resistance results to estimate resistance and power for the ship would be carried out by using either the Froude coefficients or the ATTC 1947 line, the latter being based upon the work of Schoenherr. In using this latter line, a ship correlation allowance is usually made of +0.0004 on C_F .

The 1948 Conference also set up a Skin Friction Committee which was instructed, inter alia, "to survey the problem of skin friction in general, and in particular to recommend what further research should be carried out to establish the minimum turbulent friction line for both model and ship use."⁷⁰

This committee finally reported to the 8th ITTC in Madrid in 1957, making two alternative proposals. Both were designed to increase the slope of the ATTC line at the low values of Reynolds number associated with the use of small ship models while giving values close to the ATTC line at high Reynolds numbers. One of these proposals was, in effect, adopted by the Conference, which decided that "the line given by the formula

$$C_f = \frac{0.075}{(\log_{10} R_n - 2)^2}$$

is adopted as the ITTC 1957 model-ship correlation line, it being clearly understood that this is to be regarded only as an interim solution to this problem for practical engineering purposes."⁷¹

Tables of values of C_F derived from this formula have been given at various times (see for example Reference 72), and the differences between them and those represented by the ATTC 1947 line can be illustrated by the following figures:

$\log_{10} R_n$	Values of $C_F \times 10^3$		
	ATTC 1947 Line	ITTC 1957 Line	Difference
6.0	4.410	4.688	+0.278
7.0	2.934	3.000	+0.066
8.0	2.072	2.083	+0.011
9.0	1.531	1.531	---
10.0	1.173	1.172	-0.001

*Then called the "International Conference of Ship Tank Superintendents."

One or two points are worth mentioning in connection with this new formulation.

In the first place, the Conference was careful to label the line a "model-ship correlation line," thereby emphasising that the members did not consider it to be a line representing the skin friction of the hull nor of an equivalent plank. It is, as the resolution states, "for practical engineering purposes," and may be taken as including some allowance for form effect. At the time of the 1957 Conference, a great deal of research was in progress on the problem of extrapolation from model to ship, and it was generally felt that great developments were likely in the not too distant future—hence the emphasis on an "interim solution." These will probably take the shape of a three-dimensional system of extrapolation, allowing for the effects of hull form and proportions upon the viscous resistance. Such methods have been proposed, but the profession will no doubt wish to gain experience in their use before making what will be, after all, a radical departure from the practice of nearly a hundred years.

Secondly, the values of C_F quoted above show that the 1957 ITTC line is everywhere steeper than the 1947 ATTC line, and it is this slope which is important in the extrapolation problem. Since the ITTC line is higher over the model range, the C_R values derived from the model results will be smaller. When added to the ITTC C_F values over the ship range, which are nearly equal to or less than the ATTC values, those C_R values will result in a lower prediction of the total "smooth" ship resistance and corresponding ehp. This will apply whatever the model scale, but the effect will be larger with small models run at low Reynolds numbers.

In the third place, in adopting the new correlation line, the ITTC made no recommendation regarding the ship correlation allowance to be used in predicting ehp for the actual ship, contenting itself merely with a general recommendation to continue work "to improve model and ship correlation" and "to determine roughness allowances." In adopting its line in 1947, the ATTC considered a number of model-ship correlations available at that time and while recognizing the sparseness of the data and the possible dependence of the allowance on a number of factors other than roughness, did finally recommend a "roughness" allowance of +0.0004 for all ships; this allowance has been used since in all published work based on the ATTC 1947 line. For most merchant ships of the seagoing types, the resultant ship ehp did not differ much from that obtained using the same model results and the Froude coefficients. For the same model results and the same full-scale ship trial results, the use of the ITTC line will call for a somewhat greater correlation allowance than would the use of the ATTC line in order to obtain the same agreement. If a new three-dimensional method of extrapolation is devised in the future, the value of the correlation allowance necessary to reconcile the same model and ship results will have a still different value. It is very obvious, as pointed out by the present author in 1957, that this factor is not just an allowance for the relative roughnesses of model and ship but involves such things as the method of extrapolation used, the relative sizes of model and ship, scale effect on wake, thrust deduction, and propeller

efficiency, factors which are involved in the comparison of the resistance of the model with that of the ship as deduced from shaft horsepower measurements made on trial—and other quantities besides hull surface finish.⁷³ The term “roughness” allowance is therefore very misleading, and for this reason has not been used in the present text. The more rational name “ship correlation allowance” or “factor” has been suggested and the ITTC Presentation Committee has proposed the symbol C_A , where the suffix stands for “additional.” In Great Britain, where the Froude coefficients are still in general use, the NPL tanks have for some years used a “ship correlation factor” which has different values for different types of shell construction, these values being derived from comparisons of actual ship trial results with corresponding predictions from model tests. The British Admiralty tanks use a similar method of correlation in the form of a quasi-propulsive coefficient factor. The weight of evidence today is that the allowance of +0.0004 above the ATTC line is somewhat too high for modern merchant ships of good welded construction, with a clean, newly painted hull surface, using a standard commercial paint.

Hadler et al have recently given correlation allowances for 13 merchant ships for which good full-scale and model data were available.⁷⁴ They found that the correlation allowances decreased in magnitude both with increase of length of ship and with the date of construction, but were unable to disentangle the relative importance of these two effects because of the small number of ships available. The newer the ship, the better the probable finish of hull surface, but also the newer ships in general are longer. When they considered only seven ships built since World War II, they found the average values of C_A were +0.00015 for the ATTC line correlation and +0.00020 for the ITTC. This difference is small, and will be so for correlations carried out from experiments with large models of the order of 20 ft in length. Because of the divergence of the ATTC and ITTC lines at low Reynolds numbers, the differences in correlation allowances for the two methods will increase with the use of smaller models.

A large number of ship trials have been correlated with model experiments in Great Britain.⁷⁵ The trials were carried out on some 69 single-screw and 21 twin-screw ships by the British Ship Research Association and the models were run in the NPL tanks. There was some variation in C_A with speed, but no length effect was obvious. For all-welded hulls, the average value of C_A using the ITTC line was +0.00015 (with a total scatter of 0.0004) and for half-welded hulls (generally welded butts and riveted seams) +0.0004 (with a total scatter of 0.0007). Using the ATTC line, the corresponding C_A values were +0.00005 and +0.0003. Clements pointed out in this paper that the best results achieved to date correspond to a correlation allowance C_A of zero.

More recently, results of British ship trials embracing modern large tankers have suggested a definite trend towards lower correlation allowances with increasing length, and a proposal to represent this by the straight line

$$C_A = 0.00160 - 0.0000023 \cdot L_{BP}$$

has been made by Moor (discussion on Reference 74). This equation leads to a value of +0.00045 for a ship with an *LBP* of 500 ft, zero for 700 ft, and negative values for longer lengths, all based on the ITTC line.

In order that the Series 60 results based upon the ATTC line can be compared with others derived from model tests by the use of the ITTC line, it is desirable to provide a rapid method of conversion from one method to the other. This involves the choice of a correlation allowance C_A . In view of the above discussion, the ATTC allowance of +0.0004 would appear too high for modern ships, and moreover it should quite possibly be varied with length of ship, but there is no finality in these matters at present. Since there is little difference in the ship prediction from the Series 60 models whichever line is used for extrapolation, the only logical choice would seem to be to use the same allowance of +0.0004 with the ITTC line until such time as a more definite value is recommended by the ITTC.

A second nomograph has therefore been prepared on the basis of the ITTC line using a correlation allowance of +0.0004; see Figure E1. In any individual case, if some other value of C_A is preferred, an appropriate allowance can be made.

The relative values of the frictional and residuary resistances for a given model total resistance will be different when using the ATTC and ITTC lines, so that it is not sufficient merely to correct the frictional part of the total.

Using the suffixes *t*, *r*, and *f* for total, residuary and frictional, *m* and *s* for model and ship and C and C' for resistance coefficients using ATTC and ITTC lines, respectively, we can write

$$C_{tm} = C_{rm} + C_{fm} = C'_{rm} + C'_{fm}$$

and

$$C'_{rm} = C_{rm} + C_{fm} - C'_{fm}$$

also

$$\begin{aligned} C'_{ts} &= C'_{rs} + C'_{fs} \\ &= C'_{rm} + C'_{fs} \\ &= C_{rm} + C_{fm} - C'_{fm} + C'_{fs} \\ &= C_{rs} + C'_{fs} + (C_{fm} - C'_{fm}). \end{aligned}$$

C_{rs} is the residuary resistance coefficient as obtained using the ATTC line, and so the values of $\frac{R_R}{\Delta}$ can be lifted from the contours and inserted in Column G of Table D3 as before. The frictional resistance coefficient to use with the nomograph for the ITTC line will now be

$$C'_{fs} + (C_{fm} - C'_{fm})$$

i.e., ITTC ship coefficient + (ATTC model coefficient - ITTC model coefficient).

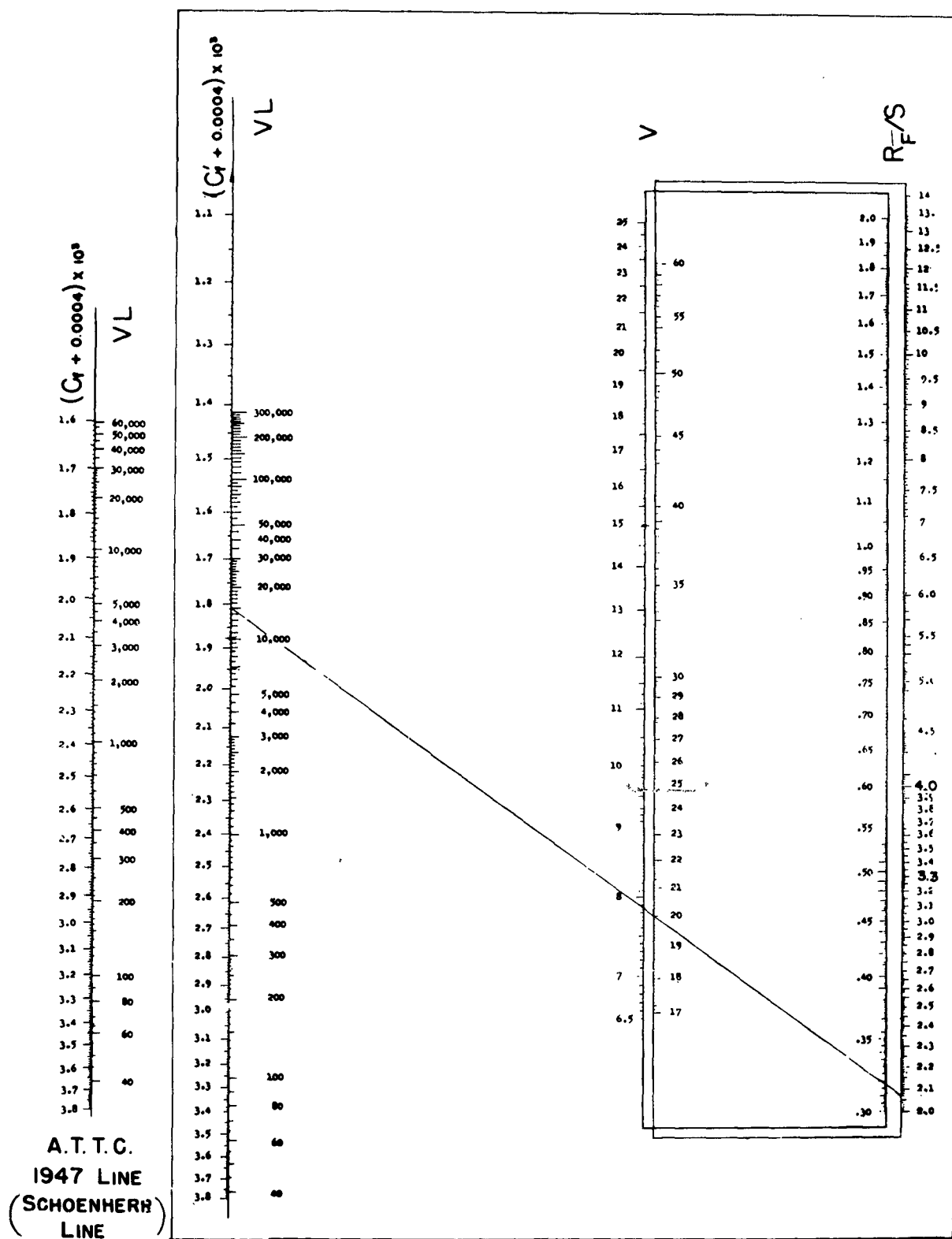


Figure E1 - Nomograph for $\frac{R_F}{S}$ Computation based on ITTC 1957 Model-Ship Correlation Line

In Figure E1 the $V \cdot L$ and C'_{f_s} scales have been extended to cover model values, so that C'_{f_m} can be found. For convenience, extended scales of VL and C_f for the ATTC line are also given at the left-hand side, but these form no part of the nomograph itself.

As an example, consider a ship 500 ft in waterline length with a speed of 20 knots.

$$V = 20 \text{ knots}$$

$$L_{WL} = 500 \text{ ft}$$

$$V \cdot L = 10,000$$

The Series 60 models have a WL length of 20.388 ft, so that the scale will be

$$\lambda = \frac{500}{20.388} = 24.52$$

For the model,
$$V = \frac{20}{\sqrt{\lambda}} = \frac{20}{\sqrt{24.52}} = \frac{20}{4.952} = 4.039 \text{ knots}$$

and
$$L = 20.388,$$

whence
$$VL = 4.039 \times 20.388 = 82.34.$$

For $VL = 82.34$, from Figure E1

$$C_{f_m} + 0.0004 = 0.00330 \text{ for ATTC line}$$

$$C'_{f_m} + 0.0004 = 0.00337 \text{ for ITTC line}$$

and for $VL = 10,000$

$$C'_{f_s} + 0.0004 = 0.001879 \text{ for the ITTC}$$

Hence the final value of the resistance coefficient to be used is

$$\begin{aligned} C'_{f_s} + (C_{f_m} - C'_{f_m}) &= 0.001879 + (0.00330 - 0.00337) \\ &= 0.001879 - 0.00007 \\ &= 0.001809 \end{aligned}$$

On Figure E1, starting with this value of C'_{f_s} for the ITTC line, a straight line through a speed of 20 knots on the V scale will give a value of $\frac{R_F}{S}$ of 2.069, which will be inserted in Column J of Table D3 and the calculation completed in the usual way.

REFERENCES

The following standard abbreviations are used in these references:

Trans. INA	- Transactions, Institution of Naval Architects, London
SSPA	- Statens Skeppsprovings Anstalt (Swedish State Shipbuilding Experimental Tank), Goteborg
Trans. NECI	- Transactions, North East Coast Institution of Engineers and Shipbuilders, Newcastle, England
Trans. IME	- Transactions, Institute of Marine Engineers, London
Trans. IESS	- Transactions, Institution of Engineers and Shipbuilders in Scotland, Glasgow
NSMB	- Netherlands Ship Model Basin, Wageningen
SNAME	- Society of Naval Architects and Marine Engineers, New York
TMB	- David Taylor Model Basin

1. Project 2 of the Hydromechanics Subcommittee of the Society of Naval Architects and Marine Engineers, "Model and Expanded Resistance Data Sheets."
2. Taylor, D.W., "Speed and Power of Ships," published by the Department of Commerce, Washington, D.C. (1933).
3. Kent, J.L., "Model Experiments on the Effect of Beam on the Resistance of Mercantile Ship Forms," Trans. INA (1919).
4. Lindblad, A., "Experiments with Bulbous Bows," Pub. 3, SSPA (1944).
5. Lindblad, A., "Further Experiments with Bulbous Bows," Pub. 8, SSPA (1948).
6. Nordstrom, H.F., "Some Systematic Tests with Models of Fast Cargo Vessels," Pub. 10, SSPA (1948).
7. Nordstrom, H.F., "Further Tests with Models of Fast Cargo Vessels," Pub. 14, SSPA (1949).
8. Nordstrom, H.F., "Systematic Tests with Models of Cargo Vessels with Block Coefficient = 0.575," Pub. No. 16, SSPA (1950).
9. Edstrand, H., et al., "Experiments with Tanker Models I," Pub. 23, SSPA (1953).
10. Edstrand, H., et al., "Experiments with Tanker Models II," Pub. 26, SSPA (1953).
11. Edstrand, H., et al., "Experiments with Tanker Models III," Pub. 29, SSPA (1954).
12. Lindgren, H., "Experiments with Tanker Models IV," Pub. 36, SSPA (1956).
13. Edstrand, H., et al., "Experiments with Tanker Models V," Pub. 37, SSPA (1956).
14. Warholm, A.O., "Tests with Models of Coasters," Pub. 24, SSPA (1953).
15. Lindgren, H. and Warholm, A.O., "Further Tests with Models of Coasters," Pub. 35, SSPA (1955).

16. Edstrand, H. and Lindgren, H., "Systematic Tests with Models of Ships with $\delta_{pp} = 0.525$," Pub. 38, SSPA (1956).
17. Freimanis, E. and Lindgren, H., "Systematic Tests with Ship Models with $\delta_{pp} = 0.675$ - Part I," Pub. 39, SSPA (1957).
18. Freimanis, E. and Lindgren, H., "Systematic Tests with Models of Ships with $\delta_{pp} = 0.675$ - Part II," Pub. 41, SSPA (1957).
19. Freimanis, E. and Lindgren, H., "Systematic Tests with Models of Ships with $\delta_{pp} = 0.675$ - Part III," Pub. 42, SSPA (1958).
20. Freimanis, E. and Lindgren, H., "Systematic Tests with Ship Models with $\delta_{pp} = 0.600$ to 0.750 ," Pub. 44, SSPA (1959).
21. Lindblad, A., "Some Experiments with Models of High-Speed Cargo Liners," Pub. 25, Trans. of Chalmers University Goteborg (1943).
22. Lindblad, A., "Experiments with Models of Cargo Liners," Trans. INA (1945).
23. Lindblad, A., "Some Experiments with Models of High-Speed Ships," Trans. INA (1948).
24. Lindblad, A., "Further Experiments with Models of High-Speed Ships," Trans. INA (1950).
25. Todd, F.H., "Further Model Experiments on the Resistance of Mercantile Ship Forms - Coaster Vessels," Trans. INA (1931).
26. Todd, F.H., "Screw Propeller Experiments with Models of Coasters - the Effect of a Cruiser Stern," Trans. NECI (1934).
27. Todd, F.H. and Weedon, J., "Further Resistance and Propeller Experiments with Models of Coasters," Trans. INA (1938).
28. Todd, F.H. and Weedon J., "Experiments with Models of Cargo-Carrying Type Coasters," Trans. IME (1940).
29. Todd, F.H. and Weedon, J., "Further Experiments with Models of Cargo-Carrying Coasters," Trans. NECI (1942).
30. Dawson, J., "Resistance of Single-Screw Coasters, Part I," Trans. IESS (1952-1953).
31. Dawson, J., "Resistance of Single-Screw Coasters, Part II," Trans. IESS (1954-1955).
32. Dawson, J., "Resistance of Single-Screw Coasters, Part III," Trans. IESS (1955-1956).
33. Dawson, J., "Resistance of Single-Screw Coasters, Part IV," Trans. IESS (1959-1960).
34. Haaland, A., "Some Systematic Variations in the Shape of Coasting Vessels, Etc.," Report 4, Norwegian Tank, Trondheim (1951).

35. Koning, J.G., "E.H.P. of Small Seagoing Cargo Ships," Pub. 37, NSMB.
36. Ackerson, J.L., "Test Results of a Series of 15 Models," Trans. SNAME (1930).
37. Davidson, K.S.M. and Suarez, A., "Tests of Twenty Models of V-Bottom Motor Boats, EMB Series 50," TMB Report R-47 (Mar 1949).
38. Almy, N.V. and Hughes, G., "Model Experiments on a Series of 0.65 Block Coefficient Forms, Part I," Trans. INA (1954).
39. Ferguson, J.M. and Meek, M., "Model Experiments on a Series of 0.65 Block Coefficient Forms, Part II," Trans. INA (1954).
40. Ferguson, J.M. and Parker, M.N., "Model Resistance Tests on a Methodical Series of Forms $C_B = 0.65$ to 0.75 ," Trans. INA (1956).
41. Balckwell, R.E. and Goodrich, G.J., "Model Experiments on a Series of 0.70 Block Coefficient Forms, Part I," Trans. INA (1957).
42. Blackwell, R.E. and Doust, D.J., "Model Experiments on a Series of 0.70 Block Coefficient Forms, Part II," Trans. INA (1957).
43. Moor, D.I., Parker, M.N., and Pattullo, R.N.M., "The B.S.R.A. Methodical Series - An Overall Presentation," Trans. INA (1961).
44. Todd, F.H. and Forest, F.X., "A Proposed New Basis for the Design of Single-Screw Merchant Ship Forms and Standard Series Lines," Trans. SNAME (1951).
45. Todd, F.H., "Some Further Experiments on Single-Screw Merchant Ship Forms - Series 60," Trans. SNAME (1953).
46. Hughes, G. and Allan, J.F., "Turbulence Stimulation on Ship Models," Trans. SNAME (1951).
47. Gertler, M., "A Method for Converting the British C Coefficient Based on the Froude '0' Values to an Equivalent C Coefficient Based on the Schoenherr Frictional Formula," TMB Report 657, Rev. Ed. (Jun 1949).
48. Troost, L., "A Simplified Method for Preliminary Powering of Single-Screw Merchant Ships," SNAME, New England Section (Oct. 1955).
49. van Lammeren, W.P.A., Troost, L., and Koning, J.G., "Resistance, Propulsion and Steering of Ships," H. Stam, Haarlem, Holland (1948).
50. Volker, H., "Optimum Location of L.C.B. of Merchant Ships," Schiff und Hafen, Jahrgang 5, Heft 3 (Mar 1953).
51. Bocler, H., "The Position of LCB for Minimum Resistance," Trans. IESS (1953).
52. Heckscher, E., "Erfahrungen uber Formgebung von Seeschiffen," Hydromechanische Problem des Schiffsantriebs, Hamburg, Germany (1940).

53. Ayre, Sir Amos, "Approximating EHP," Trans. NECI (1947-48).
54. Todd, F.H., "Fundamentals of Ship Form," Trans. IME (1940).
55. Dawson, J., "Resistance of S. S. Coasters," Trans. IESS (1952-53).
56. Lap, A.J.W., "Diagrams for Determining the Resistance of Single-Screw Ships," Pub. 118, NSMB (1954).
57. Troost, L., "Open Water Test Series with Marine Propeller Forms," Trans. NECI (1951).
58. Saunders, H.E. "The Prediction of Speed and Power of Ships by Methods in Use at the U.S. Experimental Model Basin, Washington," C & R Bulletin No. 7, U.S. Government Printing Office, Washington, D.C. (1933).
59. Gertler, M., "The Prediction of the Effective Horsepower of Ships by Methods in Use at the David Taylor Model Basin," TMB Report 576, Second Edition, (Dec 1947).
60. Gertler, M., "A Reanalysis of the Original Test Data for the Taylor Standard Series," TMB Report 806 (Mar 1954).
61. Hadler, J.B., Stuntz, G.R., and Pien, P.C., "Propulsion Experiments on Single-Screw Merchant Ship Forms--Series 60," SNAME (1954).
62. Todd, F.H. and Pien, P.C., "Series 60 - The Effect upon Resistance and Power of Variation in LCB Position," SNAME (1956).
63. Todd, F.H., Stuntz, G.R., and Pien, P.C., "Series 60 - The Effect upon Resistance and Power of Variation in Ship Proportions," SNAME (1957).
64. Stuntz, G.R., Pien, P.C., Hinterthan, W.B., and Ficken, N.L., "Series 60 - The Effect of Variations in Afterbody Shape upon Resistance, Power, Wake Distribution, and Propeller-Excited Vibratory Forces," SNAME (1960).
65. Harvald, S.A., "Wake of Merchant Ships," The Danish Technical Press, Copenhagen (1950).
66. Doust, D.J. and O'Brien, T.P., "Resistance and Propulsion of Trawlers," NECI, Vol. 75, (1958-59).
67. Kerwin, J.E., "Polynomial Surface Representation of Arbitrary Ship Forms," Journal of Ship Research, Vol. 4, No. 1 (1960).
68. Gerritsma, J., Kerwin, J.E., and Newman, J.N., "Polynomial Representation and Damping of Series 60 Hull Forms," International Shipbuilding Progress, Vol. 9, No. 95 (Jul 1962).
69. Hess, J.L. and Smith, A.M.O., "Calculation of Non-Lifting Potential Flow about Arbitrary Three-Dimensional Bodies," Douglas Aircraft Division Report E.S. 40622 (Mar 1962).

70. Fifth International Conference of Ship Tank Superintendents, London, 1948, p. 114, H.M. Stationery Office, London (1948).
71. Eighth International Towing Tank Conference Proceedings, Madrid, 1957, p. 324, Canal de Experiencias Hidrodinamicas, El Pardo, Madrid (1959).
72. Hadler, J.B., "Coefficients for International Towing Tank Conference 1957 Model-Ship Correlation Line," TMB Report 1185 (Apr 1958).
73. Todd, F.H., "Skin Friction and Turbulence Stimulation," Eighth International Towing Tank Conference Proceedings, Madrid 1957, p. 88-89, Canal de Experiencias Hidrodinamicas, El Pardo, Madrid (1959).
74. Hadler, J.B., Wilson, C.J., and Beal, A.L., "Ship Standardization Trial Performance and Correlation with Model Predictions," SNAME, Chesapeake Section (Dec 1961).
75. Clements, R.E., "An Analysis of Ship-Model Correlation Data Using the 1957 I.T.T.C. Line," Trans. INA (1959).

SERIES 60 PAPERS

- I. "A Proposed New Basis for the Design of Single-Screw Merchant Ship Forms and Standard Series Lines," Todd, F.H. and Forest, F.X., SNAME (1951).
- II. "Some Further Experiments on Single-Screw Merchant Ship Forms-Series 60," Todd, F.H., SNAME (1953).
- III. "Propulsion Experiments on Single-Screw Merchant Ship Forms-Series 60," Hadler, J.B., Stuntz, G.R., and Pien, P.C., SNAME (1954).
- IV. "Series 60-The Effect upon Resistance and Power of Variation in LCB Position," Todd, F.H. and Pien, P.C., SNAME (1956).
- V. "Series 60-The Effect upon Resistance and Power of Variation in Ship Proportions," Todd, F.H., Stuntz, G.R., and Pien, P.C., SNAME (1957).
- VI. "Series 60-The Effect of Variations in Afterbody Shape upon Resistance, Power, Wake Distribution and Propeller-Excited Vibratory Forces," Stuntz, G.R., Pien, P.C., Hinterthan, W.B., and Ficken, N.L., SNAME (1960).

INITIAL DISTRIBUTION

Copies

- 8 CHBUSHIPS
 - 3 Tech Lib (Code 210L)
 - 1 Lab Mgt (Code 320)
 - 1 Appl Res (Code 340)
 - 1 Prelim Des (Code 420)
 - 1 Hull Des (Code 440)
 - 1 Sub (Code 525)
- 3 CHBUWEPS
 - 1 Aero & Hydro Br (Code RAAD-3)
 - 1 Ship Instal & Des (Code SP-26)
 - 1 Dyn Sub Unit (Code RAAD-222)
- 4 CHONR
 - 1 Nav Analysis (Code 405)
 - 1 Math Br (Code 432)
 - 2 Fluid Dyn (Code 438)
- 1 ONR, New York
- 1 ONR, Pasadena
- 1 ONR, Chicago
- 1 ONR, Boston
- 1 ONR, London
- 1 CDR, USNOL, White Oak
- 2 DIR, USNRL (Code 5520)
 - 1 Mr. Faires
- 1 CDR, USNOTS, China Lake
- 1 CDR, USNOTS, Pasadena
- 1 CDR, USNAVMISCEN, Point Mugu
- 1 DIR, Natl BuStand
 - Attn: Dr. Schubauer
- 20 CDR, DDC
 - 1 DIR, APL, Johns Hopkins Univ, Silver Spring
 - 1 DIR, Fluid Mech Lab, Columbia Univ
 - 1 DIR, Fluid Mech Lab, Univ of Calif, Berkeley
- 5 DIR, DL, SIT
 - 1 DIR, Exptl Nav Tank, Univ of Mich
 - 1 DIR, Inst for Fluid Dyn & Appl Math, Univ of Maryland
 - 1 DIR, Hydrau Lab, Univ of Colorado
 - 1 DIR, Scripps Inst of Oceanography, Univ of Calif

Copies

- 1 DIR, Penn St. Univ, University Park
- 1 DIR, WHOI
- 1 Admin, Webb Inst of Nav Arch, Glen Cove
- 1 DIR, Iowa Inst of Hydrau Research
- 1 DIR, St Anthony Falls Hydrau Lab
- 3 Head, NAME, MIT, Cambridge
 - 1 Prof. Abkowitz
 - 1 Prof. Kerwin
- 1 Inst of Mathematical Sciences, NYU, New York
- 2 Dept of Engin, Nav Architecture, Univ of Calif
 - 1 Dr. J. Wehausen
- 1 Dr. E.H. Kennard, LaVerne, Calif
- 1 Dr. H.H. Jasper, US Navy Mine Def Lab
Panama City
- 1 Dr. Willard J. Pierson, Jr.,
Col of Engin, NYU, New York
- 1 Dr. Finn Michelsen, Dept of Nav Arch,
Univ of Mich, Ann Arbor
- 1 Prof. Richard MacCamy, Carnegie Tech,
Pittsburgh 13
- 1 Dr. T.Y. Wu, Hydro Lab, CIT, Pasadena
- 1 Dr. Hartley Pond, 4 Constitution Rd,
Lexington 73, Mass
- 1 Dr. J. Kotik, TRG, 2 Aerial Way,
Syosset, N.Y.
- 1 Prof. Byrne Perry, Dept of Civil Eng,
Stanford Univ, Palo Alto, Calif
- 1 Prof. B.V. Korvin-Kroukovsky,
East Randolph, Vt
- 1 Prof. L.N. Howard, Dept of Math, MIT,
Cambridge 39, Mass
- 1 Prof. M. Landahl, Dept of Aero & Astro,
MIT, Cambridge 39, Mass
- 1 Pres, Oceanics, Inc, 114 E 40 St, N.Y. 16

David Taylor Model Basin. Report 1712.

SERIES 60. METHODOICAL EXPERIMENTS WITH MODELS OF SINGLE-SCREW MERCHANT SHIPS, by F.H. Todd. Jul 63. vii. 1 vol. illus., diagr., tables, refs. UNCLASSIFIED

1. Merchant vessels--Hydrodynamic characteristics--Model tests
2. Effective horsepower (EHP)
3. Merchant vessels--Design--Requirements
4. Merchant vessels--Resistance--Model tests
5. Merchant vessels--Propulsion--Model tests
6. Ship Models--Model TMB Series 60
- I. Todd, Frederick H.
- III. Methodical experiments with models of single-screw merchant ships

David Taylor Model Basin. Report 1712.

SERIES 60. METHODOICAL EXPERIMENTS WITH MODELS OF SINGLE-SCREW MERCHANT SHIPS, by F.H. Todd. Jul 63. vii. 1 vol. illus., diagr., tables, refs. UNCLASSIFIED

1. Merchant vessels--Hydrodynamic characteristics--Model tests
2. Effective horsepower (EHP)
3. Merchant vessels--Design--Requirements
4. Merchant vessels--Resistance--Model tests
5. Merchant vessels--Propulsion--Model tests
6. Ship Models--Model TMB Series 60
- I. Todd, Frederick H.
- III. Methodical experiments with models of single-screw merchant ships

David Taylor Model Basin. Report 1712.

SERIES 60. METHODOICAL EXPERIMENTS WITH MODELS OF SINGLE-SCREW MERCHANT SHIPS, by F.H. Todd. Jul 63. vii. 1 vol. illus., diagr., tables, refs. UNCLASSIFIED

1. Merchant vessels--Hydrodynamic characteristics--Model tests
2. Effective horsepower (EHP)
3. Merchant vessels--Design--Requirements
4. Merchant vessels--Resistance--Model tests
5. Merchant vessels--Propulsion--Model tests
6. Ship Models--Model TMB Series 60
- I. Todd, Frederick H.
- III. Methodical experiments with models of single-screw merchant ships

David Taylor Model Basin. Report 1712.

SERIES 60. METHODOICAL EXPERIMENTS WITH MODELS OF SINGLE-SCREW MERCHANT SHIPS, by F.H. Todd. Jul 63. vii. 1 vol. illus., diagr., tables, refs. UNCLASSIFIED

1. Merchant vessels--Hydrodynamic characteristics--Model tests
2. Effective horsepower (EHP)
3. Merchant vessels--Design--Requirements
4. Merchant vessels--Resistance--Model tests
5. Merchant vessels--Propulsion--Model tests
6. Ship Models--Model TMB Series 60
- I. Todd, Frederick H.
- III. Methodical experiments with models of single-screw merchant ships